WHITE PAPER

Astrophysics with the Laser Interferometer Space Antenna

**Pau Amaro-Seoane · Jeff Andrews · Manuel Arca Sedda · Abbas Askar ·
Quentin Baghi · Razvan Balasov et al.** *[full author details at the end of the
article]*

Abstract

The Laser Interferometer Space Antenna (LISA) will be a transformative experiment
for gravitational wave astronomy, and, as such, it will offer unique opportunities to
address many key astrophysical questions in a completely novel way. The synergy
with ground-based and space-born instruments in the electromagnetic domain, by
enabling multi-messenger observations, will add further to the discovery potential of
LISA. The next decade is crucial to prepare the astrophysical community for LISA's
first observations. This review outlines the extensive landscape of astrophysical
theory, numerical simulations, and astronomical observations that are instrumental
for modeling and interpreting the upcoming LISA datastream. To this aim, the
current knowledge in three main source classes for LISA is reviewed; ultra-compact
stellar-mass binaries, massive black hole binaries, and extreme or interme-diate mass
ratio inspirals. The relevant astrophysical processes and the established modeling
techniques are summarized. Likewise, open issues and gaps in our understanding of
these sources are highlighted, along with an indication of how LISA could help
making progress in the different areas. New research avenues that LISA itself, or its
joint exploitation with upcoming studies in the electromagnetic domain, will enable,
are also illustrated. Improvements in modeling and analysis approaches, such as the
combination of numerical simulations and modern data science techniques, are
discussed. This review is intended to be a starting point for using LISA as a new
discovery tool for understanding our Universe.

Abbreviations
AGN   Active galactic nucleus/nuclei
AM CVn   AM Canum Venaticorum

Extended author information available on the last page of the article

AU	Astronomical Unit
BD	Brown dwarf (plural: BDs)
BH	Black hole (plural: BHs)
BH+BH	(Stellar-mass) binary black hole (plural: BH+BHs)
CDM	Cold dark matter
CE	Common envelope
CO	Compact object
COM	Centre-of-mass
CV	Cataclysmic variable
DM	Dark matter
ELM	Extremely low-mass
EM	Electromagnetic
EMRI	Extreme mass ratio inspiral
EOS	Equation of state
GR	General relativity/relativistic
GW	Gravitational wave (plural: GWs)
HMXB	High-mass X-ray binary
IMBH	Intermediate-mass black hole
IMF	Initial mass function
IMRI	Intermediate mass-ratio inspiral
IR	Infra-red
ISCO	Innermost stable circular orbit
LMXB	Low-mass X-ray binary
MBH	Massive black hole
MBHB	Massive black hole binary
MHD	Magnetohydrodynamics/magnetohydrodynamic
MSP	Millisecond radio pulsar
MW	Milky Way
MS	Main sequence
NFW	Navarro–Frenk–White
NS	Neutron star (plural: NSs)
NS+NS	Double neutron star (plural: NS+NSs)
NSC	Nuclear star cluster
PN	Post-Newtonian
Pop III	Population III
PTA	Pulsar timing array
RF	Radiative feedback
RLO	Roche-lobe overflow
SFH	Star-formation history
SGWB	Stochastic gravitational wave background
SMBH	Supermassive black hole
SMS	Supermassive star
SN	Supernova (plural: SNe)
SNR	Signal-to-noise ratio
SPH	Smoothed-particle hydrodynamics

SSO	Substellar object
TDE	Tidal disruption event
UCB	Ultra-compact binary
UCXB	Ultra-compact X-ray binary
UV	Ultra-violet
WD	White dwarf (plural: WDs)
WD+WD	Double white dwarf (plural: WD+WDs)
XMRB	Extremely large mass-ratio burst
XMRI	Extremely large mass-ratio inspiral
ZKL	Von Zeipel–Kozai–Lidov
b-EMRI	Binary-extreme mass ratio inspiral

Contents

General introduction

Gravitational wave (GW) observations have opened a new way to observe and characterize compact objects throughout the Universe and at all cosmic epochs. The Laser Interferometer Space Antenna (LISA; Amaro-Seoane et al. 2017), with its low-

frequency band coverage spanning nearly three decades, will allow the detection and study of signals from a strikingly large variety of sources, ranging from stellar-mass binaries in our own galaxy to mergers between nascent massive black holes (MBH), called black hole (BH) *seeds*, at high redshift. LISA is expected to revolutionize our understanding of these astrophysical sources by allowing reconstruction of their demographics and dynamical evolution, as well as discovery of new types of sources, including some that have been theorized but not yet detected by conventional means. Since the first detection of GWs by the Laser Interferometer GW Observatory (LIGO)/Virgo collaboration in 2015 (Abbott et al. 2016c), ground-based GW observations already had a remarkable impact on astrophysics. For instance, the gravitational-wave facilities LIGO and Virgo have observed the mergers of stellar BHs in the range ~ 6–$95\,M_\odot$ (Abbott et al. 2021), greatly expanding our knowledge of the mass spectrum of BHs. Recently, the first intermediate mass black holes (IMBH), with masses of $\sim 142\,M_\odot$, has been discovered (GW190521, see Abbott et al. 2020c). The existence of stellar-mass BHs with masses higher than observed before, as well as the discovery of an IMBH, have fostered new exciting developments in theoretical models for the formation and evolution of stellar-origin black holes. The discovery of the double neutron star (NS+NS) merger GW170817 with accompanying electromagnetic observations (Abbott et al. 2017b) has had a great impact on our understanding of dense matter and the origin of heavy elements. These discoveries showcase the huge potential that gravitational wave astronomy has to revolutionize our understanding of astrophysical objects and processes.

At the lower frequencies in LISA's observing band, the stellar-mass systems, in binaries or multiples, provide a very rich source population. The population in the Milky Way is expected to consist of millions of double white dwarf (WD+WD) binaries, with a smaller population of neutron star (NS)/BH binaries, and possibly some of the heavy BHs that LIGO/Virgo have already detected. LISA observations of the BH populations will capture a snapshot of BH systems when their orbital periods are tens of minutes, a few years before their coalescence at the high frequencies observed by LIGO-Virgo. Overall, LISA observations of Galactic binaries will address many open questions in stellar astrophysics, such as the evolution of binary star systems, the origin of different transient phenomena, the origin of the elements and even the structure of the Galaxy. It should be noted that among the stellar-mass binaries in the Milky Way, a few are already known from electromagnetic observing campaigns, and can be used as LISA verification sources. While the vast majority of the stellar-mass binaries are expected to be too dim to be detected by electromagnetic instruments, there will be a substantive number that will be excellent targets for electromagnetic follow-up after LISA discovers them.

The observed BH mass spectrum spans ten orders of magnitude, ranging from a few $M_\odot$ for stellar-mass BHs to up to $10^{11}\,M_\odot$ for the most extreme MBHs. Many of the most massive MBHs, with $M_{\mathrm{BH}} \gtrsim 10^8\,M_\odot$, have been discovered in the high-redshift Universe, at $z > 6$, powering some of the brightest quasars (Fan et al. 2003; Mortlock et al. 2011; Yang et al. 2020a). LISA will open up a wide discovery space for BHs. BH systems that merge at the millihertz frequencies, where LISA is most sensitive, are typically hosted in the most common type of galaxies, namely dwarf

and massive spiral galaxies. The fact that LISA observations straddle the frequency bands of merging IMBHs and MBHs suggests that the potential impact on many fields of extragalactic astrophysics is huge. Such foreseen impact, however, relies heavily on our understanding of the astrophysical processes preceding and accompanying the evolution of the binaries during inspiral and into merger (De Rosa et al. 2019b). For MBHs, this knowledge is tightly entangled with the knowledge of the environments in which they evolve, namely their host galaxies and galactic nuclei. It follows then that LISA sources associated with MBH binaries cannot be understood without a robust knowledge of the landscape of galaxy formation and evolution, and in particular without a detailed knowledge of stellar dynamical processes and the interstellar medium inside galactic nuclei. There is thus an inherent multi-disciplinarity in the approach needed to understand these sources, which will naturally bring together various fields of galactic and extra-galactic astrophysics. Furthermore, since LISA will be able to detect MBH binary sources up to very high redshift ($z \sim 10$–15), one also needs ancillary knowledge of cosmic structure formation, as galaxies, and thus their relevant environments, evolve significantly from high to low redshift (Woods et al. 2019). The endeavour then extends into cosmology, and hints at great possibilities for derivative knowledge, some already expected and others not, coming from the future discovery and characterization of LISA MBH binaries.

The stellar dynamics of the central cluster of stars at the galactic centre (the S-stars, or S0-stars), provides compelling evidence for the existence of a MBH of mass $\sim 4 \times 10^6 \, M_\odot$, Sgr A* (see for a review Genzel et al. 2010, and references therein). The stars in the centres of galaxies have the potential to interact with MBHs, but only if their pericentres are small enough. LISA will be able to observe the inspiral of a compact object such as a stellar-mass BH, a NS or a WD onto a (light) MBH, i.e., one with a mass between $\sim 10^4 \, M_\odot$ and $\sim 10^7 \, M_\odot$. Because of the difference in mass between the MBH and the $\lesssim$ few–tens of solar masses of the compact object, we call these *extreme mass-ratio inspirals* (EMRIs)—where the mass ratio is $10^{-8} \lesssim q \lesssim 10^{-5}$ (Amaro-Seoane et al. 2007). There is also a potential population of IMBHs with masses between $10^2 \, M_\odot$ and $10^4 \, M_\odot$, which, through inspiral onto the central MBH, would generate GWs detectable by LISA, this being a class of sources dubbed *intermediate mass-ratio inspirals* (IMRIs) (Amaro-Seoane et al. 2007). In principle, EMRIs and IMRIs could occur in the nuclei of any galaxy hosting a central MBH. They should be ubiquitous, since most galaxies host a central MBH and undergo a variety of merger events with other galaxies throughout their lives. IMRIs might also occur outside galactic nuclei, for example in a star cluster cannibalizing its own population of compact objects. For EMRIs and IMRIs, astrophysical modelling of their origin are in their earliest theoretical stages; in recent years a number of new astrophysical scenarios have been proposed in which they could form even outside the conventional stellar-dynamical scenarios in the galactic centre or in star clusters. These scenarios have been, for the most part, detached from the notion that their host galaxies are highly dynamical systems with a diverse range of properties, at large scales as well as at the level of galactic nuclei and star clusters. From the astrophysical perspective, this is thus the least explored, albeit potentially most

exciting, class of sources in the LISA band. An assessment of the current knowledge and upcoming developments in this area is of paramount importance, to propel new research on the astrophysical impact that the discovery of EMRIs and IMRIs by LISA can have.

The joint exploitation of LISA data with data from terrestrial GW detectors and electromagnetic observations across essentially all possible wavelengths, from infrared and radio to X-ray and gamma-rays, will further enhance its astrophysical impact (Mangiagli et al. 2020). Indeed, essentially all of LISA's individual sources have potential electromagnetic counterparts. Achieving a quantitative characterization of such counterparts, determining the feasibility of detecting them in one or more wavebands, and assessing the stage at which they would be detectable, relative to the inspiral and/or merger stage of the corresponding GW signal, are the main objectives ahead for current and upcoming research. An assessment of the current knowledge in this area is another important task.

The challenge to bring all these different pieces of knowledge into a coherent, robust picture within the next decade is huge, perhaps the most ambitious that the astrophysical community has ever faced. This review attempts to aid this ambitious, community-wide effort by assessing the status of knowledge in the modelling of LISA sources, and it summarizes our understanding of the astrophysical processes and environments relevant for the interpretation of the LISA data. Furthermore, it discusses the most important challenges ahead of us in the research of galactic binaries/multiples, massive and intermediate-mass black hole binaries, and EMRIs/IMRIs. Among these are the quest for identifying the different astrophysical formation channels for these various sources, including how these might be encoded in the LISA data stream, and the daunting multi-scale modelling needed to reconstruct the full dynamical history of such sources, from their emergence to the final inspiral phase and merger driven by GW radiation. The review material presented will help foster a critical discussion of the major gaps in our knowledge that need to be filled in the next decade, highlighting where disagreement exists between results, and what should be done next to reach beyond the current state of the art. This brings the discussion to important methodological tasks for the immediate future, from exploiting electromagnetic (EM) observations in the next decade, to improving simulation and semi-analytical techniques employed to build astrophysical models for the sources, and to refurbishing analysis and interpretation techniques for the models, for example by employing machine learning, neural networks and other modern inference strategies.

1 Stellar compact binaries and multiples

*Coordinators:* **Silvia Toonen, Tassos Fragos, Thomas Kupfer, Thomas Tauris**

1.1 Introduction and summary

Contributors: **Silvia Toonen, Tassos Fragos, Thomas Kupfer, Thomas Tauris**

Detection of GW emission from binary compact stars is one of the key drivers for the LISA mission. There are already at the time of writing (July 2022) about two dozen known Galactic sources, most of which are guaranteed to be detectable with LISA within a few years of its operation (Sect. 1.2). These are tight binaries (typically with orbital periods of $P_{orb} \simeq 5-30$ min) of WD+WDs which give rise to continuous emission of GWs. Unlike binaries consisting of NSs and BHs, WD binaries (with their larger radii and thus lower orbital frequencies at merger) are not readily detectable by ground-based high-frequency (Hz–kHz) GW observatories, such as LIGO/Virgo/KAGRA, nor by the planned third generation of such detectors. These high-frequency detectors can observe the final a few—a few thousands orbits of inspiral (lasting a fraction of a second–minutes) and the merger event itself for NSs and BHs. Such merger events, however, are rare (of order a dozen events Myr^{-1} for a Milky Way equivalent galaxy) and therefore they are only anticipated to be detected as extra-galactic sources, across volumes that encompass large numbers of galaxies. A major advantage of LISA is that the inspiral phase (due to orbital GW damping in the compact binaries) of the vast population of tight Galactic double WDs, NSs and BHs is in the low-frequency ($\sim$ mHz) GW window for up to $\sim 10^6$ year prior to their merger event. Thus a significant number of such local sources are anticipated to be detected by LISA, even though their emitted GW luminosity is relatively small compared to that of the final merger process. The possibility that LISA can measure sky locations of its sources will allow for EM follow-up observations which may result in much more precise compact object component masses, e.g., compared to high-frequency GW mergers.

Binary population synthesis studies and early data-analysis work predicts of order 10^4 resolved Galactic WD+WD may be detected with LISA. This population includes both detached WD+WD and those undergoing mass transfer (the so-called AM Canum Venaticorum binaries or AM CVns, see Sect. 1.2.3.1). NS+NS systems are also expected to be detected by LISA. Based on the known Galactic population of tight-orbit radio pulsar binaries in combination with population synthesis predictions, an estimated number of 10^1–10^2 NS+NS systems with a significant signal-to-noise ratio (SNR) may be detected by LISA within a 4-year mission (Sect. 1.2.2.3). An even larger number of NS+WD systems is expected to be detected too, including ultra-compact X-ray binaries (UCXBs, see Sect. 1.2.3.2, a sub-class of low-mass X-ray binaries, LMXBs). Binary BHs (BH+BH) detectable by LISA are strong candidates to become the first discoveries of such systems in the Milky Way. Given that LISA's volume sensitivity for a constant SNR scales with chirp mass to the fifth power, $\mathcal{M}_{chirp}^5$, BH+BH sources may be detected in distant galaxies, located several hundreds of megaparsecs away (see examples in Fig. 1). Interestingly enough, this fortuitous condition will therefore allow LISA to discover extra-galactic BH+BHs several years before the final merger events that LIGO/Virgo/KAGRA or Einstein Telescope/Cosmic Explorer will detect. Finally, LISA is also expected to detect rare Galactic systems such as (see Sect. 1.2.4): triple stellar systems, tight systems of WDs with exoplanets, or helium star binaries.

The LISA mission will provide opportunities to learn new physics and answer key scientific questions related to formation and evolutionary processes of tight binary
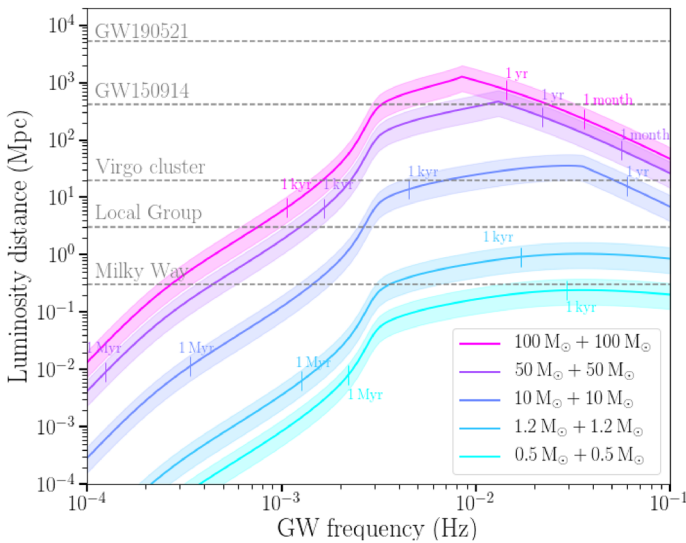
Fig. 1 Distance to which LISA binaries can be detected as a function of GW frequency. The coloured lines represent the SNR threshold of 7 (here computed assuming a mission duration of 4 year with 100% duty cycle) for (quasi-)stationary equal-mass circular binaries of different total masses in the distance–GW frequency parameter space. The shaded range represents angle-averaged curve limits for the optimal and worst binary orientation. The ticks on the curves represent binary merger times: for merger times $\gg 4$ year the binary will be seen by LISA as a monochromatic GW source, whereas for merger times < 4 year the binary will be seen as evolving. Note in particular that evolving sources like GW190521 and GW150914 remain within the LISA band for less than the mission lifetime. Image credit: Antoine Klein & Valeriya Korol

and multiple stellar systems containing compact objects. This includes questions related to the stability and efficiency of mass transfer, common envelopes (CEs), tides and stellar angular momentum transport, irradiation effects, as well as details of their formation and destruction in core-collapse supernovae (SNe) and Type Ia SNe (and related transients), respectively. Furthermore, information about the environments of these sources will be available too, and the number and Galactic distribution of LISA sources are excellent probes to gain new knowledge on the star formation history and the structure of the Milky Way. Finally, the sheer numbers of LISA sources will provide crucial knowledge concerning their formation and evolution processes and help to place constraints on key physical parameters related to binary (and triple-star) interactions.

The current catalogue of known LISA "guaranteed sources" consists of detached WD+WDs, accreting AM CVn binaries, a hot subdwarf binary, and an UCXB. Although the sample is still small and inhomogeneous, binary population synthesis predicts a large population of multi-messenger sources that are EM bright and also detectable by LISA. This includes up to a few thousand detectable WD+WDs as well as a few tens of NS or BH binaries, with a population strongly peaking towards the Galactic Plane/Bulge. Many sources will be detected across different EM bands. Detached WD+WDs and NS+WDs are typically seen in optical and UV bands, whereas AM CVn systems and UCXBs are also seen in X-rays. NSs in compact

binaries can potentially be detected as pulsars in the radio band. Therefore, in parallel with the LISA mission, we expect an EM bright future of thousands of resolved Galactic LISA binaries.

Systems with orbital periods <20 min will be the strongest Galactic LISA sources and will be detected by LISA within weeks after science operations begin. These verification binaries, as well as other so far unknown loud sources, are crucial in facilitating the functional tests of the instrument and maximize LISAs scientific output. Combined GW and EM multi-messenger studies of UCXBs will allow us to derive population properties of these systems with unprecedented quality including for the first time the effects of tides compared to GW radiation. Tides are predicted to contribute up to 10% of the orbital decay. For accreting WDs as well as NS binaries, multi-messenger observations give us the possibility to study the angular momentum transport due to mass transfer. In particular for monochromatic GW sources, EM observations are required to break degeneracies in the GW data (e.g. between masses and distance).

1.2 Classes of LISA binaries

1.2.1 Known binaries—LISA verification sources

Coordinators: **Thomas Kupfer, Thomas Tauris**

Contributors: **Thomas Kupfer, Thomas Tauris, Silvia Toonen, Tassos Fragos**

The most abundant sources in the LISA band will be binary stars with orbital periods <60 min, so-called ultra-compact binaries (UCBs). They are a class of binary stars with ultrashort orbital periods, consisting of a WD or NS primary and a compact helium-star/WD/NS secondary. A subset of the known UCBs have predicted GW strains high enough that they will be individually detected due to their strong GW signals (e.g. Burdge et al. 2020b). These LISA guaranteed sources are termed *verification binaries* with some being expected to be detected on a timescale of weeks or a few months (Stroeer and Vecchio 2006). Currently, we know of only about two dozen of these systems although hundreds are predicted by theory to be detectable in our Galaxy (e.g. Nelemans et al. 2004b; Timpano et al. 2006; Littenberg et al. 2013; Korol et al. 2017; Kremer et al. 2017; Kupfer et al. 2018; Lamberts et al. 2019).

At present, the catalogue of verification binaries include 13 WD+WDs, 11 semi-detached accreting WDs (AM CVn binaries, a subclass of Cataclysmic Variables, CVs), one hot subdwarf star with a WD companion, and one semi-detached UCXB. Tables 1 and 2 present an overview of the known systems with observed EM properties. Figure 2 shows the characteristic strain of the known verification binaries which reach a predicted SNR ≥ 5 in LISA assuming an optimistic 10 year mission with an 80% duty cycle. So far large-scale searches for verification binaries have been conducted almost exclusively in the northern hemisphere, because large-scale survey instruments (e.g., the Sloan Digital Sky Survey, SDSS, and the Zwicky

Table 1 Physical properties (orbital periods, component masses, inclination angles) of the known verification binaries which reach a SNR > 5 after a 10 year LISA mission with 80% duty cycle

Source	$P_{orb}(s)$	$M_1 (M_\odot)$	$M_2 (M_\odot)$	ι (deg)	References
AM CVn type					
HM Cnc	321.5	0.55	0.27	$\approx$38	1, 2
V407 Vul	569.4	[0.8 ± 0.1]	[0.177 ± 0.071]	[60]	3
ES Cet	620.2	[0.8 ± 0.1]	[0.161 ± 0.064]	[60]	4
SDSS J135154.46−064309.0	943.8	[0.8 ± 0.1]	[0.100 ± 0.040]	[60]	5
AM CVn	1028.7	0.68 ± 0.06	0.125 ± 0.012	43 ± 2	6, 7
SDSS J190817.07+394036.4	1085.7	[0.8 ± 0.1]	[0.085 ± 0.034]	10–20	8, 9
HP Lib	1102.7	0.49–0.80	0.048-0.088	26–34	10,11
PTF1 J191905.19+481506.2	1347.3	[0.8 ± 0.1]	[0.066 ± 0.026]	[60]	12
CXOGBS J175107.6−294037	1375.0	[0.8 ± 0.1]	[0.064 ± 0.026]	[60]	13
CR Boo	1471.3	0.67–1.10	0.044–0.088	30	10,14
V803 Cen	1596.4	0.78–1.17	0.059–0.109	12–15	11
Detached double WDs					
ZTF J1539+5027	414.8	$0.610^{+0.017}_{-0.022}$	0.210 ± 0.015	$84.15^{+0.64}_{-0.57}$	15
ZTF J2243+5242	527.9	$0.349^{+0.093}_{-0.074}$	$0.384^{+0.114}_{-0.074}$	$81.88^{+1.31}_{-0.69}$	16
SDSS J065133.34+284423.4	765.5	0.247 ± 0.015	0.49 ± 0.02	$86.9^{+1.6}_{-1.0}$	17, 18
ZTF J0538+1953	866.6	0.45 ± 0.05	0.32 ± 0.03	$85.43^{+0.07}_{-0.09}$	19
SDSS J093506.92+441107.0	1188.0	0.312 ± 0.019	0.75 ± 0.24	[60]	20, 21
SDSS J2322+0509	1201.4	0.34 ± 0.02	> 0.17	[60]	22
PTF J0533+0209	1234.0	$0.652^{+0.037}_{-0.040}$	0.167 ± 0.030	$72.8^{+0.8}_{-1.4}$	19, 23
ZTF J2029+1534	1252.0	0.32 ± 0.04	0.3 ± 0.04	$86.64^{+0.70}_{-0.40}$	19
ZTF J0722−1839	1422.5	0.38 ± 0.04	0.33 ± 0.03	89.66 ± 0.22	19
ZTF J1749+0924	1586.0	$0.40^{+0.07}_{-0.05}$	$0.28^{+0.05}_{-0.04}$	$85.45^{+1.40}_{-1.15}$	19
SDSS J163030.58+423305.7	2389.8	0.298 ± 0.019	0.76 ± 0.24	[60]	20, 24
SDSS J1235+1543	3172.6	0.35 ± 0.01	$0.27^{+0.06}_{-0.02}$	27 ± 3.8	25, 26
SDSS J092345.59+302805.0	3883.7	0.275 ± 0.015	0.76 ± 0.23	[60]	20, 27
Hot subdwarf binaries					
CD−30°11223	4231.8	0.54 ± 0.02	0.79 ± 0.01	82.9 ± 0.4	28
Ultracompact X-ray binaries					
4U1820−30	685.0	[1.4]	[0.069]	[60]	29, 30

Masses and inclination angles in brackets are assumed and based on evolutionary stage and mass ratio estimations

[1] Strohmayer (2005), [2] Roelofs et al. (2010), [3] Marsh and Steeghs (2002), [4] Espaillat et al. (2005), [5] Green et al. (2018a), [6] Skillman et al. (1999), [7] Roelofs et al. (2006), [8] Fontaine et al. (2011), [9] Kupfer et al. (2015), [10] Roelofs et al. (2007b), [11] Solanki et al. (2021), [12] Levitan et al. (2014), [13] Wevers et al. (2016), [14] Provencal et al. (1997), [15] Burdge et al. (2019a), [16] Burdge et al. (2020a), [17] Brown et al. (2011), [18] Hermes et al. (2012), [19] Burdge et al. (2020b), [20] Brown et al. (2016), [21] Kilic et al. (2014), [22] Brown et al. (2020a), [23] Burdge et al. (2019b), [24] Kilic et al. (2011), [25] Breedt et al. (2017), [26] Kilic et al. (2017), [27] Brown et al. (2010), [28] Geier et al. (2013), [29] Stella (1987), [30] Chen et al. (2020a)

Table 2 Measured EM properties (Galactic coordinates, GW frequency, magnitudes and parallaxes from Gaia early data release 3 (Gaia Collaboration et al. 2021) of the known verification binaries which reach a SNR > 5 after a 10 year LISA mission with 80% duty cycle

Source	f_{GW} (mHz)	l_{Gal} (deg)	b_{Gal} (deg)	Gaia G (mag)	ϖ (mas)
AM CVn type					
HM Cnc	6.22	206.9246	23.3952	20.92	–
V407 Vul	3.51	57.7281	6.4006	19.36	0.0978 ± 0.2384
ES Cet	3.22	168.9684	− 65.8632	16.80	0.5606 ± 0.0677
SDSS J135154.46−064309.0	2.12	328.5021	53.1240	18.72	0.6584 ± 0.2197
AM CVn	1.94	140.2343	78.9382	14.06	3.3106 ± 0.0303
SDSS J190817.07+ 394036.4	1.84	70.6664	13.9349	16.22	1.0232 ± 0.0335
HP Lib	1.81	352.0561	32.5467	13.60	3.5674 ± 0.0313
PTF1 J191905.19+ 481506.2.	1.48	79.5945	15.5977	19.75	0.6229 ± 0.2385
CXOGBS J175107.6 −294037	1.45	359.9849	− 1.4108	16.27	0.8591 ± 0.1733
CR Boo	1.34	340.9671	66.4884	15.47	2.8438 ± 0.0367
V803 Cen	1.25	309.3671	20.7262	15.73	3.4885 ± 0.0599
Detached double WDs					
ZTF J1539+5027	4.82	80.7746	50.5819	20.40	− 0.4926 ± 0.5726
ZTF J2243+5242	3.79	104.1514	− 5.4496	20.55	− 1.2372 ± 0.6578
SDSS J065133.34+ 284423.4	2.61	186.9277	12.6886	19.28	1.0071 ± 0.3091
ZTF J0538+1953	2.31	186.8104	− 6.2213	18.80	0.9617 ± 0.2866
SDSS J093506.92+ 441107.0	1.68	176.0796	47.3776	17.80	2.7034 ± 0.6648
SDSS J2322+0509	1.66	85.9507	− 51.2104	18.75	1.1558 ± 0.2244
PTF J0533+0209	1.62	201.8012	− 16.2238	19.05	0.7902 ± 0.2396
ZTF J2029+1534	1.60	58.5836	− 13.4655	20.47	0.1240 ± 0.9893
ZTF J0722−1839	1.40	232.9930	− 1.8604	19.05	0.6996 ± 0.2457
ZTF J1749+0924	1.26	34.5093	17.9025	20.47	− 0.2961 ± 0.8222
SDSS J163030.58+ 423305.7	0.84	67.0760	43.3604	19.18	1.1748 ± 0.1952
SDSS J1235+1543	0.63	284.5186	78.0320	17.52	2.2504 ± 0.1389
SDSS J092345.59+ 302805.0	0.51	195.8199	44.7754	15.92	3.4795 ± 0.0648
Hot subdwarf binaries					
CD–30°11223	0.47	322.4875	28.9379	12.30	2.8198 ± 0.0516
Ultracompact X-ray binaries					
4U1820−30	2.92	2.7896	− 7.9144	15.41	− 0.7676 ± 0.2164
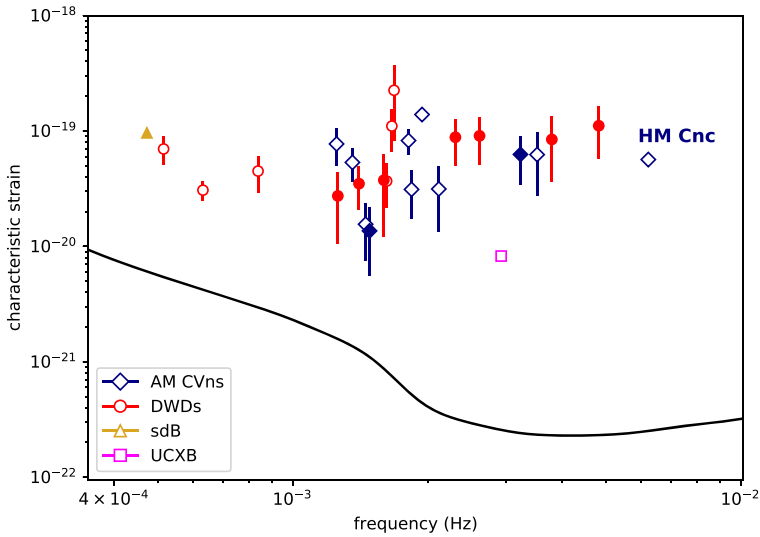
Fig. 2 Sensitivity plot for LISA assuming 10 year of observation with an 80% duty cycle showing the known binaries which reach a SNR $\geq$ 5. Filled symbols represent eclipsing sources and open symbols represent non-eclipsing sources from Kupfer et al. (2018). The black lack solid line represents the LISA sensitivity curve. Acronyms for binaries: AM Canum Venaticorum (AM CVns), WD+WD (DWDs), subdwarf B-star (sdB) and ultracompact X-ray binary (UCXB). Image credit: Thomas Kupfer
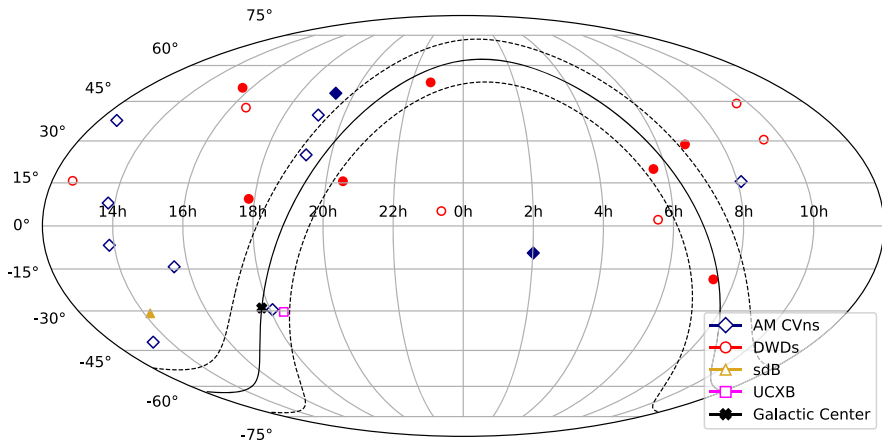
Fig. 3 Sky position of the verification binaries. The sky positions show a clear bias towards the northern hemisphere and to higher Galactic latitudes. The black line indicates the Galactic equator and $|b| = 10$ deg, with the Galactic Centre located at the black cross. See caption in Fig. 2 for explanation of acronyms. Image credit: Thomas Kupfer

Transient Facility, ZTF) are located in the Northern Hemisphere, and mostly at high Galactic latitudes, to avoid stellar crowding. Figure 3 shows the sky location of the known verification systems which presents the strong bias towards sources in the Northern Hemisphere.

In 2018, Gaia data release 2 (Gaia Collaboration et al. 2018a) announced parallaxes for $\approx$ 1.3 billion sources. The Gaia catalogue contains the distances of many of the known LISA verification binaries, allowing accurate prediction of their GW strains. Using the Gaia distances, Kupfer et al. (2018) found 13 sources will exceed an SNR of 5 after 4 year of LISA observations. This sample consists of 13 verification binaries from the current, known list; it is strongly biased and incomplete. It includes AM CVn, CR Boo, V803 Cen and ES Cet, which were all found as outliers in surveys for blue, high-Galactic latitude stars. HM Cnc and V407 Vul are the most compact known AM CVn systems and were discovered during the course of the ROSAT All-Sky Survey showing an on/off X-ray profile modulated on a period of 321 and 569 s respectively. The known WD+WD verification binaries, such as SDSS J0651 and SDSS J0935, were found as part of the extremely low-mass (ELM) WD survey (Brown et al. 2020b and references therein).

More recently, more systematic searches for UCBs were performed. UCBs show up in lightcurves with variations on timescales of the orbital period (e.g. due to eclipses or tidal deformation of the components). Therefore, photometric surveys are well suited to identify UCBs in a homogeneous way. A number of fast cadence ground-based surveys, including the Rapid Temporal Survey (RATS; Ramsay and Hakala 2005; Barclay et al. 2011), OmegaWhite (Macfarlane et al. 2015) survey as well as the ZTF high-cadence Galactic plane survey (Masci et al. 2019; Kupfer et al. 2021), have been executed to study the variable sky down to a few minute period aiming to find UCBs and increase the number of known verification binaries. The ELM survey targets a colour-selected sample of B-type hypervelocity candidates from SDSS (Anderson et al. 2005; Roelofs et al. 2007c), which are being followed up systematically (Brown et al. 2020b and references therein). ELM WDs can be separated efficiently from the bulk of WDs with a colour selection (Brown et al. 2010).

Over the last few years the number of known verification binaries has almost doubled thanks to these large scale surveys. The two most significant contributors were the ELM survey (Brown et al. 2020b and references therein) and ZTF (Burdge et al. 2019a, 2020b, a). The ELM survey discovered six WD+WD verification binaries including SDSS J0651: a detached eclipsing system with an orbital period of 12 min. Most recently ZTF released seven new WD+WD verification binaries, five systems found as eclipsing sources. Remarkably, one of the first ZTF discoveries was the shortest orbital period eclipsing WD+WD known to date, ZTF J1539+5027, with an orbital period of just 6.91 min (Burdge et al. 2019a).

1.2.2 Detached binaries

***Coordinators:* Ashley Ruiter, Ross Church**

***Contributors:* Ashley Ruiter (1.2.2.1), Thomas Tauris (1.2.2.2–4), Jeff Andrews (1.2.2.3), Simone Bavera (1.2.2.4), Ross Church (1.2.2.2), Tassos Fragos (1.2.2.4), Gijs Nelemans (1.2.2.1), Milton Ruiz (1.2.2.3), Alberto Sesana (1.2.2.4), Antonios Tsokaros (1.2.2.3), Shenghua Yu (1.2.2.3)**

1.2.2.1 WD+WD systems   For over three decades it has been known that WD+
WD binaries will be the dominant contributor to signals detected by a space-based
GW observatory (Hils et al. 1990). While most extra-galactic sources (Farmer and
Phinney 2003) as well as a significant fraction of those in the Galactic halo (Rosswog
et al. 2009a) are likely too distant to be individually detected by LISA, a large portion
of the frequency band observed by LISA will be swamped with GWs from millions
of WD+WDs existing in the Galactic disc and bulge. At low frequencies, the
combined signal of these millions of WD+WDs will populate just a few frequency
bins and merge to form an unresolved confusion foreground (often referred to as the
galactic foreground or the galactic confusion noise), with louder resolvable sources
standing out above the confusion (see also Sect. 1.6.2). Together with high-frequency
sources a large number these form $\sim 10^4$, (e.g., Nelemans et al. 2001c; Farmer and
Phinney 2003; Ruiter et al. 2010; Korol et al. 2017) of resolved WD+WDs and we
now discuss these key sources in more detail.

WD+WDs were discovered in the late 1980s and initially were dominated by
low-mass ($\lesssim 0.4\,M_\odot$) helium-core (He-core) WDs that cannot be formed in single-
star evolution within a Hubble time, and, thus, were the targets for radial velocity
searches for binarity amongst known WDs (Marsh et al. 1995). Later, (more)
unbiased surveys were done, e.g. the Supernova Ia Progenitor surveY (SPY,
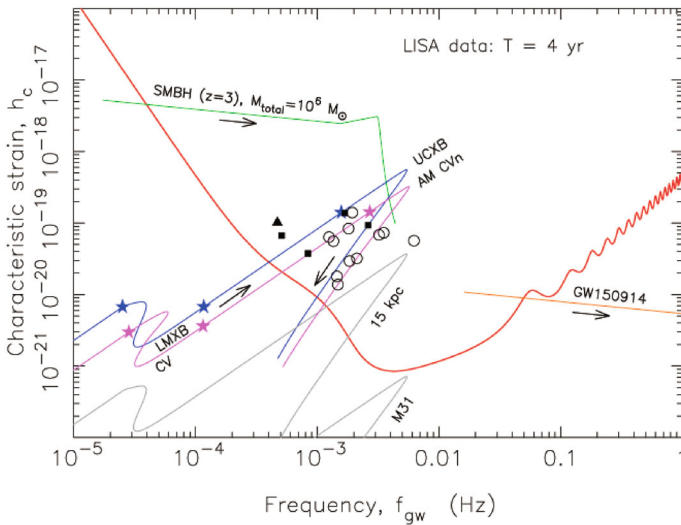
Fig. 4 Characteristic strain amplitude vs GW frequency for LISA. Evolutionary tracks are for an UCXB
(blue) and an AM CVn system (magenta) at a distance of $d_L = 1$ kpc. Their slope on the inspiral leg is
$\propto f_{gw}^{7/6}$. The stars along the tracks represent (with increasing GW frequency) onset LMXB/CV stage,
termination LMXB/CV stage, and onset UCXB/AM CVn stage. The evolutionary timescales along these
tracks are shown in Fig. 5. The LISA sensitivity curve (red line, SNR = 1) is based on 4 years of
observations. The grey curves are for the UCXB at $d_L = 15$ kpc and 780 kpc (M31), respectively.
Comparison tracks are shown for an MBH merger (green) and GW150914 (orange). Their inspiral slopes
are $\propto f_{gw}^{-1/6}$. Data from LISA verification sources (Kupfer et al. 2018) include detached double WD
binaries (solid squares), AM CVn systems (open circles), and a hot subdwarf binary (solid triangle). Image
reproduced with permission from Tauris (2018), copyright by APS
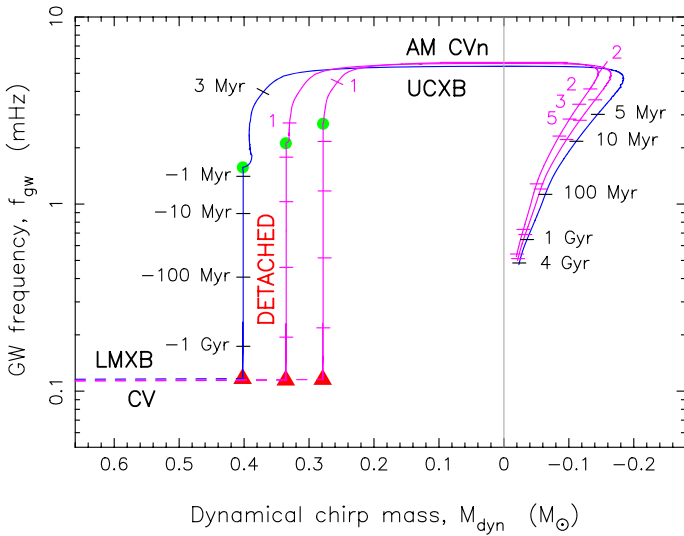
Fig. 5 GW frequency vs dynamical chirp mass for an UCXB and two AM CVn systems, based on detailed mass transfer calculations (including finite-temperature effects of the WD donor star) using the MESA code (Tauris 2018). The end points of the first mass-transfer phases (LMXB and CV) are indicated by red triangles; the starting points of the second mass-transfer phases (UCXB and AM CVn) are indicated by green circles. The time marks along the AM CVn tracks are for the same values as indicated for the UCXB system, unless stated otherwise (in Myr). Time zero is defined at the onset of the second mass-transfer phase. The maximum GW frequencies (strongest LISA signal) in these three examples are 5.45 mHz (UCXB), 5.64 mHz (AM CVn1), and 5.72 mHz (AM CVn2) corresponding orbital periods of 6.12 min, 5.91 min and 5.83 min, respectively. The frequency at the onset of the RLO (green circles) depends on the temperature of the low-mass He WD donor (T_{eff} = 10 850 K, 9 965 K and 8 999 K, respectively)

Napiwotzki et al. 2020, and references therein) and studies using SDSS, discovering also more massive WDs. Over the last decade, it has become more clear that previously-undetected WD+WD systems (and their progenitors, e.g. double-core planetary nebulae) are more easily detectable with today's sophisticated instrumentation (Wesson et al. 2018). A dramatic increase in the number of WD+WDs has come from the ELM WD survey (Kilic et al. 2012; Bell et al. 2017; Brown et al. 2020b) that targets a part of the parameter space in colour–colour diagrams that is occupied by (subdwarf) B-stars, but also by very low mass (below $\sim 0.3\,M_\odot$) proto-WDs that are still approaching the cooling track and are thus relatively large and bright (Istrate et al. 2014b, 2016). In total, the ELM survey alone has discovered 98 WD+WDs so far (Brown et al. 2020b).

Over the past couple of years, ZTF (Bellm et al. 2019) has facilitated a rapid growth in the population of known WD+WDs with orbital periods under an hour. Three of the sources discovered by ZTF so far (Burdge et al. 2020a), the eclipsing WD+WDs: ZTF J1539+5027 ($P_b = 6.91$ min), ZTF J2243+5242 ($P_b = 8.80$ min) and ZTF J0538+1953 ($P_b = 14.4$ min), should all be detected by LISA with a high SNR, enabling precise parameter estimation using GWs (Littenberg and Cornish 2019).

The detached WD+WDs may consist of a pair of He-core WDs, carbon/oxygen-core (C/O-core) WDs, oxygen/neon/magnesium-core (O/Ne/Mg-core) WDs, or any mixed combination thereof. For some systems, LISA measurements of the orbital-decay rate will yield the chirp mass for a given system, which can be combined with EM observations to reveal individual WD component masses. The distribution of WD masses (and their mass ratios), along with the number of detectable sources in a local volume, will provide important information to help understand their formation history (see Sect. 1.3). With enough detached WD+WDs in a sample, it may even be possible to set limits on mass-transfer efficiencies and CE physics (Sect. 1.7) through characterisation of chirp mass distributions (Ruiter et al. 2019). Furthermore, the detected WD+WDs will provide unique information on the formation of progenitors of R Coronae Borealis stars, thought to be formed by the merger of two WDs (e.g., Tisserand et al. 2020), massive carbon-enhanced WDs (Kawka et al. 2020), Type Ia SNe (see Sect. 1.7.1.6), and other transients.

Over the last three decades, several works have made predictions about the scientific impact of LISA detections of Galactic WD+WDs. Different binary evolution population synthesis studies have uncovered how the WD+WD population will look to LISA in terms of characteristic strain amplitude (Nelemans et al. 2001b, 2004b; Yu and Jeffery 2010; Lamberts et al. 2019; Korol et al. 2020), spectral density (Breivik et al. 2020b), as well as how different populations of WD+WDs contribute to the spectral amplitude signal (Rosswog et al. 2009a; Ruiter et al. 2010).

Detached WD+WD binaries that are resolvable with LISA are expected to be on par with or slightly outnumber the resolvable interacting WD+WD binaries (Nelemans et al. 2001a, 2004b; Ruiter et al. 2010), and will be the sole WD+WD contributers to the LISA signal at GW frequencies below $\sim 2 \times 10^{-4}$ Hz. Kremer et al. (2017) found that a number of *mass-transferring* WD+WDs (Sect. 1.2.3) will be resolvable with LISA ($\sim$ 200–3000 for SNRs between 10 and 5, respectively), many of which are likely to exhibit a negative chirp (caused by orbital widening)—a diagnostic not applicable for detached WD+WDs. Finally, we expect that the number of detached WD+WDs, composed of a light He-core WD and a more massive C/O-core WD (or possibly an O/Ne/Mg-core WD) detected by LISA must be in accordance with the number of similar interacting AM CVn systems that LISA will detect, given their evolutionary connection (the detached systems being the precursors of the interacting WD+WDs, see Fig. 6). The transitional GW frequency between these two populations (detached and interacting) depends on the mass and temperature of the lighter (last-formed) WD, see examples in Figs. 4 and 5.

1.2.2.2 NS+WD and BH+WD systems The known population of Galactic NS+ WD systems can be divided into two classes. Systems with: (i) massive WDs (O/Ne/ Mg-core or C/O-core WDs, typically more massive than $0.7 M_\odot$), and (ii) low-mass He-core WDs (typically less massive than $0.3 M_\odot$). The massive NS+WD systems can again be subdivided into two populations, depending on the formation order of

---

[1] The empirical rate and its uncertainty measured by the LIGO network of detectors is currently based on only two events (GW170817 and GW190425) but is anticipated to improve substantially in the coming decade.

the WD and the NS. The NS+WD systems are observed as binary radio pulsars and the formation order can be clearly distinguished from the properties of the pulsar: if the pulsar has a strong B-field and an eccentric orbit (e.g. Tauris and Sennels 2000; Church et al. 2006), it is the last-formed compact object, whereas if the pulsar is (mildly) recycled with a low-B-field and a fairly rapid spin, and in a near-circular orbit, it is the first-formed compact object (Tauris et al. 2012). For LISA detections, the formation order is irrelevant and among both types of systems examples are known to merge within a Hubble time, thus producing a bright LISA source well before their final merger.

Among the detached low-mass He-core WDs with NS companions, the systems in relatively tight orbits are completely dominated by millisecond radio pulsars. According to the ATNF Pulsar Catalogue (Manchester et al. 2005), there are about 120 such systems known in the MW disc, a handful of which will merge within a Hubble time, producing a bright detached LISA source (depending on their distance) for approximately the last several tens of Myr of the inspiral, before an UCXB is formed (Sect. 1.2.3.2). Based on the observed population of radio pulsars and their selection effects, Tauris (2018) argue that LISA could detect about 50 of these systems while still detached, before they become UCXBs and widen their orbits again, resulting in a negative chirp of the GW signal (see Figs. 4 and 5).

At present, we do not know of any detached BH+WD binaries. However, this is probably due to observational selection effects since the only EM radiation we would expect from such detached systems would be from the cooling of the WD companion —unlike the situation for semi-detached systems or systems containing NSs, which can be detected in X-rays and radio waves, respectively. Nevertheless, several Galactic LMXBs are known with low-mass donor stars and BH accretors (McClintock and Remillard 2006) and thus we expect many of these systems to leave detached BH+WD systems, possibly (although still to be proven) in tight orbits that LISA will detect. A more viable formation channel for more massive WDs in tight orbits with BHs is formation via a CE. Optical follow-up observations of the WD companion, in combination with the measured chirp mass, will constrain the BH mass in these systems. Early simulations (Nelemans et al. 2001b) predict a Galactic merger rate of BH+WD binaries of order $\sim 100\,\mathrm{Myr}^{-1}$ and thus roughly ~ 100 such systems detectable by LISA.

1.2.2.3 NS+NS systems The known population NS+NS systems so far only manifest themselves as radio pulsars. The first one of these (PSR B1913+16, the *Hulse–Taylor Pulsar*) was discovered in 1974 (Hulse and Taylor 1975). According to the ATNF Pulsar Catalogue (Manchester et al. 2005), there are currently about 20 NS+NS systems detected in our Galaxy. Except for one case, the *double pulsar* PSR J0737−3039 (Lyne et al. 2004), only one of the two NSs is detected—usually the recycled pulsar (Tauris et al. 2017). The other NS, is either not an active radio pulsar anymore or it is not beaming in our direction.

Given the small merger rate of NS+NS systems in our Galaxy[1] (most likely somewhere in the range from a few events up to a hundred events per Myr), it is statistically highly improbable that ground-based high-frequency detectors (LIGO–

Virgo–KAGRA) will detect a NS+NS merger in the Local Group earlier than the LISA era. The advantage of LISA is that it can follow the inspiral of Galactic NS+NS systems up to $\sim 10^6$ year prior to their merger event, and thus a significant number of NS+NS sources are anticipated to be detected in GWs by LISA.

About half of the 20 known NS+NS systems have orbital periods small enough (or eccentricities sufficiently large) to merge within a Hubble time. As an example, a "standard" NS+NS system with NS masses of $1.35 \, M_\odot$ and e.g. an orbital period of 16 h will merge in: 11.8 Gyr, 4.4 Gyr or 0.35 Gyr for an initial eccentricity, e_0 of 0.1, 0.5 or 0.8, respectively. The number of NS+NS sources that LISA will detect can be evaluated, approximately to first order, from a combination of the Galactic NS+NS merger rate and the distribution of these sources within the Milky Way. The above three standard NS+NS systems will have a remaining lifetime of between ~ 247 kyr (~ 243 kyr for $e_0 = 0.8$) and 1.57 Myr (1.48 Myr for $e_0 = 0.8$) by the time they enter the LISA band, if this occurs at a GW frequency of about 2 mHz and 1 mHz, respectively. Thus, if the Galactic merger rate is, say, 10 Myr^{-1}, we can roughly expect to detect between a few and a dozen LISA sources. Of course, the details depend on the Galactic distribution of these sources, the SNR required for a detection, and the duration of the LISA mission. The merger rate can be estimated from population synthesis, but its value is uncertain by, at least, one or two orders of magnitude (Abadie et al. 2010). The merger rate derived from an extrapolation of the LIGO/Virgo empirical merger rate of NS+NSs still has very large error bars due to small number statistics.

Recent works by Lau et al. (2020), Andrews et al. (2020) suggest that LISA may even detect up to $\sim 50-200$ Galactic NS+NS sources with a SNR greater than 7 within a 4 year mission. Given that LISA's volume sensitivity for a constant SNR scales with $\mathcal{M}_{\mathrm{chirp}}^5$, unlike double BH sources, very few NS+NS sources are anticipated to be detected outside the Milky Way, although a few such binaries may be found in both the LMC and M31 (Seto 2019). Applying a more conservative number, however, for the merger rate of Galactic NS+NS system of about $3-14$ Myr^{-1} (Kruckow et al. 2018) would lead to a substantial reduction in the predicted number of LISA detections. The Galactic merger rate is expected to be significantly better constrained in the coming decade such that we will have a clear idea about the expected number of NS+NS sources detected by LISA prior to its operation. Finally, an expected reduction in LISA SNR for detecting eccentric NS+NS systems, compared to circular NS+NS systems with similar orbital period and NS masses, should be noticed (Randall et al. 2021).

LISA may give us the opportunity to probe a hidden subpopulation of NS+NS systems with different properties compared to those of the well-known radio pulsar NS+NSs. The nature of GW190425, a presumed NS+NS merger detected by the LIGO/Virgo network with a total mass of $3.4 \, M_\odot$ (Abbott et al. 2020a), is still a mystery. With such a large total mass, GW190425 stands at five standard deviations away from the total mass distribution of Galactic NS+NSs detected in the Milky Way as radio pulsars (Farrow et al. 2019). If a subpopulation of heavy GW190425-

---

² Notice, the $2.6 \, M_\odot$ compact object in GW190814 might well have been a massive NS rather than a BH.

like NS+NSs exists in our Galaxy, it is not yet clear why it should be radio-quiet (e. g. Safarzadeh et al. 2020b). Thus, LISA may actually be the most suited instrument for detecting the population of GW190425-like binaries (Galaudage et al. 2021; Korol and Safarzadeh 2021). In particular, Korol and Safarzadeh (2021) demonstrated that if GW190425-like binaries constitute a fraction larger than 10% of the total Galactic population, LISA should be able to recover this fraction with better than $\sim 15\%$ accuracy, assuming the merger rate of 42 Myr^{-1}.

Additional recent investigations (Thrane et al. 2020; Kyutoku et al. 2019) have discussed the importance of sky-localization on LISA NS+NS sources for multi-messenger follow-ups that may allow to impose constraints on the equation-of-state of NSs by measuring the Lense–Thirring precession (Thrane et al. 2020) or test general relativity through the detection of radio pulses from Galactic NS+NS binaries in a very tight orbit with the period shorter than 10 min (Kyutoku et al. 2019). Sky-localization may also help disentangle NS+NS systems from others sources by either knowing their position in the Milky Way, or in nearby galaxies, thus enhancing the possibility of EM follow-ups (e.g. Lau et al. 2020). In particular, in addition to differences in chirp masses, it will allow us to distinguish between eccentric NS+NS and eccentric WD+WD systems—the latter only expected to be formed in globular clusters and ejected into the Galactic halo via dynamical interactions, while the former systems have an eccentricity encoded from the last SN explosion.

1.2.2.4 BH+NS and BH+BH systems For several decades, a number of high-mass X-ray binaries (HMXBs) containing BH accretors have been identified in the Milky Way and nearby galaxies (e.g. Cyg X-1, LMC X-1, LMC X-3, MCW 656, M33 X-7, see van den Heuvel 2019). It has been shown that a fraction of these known wind-accreting HMXBs may eventually form BH+BHs or BH+NS systems (Belczynski et al. 2012, 2013, see also Fig. 9), while others will merge in an upcoming CE phase (Sect. 1.7.1.3), once the companion star evolves to a giant-star size and possibly initiates dynamically unstable Roche-lobe overflow (RLO), depending on its stellar

Fig. 6 Illustration of the formation of an AM CVn system and a detached WD+WD binary. LISA sources are indicated with waves. Acronyms. ZAMS: zero-age main sequence; RLO: Roche-lobe overflow (mass transfer); CE: common envelope; He star: helium star; WD: white dwarf; CV: cataclysmic variable; AM CVn: AM Canum Venaticorum binary. Image reproduced with permission from Tauris and van den Heuvel (2023), copyright by PUP
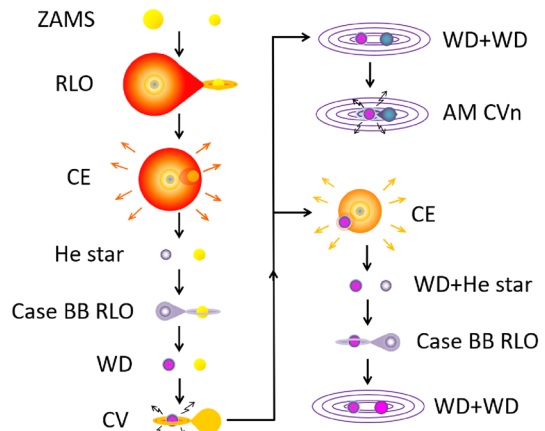
structure and the mass ratio between the two binary components. The masses of compact objects in X-ray binaries can be estimated with astrometry and the Galactic stellar-mass BHs are found to have masses between roughly $5 - 21\,M_\odot$ (Gandhi et al. 2019; Arnason et al. 2021; van den Heuvel 2019; Miller-Jones et al. 2021). The astrometric satellite Gaia, can also be used to detect optical emission from the HMXB companion stars (Barstow et al. 2014; Kawanaka et al. 2017; Mashian and Loeb 2017; Breivik et al. 2017; Yamaguchi et al. 2018). Finally, non-interacting binaries with a BH component have also been discovered by combining radial velocity measurements with photometric variability data (Breivik et al. 2017; Thompson et al. 2019; Liu et al. 2019a), although their interpretations can, in some cases, be subject to alternative explanations (van den Heuvel and Tauris 2020).

The LIGO–Virgo GW detectors have detected BH+BH mergers in distant galaxies, out to ~ 5 Gpc. (Abbott et al. 2021). The inferred BH masses[2] of their inspiralling BH components potentially range all the way from $\sim 2.6 \pm 0.1\,M_\odot$ (Abbott et al. 2020b) to $\sim 95 \pm 10\,M_\odot$ (Abbott et al. 2021), thus significantly more massive than the known Galactic stellar-mass BHs. This difference is mainly attributed to the relatively high metallicity content of the Galaxy (Belczynski et al. 2016a; Kruckow et al. 2018). The LIGO–Virgo GW detectors have also identified two sources in close proximity or within the mass ranges expected for BH+NS binaries: GW190426 and GW190814. The first event has marginal significance (i.e. a high false-alarm rate, FAR = 1.4 year^{-1}) and the second is likely to be a BH+BH, not a BH+NS. Nevertheless, LISA like LIGO is much more sensitive to the masses (as opposed to matter content) of the binaries, so the presence of similar binaries suggests LISA will copiously find similar sources.

Interestingly enough, although the LIGO–Virgo GW sources are located in distant galaxies at Gpc distances, their low-frequency GWs during the last few years of inspiral prior to the merger event is often so luminous that it allows for detection with LISA (Sesana 2016). For example, the very first GW source (GW150914) would have been observable by LISA several years before its merger (see Fig. 4). Similarly, the extreme event GW190521 (Abbott et al. 2020c; Toubiana et al. 2021), with a total stellar mass of $\sim 160\,M_\odot$ and located at a distance of about 5 Gpc, would also have been detected during its inspiral in the LISA band.

1.2.2.5 Stochastic background   As discussed above, stellar-mass compact binaries (BH+BH, BH+NS, NS+NS) are one of the primary targets for LISA, with expected detection rates of between a few and a few thousands per year, as summarized in Sect. 1.4. Nevertheless, many of these sources will not be detected, either because they are too distant and thus have a low SNR, or because the signals from multiple long-lived sources will overlap in time and will be difficult to disentangle. These unresolved signals will combine incoherently and produce a stochastic GW background (SGWB). Current predictions of the amplitude of this background typically rely on the merger rates measured in the local Universe by LIGO-Virgo (Abbott et al. 2016a, 2018b), but since most of the unresolved sources reside at higher redshifts, these predictions depend on the detailed population synthesis and galaxy evolution models.

The expected amplitude of the SGWB from BH+BH binaries in the LISA band (without source subtraction) varies in the range $\Omega_{GW}(f) \sim 10^{-13} - 10^{-11}$ at $f = 3$ mHz (Sesana 2016; Dvorkin et al. 2016a; Cusin et al. 2020; Périgois et al. 2021). Up to a few thousands of these binaries (likely responsible for about 10% of the background) will be individually detected by LISA (Sesana 2016; Périgois et al. 2021). The prediction for the background from NS+NS is significantly lower at $\Omega_{GW}(f) \sim 10^{-14}$ at $f = 3$ mHz (Périgois et al. 2021), and the background from BH+ NS in the model of Périgois et al. (2021) is slightly higher but similar to that of NS+ NS. The uncertainties on these rates will be significantly reduced in the coming years with more detections of stellar-mass binaries by ground-based detectors, and improved modelling of source formation and evolution. Detection of this background and in particular its shape, will provide important information about the population at periods too short to be directly observed, but before the merger phase probed by ground-based detectors (see Sect. 1.5.2.1).

1.2.3 Interacting binaries

Coordinators: **Shenghua Yu, Thomas Tauris**

Contributors: **Ashley Ruiter (1.2.3.1), Thomas Kupfer (1.2.3.1), Thomas Tauris (1.2.3.1–2), Gijs Nelemans (1.2.3.1), Shenghua Yu (1.2.3.2)**

1.2.3.1 AM CVn binaries (AM Canum Venaticorum binaries—accreting WDs)
AM CVn binaries consist of a WD accreting from a hydrogen-deficient star (or WD) companion (Warner 1995; Solheim 2010). In their formation history (Fig. 6 and Sect. 1.3.1.1), AM CVns form after at least one CE phase of their progenitor system. The current RLO is initiated, due to orbital damping caused by GW radiation, at orbital periods of typically 5–20 min (depending on the nature and the temperature of the companion star), and the mass-transfer rate is determined by a competition between orbital angular momentum loss through emission of GWs and orbital widening due to RLO from the less-massive donor star to the more-massive WD accretor.

If the system survives the onset of the semi-detached phase, a stable accreting AM CVn binary is formed in which the orbital separation widens shortly after onset of RLO (Fig. 5), and the system evolves to longer orbital periods (see Fig. 5). When they reach an orbital period of ~ 60 min (after a few Gyr), the donor star has been stripped down to about 5 Jupiter masses ($5\,M_J$, Tauris 2018). These systems have been hypothesised to be possible progenitors of faint thermonuclear explosions (flashes, or Type ".Ia" SNe, Nelemans et al. 2001a; Bildsten et al. 2007).

Figure 4 shows examples of computed evolutionary tracks of AM CVn (and UCXB) systems in the characteristic strain amplitude vs GW frequency diagram. As can be seen, AM CVn systems are indeed anticipated to be detected by LISA—in some cases even with a SNR > 100 (for the sources located within 1 kpc).

Though there are currently ~ 65 AM CVn binaries known in the Galaxy (Ramsay et al. 2018), their formation pathways are still a puzzle (Green et al. 2018b). Their compact orbits and the lack of hydrogen in their spectra, led to three different proposed formation channels: (i) the donor is a low-mass (likely He-core) WD (Paczyński 1967; (ii) the donor is a semi-degenerate hydrogen-stripped, helium-burning star (e.g. main-sequence helium star, or hot subdwarf); or (iii) the donor is a helium-rich core of a main-sequence star that has not undergone helium-burning since it had a rather low mass to begin with (see Solheim 2010). Further discussions on their formation is given in Sect. 1.3.1.1.

Only for eclipsing AM CVns is it possible to fully determine all binary parameters and put constraints on the donor type. Recent results from eclipsing systems revealed that the donor stars are likely larger and more massive than previously assumed (Copperwheat et al. 2011; Ramsay et al. 2018), implying that a semi-degenerate donor is more likely for such systems, unless the donor star is a low-mass He-core WD which can remain bloated on a Gyr timescale (Istrate et al. 2014b). If that is the norm rather than the exception, it will lead to more AM CVn GW sources than previously predicted.

Based on binary population synthesis, Nelemans et al. (2001a) predicted a space density of AM CVn stars in a range of 0.4–$1.7 \times 10^{-4} \, \mathrm{pc}^{-3}$ and a number of resolvable AM CVn systems for LISA roughly equal to the number of detached WD+WDs (Nelemans et al. 2004b). More recently, Kremer et al. (2017) predicts that ~ 2700 systems will be observable by LISA with a negative chirp of $0.1 \, \mathrm{year}^{-2}$ (i.e. $\dot{f}_{\mathrm{gw}} < 0$, resulting from orbital expansion due to mass transfer, see Figs. 4 and 5). Until very recently, when ZTF reported a large number of eclipsing WD+WDs (Burdge et al. 2019a, 2020a), the majority of known LISA verification binaries was dominated by AM CVn systems (Roelofs et al. 2007a, 2010; Kupfer et al. 2015; Green et al. 2018a; Kupfer et al. 2018). However, observational space density estimates from SDSS data are in strong disagreement with theoretical predictions from these binary population studies. Roelofs et al. (2007c), Carter et al. (2013) derived an observed space density about an order of magnitude below the prediction by Nelemans et al. (2001a), Kremer et al. (2017) which would result in only $\lesssim 1000$ resolvable systems in the LISA band. The discrepancy could be real with the population synthesis predicting too many systems, related to assumptions in binary evolution physics (especially the treatment of mass transfer in close binaries), and/or possibly because some of the systems that are predicted to evolve into AM CVn binaries in fact merge in a CE shortly after the less-massive star fills its Roche lobe. On the other hand, it could also be that AM CVn stars are more difficult to find than expected (when not in outburst) or that they are distributed with relative high concentration in the thick disc (Nissanke et al. 2012). Ramsay et al. (2018) argued, based on Gaia data release 2 parallaxes, that a significant fraction of AM CVn systems, even within 100 pc, could still be undiscovered. Future transient sky surveys, such as LSST using the Vera C. Rubin Observatory, could have great success in detecting short-period binary systems with the implementation of appropriate cadence intervals (e.g. very short, ~ 15 s sub-exposures). Indeed already some AM CVn systems are thought (or known) to be eclipsing (Burdge et al. 2020b).

Nonetheless, AM CVn binaries are expected to be extremely useful for LISA because they simultaneously provide EM information across different wavelengths, as well as being observable in LISA's GW frequency range. For this reason, AM CVn systems have been cited as being important verification sources for LISA (e.g. Kupfer et al. 2018). In other words, AM CVn binaries will be multi-messenger sources once LISA flies. See Sect. 1.5.1 for further discussion on the multi-messenger opportunities for LISA.

1.2.3.2 UCXBs (ultra-compact X-ray binaries)

It has been known for many years that tight-orbit post-LMXB systems, leaving behind a NS+WD binary that spirals-in due to GW radiation, may avoid a catastrophic event, once the WD fills its Roche lobe. The outcome is expected to be a long-lived UCXB (Webbink 1979; Nelson et al. 1986; Podsiadlowski et al. 2002; Nelemans et al. 2010; van Haaften et al. 2012; Heinke et al. 2013). These sources are tight X-ray binaries observed with an accreting NS and a typical orbital period of less than 60 min. Because of the compactness of UCXBs, the donor stars are constrained to be either a WD, a semi-degenerate dwarf or a helium star (Rappaport et al. 1982). UCXBs are not only excellent laboratories for testing binary-star evolution, but also important GW sources. Studies of their orbital parameters (mass, orbital period and eccentricity), chemical composition and spatial distribution may provide important information and clues to understand both the accretion processes of compact binaries (including spin-orbit and tidal interactions) and the long-term evolution of double compact object binaries.

Depending on the mass-transfer rate, the UCXBs are classified in two categories: persistent and transient sources (e.g. Heinke et al. 2013). Only about 14 UCXBs have been confirmed so far (9 persistent, 5 transient), and an additional ~ 14 candidates are known. Thus UCXBs are difficult to detect or represent a rare population. Earlier studies (e.g. Istrate et al. 2014a) have suggested the need for extreme fine tuning of initial parameters (stellar mass and orbital period of the LMXB progenitor systems) in order to produce an UCXB from an LMXB system. UCXBs are detected with different chemical compositions in the spectra of their accretion discs (e.g. H, He, C, O and Ne, see Nelemans et al. 2010). To explain this diversity requires donor stars which have evolved to different levels of nuclear burning and interior degeneracy, and therefore to different scenarios for the formation of UCXBs. Since a large fraction of the UCXBs are found in globular clusters, some of these UCXB systems could also have formed via tidal captures, direct collisions or stellar exchange interactions (Fabian et al. 1975; Sutantyo 1975; Hut and Bahcall 1983).

Figure 5 displays the evolution of AM CVns and UCXBs in the GW frequency vs dynamical chirp mass diagram. These systems undergo stable RLO and will start to widen their orbits again within a few Myr after the onset of the mass transfer. LISA will detect such Galactic systems continuously both during the inspiral phase for a few tens of Myr, while the systems are still detached, and after the onset of RLO on a timescale of up to 100 Myr (depending on their distance).

The long-term stability of UCXBs has been a topic of debate. From an analytical investigation, van Haaften et al. (2012) argued that for a 1.4 $M_\odot$ NS accretor, only C/

O-core WDs with a mass of $\lesssim 0.4\,M_\odot$ lead to stable UCXB configurations. Subsequent hydrodynamical simulations suggested that this critical WD mass limit could be lower (Bobrick et al. 2017). The first successful numerical calculations of RLO from a WD to a NS were presented by Sengar et al. (2017), and they were able to follow the entire evolution until the low-mass He-core WD donor star has become a $\sim 0.005\,M_\odot$ planet-like companion. These systems were further evolved (Tauris 2018), including the finite-temperature (entropy) effects of the WD donor stars, and the first evolutionary tracks of such sources across the LISA GW band were produced, see e.g. Figs. 4 and 5. Further independent studies on the detectability of UCXBs as LISA sources have been provided by e.g. Chen et al. (2020a), Yu et al. (2021).

It is also anticipated that LISA may detect interacting BH+WD systems (Bahramian et al. 2017; Sberna et al. 2021). It has been estimated in some studies (Yungelson et al. 2006) that the Galaxy contains some 10^4 of these systems. However, their formation process (especially those with low-mass WD companions) remains uncertain (Podsiadlowski et al. 2003).

1.2.4 Other potential sources

Contributors: Camilla Danielski (1.2.4.1-2), Silvia Toonen (1.2.4.2), Thomas Kupfer (1.2.4.4), Jan van Roestel (1.2.4.3), Nicola Tamanini (1.2.4.1), Valeriya Korol (1.2.4.1)

1.2.4.1 Helium-star binaries   Subdwarf B stars (sdBs) are stars of spectral type B with luminosities below that of main-sequence stars. The formation mechanism and evolution of sdBs are still debated, although most sdBs are likely He–burning stars with masses $\sim 0.5\,M_\odot$, radii as small as $\sim 0.1\,R_\odot$ and thin hydrogen envelopes (Heber 2016). A large fraction are found in binary systems and, due to their compact nature, the most compact ones have orbital periods $\lesssim 1$ h (Vennes et al. 2012; Geier et al. 2013; Kupfer et al. 2017, 2020b, a), making them potentially detectable sources for LISA.

The most compact systems have WD companions and as such they are prime progenitor systems for double detonation Type Ia SNe. In this scenario a WD is orbited by a core He-burning sdB star in an ultra-compact orbit ($P_{orb} < 80$ min). Due to the emission of GWs, the binary shrinks until the sdB star fills its Roche lobe and starts mass transfer. He-rich material is then transferred to the C/O-core WD companion which will lead to the accumulation of a He-layer on top of the WD. After accreting about $0.1\,M_\odot$, He-burning is predicted to be ignited in this shell. This in turn triggers the ignition of carbon in the core, even if the WD mass is significantly lower than the Chandrasekhar limit (Fink et al. 2010). So far, the only known candidate for this scenario is the ultra-compact sdB+WD binary CD$-30°11223$ with an orbital period of $P = 71$ min (Vennes et al. 2012; Geier et al. 2013). This system was also found to be detectable for LISA with an expected SNR of ~ 5 after 4 years of LISA observations (Kupfer et al. 2018). More recently, the first members of ultra-compact sdB binaries which have started to transfer material to the WD companion

were discovered. The most compact system, ZTF J2130+4420, consisting of a low-mass sdB star with $M_{sdB} = 0.337 M_{\odot}$ has an orbital period of 39 min. The system has well measured properties from EM observations and is expected to have a SNR of ~ 3 after 4 years of LISA observations, adding to the growing number of LISA detectable He-burning stars.

Götberg et al. (2020) modelled the Galactic population of stripped stars, which contain the low-mass sdB stars as well as more massive He-core burning stars, in tight orbits with compact companions, focusing on those that will be detectable by LISA. Their analysis predicts up to 100 stripped star + WD binaries and up to 4 stripped star + NS binaries with SNR > 5 after 10 years of observations with LISA. Although the expected numbers are significantly smaller than for WD+WDs or AM CVns, Götberg et al. (2020) finds that all of the LISA detectable sources are within 1 kpc and therefore bright in EM flux which makes them ideal targets for multi-messenger studies (see Sect. 1.5.1 for more details on multi-messenger opportunities).

1.2.4.2 Period bouncing CVs   Period bouncing CVs are highly evolved cataclysmic variables where the donor has lost almost all of its mass and has become degenerate. These systems have reached the minimum orbital period for a hydrogen donor (70 min) and are evolving to longer orbital periods (up to 100 min). Model predictions are that 40–70% of all CVs are period bouncers (Kolb 1993; Knigge et al. 2011). However, only a few have been identified so far because of the low accretion rate and low temperature of the WD and donor (e.g. Pala et al. 2018). While the donor-mass is low and the orbital periods are relatively long, nearby period bouncers are detectable with LISA. Given their high space density, a dozen of these systems are close enough to be detected by LISA.

1.2.4.3 Exoplanets, brown dwarfs and substellar companions   In the Galaxy, due to the slope of the Salpeter-like initial mass function (IMF), more than 97% of all stars will terminate their lives as a WD, meaning that the vast majority of the known 4000+ planet-hosting stars will end their lives as WDs. In the last couple of decades, most of the attention in exoplanetary searches has been focused on the formation and characterisation of exoplanets orbiting host stars on the main sequence, but very little is known on planetary systems in which the host star evolves off the main sequence, to become a red giant. Theoretical models indicate that, if planets avoid engulfment and evaporation throughout the red-giant or/and the asymptotic-giant branch phases of the host star, they can survive (see e.g. Livio and Soker 1984; Duncan and Lissauer 1998; Nelemans and Tauris 1998). This is expected to be the fate of the planet Mars, and other planets orbiting further out in our Solar System (Schröder and Smith 2008). Observational evidence, in the form of photospheric contamination by the accreted debris (Zuckerman et al. 2010; Koester et al. 2014), dusty (Farihi et al. 2009) and gaseous circumstellar discs (Gänsicke et al. 2006; Manser et al. 2016), supports the existence of dynamically active planetary systems around WDs. Up to very recently, only two planetesimals had been observed orbiting a WD (Vanderburg et al. 2015; Manser et al. 2019). However, within the last years, two giant planets

have been detected orbiting single WDs (Gänsicke et al. 2019; Vanderburg et al. 2020), showing that planets can survive single host-star evolution.

Today, over 1000 brown dwarfs (BDs) have been detected in the Solar neighbourhood (Burningham 2018). Some of them have been discovered also around single WDs, and examples of BDs orbiting at distances beyond the tidal radius of the asymptotic-giant branch progenitor (but also within it, e.g. WD 0137 −349 B, Maxted et al. 2006), show that BDs can survive stellar evolution of their host star, whether or not they are engulfed by its expanding envelope. Farihi et al. (2005) predicted that few tenths of percent of Galactic single WDs hosts a BD.

The most straightforward way with which LISA could detect sub-stellar objects, such as planets or BDs, would be the direct detection of GWs emitted by a binary system composed of a sub-stellar object in an tight orbit around a single star. However, the absolute orbital period minimum for a hydrogen-rich body (i.e. a star, BD or a gas giant planet) in a binary system is about $P_{\rm orb} \simeq 37$ min (Rappaport et al. 2021). This corresponds to a GW frequency of at most $f_{\rm GW} \simeq 0.9$ mHz. Such a system could be detected only at close distances (say, within 1 kpc) and only for relatively high sub-stellar masses ($M \gtrsim 13\, M_{\rm J}$), possibly excluding all exoplanets. Furthermore, the mass of the sub-stellar object cannot be directly inferred from direct detection, and at best only the chirp mass of the binary system can be retrieved. Further investigations and EM observations are necessary to better understand the detectability and the rates of these sub-stellar objects, although at the moment it seems unlikely that a large number of these systems will be observed by LISA (Wong et al. 2019b).

Another option is to search for circumbinary planets around WD+WD through a modulation of the WD+WD signal (Tamanini and Danielski 2019), that can probe regions of parameter space not probed by EM observations (far away and not towards the Galactic Centre). The discovery of evolved planetary systems will statistically increase the current sample of post-main-sequence planets, filling an area of the planetary Hertzsprung–Russell diagram that is currently not explored (Tamanini and Danielski 2019). LISA will provide observational constraints on both planets that can survive two CE stellar evolution phases and on a possible second-generation planet population produced from CE ejecta material (Schleicher and Dreizler 2014). Even in the case where LISA will prove no detection anywhere in the Milky Way, it will be possible to set strong unbiased constraints on planetary evolution and dynamical theories, and in particular on the fate of exoplanets bound to a binary that undergoes two CE phases.

1.2.4.4 Triples and multiples   LISA's stellar sources will also contain multiple body systems, such as triples and quadruples. Hierarchical systems that consist of nested orbits represent stable configurations that can remain intact for several Gyr and throughout (despite) the evolution of the stellar components, as evidenced by observations. Within 20 pc of the Sun, there are already two such systems that harbor close WD+WDs. These are WD 0326−273 (Luyten 1949; Poveda et al. 1994; Nelemans et al. 2005; Giammichele et al. 2012; Toonen et al. 2017) and WD 0101+ 048 (Saffer et al. 1998; Maxted et al. 2000a; Caballero 2009; Giammichele et al.

2012; Toonen et al. 2017). The former is a triple that consists of a close WD+WD with a period of ~ 1.8 d, and an M5 star in a wide orbit. The latter is a quadruple consisting of a close WD+WD (with a period of ~ 1.2 d, but see (Maxted et al. 2000a) and a MS+MS binary. Two triple systems with *three* WD components are known as well, J1953−1019 (Perpinyà-Vallès et al. 2019) and WD 1704+481 (Maxted et al. 2000b). The inner binary of the latter system has a period of ~ 0.15 d, just inside the LISA frequency range. Even millisecond pulsars have been found to be part of triple-architectures; the PSR J0337+1715 system harbors a compact NS+ WD (1.6 d orbital period) inner binary which is orbited by another (tertiary) WD every 327 d (Ransom et al. 2014; Tauris and van den Heuvel 2014). The globular cluster (M4) pulsar B1620−26 has a WD companion in a half-year orbit, and a planetary companion in a 100-year orbit (Thorsett et al. 1999; Sigurdsson et al. 2003).

Theory suggests that exoplanets (and BDs) also exist around WD+WDs in the Galactic disc, and that such objects are more likely to survive around evolving close binary stars than around evolving single stars (Kostov et al. 2016). The eclipse timing variation technique allowed the detection of a few post-CE systems (that is WD+ low-mass star), and a BD companion(s) (see e.g. Goździewski et al. 2015; Beuermann et al. 2012; Almeida et al. 2019), nevertheless today no BDs or exoplanets orbiting WD+WDs have been observed yet.

LISA will be able to detect outer companions to compact (inner) binaries when they impose eccentricity oscillations in the inner orbit due to three-body dynamics (von Zeipel 1910; Lidov 1962; Kozai 1962; Naoz 2016). In particular Hoang et al. (2019) showed such oscillations would be observable with LISA to distances up to a few Mpc for compact binaries near supermassive BHs, which can also be considered a three-body system. Furthermore, LISA can detect outer companions by exploiting the Doppler frequency modulation on the GW waveform due to their gravitational pull (Robson et al. 2018). The acceleration imparted by the hierarchical companions can be detected in the GW signal for outer periods as large as 100 year (Robson et al. 2018; Tamanini et al. 2020). For systems with orbital periods that are shorter than, or comparable to, the mission lifetime, the perturbation allows for the determination of the orbital period, eccentricity, initial orbital phase and radial velocity parameter of the companion (Robson et al. 2018; Tamanini and Danielski 2019). On a general level, the sensitivity of LISA will be able to detect WD+WDs companions with masses down to $\sim M_J$ (Danielski et al. 2019), and therefore allow not only for the detection of stellar companion and compact objects, but also BDs and exoplanets. This being an indirect detection, i.e. the observation of a periodic Doppler shift modulation of an existing strong binary GW signal, we are able to probe a wider mass range, whose inferior limit also covers the giant planets range. The novelty of using LISA for the detection of planetary/low-mass companions is that GWs provide a much larger spatial coverage than the one provided by EM techniques, enabling us to probe regions of our Galaxy currently not accessible to other methods. More specifically, Danielski et al. (2019) showed that during a 4 year nominal mission LISA will detect from 3 to 83 exoplanets, and from 14 to 2218 BDs everywhere in the Milky Way. The sensitivity of LISA is such that in the most optimistic cases exoplanets could be detected orbiting WD+WDs in the Milky Way's satellites, in

particular in the Large Magellanic Cloud (LMC, Danielski and Tamanini 2020). Such an observation could represent the first detection of an extra-galactic bound exoplanetary system.

1.2.4.5 Capturing the inspiral of a CE system   It has been suggested by Renzo et al. (2021) that LISA may be able to detect the inspiral of binaries undergoing a CE phase. Depending on various assumptions, they anticipate that LISA could detect between 0.1 and 100 such GW sources in the Galaxy during the mission duration. Detecting this GW signal would provide direct insight into the gas-driven physics of CE evolution.

1.3 Formation of LISA binaries

***Coordinators:* Katelyn Breivik**

***Contributors:* Michela Mapelli (1.3.2-3), Simone Bavera, Katelyn Breivik, Martyna Chruslinska, Gijs Nelemans, Pau Amaro Seoane (1.3.2), Manuel Arca Sedda (1.3.2-3), Thomas Tauris, Silvia Toonen (1.3.2-3), Jeff Andrews, Tassos Fragos (1.3.1), Luca Graziani, Daryl Haggard (1.3.2), Melvyn B. Davies (1.3.2-3)**

In the following section, we discuss the formation of LISA binaries. For a review and broader description of the many physical aspects of stellar evolution and binary star interactions that are referred to below in the context of the formation of compact object binaries, we refer to the textbooks by, for example, Shore et al. (1994), Hilditch (2001), Eggleton (2006), Chaty (2022), Tauris and van den Heuvel (2023).

1.3.1 Isolated binaries

The formation pathways of isolated binaries observable by LISA are marked with several phases of mass loss or exchange. In the following Section, we refer to the initially more massive star as the primary and the initially less massive star as the secondary. Stable mass transfer can occur either through wind mass loss/accretion or RLO. Wind mass loss is generally assumed to be non-conservative across all phases of stellar evolution, with mass accretion efficiency ranging from $\lesssim 10\%$ for the Bondi–Hoyle–Lyttleton mechanism and $20-50\%$ if the accretion is focused (de Val-Borro et al. 2017). In this case, the orbit widens as the mass lost from the system causes an increase of the remaining specific angular momentum. In practice, the dynamics are complicated and dependent on physics related to the geometry and structure of the wind, tidal effects, orbital characteristics and in some cases magnetic fields and radiation transport, thus calling for three-dimensional, multi-physics, hydrodynamical simulations (e.g. Saladino et al. 2018, 2019).

RLO occurs when the donor star expands to the point that its radius exceeds the Roche radius (Eggleton 1983). RLO mass transfer can proceed in a dynamically stable or unstable fashion, depending on the structure of the donor and accretor as well as their mass ratio. The stability of RLO mass transfer is commonly described

using the Webbink radius–mass exponents (Webbink 1985) that determine the timescales on which mass transfer will become unstable. In the case of dynamically stable mass transfer, the orbital evolution depends strongly on the mass ratio of the binary: if $M_{\text{donor}}/M_{\text{accretor}} > 1$, the orbit tightens (for fully conservative mass-transfer), while in the converse case the orbit widens. Mass-transfer efficiency, as well as the assumed specific angular momentum carried away from mass lost from the system, play a crucial role in mass-transfer stability and the orbital evolution of the binary.

Dynamically unstable mass transfer is believed to generate a CE phase where the donor star's core and companion are enshrouded in the donor's envelope (for a review see Ivanova et al. 2013). The precise dynamics of how CE proceeds are still not fully understood. In the context of compact object binary formation and population synthesis studies, energy budget arguments are most often employed to estimate the post-CE properties of a binary. In the "α_{CE}" prescription, it is assumed that a fraction α_{CE} of the released orbital energy is used to unbind the donor's envelope and eject it from the system (van den Heuvel 1976; Webbink 1984). Several recent studies have suggested that other sources of energy may be needed to successfully eject the envelope, including recombination energy (e.g. Zorotovic et al. 2014; Nandez and Ivanova 2016) or jets launched by the companion (e.g. Shiber et al. 2019). Each of these will change the overall energy budget of the CE evolution and lead to differences in the final orbital separation (e.g. Iaconi et al. 2018). Alternatively, in the "γ_{CE}" prescription, angular momentum conservation arguments, which lead to less dramatic inspiral, have been considered to explain the orbital period distribution of WD+WDs (Nelemans et al. 2000).

1.3.1.1 WD+WD systems and AM CVn binaries The progenitors of isolated WD+WD and AM CVn binaries begin with zero age main sequence stars with masses below $8 - 10\,M_\odot$. The formation pathways of close WD+WD and AM CVn binaries contain several stages of stable and unstable mass transfer, or CE (see Fig. 6). The uncertain outcomes of these interactions determine whether the progenitor binary


Fig. 7 Illustration of the formation of a detached NS+WD binary and an UCXB system. See Fig. 6 for details. Additional acronyms: SN: supernova; NS: neutron star; LMXB: low-mass X-ray binary; BH: black hole. Image reproduced with permission from Tauris and van den Heuvel (2023), copyright by PUP
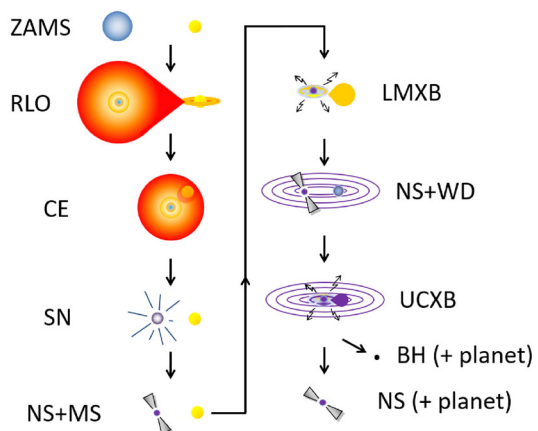
continues on in its evolutionary path toward becoming a LISA source or if it merges with its companion. Conversely, LISA observations of the populations of WD+WD and AM CVn sources will constrain these interactions.

Virtually all close WD+WD and AM CVn progenitors experience an interaction as the primary star advances off the main sequence and fills its Roche lobe. This interaction can either proceed stably or unstably on dynamical timescales. In either case, the orbit will shrink because of the donor's higher mass relative to the accretor. For systems with late red giant and asymptotic giant branch donors, initially dynamically stable but thermally unstable mass transfer can produce mass loss from the L2 Lagrange point, which leads to a delayed dynamical instability and a CE phase (Ge et al. 2020; Misra et al. 2020). In the rare case of close WD+WDs where the more massive WD forms second (converse to stellar lifetime expectations), a phase of stable mass transfer, followed by a CE generated by the initially lower mass star could be necessary (Woods et al. 2012).

After each interaction, the star which donates mass becomes stripped leaving behind a He core that can have varying structure depending on the evolutionary phase at which the donor filled its Roche lobe. Such stripped stars orbiting main sequence companions have been widely observed throughout the Galaxy (Rebassa-Mansergas et al. 2007) and been used to constrain CE ejection efficiencies (Zorotovic et al. 2010; Toonen and Nelemans 2013).
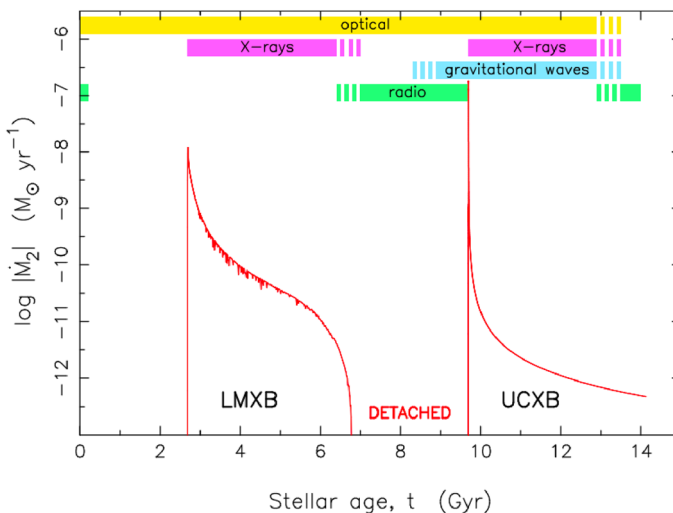
Fig. 8 Evolutionary sequence showing how ultra-compact X-ray binaries (prime LISA source candidates) are formed from merging NS+WD binaries, descending from LMXBs. Plotted here is mass-transfer rate of the donor star as a function of stellar age. The initial MS star + NS binary has components of $1.40\,M_\odot$ and $1.30\,M_\odot$, respectively. The system evolves through two observable stages of mass transfer: an LMXB for 4 Gyr, followed by a detached phase lasting about 3 Gyr where the system is detectable as a radio millisecond pulsar orbiting the helium WD remnant of the donor star, until GW radiation brings the system into contact again, producing a UCXB. The colour bars indicate detectability in different regimes resulting in synergies between LISA and EM detectors. Image reproduced with permission from Tauris (2018), copyright by APS

Fig. 9 Illustration of the formation of a tight BH+NS binary that evolves towards a merger. See Figs. 6 and 7 for explanation of acronyms. Image reproduced with permission from Tauris and van den Heuvel (2023), copyright by PUP
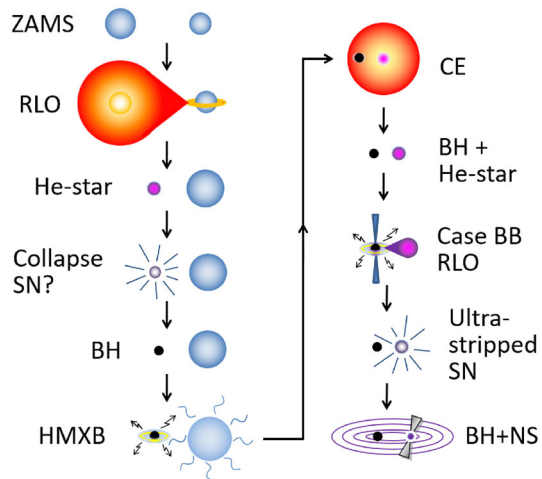
Since the previous interaction brings the two stars together, further interactions are likely. Interactions can occur while the secondary is still on the main sequence. In this case, if the mass transfer is stable, a cataclysmic variable is formed (Zorotovic et al. 2011). Conversely, mass transfer can also occur as the secondary advances up the giant branch. Due to previous envelope stripping, the mass ratio of the secondary donor to the WD accretor can be either greater or less than one. If the secondary is already less massive than the WD, stable mass transfer will occur and widen the orbit, removing the possibility of detection by LISA. However, if the secondary is more massive than the WD companion, the mass exchange will lead to orbital tightening. If the mass transfer is unstable, another CE phase takes place, potentially bringing the stars even closer together and leaving behind a WD with a stripped He core companion. The structure of the He core again depends on the evolutionary phase at which the secondary overflows its Roche lobe. At this point, a close WD+ WD binary is assured and the slow evolution due to GW emission brings the WD+ WD toward the LISA band.

A key uncertainty in the formation pathways of AM CVn binaries is the nature of the donor star. AM CVn binaries consist of a WD accreting He-rich material originating from a WD, semi-degenerate helium star, or evolved MS donor (Solheim 2010). Indeed, it could be the case that the observed AM CVn population is a combination of all three with different relative contributions (Nelemans et al. 2004b). If the donor star is a non-degenerate evolved star, magnetic braking is required, along with GW emission, to maintain the ultra-short periods of observed AM CVn systems (van der Sluys et al. 2005). Magnetic braking is a process in which orbital angular momentum in a tight synchronized binary is converted into spin angular momentum via a magnetic stellar wind (a process that therefore requires a low-mass stellar component with a convective envelope). The ultra-compact orbital configuration is less problematic for semi-degenerate and fully-degenerate donors which originate from the ejection of a second CE, with tighter orbits allowed by more degenerate donors (Yungelson 2008). In the case of fully-degenerate He-core WD donors, the

orbit can become so small that the mass lost from the donor directly impacts the accretor leading to a rapid decrease in orbital size followed by a long-lived phase of accretion which widens the orbit (Nelemans et al. 2004b; Marsh et al. 2004; Deloye and Taam 2006; Kremer et al. 2017). Regardless of the donor, a significant uncertainty still remains in how much He-rich material the accretor can handle until novae erupt on the WD's surface. While detailed binary evolution calculations (e.g. Tauris 2018) have shown that RLO mass transfer in WD+WD can be stable, it has been suggested that interactions of the donor star with the expanding nova shells will likely lead to a rapid orbit shrinkage and eventually a merger (Shen 2015).

1.3.1.2 White-dwarf binaries with neutron-star or black-hole companions

Compared to WD+WDs, the formation of detached binaries with WD and NS or BH companions occur in binaries with stars that are massive enough to explode in a SN (see Fig. 7). Similar to WD+WD formation, the more massive primary evolves first and, because of the relatively large mass ratio, begins RLO mass transfer that is often expected to be unstable and lead to a CE. Soon after, the primary evolves to become a compact object, through either a supernova explosion (NS or BH) or direct collapse (BH only). Since a NS is thought to receive a kick during its formation, there is a significant probability that the binary disrupts at this point.

The subsequent evolution, of a lower-mass non-degenerate star with a NS or BH, will typically go through a phase of stable mass transfer in which the binary becomes observable as X-ray binary, due to the strong heating of the accretion disc in the deep potential of the NS or BH. When the onset of the mass-transfer occurs after the secondary star has evolved past its main sequence, the core of the star has already contracted. Thus after the X-ray binary phase, when the envelope of the expanding star has been completely transferred, the NS or BH is left with a WD companion that was the core of the donor star.

In some cases, the NS/BH+WD binary is tight enough that angular momentum loss due to GW emmission will bring the two objects together as LISA sources (Fig. 8). At periods of $\sim$ 10–20 min, i.e. within the LISA band, the WD will start to transfer mass to the NS/BH, forming an X-ray binary again, but now of ultra-short period, called an UCXB. Detailed numerical calculations, including finite-temperature (entropy) effects, have shown that UCXBs can indeed form via stable RLO from post-LMXBs systems (Sengar et al. 2017; Tauris 2018).

1.3.1.3 Double neutron star/black hole binaries

NS+NS formation has been extensively discussed in the literature (see Tauris et al. 2017, for a review). The standard scenario (see Fig. 9 for a schematic diagram) involves several phases of interaction, starting with a stable RLO, during which the primary loses part of its envelope before it undergoes a SN to form a NS. The newly formed NS HMXB is likely too dim to be detectable in X-rays, as the orbital separation is still large and the NS may only be able to capture an appreciable fraction of the companion's stellar wind when the latter evolves to the giant phase. During the subsequent evolution the orbital separation needs to decrease from $\sim 10^3 \, R_\odot$ to a few $R_\odot$ for the final binary to merge within the Hubble time. Significant tightening is typically achieved through a

CE phase that occurs when the secondary this time fills its Roche lobe. The post-CE binary is expected to encounter another phase of mass transfer, initiated by a stripped helium-burning secondary (i.e., so-called Case BB mass transfer, often initiated when a ~ 2.5–$3.5\,M_\odot$ helium star expands during shell-helium burning, Habets 1986). This leads to further orbital tightening, stripping of the secondary's envelope, and NS spin-up. If this last mass-transfer episode is unstable and leads to a second CE phase, a fast merging NS+NS will be formed; a scenario invoked to explain r-process element enrichment observed in some stellar systems (Safarzadeh et al. 2019; Zevin et al. 2019a). Such NS+NSs would be effectively unobservable with current radio surveys, and if they exist within the Galaxy, their presence will be revealed by LISA (Kyutoku et al. 2019; Andrews et al. 2020). However, recent detailed binary evolution calculations have shown that this last phase of Case BB mass transfer is expected to be stable (Tauris et al. 2015; Vigna-Gómez et al. 2018) and do not support the existence of the aforementioned fast-merging channel (in contrast to earlier works Ivanova et al. 2003; Dewi and Pols 2003).

Besides the pre-HMXB evolution, the most important and uncertain aspects of our current understanding of NS+NS and mixed BH+NS formation are related to: (i) CE evolution and spiral-in of the NS, (ii) momentum kicks (magnitude and direction) imparted onto newborn NSs, and (iii) the mass distribution of NSs.

From an energetics point of view, it has been shown that an inspiralling NS may indeed be able to eject the envelope of its massive star companion (e.g. Xu and Li 2010; Loveridge et al. 2011; Wang et al. 2016a; Kruckow et al. 2016). However, predicting the final post-CE separation is difficult for several reasons, including: estimating the location of the bifurcation point within the massive star (Tauris and Dewi 2001), separating the remaining core from the ejected envelope (Tauris and Dewi 2001; Fragos et al. 2019), additional energy sources such as accretion energy (MacLeod and Ramirez-Ruiz 2015; Murguia-Berthier et al. 2020), energy and radiation transport during the CE inspiral (Fragos et al. 2019) and the effect of an inflated envelope of the exposed naked helium core (Sanyal et al. 2015, see also Sect. 1.7.1.3).

Newly formed NSs gain velocity (natal kicks; e.g. Gunn and Ostriker 1970; Hobbs et al. 2005; Verbunt et al. 2017) due to asymmetries arising during their formation (e. g. Janka 2012). The properties of the modelled NS+NS population (e.g. number of systems formed, orbital parameters, merger locations relative to formation site) are highly dependent on the adopted natal kick prescription (e.g. Portegies Zwart and Yungelson 1998; Bloom et al. 1999; Chruslinska et al. 2018; Giacobbo and Mapelli 2018; Andrews and Zezas 2019). To match the current observational constraints on the NS+NS merger rate and parameters of several of the observed systems (e.g. van den Heuvel 2007), it is necessary to assume that a fraction of NS forms with natal kicks smaller than typically found for young single pulsars. Some scenarios involve low-mass NS progenitors and electron-capture triggered explosions (e.g. Dessart et al. 2006; Jones et al. 2013). Others postulate a link between the natal kick magnitude and the mass of the NS progenitor and SN ejecta (e.g. Beniamini and Piran 2016; Bray and Eldridge 2016; Janka 2017). These claims have been supported by 3D NS simulations of ultra-stripped stars (Müller et al. 2019). In fact, it has been demonstrated that close-orbit, low-eccentricity NS+NS and BH+NS systems most

Fig. 10 Illustration of the formation of LISA sources via examples of exchange encounters. See Figs. 6 and 7 for explanation of acronyms. Image reproduced with permission from Tauris and van den Heuvel (2023), copyright by PUP
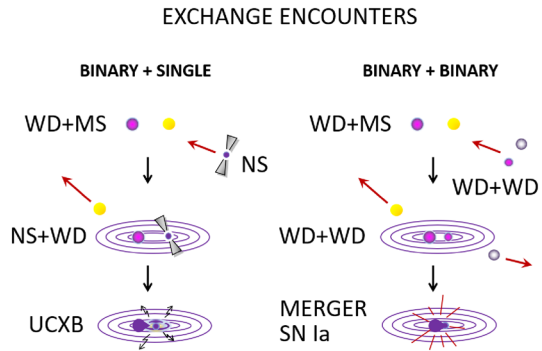
likely form via ultra-stripped SNe when the last star explodes (Tauris et al. 2013, 2015). The reason being that the last Case BB RLO mass-transfer phase causes the NS to significantly strip its evolved helium-star companion, almost to a naked metal core prior to its explosion, and thus there is very little SN ejecta (see also Sect. 1.7.1.7).

Finally, a clear correlation has been predicted between the spin period of the recycled pulsar and the orbital period of the system after the second SN (Tauris et al. 2017). This correlation can be tested in LISA binaries, if the spin period is measured, since only short orbit systems will enter the LISA band within a Hubble time, and these binaries should therefore contain the most rapidly spinning NSs of this population. Another hypothesis that can be tested by LISA, is the resulting mass distribution among NS+NS systems (e.g. Özel and Freire 2016, and references therein).

Merging BH+BHs and NS+BHs in the field are thought to occur under some specific binary interactions which either (i) bring the parent stars closer together during their evolution or (ii) prevent stars in close obits from expanding.

The former one (i) occurs in a similar manner to the formation of NS+NSs described above, and involves many of the main uncertainties. In contrast to NS+NS formation, BH+BHs and to a lesser degree BH+NSs are sensitive to the metallicity of the progenitor stars, and they favor low-metallicity environments. In addition the second mass transfer episode, after the first compact object formation, can be either dynamically stable (e.g. van den Heuvel et al. 2017; Inayoshi et al. 2017a; Neijssel et al. 2019) or unstable (e.g., Smarr and Blandford 1976; van den Heuvel 1976; Tutukov and Yungelson 1993; Kalogera et al. 2007; Postnov and Yungelson 2014; Belczynski et al. 2016a). In the latter case this leads to a CE phase. The resulting tight system composed of a compact object and a Wolf–Rayet star can eventually undergo a tidal spin up of the star (Qin et al. 2018; Bavera et al. 2020). On the other end, if the second mass transfer is stable the binary will result in wider orbits compared to the evolution through CE and avoid a subsequent tidal spin up phase (Bavera et al. 2021). Eventually, following wind-driven mass loss, the secondary will collapse to a compact object. This leave us with either a BH+BH system or a NS+BH system with either a first- or second-born NS.

The latter possibility (ii) occurs when two massive stars are born in a tight orbit (orbital periods less than 4 days) in low-metallicity environments which due to their tidal interactions can maintain the stars at almost critical rotation. Such rapidly rotating stars develop a temperature gradient between the poles and the equator leading to chemical homogeneous evolution (e.g., de Mink et al. 2009; Mandel and de Mink 2016; Marchant et al. 2016; du Buisson et al. 2020). In these stars meridional circulation transport hydrogen from the surface into the core and helium out into the envelope until nearly all the hydrogen in the star is fused into helium. At the end of their main sequence these stars are essentially Wolf–Rayet stars and do not expand, hence, avoiding any additional mass-transfer phase.

LISA may answer whether or not mixed binaries of BHs and NSs, in which the NS formed first, are produced in the Galaxy. It is possible that the in-spiralling NS is unable to eject the envelope of the relatively massive BH progenitor star (Kruckow et al. 2018). Since we currently do not know of the existence of mixed BH+NS systems in the Galacy, any LISA detections of such systems, as well as double BH systems, will provide crucial information about their formation process.

1.3.2 Sources in clusters

The inner regions of stellar clusters are cosmic factories of compact binaries (i.e., binaries containing two compact objects; BHs, NSs or WDs), owing to the dominant role played by stellar dynamics in such environments. Massive stars in stellar clusters lose kinetic energy to lighter stars and accumulate into the cluster centre. In just a few Myr, these stars evolve into stellar BHs and NSs.

The production of compact binaries can take one of two routes. If only a small fraction of BHs are retained within a cluster, encounters between BHs and binary stars lead to dynamical exchanges, where the BH replaces a less massive star within the binary (Hills and Fullerton 1980). Globular clusters have a considerably-enhanced population of X-ray binaries (Heinke et al. 2003), which might have formed when a NS or a BH exchanges into a binary star (e.g., Hills 1976). After the first exchange, evolution of the stellar companion (which might also become a BH or a NS) or a second dynamical exchange can produce a compact binary. Binary-single interactions represent an efficient mechanism to harden these binaries (Heggie 1975) to the point where they can merge via the emission of gravitational radiation (see Fig. 10 for a schematic representation).

Alternatively, if a large fraction of BHs are retained in the cluster, they can form a BH subsystem (Spitzer 1969; Mackey et al. 2007, 2008; Arca Sedda et al. 2018; Kremer et al. 2020b, but see Breen and Heggie 2013). BHs in the subsystem tend to strongly interact with each other, undergoing frequent pairing, exchanges, and ejections. The most efficient mechanism driving binary formation in globular clusters is via three-body scatterings (e.g., Morscher et al. 2015). After formation, a binary can undergo dozens of interactions with passing stars and binaries, which can lead to the production of very hard binaries, capable of merging via the action of GW emission (Portegies Zwart and McMillan 2000). If the star cluster centre harbours a BH subsystem, the BHs dominate the dynamics, quenching mass segregation and preventing the formation of binaries containing other compact objects (see e.g. Ye

Fig. 11 Illustration of the formation of a LISA source in a triple system. See Figs. 6 and 7 for explanation of acronyms. Image reproduced with permission from Tauris and van den Heuvel (2023), copyright by PUP
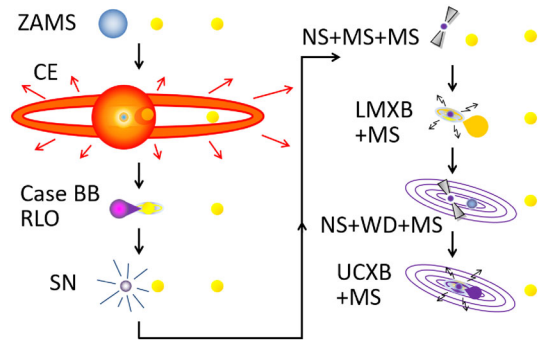
et al. 2020). However, dynamically evolved clusters can lose a substantial fraction of the BHs. In these BH-poor clusters, binary-single interactions can allow the formation of binary NS and BH+NS binaries. Furthermore, it has been proposed that a parabolic encounter between two compact objects could potentially lead to the formation of a binary due to an abrupt loss of energy emitted as gravitational radiation (e.g. Hansen 1972; Quinlan and Shapiro 1989; Kocsis et al. 2006; Hong and Lee 2015). However, the event rate of this mechanism, which is often referred to as the "gravitational brake" capture, is very likely to be negligible due to the small cross-section (Kochanek et al. 1990).

Old BH-poor clusters may also be ideal for dynamical formation of WD+WD binaries as well as BH/NS+WD binaries (Kremer et al. 2020b), see Fig. 10. In old globular clusters, WDs are by far the most abundant type of compact object (roughly 10^5 WDs are expected in a $10^6 \, M_\odot$ cluster). A number of analyses have studied ways WD binaries, both accreting and detached, may be dynamically assembled in stellar clusters (Grindlay et al. 1995; Ivanova et al. 2006; Belloni et al. 2016; Kremer et al. 2018b). Furthermore, a handful of the stellar-mass BH binary candidates observed in Galactic globular clusters are suspected to be ultra-compact accreting BH+WD binaries (Strader et al. 2012; Bahramian et al. 2017; Church et al. 2017). Overall, up to a few dozen dynamically formed WD binaries are expected to be resolved by LISA in the Galactic globular clusters, likely constituting the largest class of dynamically-formed LISA sources in the Galaxy (Willems et al. 2007; Kremer et al. 2019b). Currently two candidates to AM CVns in globular clusters have been identified (Zurek et al. 2016; Rivera Sandoval et al. 2018) and several more are expected to be discovered in upcoming globular cluster surveys.

Comparing nuclear stellar clusters with globular clusters, the former tend to have somewhat larger escape speeds (due in part to the presence of a central massive BH, MBH: Graham and Spitler 2009). This means that a larger fraction of BHs are likely to be retained (e.g. Miller and Lauburg 2009), while the higher dispersion velocity inhibits both exchange encounters and the dynamical formation of binaries (e.g. Heggie and Hut 2003). The presence of a dense nuclear cluster surrounding the MBH can significantly affect the formation process of compact binaries in a number of ways. Dynamical three body encounters can form at least one compact BH+BH if the nuclear cluster-to-MBH mass ratio exceeds 10, whereas at lower values the

reservoir of compact binaries might be replenished via star cluster inspiral (e.g. Arca Sedda 2020a). The presence of an MBH can leave significant imprints on the BH+ BH evolution, owing to the possible development of von Zeipel–Kozai–Lidov cycles (von Zeipel 1910; Kozai 1962; Lidov 1962), which can boost the rate of BH+BH mergers (Blaes et al. 2002; Antonini and Perets 2012; Hoang et al. 2018; Fragione et al. 2019; Arca Sedda 2020a) and significantly affect the BH mass spectrum in these extreme environments (e.g. Arca Sedda 2020a).

Young star clusters and open clusters, because of their relatively low total masses (10^2–$10^5\,M_\odot$), host a smaller population of BHs with respect to globular and nuclear clusters (e.g., Portegies Zwart and McMillan 2000; Banerjee et al. 2010; Banerjee 2017, 2021). BH+BHs in young/open star clusters mostly originate from dynamical exchanges or even from the evolution and hardening of primordial binaries (Ziosi et al. 2014; Di Carlo et al. 2019, 2020b; Kumamoto et al. 2019, 2020). Furthermore, dynamical exchanges favour the formation of BH+NS binaries in young and open clusters (Rastello et al. 2020).

Finally, hierarchical mergers in globular/nuclear clusters (e.g. Miller and Hamilton 2002a; Rodriguez et al. 2019; Antonini et al. 2019; Arca Sedda 2020a; Arca Sedda et al. 2020b) or runaway collisions of massive stars (e.g. Portegies Zwart et al. 2004; Giersz et al. 2015; Mapelli 2016; Rizzuto et al. 2020) and binary star mergers in young star clusters (Di Carlo et al. 2020a) might even lead to the formation of intermediate-mass BHs (Graham et al. 2019) and BHs with mass in the pair-instability gap (e.g. Arca Sedda et al. 2020b), similar to GW190521 (Abbott et al. 2020c, d).

1.3.3 Triple stellar systems

Some of the LISA sources may form as part of triples and higher-order multiples. This includes sources in the Galactic disc (formed through e.g. isolated triple evolution) as well as those in dense environments. Three-body (or more) interactions are important in the formation of compact sources in two ways: during short-lived dynamical interactions and in hierarchical triple systems (Fig. 11).

Hierarchical triples, in which two bodies orbit each other, and a third body orbits the centre of mass of the inner orbit, can remain stable for secular timescales, and therefore stay intact for Hubble times (Kiseleva et al. 1994; Mardling and Aarseth 1999; Georgakarakos 2008; He and Petrovich 2018). They may form in clusters (where they may interact with interloper stars in the densest environments) or exist in the Galactic disc (and evolve in pure isolation). Their evolution differs from that of isolated binaries due to three-body effects. Hence, triples that live their lives in isolation bridge the gap between classically isolated LISA sources and dynamically-evolving sources (often used to mean cluster sources). The importance of three-body interactions in hierarchical systems has been recognised for the evolution of stellar triples (Thompson 2011; Hamers et al. 2013; Silsbee and Tremaine 2017; Antonini et al. 2017; Liu and Lai 2017; Toonen et al. 2018; Fragione and Loeb 2019; Fragione and Kocsis 2019; Toonen et al. 2020), triples that consists of a combinations of stars and planets (Hamers and Portegies Zwart 2016; Hamers 2017; Veras et al. 2018;

Stephan et al. 2018, 2020), as well as stellar binaries in dense environments (Antonini and Perets 2012; Antonini et al. 2016; Petrovich and Antonini 2017; Stephan et al. 2016, 2019; Hamilton and Rafikov 2019b, a; Fragione et al. 2020; Martinez et al. 2020; Fragione et al. 2020).

The general formation of binaries and multiples (compact and wide) in clusters is boosted during the collapse of the dense cluster core, which is halted by frequent stellar interactions (Spitzer 1987; Hut et al. 1992). The formation of the first binaries takes place most likely via three-body scatterings, involving three initially unbound objects (Goodman and Hut 1993; Lee 1995). As soon as binaries start forming, binary–single (Hut and Bahcall 1983; Sigurdsson and Phinney 1993) and binary-binary (Mikkola 1983; Miller and Hamilton 2002a) interactions take over and become the dominant dynamical processes at play. Even for relatively low triple fractions, dynamical interactions involving triples occur roughly as often as encounters involving either single or binary stars alone, particularly in low-mass star clusters (Leigh and Geller 2013). When the objects involved in the interaction cross their mutual sphere of influence, a strong interaction can trigger the formation of a short-lived bound triple system (Goodman and Hut 1993). During these chaotic resonances, a pair of objects has a non-negligible probability of experiencing a very close passage, triggering the formation of a compact binary and subsequent merger (Samsing et al. 2014). Depending on the cluster structure, binary mergers developing through resonant interactions can be highly eccentric at LISA frequencies and even still when entering the frequency range typical of ground-based detectors (Samsing 2018; Samsing and D'Orazio 2018; Arca Sedda et al. 2021b). Binary–binary interactions (Mikkola 1984; McMillan et al. 1991; Miller and Hamilton 2002a) represent another efficient mechanism to form triples, either in the form of short lived, resonant unstable triples (Hut and Bahcall 1983; Zevin et al. 2019b; Arca Sedda et al. 2021b), or in a hierarchical configuration (Antonini et al. 2016; Zevin et al. 2019b; Arca Sedda et al. 2021b; Martinez et al. 2020; Fragione et al. 2020).

The best known manifestation of three-body dynamics are the von Zeipel–Kozai–Lidov cycles (von Zeipel 1910; Lidov 1962; Kozai 1962) regime in which the inner orbit eccentricity and the inclination between the two orbits vary periodically. Strictly speaking this applies to the (inner) test particle regime, an axisymmetric outer potential and the lowest-order expansion of the Hamiltonian (i.e., quadrupole). Relaxing either one of these assumptions leads to qualitative different dynamical evolution, which include extreme eccentricity variations and orbital flips (see Naoz 2016, for a review). The high eccentricities can lead to close passages between the bodies, mass transfer, and enhancement of dissipative processes such as from tides or by GW emission. Over time, the latter can lead to a significant reduction of the inner orbital separation during the nuclear burning stages or during the compact object phase of the stars (Mazeh and Shaham 1979; Kiseleva et al. 1998; Fabrycky and Tremaine 2007; Thompson 2011). Through the internal stellar evolution, a triple may transition from one dynamical regime to another, enhancing (or diminishing) the three-body effects (Shappee and Thompson 2013; Michaely and Perets 2014; Toonen et al. 2016).

1.4 Expected LISA observations: numbers and rates

Coordinators: **Abbas Askar, Simone Bavera**

Contributors: **Abbas Askar, Quentin Baghi, Simone Bavera, Tassos Fragos, Valeriya Korol, Kyle Kremer, Manuel Arca Sedda**

1.4.1 Binary's detectability

The detectability of Galactic stellar binaries with LISA primarily depends on the parameters involved in the GW amplitude:

$$\mathcal{A} = \frac{2(G\mathcal{M})^{5/3}(\pi f)^{2/3}}{c^4 d}, \tag{1}$$

where f is the binary's GW frequency, $\mathcal{M} = (m_1 m_2)^{3/5}/(m_1 + m_2)^{1/5}$ is the chirp mass (with m_1 and m_2 being the primary and secondary masses), d is the luminosity distance, G and c are respectively the gravitational constant and the speed of light. This follows from the fact that the signal-to-noise ratio scales linearly with amplitude $\rho \propto \mathcal{A}\sqrt{T}$ with T being the observation time (Babak et al. 2021). Besides, in contrast

Table 3 Estimated absolute number of compact binaries from *isolated binary evolution* in the Milky Way

Source	N	N^{detected}
WD+WD	$\sim 10^8$	6000–10,000
NS+WD	$\sim 10^7$	100–300
BH+WD	$\sim 10^6$	0–3
NS+NS	$\sim 10^5$	2–100
BH+NS	$\sim 10^4 - 10^5$	0–20
BH+BH	$\sim 10^6$	0–70

The columns show the source type, the total number of binaries in the galaxy at any frequency and the total number of estimated sources detected by LISA. We report values from indipendent studies which assume different LISA mission lifetimes and SNR. WD+WD models assume a frequency range 0.5–10 mHz while models for the other sources assume a frequency range 0.1–10 mHz. At lower frequencies the total number of LISA sources is so high that it might become impossible to distinguish individual sources from the GW foreground. The ranges of the expected intrinsic number of each binary type are extracted from Nissanke et al. (2012), Breivik et al. (2020a), Belczynski et al. (2010a), Kruckow et al. (2018), Nelemans et al. (2001c), van Oirschot et al. (2014), Lamberts et al. (2018) while the ranges of the expected number of LISA sources are extracted from Nelemans et al. (2001b), Korol et al. (2017), Lamberts et al. (2019), Korol et al. (2018), Liu et al. (2010), Ruiter et al. (2010), Tauris (2018), Breivik et al. (2020a), Belczynski et al. (2010a), Kruckow et al. (2018), Lau et al. (2020), Andrews et al. (2020), Sesana et al. (2020)

Table 4 Estimated absolute number of compact binaries in *globular clusters* in the Milky Way

Source	N	N^{detected}
WD+WD	$\sim 2 \times 10^4$	4–20
NS+WD	$\sim 10^3$	3–6
BH+WD	$\sim 10^2$	2–4
NS+NS	~ 40	1
BH+NS	~ 4	0
BH+BH	$\sim 2 \times 10^2$	4–7

The columns show the source type, the total number of binaries in the galaxy at any frequency and the total number of estimated sources detected by LISA assuming a frequency range of 10^{-5}–1 Hz and a mission lifetime of 4 years with a SNR ranging between 2 and 7 (Kremer et al. 2018a)

with electromagnetic observations, the observed GW signal scales as $1/d$, rather than $1/d^2$.

The GW frequency, defined as $f = 2/P$ with P being the binary's orbital period, has the strongest impact on the signal's detectability. Binaries emitting at $f > 3\,\text{mHz}$ fall in the most sensitive part of the LISA frequency band (Amaro-Seoane et al. 2017). As a result, these high-frequency binaries—even if consisting of the lowest-mass WD components—can be detected across the Milky Way also reaching satellite galaxies (cf. Figs. 1 and 15). At a set frequency, the maximum distance at which the binary can be detected increases with its chirp mass, as shown in Fig. 1. In addition, the chirp mass defines how fast the GW frequency changes during the in-spiral phase. This so-called chirp is given by

$$\dot{f} = \frac{96}{5} \pi^{8/3} \left(\frac{G\mathcal{M}}{c^3} \right)^{5/3} f^{11/3}. \tag{2}$$

The chirping rate for stellar binaries in the LISA band is generally very slow ($\dot{f} < 10^{-15}\,\text{Hz}^2$ for typical WD+WD and NS+NS binaries emitting at frequencies lower than a few mHz). Note that the frequency derivative (not the chirp mass) can be measured directly from GW data. The measurements is possible for binaries emitting at sufficiently large frequencies ($f > 3\,\text{mHz}$; Roebber et al. 2020), such that during the observation time (T) with LISA the binary sweeps through at least a few frequency bins ($1/T$) . If $\dot{f}$ is measured and assuming that the inspiral is driven by radiation reaction only, the luminosity distance can be recovered by plugging in the measured value of the chirp mass into Eq. (1). At lower frequencies, binaries will be effectively "seen" by LISA as monochromatic. In which case, only measurements of f and $\mathcal{A}$ will be possible, while the chirp mass estimate will be degenerate with that of the distance (cf. Eq. 1).

Unlike circular binaries, eccentric ones emit GWs at multiple harmonics. Each signal can be thought as a collection of n signals from circular binaries emitting at $f_n = nf/2$ and the amplitude $\mathcal{A}_n = \mathcal{A}(2/n)^{5/3} g(n, e)^{1/2}$, where $g(n, e)$ is given in Peters and Mathews (1963). The total signal-to-noise ratio can be estimated as the

quadrature sum of the individual harmonics' signal-to-noise ratios. Thus, to measure the chirp mass in case of the eccentric binary, in addition to $\dot{f}$, one needs to simultaneously measure the eccentricity. This is possible when at least two harmonics are detected (e.g. Seto 2016), otherwise only an upper limit on the chirp mass can be derived.

Another aspect of Galactic binaries' detectability is that they will be observed continuously during the course of the mission. However, it is likely that the measurements will undergo occasional interruptions due to communication antenna re-pointing or spacecraft housekeeping. Additionally, spurious disturbances may affect the interferometer signals, such as the transient glitches observed in LISA Pathfinder (Armano et al. 2022; Baghi et al. 2022), leading to corrupted data spans. These operating conditions may impact the duty cycle of the mission, with a minimum requirement of 89% at the time of writing. If the masking events are frequent, they could impact the detection of low-frequency sources (around 0.1 mHz and below). However, mitigation techniques have been developed and show promising results for restoring the optimal detectability (Baghi et al. 2019; Blelly et al. 2022).

1.4.2 Detection and parameter estimation expectations

It is expected that the Galactic stellar binaries will dominate the number of individually detected GW sources at mHz frequencies (Table 3). Out of $\sim \mathcal{O}(10^7)$ stellar binaries emitting in the LISA frequency band, LISA is expected to deliver $\sim \mathcal{O}(10^4)$ individual detections (e.g. Littenberg et al. 2020; Karnesis et al. 2021). Current estimates suggest that at frequencies >3 mHz, Galactic WD+WD detectable by LISA will be counted in thousands, NS+NSs in few up to hundreds and BH+BHs in a few (see Tables 3 and 4). At frequencies <3 mHz the number of stellar binaries is so large, that only a small fraction—the closest and more massive ones—will be individually detected, while the rest of the population will form an unresolved stochastic foreground (see Sect. 1.6.2).

Amongst the resolvable systems, population synthesis simulations suggest that hundreds will be exceptionally strong LISA sources (e.g. Karnesis et al. 2021). These binaries will be detectable within weeks from the start of mission operations, and over the full mission lifetime can accumulate SNRs up to 10^3. Based on an SNR evaluation via an iterative scheme for the estimate of the confusion foreground generated by Milky Way's GW sources (e.g. Littenberg et al. 2020; Karnesis et al. 2021), synthetic population analysis (e.g. Korol et al. 2017; Lamberts et al. 2019) yields about up to 10^4 binaries detectable with SNR > 20, several 10^3 with SNR > 100, a few with SNR > 1000. For all binaries, frequencies predicted be measured very accurately with $\sigma_\mathrm{f}/f < 10^{-5}$, which corresponds to $\sigma_\mathrm{P} < 0.025$ ms for a typical mHz WD+WD binary. Frequency derivative is estimated to be measured to better than 30% for up to 10^4 binaries, leading to the measurement of the chirp mass via Eq. (2). Consequently, also distances can be derived to better than 30% for several 10^3 binaries. The sky localisation uncertainty depends strongly on the SNR and GW frequency ($\propto \rho^{-2} f^{-2}$). Additionally, it is also dependent on the ecliptic

latitude: a source on the ecliptic has an order of magnitude more uncertainty than a source at the poles (Roebber et al. 2020). On average, sky localisation error for Galactic WD+WD systems is expected to be of several deg^2, improving with increasing GW frequency and SNR down to sub-square degree precision and below. These expectation are well supported by Bayesian-based data analysis exercises (Littenberg et al. 2020) with mock data simulating observations over 1 year, and including 30 millions of injected Galactic sources. Consolidation of these results are expected once more realistic data simulations featuring mixed source types are analysed (see https://lisa-ldc.lal.in2p3.fr).

Beyond the Milky Way, the Local Group galaxies are expected to harbour from a few to a few hundreds LISA sources (mainly WD+WDs and some NS+NSs) depending on the total mass and the distance of the galaxy (Seto 2019; Andrews et al. 2020; Korol et al. 2020; Lau et al. 2020) (see Fig. 1). For instance, the number of WD+WDs and NS+NS in the largest Milky Way satellites, the Large and Small Magellanic Clouds, will be high enough to overcome Galactic foreground and to unambiguously identify these galaxies in the LISA data (Roebber et al. 2020). Even further away, with the total mass comparable to the Milky Way's mass, the Andromeda galaxy could also be visible on the LISA sky as a group of GW sources (Korol et al. 2018).

The outside limits of the Local Group, LISA can access distances up to ~ 1 Gpc through GW signal from stellar-mass BH+BHs, which will ultimately be observable during merger to ground-based detectors (see Sect. 1.5.1). Studies based on cosmological simulations of galaxies at $z = 0$ find that the present-day dwarf galaxies can accommodate a larger BH+BH merger rate compared to massive galaxies (O'Shaughnessy et al. 2017). Specifically, for massive BH+BHs similar to GW150914, about 40% of mergers are expected to be in galaxy progenitors of Milky Way-like systems and the rest in smaller satellite or isolated dwarf galaxies (Marassi et al. 2019). This translates into a large number of potential hosts within the estimated LISA horizon distance. Not only BH+BHs formed from the evolution of isolated binaries, but also BH+BHs formed in extragalactic globular clusters may be detectable by LISA, with initial studies predicting the number of such sources to be in the range of 1–10^2 (Kremer et al. 2018a).

Given LISA's selection effects, extra-galactic LIGO-like BH+BH are expected to have quite low signal-to-noise ratios (~ 10). For this class of stellar binaries, Buscicchio et al. (2021) report sky localisation errors of a few tens of squared degrees and constrains on the detector-frame chirp mass down to $\pm 0.01\,M_\odot$. They also show that at 10 mHz the eccentricity for these binaries can be measured down to 10^{-3}, while the merger time can be determined within a time window of 1 h.

For sources that form through isolated binary evolution, the rates (such as those mentioned above and in Table 3) are often estimated with the population synthesis approach. There are many uncertainties that affect the rate calculations. These uncertainties can be divided in five broad categories: (i) binary evolution physics (e. g., CE evolution, mass transfer stability, mass-accretion efficiency, etc.), (ii) stellar evolution physics (e.g., metallicity dependent stellar winds, core-collapse mechanisms, natal kicks, pair-instability SN and pulsational pair instability, etc.), (iii) initial

stellar and binary properties (e.g., initial mass function, binary fraction, initial distribution of separation, mass ratio, eccentricity, etc.), (iv) different assumptions for the Galactic spacial distribution (thin/thick disc and bulge) and star-formation history and (v) LISA selection effects (e.g., GW foreground, mission length, sensitivity curve and SNR detection threshold).

As discussed in Sect. 1.3.2, LISA sources may also form dynamically in dense stellar environments such as globular clusters (and may have markedly different features compared to sources that form through isolated binary evolution, Sect. 1.3.1). In Table 4, we show the estimated number of sources expected to be found in globular clusters in a Milky Way-like galaxy (Kremer et al. 2018a). The number of detectable LISA BH+BHs originating from young massive clusters and open clusters is expected to be several tens to ~ 100 (or about 0.5–3 times the density of those clusters in the local volume in units of Mpc^{-3}; Banerjee 2020). Merger rate estimates for GW sources produced in dynamical environments from cluster simulations, can also be influenced by many uncertain physical processes, some of which are common to the ones outlined for sources formed via isolated binary evolution. For instance, natal kicks for compact objects have a direct impact on retention of those objects in stellar clusters (Morscher et al. 2013; Arca Sedda et al. 2018; Webb et al. 2018; Pavlík et al. 2018; Banerjee et al. 2020) which influences the number of dynamically formed binary systems. The number of compact objects that form in dense environments also depends on their metallicity and the initial mass function of their stars which may vary with their formation environment (Dabringhausen et al. 2009; Geha et al. 2013; Krumholz 2014; Chruślińska et al. 2020). Additionally, dissolved or tidally disrupted open and globular clusters can also contribute to the number of GW sources that may have dynamically formed (Muratov and Gnedin 2010; Fragione et al. 2018; Giersz et al. 2019).

Apart from population synthesis-like simulations, another approach to predict the expected LISA rates is to derive empirical estimates from the already observed population of sources. For NS+NSs for instance, one can use the inferred merger rate coming from the known Galactic NS+NS population, and accounting for survey selection effects (Phinney 1991; Kim et al. 2003), or the inferred merger rate from LIGO–Virgo (Abbott et al. 2021b), to predict that LISA should be able to detect 50–300 NS+NSs in the Milky Way (Andrews et al. 2020). In a similar manner, based on O1 LIGO–Virgo detections, it was estimated that LISA maybe able to detect up to ~ 50 BH+BHs (Sesana 2016), but the inferred BH+BH merger rate density decreased in the most recent O3 run by a factor of ~ 2. Empirical estimates of the Galactic NS+WD population have been derived, based on the observed pulsar population, with 100–150 being predicted to be observable by LISA (Tauris 2018).

1.5 Synergies

1.5.1 Synergies with EM observations

Coordinators: **Thomas Kupfer**

Contributors: **Thomas Kupfer, John Tomsick, Nicole Lloyd-Ronning, John Quenby, Thomas Tauris, Thomas J. Maccarone**

Many new verification binaries are expected to be discovered before the launch of LISA, in particular with wide-field optical surveys such as ZTF, BlackGEM and LSST on the Rubin Observatory. Once flying, LISA will be complemented with surveys across different frequency bands (radio to gamma-rays). New sources discovered by LISA can be studied with the next generation of follow-up facilities such as ESO/ELT, CTA, SKA, ngVLA or even Athena as well as smaller space missions which could be approved, built and launched in the early 2030s (eXTP or STROBE-X). This provides a plethora of large-scale follow-up resources for detailed multi-messenger studies but it requires a well planned follow-up strategy to generate the most useful results.

The large number of facilities running in the 2020s and 2030s will provide a bright future for the research on compact Galactic binaries, with hundreds of additional EM discovered systems ready to be studied in detail through EM+GW observations as soon as LISA is operational. A significant sample of binaries, observed with EM+GW observations, will open up possibilities to explore and study astrophysical phenomena which are crucial to our understanding of the Universe. This includes the long-standing questions of the progenitors of SNe Ia, the formation and evolution of compact objects in binaries and accretion physics under extreme conditions.

1.5.1.1 UV/Optical/IR observations   Previous studies predict that we will be able to observe several thousand Galactic binaries in both GW and optical emission (Littenberg et al. 2013; Korol et al. 2017). A subset of the known UCBs have orbital periods that lie in the LISA band and these will be individually detected by LISA due to their strong GW signals, some on a timescale of weeks or a few months. Combined GW and EM multi-messenger studies of UCBs will allow us to derive population properties of these systems such as masses, radii, orbital separations, and inclination angles but in many cases EM observations are required to complement GWs and break degeneracies in the GW data. Shah et al. (2012), Shah et al. (2013), Shah and Nelemans (2014b) and Kupfer et al. (2018) present several studies on how EM observations can complement LISA GW data and vice versa. The GW amplitude and inclination is strongly correlated, but the GW amplitude can be improved by a factor of six when including EM constraints on the inclination and the sky position and inclination can reduce the uncertainty in amplitude by up to a factor of 60 (Shah and Nelemans 2014b).

Additionally, knowing the distance from EM, e.g., from parallaxes measured by Gaia, will help to derive a chirp mass from GWs even for non-chirping sources because for many LISA sources only the frequency and amplitude will be measured. This leaves a degeneracy between chirp mass and distance and inclination, since a more massive binary further away can have the same amplitude as a lower mass one that is closer by and inclined systems closer by look like face on systems further away (Shah et al. 2012; Shah and Nelemans 2014a).

If the chirp mass has been measured from GWs using, e.g., Gaia parallaxes and the mass ratio has been measured from EM, through radial velocities or ellipsoidal
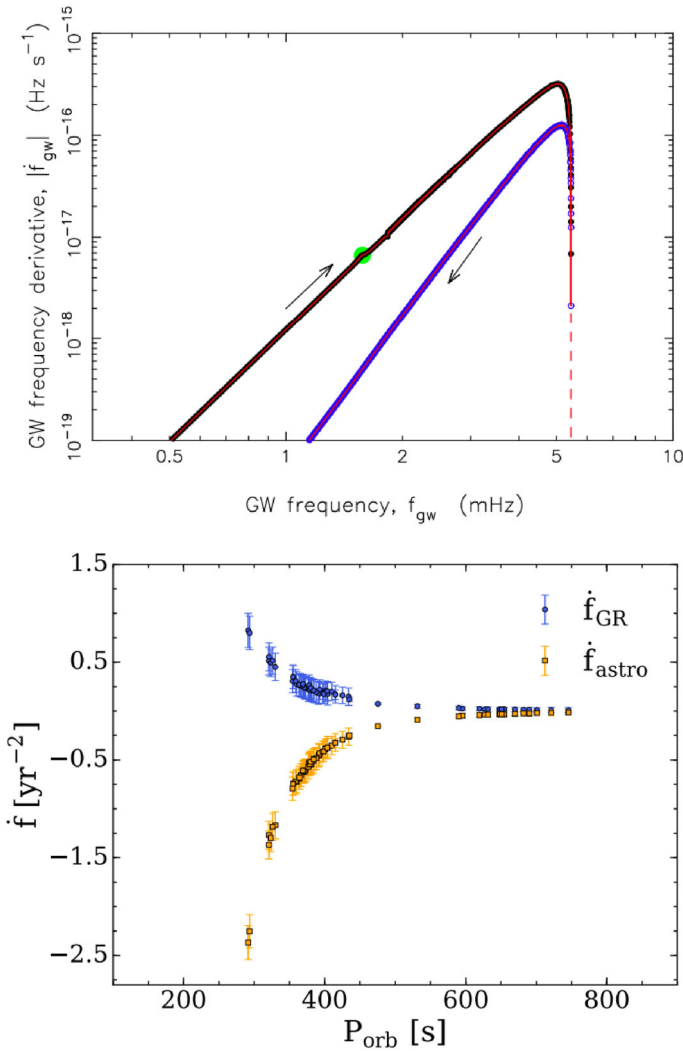
Fig. 12 Upper panel: GW frequency derivative, $|\dot{f}_{GW}|$ as a function of GW frequency, f_{GW} for the UCXB shown in Figs. 4 and 5. The black coloured points correspond to the inbound leg (orbital shrinking) and the blue points correspond to the outbound leg (orbital expansion, after reaching the orbital period minimum) including mass transfer/loss from the system and finite-temperature effects of the WD donor. Each point represents a binary stellar MESA model. The green solid circle indicates the onset of the UCXB stage. (Before this point, the system is a detached NS+WD binary). Bottom panel: pure general relativistic (GR, blue) and astrophysical (orange) chirps as a function of GW frequency for WD+WD (AM CVn) systems. The astrophysical contribution from mass transfer and tides leads to a significant deviation from the contribution from GR alone and will cause the systems to widen their orbit upon mass transfer. The decoupling of the astrophysical chirp from the GR chirp will be possible with *combined measurements* from LISA and Gaia. The error bars show the anticipated 1σ measurement errors. On average, Breivik et al. (2018) find that about 50 AM CVn systems in the Mikly Way with $P_{orb} < 800$ s have resolvable GR and astrophysically driven chirps. Images reproduced with permission from [top] Tauris (2018), copyright by APS; and [bottom] Breivik et al. (2018), copyright by AAS

deformation of one component, both measurements can be combined to the measure the masses of both components with a few percent precision. Comparing the measured orbital decay with the predicted orbital decay from general relativity will allow us to measure the effects of tides compared to GWs. Tides are predicted to contribute up to 10% of the orbital decay (Piro 2011) but has not been measured so far and is very difficult with GW and EM alone. Some of the known AM CVn and detached WD+WD binaries have well constrained distances from Gaia (Kupfer et al. 2018; Ramsay et al. 2018). Measuring the distance from EM constrains the uncertainty in chirp mass to 20%, whereas adding the period derivative $\dot{P}$ reduces it to 0.1% (see e.g. Fig. 12). A GW chirp mass measurement would provide the first detection of tidal heating in a merging pair of WDs from the deviations in predicted $\dot{P}$ (Shah and Nelemans 2014b). With a large enough sample of WD+WD binaries whose chirp masses can be determined, we can plausibly extract constraining information about CE phase evolution physics. In studying massive WD+WD binaries that are likely progenitors of merger-induced collapse NSs (Ruiter et al. 2019), chirp mass distributions had different shapes depending on the adopted CE phase prescription in the binary evolution population synthesis model.

Several studies have shown that spectral and photometric analysis of detached WD+WD can provide precise sky positions, orbital periods and in some cases mass ratios, inclinations, and the rate of orbital period decay (e.g. Maxted et al. 2002; Brown et al. 2011; Hermes et al. 2012; Burdge et al. 2019a). All of the known verification binaries have precise sky positions and orbital periods and five systems have a measured orbital decay from photometric monitoring (Kupfer et al. 2018). SDSSJ0651, a 12 min orbital period detached WD+WD (Brown et al. 2011), and ZTFJ1539, a 7 min orbital period detached WD+WD (Burdge et al. 2019a), are prime example of what can be accomplished. Using only 1 year of eclipse timing measurements, Hermes et al. (2012) found an orbital decay of $\dot{P} = (-9.8 \pm 2.8) \times 10^{-12}$ s s^{-1} in SDSSJ0651 which has not been updated since then. Burdge et al. (2019a) used photometric data from PTF/iPTF and ZTF covering a total of 10 years and measured a very precise orbital decay of $\dot{P} = (-2.373 \pm 0.005) \times 10^{-11}$ s s^{-1}. However, neither of the two systems has a precision of WD component masses good enough from optical observations to see if their $\dot{P}$ differs from the predictions of the theory of General Relativity (GR). GW observations can solve that. Tidal theory predicts a 10% deviation from GR if the WDs are tidally heating up. Which means that combining EM+GW observations from LISA will allow a measurement of the amount of tidal heating in these merging pairs of WDs for the first time.

Combined EM+GW observations of the Galactic WD+WD population will help to solve another major problem in astrophysics: the SNe Ia progenitor problem. Although only the thermonuclear explosion of a WD following the interaction with a binary companion can explain the observed features in the SN light, much less is known about their progenitors. Recent results have shown that SN Iae show a large range of explosion energies and decay times, photometric and spectroscopic signatures indicating different progenitor systems (Jha et al. 2019). Several different explosion scenarios are under discussion, including the merger and subsequent

explosion of an ultra-compact WD+WD system (double-degenerate model) or the explosion triggered by ignition of an helium shell accreted from a helium star in a UCB (double-detonation scenario). However, the number of known progenitor systems is limited. Rebassa-Mansergas et al. (2019) studied the probability of finding WD+WD progenitors of SNe Ia using a binary population synthesis approach, and found that the chance of identifying such progenitors purely in EM data is $\sim 10^{-5}$. These include both double-lined spectroscopic binaries and the eclipsing systems. Even with the next generation of 30-m class telescopes, the probability for detection only goes up by a factor of ~ 10. Korol et al. (2017) predicts that LISA will individually resolve $\sim 25,000$ detached WD+WD systems including the most massive systems. EM follow-up observations in combination with GW measurements will allow us to measure masses of individual systems and find and characterize the population of double degenerate SN Ia progenitors.

Kilonovae (see Metzger 2019) are optical/IR emission accompanying the merger of NS+NS, possibly NS+BH, and in special cases, WD+WD mergers (Rueda et al. 2019). Although LISA is not sensitive to the actual merger that can produce a kilonova, it is sensitive to the GW emission from their progenitors. Therefore it is worthwhile to consider kilonova events in the nearby universe because they allow constraints on these degenerate stellar populations.

1.5.1.2 X-ray observations Many of the LISA sources also emit X-rays, thus allowing for a number of joint LISA + X-ray investigations. The donor stars in UCXBs appear to be a mixture of C/O-core and He-core WDs and abundance measurements can help identify their formation scenario (Nelemans et al. 2010). In the oxygen-rich systems, oxygen is the dominant coolant in the accretion discs, and the iron emission lines are suppressed; the strength of the iron lines is broadly in agreement with the thermonuclear burst properties of the sources, strengthening the case that this donor classification process works reasonably well even in its simplest form (Koliopanos et al. 2020). However, in some cases, the abundances of the WD inferred from X-ray data are at odds with those inferred from Type I burst properties. In a few cases, the inference has been made from neon-to-oxygen rations (Juett et al. 2001), and for this scenario, it has been shown that there is a channel of binary evolution that allows a He-core WD to have such neon-to-oxygen ratios (in't Zand et al. 2005). Alternatively, Bildsten et al. (1992) show that spallation of CNO elements in a NS atmosphere is quite likely. The combination of LISA measurements with X-ray (and optical) abundance measurements thus opens a window to determining which of these scenarios is correct. If the apparent C/O-core WD donors are paired with high mass NSs, then the spallation scenario is strongly preferred.

More detailed X-ray spectroscopy should potentially be able to make detailed abundance estimates for the donor stars, allowing, e.g., identification of systems in which the CNO processing may not have gone to completion, and perhaps estimating the time of formation through estimates of the abundances of non-CNO elements,

---

[3] Most imaging X-ray telescopes will not be able to make such measurements because of pile-up or deadtime issues.

which could yield the initial metallicity of the star. The X-ray measurements are essential given that a large fraction of the UCXBs are located in globular clusters, or deep in the Galactic Plane where ultraviolet and optical spectroscopy are more challenging. Substantive work has also been done in the optical wavebands (see e.g. Nelemans et al. 2004a, 2006). Furthermore, when combined with LISA data the UCBs then may provide a means of testing how conservative accretion onto NSs is; C/O-core WD donors must start at masses of at least $\approx 0.5 M_\odot$, but are generally observed with masses of $0.1 M_\odot$ or less. If the early stages of mass transfer in these systems are conservative, the NSs should typically be about $1.8 M_\odot$, while if they show much lower masses, this implies that the mass transfer was strongly non-conservative.

Additionally, for 4U 1820−30, X-ray measurements provide a straightforward way to monitor the source's period derivative (Tan et al. 1991), as the source is deep in the potential well of a globular cluster whose gravitational acceleration leads to its negative period derivative. It is easy to track the source's orbital period in the X-ray band (Stella et al. 1987; Tan et al. 1991), and hard in other bands, due to the crowding in the cluster. With more intensive X-ray data, the period derivative of 47 Tuc X-9, the best candidate BH+WD binary in the Milky Way (Bahramian et al. 2017), could be tracked. Imposing these constraints, which are likely to lie outside the range of normal templates, can help improve the quality of the LISA GW detection. Globular clusters are likely good hosts for LISA sources, but the globular cluster sources' periods have come from ultraviolet photometry (Dieball et al. 2005; Zurek et al. 2009) and the best non-cluster source's period comes from optical spectroscopy (Madej et al. 2013). Additional intensive monitoring campaigns would be required for the period derivative to be estimated.

For the AM CVn systems, X-ray emission is also valuable. The same abundance issues can be studied in the X-ray band in AM CVn systems, although primarily from the emission lines from the boundary layer of the accretor, rather than disc reflection. Relatively short period AM CVn systems will be detectable to large distances, where reddening may be important, and in these cases, restricting the set of sources to those which are in a reasonable range of fluxes. For the faintest AM CVn sources with periods less than half an hour, the X-ray luminosities are typically about 10^{31} erg s^{-1} (e.g. Nelemans et al. 2004b; Strohmayer 2004; Ramsay et al. 2005, 2006; Zurek et al. 2016), meaning that eROSITA should detect them to distances of about 3 kpc. Combining with radio surveys to remove background Active Galactic Nuclei (AGN), and optical surveys to remove foreground stars and CVs should then yield a much more manageable list of candidates for high time resolution optical follow-up (which usually has limited fields of view) than without the X-ray data and potentially add more LISA verification sources.

X-rays are also likely to provide the best EM distance estimators for many of these UCXBs (see Fig. 8) complementing LISA data. Some are located in globular clusters, where the cluster distance can be used. None of the Galactic field UCXBs is bright enough for Gaia in the optical, and most are also too faint for radio parallaxes with current facilities. Thermonuclear bursts with radius expansion can be used to estimate the Eddington luminosities (Kuulkers et al. 2003), and these can then be

used in conjunction with the GW estimates of the masses to establish self-consistent properties for the sources. For the persistent sources that burst in an appropriate manner, these data are already in hand, but obtaining such data for transients would require instruments with large collecting area and small deadtime (e.g., NICER, STROBE-X, eXTP Gendreau et al. 2016; Ray et al. 2019; Zhang et al. 2019).[3] The other approach that can be used to estimate distances is that of dust-scattering halos (Trümper and Schönfelder 1973), something that requires good angular resolution, good collecting area, and the ability to observe bright sources; while Chandra has done some work in this area, Athena should be able to help dramatically (Corrales et al. 2019).

Some UCXBs may contain BHs as well. The first strong globular cluster BH candidate (Maccarone et al. 2007) in NGC 4472 is an ultracompact system (Zepf et al. 2008), probably with an orbital period near 5 min, and 47 Tuc X-9 (Miller-Jones et al. 2015; Bahramian et al. 2017) is also a strong candidate ultracompact BH X-ray binary. At the shortest orbital periods, BH+WD binaries should be detectable by LISA to distances of a few megaparsecs. For these cases, imaging X-ray data would be needed, along with follow-up optical spectroscopy to look for [O III] nebulae as well as hydrogen emission similar to that in the globular cluster RZ 2109 in NGC 4472 (Zepf et al. 2008; Steele et al. 2014; Dage et al. 2019). In the Milky Way, UCXBs with BH accretors at relatively long orbital periods could be quite faint X-ray sources in quiescence (being considerably fainter than accreting NSs at the same mass transfer rate due to advection dominated accretion, Narayan and Yi 1994). They could also exhibit only rare outbursts, meaning that sensitive X-ray observations would be needed to detect their counterparts. Furthermore, these objects may be preferentially in globular clusters, meaning that excellent angular resolution, from Chandra or a Chandra successor mission like Lynx or AXIS would be needed to find their counterparts. If some new BH UCXBs are discovered with X-ray outbursts, they may become bright enough to make BH spin estimates using reflection and/or disc continuum modelling.

For most of the topics related to accretion, there is a need for developing better spectral models that treat unusual abundances. Development of reflection models that include both the reflection from the surface of the WD, and discs made from hydrogen-poor material is thus vital. It has already been found that details of how atomic physics is incorporated into the disc models can affect inferred spins and abundances (García et al. 2016; Tomsick et al. 2018).

X-ray observations are also vital for understanding the detached systems with NS members. In most of these systems, the older NS will have experienced significant spin-up, and will be a millisecond pulsar. Pulsar beam opening angles are larger at high energy than at radio wavelengths (a phenomenon exhibited by objects like Geminga (Halpern and Holt 1992) and many of the Fermi-discovered pulsars), meaning that some fraction of these objects will be radio-quiet pulsars (Marelli et al. 2015). X-ray observations will then provide the most comprehensive means for estimating the spins of these systems and determining what fraction of them have become recycled. Furthermore, in combination with radio searches for pulsations, having a gravitationally-selected sample will allow a clean determination of the ratio of pulsars with radio and X-ray emission, allowing an important constraint for

developing a full picture of the pulsar beam geometry. In an ideal case we may identify an object with thermal cap emission from the NS, such that pulse-profile measurement and modelling could be done to estimate its radius. If this comes in conjunction with sufficiently good LISA GW measurements to provide an independent, precise, estimate of the NS's mass, this would give a constraint on the equation of state for NSs, even from a single object (Watts 2019).

1.5.1.3 Radio observations   The synergies from joint, multi-messenger observations of radio pulsar binaries entering the LISA band are very promising and will provide significantly more information than observations in the EM or GW bands alone (see Fig. 8). Such benefits include better measuring the orbital inclination angle (Shah et al. 2012) and sky position (Shah et al. 2013) and potentially even constraining the NS mass-radius relation to within $\sim 0.2\%$ (Thrane et al. 2020). Additionally, radio astrometry can give parallax distances out to a few kpc already, and with ngVLA (Murphy et al. 2018), that should increase dramatically. Most LISA sources would be nearby enough that with ngVLA, one would be able to get 10% or better geometric parallaxes over about 3/4 of the sky.

Binary NSs in NS+NS and NS+WD systems enter the LISA band at a GW frequencey of order 1 mHz (depending on their distance), corresponding to orbital periods of about 30 min. Doppler smearing of radio pulsations from pulsars in such tight binary orbits (Eatough et al. 2013) could cause a selection bias against detection of e.g., rapidly spinning millisecond radio pulsars in many previous and present day acceleration searches (at least for dispersion measures, $< 100\,\mathrm{cm}^{-3}$ pc). However, using neural networks, Pol et al. (2021) develop accurate modelling of the observed binary pulsar population and argue for a ~ 50–80% chance of detecting at least one of these systems with $P_{orb} \leq 15$ min using data from surveys with the Arecibo radio telescope, and ~ 80–95% using optimal integration times of ~ 50 s in the next several years. The chances of a radio detection of a binary pulsar in the LISA GW band is expected to be significantly enhanced by the completion of the Square Kilometre Array (Keane et al. 2015).

It has been argued (Pol et al. 2021) that unequal mass NS+WD systems are easier to detect compared to the usually near-equal mass NS+NS systems. It should be kept in mind that RLO from these (often bloated) WD companions begins when P_{orb} has decreased to $25 - 15$ min, depending on their temperature (Tauris 2018) (see also Figs. 4 and 5). This will exclude radio detection of such pulsar binaries once accreted plasma enters the NS magnetosphere.

1.5.1.4 Particle observations   For high-frequency GW detections, there are prospects for detection of neutrino's or cosmic rays, from jets produced in mergers or from supernovae (Adrián-Martínez et al. 2016). For LISA, the prospects are not so clear, even though associations of LISA GW sources with AGN jets and tidal disruption events could be possible.

1.5.2 Synergies with other GW detectors

Coordinators: **Lijing Shao; Paul Groot**

Contributors: **Ilya Mandel (1.5.2.1), Alberto Sesana, Emanuele Berti, Lijing Shao (1.5.2.4), Davide Gerosa (1.5.2.1), Pau Amaro Seoane, Paul Groot, Thomas Tauris (1.5.2.2), Valeriya Korol (1.5.2.3)**

1.5.2.1 High-frequency GW merger precursors seen by LISA LISA has a unique capability of covering the full frequency spectrum for stellar-mass binary BHs and NSs when combined with the higher-frequency ground-based GW detectors advanced LIGO (Aasi et al. 2015) and Virgo (Acernese et al. 2015), and their third generation successors such as the proposed Einstein Telescope (Punturo et al. 2010) and Cosmic Explorer (Abbott et al. 2017a).

Some individual sources can be tracked on human timescales from the LISA band to the $\gtrsim$ few Hz ground-based detector sensitive frequency band (Sesana 2016). The GW driven merger timescale for a circular binary with components of equal mass m from a starting frequency f is (Peters 1964a)

$$\tau_{\rm GW} \simeq 5 \left(\frac{f}{0.01 \; {\rm Hz}} \right)^{-8/3} \left(\frac{m}{68 \; M_\odot} \right)^{-8/3} \; {\rm year}. \qquad (3)$$

Thus, a signal like GW190521 (Abbott et al. 2020c) could be tracked from 10 mHz to merger across the the full range of frequencies with the combination of LISA and ground-based detectors. Rate estimates have been presented by Shannon et al. (2015), Kyutoku and Seto (2016), Sesana (2016, 2017), Gerosa et al. (2019) and Moore et al. (2019), with predictions ranging from 0 to roughly a dozen detections during the LISA mission.

The high mass and correspondingly rapid orbital evolution of IMBHs with masses in the 100–1000 $M_\odot$ range makes them particularly appealing targets for tracking across the LISA and ground-based detector frequency bands. IMBHs with these masses are a challenge for EM observations: their dynamical signature is relatively insignificant, while their X-ray emission can be confused with that of super-Eddington accretors (e.g., Miller and Colbert 2004; Feng and Soria 2011; Greene et al. 2020). On the other hand, IMBH mergers have been proposed in the context of both isolated binary evolution of very massive stars (Belczynski et al. 2014) and globular cluster dynamics (Amaro-Seoane and Freitag 2006). The latter can also be responsible for intermediate-mass ratio inspirals of stellar-mass compact objects into IMBHs (Mandel et al. 2008; Haster et al. 2016a). Meanwhile, hierarchical mergers of few-hundred $M_\odot$ seeds have been proposed as seeds of today's massive BHs (Volonteri et al. 2003a, see Sect. 2). Joint observations with LISA and third-generation ground-based detectors (Sesana et al. 2011a; Gair et al. 2011) would provide the perfect tools for studying these elusive IMBHs.

Observations of the same individual source across a broad range of frequencies can improve the accuracy of source parameter measurement. Some parameters are

likely to be best measured at low frequencies. For example, sky localisation accuracy depends on timing precision (Fairhurst 2009; Wen and Chen 2010; Grover et al. 2014). The sky localization accuracy can be estimated as the timing accuracy divided by the light travel time across the detector baseline (Mandel et al. 2018), which is $\sim$ astronomical unit (AU) for LISA, yielding a relative position error of:

$$\sigma_\theta \sim 0.025 \left(\frac{0.01 \text{ Hz}}{f} \right) \left(\frac{8}{\rho} \right), \tag{4}$$

where ρ is the detection signal-to-noise ratio. For heavier sources that can evolve faster than the LISA observing duration, the LISA frequency bandwidth $f_{\text{bandwidth}}$ should be used in place of f. The angular resolution scales inversely with baseline. Therefore, despite the lower observing frequency (lower bandwidth), for high SNR sources, LISA sky localisation is likely to be superior to the capabilities of ground-based detectors, whose baseline, even in a network, is limited by the size of the Earth (unless the signal is sufficiently long-lived to allow the effective baseline to be extended by the detector motion over the duration of the observation).

On the other hand, some source parameters will be better measured at higher frequencies, allowing ground-based detectors to provide complementary information to LISA observations. These include measurements of the ringdown of the post-merger BH, which yield the final mass and spin, and the tidal effects for NSs.

Yet other measurements could benefit from the joint constraints placed by low-frequency and high-frequency observations. These include measurements of spin magnitudes and spin-orbit misalignment angles, which could carry information about formation scenarios (e.g., Gerosa et al. 2013; Vitale et al. 2017; Stevenson et al. 2017a; Zevin et al. 2017; Farr et al. 2017; Gerosa et al. 2018a). Spin-orbit and spin-spin coupling enter the waveform at higher post-Newtonian orders in an expansion in the orbital frequency (Poisson and Will 1995), and so may be better measured at higher frequencies by ground-based detectors. On the other hand, massive binaries like GW190521 may spend a million cycles in the LISA band (only 4 cycles were observed in the LIGO band when this signal was detected in 2019; Abbott et al. 2020c). Further analysis is necessary to explore the quantitative benefits of LISA for parameter estimation of such signals (but see e.g. Vitale 2016; Moore et al. 2019; Mangiagli et al. 2019; Cutler et al. 2019)

Lower-mass GW sources such as double NSs (Lau et al. 2020; Andrews et al. 2020) will not be individually trackable on a human timescale from the LISA band to the band of ground-based detectors. However, they may still benefit from tracking the entire population of sources as the sources evolve from the LISA frequency band to the frequency band of ground-based detectors. For example, binaries circularise through GW emission (very roughly, the eccentricity scales inversely with the increase in frequency), making eccentricity challenging to observe with ground-based detectors (e.g., Romero-Shaw et al. 2019; Lenon et al. 2020). Thus, LISA observations at lower frequencies, where eccentricities are still significant, could help to distinguish compact binary formation scenarios (Breivik et al. 2016; Nishizawa et al. 2016, 2017).

This can be further aided by the detection of a stochastic background from a superposition of GWs emitted by multiple individually unresolvable binaries (see Sect. 1.2.2.6). For circular binaries, the stochastic background should be a simple power-law in frequency, and any deviations from that could indicate the emergence of new binaries, particularly eccentric binaries, at high frequencies. Moreover, the combined low-frequency and high-frequency stochastic background observations may make it easier to subtract the astrophysical background and reveal a possible GW background of cosmological origin (e.g. Mandic et al. 2012; Lasky et al. 2016; Callister et al. 2016).

LISA precursors to ground-based detector mergers could also have important repercussions in fundamental physics, allowing stringent tests of the BH no-hair theorems, as well as more stringent bounds on low-Post-Newtonian deviations from GR (Toubiana et al. 2020; Barausse et al. 2016; Tso et al. 2019; Gnocchi et al. 2019; Carson and Yagi 2020; Shao et al. 2017).

1.5.2.2 Dual-line GW sources   A possibility in upcoming GW astronomy will be the potential discovery of a *dual-line* Galactic GW source (Tauris 2018), where ground-based detectors detect the continuous high-frequency GW emission from the rapid spinning (recycled) NS (Andersson 2019) and LISA simultaneously detects the gravitational damping of the system's orbital motion via continuous low-frequency GW emission. Such a system could very well be a UCXB (e.g. van Haaften et al. 2012; Heinke et al. 2013). Combining the expressions for the strain amplitudes of the ground-based and LISA observations (h_{spin} and h_{orb} respectively) yields (Tauris 2018):

$$I_{zz}\,\varepsilon = \sqrt{\frac{2}{5}} \left(\frac{\sqrt{G}}{2\pi}\right)^{4/3} \left(\frac{f_{\mathrm{orb}}^{1/3}}{f_{\mathrm{spin}}}\right)^2 \mathcal{M}^{5/3} \left(\frac{h_{\mathrm{spin}}}{h_{\mathrm{orb}}}\right). \tag{5}$$

Once the right-hand-side of this equation is determined observationally, and assuming that the NS mass, M_{NS} can be determined from the chirp mass, $\mathcal{M}$ (see required assumptions on component mass determinations in Tauris 2018), constraints can be made on the NS moment of inertia, I_{zz}, and thus the NS radius (Ravenhall and Pethick 1994). Suvorov (2021) recently examined the dual-line detectability of tight Galactic binaries, and found that at least two of the known systems (4U 1820-30 and 4U 1728-34) may be visible to both ground-based and space-based instruments simultaneously. Although only measuring the moment of inertia in combination with the ellipticity, ε, it will still help in pinning down the long sought-after equation of state (EOS) of NS matter. The maximum spin rate and ε for accreting NSs (Andersson 2019) remain to be constrained firmly.

1.5.2.3 TianQin   TianQin is a space-based GW observatory conceived as an equilateral triangle constellation of three drag-free satellites with frequency sensitivity at 10^{-3}–10^{-1} Hz (Luo et al. 2016), between LISA and DECIGO. Unlike LISA, TianQin will follow a geocentric orbit with a radius of about 10^5 km (Hu et al. 2018; Ye et al. 2019). Its constellation plane will be nearly perpendicular to the

ecliptic plane and will have a fix orientation pointing toward RX J0806.3+1527 (Strohmayer 2005), a 5-min orbital period Galactic binary that is expected to be the strongest GW source among currently known systems (Kupfer et al. 2018). Planned for the launch around 2035, TinQin will see the same GW sources as LISA (Mei et al. 2020). Consequently, many synergies can be envisioned between the two missions. For instance, TianQin and LISA will simultaneously detect several thousand Galactic WD+WD binaries, which will improve the parameters estimation including the amplitude, inclination and sky localisation for these binaries (Huang et al. 2020).

1.5.2.4 Mid-band observatories, e.g., DECIGO   After the discovery of GW150914 (Abbott et al. 2016c), it was realized that massive stellar-mass BHs will be detectable in both LISA and LIGO/Virgo bands (Sesana 2016; Amaro-Seoane and Santamaría 2010). However, the SNRs are not expected to be large in the mHz band, and because of the use of template bank searching, in order to claim a confident detection, BH+BH signals in LISA require a larger SNR threshold than 15 (Moore et al. 2019). Fortunately, these sources will have large SNRs if they are seen in the decihertz band (Isoyama et al. 2018; Arca Sedda et al. 2020a; Liu et al. 2020). DECihertz laser Interferometer Gravitational wave Observatory (DECIGO) is a representative GW detector in the relevant frequency band (Yagi and Seto 2011; Kawamura et al. 2011, 2020). Studies showed that, not only will observations in the decihertz band provide profound insights to astrophysics (see Arca Sedda et al. 2020a, for a comprehensive discussion), they will also provide unprecedented playgrounds for fundamental physics (e.g., testing the dipolar radiation (Barausse et al. 2016; Liu et al. 2020). The mid-band observations of decihertz frequency are natural means to bridge the gap between LISA and LIGO/Virgo observatories.

1.6 Technical aspects

Coordinators: **Irina Dvorkin**

Contributors: **Emanuele Berti, Sylvain Chaty, Astrid Lamberts, Alberto Sesana, Kinwah Wu (1.6.3), Shenghua Yu, Shane Larson, Irina Dvorkin (1.6.1, 1.6.3, 1.6.5), Kinwah Wu already cited above, Pau Amaro Seoane, Giuseppe Lodato, Xian Chen, Valeriya Korol (1.6.2), Silvia Toonen (1.6.5)**

1.6.1 How to distinguish between different compact binaries?

One of the outstanding challenges of LISA will be to analyze a datastream that consists of multiple overlapping signals from astrophysical and possibly cosmological sources as well as instrumental noise. Since many LISA sources will remain in band for multiple orbits, from several days or months up to the entire duration of the mission, there will be an overlap between multiple sources in any given data stretch. Data analysis techniques suitable for this unique problem are currently under development, including in the context of the LISA Data Challenge (Babak et al.

2010; Cornish and Shuman 2020; Littenberg et al. 2020). A standard procedure that allows us to extract WD+WD signals from a noisy datastream uses waveform templates that span a large parameter space (Owen 1996). The most studied case (and the only class detected so far by LIGO-Virgo) is that of isolated compact binaries (see Sect. 1.2.2), which are characterized by the component masses, the distance to the binary, its position on the sky and the orbital eccentricity, as well as the orbital frequency. Contrary to the case of ground-based interferometers, these binaries are long-lived LISA sources. In other words their orbital evolution timescale due to the emission of GW is very slow compared to the mission duration. This will allow us to collect data from many cycles of each binary, increasing the SNR, but also puts stringent requirements on the accuracy of the template waveform. The waveform of quasi-monochromatic sources, such as WD+WD binaries, is relatively simple and can be quite accurately described by the leading order terms in the orbital dynamics (Littenberg et al. 2020). On the other hand, binaries that evolve in the LISA band (such as BH+BH) require a more detailed computation to higher Post-Newtonian order (Mangiagli et al. 2019). Accurate waveform templates are crucial for measuring the source parameters and distinguishing between various source classes since any error in the predicted phase of the template waveform will accumulate over the many cycles the binary stays in band.

The main parameter that can help to distinguish the different classes of isolated compact binaries is the chirp mass of the system. In order to establish the class of a quasi-monochromatic source one may use the fact that the chirp mass distribution of WD+WD binaries peaks around $\simeq 0.25\,M_\odot$ (Korol et al. 2017) with the tail up to $1\,M_\odot$, while the chirp mass of NS+NS systems is expected to lie around $\simeq 1.2\,M_\odot$. BH+NS and BH+BH systems will have higher chirp masses. However, high-mass WD+WD systems at the tail of the distribution with chirp masses of up to $\simeq 1.2\,M_\odot$ may be confused for a NS+NS or a NS+WD binary. Similarly, BH+NS binaries may be confused with NS+NS if the NS has an extremely high mass, or the BH has an extremely low mass. Indeed, the discovery by LIGO-Virgo of GW190814, a binary consisting of a $23\,M_\odot$ BH and a $2.6\,M_\odot$ compact object (Abbott et al. 2020b) is very difficult to interpret: the secondary component is either the lightest BH or the heaviest NS discovered to date.

Additional clues as to the identity of the source are somewhat model-dependent, although priors from copious ground-based observations will help with NS+NS, NS+BH, BH+BH scale events. Thus, it may be possible to use eccentricity measurements to distinguish between WD+WDs and NS+NSs (Lau et al. 2020). Since WD+WDs are expected to have formed via isolated binary evolution, their progenitors are expected to have circularised via multiple mass transfer episodes (see Sect. 1.3.1.1). This assumption is supported by the lack of observed eccentric galactic WD+WD binaries. On the other hand, NS+NSs in the LISA band could have measurable eccentricities: e.g. in the fiducial model by Lau et al. (2020) half of LISA NS+NS sources have eccentricities $e > 0.1$. Thus, a detection of an eccentric source with chirp mass of around $\simeq 1.2\,M_\odot$ can be interpreted as a likely NS+NS. Nevertheless, some rare eccentric WD+WD can be produced in globular clusters of the Milky Way, or via triple interactions (e.g. Kremer et al. 2018a).

The case of interacting binaries (see Sect. 1.2.3) is potentially even more complex, since their orbital evolution is influenced not only by gravity, but also mass transfer and magnetic braking, which lead to qualitatively different waveforms (such as anti-chirping phases) depending on the evolution stage of the binary (e.g. Kremer et al. 2017; Tauris 2018). For example, as discussed in Sects. 1.2.3.1 and 1.2.3.2, AM CVns and UCXBs can be detectable by LISA either during their inspiral phase (when the binary components are detached and the orbits shrinks) or during mass transfer (when the orbit expands). The upside of this complexity is that anti-chirping signals are easier to distinguish from isolated compact binaries.

Clearly, an EM counterpart to a GW detection will help to identify the source. Indeed, as discussed in Sect. 1.5.1, EM observations can help in distinguishing between interacting and isolated sources, as well as identifying NS+NS or BH+NS binaries. For the technical aspects of EM synergies, see Sect. 1.5.1.

1.6.2 Foreground sources

The Milky Way hosts a large variety of stellar binaries (Sect. 1.2), numbering in the millions below mHz frequencies (Table 3). They will appear as nearly monochromatic (constant frequency) sources emitting over the whole duration of the mission (continuous GW sources). Up to tens of thousands—those with frequencies larger than a few mHz and/or located closer than a few kpc—will be individually resolvable. The rest of Galactic binaries will blend together into the confusion-limited foreground that is expected to affect the LISA data stream at frequencies below 3 mHz (e.g. Bender and Hils 1997; Edlund et al. 2005; Ruiter et al. 2010; Cornish and Robson 2017). The optimal detection, characterization, and subtraction

Table 5 Population synthesis codes used by the community at the time of writing

Code name	References	Publicly available
Binary_c	Izzard (2004), Izzard et al. (2006, 2009)	No
BSE	Hurley et al. (2002)	Yes
BPASS	Stanway and Eldridge (2018)	No
ComBinE	Kruckow et al. (2018)	No
COMPAS	Stevenson et al. (2017b)	Yes
COSMIC	Breivik et al. (2020a)	Yes
MOBSE	Giacobbo et al. (2018)	No
POSYDON	Fragos et al. (2022)	Yes
Scenario Machine	Lipunov et al. (1996, 2009)	No
SEVN	Spera et al. (2015)	Yes
SeBa	Portegies Zwart and Verbunt (1996), Toonen et al. (2012)	Yes
StarTrack	Belczynski et al. (2008)	No
TRES	Toonen et al. (2016)	Yes

Binary_c, COSMIC, MOBSE are based on the BSE code (Hurley et al. 2002)

of Galactic binaries from the data stream has been recognized as one of the fundamental tasks for the LISA analysis. Over-fitting the population of Galactic binaries can result in a large contamination fraction in the catalogue of detected sources, while under-fitting it can degrade the analyses of extra-galactic GW sources in the data due to the excess residual.

The waveforms for Galactic binaries are well predicted using only leading order terms for the orbital dynamics of the binary (Peters and Mathews 1963) and can be computed at low computational cost using a fast/slow decomposition of the waveform combined with the instrument response (Cornish and Littenberg 2007). Nevertheless, their identification in the LISA data will be laborious due to the sheer number of sources expected to be in the measurement band ($\sim 10^4$) and the large number of parameters required to model each source (between 5 and 10, depending on if the source is chirping and if spins are important in the modelling of one or both of the components). In addition, the high density of Galactic binaries in the LISA band (to the extent that sources are overlapping) and the modulation effects caused by LISA's orbital motion, which spreads a source's spectral power across multiple frequency bins, makes the true number of signals at a given frequency difficult to identify. Several techniques have been developed to address this challenge.

A hierarchichal/iterative scheme The detectable binaries can be identified by using an iterative process that utilizes a median smoothing of the power spectrum to estimate the effective noise level at each iteration, regresses binaries from the data with signal-to-noise ratios above the established threshold as detected sources, repeating the process until the convergence (Cornish and Larson 2003; Timpano et al. 2006; Nissanke et al. 2012). However, each iteration can leave behind some residual due to "imperfect subtraction" that can affect further analysis and bias parameter estimation. In practice, the stochastic signal is not actually subtracted but rather included in the covariance matrix during the likelihood calculation.

Global fit A number of studies show that a global fit to the resolvable binaries, while simultaneously fitting a model for the residual confusion or instrument noise and using Bayesian model selection to optimize the number of detectable sources can provide an effective solution to the Galactic binaries challenge (Cornish and Crowder 2005; Umstätter et al. 2005). These global fit methods have been demonstrated on the

Table 6 N-body and few-body dynamics codes used by the community at the time of writing

Code name	References	Publicly available
NBODY6/NBODY6++GPU/ NBODY7	Aarseth (2012), Nitadori and Aarseth (2012), Wang et al. (2015)	Yes
phiGRAPE/phiGPU	Berczik et al. (2013, 2011)	No
HiGPU	Capuzzo-Dolcetta et al. (2013)	No
CMC	Kremer et al. (2020b, 2019b, 2018a)	Yes
MOCCA	Hypki and Giersz (2013), Giersz et al. (2013)	No
clusterBH	Antonini and Gieles (2020)	No

Galactic binaries using data from the LISA Data Challenges (Littenberg et al. 2020), but work still needs to be done to extend this into a fully-developed analysis pipeline with the full variety of overlapping LISA sources.

It should be noted that there will possibly be SGWBs of unresolved extragalactic sources or of cosmological origin (see Sect. 1.2.2.5). Such backgrounds will similarly be a broadband confusion signal, and similar considerations to identify and characterize SGWB in LISA data may be needed in order to reveal some of the fainter signals from astrophysical and cosmological sources. Techniques to identify and subtract the SGWB in LISA data are currently being developed by several groups (Karnesis et al. 2020; Caprini et al. 2019; Pieroni and Barausse 2020).

1.6.3 Tools

1.6.3.1 Modelling isolated binary evolution and populations The long-term evolution of stars and binaries is typically modelled in either of two methods; by solving the stellar structure equations, i.e. referred to as detailed calculations, or by faster approximate methods typically aimed at the population synthesis approach. The latter either interpolates in a grid of detailed calculations or uses parametrised stellar evolution tracks which are fitted to detailed calculations. The advantage of this method is the highly boosted computational speed (the simulation of the evolution of a single binary takes a fraction of a second in stead of hours or days), at the cost of detail; one only has access to those parameters included in the grid of tracks. Due to the speed, the effect of different assumptions for poorly understood stellar physics (e. g., stellar mass-loss, interaction physics, supernova kick physics) can be tested in a statistical way, which leads to a deeper understanding of the underlying physical processes involved. The population synthesis approach has proven to work well in retrieving the general characteristics of large binary populations (Toonen et al. 2014) and has led to many insights in binary evolution.

Population synthesis codes are crucial for LISA science, both in order to make forecasts for source rates, but also to develop data analysis pipelines. Indeed, ongoing work on building fast and reliable waveforms relies on the knowledge of the expected properties of the sources (masses, spins, eccentricities) and the accuracies required to detect them and measure these properties. The codes currently in use by the LISA community are listed in Table 5. Further development of these codes, in particular the inclusion of additional physical processes as well as cross-checks between the codes will help to prepare for LISA observations.

1.6.3.2 Modelling binary evolution in dense environments Stellar-origin LISA GW sources can also be formed in dense stellar environments through dynamical interactions. Hence simulation codes that follow the evolution of dense stellar systems, either by direct integration or using Monte–Carlo techniques, are crucial for their study. Many of these codes follow simultaneously the evolution of single and binary stars within the dense stellar system, using one of the tools described in the previous Section. A list of stellar dynamics codes currently used in the community

for the study of the formation of stellar-origin LISA GW sources can be fount in Table 6.

1.6.3.3 GW signal tools   In order to calculate the GW signal of Galactic binary systems there are a number of approaches that can be used, ranging from detailed TDI based methods, e.g., via codes from the LISA Data Challenges (LDC, https:// lisa-ldc.lal.in2p3.fr) to (more) analytic methods to calculate the signal and SNR of specific objects (e.g. Cornish and Larson 2003; Robson et al. 2019; Korol et al. 2017; Kupfer et al. 2018; Smith and Caldwell 2019). There are also some web-based tools to explore sensitivity of different GW detectors, including LISA and also detectability of sources in LISA, such as https://gwplotter.com (Moore et al. 2015) and the Gravitational Wave Universe Toolbox (https://www.gw-universe.org, Yi et al. 2022)

1.7 Scientific objectives

1.7.1 Constraining stellar and binary interaction physics

Coordinators: **Fritz Röpke, Alina Istrate**

Contributors: **Karel Temmink (1.7.1.1), Mike Lau (1.7.1.1, 1.7.1.7-8), Stephan Rosswog (1.7.1.2, 1.7.1.6), Vasileios Paschalidis (1.7.1.2), Alina Istrate (1.7.1.2), Fritz Röpke, (1.7.1.3,1.7.1.6), Kinwah Wu (1.7.1.4-5), Stéphane Mathis (1.7.1.4), Thomas Tauris (1.7.1.5), Stéphane Blondin (1.7.1.6), Ashley Ruiter(1.7.1.6, 1.7.1.8), Chris Fryer (1.7.1.7), Thierry Foglizzo (1.7.1.7) Manuel Arca Sedda (1.7.1.8), Kyle Kremer (1.7.1.8), Simone Bavera (1.7.1.8), Abbas Askar (1.7.1.8), Silvia Toonen (1.7.1.8), Gijs Nelemans (refs for 1.7.1.8), Irina Dvorkin (refs for 1.7.1.8), Valerya Korol (refs for 1.7.1.8), Astrid Lamberts (refs for 1.7.1.8)**

Throughout this section, we will highlight science questions related to LISA that can/ should be addressed before the launch of the mission with the label **pre-LISA-launch objective**, while science questions that can only be addressed by using LISA data will be highlighted with the label **post-LISA-launch objective**. It should be emphasized, that in most cases LISA detection of individual binaries is limited to GW frequency and a somewhat poor sky location. For a fraction of these thousands of systems, however, high SNR and/or high frequency will enable the measurement of the GW frequency derivative, a good sky localization, and possibly constraining the eccentricity of the binary system. The GW frequency derivative will reveal the chirp mass of the binary and thus the distance. Although these cases will be exceptional systems in the overall global perspective, they will be the key science drivers that deliver deep insight and new breakthroughs in our understanding of binary compact object systems—often because of the enhanced chances of finding the EM counterpart of these well-localized systems.
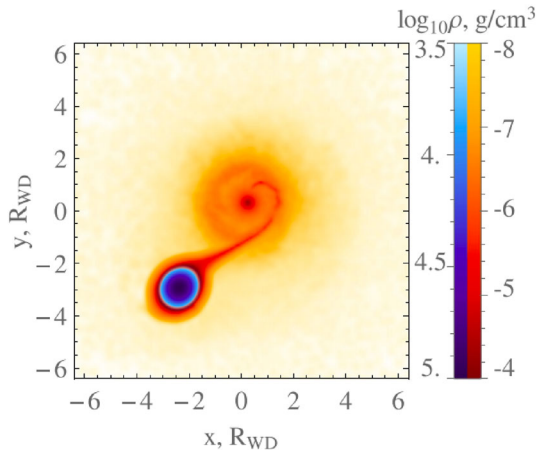
Fig. 13 Hydrodynamical investigation of dynamical stability in a UCXB with a $0.15\,M_\odot$ WD donor star and a $1.4\,M_\odot$ accreting NS, in an orbit with an initial eccentricity of 0.04. Plotted here is the mass density in the orbital plane after roughly 13 orbits of RLO. The density plot shows eccentric structures in the accretion disc, the complex character of the flow near the circularization radius and a strong density cusp near the NS. The envelope surrounding the binary is sparse but its total mass is significant compared to the disc. Image reproduced with permission from Bobrick et al. (2017), copyright by the authors

1.7.1.1 Dynamical stability and efficiency of mass transfer in the formation of LISA sources

The formation of compact binary systems with two compact objects is still relatively poorly constrained. Typically, at least two phases of mass transfer are required to form a general observable stellar LISA system: one for each component star to lose their hydrogen envelope, and additional phases are possible to remove the helium-rich envelope. To explain the compactness of the orbit, typically one or more of these mass-transfer phases are considered to proceed in an unstable fashion in order to get the necessary amount of orbital shrinkage i.e. a CE phase (e.g. Paczyński and Sienkiewicz 1972; Paczynski 1976; Webbink 1984). Hence, it is crucial to understand for which binary configurations mass transfer proceed stably, and for which it will be unstable.

Pre-LISA-launch objective The precise value of the stability boundary (i.e. a critical mass ratio, q between the two stellar components above which no stable mass transfer is possible) remains under debate. Theoretical work has shown that mass transfer can proceed significantly more stable than classical results have previously implied (e.g. Hjellming and Webbink 1987; Chen and Han 2008; Woods and Ivanova 2011; Passy et al. 2012b; Pavlovskii and Ivanova 2015; van den Heuvel et al. 2017; Misra et al. 2020). Similarly, the mass-retention fraction of the accreting companion remains relatively poorly understood (e.g. Paczyński and Sienkiewicz 1972; Kato and Hachisu 1999; Hachisu et al. 1999; Tauris et al. 2000; Hurley et al. 2002; Nomoto et al. 2007; Vinciguerra et al. 2020). These issues severely affect the predicted formation details of compact binaries, and determine which evolutionary pathways are dominating in the formation rate of LISA sources (Sect. 1.4), and hence would leave characteristic imprints on the numbers and properties (orbital periods, masses) of the resulting LISA population (e.g. Korol et al. 2017; Ruiter et al. 2019).
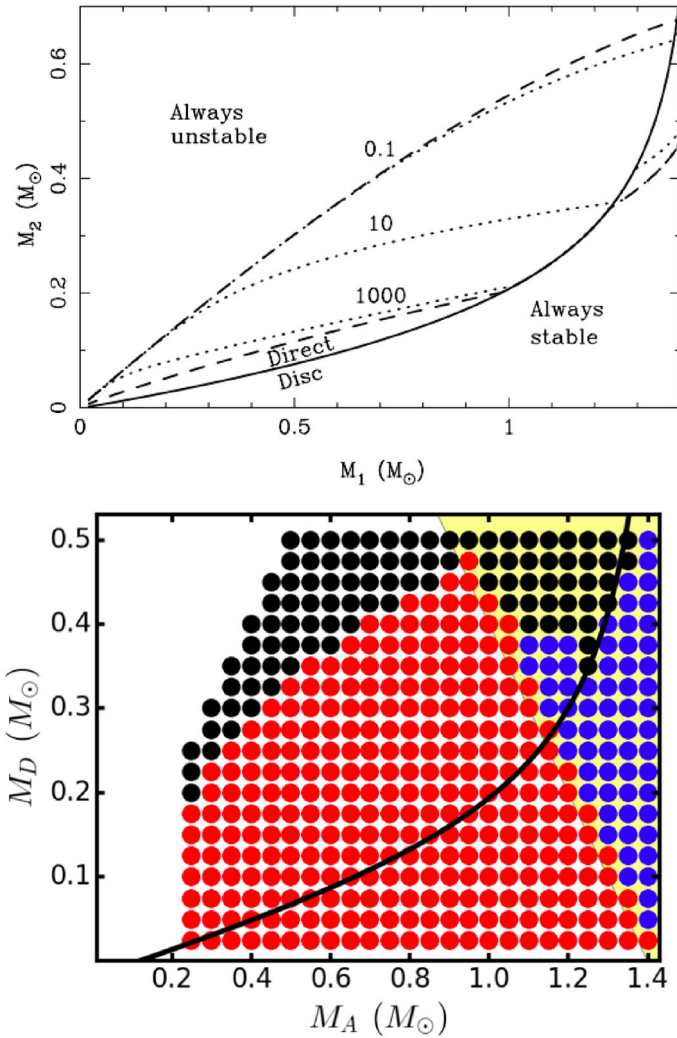
Fig. 14 Stability regions in the donor mass—accretor mass plane of WD+WDs and UCXBs. Donor star masses are on the vertical axes, accretor star mass on the horizontal axes. Upper panel: analytical results of Marsh et al. (2004) where the solid line marks the transition between disc and direct impact accretion, and the other lines show how the strict stability limit of Nelemans et al. (2001a) is relaxed when dissipative torques feed angular momentum from the accretor back to the orbit. Bottom panel: ballistic calculation approach by Kremer et al. (2017) using zero-temperature mass–radius relations for the WD donor. Red systems are stable throughout their lifetimes, through stages of both direct-impact and disc accretion; black systems are unstable; and blue systems have an accretor that exceeds the Chandrasekhar limit during their evolution. The solid black line marks again the boundary between disc and direct-impact accretion for initially synchronous and circular binaries. The yellow region indicates systems with a total mass in excess of the Chandrasekhar limit, i.e. potential SN Ia progenitors. It is evident from these figures that UCXBs with low-mass ($\lesssim 0.2\,M_\odot$) He WD donor stars, and NS accretors, are always dynamically stable. Images reproduced with permission from [top] Marsh et al. (2004), copyright by RAS; and [bottom] from Kremer et al. (2017), copyright by AAS

For instance, whether or not the first phase of mass transfer in the formation of a WD+WD leads to a shrinkage or widening of the orbit (i.e. unstable or stable mass transfer) determines to which size the secondary star can evolve before filling its Roche lobe, which dictates the mass of its core at RLO, i.e. the mass of the resulting WD, and hence the mass ratio of the WD+WD (Nelemans et al. 2000, 2001c; van der Sluys et al. 2006; Toonen et al. 2012).

Stability of mass transfer depends rather sensitively not only on the intricate details of the structure of the donor star, but also on the transfer and potential loss of mass and angular momentum (Soberman et al. 1997). **Pre-LISA-launch objective** Hydrodynamical simulations can help settle the question of dynamical stability (see Fig. 13). The mass that is transferred to the companion can not always be fully accreted by the companion star: spin-up to critical rotation rates and/or strong optically thick winds or outflows (including jets) can result in significant fractions of transferred material being lost from the accreting star. Since mass that is not accreted leaves the binary system, carrying with it an amount of orbital angular momentum, the efficiency of accretion and the stability of mass transfer are linked. In the case of compact object accretors, it is expected that less conservative mass transfer is typically more stable than mass transfer where all mass is accreted (Soberman et al. 1997).

Post-LISA-launch objective Observed samples are required to reverse-engineer the progenitor evolution, and constrain the evolutionary pathways (e.g. Nelemans et al. 2000; van der Sluys et al. 2006; Zorotovic et al. 2010; De Marco et al. 2011; Portegies Zwart 2013). On the EM side, only relatively small samples exist currently, with relatively large biases towards the lower-mass and hotter WDs, since they have longer (observational) lifetimes and are brighter. However, LISA will be sensitive to WD+WDs throughout the whole Galaxy and will be able to provide properties of the entire WD+WD population with relatively few selection biases. This will allow for stronger and more meaningful statistical analyses. Additionally, LISA will be able to almost directly measure the Galactic rate and masses of merging WD+WDs, which is another useful tool in constraining progenitor evolution.

The detection of NS+NSs (and potentially NS+BH systems) with LISA allow for a direct view of their formation pathways through their eccentricity, that is induced by the supernova kick associated with the formation of the second NS (Vigna-Gómez et al. 2018; Lau et al. 2020). The population of eccentric LISA NS+NS binaries originate from NS+NS binaries born right in or near the sensitivity window of LISA, so that there is little time for GWs to circularise the orbit. The tight orbit prior to the second SN, leading to NS+NS formation, is characterized by the last phase of mass transfer (see Sect. 1.3.1.3 and Fig. 9). This is Case BB mass RLO initiated by the expansion of the naked helium-star after core-helium depletion. The Case BB mass transfer episode is believed to be predominantly stable from detailed simulations (Tauris et al. 2015) and in order to match the observed period distribution of Galactic NS+NS systems (Vigna-Gómez et al. 2018). However, unstable Case BB RLO would lead to an additional CE phase that produces NS+NSs with sub-hour periods. Yet, because such NS+NSs that have gone through unstable Case BB RLO prior to the second SN are formed with higher GW frequencies, they also have a more rapid

GW frequency evolution ($f_{GW}/\dot{f}_{GW} \propto f_{GW}^{-8/3}$), which disfavours their detection by LISA (Lau et al. 2020; Andrews et al. 2020). **Pre-LISA-launch objective** A deeper understanding of whether or not mass transfer is stable or unstable in Case BB RLO is needed, and should be investigated further.

1.7.1.2 Dynamical stability and efficiency of mass transfer in accreting LISA sources

A remarkable property of Roche-lobe filling stars is that, for mass ratios < 0.8, their average density is related to their orbital period (see e.g. Frank et al. 2002). For mass ratios, $M_{donor}/M_{accretor} < 0.8$ the relation is given by:

$$P_{orb} = 10.5 \text{ hr} \left(\frac{\bar{\rho}}{\text{g cm}^{-3}} \right)^{-1/2}, \tag{6}$$

As an example, Roche-lobe filling stars with orbital frequencies of 0.1 mHz ($f_{GW} = 0.2$ mHz) have $\bar{\rho} \sim 10$ g cm^{-3}, while those at 1 Hz possess an average density of $\bar{\rho} \sim 10^9$ g cm^{-3}. In other words, mass-transferring WDs are located right inside LISA's frequency band. For NS donors, mass transfer only sets in at much smaller separations when the frequencies are already close to the kHz-regime (Shibata and Taniguchi 2011).

For a LISA stellar source, there are at least two possible scenarios for the subsequent evolution after the onset of mass transfer: a) after an initial brief phase of continued orbital shrinkage after RLO is initiated (Tauris 2018), mass flows on a much longer timescale from the WD toward the accretor star while the binary separation increases. This process is commonly referred to as a form of stable mass transfer (see Fig. 14); b) The WD becomes tidally disrupted by the accretor, resulting in the binary merger. This process occurs on a dynamical (orbital) timescale. **Pre-LISA-launch objective** Whether the binary undergoes stable mass transfer vs a merger may have important implications on the type of GW templates that are necessary to detect these binaries with LISA.

The above discussion makes it clear that for WD+WD, NS+WD, and BH+WD binaries the onset of mass transfer marks a turning point since the stability of mass transfer decides whether the binary can survive or will inevitably merge. As mentioned in the previous Sections, its fate depends sensitively on the internal structure of the mass-donating star, on the mass ratio and on the involved angular momentum exchange mechanisms, which here depend primarily on whether mass transfer takes place with or without an accretion disc around the accretor (Rappaport et al. 1982; Hut and Paczynski 1984; Marsh et al. 2004; Gokhale et al. 2007; Motl et al. 2007; Paschalidis et al. 2009; Dan et al. 2011; Shen 2015). Since fully degenerate WDs possess an inverted mass-radius relation, i.e. they grow in size as mass is removed, the mass-donating star will expand and thereby tend to speed up the mass transfer. However, since the mass is transferred to the heavier star, the orbit will tend to widen, and therefore stabilize the mass transfer (Soberman et al. 1997; Tauris and Savonije 1999).

The way the transferred mass settles onto the accretor star has a decisive impact on the orbital evolution. If the circularization radius of the transferred matter is smaller

than the radius of the accretor, it will directly impact onto the stellar surface and spin up the accreting star—this scenario is referred to as direct impact accretion. That means that orbital angular momentum is not fed back into the orbit, and therefore the orbital separation shrinks and mass transfer accelerates. If instead the circularization radius is larger than the radius of the heavier WD accretor, a disc can form and—via its large lever arm—the disc can feed back angular momentum into the orbital motion, increase the orbital separation, and thus stabilize the binary system (Iben et al. 1998; Piro 2011; Paschalidis et al. 2009).

The majority of studies of mass-transfer stability to date assume that the mass-transferring WD is tidally locked. However, as pointed out by Iben and Webbink (1987), spinning up a WD while being tidally locked from some initial separation down to the Roche limit is accompanied by tremendous energy release that, depending on the dissipation mechanism, could potentially lift the degeneracy throughout the star. Given that the dissipation mechanisms in WD interiors are not well understood, this makes things even more complex: The tidal interaction between the stars can substantially heat up the mass-donating WD, change its internal structure, and thereby its response response to mass loss.

For LISA this means that the measured chirp of a mass-transferring binary is not only set by the decay of the orbit due to GW, but also due to mass transfer and tidal interactions, and therefore the chirp mass can not be directly measured as in the case of detached (chirping) binaries. However, for an assumed cold equation-of-state mass-radius relation of the donor star, both the mass of the donor star and the model mass-transfer rate can be derived, as these are fully set by the orbital period (Faulkner 1971; Vila 1971, see also Eq. 6). **Pre-LISA-launch objective** Future work should aim at including finite-temperature effects in the WD EOS consistently, e.g. by using detailed stellar structure calculations following the formation and evolution of the system—from the detachment of the CV/LMXB phase until onset of the AM CVn/UCXB phase (Fig. 8).

Post-LISA-launch objective We do not expect the second derivative ($\dddot{f}_{\mathrm{GW}}$) of the GW frequency an AM CVn system to be measurable with LISA, as the low mass ratios required from mass transfer stability considerations ($M_{\mathrm{donor}} \ll M_{\mathrm{accretor}}$), imply a low-mass WD donor, whose large radius prevents the AM CVn system from penetrating into the highest frequency range where the second derivate is large (Nelemans et al. 2004b). The combination of LISA with EM surveys, such as Gaia, is particularly promising for AM CVn sources. If their distance is known, the chirp mass can be constrained, which allows for the orbital chirp to be decoupled into its different components (Breivik et al. 2018).

Apart from determining the orbital evolution, mass transfer in a WD+WD also leads to an accumulation of helium (possibly also carbon and oxygen) on the surface of the accreting WD. If (or when) nuclear fusion commences in this layer, rapid burning follows that causes a nova outburst or, in case of persistent fusion, X-ray emission may be observed as for supersoft X-ray sources (Kahabka and van den Heuvel 1997). Rapid accretion during the last tens of orbits before a merger and the interaction with the incoming accretion stream can trigger surface detonations that cause weak SN Ia-like transients (Guillochon et al. 2010). A (tidal) disruption of a

WD by a NS or BH could potentially lead to nuclear-dominated accretion flows (Metzger 2012; Fernández and Metzger 2013).

Post-LISA-launch objective The probability of detecting a Galactic WD+WD merger during the LISA mission is small (since the Galactic WD+WD merger rate is of order one per century (Nelemans et al. 2001b), let alone that this number includes all the WD+WD "mergers" giving rise to stable RLO after contact, i.e. the AM CVn systems). Yet, the case of merging WD+WD binaries deserves a separate mention, because of the exciting possibility of multiband and/or multiwavelength observations: the inspiral phase would be detectable by LISA or a similar mission, and the merger phase by a future observatory such as DECIGO (Sato et al. 2017). If the merger gives rise to an optical transient (e.g. a SN of Type Ia/Iax), these can be observed by EM transients surveys such as ZTF and the Vera Rubin Observatory. For NS+WD, the post-merger phase would be detectable by ground-based high-frequency GW observatories, such as LIGO, Virgo, KAGRA and future facilities like Cosmic Explorer (Abbott et al. 2017a) and the Einstein Telescope (Punturo et al. 2010), due to either the eventual collapse of the NS core or post-merger oscillations of the remnant (Paschalidis and Stergioulas 2017). Therefore, NS+WD systems offer the unique opportunity not only to study the dynamics/stability of mass-transfer, but also the potential to place constraints on the nuclear equation of state. Nevertheless, once again, we emphasize the small probability for a Galactic WD+WD merger event during the lifetime of the LISA mission.

Post-LISA-launch objective In summary, mass transfer is crucial for determining the final fate of interacting close binaries, but many details and many questions still remain unanswered related to e.g. formation and evolution of AM CVn and UCXB systems and their ultimate fates, and for related questions such as the progenitor systems of Type Ia/Iax supernovae. Observations with LISA may therefore bring a major leap forward in our understanding of the physics of this crucial evolutionary phase of close-orbit stellar binaries with compact objects.

1.7.1.3 Common envelopes   CE phases are one of the greatest uncertainties in binary stellar evolution theory (Ivanova et al. 2020) and LISA will provide important measurements. **Pre-LISA-launch objective** The inspiral of the secondary star into the envelope of the primary lacks obvious symmetries and is therefore not accessible to classical one-dimensional stellar evolution modelling approaches. At least some part of CE interaction takes place on a dynamical timescale. Therefore, parametrized prescriptions for CE evolution are used in stellar evolution modelling. Three-dimensional hydrodynamic simulations have been employed to study the process in more detail (Passy et al. 2012a; Iaconi et al. 2018; Sandquist et al. 2000; Ricker and Taam 2012; Nandez et al. 2015; Nandez and Ivanova 2016; Kuruwita et al. 2016; Ohlmann et al. 2016a, b; Chamandy et al. 2018; Reichardt et al. 2019; Rasio and Livio 1996; Prust and Chang 2019; Kramer et al. 2020; Sand et al. 2020; Law-Smith et al. 2020), but they are numerically challenging due to the large dynamical range of spatial and temporal scales of the problem. Furthermore, most often three-dimensional hydrodynamic simulations do not incorporate modelling of physical processes like convection and radiation transport, which are thought to be important

especially in the later phases of the inspiral. Complementing the global three-dimensional CE simulations with local, wind-tunnel type, simulations that study the details of the flow around the inspiraling object (e.g. MacLeod et al. 2017; De et al. 2020; Everson et al. 2020), as well as one-dimensional but multi-physics hydrodynamic simulations (e.g. Clayton et al. 2017; Fragos et al. 2019) is a promising avenue to more physically accurate predictions of post-CE binary properties. Lastly, studies of post-CE binaries that are found observationally will provide insights into the CE phase. Valuable constraints on the CE mechanism have come from this method previously (Nelemans et al. 2000; van der Sluys et al. 2006; Zorotovic et al. 2010; Toonen and Nelemans 2013).

Because the actual interaction is short (up to about 10^3 years), direct observations in optical astronomy are difficult. Some of the fainter optical transients (luminous red novae; Soker and Tylenda 2003; Tylenda et al. 2011; Kulkarni et al. 2007; Howitt et al. 2020; Stritzinger et al. 2020) have been associated with CE events. The two fundamental, and to date unanswered, questions are: (i) Which systems manage to eject the CE? (ii) What is the final orbital separation of the two stellar cores in this case? **Post-LISA-launch objective** The LISA mission is instrumental for clarifying many aspects of the physics of CE phases in two main directions:

1. **Direct observations of events related to CE interaction.**

    The secondary star may be a compact object, but the primary (donor) is typically in a giant phase. Therefore, a generation of sufficiently strong GW signals during inspiral can only be expected if the core of the primary star is also relatively compact, and if the secondary (a compact object) comes close enough during the inspiral.

    The prospects to observe GW signals from the inspiral phase, however, do not seem very promising in current models. While based on a parametrized description of CE inspiral, Ginat et al. (2020) predict about one detection in a few centuries with LISA. The full three-dimensional hydrodynamic CE simulations of Ohlmann (2016) find weaker signals. The rates for the slower self-regulated phase that proceeds on a thermal timescale are more promising, with a rate of $\approx 0.1 - 100$ events in the Galaxy during the LISA mission duration (Renzo et al. 2021).

    The detectability, however, depends on how close the stellar cores come to one another during the evolution. This is uncertain and depends on the above questions (i) and (ii). Due to the inspiral of the secondary into the primary star's envelope, orbital energy and angular momentum are transferred to this (now) CE. Some material becomes unbound and is ejected from the system. Simulations, however, show that this process alone is inefficient and other energy sources (such as the ionization of envelope material, Nandez et al. 2015; Prust and Chang 2019; Sand et al. 2020) have to be tapped to achieve full envelope removal. The exact parameters allowing for such a successful CE ejection are still unknown, but it is likely that most initial configurations may fail. Such failed events, however, may produce stronger GW signals. Moreover, more exotic cases in which, for instance, triple systems enter CE evolution (Comerford and Izzard

2020; Glanz and Perets 2021), may potentially also be sources of detectable GW signals.

2.   **Indirect information from detecting post-CE sources**

Since all stellar mass LISA sources have presumably gone through a CE phase (disregarding here sources produced in dense clusters via dynamical interactions), comparison of LISA populations with model predictions naturally test CE physics. Specifically, the occurrence (and detection) rates of these binary populations depend critically on the orbital separation of the stellar cores after the CE phase. In this sense, the LISA mission will statistically sample the outcome of CE events and the results provide valuable information for answering the above question (ii). Moreover, if CEs produce binaries with sufficiently short orbital periods, such that they are within the LISA band immediately at envelope ejection, they will act as a source term for the population of LISA binaries. In the absence of this injection of sources, evolution of the orbits due to GWs produce a predictable expectation for the orbital period distribution of binaries, any deviations from that expectation could be ascribed to an injected population of post-CE systems. By simultaneously modelling the LISA noise curve, the GW foreground from unresolved Galactic sources, and the effect of GWs on a binary population, the initial post-CE separations for the shortest period binaries can, in principle, be derived, and thereby deliver important insight into CE physics.

Contributing to these two aspects, the LISA mission will help to constrain physics of the mysterious, and yet crucial, CE phase in binary stellar evolution. Its results will be used to validate hydrodynamic simulations and to develop new efficient prescriptions of CE interactions that are to be used in binary stellar evolution and population synthesis studies.

1.7.1.4 Tides and angular momentum transport   The orbital evolution of detached binaries is practically determined by the loss of orbital angular momentum and the exchanges of angular momentum between the stars and the orbit, and also in some situations, the mass loss from the system. For binaries with only BH or NS components, tidal effects are completely insignificant (except for the few final orbits before a merger event) and the orbital evolution is entirely determined by GWs alone. An example of such a system is the radio pulsar binary PSR B1913+16 (see Weisberg and Huang 2016). For binaries with non-degenerate stars, or tight systems with WDs, tides can be important, leading to measurable differences in the LISA signal. The orbital dynamics of the wide-orbit systems is relatively simple, as the orbital angular momentum is decoupled from the spin of the two stars. The orbital evolution of these binaries is therefore simply driven by the wind-mass loss of the stars and, in principle, GWs, which nevertheless is negligible in such wide systems. The situation is very different for the systems with a sufficiently short orbital period. First of all, the timescale for the loss of orbital angular momentum via GWs (Peters and Mathews 1963) could be comparable to or shorter than the evolution of the stars and the tidal evolution of the system (Bildsten and Cutler 1992). Secondly, the sizes of the stars are no longer negligible compared with the orbital separation, and torques can be exerted on the stars effectively (Lai et al. 1994; Hut 1981). Hence, the

structures and the hydrodynamical properties of the stars would play an important role in determining the orbital dynamics and the orbital evolution of these systems (Benacquista 2011; Fuller and Lai 2012; Shah and Nelemans 2014a). These have, at least, two immediate consequences on the LISA science: (i) the number density of persistent GW sources associated with these binaries observable within the LISA band, and (ii) the event rate of burst sources associated with coalescence or merging, resulting from the orbital decay of these binaries, although these bursts are very rare in our Galaxy.

The exchange of angular momentum between the binary orbit and the spin of the stars can be facilitated by the viscous torque (Zahn 1977), but in the compact star binaries this coupling is less efficient than the coupling caused by a stellar bulge cause by the tidal deformation of the star (Bildsten and Cutler 1992; Dall'Osso and Rossi 2013; Kochanek 1992). The degree of tidal deformation of a star depends on its internal structure and dynamics (e.g. Flanagan and Hinderer 2008; Ogilvie 2014; Mathis 2019). Thus, even in the absolute absence of viscosity, WDs and NSs would respond differently to tidal deformations (cf. the studies of Vick and Lai 2019; Lai and Shapiro 1995; Dall'Osso and Rossi 2013; Bildsten and Cutler 1992; Dall'Osso and Rossi 2013; Kochanek 1992). The presence of the close companion will trigger a large-scale flow induced by the hydrostatic adjustment of the studied primary to the tidal perturbation, the equilibrium tide (e.g. Zahn 1966; Remus et al. 2012; Ogilvie 2013), and a broad diversity of tidal waves (i.e., gravity waves, inertial waves, gravito-inertial waves), and the dynamical tide (e.g. Xu and Lai 2017; Yu et al. 2020). Their dissipation and the quadrupolar moment they induce modify the inspiral and cause changes in orbital frequency and phase shifts (e.g. Bildsten and Cutler 1992; Wang and Lai 2020; McNeill et al. 2020). Thus, WD binaries and NS binaries will behave and evolve differently, which will manifest in the LISA GW background. Their orbital evolution will also imprint signatures in the GWs that they emit (Vick and Lai 2019; McNeill et al. 2020; Dall'Osso and Rossi 2013, 2014; Shah and Nelemans 2014b). The situation can be more complicated if the compact stars have a large magnetic moment, which is not uncommon among magnetic WDs (Ferrario et al. 2015). The magnetic moments of NSs may not be as large as those of WDs since NSs are more compact. Direct magnetic interactions between two magnetised components should be taken into account and may compete with tidal interactions in LISA sources.

Post-LISA-launch objective Our understanding of the interplay between tidal interaction, feedback magnetic-field amplification and orbital angular momentum extraction by GWs is currently very primitive. The observations of GWs from such systems will surely expand our knowledge on this subject substantially (e.g. King et al. 1990; Piro 2012; Wu et al. 2002; Wang et al. 2018).

1.7.1.5 Irradiation of companion star

Feedback irradiation effects on companion stars caused by the intense X-ray flux emitted from accreting compact objects may influence the evolution of the orbits of binary stars (Podsiadlowski 1991; Benvenuto et al. 2014). In detached systems, energetic millisecond pulsars (MSPs, recycled to high spin frequencies from a previous recycling phase; Bhattacharya and van den

Heuvel 1991) may irradiate their companion star with a pulsar wind of relativistic particles and hard photons (Tavani and Brookshaw 1992). Observations have revealed a growing number of such MSPs with a non- or semi-degenerate companion star which is being ablated by the pulsar wind, the so-called black widows and redbacks (Roberts 2013). This is evidenced by the radio signal from the pulsar being eclipsed for some fraction of the orbit (Fruchter et al. 1988). Tidal dissipation of energy in the donor star envelope (Applegate and Shaham 1994) may cause the companion star to be thermally bloated and thereby evaporate more easily. For LISA binaries, such mass loss via ablation/evaporation will modify their orbital evolution (e.g. Chen et al. 2013; Hui et al. 2018), which is otherwise dictated by GWs and tides. For this reason, we may gain new insight on irradiation efficiency from LISA detections of such systems and precise measurements of their orbital frequency. **Pre-LISA-launch objective** The impact and the modelling of this effect, often leading to cyclic accretion, is still unclear needs to be improved before LISA flies.

Post-LISA-launch objective For accreting LISA sources, the irradiation will lead to disturbance of the thermal equilibrium of the companion star (Büning and Ritter 2004) and, in the extreme situation, geometrical deformation (Phillips and Podsiadlowski 2002), thereby affecting its mass-transfer rate and thus the orbital evolution of the binary. Such an effect may indeed be measured by LISA via its impact on the orbital frequency derivative, and thus the chirp mass of the system. Hence, detection of a number of mass-transferring UCXBs and AM CVn systems by LISA could provide us with unique ways of probing the physics governing close compact object binaries (Jia and Li 2016; Kremer et al. 2017).

1.7.1.6 Type Ia supernovae and other transients   Stellar interactions in binary systems containing at least one WD are thought to trigger Type Ia supernovae (SN Ia) and likely a variety of other transients (see e.g. Wang and Han 2012, forareview). SN Ia were of paramount importance for the discovery of the accelerated expansion of the Universe and they significantly contribute to cosmic nucleosynthesis, but the lack of a clear observational connection between a progenitor system and the observable phenomenon has made their understanding difficult. Without proper initial conditions their modelling remains uncertain.

The properties of the ensuing explosion are determined by the pre-explosion state of the WD, but is it triggered when approaching the Chandrasekhar-mass limit, or well before? The occurrence rate, the delay time between binary formation and SN explosion, and the ignition process are all determined by the nature of the progenitor system, and they have a strong impact on the contribution of thermonuclear SNe to galactic chemical evolution. A traditional broad classification is to distinguish between single-degenerate systems, where the companion of the exploding WD is a non-degenerate star—and the double degenerate systems—where the interaction of two WDs (mergers, or in rare cases collisions) triggers the SN explosion (see Ruiter 2020, for a breakdown of binary star progenitor configurations).

None of the progenitors and explosion mechanisms is established beyond doubt. The single-degenerate Chandrasekhar-mass model, that served as a reference for a long time, has several shortcomings, but it seems to be needed to explain observed

abundance trends (Seitenzahl et al. 2013). However, both population synthesis models and observations indicate that single degenerate explosions fall short of explaining the observed SN Ia rate. GW signals were derived from explosion simulations of near-Chandrasekhar mass WDs (Falta et al. 2011; Seitenzahl et al. 2015), but the prospect of measuring individual events is low.

The major competing double-degenerate scenario received increased attention over the past years and is of particular interest in the context of LISA. In this scenario, however, the process initiating the actual thermonuclear explosion is unclear. For massive WDs, the remnant can reach or exceed the Chandrasekhar-mass, but the explosion could also be triggered in the merger process itself while the more massive WD is well below the Chandrasekhar mass limit (Pakmor et al. 2010, 2012). Apart from GW-driven (close-to-circular) mergers, *collisions* can also (likely to a much smaller extent) contribute to the SN Ia rate (Rosswog et al. 2009a; Raskin et al. 2009). They may occur in locations with large stellar number densities such as globular cluster cores or galactic centres, but they are generally thought to occur too infrequently to explain the bulk of SN Ia (Toonen et al. 2018, but seeKushnir et al. 2013 for more optimistic claims). Such collisions, however, have the advantage of a very robust and physically understood explosion mechanism: WDs of the most common type ($\sim 0.6\,M_\odot$), that collide with velocities given by their mutual gravitational attraction, cause strong shocks in the collision and nuclear burning occurs in the right density regime, so that the resulting explosions appear as rather common Type Ia SNe (Rosswog et al. 2009a). Before the final collision causes a thermonuclear explosion, the two WDs may undergo several close encounters causing a sequence of GW bursts in the LISA band of increasing amplitude.

Further clarification of the double-degenerate progenitor channel of Type Ia SNe requires the determination of the exact demographics of WD merger events—what is their occurrence frequency for different WD masses? It is further crucial to understand whether the explosion is triggered during the merger itself or, maybe, already during the inspiral phase when mass transfer between both WDs sets in. Even if only small amounts of mass are exchanged, the re-distribution of angular momentum can have a substantial impact on the orbital dynamics and therefore on the GW signal (Dan et al. 2011). **Post-LISA-launch objective** The LISA mission has great potential to contribute here and to provide important clues to the mechanism of Type Ia SN explosions. Ruiter et al. (2010) found that on the order of ~ 500 WD+ WD pairs—whose total mass exceeds the Chandrasekhar mass limit and will merge within a Hubble time—could be resolvable by LISA in our own Galaxy. While most likely no such systems will merge and give rise to a SN Ia during LISA's operation, much can be learned about SN Ia (and more generally transient) demographics from detecting these plausible progenitor systems.

1.7.1.7 Core-collapse and supernova kicks

Observations of compact objects, from pulsar proper motions (Hobbs et al. 2005) to compact binary properties (Dewi et al. 2005; Mirabel 2017), argue that many NSs and some BHs receive natal kicks during the collapse and explosion of the massive star that forms them. Asymmetries in the explosion mechanism, manifested either through asymmetries in the mass ejecta

(Wongwathanarat et al. 2013) or neutrino emission, have been studied as a source of these kicks. The different mechanisms (Lai et al. 2001) produce different predictions for the distribution of their magnitude (Scheck et al. 2006), their orientation with respect to the orbital angular momentum (Blaauw 1961), to the stellar spin (Wang et al. 2006; Noutsos et al. 2012; Wongwathanarat et al. 2013), and to the distribution of heavy elements (Wongwathanarat et al. 2013; Grefenstette et al. 2014). The asymmetries produced by strongly magnetized explosions are generally aligned with the angular momentum in the collapsing star (Sawai et al. 2008; Obergaulinger and Aloy 2020; Kuroda et al. 2020) and these mechanisms will produce kicks with directions aligned with the rotation axis, which typically is also aligned with the orbital angular momentum axis. Mechanisms produced by the large-scale convective eddies in the neutrino driven mechanism can produce kicks that are distributed more isotropically (Wongwathanarat et al. 2013; Müller et al. 2019).

Different kick mechanisms also predict different kick magnitudes as a function of the compact remnant mass (Tauris et al. 2017; Mandel and Müller 2020, and references therein). These kick distributions, in turn, predict different properties in compact object binaries (Voss and Tauris 2003; Lau et al. 2020). The NS kick properties can thus affect the number of NS+NS, BH+NS and BH+BH binaries detectable by LISA and LIGO/Virgo (Voss and Tauris 2003; Belczynski et al. 2016b; Vigna-Gómez et al. 2018; Kruckow et al. 2018; Giacobbo and Mapelli 2020; Lau et al. 2020), as well as EMRIs (Bortolas and Mapelli 2019).

For example, it has been demonstrated (Tauris et al. 2013, 2015) that ultra-stripped SNe are at work in close-orbit NS+NS and BH+NS systems that LISA and LIGO will eventually detect. The reason being that extreme stripping of the companion star by the accreting NS or BH during the last mass-transfer stage (Case BB RLO), produces an almost naked metal core prior to the second SN. This has an important effect on the magnitude of the kick added onto the newborn (second) NS, which affects the survival probabilities. It was argued qualitatively and quantitatively (Tauris et al. 2017) that the resulting kicks are often, but not always, small—depending on the mass of the collapsing metal core and thus on the resulting NS mass—which enhances the survival probability.

Post-LISA-launch objective The overall detection rate of Galactic NS+NS systems by LISA is thus directly affected by the magnitude of the kick, since a large kick can disrupt the binary during the SN. A large kick may also produce moderately more eccentric LISA NS+NS sources (Lau et al. 2020). The systemic velocity imparted by the two SN kicks displaces a binary from its birth position in the thin Galactic disc. LISA's ability to localise Galactic NS+NS sources on the sky to within a few degrees (Kyotoku et al. 2019; Lau et al. 2020) may therefore constrain the kick distribution by measuring the Galactic NS+NS scale height. By increasing the sample of observed compact binaries, LISA can thus be used to constrain the kick mechanism. In turn, this constrains the nature of SN explosions in binary system Podsiadlowski et al. (2004).

1.7.1.8 Neutron star equation of state
Matter in the interior of a NS is compressed to densities exceeding those in the centre of atomic nuclei, providing a unique

possibility to probe the nature of the strong interaction and to determine the NS composition. Via the EOS, matter properties determine the star's radius for a given mass (Lattimer and Prakash 2016; Özel and Freire 2016). Candidate EOSs can be tested by measuring the mass and radius for a NS or via the accurate measurement of a NS with a high mass because each EOS has a corresponding maximum allowed mass. Thus, finding a NS with a mass above the maximum allowed for an EOS rules out that EOS, and the radio measurement that PSR J0740+6620 has a mass of 2.14 solar masses rules out many EOSs (Cromartie et al. 2020). In addition, the Neutron Star Interior Composition Explorer (NICER) has enabled the measurement of the mass and radius for PSR 0030+0451. In particular, M/R is measured to 5%, but M and R separately are known to $\approx 10\%$ (Riley et al. 2019; Miller et al. 2019), and the uncertainties still do not allow for the determination of a unique EOS. STROBE-X and eXTP could do the same work as NICER to even to a larger distance. Masses provided by GW measurements would help dramatically, since for the pulsars observed using NICER the pulse profile fitting is mostly sensitive to M/R, and having data points with M and M/R measured well is much more valuable than just having M/R. With GW measurements, the determination of the tidal deformability for merging NSs is another measurable parameter that can constrain the EOS, as has been shown for GW170817 (Abbott et al. 2018a). Given the small number of constraining measurements to date, it is clear that additional EM measurements of pulsars and GW measurements of merging NSs are both necessary (Raaijmakers et al. 2020) to obtain conclusions that will affect our understanding of fundamental physics.

Post-LISA-launch objective Many binary systems with NSs produce GWs that will be detectable by LISA, leading to NS mass distributions for various binary populations, and some of these populations may have high mass NSs to further constrain the EOS. While NS+NSs are somewhat rare, binaries with a WD and a NS are expected to be plentiful. LISA will also detect binaries that are approaching mergers, and predicting mergers will allow for EM observations to be planned at the time of the merger. UV, optical, and near-IR observations to determine the remnant type and to constrain the mass and velocity of the ejecta will be very powerful for constraining the EOS (Coughlin et al. 2018; Margalit and Metzger 2019), especially with a facility like STROBE-X.

1.7.1.9 Disentangling formation environments based on LISA data

One of the exciting prospects of LISA observations is the possibility to disentangle the formation channels from compact sources in different environments based on their distinctive properties/demographics; most importantly isolated binary evolution in the Galactic disc or dynamical interactions in dense environments (e.g. open, globular and nuclear star clusters) or isolated triple evolution (Sect. 1.3). Whereas the majority of LISA binaries are expected to form in isolation (Sect. 1.4), several key properties, in particular orbital eccentricity and component masses, can reveal deviating birth environments. If LISA is able to constrain these source properties from the GW signal for a given resolved system, the formation channel for that particular system may be inferred. Here, we describe briefly ways these properties

may differ between different formation channels and describe applications to particular classes of binaries.

In general, BH and WD binaries that form as isolated systems through standard binary evolution processes are expected to be nearly circular by the time they enter the LISA frequency band. This is a consequence of the various dissipative forces expected to operate throughout the binary evolution that circularize the binary orbit, namely CE (Ivanova et al. 2013; Kruckow et al. 2016; Giacobbo and Mapelli 2018; Vigna-Gómez et al. 2020) and tidal interactions (Zahn 1977; Postnov and Yungelson 2014; Belczynski et al. 2020). In contrast, LISA binaries that formed dynamically in dense stellar environments may have relatively high eccentricities. In the dense star clusters, frequent dynamical encounters impart large eccentricities to binaries (Heggie and Hut 2003), whereas the formation of triple systems with an inner double compact object can reach high eccentricities via von Zeipel–Kozai–Lidov cycles (Antonini et al. 2016; Arca Sedda et al. 2021b; Rastello et al. 2019; Martinez et al. 2020), which induce a secular variation of the inner binary eccentricity (von Zeipel 1910; Kozai 1962; Lidov 1962).

Dynamically formed binaries are expected to feature several distinct sub-classes of formation channels that may also be distinguished by their eccentricities. In order of increasing characteristic formation frequency, these dynamical sub channels include: binaries dynamically *ejected* from their host cluster that merge as isolated binaries ($f_{\mathrm{GW}} \approx 10^{-5}$ Hz), binaries that merge *in cluster* between strong dynamical encounters ($f_{\mathrm{GW}} \approx 10^{-3}$ Hz), and finally binaries that merge in cluster through *GW capture* during single–single ($f_{\mathrm{GW}} \approx 10^{-1}$ Hz) or few-body dynamical encounters encounters ($f_{\mathrm{GW}} \approx 1$ Hz) (Breivik et al. 2016; Banerjee 2018; Kremer et al. 2018a; Samsing and D'Orazio 2018; D'Orazio and Samsing 2018; Arca Sedda et al. 2021b; Samsing and D'Orazio 2019; Kremer et al. 2019b; Zevin et al. 2019b; Banerjee 2020; Arca Sedda et al. 2020b). **Post-LISA-launch objective** Binaries formed through the ejected and in-cluster merger channels are expected to have eccentricities at GW frequencies of 10^{-2} Hz of roughly 10^{-3} and 10^{-2}, respectively, which are expected to be measurable by LISA (Nishizawa et al. 2016). Furthermore, the likelihood of an eccentric merger is dependent on the eccentricity and orbital separation of the outer perturber's orbit and the mutual orientation of the outer and inner orbit (Liu and Lai 2018; Arca Sedda et al. 2021b). Since the typical binary architecture can be connected with the cluster structure, in terms of either mass and radius or velocity dispersion, the detection of binaries with given orbital properties can carry insights on the type of cluster that harboured the merger.

In nuclear star clusters and, more in general, galactic nuclei, the formation and evolution of compact binaries can be substantially affected by the presence of an MBH (Lee 1995; Blaes et al. 2002; Miller and Lauburg 2009; Arca Sedda 2020a). MBHs are not only a common occurrence in nuclear star clusters (e.g., Graham and Driver 2007; González Delgado et al. 2008), but their masses are correlated (Graham and Spitler 2009; Scott and Graham 2013; Graham 2016a). The binary can develop ZKL oscillations as a result of secular perturbations exerted by the MBH tidal field (Antonini and Perets 2012; Hoang et al. 2018; Fragione et al. 2019; Arca Sedda 2020a). Up to 40% of binaries undergoing ZKL oscillations in galactic nuclei transit

into the LISA band with an eccentricity > 0.1 (Arca Sedda 2020a). LISA has the potential to measure the eccentricity oscillations driven by an MBH onto a stellar BH+BH binary out to a few Mpc (Hoang et al. 2019) thus offering a unique way to probe the KL mechanism in galactic nuclei and to disentangle this sub-channel of the dynamical formation scenario. **Post-LISA-launch objective** Thus, if measurable by LISA, eccentricities (or lack thereof) may serve as a strong fingerprint pointing toward the specific formation channel (Breivik et al. 2016; Nishizawa et al. 2017; Randall and Xianyu 2019a; Kremer et al. 2019b).

In the case of NS binaries, NS natal kicks (e.g., Hobbs et al. 2005) may result in high-eccentricities for binaries that form through isolated binary evolution. In this case, eccentricity may no longer be useful for distinguishing between the dynamical and isolated formation channels. However, even in this case, dynamical and disc binary NSs may still have distinguishable eccentricity distributions that can potentially be differentiated with LISA (Andrews et al. 2020).

Although rare, dynamically-formed NS+BH systems represent a class of GW sources that potentially offer the widest range of peculiarities compared to the isolated channel in terms of total mass, primary mass, and high eccentricity at mHz frequencies (Arca Sedda 2020b). Isolated NS+BH systems (Kruckow et al. 2018) are mostly characterised by BHs with masses of $6-10\,M_\odot$ at high, Milky Way-like metallicity ($Z = 0.0088$), or BH masses of $10-25\,M_\odot$ at low metallicity, ($Z = 0.0002$), and nearly zero eccentricity at merger (Giacobbo and Mapelli 2018). Dynamical formation of these systems is not generally relevant for isolated LISA sources in the Milky Way, but in globular and nuclear clusters up to 50% of dynamically formed compact NS+BH feature BH masses $> 10\,M_\odot$, and a large probability ($\sim 50\%$) will have an eccentricity > 0.1 when transiting into the mHz frequency band of LISA (Arca Sedda 2020b).

In general, GW sources forming through dynamical channels may contain compact objects with masses that differ or that are even not expected to form at all from isolated binary evolution of Galactic disc sources. For instance, BHs with masses between $\sim 55\,M_\odot - 120\,M_\odot$ are not expected to form from the evolution of single massive stars due to pair-instability SNe (Woosley et al. 2007; Fryer et al. 2012; Belczynski et al. 2016a; Spera and Mapelli 2017; Farmer et al. 2019; Woosley and Heger 2021). This range has been described as the upper-mass-gap for BHs. It may be possible to form binaries containing BHs in this mass range through dynamical processes in stellar clusters (Di Carlo et al. 2020a). One channel to form such BHs could be through hierarchical mergers of stellar-mass BHs in nuclear and globular clusters (Miller and Hamilton 2002b; Rodriguez et al. 2019; Arca Sedda et al. 2020b; Arca Sedda 2020a; Samsing and Hotokezaka 2021; Mapelli et al. 2021). Hierarchical mergers are most likely to happen in the densest stellar clusters with the highest escape velocities, such as nuclear star clusters, as these clusters can retain the binary despite the GW recoil kick from the merger (Fragione et al. 2018; Antonini et al. 2019; Fragione and Silk 2020; Neumayer et al. 2020; Arca Sedda 2020a). In these extreme environments, binaries at formation are tighter, on average, than in normal clusters, and the interactions with flyby stars and the possible long-term effect of a central MBH can boost stellar collisions and BH mergers, thus possibly inducing a significant modification of the BH mass spectrum. Another possibility to form more massive BHs could be through collisional

runaway mergers of BH progenitors in dense star clusters (Portegies Zwart and McMillan 2002; Portegies Zwart et al. 2004; Freitag et al. 2006b, a; Giersz et al. 2015; Mapelli 2016; Di Carlo et al. 2020a; Kremer et al. 2020a).

Post-LISA-launch objective Such runaway mergers and collisions in dense clusters can also lead to the formation of IMBHs in the mass range 10^2–$10^4 \, M_\odot$ (Ebisuzaki et al. 2001; Portegies Zwart et al. 2006; Gürkan et al. 2006; Amaro-Seoane et al. 2007; MacLeod et al. 2016b; Arca Sedda and Mastrobuono-Battisti 2019; Askar et al. 2021; Hong et al. 2020; Arca Sedda et al. 2020b; Mapelli et al. 2021), and mergers of IMBH+IMBH with component masses in the range 10^3–$10^4 \, M_\odot$ can be observed with LISA up to redshift $z \lesssim 3$ (Arca Sedda and Mastrobuono-Battisti 2019; Arca Sedda et al. 2020a, 2021a; Jani et al. 2019). The number and characteristics of BHs in the upper mass-gap could shed a light on the relative contribution of dynamically-formed or isolated sources to the overall population of BH+BH mergers.

Lastly, the evolution of isolated triples can also lead to a mass distribution that deviates from that of isolated binary evolution. This is mainly due to two effects. Firstly, to form a LISA source, isolated binary evolution relies on one or more mass-transfer phases that reduce the orbital period (Sect. 1.3) down to the range observable by LISA. Mass transfer can also occur in triples (even a larger fraction of triples experiences RLO; Toonen et al. 2020) (Sects. 1.2.4.4 and 1.3.3), however orbital shrinkage can also be achieved by the combination of three-body dynamics with dissipative processes. The increased eccentricities during von Zeipel–Kozai–Lidov cycles reduce the GW inspiral time (e.g. Thompson 2011; Antonini et al. 2017; Rodriguez and Antonini 2018; Fragione and Loeb 2019). Moreover, if a star does not fill its Roche lobe, and does not lose its envelope prematurely, it typically will form a more massive remnant compared to the case of RLO mass stripping. Such triples will on average contain stars that are more massive than those formed through isolated binary evolution (Hamers et al. 2013; Toonen et al. 2018), and will not contain He-core WDs (which have masses $\lesssim 0.45 M_\odot$ which can only be formed in a Hubble time through mass stripping). Secondly, similar to the evolution in star clusters, sequential mergers in multiples give rise to higher stellar masses (Safarzadeh et al. 2020a; Hamers and Safarzadeh 2020; Lu et al. 2020). In addition, the effect of a tertiary perturber can induce precession of the spins and lead to spin misalignment (Antonini et al. 2018; Liu and Lai 2018; Rodriguez and Antonini 2018).

1.7.2 LISA sources as galactic probes

Coordinators: **Valeriya Korol**

Contributors: **Valeriya Korol, Raffaella Schneider, Luca Graziani, Astrid Lamberts, Samuel Boissier, Martyna Chruslinska, Alberto Sesana, Katelyn Breivik, Shane Larson, Michela Mapelli**

Stellar binaries detectable by LISA bear the imprint of the properties of their native stellar environments (galaxies and stellar clusters) such as the total stellar mass, IMF,

star formation history (SFH), age and metallicity (Z). These properties can be investigated by combining binary population synthesis (BPS) models (Sect. 1.6.3) with models of galaxy formation and evolution. Several methods have been developed to achieve this goal. The combination of BPS models with theoretical semi-analytic or observationally inferred cosmic star formation rate densities provides a fast way of predicting the evolution of the overall birth and merger rates with redshift (Schneider et al. 2001; Regimbau 2011; Marassi et al. 2011; Dominik et al. 2013; Belczynski et al. 2016a; Dvorkin et al. 2016b; Lamberts et al. 2016; Elbert et al. 2018; Chruslinska and Nelemans 2019; Boco et al. 2019). In particular, observation-based approaches allow one to account for the current observational uncertainties on the birth metallicity distribution of stars forming over the cosmic history and evaluate the related uncertainty on the predicted properties of mergers (e.g. Chruslinska and Nelemans 2019). A detailed understanding of the properties of galaxies hosting GW sources can be gained from cosmological simulations, which provide a detailed description of the cosmic star formation in a more accurate context of the galaxy evolution. Galaxy catalogues from the Illustris (Vogelsberger et al. 2014), GASOLINE (Stadel 2001; Wadsley et al. 2004), EAGLE (Schaye et al. 2015) simulations have been used for predicting NS+NS and BH+BH mergers (e.g. Mapelli et al. 2017; O'Shaughnessy et al. 2017; Artale et al. 2019). Similarly, the Latte simulation of Milky Way-like galaxies of the FIRE hydrodynamical simulation project (Hopkins et al. 2014; Wetzel et al. 2016) was adopted to study the properties of Galactic WD+WDs and BH+BHs accessible to LISA (Lamberts et al. 2018, 2019). Alternative hybrid pipelines such as GAMESH (Graziani et al. 2015, 2017; Graziani 2019), combining a dark matter simulation with semi-analytic star formation, chemical enrichment and numerical radiative transfer, represent an advantageous alternative to study the redshift evolution of compact binaries along the assembly of a Milky Way-like galaxy and in its local volume dwarf satellites (Schneider et al. 2017; Marassi et al. 2019; Graziani et al. 2020).

Effect of the IMF The IMF is one of the key ingredients in the BPS that sets the distribution of initial masses and the relative proportions of stars forming in different mass ranges. Therefore it has a direct impact on the observed merger rates and properties of the LISA sources. Studies often adopt the IMF inferred from the observations of stars in the local Galactic neighborhood (e.g. Kroupa 2001; Chabrier 2003). However the universality of this assumption is one of the fundamental open questions in astronomy and is still debated (e.g. Bastian et al. 2010). Theoretical studies show that with the assumption of the Milky Way-like IMF one may underestimate the number of WD and NS progenitors forming at redshifts $\lesssim 1$, especially at low metallicities (Chruślińska et al. 2020), and, therefore, underestimate the predicted number of individual LISA detections and background/foreground noise.

Post-LISA-launch objective LISA's observations of stellar remnants—invisible to EM observatories—will offer us an alternative way of probing the IMF. For instance, hundreds of Galactic WD+WDs with measured chirp mass (Rebassa-Mansergas et al. 2019) can be used to constrain the low-mass end of the IMF in different Galactic habitats. In addition, numerous LISA detections in the Magellanic
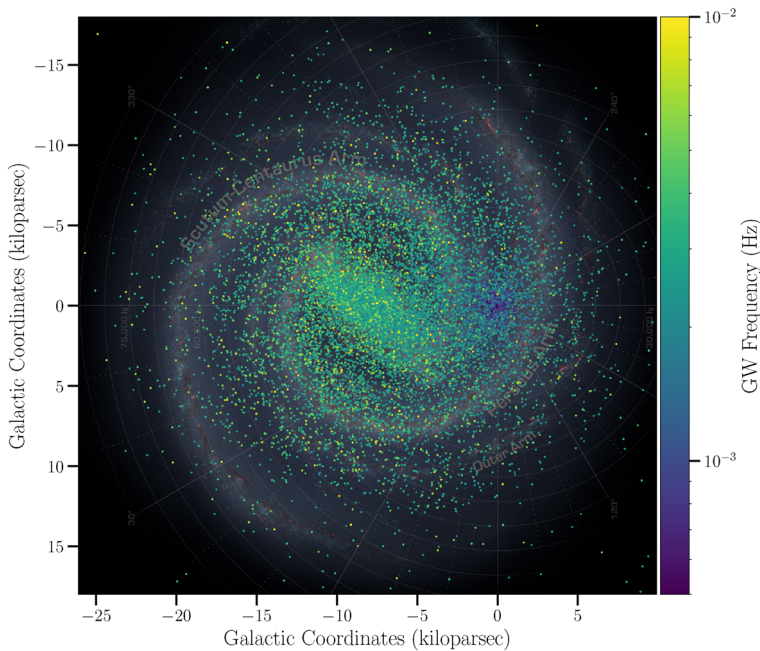
Fig. 15 Numerous WD+WDs detectable by LISA will enable the mapping of our Galaxy. In the background the artist impression of our current view of the MW. Over-plotted in colour WD+WD with SNR > 7 from Wilhelm et al. (2021). LISA's position is at (0, 0). The selection effect due to GW frequency in visible in colour. Image credit: Valeriya Korol

Clouds will enable the studies of the IMF with GWs in alternative environments (Korol et al. 2020).

Effect of metallicity The metallicity is another important assumption of the models that affects different types of stellar binaries in different ways (Chruslinska et al. 2019). The predicted metallicity dependence of the formation efficiency of merging BH/NS binaries is a complex function of numerous poorly constrained phases of binary evolution. Specifically, BH+BH mergers resulting from isolated stellar evolution are typically found to form much more efficiently at low metallicity ($\lesssim 0.1$–$0.3\,Z_\odot$) than at solar metallicity (Belczynski et al. 2010b; Eldridge and Stanway 2016; Stevenson et al. 2017b; Schneider et al. 2017; Klencki et al. 2018; Giacobbo et al. 2018). The differences in formation efficiency reach up to two orders of magnitude and consequently, the size of the observable BH+BH population is sensitive to the amount of star formation happening at low metallicity (Dominik et al. 2013; Mapelli et al. 2017; Marassi et al. 2019; Chruslinska et al. 2019; Neijssel et al. 2019; Graziani et al. 2020; Santoliquido et al. 2020, 2021). Furthermore, the most massive BH+BH are expected to form at low metallicity and their mass distribution could potentially be linked to the metallicity distribution of their progenitors. Metallicity dependence of the formation efficiency of NS+NS mergers is typically found to be much weaker than for BH+BH, with the mixed systems falling in between. For the case of WD+WD, the metallicity mainly changes the total number
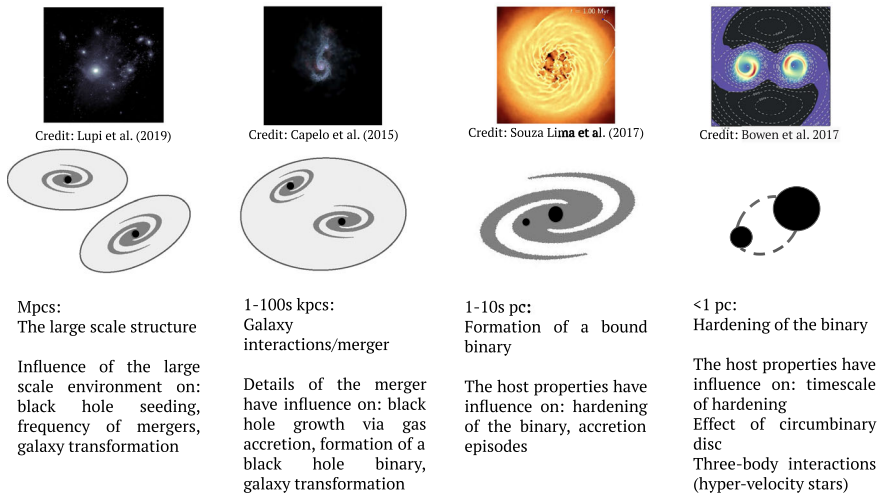
of WD+WDs by allowing lower masses for a star to reach the WD stage in a Hubble time with decreasing metallicity. This results in a moderate increase (few tens of percents) in the number of resolved LISA sources (Yu and Jeffery 2010; Korol et al. 2020).

Effect of star formation histories The merger rate of compact stellar binaries across cosmic time is a direct consequence of the SFH (Madau and Fragos 2017; Artale et al. 2019; Dominik et al. 2013; Mapelli et al. 2017; Mapelli and Giacobbo 2018; Vitale et al. 2019; Neijssel et al. 2019; Santoliquido et al. 2020). Together with BPS models, SFH regulates the content of stellar binaries in the LISA band at a given time. Galactic WD+WDs can be used as a tool to study the SFHs of the MW components: due to the different timescales to reach the mHz frequencies, WD+WDs of different core composition dominate different parts of the Galaxy due to their distinct SFHs. Specifically, double He-core WDs with formation times that can exceed 10 Gyr populate the Galactic bulge, thick disc and stellar halo; double C/O-core WDs, typically form on timescales shorter than 2 Gyr and are associated with a much younger populations present in the thin disc; mixed He-C/O-core binaries present an intermediate distribution (Yu and Jeffery 2010; Lamberts et al. 2019). In addition, SFH has significant effects on the LISA detection rates in the Milky Way satellites (Korol et al. 2020).

Structure of the Milky Way with resolved and unresolved sources It is expected that the Galactic GW population at mHz frequencies will be largely dominated by WD+WDs and will have two components in the LISA data: population of high-frequency individually resolved binaries and unresolved stochastic foreground from low-frequency binaries (Sect. 1.6.2). Both resolved and unresolved WD+WDs encode global properties of Galactic stellar populations, and can thus be used as a tool to study the Milky Way's stellar content and shape.

Post-LISA-launch objective Affected by different selection biases than EM observatories, LISA can probe the entire volume of the Milky Way and therefore will facilitate detailed studies of its the far side (Fig. 15). Moreover, unaffected by the dust extinction and stellar crowding, LISA can also probe the inner Galaxy at all latitudes. For several thousands WD+WDs measurements of the sky positions and distances will enable the mapping of the Galaxy. Reconstructed density profiles of WD+WDs will provide unbiased constraints on the scale length parameters of Galactic bulge/bar and disc that are both accurate and precise, with statistical errors of a few % to 10% level (Adams et al. 2012; Korol et al. 2019; Wilhelm et al. 2021). The Galactic stellar halo is also expected to host up to a few thousand WD+WDs, and therefore can potentially be studied with WD+WDs in a similar way (Ruiter et al. 2009; Yu and Jeffery 2010; Lamberts et al. 2019). Furthermore, the LISA sample is found to be sufficient to disentangle between different commonly used disc density profiles, by well covering the disc out to sufficiently large radii. The stellar bar will also clearly appear in the GW map of the bulge. LISA's WD+WDs can accurately characterise the bar's physical parameters: length, axis ratio and orientation angle with respect to the Sun's position (Wilhelm et al. 2021). However, because of the low density contrast compared to the background disc, the spiral arms will be elusive to LISA. Finally, building upon the analogy with simple stellar population models used for inferring stellar masses of galaxies based on their total

Credit: Lupi et al. (2019)　　Credit: Capelo et al. (2015)　　Credit: Souza Lima et al. (2017)　　Credit: Bowen et al. 2017

Mpcs:
The large scale structure

Influence of the large scale environment on: black hole seeding, frequency of mergers, galaxy transformation

1-100s kpcs:
Galaxy interactions/merger

Details of the merger have influence on: black hole growth via gas accretion, formation of a black hole binary, galaxy transformation

1-10s pc:
Formation of a bound binary

The host properties have influence on: hardening of the binary, accretion episodes

<1 pc:
Hardening of the binary

The host properties have influence on: timescale of hardening
Effect of circumbinary disc
Three-body interactions (hyper-velocity stars)

Fig. 16 A schematic view of the complex and multi-scale processes affecting the formation of a hard MBH binary system. Image credit: Silvia Bonoli and Alessandro Lupi

light, the total stellar mass of the Galaxy can be estimated from the number of LISA events. Using a simplified example of Milky Way satellites, Korol et al. (2021) showed that based on BPS models of LISA sources satellite masses can be recovered within (1) a factor two if the SFH of the satellite is known and (2) within an order of magnitude even when marginalising over alternative SFHs. When also accounting for the unresolved Galactic foreground, this method could be extended for measuring the total stellar mass of the Milky Way.

Post-LISA-launch objective The power of constraining the overall properties of the Galactic potential will be significantly enhanced by using LISA detections in combination with EM observations of binaries motions. BPS studies forecast up to 150 detached and interacting WD+WDs detectable through both EM and GW radiation (e.g. Korol et al. 2017; Breivik et al. 2018, see also Sect. 1.4). For these multi-messenger binaries 3D positions provided by LISA can be combined with proper motions—for example, provided by Gaia or Vera Rubin Observatory—into the rotation curve, which allows the derivation of the stellar masses of the Galactic baryonic components (Korol et al. 2019).

The unresolved Galactic foreground will provide complementary constraints on the Galactic structure. For example, the Galactic foreground will show whether the WD+WD population traces the spatial distribution of young, bright stars (and thus do experience significant kicks), or traces a vertically heated spatial distribution associated with Galaxy's oldest stellar populations. This can be understood from the shape of Galactic power spectral density that depends on the characteristic scale height of the WD+WD population (Benacquista and Holley-Bockelmann 2006). **Post-LISA-launch objective** In addition, using the spherical harmonic decomposition of the LISA data streams, the structure of the disc population of Galactic WD+WDs can be constrained with an accuracy of 300 pc (Breivik et al. 2020b). The

relative poor resolution compared with the resolved sources is a direct consequence of LISA's poor spatial resolution at low frequencies. Nevertheless, an independent measurement at low frequencies will either help to confirm the structure of the resolved sources or point to frequency-dependent Galactic structure.

2 Massive black hole binaries

Coordinators: **Elisa Bortolas, Pedro R. Capelo, Melanie Habouzit**

Reviewers: **Laura Blecha, Massimo Dotti, Zoltan Haiman**

2.1 Introduction

Contributors: **Elisa Bortolas, Pedro R. Capelo, Melanie Habouzit**

The observed BH mass spectrum spans ten orders of magnitude, ranging from a few $M_\odot$ of stellar-mass BHs to more than $10^{10}\,M_\odot$ for the most extreme MBHs. Our knowledge of the mass spectrum has expanded over the past decade. On the low-mass end, the GW facilities Laser Interferometer Gravitational-wave Observatory (LIGO) and Virgo have observed the mergers of low-mass BHs in the range ~ 6–$80\,M_\odot$ (Abbott et al. 2020c). At the high-mass end, we have discovered in the high-redshift Universe extremely bright objects, called quasars, powered by MBHs with masses similar to those of the most massive MBHs around us ($M_{\mathrm{BH}} \geqslant 10^8\,M_\odot$ at $z > 6$, e.g. Mortlock et al. 2011; Bañados et al. 2018b; Yang et al. 2020a). LISA has the ability to detect MBHs of $M_{\mathrm{BH}} = 10^3$–$10^7\,M_\odot$ through the last stages of in-spiral and merger up to $z \sim 20$, bridging these extremes of the mass spectrum.

The mass-redshift regime that LISA can probe is key to constraining the origin and growth of MBHs, and is one of LISA's main science goals. Considering the current state of observations, theory, and simulations, we still do not know how MBHs form and evolve in the early Universe. We do not know how they assemble with time and become present in almost all the galaxies in the local Universe, from dwarf galaxies (with stellar masses of $\leqslant 10^{9.5}\,M_\odot$, e.g. Mezcua and Domínguez Sánchez 2020; Greene et al. 2020; Chilingarian et al. 2018; Mezcua et al. 2018; Baldassare et al. 2015; Reines et al. 2013) to large ellipticals (e.g. Magorrian et al. 1998; Gültekin et al. 2009; McConnell et al. 2011; Kormendy and Ho 2013; Graham 2016b; Davis et al. 2019a; Sahu et al. 2019a). LISA observations will play a key role in addressing these enigmas. In this section, we only discuss MBHs, which we define as BHs with $\gtrsim 100\,M_\odot$. Additionally, we do not make an explicit distinction within that range, i.e. we do not distinguish between intermediate-mass BHs, massive black holes, and supermassive BHs.

In the hierarchical paradigm of galaxy formation, we expect central MBHs to coalesce after the merger of their host galaxies. As shown in Fig. 16, MBHs will have to cross an impressive range of scales, from when they are hosted in separate galaxies at early times to the end of their dance, when they coalesce with each other

(Begelman et al. 1980; Milosavljević and Merritt 2001; Dullo and Graham 2014). Following a galaxy merger, while MBHs are still separated by kpc to tens of kpc scales, they will start losing orbital energy and angular momentum via gravitational drag from background gas and stars, causing them to sink to the centre of the remnant galaxy (a process referred to as dynamical friction). On $\lesssim$ pc scales, the MBHs will form a gravitationally-bound binary and evolve further via interactions with gas and individual stars (the so-called binary hardening phase). This may include interactions with a circumbinary disc on $\sim 10^{-3}$ pc scales. Finally, the MBHs enter the last stage of the dance, i.e. the GW regime ($\leqslant 10^{-5}$ pc scale).

To maximize the scientific return of LISA, advances are needed in our theoretical understanding of MBH formation, dynamics, and evolution, a field of research that started in the 1980s (Begelman et al. 1980). Building powerful tools such as semi-analytical models, N-Body and hydrodynamic simulations is crucial to predict the MBH mergers that LISA will detect as a function of the intrinsic properties that describe both the MBH and galaxy. Currently, the predicted MBH merger rate spans more than one order of magnitude, from a few LISA detections per year to tens. Rate predictions depend on computational methods, and on the modelling of the relevant physics. In the coming years we will improve on the dynamical range of scales that we can resolve, and address how different mechanisms of MBH formation, galaxy environments, MBH growth models, and MBH dynamics can shape the merger rates of MBHs, thus paving the way for the interpretation of LISA data.

In the near future, several space missions will be launched with the goal of constraining the formation and evolution of MBHs and their environments. These missions will complement LISA in the EM domain, and will provide unprecedented constraints on the entire population of MBHs. The James Webb Space Telescope (JWST; Gardner et al. 2006) and the Roman-Wide Field Infra-red Survey Telescope (Spergel et al. 2015) will image the first galaxies (e.g. Williams et al. 2018), the cradles of the first MBHs. The assembly of galaxies will also be witnessed by the new thirty-meter telescopes such as E-ELT, TMT, and GMT. New X-ray facilities such as Athena (Nandra et al. 2013), as well as the LynX (The Lynx Team 2018) and AXIS (Mushotzky 2018) concept missions, will aim at uncovering the population of accreting young MBHs at high redshift ($z > 6$).

With LISA and the aforementioned new instruments working in the EM domain, we will enter the new multimessenger era for MBHs. By performing synergistic observations that combine low-frequency GW signals with EM signals from the same source, we will uncover previously unavailable information. These combined observations will precede, accompany, or follow, the MBH merger events, helping us to constrain MBH activity, understand their immediate surroundings (e.g. the nature of the accretion disc, jets, and the accreted/ejected material), and its relation with the host galaxy. One challenge of multimessenger observations is the localization of the sources, and the confirmation that they are indeed MBH binaries. Before the launch of LISA, we will have to better understand, among other aspects, how the different potential observational EM signatures of coalescing systems are originated, and develop new analysis tools to identify these GW source candidates in large datasets.
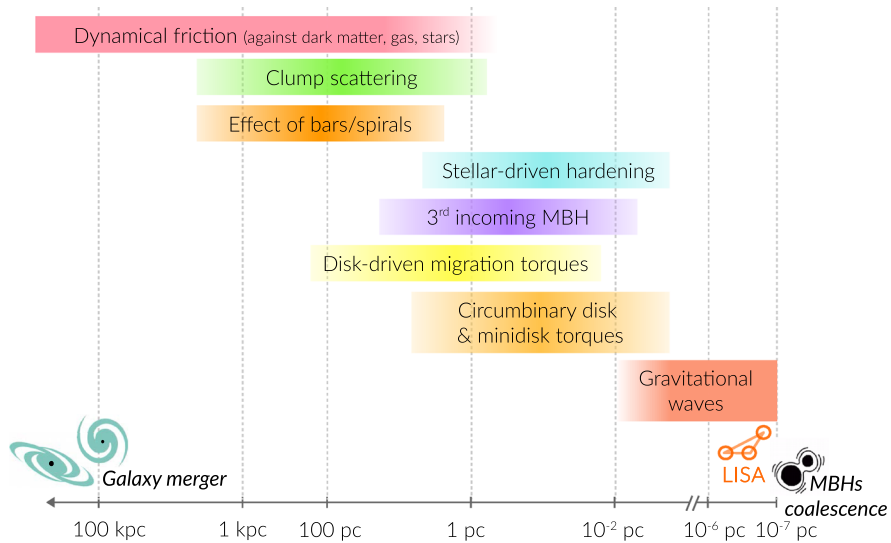
Fig. 17 Illustration of the physical processes affecting two coalescing MBHs after the merger of their host galaxies. The cartoon reports the typical physical scales associated to each process for a nearly equal mass MBH pair of about $10^6 M_\odot$. Scales vary depending on the exact mass, mass ratio and host galaxy properties. These physical processes are described in Sects. 2.2.1.1, 2.2.1.2 (dynamical friction); Sect. 2.2.1.3 (clump scattering, effect of bars/spirals); Sect. 2.2.2.1 (stellar-driven hardening); Sect. 2.2.2.4 (3rd incoming MBH); Sect. 2.2.2.2 (disc-driven migration torques; circumbinary disc and minidisc torques); Sect. 2.2.3 (gravitational waves). Image credit: Elisa Bortolas

LISA will also constitute a bridge between the two GW frequency regimes that are already being investigated: the highest GW frequencies (LIGO/Virgo/KAGRA), and the lowest GW frequencies which build the GW background (observed by Pulsar Timing Arrays; PTAs). In the coming years, we will have to fully exploit these missions to, e.g. select, monitor, confirm and characterise MBH binaries (MBHBs), but also understand their small-scale to galactic and large-scale environments, and how they fit within the full MBH population.

Sections 2.2 and 2.3 review the theoretical background and highlight pre-launch objectives for the LISA community that can sharpen our preparation for the mission. Section 2.4 distills the theoretical picture into LISA's observables and highlights uncertainties. The pre-launch objective is to compare different approaches to obtain realistic predictions that can be used, post-launch, to interpret LISA's data. The pre-LISA theoretical development is of paramount importance because the expectation is that LISA's event properties will be compared to theoretical models through a Bayesian framework in order to perform astrophysical inference (Sesana et al. 2011a). Section 2.5 focuses on EM signatures of MBHs, highlighting both pre-launch (improve theoretical models, search for EM emission from MBHBs) and post-launch (devise strategies for searches of EM counterparts to MBHBs detected by LISA) objectives. Finally, Sect. 2.6 shows how LISA's results can be strengthened by complementary campaigns performed by different instruments and facilites,

straddling pre-launch and post-launch objectives dependent on whether missions overlap or not.

2.2 MBHs and their path to coalescence

Coordinators: **Matteo Bonetti, Hugo Pfister**

Contributors: **Emanuele Berti, Tamara Bogdanovic, Elisa Bortolas, Pedro R. Capelo, Monica Colpi, Pratika Dayal, Massimo Dotti, Alessia Franchini, Davide Gerosa, Zoltan Haiman, Peter Johansson, Fazeel Mahmood Khan, Giuseppe Lodato, Lucio Mayer, David Mota, Vasileios Paschalidis, Alberto Sesana, Nicholas C. Stone, Tomas Tamfal, Marta Volonteri, Lorenz Zwick**

There is observational evidence that a significant fraction of galaxies host MBHs in their centres (Kormendy and Ho 2013), and at least some of them harbour an MBH since the dawn of structure formation (e.g. Bañados et al. 2014; Wu et al. 2015; Bañados et al. 2018b). This, combined with the notion that galaxies aggregate via repeated mergers of smaller structures (Fakhouri et al. 2010; O'Leary et al. 2021), leads to the conclusion that a number of MBHBs should have formed across cosmic epochs, and that their ultimate coalescence phase could be observed by LISA (e.g. Klein et al. 2016; Dayal et al. 2019; Chen et al. 2020b; Barausse et al. 2020b; Valiante et al. 2021; Bonetti et al. 2019).

The exact number of detectable MBHB mergers and their properties (Sect. 2.4) will depend on still poorly understood parameters, such as the low-mass end of the MBH mass function and their seeding mechanism (Sect. 2.3), or the host galaxy structure and environment. However, as a start, we can try to address the following questions for MBHs in the LISA mass-redshift range: *(i)* What are the mechanisms which bring two MBHs in distinct galaxies separated by tens of kpc close enough, so that they emit GWs and merge when they are at separations of the order of their gravitational radii, $\sim 10^{-6}\,(M_{\mathrm{BH}}/10^7 M_\odot)$ pc? *(ii)* Given the variety of galaxy types, MBH masses, and orbits they can have, are these mechanisms always efficient enough that a galaxy merger results in an MBH merger within the age of the Universe? We begin by considering two galaxies with a range of properties hosting an MBH in their centre. We will then describe the different steps that may or may not lead to the MBH merger following the merger of the two galaxies.

In a seminal work, Begelman et al. (1980) were the first to explore the dynamics of MBH pairs in merging galaxies. In their study they highlighted the occurrence of three steps, which we will use as the foundation of this section: the initial *dynamical friction phase* (Sect. 2.2.1; kpc scale), when MBHs and their hosts sink toward the centre of the remnant galaxy losing orbital energy and angular momentum until they

---

[4] The Coulomb term Λ is the ratio of the maximum and minimum relevant impact parameters for encounters between stars in the background, and the perturber. Λ is often estimated as the ratio of two global quantities characterizing the system: for example, the mass of the galaxy over the mass of the MBH, or the mass of the MBH over the mass of individual stars, with the first choice being more applicable to systems comprising both stars and dark matter.

are gravitationally bound and form a binary; the *binary hardening phase* (Sect. 2.2.2; pc scale), when the binary mainly interacts with single stars and/or gas; and finally the *relativistic phase* (Sect. 2.2.3; mpc scale), when the dynamics is dominated by GW emission.

Throughout the years, this initial picture has been enriched by many different aspects, highlighting different astrophysical regimes for MBH orbital decay determined by the nature of the galactic environment, with associated different times-cales which depend on the MBHs mass, mass ratio, mass distribution and thermodynamics in the galactic nucleus etc. (see Fig. 17). Below we focus on the recent developments on the aforementioned stages of the orbital decay, and we highlight the prospects for future research in the context of the science relevant to LISA. We refer the reader to the many existing reviews for a more complete presentation of the topic (e.g. Mayer 2013; Colpi 2014; Dotti et al. 2012; De Rosa et al. 2019b).

2.2.1 The galaxy merger and the large-scale orbital decay at kpc scales

In order to make forecasts for the LISA event rates the first step is to quantify robustly the range of decay time-scales at kpc scales, where the BH pair is expected to spend most of its time.

2.2.1.1 Dynamical friction in collisionless media

When a massive perturber, such as an MBH, with mass $M_{\rm BH}$ moves in a medium composed of collisionless particles (stars or dark matter, DM) with masses $m_\star \ll M_{\rm BH}$, it deflects such particles from their unperturbed trajectories. As a result a trailing overdensity is generated, often referred to as "wake", which then pulls the perturber towards it owing to its gravitational force, namely it causes a deceleration directed opposite to its motion. Such drag force is the so-called dynamical friction (Chandrasekhar 1943). Under the assumption of an infinite homogeneous medium with density ρ, if the background is characterized by an isotropic Maxwellian velocity distribution with velocity dispersion σ, Chandrasekhar (1943) showed the force acting on the perturbing body is:

$$\mathbf{F}_{\rm DF} \propto -M_{\rm BH}^2 \rho \mathcal{G}\left(\frac{v}{\sigma}\right) \ln \Lambda \frac{\mathbf{v}}{v^3} \,, \tag{7}$$

where v is the perturber velocity relative to the surrounding background, $\ln \Lambda \sim 10$ is the Coulomb logarithm[4] and the function $\mathcal{G}(x), x = v/\sigma$ depends on the underlying velocity distribution; if the latter is Maxwellian, as typically assumed, $\mathcal{G}(x)$ scales as x^3 for $x \ll 1$ and as ~ 1 for $x \gtrsim 2$. When Eq. (7) is applied locally to the case of an MBH moving on a circular orbit of radius r in the stellar background of a singular isothermal sphere ($\rho \propto \sigma^2 r^{-2}$), a calculation (Binney and Tremaine 1987) shows that the orbital decay of $M_{\rm BH}$ occurs on a time-scale

$$\tau_{DF} \approx \frac{8\,\text{Gyr}}{\ln \Lambda} \left(\frac{r}{\text{kpc}}\right)^2 \frac{\sigma}{200\,\text{km/s}} \frac{10^7 M_\odot}{M_{BH}}. \tag{8}$$

If we assume MBHs at kpc scale separations and a $10^6\,M_\odot$ black hole in a galaxy with $\sigma = 100$ km/s, this calculation shows that dynamical friction plays an important role in causing a rapid sinking of MBHs with masses in the range accessible to LISA as the process can take less than a Hubble time (in the early stage of a galaxy merger, M_{BH} may be replaced by the mass of a residual galactic core embedding the MBHs, resulting in much shorter time-scales, Yu and Tremaine 2002). Two $10^6\,M_\odot$ black holes are indeed expected to bind gravitationally and form a binary once their separation is reduced to a few pc. In the following, we detail how this simplified picture is enriched when some of the assumptions made above are relaxed. Overall, more complex dynamics lead to a much broader range of time-scales than expected based on the previous discussion, and render the formation of a binary a more uncertain outcome.

  • **Global asymmetries**

The description of dynamical friction given above implies that the drag is local, caused by the overdensity trailing the perturber, thus it neglects the global exchange of orbital angular momentum and energy between the MBH and the host system. Global asymmetries triggered in the mass distribution of the host system (called *modes*; see, e.g. Tremaine and Weinberg 1984; Weinberg 1986, 1989) can give rise to global torques, and these can be enhanced at resonances between the perturber's orbital frequency and the orbital frequency of the background matter. Owing to new observational data (Gaia Collaboration et al. 2018b), as well as recent theoretical (Hamilton and Heinemann 2020) and numerical work (Garavito-Camargo et al. 2019; Cunningham et al. 2020; Tamfal et al. 2021; Garavito-Camargo et al. 2021), the global halo mode theory has gained renewed attention. Accounting for the corrections to the dynamical friction time-scale introduced by global torques is likely important in order to provide robust estimates of the initial phase of black hole binary formation and sinking. Studies specifically for LISA MBHBs are required to ultimately assess the importance of these processes in the context of LISA's science.

  • **Power-law density profiles: cusps and cores**

The assumption of an isothermal sphere used to derive Eq. (8) is also a simplification: all real galaxies feature much more complex profiles. Even referring only to the DM distribution, its inner density profile is typically believed to behave as a Navarro–Frenk–White (NFW) profile $\rho \propto r^{-\gamma}$ with $\gamma = 1$, or even shallower in low-mass dwarf galaxies (see, e.g., the evidence on constant density cores in Oh et al. 2015). This shallower core could be the result of baryonic feedback effects (Governato et al. 2010), or of the phase-space density structure inherent to a specific DM model such as self-interacting DM or fuzzy DM (Hui et al. 2017). LISA will be particularly sensitive to MBHBs in the range of masses 10^4–$10^6\,M_\odot$ mainly hosted in low-mass dwarf galaxies; since many dwarfs appear to be DM cored (at least at low redshift; see, e.g., Moore 1994; Contenta et al. 2018; Leung et al. 2020), this motivates a thorough study of the dynamics in shallow inner density profiles.

Tamfal et al. (2018) modelled numerically the orbital dynamics of a pair of $10^5 M_\odot$ BHs during the equal-mass merger of two dwarf galaxies. They showed that, if the merging galaxies have kpc-sized cores, or at least a profile shallower than NFW (inner slope $\gamma \sim 0.6$ or lower), the pair of MBHs would stall at separations of 50–100 pc (i.e., when the bound binary is not formed yet) and the coalescence would be aborted. In a halo with an NFW profile, stalling does not occur, rather the MBHs sink very fast to sub-pc separations in less than a few 10^8 year after the two host galaxies have merged. In self-interacting DM models, in which cores can be > 1 kpc in size assuming a large specific cross section of interaction of $10 \, \mathrm{cm}^2/g$, and which are under-dense compared with Cold Dark Matter (CDM) control cases, an analogous suppression of dynamical friction was found to occur at even larger scales, when galaxies are still in the process of merging, leading to many wandering MBH pairs with few kpc separation (Di Cintio et al. 2017). This opens the possibility that the event rate of MBH mergers detected by LISA could constrain the density profile of dark matter halos of their host galaxies, which in turn can shed light on the physical properties of dark matter particles.

Gas dissipation and stellar feedback were not taken into account in the aforementioned studies; those could delay the binary formation even more. On the other hand, if at least one of the sinking MBHs is surrounded by a massive nuclear star cluster, as in the case of a captured ultra-compact dwarf galaxy, this may enhance the dynamical friction and aid the binary formation and shrinking even in cored DM profiles. These aspects should be investigated in detail in preparation for LISA.

- **MBHBs with very unequal mass ratio**

When the mass enclosed within the binary orbit becomes of order the mass of the secondary, dynamical friction is not effective anymore, and different processes are required to shrink the binary further (see Sect. 2.2.2). For equal mass binaries this critical separation roughly corresponds to the distance at which the binary becomes effectively bound, but for binaries in which the secondary MBH is much lighter than the primary, dynamical friction remains the main driver for the MBHB shrinking well below the separation at which the secondary becomes bound. In this situation, the fact that (Eq. (7)) considers only the contribution of stars moving slower than the secondary MBH (Chandrasekhar 1943) can be a major limitation. Antonini and Merritt (2012) found that, if the inner density profile scales as $\rho \propto r^{-\gamma}$, the conventional application of Chandrasekhar's formula works reasonably well if $\gamma > 1$, but does not reproduce the inspiral of the secondary if the profile is very shallow ($\gamma \sim 0.6$). The reason is that, in the latter case, stars that move faster than the secondary MBH contribute to most of the force. As a consequence, conventional dynamical friction would predict stalling of the secondary MBH, while the orbit can keep shrinking, albeit at a much slower pace (Dosopoulou and Antonini 2017). However, this has only been verified when the secondary MBH is significantly smaller than the primary ($q \lesssim 0.01$, i.e. close to the IMRI regime) and orbits inside a nearly spherical and isotropic nucleus without net rotation. Assessing the outcome for a more realistic profile of the nucleus will be needed in the near future to prepare for LISA.
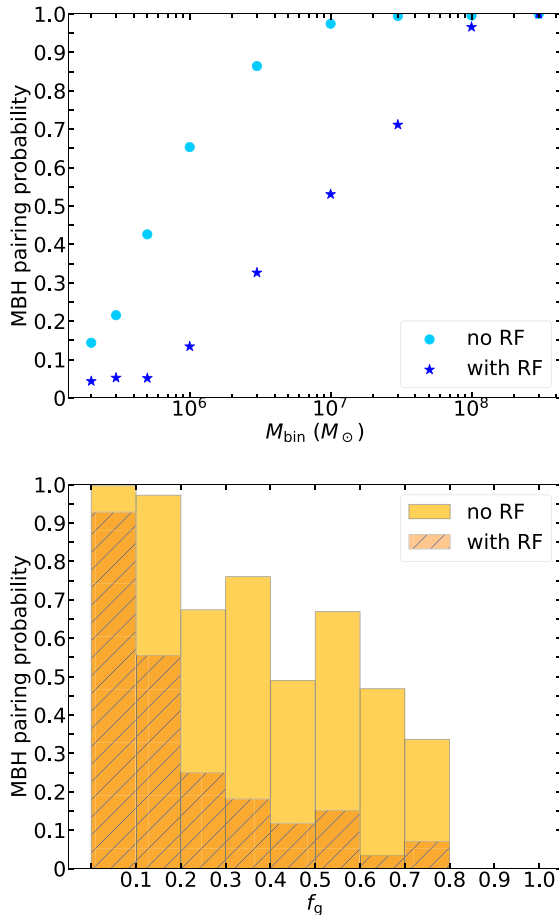
Fig. 18 MBH pairing probability as a function of the MBH pair mass (left) and the gas fraction of the host galaxy (right) in models with and without radiative feedback (RF). In the presence of radiative feedback, the suppression of MBH pairing is most severe in galaxies with MBH pairs with mass $< 10^8 \, M_\odot$ and $f_g \geq 0.1$. The pairing probability is calculated as a fraction of models in which the two MBHs reach a minimum separation of 1 pc within a Hubble time. Figure adapted from Li et al. (2020b)

2.2.1.2 Dynamical friction in a gaseous medium   In the previous sections, we considered orbital decay of a pair of MBHs in a collisionless background of stars and dark matter. However, gas constitutes a significant fraction of mass in many galaxies, especially at high-redshift (Tacconi et al. 2018; Decarli et al. 2020). Similarly to stars, the gaseous wake lagging behind a massive perturber tends to slow it down but the details of the interaction depend on the geometry of the gas wake, which in the case of gas is subject to the additional effect of pressure.

For comparable densities gas-driven dynamical friction is larger by a factor of ~ 5 than that of stars in the transonic regime, i.e., when the Mach number of the perturber is around unity (Ostriker 1999), while it is of similar order in the supersonic regime, i.e., for Mach numbers much larger than unity, and it is suppressed in the subsonic

regime, i.e., below Mach numbers of order unity. However, the overall contribution of the gas-driven component to the total drag force suffered by an MBH in a galactic nucleus is still debated, as it depends sensitively on the dynamical and thermodynamical state of the medium as well as on its density and cooling properties in the vicinity of the perturber.

Hot, low-density gas in gas-poor galaxies is virialized and thus gives little contribution to the drag. However, the central cold and dense region may play an important role. Using semi-analytical models, Li et al. (2020a) find that galaxies with low gas fraction and a large stellar bulge favour the formation of binary MBHs, and that their dynamics is dominated by stellar dynamical friction. Hydrodynamical simulations find quite a range of results, whose often large differences are likely driven by the different setups, astrophysical as well as numerical, considered by different simulations.

For example, Pfister et al. (2017) also find that the contribution from gas friction is negligible compared to that from stars as in their case *(i)* the gas density is lower than stellar density; and *(ii)* the stellar density profile is more regular than the gas one, so that stars act as a smooth background, which is conceptually consistent with the theory of dynamical friction. On the other hand, numerical simulations and observations also show that stellar morphology in merging systems is often highly disturbed and rapidly varying, which complicates this picture and suggests that galactic substructure might be important to take into account. Chapon et al. (2013) find that the collision between the two massive equal mass gas-rich galactic discs drives rapid sinking, primarily owing to gas-driven friction, of the MBHs that pair into a binary. Note that, in equal mass galaxy mergers, funnelling of gas to the centre of the merger remnant via gravitational torques and shocks is maximized relative to the unequal mass merger case considered by Pfister et al. (2017), and this leads to a much higher central gas density. It is therefore not surprising that the two studies reach different conclusions on the relative importance on gas-driven and stellar-driven friction. All this shows that the processes leading to the formation of LISA binaries in realistic gaseous and stellar environments deserves future investigations before LISA flies.

2.2.1.3 More complex mass distributions and additional physical phenomena   We expect galaxies to not be realistically represented by the spherical, power-law, and smooth density profiles. As already mentioned in the previous section, global asymmetries affect the sinking time-scale. In order to prepare for LISA, we need to investigate the effects of more complex structures onto the dynamics of MBHs. We summarize below the recent results of several groups studying these effects and highlight some areas of particular interest for future study.

• **Effects of discs** The question of the effects of large-scale galactic discs (~ 1–10 kpc) and circumnuclear discs (~ 100 pc) on the formation of gravitationally bound MBH pairs is closely related to the question of what types of galaxies are the most likely progenitors of LISA sources. Simulations have already addressed the effect of dynamical friction in composite, rotationally supported environments; they suggested that, quite independently of whether the background is mainly stellar or gaseous

(Dotti et al. 2007), dynamical friction acting in rotating discs usually induces the circularization of initially prograde and eccentric orbits, while it reverses the angular momentum of counter-rotating trajectories, then again promoting circularization (see, e.g. Dotti et al. 2006; Callegari et al. 2011; Fiacconi et al. 2013; Bonetti et al. 2020a).

Using a different approach, Li et al. (2020a) studied this aspect adopting a semi-analytical model to describe the orbital evolution of MBHs from separations of ~ 1 kpc to ~ 1 pc, under the influence of stellar and gaseous dynamical friction. Their study of the parameter space suggests that the dominant drivers of the MBH orbital evolution are the stellar bulge and galactic gas disc. They find that the chance of MBH pairing within a Hubble time is nearly 100 per cent in host galaxies with a gas fraction of < 0.2, as shown in the right-hand panel of Fig. 18. They also find that the orbital evolution sensitively depends on the relative speed between the gas disc and the MBHs. Semi-analytical models, however, are quite limited in their predictive power when it comes to the effect of gas as they cannot account for the multi phase nature of the interstellar medium and the concurrent star formation in the galactic nucleus, which are bound to have an impact on both the local drag and the global torques, motivating the investigation of this problem with various approaches in order to assess the impact on LISA's MBH mergers.

● **Effects of feedback** The distribution of gas in the host galaxy and its contribution to the total dynamical friction force on MBHs is likely to be strongly impacted by radiative feedback (e.g. Sijacki et al. 2011; Souza Lima et al. 2017). More specifically, it was recently shown for MBHs evolving in gas-rich backgrounds that ionizing radiation that emerges from the innermost parts of the MBHs' accretion flows can strongly affect their gaseous dynamical friction wake and render gas friction inefficient for a range of physical scenarios. Combined with the effect of radiation pressure, the radiative feedback creates an ionized region larger than the characteristic size of the dynamical friction wake and a dense shell of gas in front of the MBH, as a consequence of the snowplow effect. In this regime, the dominant contribution to the MBH acceleration comes from the dense shell and such MBHs experience a positive net force, meaning that they speed up, contrary to the expectations for gaseous dynamical friction in absence of radiative feedback (Park and Bogdanović 2017; Gruzinov et al. 2020; Toyouchi et al. 2020). This effect was dubbed "negative dynamical friction".

If prevalent in real merging galaxies, negative gaseous dynamical friction can lengthen the inspiral time of MBHs and even offset the action of stellar dynamical friction. Its full implications for the formation and coalescence rate of MBHBs in galactic and cosmological settings for MBHs in the LISA mass range are however yet to be understood. Some early insights into this question are provided by Li et al. (2020b), who used a semi-analytical model to study the impact of negative dynamical friction on pairs of MBHs in merger remnant galaxies evolving under the combined influence of stellar and gaseous dynamical friction. They found that, for a wide range of galaxy mergers and MBH properties, negative dynamical friction reduces the MBH pairing probability to ~ 50 per cent of that found in absence of radiative feedback (Fig. 18, left). This effect is particularly prevalent in systems with

---

[5] The main galaxy forming in the cosmological zoom-in simulation Ponos (Fiacconi et al. 2017).

a gas fraction above 0.1, especially if the disc rotational velocity is comparable to the circular velocity (Fig. 18, right). Importantly, the pairing probability in the presence of radiative feedback decreases five-fold (to $\lesssim 0.1$) for MBHBs with mass $\lesssim 10^6\,M_\odot$ (Li et al. 2020b), implying that the pairing of the very population of MBHBs targeted by LISA may be greatly affected by it.

Dayal et al. (2019) on the other hand point out that many MBHs in the LISA mass range ($\lesssim 10^6\,M_\odot$) MBHs would reside in low mass haloes, in which SN feedback and radiation background due to reionization will expel and photo-evaporate most of the gas, thus curbing the growth of the MBHs and suppressing the effect of gas on their orbital evolution (see Sect. 2.3.2.2 for a related discussion). It is therefore crucial to understand how feedback affects gas dynamical friction in realistic merger remnants. If pairing and merger rates of MBHBs in gas-rich environments are reduced, this has important implications for the likelihood of detection of multimessenger events with LISA and the contemporary EM observatories. For this reason, a much wider range of scenarios needs to be explored to investigate the complex role of radiative feedback and gaseous dynamical friction for MBHs in the LISA mass/redshift range, exploring the impact of a different feedback geometry, energetics, mass loading, momentum injection, etc.

• **Effects of bars** A large fraction of disc galaxies at low redshift show clear deviations from axisymmetry in their stellar distribution. At least at low redshift, about half of massive ($M_* \gtrsim 10^{10}\,M_\odot$) discs (e.g. Consolandi 2016, and references therein) host a prominent overdensity approximately symmetric with respect to the centre with constant phase, e.g. a bar, that can significantly affect the dynamical evolution of the different components of the host galaxies (Athanassoula 2002; Sellwood 2014). Quantifying the fraction of barred galaxies at high redshift is still challenging (see, e.g. Sheth et al. 2008; Melvin et al. 2014; Simmons et al. 2014), but
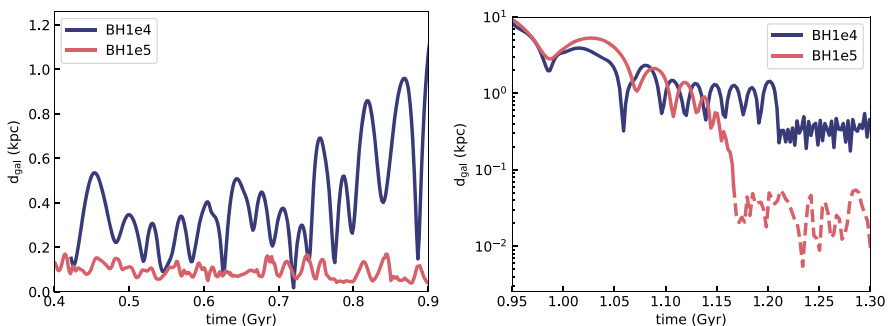
Fig. 19 Distance between an MBH and a galaxy as a function of time for two cosmological simulations which only differ by the mass of the MBHs ($10^4 M_\odot$ in blue and $10^5 M_\odot$ in pink). Left: We show the results for the central MBH of the galaxy. In both cases MBHs are smoothly off-centred due to inhomogeneities of the potential, but the more massive one remains in the centre, since dynamical friction is efficient, and the lighter one is instead displaced to kpc distances. Right: We show the results for the central MBH embedded in a satellite galaxy sinking towards the primary galaxy. The initial phase is similar in both cases as the whole satellite suffers dynamical friction, but as soon as material surrounding MBHs has been stripped, the light MBH stalls while the more massive one keeps sinking until it merges with the central MBH of the primary galaxy (subsequent evolution in dashed line). Adapted from Pfister et al. (2019b)

(a) it has been observationally proposed that bars could be frequently hosted in massive galaxies at all redshifts, with an increasing mass threshold for entering in the bar unstable regime as a function of redshift (Gavazzi et al. 2015), and *(b)* bar formation has been found as early as at $z \sim 7$ in cosmological zoom-in simulations (Fiacconi et al. 2017).

Being such strong perturbations to the host potential, bars could significantly affect the pairing of MBHs during galaxy mergers. The occurrence of such effect could be increased when the actual merger is responsible for the triggering of a bar (Byrd et al. 1986; Mayer and Wadsley 2004; Romano-Díaz et al. 2008; Martinez-Valpuesta et al. 2016; Zana et al. 2018a, b; Peschken and Łokas 2019), even when this is short-lived and not sustained by the galactic potential, e.g. if the galaxy stellar disc is below the threshold for bar instability.

The effect of a forming and growing bar on the pairing of MBHs within LISA's reach has been recently explored by Bortolas et al. (2020). They populated a main-sequence $z \sim 7$ galaxy[5] with secondary MBHs at different radii and at different angles with respect to the forming bar, and found a stochastic behaviour in the pairing time-scales, with some of the secondary MBHs being pushed towards the centre of the main galaxy, and others being ejected by a slingshot with the bar. Noticeably, it was found that the orbital decay of the secondary MBHs was dominated by the global torque provided by the bar rather than by the local effect of dynamical friction. This points to the need of including the effect of global torques in future recipes for sinking time-scales of MBH pairs at $\sim$ kpc distances. A first semi-analytical attempt to explore the broad parameter space of MBH pairs/bar interaction is currently ongoing (Bortolas et al. 2022), in which a time-dependent bar potential has been added to the integrator of orbits in disc galaxy potentials presented in Bonetti et al. (2020a, 2021). A much more thorough analysis, considering (a) different galactic properties, different bar potentials and bar precession velocities, (b) the dependence of the fraction of barred discs as a function of redshift and in recent mergers, and (c) the host galaxy evolution during the MBH pairing is needed to better evaluate the effect of bars on the population of MBH binaries in the LISA band.

• **Effects of clumps** If an MBH happens to get close to a massive interstellar cloud or dense star cluster, its orbit can be severely affected, and this effect is particularly strong in a clumpy interstellar medium. The typical masses of the perturbers depend on the background gas density which determines the conditions of fragmentation in the framework of the Toomre instability. These masses are $\sim 10^5$–10^7 $M_\odot$ for giant molecular clouds in present-day galaxies; and 10^7–10^8 $M_\odot$ for giant star-forming clumps in galactic discs at higher redshift, which have a much larger gas fraction (Tamburello et al. 2015, 2017a, b). As clumps have to be massive enough to have a dynamical impact on the MBH, this suggests that the effect of a clumpy medium is irrelevant for MBHs with masses $> 10^8 M_\odot$ (Fiacconi et al. 2013), but is likely relevant for the MBHs that are targeted by LISA. This is especially important considering that a significant fraction of galaxies at $z \approx 1$–3 (i.e. an epoch in which galaxy mergers are supposedly frequent, Fakhouri et al. 2010) appears to be clumpy (Ceverino et al. 2010; Shibuya et al. 2016). Several numerical

simulations show that the clumpiness of the gaseous medium renders the orbital decay highly stochastic (De Rosa et al. 2019b): in some situations, the MBH separation does not shrink (Roškar et al. 2015), in others the decay is promoted (Fiacconi et al. 2013; del Valle et al. 2015).

When the decay stalls, it is often because the lighter secondary MBH is scattered away from the disc plane (galactic or circumnuclear), ending up in a region of much lower stellar and gas density, where dynamical friction becomes inefficient. This effect is even more emphasized when stellar and AGN feedback are included, as they can open cavities of low density gas (Souza Lima et al. 2017). Note that this is not a definitive effect, as a scattered MBH can eventually be dragged back to the disc: the net effect is to delay the formation of the binary which takes 10–100 times longer (Roškar et al. 2015), but this will contribute in shaping the redshift distribution of MBH coalescences (Volonteri et al. 2020).

In summary, while stalling of the MBH pair is an extreme outcome that cannot be verified due to the limited time-scales probed by current simulations, it is clear that the range of orbital decay time-scales of MBH pairs in a clumpy medium, from kpc scales to separations of order pc and below, can be widened by up to two orders of magnitude. In addition, the induced delay likely depends on the number and mass distribution of clumps within their hosts. Since LISA can detect MBHs up to high redshift, when clumpy galaxies were more common, future, better resolved observations of clumpy galaxies at $z > 1$ would be beneficial for the community. The latter, aided by more accurate simulations of the same systems, will help in better constraining the effect of clump-driven perturbations on the orbital decay of MBHs, especially their impact on the rates and properties of the MBHBs that LISA will detect.

2.2.1.4 Is there a final kpc problem?   In the previous sections we discussed several mechanisms that can cause complete stalling, or at least a significant delay of the orbital decay of a MBH pair. These mechanisms can essentially stifle the formation of an MBH binary in the first place, and the orbital evolution seems to be highly sensitive to the physical parameters involved.

To exemplify this, we show in Fig. 19 the outcome of two cosmological simulations (Pfister et al. 2019b) which only differ by the mass of the MBHs. In the case of a light MBH ($10^4 M_\odot$ in blue), not only the sinking MBH stalls at $\sim$ kpc distances, similarly to Tamfal et al. (2018), but even the central one is smoothly off-centred due to inhomogeneties and never sinks back, as the dynamical friction time-scale is very long. While in this particular case, the massive MBH ($10^5 M_\odot$ in pink) behaves smoothly in agreement with the classic picture of dynamical friction, we recall that Bortolas et al. (2020) have shown that massive MBHs can wander for a long time because of bars.

Perturbations, and the subsequent stalling, appear to be more relevant and likely to occur at higher redshift ($z > 1$), as host galaxies have clumpier, more turbulent, and

---

[6] The sphere of influence of an MBH of mass M can be defined in different ways, but generally it is considered as the sphere with radius equal to $\sim GM/\sigma^2$, with σ the velocity dispersion of the nearby stellar background.

more inhomogeneous gas and stellar density profiles (Pfister et al. 2019b). At lower redshift, stalling is more likely to occur in low-mass/dwarf galaxies that have low background density (Tremmel et al. 2015; Bellovary et al. 2019) or cored DM profiles (Tamfal et al. 2018), or in high-mass galaxies with core-Sérsic profiles (Graham et al. 2003). Some isolated simulations of 1:4 massive spirals mergers (Callegari et al. 2009, 2011) also show a delayed inspiral with respect to the estimate of Eq. 8. However, the exact physics of the inspiral crucially depends on the details of gas accretion and star formation about the MBHs, as e.g. the formation of a dense stellar nucleus about the secondary may accelerate its orbital decay (Van Wassenhove et al. 2014; Ogiya et al. 2020).

On the observational side, recent radio observations of AGN in local dwarf galaxies (Reines et al. 2020) have highlighted that at least some of these objects are not located in the centre of their host, which is often not easy to define, due to irregular galactic morphologies, in line with the results of the simulations presented above. Known offsets of nuclear star clusters offer further insight (Binggeli et al. 2000). If the reason for the observed displacement is a failed inspiral (instead of e.g. the effect of a GW recoil following an MBH merger, or the interaction with a third MBH), it is easy to imagine that the formation of a bound MBH binary may become very unlikely. All the above suggests that the large-scale decay of MBHs is likely to be a stochastic process, highly dependent on the environmental conditions of the host galaxy nucleus, and on the orbital configuration of the MBH pair.

Modelling such stochasticity in a way simple enough that can be incorporated in population synthesis models for LISA MBHs, but at the same time accurate enough to account for the relevant physical processes shaping the inspiral, is a key challenge ahead of us (see Barausse et al. 2020b, for an example investigating the effect on LISA's coalescences). Furthermore, it is practically hard to set the boundary between dynamical friction (thought as the response of the host to the perturber's passage) and different torquing mechanisms related to the galaxy mass distribution. For this, an effort towards a detailed and realistic characterization of MBHs, along with the effect of their feedback, in a variety of systems at all redshifts is vital to properly model the MBH merger population that LISA is going to probe. In order to interpret LISA's data it is crucial to develop well-motivated models that can be compared with the detected events in order to extract astrophysical information.

2.2.2 Orbital decay after binary formation at pc scales

As dynamical friction drives the orbital decay of the MBHs, they eventually find themselves inside their mutual sphere of influence,[6] resulting in the formation of an MBHB (Begelman et al. 1980; Milosavljević and Merritt 2001). The subsequent evolution of the newborn binary can be driven by several processes. In general, the efficiency of these processes is critically connected to the characteristics of the environment surrounding the MBHB, and every MBHB will follow its own different evolutionary path. As for the larger-scale dynamics at kiloparsec scales, we can broadly identify two classes of physical processes that shape the further shrinking of the binary separation in galactic nuclei: those that operate in gas-poor stellar environments and those that instead work when a consistent reservoir of gas is
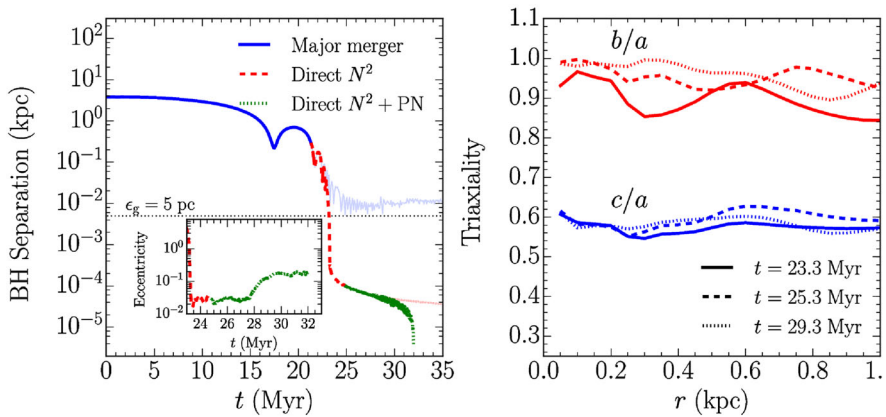
Fig. 20 Evolution of an MBH pair in direct N-body simulations of a galaxy merger (obtained from cosmological simulations) at redshift $z \sim 3$. Left: MBH separation as a function of time; the small plot shows the time evolution of the Keplerian eccentricity past the binary formation. Right: Merger remnant axis ratios as a function of the radius for different simulation times. Figure adapted from Khan et al. (2016)

present. The boundary between the two classes is definitely not strict, and although most studies available today focus on only one of the two environments at a time, both stellar and gaseous hardening can operate at the same time (see e.g. Kelley et al. 2017a; Bortolas et al. 2021). In the following we outline the key physical aspects featured by each shrinking mechanism, since they can all operate for LISA's MBHs, which are expected to dwell in environments rich in both gas and stars.

2.2.2.1 Hardening in stellar environments   As soon as two MBHs form a bound binary system, dynamical friction gradually ceases to be effective since at such small scales, of order a parsec, the surrounding background mass is too low to generate a significant back-reaction to the perturbation induced by the MBHB itself. In a galactic nucleus whose density is dominated by stars, then, the prevalent mechanism that can continue to shrink the orbit of the binary is three-body encounters of individual stars with the MBHB (Mikkola and Valtonen 1992; Quinlan 1996; Sesana et al. 2006). After a first rapid decay of the MBHB orbit in which dynamical friction and three-body encounters act in tandem, the binary shrinking starts to proceed at a slower but almost constant rate. The transition occurs around a separation commonly known as the hard binary separation, $a_{\rm h}$, corresponding to a semi-major axis (Merritt and Milosavljević 2005)

$$a_{\rm h} \leq \frac{G\mu}{4\sigma^2},$$ (9)

with μ denoting the reduced mass of the binary and σ the local velocity dispersion of the surrounding stellar distribution. Physically, this scale approximately denotes the point at which the binary orbital velocity exceeds the characteristic speed of the stellar background, therefore representing a sort of decoupling length below which the dynamics is strongly dominated by the self-gravity of the two black holes. During

the process stars are generally ejected out of galaxy centre with high velocities as a result of the interaction with the binary. Therefore, ejections of stars by the MBHB result in a decrease of stellar density in the vicinity of the MBHB, with the damage extending typically up to a few influence radii (Ebisuzaki et al. 1991; Volonteri et al. 2003b; Khan et al. 2012) and effectively translating into less frequent stellar encounters. This mechanism possibly justifies the almost ubiquitous presence of stellar cores at the centre of the most massive galaxies (i.e. the ones that likely experienced the largest number of mergers; Bonfini et al. 2018).

• **The final parsec problem**

As the MBHB enters in the hard binary regime, it is expected to shrink at a rate determined by

$$\frac{d}{dt}\left(\frac{1}{a}\right) = \frac{G\rho}{\sigma}H, \tag{10}$$

where ρ is the density of the stellar background, σ is the velocity dispersion, a is the binary Keplerian semi-major axis and $H \approx 15$–20 is a numerical coefficient weakly dependent on the properties of the binary (mass, mass ratio, and eccentricity; Mikkola and Valtonen 1992; Quinlan 1996; Sesana et al. 2006, but see Ogiya et al. 2020). The equation above shows that the shrinking rate would be constant for fixed ρ and σ; however, the binary surroundings get perturbed by its scouring action, resulting typically in a mildly declining hardening rate (Vasiliev et al. 2015; Bortolas et al. 2018a). Equation 10 applies so long as the MBHB loss cone (the region of phase space containing stars with angular momentum low enough to interact with the binary) remains populated with stars. However, the loss cone is generally depleted within a typical stellar orbital period at the beginning of the hardening phase, and further MBHB shrinking crucially depends on the existence of processes able to repopulate it. In principle, the loss cone can be replenished by means of two-body relaxation. Unfortunately, this process acts on a time-scale much longer than a Hubble time if one considers the average properties of galactic nuclei, assuming a spherically symmetric potential (Binney and Tremaine 1987, although it may be short enough for dwarf galaxies hosting low mass MBHs in the LISA band). For this, the possibility of an MBHB stalling at pc scales has been put forward from both numerical (Makino and Funato 2004; Berczik et al. 2005) and theoretical grounds (Begelman et al. 1980), and has been referred to as the final parsec problem.

• **The final parsec problem is not a problem** Throughout the last decades, evidence has been building up that the final parsec problem would only occur in perfectly spherical, idealized galaxies; in fact, in these systems stars are bound to conserve all components of their specific angular momentum. If the stellar bulge is triaxial—as in real systems—stellar orbits can be torqued by the asymmetric mass distribution and their angular momentum does not have to be conserved in time, meaning that the loss cone can be easily repopulated in a collisionless fashion (Yu 2002; Merritt and Poon 2004; Merritt and Vasiliev 2011). Berczik et al. (2006) first adopted numerical simulations to point out how rapid the MBHB coalescence can be in triaxial nuclei, which are themselves a natural outcome of the merger of two stellar bulges (Khan et al. 2011; Preto et al. 2011, see the right-hand panel in Fig. 20). Those

findings were confirmed and extended to systems with different MBHB mass ratios, galaxy density profiles, and orbits, and were generalized to galaxies with realistic two body relaxation rates (Khan et al. 2012; Vasiliev et al. 2015; Sesana and Khan 2015; Khan et al. 2016; Gualandris et al. 2017; Bortolas et al. 2018a).

The general consensus is that MBHBs in realistic merger remnants can reach the GW-driven coalescence through stellar hardening alone. The time-scale on which this happens, though, depends heavily on the details of the stellar density profile and the eccentricity growth of the binary, both of which are hard to pin down. For instance, (galaxy-morphology)-dependent scaling relations that correlate the MBH mass with many host galaxy quantities (e.g. Gültekin et al. 2009; McConnell et al. 2011; Kormendy and Ho 2013; Reines and Volonteri 2015; Graham and Scott 2015; Davis et al. 2018) can be used to probe the binary lifetimes. Biava et al. (2019) found they can range between 10^{-2} Gyr to more than 10 Gyr for MBHs of 10^5–$10^7 M_\odot$. When hosts are scaled to bulges of local galaxies, the merger times of MBHBs derived from simulations are typically less than 500 Myr (Khan et al. 2018b), but can reach ~ 1 Gyr depending on central density, which is varied in a realistic range (Khan et al. 2018c, 2016). Time-scales, however, have also been shown to depend strongly on redshift because the scaling of mass density and velocity dispersion, which both affect hardening, is a rather steep function of redshift (Mayer 2017). This is the reason behind the extremely short MBH merging time-scales found in cosmological simulations of massive galaxies at redshift ~ 3.3 (Khan et al. 2016, see Fig. 20), and is naturally explained if one considers the scaling of structural properties of galaxies with respect to their host CDM halos as a function of redshift (Mayer 2017). A detailed knowledge of the properties of stellar dominated galaxies hosting LISA MBHs at different redshifts appears thus to be important in order to derive a realistic distribution of hardening times for LISA MBHB evolving inside such hosts.

An acceleration of the MBHB shrinking can be induced by a non-zero orbital eccentricity during the hardening stage, as this would shorten the time-scale needed by the binary to enter the GW-dominated evolutionary stage (Peters 1964a, but see Sect. 2.2.3). For example, Sesana and Khan (2015) find that the typical time spanning from the onset of the hardening to the GW-induced coalescence is ≈ 30 times shorter for binaries with $e = 0.99$ compared to circular ones. Eccentricity evolution in the hardening phase depends on a fine balance between energy and angular momentum exchange, and it is sensitive to a number of factors. Three-body scattering experiments in a non-rotating stellar system find that eccentricity tends to grow as the binary shrinks (Quinlan 1996), and the growth is more prominent for binaries with moderately low mass ratio ($q \gtrsim 0.01$) residing in steeper stellar density cusps (Sesana et al. 2008a). For binaries with even lower mass ratio, the evolutionary trend is less clear, and below $q \sim 0.001$ the scattering process seems to even circularise binaries (Rasskazov et al. 2019; Bonetti et al. 2020b). Khan et al. (2012) also noticed that mergers of cuspy galaxies result in lower binary eccentricities at the time of binary formation, whereas galaxy mergers with shallower central density end up with higher eccentricity values. MBH mergers in the mass range 10^4–$10^7 M_\odot$, around the peak of the LISA sensitivity window, are generally observed to be hosted by galactic nuclei

with steep density profiles, which might favour relatively low eccentricities. However, the situation may greatly vary once the hosts rotation is taken into consideration, as discussed below. The expected eccentricity of binaries close to merger is not only important to estimate the merger time-scale, but it has repercussions on what type of waveforms should be developed for LISA data analysis.

● **The host rotation**

Recent numerical studies investigated the impact of rotation in galactic nuclei on the evolution of MBHBs, showing that it can profoundly affect the orbital parameters of the bound binary (Mirza et al. 2017; Rasskazov and Merritt 2017). MBHs sink significantly faster in orbits co-rotating with galaxy rotation, because of the longer time for the encounter between the MBHs and the incoming stars, results in a more efficient extraction of energy from the orbit (Holley-Bockelmann and Khan 2015). Moreover, MBHs in co-rotating orbits circularise efficiently prior to binary formation, whereas those on counter-rotating ones tend to maintain their eccentricity, which starts to grow as the two MBHs approach the binary formation phase (Sesana et al. 2011b; Khan et al. 2020). Before a hard binary forms, MBHBs in counter-rotating orbits attain very high values of the orbital eccentricity ($e \simeq 1$) and also flip their plane to align themselves with the orientation of the galactic angular momentum (Gualandris et al. 2012; Rasskazov and Merritt 2017). This means that, in principle, MBHBs evolving in rotating environments may typically end up being close to co-rotating with their background and having a very low eccentricity; however, more studies on the modelling of MBHBs in rotating systems is needed in this direction in order to get a more complete picture of the phenomenon before LISA flies.

● **Substructure in galactic nuclei**

The evolution of an MBHB in its hardening stage can also be affected by the presence of perturbers near the galaxy nucleus. In the case of low-mass perturbers,

Fig. 21 Illustration of the geometry of a circumbinary disc, with minidiscs surrounding each of the MBHs in the binary, a gap opened by the MBHs gravitational torques, and gas streams connecting the circumbinary disc to the minidiscs. Adapted from Bowen et al. (2018, the central larger black circle at the coordinate origin marks a central excision and is not physical). Image concept: Julian Krolik. Figure realization: Marta Volonteri
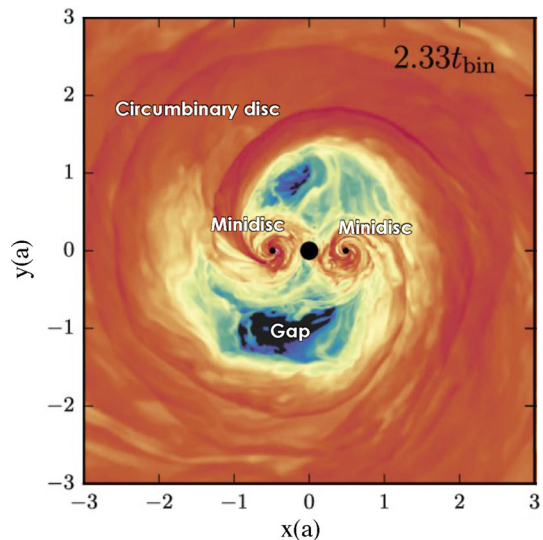
such as the nearby stars, this results in Brownian wandering. The MBHB instantaneous centre-of-mass velocity gets continuously perturbed by gravitational three-body encounters with the nearby stars (Merritt 2001), and is balanced by dynamical friction, which acts as a restoring force. As a result, the MBHB centre of mass wanders about the centre of the galaxy. As the MBHB gets displaced from the centre, the MBHB loss-cone re-population can be enhanced, resulting in a possible boost of the MBHB hardening rate in spherically symmetric systems (Quinlan and Hernquist 1997; Chatterjee et al. 2003; Milosavljević and Merritt 2003). For triaxial systems, where an almost full MBHB loss cone is usually expected (Gualandris et al. 2017), the MBHB shrinking rate can be impacted by the MBHB's wandering only if $M_{\mathrm{BH}}/m_{\star} \lesssim 10^3$ (being $m_{\star}$ the typical mass of stars, see Bortolas et al. 2016). This suggests that the MBHB's wandering would not significantly affect the hardening rate of LISA MBHBs.

In the case of perturbers with mass much larger than the stellar one, the effects can be more significant (Perets et al. 2007; Perets and Alexander 2008). Massive perturbers may be in the form of star clusters, giant molecular clouds or even a further inspiralling MBH, and may have masses up and above that of MBHs in the LISA band. Such objects can reach the galaxy centre and affect the binary inspiral in different ways. Due to their large mass, they scatter new stars into the loss cone, thus indirectly enhancing the MBHB shrinking rate, somehow acting as boosters for two body relaxation (Spitzer and Schwarzschild 1951). In addition, if they come close enough to the binary, they may displace it from the galaxy centre, thus again affecting the flux of stars in the loss cone; furthermore, if the massive perturber is a stellar cluster, once the object reaches the binary, it delivers new stars onto it, thus directly promoting its shrinking (Bortolas et al. 2018b; Arca Sedda et al. 2019b). Thus, in principle, massive perturbers may have a significant effect on the orbital evolution of an MBHB. In order to properly model their impact on a population of LISA MBHBs, more studies are needed to pinpoint the rate at which different massive perturbers may interact with hardening binaries in different host environments. This regime bears similarities with the clumpy medium regime in gas-rich galaxies and in circumnuclear discs as far as the dynamical interaction with the MBHB is concerned.

2.2.2.2 Hardening in gaseous environments

We now turn to the evolution of MBHBs embedded in a gas-dominated galactic nucleus. This is of great relevance for LISA, since it will detect low mass MBHs, which are expected to reside in high-redshift gas-rich galaxies. In Sect. 2.2.1 we have already discussed extensively the dynamics of MBH pairs, until MBHB formation, in gas-rich galaxies, from kpc scales in the galactic disc, to pc scale separations in the circumnuclear disc, showing how various effects can both hamper or promote the sinking of the MBHs. We now continue our investigation in gas-rich nuclei for smaller separations, namely following MBHB formation.

One first effect of gas which is relevant also at such small separations is related to accretion. In the limiting case that the gas accreting on to the MBHs has zero angular momentum, the gas inflow will be purely radial and accretion on to the binary will be

Bondi–Hoyle–Lyttleton-like (hereafter Bondi; Hoyle and Lyttleton 1939; Bondi and Hoyle 1944; Bondi 1952). Bondi accretion onto a binary has been studied in, e.g. Farris et al. (2010), Antoni et al. (2019), Comerford et al. (2019) and, with the inclusion of magnetic fields, in Giacomazzo et al. (2012), Kelly et al. (2017). The main conclusion is that the sinking time-scale of the binary caused by their distorted wakes remains comparable to the usual gaseous Bondi drag time-scale for a single compact object, only a factor of few smaller, at least in the parameter ranges studied in the above papers.

In reality, gas on large scales is likely to possess a specific angular momentum much larger than the one corresponding to the innermost stable circular orbit (ISCO) of the MBHs. Therefore, considerable loss of angular momentum is required to drive gas from kpc to sub-pc scales, and it is likely that some residual angular momentum remains on small scales, resulting in the formation of a disc surrounding the MBHB: the so-called circumbinary disc (for a single MBH the analogous structure is an accretion disc). An illustration of the geometry of a circumbinary disc is provided in Fig. 21. In this section we focus on the effect of the disc onto the MBH binary dynamics, while we refer to Sect. 2.2.2 for the implications on accretion.

- **The circumbinary disc**

Due to the computational burden, large scale simulations able to resolve ~ 100 pc scales have not yet managed to fully and self-consistently determine the properties of such circumbinary discs, with few exceptions (Souza Lima et al. 2020). To circumvent the limits of large scale simulations, Goicovic et al. (2016, 2017), Maureira-Fredes et al. (2018), Goicovic et al. (2018) detailed the properties of circumbinary discs through an extensive, though highly idealised, set of simulations, where the disc was built through a bombardment of gas clouds towards a central MBHB. These studies demonstrated that the detailed properties of circumbinary discs depend on the dynamical properties of the infalling material.

When the MBHB reaches a critical small separation, its gravitational torque on the surrounding disc material becomes stronger than the angular momentum losses per unit of time due to the disc dissipative processes; at this point, depending on the mass ratio of the binary, either an annular gap centred on the secondary radius (MacFadyen and Milosavljević 2008), or a large cavity encompassing both the MBHs can be opened (D'Orazio et al. 2016). It was initially suggested that the creation of such cavity would inhibit gas accretion onto the pair; more recent and resolved simulations seem instead to suggest that accretion may remain sustained through the inner edge of the disc (e.g., Farris et al. 2015a; Souza Lima et al. 2020).

If and when the binary reaches sufficiently small separations, the mass of the circumbinary disc enclosed within the MBHB orbit becomes much smaller than that of the binary itself, making the disc gravitationally stable against fragmentation (Goodman 2003). The simplest expectation in this regime is that the gas disc will cause the binary to harden on a time-scale comparable to the viscous time-scale (in analogy with Type II planetary migration; Ward 1997) down to the decoupling radius where GWs start dominating the MBHB dynamics. For typical, thin Shakura and Sunyaev discs (with ratio between the vertical length scale H and the radial extent R around $H/R \approx 0.05$) and close to equal mass MBHBs, this occurs at ~ 100 gravitational radii (Gold et al. 2014b).

At such close separations, for close to equal mass MBHBs ($q \sim 1$) the time-scale needed by the disc to refill the cavity would get longer than the GW-driven coalescence. If, on the other hand, $q \ll 1$, the ratio between the mass of the secondary MBH and the mass of the disc enclosed in the MBHB orbit, $q_{2,\text{disc}} \equiv M_2/M_{\text{disc}}$, is a key parameter. A $q \ll 1$ binary is expected to harden on the viscous time-scale of the surrounding disc, up to the binary separation when $q_{2,\text{disc}} > 1$, afterwards, the migration rate falls below the viscous rate. The MBHs separation at which $q_{2,\text{disc}}$ grows above unity can occur outside the region where the disc is stable against self-gravity-driven fragmentation (see figures 3 and 4 in Haiman et al. 2009 and Figure 6 in Lodato et al. 2009). The conclusion is that, if $q_{2,\text{disc}} \gg 1$ at large separations ($\gtrsim 0.1$–1 pc), the ensuing slow-down would preclude the merger (Lodato et al. 2009), or else it would have to occur in a self-gravitating, clumpy disc. At smaller separations, the viscous time is generally short, and rapid merger can be promoted by a stable disc, despite the slow-down occurring when $q_{2,\text{disc}} \gg 1$.

As commented earlier in the section, simulations have observed that gas continues to cross the inner edge of the circumbinary disc (e.g. D'Orazio et al. 2016), but in an unstable and strongly fluctuating fashion, and the spatial symmetry of the circumbinary gas is lost, resulting in a strongly lopsided, precessing disc, preventing analytical modelling of these processes. In the simplest case of an equal-mass binary on a circular orbit, surrounded by a locally isothermal but warm disc (with a low Mach number, or a high aspect ratio $H/R = 0.1$), several recent simulations have converged on the same conclusion: the disc causes the binary to outspiral (Tang et al. 2017; Moody et al. 2019; Muñoz et al. 2019, 2020). The outspiral rate is quite rapid, for accretion rates comparable to those of bright, near-Eddington quasars. This of course could represent an important obstacle to binary mergers, but more recent work suggests that this conclusion is peculiar, and holds only for the above, idealized, specific configuration. In particular, the sign of the torques and migration changes from positive to negative when the mass ratio is below $q \lesssim 0.05$ (Duffell et al. 2020). This means that binaries below this mass ratio may migrate inwards—at least until the secondary accretes a sufficient mass to increase q above 0.05 (after which, in the absence of any other effects, the torque would change sign, causing the binary to migrate outwards). More importantly, the disc torque has been found to strongly depend on the disc temperature (or equivalently Mach number or aspect ratio). Tiede et al. (2020) have emphasized that real AGN discs in the inner regions are expected to be thinner/colder. They measured the torques in simulations of such cooler discs, and have found that outspiral changes to inspiral, at a comparable rate, when $H/R \lesssim 0.04$. They attributed this to the importance of direct gravitational torques of the gas accumulating near the binary with an asymmetric distribution (as opposed to accretion torques).

The dependence on the disc temperature was later confirmed by Heath and Nixon (2020), who found that binaries outspiral only for $H/R \gtrsim 0.2$. However, Franchini et al. (2022) showed that, using high-resolution simulations, the result does not depend only on the disc temperature, but also on viscosity and argue that there is no threshold for expansion in terms of disc aspect ratios. However, these recent papers

all agree on the same conclusion: binaries embedded in thin ($H/R \lesssim 0.05$) locally isothermal discs do inspiral as a result of the interaction with the gas.

A good understanding of this gas-disc driven phase is important to better understand the properties of MBHBs when they enter in the LISA band. Assuming for simplicity that one can neglect accretion flows towards the binary, the viscous time-scale of the disc is the relevant evolution time-scale. This means that the MBHB will simply shrink as the disc material itself shrinks due to internal viscous stresses. Then one can define a *decoupling radius* by equating the viscous time-scale in the disc with the GW inspiral time-scale of the binary.

For an equal-mass binary at the decoupling radius, the GW observed frequency is given by

$$f_{\mathrm{GW}} \sim 10^{-4} \frac{1}{1+z} \mathrm{Hz} \left(\frac{H/R}{0.05}\right)^{6/5} \left(\frac{\alpha}{0.1}\right)^{3/5} \left(\frac{M}{10^6 \, M_\odot}\right)^{-1}, \tag{11}$$

assuming the viscous time-scale $t_v \sim R^2/v$ follows the α-disc scaling. This suggests that for typical values of the Shakura and Sunyaev viscosity parameter α and sufficiently large H/R ratios, binary-disc decoupling may occur just inside the LISA band. Gas interaction becomes even more relevant in the mHz regime for binaries with smaller component masses or lower mass ratios. Also, the binary residual eccentricity when it enters the LISA band may be determined at binary-disc decoupling (Roedig et al. 2011), suggesting that residual eccentricities of up to 10^{-2} in the LISA band are possible (see also Cuadra et al. 2009; Muñoz et al. 2019).

It is unclear, however, how realistic this way of reasoning is. Fully relativistic 3D magnetohydrodynamic (MHD) simulations (Farris et al. 2012; Gold et al. 2014b; Khan et al. 2018a) find that accretion on to the binary proceeds all the way through the binary merger, albeit at progressively slower rate, suggesting that there is never a true decoupling between disc and MBHB. These studies also showed that if the disc is cooler, then decoupling is more pronounced and the accretion on to the binary declines earlier than in hot discs. Recent 2D simulations (Farris et al. 2015a; Tang et al. 2018) are in agreement with the relativistic studies and suggest that angular momentum transport of the gas in the vicinity of the binary is driven by shocks, which enable it to flow inwards and follow the binary even well past the canonical decoupling radius.

Before the launch of LISA a number of improvements to these models are needed in order to develop tools (e.g., include eccentricity in waveforms and data analysis) and use them as guide for EM searches (see Sect. 2.5). Descriptions of the fuelling processes from large scale down to the central pc of galaxies, with a higher resolution than the one achieved in the current available studies, are needed to pin down the properties of circumbinary discs. Furthermore, current simulations of circumbinary discs are idealized in many ways (e.g. some simulations are in 2D rather than 3D, some do not include magneto-hydrodynamics, most have simplified equations of state and treatment of thermodynamics, all of them neglect radiative feedback, and disc self-gravity is rarely included except in Cuadra et al. 2009; Roedig et al. 2011, 2012; Roedig and Sesana 2014; Franchini et al. 2021). Moreover, although it is expected that discs at the decoupling radius are gravitationally stable, except for

binaries too massive to be detected by LISA (Haiman et al. 2009), eccentricity evolution would be different in a self-gravitating regime, as the disc would become strongly distorted in response to its own self-gravity. Therefore, more sophisticated models of accretion in conjunction with future observations are necessary to properly predict the residual eccentricity of binaries and other aspects of their dynamics when they enter the LISA band.

• **The formation and evolution of mini-discs**

The matter that crosses the gap/cavity region (as discussed in the previous section) can form mini-discs around each MBH (see illustration in Fig. 21). Their presence may depend on the thermal state of the circumbinary disc, with colder and thinner discs producing lower-mass and shorter-lived mini-discs than those in hotter and thicker circumbinary discs (Ragusa et al. 2016). While their masses may be small (Chang et al. 2010; Tazzari and Lodato 2015; Fontecilla et al. 2017), they mediate the rate of accretion on to the MBHs (and determine their spin evolution, see the discussion in Sect. 2.3.2.4) and may play a role in the migration rate of the binary. Present 2D simulations find that the resulting disc torque that affects the binary evolution receives a dominant or significant contribution from the gas near the edge of the mini-discs, and, from the numerical point of view, therefore depends on the treatment of mini-discs and possibly even on the sink particles, and/or the inner boundary conditions that mimic MBHs in Newtonian simulations (Tang et al. 2017; Muñoz et al. 2019; Moody et al. 2019; Tiede et al. 2020). The importance of the mini-discs torques has also been confirmed with 3D numerical simulations by Franchini et al. (2022), therefore calling for comprehensive investigations about mini-discs modeling in Newtonian numerical simulations.

Calculations partially involving relativistic corrections (Noble et al. 2012) or full GR (Farris et al. 2012; Gold et al. 2014b, a; Khan et al. 2018a) did not find persistent mini-discs. The more recent studies of Bowen et al. (2017, 2018) initialized the simulations with mini-discs already in place, and found mini-discs which are more persistent, but also found that they undergo periods of depletion and replenishment. In Gold et al. (2014b), it was argued that the reason for the absence of persistent mini-discs in relativistic simulations at small orbital separations was due to the fact that the ISCO around the individual MBHs is larger than the corresponding Hill spheres, thereby any matter that is gravitationally bound to one MBH is immediately accreted. This hypothesis was recently confirmed in fully GR simulations in Paschalidis et al. (2021).

Despite the progress made so far, studies of all these topics are at an infant state at the moment, and more sophisticated models are necessary to understand how the presence of mini-discs and a circumbinary disc affects the MBH spins, and the binary orbit as it evolves toward the LISA band.

2.2.2.3 The effect of AGN feedback in the hardening phase   Irrespective of the dominant hardening mechanism, AGN feedback, i.e. the energy injection from an accreting MBH, can affect the dynamics of an evolving MBHB, as it does in the phases before binary formation (see Sect. 2.2.1.3). For a binary migrating in a circumbinary disc, the effect of AGN feedback has been explored, with smoothed-

particle hydrodynamics (SPH) simulations, only for binaries with parsec separation, i.e. in the early stages of binary evolution (del Valle and Volonteri 2018). The effect of feedback in the late binary evolution has not been investigated explicitly yet. del Valle and Volonteri (2018) consider the two main regimes of binary evolution, one where the binary opens a gap in the disc and one where a gap does not form. As said, if viscous torques are inefficient in redistributing the angular momentum extracted from the binary, a low density cavity (gap) forms around the MBHs. In this situation, very little gas flows towards the MBHs, which have low accretion rates and AGN feedback is characterized by outflows carrying little mass and escaping through the cavity. They do not affect the binary orbital evolution which, however, is very slow exactly because of the presence of the cavities and inefficient torques. If the redistribution of angular momentum extracted from the binary is efficient, no gap forms, and the MBHs are embedded in a dense gas bath, leading to rapid migration. Under these conditions, however, gas accretion on the MBHs is also favoured. MBHs then produce mass-loaded winds that interact with the gas in the disc, shredding it and ejecting it in all directions. The ejection of gas leads to the formation of a hollow region ("feedback gap") around the MBHs, and the binary migration is stalled by the lack of gas with which to exchange torques. In these simulations feedback was injected isotropically, but outflows could be non-isotropic if launched by a disc, and the effect of a collimated outflow could be different and it would be worthwhile to explore this in future studies. These jets and collimated outflows could result in unique EM signatures, as discussed in Sects. 2.5 and 2.6.

For a binary evolving instead by stellar hardening, the effect of AGN feedback has not been explicitly studied. We can speculate that thermal or kinetic energy injection should have little effect on the distribution of existing stars, however, it can affect, and even suppress, the formation of new stars. If binary evolution is slower than star formation, persistent AGN feedback would prevent the formation of new stars that can repopulate the loss cone and further the shrinking of the binary. If the amount of gas present is very little, this effect is likely limited. If gas is copious, then this effect can become important, but then one has to consider that the dynamics of the binary will occur in a "mixed environment", where both scattering with stars and gas torques contribute to the binary migration.

In summary, this regime is still largely unexplored, and may have important consequences for the orbital evolution and the EM counterparts of LISA's detections. In the near future, both simulations including isotropic and collimated AGN feedback in the late evolution of MBHs in circumbinary discs, and simulations of the stellar hardening phase including gas, star formation and AGN feedback, will need to be developed to address/understand the impact of feedback on MBH coalescence.

2.2.2.4 The formation of triplets/multiplets of MBHs In the high-redshift Universe, the environment in which MBHs live is highly dynamical, as halo interactions and mergers are far more frequent (e.g. the Jackpot nebula, a system at $z \sim 2$ containing several AGN in the same 400 kpc-wide Ly-α nebula, see Hennawi et al. 2015). The outcome of these encounters could be either the formation of an MBHB or, at least temporarily, a wandering MBH, leading to multiple MBHs in the grown galaxy halo,

each inherited from a different merger (Pfister et al. 2019b). Failures in the binary formation process affect the specific merger rate as a function of redshift, MBH mass, and mass ratio (Klein et al. 2016; Bonetti et al. 2019; Barausse et al. 2020b).

In these situations, the formation of MBH triplets or multiplets can arise, possibly triggering a richer and more complex range of few-body dynamics (Mikkola and Valtonen 1990; Heinämäki 2001; Blaes et al. 2002; Hoffman and Loeb 2007; Amaro-Seoane et al. 2010b; Kulkarni and Loeb 2012; Rantala et al. 2017; Ryu et al. 2018; Bonetti et al. 2018; Mannerkoski et al. 2021). Triplets of MBHs generally start their evolution as spatially hierarchical systems, i.e. systems where the hierarchy of orbital separations (or semi-major axes) defines an inner (a_{in}) and an outer binary (a_{out}), the latter consisting of the newly arrived MBH coming from $\sim$ kpc scales plus the former binary (viewed as an effective single body located at its centre of mass). Under certain circumstances, these MBH systems may undergo von Zeipel–Lidov–Kozai (ZKL) oscillations (von Zeipel 1910; Kozai 1962; Lidov 1962), in which secular exchanges of angular momentum between the two binaries periodically excite the inner binary's orbital eccentricity at the expense of the relative inclination (see also Sects. 2.3.3 and 1.7.1.6 for the same process in the context of stellar-mass compact objects), resulting in efficient GW emission (see Sect. 2.2.3).

Despite the ZKL mechanism's efficiency in increasing the orbital eccentricity, it has been shown that relativistic precession (or other types of precession) can interfere with it. In practice, if the apsidal precession time-scale is shorter than that of the ZKL oscillations, then precession destroys the coherent accumulation of secular torques, hindering eccentricity growth (see e.g. Ford et al. 2000; Naoz 2016; Lim and Rodriguez 2020). In the context of MBH triplets, the ZKL mechanism can be further re-enhanced by the orbital decay of the intruder MBH, due to its interaction with the host galaxy environment, which tends to shrink its separation from the inner binary (see e.g. Bonetti et al. 2018). This produces a shortening of the ZKL oscillation period and a strengthening of the perturbing force acting on the inner binary, again promoting the increase of eccentricity with subsequent GW emission and possible coalescence (Bonetti et al. 2018).

Although ZKL oscillations may sometimes lead to a direct merger of the inner binary, there are many initial conditions under which no merger can occur during the secular evolution phase of MBH triplets. For example, the mutual inclination may not be high enough, the perturber may be too light, or the binary may be too wide for efficient emission of GWs. In this case, the triplet is likely to become Hill-unstable as the perturber's shrinking orbit brings it closer to the inner binary. The final fate of many MBH triplets is thus dynamical instability, wherein the secular interaction gives way to chaotic dynamics characterized by strong encounters, exchanges, and ejections. Again, this may not represent the end of the story, since in fact an ejected MBH may leave on a wide but bound trajectory, in which case it may return back and perturb the inner binary, this time through close energetic encounters, depending on the galactic potential (spherical, axisymmetric or triaxial), the specific outgoing trajectory and also on the dynamical friction efficiency. Repeated chaotic interactions between the ejected MBH and the leftover binary can increase the orbital eccentricity again, promoting coalescence in a non-negligible fraction of cases (see, e.g. Bonetti

et al. 2018). Still, since this is not always effective, a considerable number of ejected MBHs may keep wandering inside galaxies.

Finally, when the lifetime of hierarchical triplets is long enough, new galaxy mergers provide additional MBHs, forming hierarchical quadruplets and even higher-order multiplets. Considering quadruplets, a natural way in which they can form is when two merging galaxies each host MBHBs. In this particular case, the system can behave like a hierarchical triplet until the four-body nature of the system becomes manifest, leading again to chaotic dynamics. The dynamics of MBHs multiplets can be highly stochastic and largely non-predictable, requiring therefore numerical investigations. Still, a likely signature of MBHB coalescence triggered by dynamical interaction is the very high acquired eccentricity, that will be retained (or at least, retained in residual form) well inside the GW-dominated phase (Ryu et al. 2018; Bonetti et al. 2019).

In the context of LISA, pre-launch more work is needed to generally include triple/multiple interactions in models of MBH evolution (as done in Bonetti et al. 2019), and to assess the consequences on the need of eccentric waveforms. Post-launch, detection of highly eccentric MBHBs would point to triple/multiple interactions as important drivers of MBHB coalescences.

2.2.3 The GW-emission phase at mpc scale

As the MBHB continues to efficiently interact with the surrounding environment, which continuously drains energy and angular momentum from the MBHB system (e.g. Hills and Fullerton 1980), it eventually enters into the gravitational radiation dominated phase. During this phase, the main parameters driving the evolution are the masses and spins of the MBHs, as well as the binary separation and eccentricity.

• **Relativistic evolution**

Although relativistic effects can influence the binary evolution also in the previous hardening phase, at this stage we must necessarily take them into account. Relativistic effects can be introduced through spin-dependent post-Newtonian (PN) corrections in the equations of motion of the MBHs.

Schematically, the PN-corrected acceleration can be written as

$$\mathbf{a} = \mathbf{a}_N + \mathbf{a}_{1\,PN} + \mathbf{a}_{2\,PN} + \mathbf{a}_{3\,PN} + \mathbf{a}_{2.5\,PN} + \mathbf{a}_{3.5\,PN} + \cdots, \tag{12}$$

where, in the case of N-body numerical simulations, the Newtonian acceleration $\mathbf{a}_N$ is usually computed including the surrounding stellar particles, whereas the PN-terms only include contributions from two MBHs (see, e.g. Will 2006; Kupi et al. 2006; Brem et al. 2013; Blanchet 2014; Mannerkoski et al. 2019). The PN-correction terms are labelled so that they are proportional to the corresponding power of the formal PN expansion parameter ϵ_{PN}, i.e.

$$|\mathbf{a}_{i\,PN}| \propto \epsilon_{PN}^i \sim \left(\frac{v}{c}\right)^{2i} \sim \left(\frac{r_g}{R}\right)^i, \tag{13}$$

where v and R are the relative velocity and separation of the MBHB, while $r_g = GM/c^2$ is the gravitational radius, with c the speed of light in vacuum, G the

gravitational constant, and M the binary total mass. The PN terms of integer order are conservative, whereas the half-integer order terms are dissipative radiation reaction terms related to the emission of gravitational radiation.

The PN corrections, and thus the GW emission, are still negligibly small when the binary separation is of the order $a \sim a_h$ (see Eq. 9). The PN radiative loss terms in the equations of motion start dominating the evolution when the binary separation drops down to $a \sim a_{GW} \sim 0.01 \times a_h$ (e.g. Quinlan 1996; Sesana et al. 2006; Rantala et al. 2018). This corresponds to a typical physical separation of $a_{GW} \sim 10^{-4}$–10^{-3} pc for equal-mass binaries with individual MBH masses of $M_{BH} \sim 10^6$–10^7 M$_\odot$, with the required separation being correspondingly smaller for lower-mass MBHs. However, it is also possible for the gas component to follow the binary essentially all the way down to merger, and thus gas can be present even in this GW-emission stage (see Sect. 2.2.2.2 and Farris et al. 2015a; Tang et al. 2018). In a novel attempt to quantify the effects of environmental perturbations (such as gas friction and torques) with respect to those due to PN corrections, Zwick et al. (2021) found simple analytical expressions for the regions of phase space wherein the two are comparable.

• **The GW-driven inspiral**

If we assume that the evolution of the system is purely driven by GW emission, to leading order, the secular evolution of the Keplerian orbital parameters of the isolated MBHB can be approximated following the seminal work by Peters (1964a). While the orbital period scales as $t \sim (a/r_g)^{3/2}$ (where a is the semi-major axis), the radiation reaction time-scale scales instead as $t_{RR} \sim (a/r_g)^4$. The inequality $a \gg r_g$ implies that $t_{orb} \ll t_{RR}$: the binary is thus approximately Keplerian, and the orbital parameters a and e change slowly. Using angular brackets to denote orbit averaging, the evolution of the binary's semi-major axis is described by (Peters and Mathews 1963; Peters 1964a)

$$< \frac{da}{dt} >_{GW} = -\frac{64}{5} \frac{G^3 m_1 m_2 M}{c^5 a^3 (1-e^2)^{7/2}} \left(1 + \frac{73}{24}e^2 + \frac{37}{96}e^4\right) = -\frac{64}{5} \frac{G^3 m_1 m_2 M}{c^5 a^3} f(e),$$

(14)

where $f(e) = (1 + 73e^2/24 + 37e^4/96)(1-e^2)^{-7/2}$ is the so-called eccentricity enhancement function, whereas m_1, m_2, and M denote the masses of two bodies and the binary total mass, respectively. The evolution of the eccentricity e is instead dictated by

$$< \frac{de}{dt} >_{GW} = -\frac{304}{15} \frac{G^3 m_1 m_2 M}{c^5 a^4 (1-e^2)^{5/2}} e \left(1 + \frac{121}{304}e^2\right).$$

(15)

The overall minus sign ensures that both the semi-major axis and the eccentricity decrease as the binary evolves, resulting in an increasingly tighter and more circular binary orbit.

For $e \ll 1$, Eqs. 14 and 15 imply that the eccentricity decays faster than the orbital separation. This causes a fast circularization of initially eccentric systems and, unless

the initial eccentricity is extremely high, binaries in this GW-driven regime would mostly be circular.

An important caveat to the rather simplistic discussion presented above is that when all PN corrections up to a given order (e.g. 3.5 PN) are included in the motion of the MBHB, the standard Keplerian elements are no longer constant over an orbit, but rather they oscillate, especially near the pericentre of an eccentric orbit (e.g. Will 2006; Mannerkoski et al. 2019; Memmesheimer et al. 2004). When MBHs are spinning, their spins (both modulus and direction) also participate in shaping the dynamics of inspiraling binaries and profoundly affect the orbital motion (Cutler and Flanagan 1994; Apostolatos et al. 1994; Kidder 1995; Kesden et al. 2015; Gerosa et al. 2015a), as well the emitted GWs.

Despite the inclusion of high PN order being able to describe very well the evolution down to a few gravitational radii, at binary separation of about $a \sim 6r_\mathrm{g}$ and below, the strongly non-linear gravitational field makes the PN expansion to become unreliable, and full GR simulations are necessary (see, e.g. Pretorius 2005; Campanelli et al. 2006; Baker et al. 2006).

• **The GW inspiral time-scale**

A reasonable question to ask is the following: if the binary enters the GW-driven phase of its evolution with certain initial orbital parameters (semi-major axis and eccentricity), how much time will it take to merge?

A proper answer requires the numerical integration of the evolution Eqs. 14 and 15, as discussed above. Still, a reasonable analytical approximation, valid for mildly eccentric binaries, is given by the so-called Peters' time-scale (Peters 1964b), i.e.

$$t_\mathrm{P} = \frac{5c^5(1+q)^2}{256G^3M^3q}\frac{a_0^4}{f(e_0)} \approx 0.32\frac{(1+q)^2}{qf(e_0)}\left(\frac{a_0}{\mathrm{AU}}\right)^4\left(\frac{M}{10^6\mathrm{M_\odot}}\right)^{-3}\mathrm{year}. \quad (16)$$

where a_0 and e_0 are the initial semi-major axis and eccentricity, respectively. The interpretation of this time-scale is simple: the more massive and the more compact the binary is, the faster it will decay. Moreover, for a given semi-major axis, highly eccentric orbits decay much faster than circular ones, simply because the two MBHs at pericentre are closer to each other and the strong GW emission efficiently extracts a large amount of orbital energy.

Because of its simplicity, this formula has been widely used to estimate the decay time-scale of compact binaries, as done in many preceding sections when the efficiency of GW-induced decay must be compared against other factors that affect the orbital evolution.

While Peters's formula often suffices as an order-of-magnitude estimate for the decay time-scale, it has two major limitations that are known but often overlooked. First of all, it is only a lower bound to the results of numerical integration, and it can underestimate the numerical time-scale by a factor of 1–8 (Peters 1964a). In addition, Peters and Mathews' analysis assumes that the binary follows a Keplerian path, and that it only radiates according to the quadrupole formula: both of these assumptions are only true at the lowest order in the PN expansion. Corrections to the classic formula have been recently presented in Zwick et al. (2020) up to first order in PN theory. For orbits that are either eccentric or highly relativistic, one can expect errors

of order ten to be accounted for by the correction factors. Recently, Zwick et al. (2021) expanded further on those results, obtaining a new spin-dependent correction. The corrected formula reads, for a given total mass and mass ratio, in the case of highly eccentric orbits:

$$t_{PN}(a_0, e_0, s_1) = \underbrace{\frac{5c^5(1+q)^2}{256G^3M^3q f(e_0)} a_0^4}_{\text{Peters' formula}} \underbrace{R(e_0) \exp\left(\frac{2.8r_S}{p_0} + s_1 \frac{0.3r_S}{p_0} + |s_1|^{3/2}\left(\frac{1.1r_S}{p_0}\right)^{5/2}\right)}_{\text{eccentricity, spin and PN correction}},$$

(17)

where $p_0 = a_0(1 - e_0)$, $r_S = 2GM/c^2$, $R(e_0) = 8^{1-\sqrt{1-e_0}}$, and $s_1 \equiv S_1 \cos\theta$, with S_1 being the magnitude of the spin of the most massive MBH and θ the angle between that MBH's spin vector and the orbital angular momentum vector. Adopting more accurate GW-emission time-scales in studies devoted to LISA would be beneficial to improve the investigations of MBHB dynamics and merger rates.

- **MBH coalescence and kicks/recoils**

When MBHs finally reach coalescence, the emitted GWs are responsible for dissipating not only energy and angular momentum (causing the shrinking of the orbit), but also linear momentum (Bonnor and Rotenberg 1961; Peres 1962; Bekenstein 1973). Conservation of linear momentum implies that the MBH left behind following a merger has a non-zero recoil velocity (or "kick"), which is independent of the MBH mass and depends only on the mass ratio, spins, and eccentricity of the merging binary. While energy and angular momentum are dissipated more gradually during the inspiral, linear-momentum emission is strongly peaked during the last few orbits prior to and at merger (e.g. Brügmann et al. 2008; Gerosa et al. 2018b). This implies that, although PN predictions are possible (Fitchett 1983; Kidder 1995; Blanchet et al. 2005), kicks can be modelled accurately only using numerical-relativity simulations (e.g. Campanelli et al. 2007b; González et al. 2007a; Tichy and Marronetti 2007; Lousto and Zlochower 2011). Such kind of (very expensive) simulations show that MBH recoils can reach velocities as large as ~ 5000 km s^{-1} (the so-called "superkicks"). A variety of tools, ranging from fitting formulae (Campanelli et al. 2007a; González et al. 2007b; Lousto and Zlochower 2008, 2013; van Meter et al. 2010; Gerosa and Kesden 2016) to full surrogate models (Gerosa et al. 2018b; Varma et al. 2019) calibrated on numerical-relativity results are now available to quickly estimate MBH kicks for large parameter-space explorations.

Kicks around 1000 km s^{-1} imply that MBH merger remnants might have velocities that exceed the escape speed of their galactic hosts (Redmount and Rees 1989; Merritt et al. 2004; Gerosa and Sesana 2015). The astrophysical consequences of recoils are several. Amongst them, we find that energetic kicks can critically modify the merger rate of MBHs, induce scatter in the correlations between MBHs and galaxy hosts, deplete low-mass galaxies of MBHs, create cores in the central stellar distribution, hinder the formation of $> 10^9 M_\odot$ MBHs powering $z > 6$ quasars, and generate a population of wandering MBHs and AGN. These possibilities were explored by various authors (e.g. Haiman 2004; Boylan-Kolchin et al. 2004; Volonteri and Perna 2005; Sesana 2007; Gualandris and Merritt 2008;

Volonteri 2007; Shields and Bonning 2008; Holley-Bockelmann et al. 2008; Blecha and Loeb 2008; Blecha et al. 2011; Dunn et al. 2020; Sayeb et al. 2021). In the LISA context, the occurrence of kicks might have important consequences for the MBHB event rate, although the assessment of their impact depends very sensitively on the assumed spin directions that can be strongly affected by the interaction with the surrounding environment (Schnittman 2007; Bogdanović et al. 2007; Kesden et al. 2010a, b; Berti et al. 2012; Miller and Krolik 2013; Gerosa et al. 2015b, 2020; Dotti et al. 2010). Furthermore, recoiling MBHs would produce a post-merger EM signature that can aid in the identification of the merged MBH (Milosavljević and Phinney 2005; Schnittman and Buonanno 2007; Schnittman and Krolik 2008; Lippai et al. 2008; Corrales et al. 2010; Rossi et al. 2010).

Potential EM signatures of GW recoils are reviewed by Komossa (2012). If the recoiling MBHs carry the bound gas as they recoil, they would shine as off-nuclear AGN (Blecha and Loeb 2008; Volonteri and Madau 2008). The most characteristic signature is a set of broad emission lines, which led to the identification of several observational candidates (Komossa et al. 2008; Civano et al. 2012; Tsalmantza et al. 2011; Koss et al. 2014; Chiaberge et al. 2017; Kim et al. 2017; Kalfountzou et al. 2017) and the development of various detection strategies (Lena et al. 2014; Raffai et al. 2016; Blecha et al. 2016). Identification of such candidates is a particularly
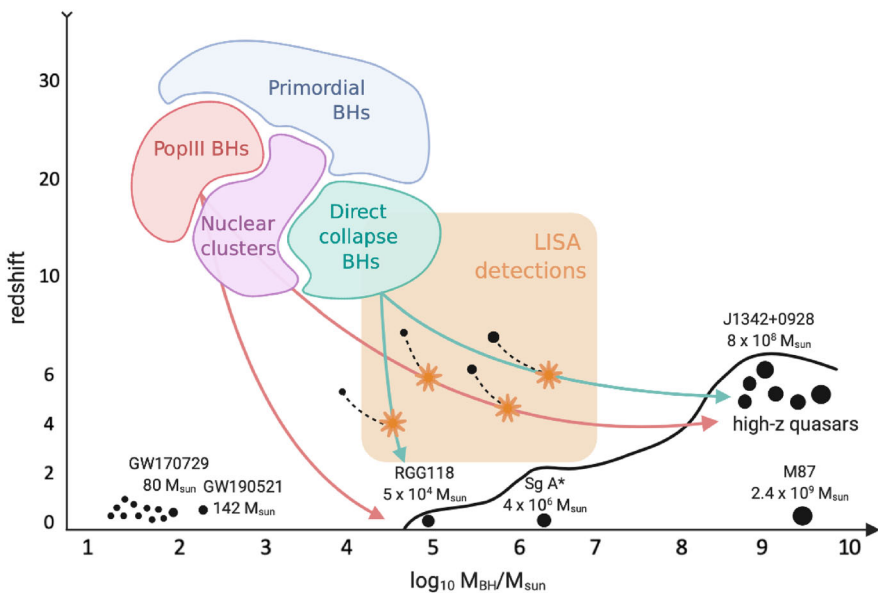
Fig. 22 Pathways towards the formation of MBHs are numerous, and include the collapse of first-generation stars (*Pop III BHs*, $M_{BH} \lesssim 10^3 M_\odot$), the collapse and/or coalescence of massive stars formed in compact stellar clusters (*nuclear clusters*, $10^2 M_\odot \lesssim M_{BH} \lesssim 10^4 M_\odot$), the collapse of SMS formed in primordial environment (*direct collapse*, $M_{BH} \gtrsim 10^3 M_\odot$), and the collapse of cosmological density perturbations (*primordial BHs*, $1 M_\odot \lesssim M_{BH} \lesssim 10^{10} M_\odot$). The shaded orange region shows the redshift and MBH mass ranges of LISA, and the orange starburst symbols the LISA detections. LISA will significantly extend the current MBH EM detections, shown below the curved solid black line (from the local Universe at $z \sim 0$ to the high-redshift quasars at $z \geqslant 6$). Image credit: Melanie Habouzit

active field of research and is a difficult task (see Sect. 2.5); some candidates cited above have already been disproved in the recent years. Detection or confirmation of some candidates would prove that indeed MBHBs merge in the Universe, supporting LISA's science case.

Recoiling systems are also expected to present GW signatures. These include a relative Doppler shift between inspiral and ringdown (Gerosa and Moore 2016), different higher-order mode content (Calderón Bustillo et al. 2018), and statistical correlation with the spin properties (Varma et al. 2020). Gerosa and Moore (2016), Calderón Bustillo et al. (2018), Varma et al. (2020) all agree that the direct detectability of GW signatures from kicked MBHs is well within the reach of LISA.

2.3 MBH origin and growth across the cosmic time

Coordinators: **Pratika Dayal, John Regan**

Contributors: **Pau Amaro-Seoane, Abbas Askar, Razvan Balasov, Emanuele Berti, Pedro R. Capelo, Laurentiu Caramete, Monica Colpi, Davide Gerosa, Melanie Habouzit, Daryl Haggard, Peter Johansson, Fabio Pacucci, Raffaella Schneider, Stuart L. Shapiro, Caner Unal, Rosa Valiante, Marta Volonteri**

MBHs are ubiquitous across space and time. Observations have revealed the likelihood that MBHs populate every massive galaxy in the Universe (e.g., Kormendy and Ho 2013), with MBHs of upwards of $10^4 \, M_\odot$ populating some, possibly large, fraction of dwarf galaxies (e.g., Baldassare et al. 2015; Chilingarian et al. 2018; Mezcua et al. 2018; Graham et al. 2019; Greene et al. 2020; Baldassare et al. 2020). At the massive end of the MBH mass function, MBHs are remarkably well-centred in the cores of galaxy bulges, and their mass is tightly correlated with many properties of the galaxy host, as the stellar mass of the bulge. Luminous quasars, powered by $10^{8-9} \, M_\odot$ MBHs, were identified when the Universe was less than a billion years old ($z \sim 7.5$, Bañados et al. 2019; Yang et al. 2020a; Wang et al. 2021a), evidence that MBH evolution started well before then.

LISA will bring a wealth of new independent information on the population census and the ability of MBH mergers to contribute to the growth of MBHs, all the way to the realm of MBH "seeds" postulated by different formation models. No telescope can search for MBHs at redshifts as high as LISA can ($z > 10$), allowing us to observe an otherwise inaccessible region of the Universe. LISA will play a crucial role in, for instance, pinpointing the main formation channel of MBH seeds at high redshift, with light seeding models (numerous but low mass BH seeds) expected to drive a significantly higher merger rate at $z \gtrsim 10$ compared to heavy seeds (rare but massive BH seeds), provided that their dynamical decay is efficient (see Sect. 2.3.2.1). Several studies (e.g. Berti and Volonteri 2008; Sesana et al. 2011a; Barausse 2012; Amaro-Seoane et al. 2017; Dayal et al. 2019; Bonetti et al. 2019; Pacucci and Loeb 2020; Barausse et al. 2020b; Valiante et al. 2021) have shown that

LISA will provide a unique view of the merger history of MBHs up to very high redshift ($z \sim 20$).

In this section, we first review our current understanding of the different seed MBH formation mechanisms, the resultant seed masses, and the outstanding questions in the field. In the second part, we examine the growth of MBHs across cosmic time under the assumption that a population of seeds, formed at $z \sim 10$–30, grow over cosmic time via the two key mechanisms of gas accretion and coalescence. Growth by accretion can typically occur by a stable influx of material, usually organised in a thin/thick accretion disc (e.g., Shakura and Sunyaev 1976; Jiang et al. 2014) or via chaotic accretion with cold gas raining from random directions (e. g. Gaspari et al. 2013, 2015; Voit et al. 2017). Coalescence between MBHs also contributes to their growth, with some small fraction of the total mass being radiated away via GWs. Through this section, we discuss how LISA will be crucial in shedding light on the origin and evolution of MBHs.

2.3.1 MBH seeds: formation mechanisms

LISA will be sensitive to the detection of MBHs with masses in excess of a few thousand solar masses out to high redshifts, and therefore uniquely able to probe how MBHs form in the first galaxies. Theoretical models show that seeding mechanisms are crucial to make detailed predictions for the number density of MBH mergers and hence for predicted detections by LISA (see detailed description in Sect. 2.4). Correctly modelling the seeding of MBHs thus becomes of paramount importance to prepare and then interpret LISA data.

In this section, we focus on formation pathways which can lead to the production of such seeds ($M_{\mathrm{BH}} = 10^2$–$10^6 \, \mathrm{M}_\odot$)—see Fig. 22. This includes *(a)* seeds from metal-free Population III (Pop III) stars; *(b)* seeds originating from the dynamical processes in dense stellar clusters; *(c)* seeds born from the collapse of supermassive stars (SMSs); and *(d)* primordial MBH seeds. More detailed information on each of these scenarios is dealt with in other reviews (e.g. Volonteri 2010; Johnson and Haardt 2016; Valiante et al. 2017; Inayoshi et al. 2020; Volonteri et al. 2021). Here we outline the mechanisms behind each pathway as well as underlining outstanding issues in the field, especially those pertinent to LISA. The consequences on the detection rate and properties of mergers identified by LISA will be discussed in Sect. 2.4.2.2.

• **Formation of MBHs as Pop III remnants** [$\mathrm{M}_{\mathrm{BH}} \lesssim 10^3 M_\odot$]

One of the popular explanations behind the formation of high-redshift MBHs is related to Pop III stars, the hypothesized first-generation stars. Pop III stars are born in $\sim 10^5$–$10^6 M_\odot$ DM "minihaloes". The primordial gas in these first haloes is cooled primarily by H_2, which allows the temperature of the gas to cool to approximately 200 K (Abel et al. 2002). This inefficient cooling channel leads to a top-heavy initial mass IMF expected for Pop III stars compared to present day star formation (Turk

---

[7] While the term direct collapse is often used in the literature to describe the formation of an MBH seed, that terminology is ambiguous and the formation of the intermediate stellar stage is expected in the general case (Inayoshi et al. 2020) except perhaps under extreme conditions (e.g. Mayer et al. 2010).

et al. 2009; Clark et al. 2011a, b), with mass values ranging from $10M_\odot$ to $10^3 M_\odot$ (Hirano et al. 2014).

Pop III stars with masses $M_* \gtrsim 260 M_\odot$ will directly collapse into BHs, losing very little of their progenitor mass in the process (Heger et al. 2003). The retention of a significant amount of the parent star mass is expected as a result of the weak stellar winds associated with metal-free stars. As a result, a large population of Pop III remnant BHs is expected to be left behind in these first minihaloes that are ubiquitous at early times. Less massive Pop III stars will explode as SNae, enriching their surroundings with metals. As metal enrichment is extended to nearby galaxies (e.g. Smith et al. 2015; Hicks et al. 2021) through both winds and halo mergers, the formation of Pop III stars declines severely and less massive Population-II stars begin to dominate the star formation history of the Universe (O'Shea et al. 2015; Xu et al. 2016). Nonetheless, this first generation of stars leaves in its wake a large number of Pop III remnant BHs, which may act as the seeds to future MBHs (Madau and Rees 2001; Hirano et al. 2014). A key open question is therefore whether these Pop III remnants can grow into a population of MBHs, and under what conditions rapid growth can be achieved (this is particularly relevant for the high-z quasars) and their mergers be expected to be detected by LISA. We will explore research in this area and the significant challenges to their growth which must be overcome in Sect. 2.3.2.

• **Formation of MBHs in dense stellar environments** $[10^2 M_\odot \lesssim M_{BH} \lesssim 10^4 M_\odot]$ Seed MBHs of 10^2–$10^4 M_\odot$ can form in dense and massive stellar clusters of $\sim 10^5 M_\odot$ through dynamical interactions (e.g., Omukai et al. 2008; Devecchi and Volonteri 2009; Reinoso et al. 2018; Schleicher et al. 2022). During the early evolution of star clusters with initial central densities $\gtrsim 10^5 M_\odot \text{pc}^{-3}$, massive stars segregate to the cluster centre due to dynamical friction, where they may undergo runaway collisions resulting in the formation of very massive stars with masses of approximately 10^2–$10^3 M_\odot$ (Portegies Zwart and McMillan 2002; Portegies Zwart et al. 2004; Gürkan et al. 2004; Freitag et al. 2006b, a). In low-metallicity clusters, such massive stars may collapse into an MBH (Katz et al. 2015; Giersz et al. 2015; Mapelli 2016; Sakurai et al. 2017; Giersz et al. 2015; Rizzuto et al. 2020).

Another possibility of forming an MBH in stellar clusters is through runaway mergers of stellar-mass BHs, which are expected to form from the evolution of massive stars. If stellar-mass BHs form with low-velocity natal kicks or are embedded in a dense gaseous halo (Belczynski et al. 2002; Mandel 2016; Giacobbo and Mapelli 2018; Davies et al. 2011), a significant fraction can be retained within the star cluster (Sippel and Hurley 2013; Morscher et al. 2013, 2015; Wang et al. 2016b; Arca Sedda et al. 2018; Askar et al. 2018; Kremer et al. 2019a). While the mergers of these stellar mass sized BHs will generate GWs, their frequency ranges put them outside of the sensitivity range of LISA - they may however be detectable by future GW detectors like the Einstein Telescope (Valiante et al. 2021). A potential barrier to this formation scenario is that the retention of any MBH will depend on the GW recoil kicks that they receive during the merger process. If recoil

---

[8] Current research is trending towards a likely overlap between the conditions necessary for a dense stellar cluster to form and for SMS formation and hence an overlap in mass scales between SMS formation and the formation of a dense stellar cluster.

kick velocities are larger than the escape speed of the cluster, then the seed MBH may be ejected out of the cluster (Holley-Bockelmann et al. 2008; Davies et al. 2011; Miller and Davies 2012; Sesana et al. 2014; Morawski et al. 2018).

It may also be possible to grow stellar-mass BHs through gas accretion (rather or in conjunction with mergers) inside stellar clusters. Retained stellar-mass BHs could effectively grow and become MBHs by accreting the interstellar gas inside massive stellar clusters (Leigh et al. 2013; Natarajan 2021). Moreover, BHs of $\sim 100 M_\odot$ can become more massive by growing through tidal capture and disruption of stars in dense nuclear star clusters (Stone et al. 2017a). Such runaway events can grow the mass of a BH from $10^{2-3} M_\odot$ to up to $10^5 M_\odot$ (Rosswog et al. 2009b; MacLeod et al. 2016a; Alexander and Bar-Or 2017; Stone et al. 2017a; Boekholt et al. 2018; Sakurai et al. 2019).

• **Formation of very massive seeds in atomic cooling haloes and primordial galaxies** [$M_{BH} \gtrsim 10^3 M_\odot$] SMSs[7] were originally invoked to explain the existence of quasars prior to their origin being understood as the accretion of matter on to MBHs. More recently, SMSs have been "reinvoked" as potential seeds for MBHs. SMSs are thought to form through the rapid accumulation of gas during the early stages of stellar evolution. If gas can be rapidly accreted with accretion rates in excess of $10^{-3} M_\odot$ year^{-1} (Haemmerlé et al. 2018; Omukai and Palla 2003), then the stellar envelope remains bloated and cool (with a temperature $T_{eff} \sim 5000$ K). Detailed numerical simulations have shown that such objects do not provide enough negative (radiative) feedback to halt accretion and the end result is an SMS (Sakurai et al. 2016; Chon et al. 2018; Sakurai et al. 2020). However, sustaining this accretion rate is nonetheless challenging, due to the complex dynamics between the gas and the stellar component (Chon and Omukai 2020; Regan et al. 2020a).

The ideal environmental conditions for SMS formation can be achieved in so-called atomic cooling haloes (Tanaka and Haiman 2009), where line-emission cooling due to neutral hydrogen allows the gas to cool and condense in a sufficiently massive halo (with a virial temperature $T_{vir} \sim 8000$ K and a virial mass $M_{vir} \sim 5 \times 10^7 M_\odot$ at $z \sim 15$). The larger mass of the atomic cooling halo, compared to the minihaloes in which Pop III stars are typically born, provides a larger baryonic reservoir for (metal-free) star formation. The key requirement for the development of an SMS is that the gas inflow onto the stellar surface remains high. Fragmentation of the gas into a (dense) stellar cluster must also be avoided for a truly SMS to form[8] (Regan et al. 2020a). Fragmentation may be avoided if the gas is sufficiently metal-poor (Chon and Omukai 2020; Tagawa et al. 2020b), with metallicities not exceeding $Z \approx 10^{-3} Z_\odot$, and perhaps also if the halo is not tidally disrupted (Chon et al. 2018). Given the difficulties in achieving monolithic SMS formation, the question of whether true SMS formation can be achieved remains an open and active research question.

Radiative feedback in the Lyman-Werner (LW) band (in the energy range 11.2–13.6 eV) allows for the dissociation of H_2, which suppresses Pop III star formation, allowing a halo to remain star-free (and hence metal-free). An attractive scenario here

---

[9] It should be noted that primordial BH mass function can also peak at BH masses higher than solar mass to form SMBHs.

is the synchronised pair (Dijkstra et al. 2008; Regan et al. 2017) mechanism, whereby a pair of halos closely separated in time and space evolve together. The first of these haloes that forms stars could then provide the second halo with a strong enough LW background (Visbal et al. 2014), the key issue with this model is that the number density of such environments may be too rare to explain the number densities of expected MBHs.

Alternative scenarios for avoiding premature star formation are to dynamically heat the gas (rather than photo-dissociating H_2). In this scenario, the gas can be shock-heated either through galactic collisions (Inayoshi et al. 2016) or through a rapid succession of minor and major mergers (Yoshida et al. 2003; Fernandez et al. 2014; Wise et al. 2019). The appeal of this scenario is that it arises more naturally through the mechanisms of DM structure formation and that the number density of MBH seed formation looks promising (e.g. Regan et al. 2020b) though further work on the expected number density of MBH seeds is required.

Finally, the collisions of massive galaxies at moderately high redshifts ($z \sim 8$–10) can lead to the direct formation of an MBH without any intermediate stage (Mayer et al. 2010, 2015). In this scenario (which, in stark contrast with the atomic cooling halo scenario, can occur also at solar metallicities) major mergers between the rare, most massive high-z galaxies funnel gas to their centre at rates exceeding $1000 \, M_\odot/$ year. The resulting accumulation of billions of solar masses of gas in a nuclear region less than a parsec in size could either induce the formation of a very large SMS, and hence a massive BH seed by direct collapse, or even directly form a large MBH via the radial general-relativistic instability of a supermassive protostellar precursor. Recent models show that an accreting SMS, owing to the much higher accretion rates occurring in the merger-driven scenario, can grow in mass much more than in the atomic cooling halo case, namely to $> 10^7 \, M_\odot$ in absence of rotation, before collapsing into an MBH seed (Haemmerlé et al. 2021).

● **Primordial Black Holes**

Primordial BHs are another plausible way to explain the formation of MBHs. Their abundance is constrained at various mass scales (Carr et al. 2021), but they can still form a considerable fraction of DM in mass ranges $1 - 10^2 M_\odot$ (Bird et al. 2016; Sasaki et al. 2016; Clesse and García-Bellido 2017) and $10^{-13} - 10^{-11} M_\odot$ (Saito and Yokoyama 2009; Garcia-Bellido et al. 2017; Domcke et al. 2017; Bartolo et al. 2019; Cai et al. 2019; Unal 2019). Moreveor, primordial BHs of mass $\mathcal{O}(10 - 10^5) M_\odot$ formed in the early universe (before recombination) could be the seeds of MBHs (Duechting 2004; Belotsky et al. 2014; Clesse and García-Bellido 2015; Nakama et al. 2016; Garcia-Bellido et al. 2016). The tail of their mass function[9] reaching a few hundred or thousand solar masses can grow many orders of magnitude (depending on formation mass) via accretion and mergers (Mack et al. 2007; Ali-Haïmoud et al. 2017; Raidal et al. 2019; Inman and Ali-Haïmoud 2019; Serpico et al. 2020; De Luca et al. 2020). This claim has been studied and found to be consistent with the current cosmological probes of cosmological history.

Primordial BHs are formed by large density contrasts, and the most likely stage to produce these large perturbations is during inflation. Although cosmic microwave background-scale perturbations must be Gaussian and nearly scale invariant with a

typical amplitude of 10^{-5}, the fluctuations at smaller scales can be larger. There exist characteristic signatures of these enhanced fluctuations in various multimessenger probes, including cosmic microwave background distortions (Chluba et al. 2012; Ali-Haïmoud and Kamionkowski 2017; Aloni et al. 2017; Inomata et al. 2017; Garcia-Bellido et al. 2017; Nakama et al. 2018; Cappelluti et al. 2022) and secondary stochastic GWs resulting from the enhanced perturbations that re-enter the horizon in the radiation (or matter) dominated era (in particular enhanced inflationary perturbations that produce $1 - 10^4 \, M_\odot$ primordial BHs) which also produce stochastic GWs at Pulsar Timing Arrays (PTA) scales (Inomata et al. 2017; Garcia-Bellido et al. 2017; Vaskonen and Veermäe 2021; Kohri and Terada 2021; De Luca et al. 2021). The next generation PTAs, which can constrain the stochastic GW Background, as well as the cosmic microwave background experiments using spectral distortions, will probe inflationary fluctuations so sensitively that they could conclusively test the existence of primordial BHs from inflationary perturbations (Byrnes et al. 2019; Inomata and Nakama 2019; Kalaja et al. 2019; Gow et al. 2021). We refer the reader to Auclair et al. (2023) for more details on primordial BHs and LISA.

Research into the seeding of MBHs remains a highly active area of research. In an era where vigorous development of both semi-analytical models and full numerical calculations continues apace (see Sect. 2.4), understanding the mechanisms of MBH seeding becomes all the more important. A definitive pathway to forming MBHs remains an open question. An important metric of success for any formation model is to explain naturally the current abundance of MBHs of all masses in the nuclei of galaxies. These have a currently measured number density of $n_{MBH} \sim (0.2 - 1.0) \times 10^{-2}$ Mpc^{-3} at $z = 0$, depending on how far down in mass function is integrated (e.g. Graham et al. 2007; Shankar 2009; Terrazas et al. 2016). A key goal in any of the seeding models discussed above is therefore a calculation of the resulting number density of MBHs in the Universe as a function of redshift. So far, calculations within the community have varied significantly between approximately 10^{-3}–10^{-9} comoving Mpc^{-3} for the very massive seeds formed in atomic cooling halos (Dijkstra et al. 2008; Agarwal et al. 2012; Dijkstra et al. 2014; Agarwal et al. 2014; Habouzit et al. 2016; Wise et al. 2019), while we expect more seeds from e.g. the Pop III remnant formation mechanism. For reference, the number density of galaxies in the Universe today is $\sim 10^{-1}$ comoving Mpc^{-3}, and the number density of quasars at $z \sim 6$ is $\sim 10^{-9}$ comoving Mpc^{-3}. MBH formation needs to explain both the population of high-redshift quasars, and the population of MBHs in the local Universe.

A central challenge of models in the next decade leading up to LISA's launch will be to reduce the number density uncertainties associated with different models of MBH seed formation. A focal point of simulations in the next decade will be to accurately model the assembly of galaxies including modelling the environments, in a cosmological context, in which MBH seeds can form. Given the large dynamical range of nonlinear physical processes required to form MBH seeds, this is challenging. The use of focused, high-resolution and relatively large-scale numerical simulations with detailed (Pop III) star formation and MBH formation prescriptions

will ultimately be required to break the current degeneracies between models which currently exist and provide models to be used for inference with LISA detections.

2.3.2 MBH growth across time and space

LISA will measure not only the masses but also the spins of massive black holes. In this section, we discuss three compelling open questions: *how do MBH seeds grow across cosmic time? What is the impact of such growth on the spin of an MBH? What can the final spin reveal about its past accretion history?* In the discussion of these issues, throughout this section, we will differentiate between *light* seeds and *heavy* seeds. *Light* seeds have masses of at most $10^3 M_\odot$ and are typically those formed by the first generation of metal-free stars, while *heavy* seeds are those with higher masses that can result from stellar dynamical processes or from the direct collapse scenarios discussed above.

2.3.2.1 How to grow light seeds   Pop III remnants are predicted to have low mass, $\leqslant 10^3 M_\odot$. In order for these seeds to grow massive enough to be in the LISA band, or to grow massive enough to even become the extremely massive quasars that we observe at $z \sim 6$–7, they would need to clear two main hurdles. If not formed in the centre of their galaxies, these seeds must sink efficiently to the centre, but also sustain efficient accretion for a significant fraction of their lifetime. To produce the population of high-redshift quasars, they have to sustain near-Eddington accretion rates for nearly a Gyr (Haiman and Loeb 2001). In the conventional picture of a spherically symmetric accretion flow whose energy loss is only controlled by radiation propagating isotropically, the Eddington limit expresses a maximum allowed accretion rate. Therefore, seeds would have to grow at near the maximum rate allowed for their entire lifetime, unless a mechanism for super-Eddington accretion is invoked by resorting to more complex configurations of the fluid flow and radiation field, and to a different energy transport mechanism.

High accretion efficiency is challenging to explain physically, given that radiative feedback both from the surrounding stellar component and MBH growth can unbind gas in the vicinity of the seed BH, thus preventing further growth. These hurdles were first examined in the early 2000s (Omukai and Inutsuka 2002; Oh and Haiman 2003; Whalen et al. 2004), with each study finding that Pop III BHs initially find themselves in low-density environments within the galaxy, where they are unable to grow. Expanding on earlier studies, Smith et al. (2018) investigated the growth of more than 15,000 light-seed BHs using the Renaissance simulations and found that none were able to grow by more than 10 percent for the 300 Myr for which their growth was followed. This time period represents a significant fraction of the Hubble time at this epoch. These predominantly numerical works have been confirmed by semi-analytical approaches which also find that light seeds struggle to achieve significant growth (e.g. Valiante et al. 2016; Pacucci et al. 2017, andreferencestherein).

A mechanism of rapid growth may be required in order to grow light seeds, both to help stabilise their orbits (see Section 2.2) within the galactic centre and to allow
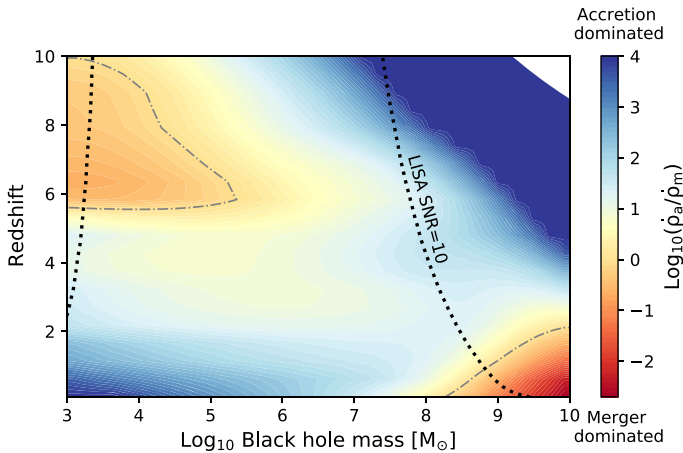
Fig. 23 Predictions on the relative importance of MBH growth by gas accretion (blue shades) and mergers (red shades). $\dot{\rho}_a$ and $\dot{\rho}_m$ are the predicted mass growth rates by gas accretion and mergers, respectively. The contour where $\dot{\rho}_a = \dot{\rho}_m$ is represented with a dash-dotted line. The region corresponding to a LISA signal-to-noise ratio ≥ 10 for MBHBs with mass ratio 0.2 is delimited within the two thick, dotted lines. The whited-out area on the top right corner indicates the region of the parameter space where no MBHs should be present (adapted from Pacucci and Loeb 2020)

them evolve into MBHs, as examined in Sect. 2.3.1. A number of studies have also shown that light seeds can grow through super-Eddington accretion given the correct environmental conditions (Alexander and Natarajan 2014; Inayoshi et al. 2016, 2020; Lupi et al. 2016; Pezzulli et al. 2016, 2017).

In either case, a growing BH must reach a critical mass before it can sink to the centre of the potential and become a central MBH. Recent investigations by Pfister et al. (2019b) have shown that MBHs with masses $M_{BH} \lesssim 10^5 M_{\odot}$ are unable to sink via dynamical friction as the stellar component of high-redshift galaxies tends to be too irregular. This leads to a population of wandering MBHs that cannot efficiently accrete gas or merge with other BHs. The idea of a population of wandering MBHs is not new; this population has been previously associated with galaxy mergers which result in off-nuclear MBHs from the failure of them to reach the centre of the merger remnant (e.g. Volonteri 2010). Nonetheless, more recent, high resolution, simulations have shown that wandering MBHs may result from seeds with masses $M_{BH} \lesssim 10^5 M_{\odot}$ that are unable to settle to the centre of the galactic potential. This result has been confirmed by other high-resolution simulations which show that a large population of wandering MBHs with $M_{BH} \lesssim 10^5 M_{\odot}$ is likely in most, if not all, galaxies (Tremmel et al. 2018a; Bellovary et al. 2019; Regan et al. 2020a). Interestingly, this result has also been tentatively confirmed by observations of off-center MBHs in galaxies (Reines et al. 2020). However, if associated with a compact massive star cluster, dynamical friction will be greater, and such off-centre MBHs may be transiting rather than stalled. Once MBHs exceed $M_{BH} \sim 10^6 M_{\odot}$, they are less prone to "jittering" (but see Ma et al. 2021), although they still remain susceptible to ejections (via triple interactions and GW recoils), the velocities of which depend on MBH mass ratios

rather than absolute mass, although of course retaining the MBHs depends on the potential well of the galaxy.

2.3.2.2 Accretion versus MBH mergers   Despite large uncertainties in the physical parameters that enable a mapping between luminosity and mass (e.g. duty cycle, matter-to-energy accretion efficiency, Eddington ratios, and bolometric corrections; see, e.g. Tanaka and Haiman 2009), a consistent picture is now emerging. Observations and theoretical models suggest that most of the mass growth over cosmic time occurred via gas accretion, and that more massive MBHs grew at earlier cosmic times, whereas lighter MBHs were still growing at $z \lesssim 1$ (Soltan 1982; Marconi et al. 2004; Merloni and Heinz 2008; Shankar et al. 2009). Assuming a combination of light and heavy MBH seeds at $z \sim 20$–30, recent studies have confirmed that growth by gas accretion is dominant for most MBH masses during a large fraction of the evolution of the Universe ($0 \leq z \leq 9$–10), especially for $M_{\mathrm{BH}} > 10^6 M_\odot$ and $z < 8$ (Pacucci and Loeb 2020; Piana et al. 2021).

Growth by mergers—which we recall can at most double an MBH mass at each merger—can become dominant for $M_{\mathrm{BH}} < 10^{4-5} M_\odot$ at $z > 6$ (Dayal et al. 2019; Piana et al. 2021), and for $M_{\mathrm{BH}} > 10^8 M_\odot$ at $z < 2$ (Pacucci and Loeb 2020). This is possible if one or more of the following conditions are met: *(a)* the number density of MBHs is large, and *(b)* the cold gas available for accretion is scarce given that the accreted mass fraction depends on the richness (over-density) of the environment (Dubois et al. 2014b). The first condition can be met at high redshifts if light seeding mechanisms are dominant, leading to a large number density of MBHs. This could in turn result in frequent mergers, although light seeds are unlikely to merge and sink to the centre as shown in Sect. 2.2. The second condition can be verified at $z \lesssim 1$ (Power et al. 2010). Predictions on the contribution of mergers to the cosmic growth of MBHs strongly depend on a multitude of parameters, many of which are unknown or loosely constrained. For example, the number density of heavy MBH seeds can vary over ~ 6 orders of magnitude (at a given redshift $z \gtrsim 8$) in modern cosmological simulations (see, e.g. Habouzit et al. 2016; Woods et al. 2019), with huge uncertainties being introduced by the time-scale on which MBHs can actually merge (e.g. Dayal et al. 2019; Barausse et al. 2020b). Nonetheless, the presence of partially-depleted cores in massive galaxies offers the promise of a substantial number of MBH mergers at least at late cosmic times (Begelman et al. 1980; Graham 2004; Dullo and Graham 2013).

Despite significant unknowns, e.g. the contribution of obscured accretion, which is invisible in all bands apart from X-rays and higher energies, (e.g. Worsley et al. 2005; Fiore et al. 2009; Comastri et al. 2015), we now have a clear picture of growth by accretion (see Fig. 23). LISA, along with future third-generation GW observatories (e.g. the Einstein Telescope and/or Cosmic Explorer), is however the only way to actually measure the merger history of the full MBH mass spectrum, and this is what is expected to be delivered after its launch. However, as stressed already, to accurately assess the role that LISA will play in constraining the relative role of MBH mergers and accretion in MBH growth, theoretical models have to be refined in order

to allow for inference on the astrophysical picture by comparing the data stream to predictions.

2.3.2.3 Feedback as a barrier to MBH growth

As detailed in Sect. 2.2, the ionizing radiation that emerges from the innermost parts of the MBHs' accretion flows can render gas dynamical friction inefficient for a range of physical scenarios (Park and Bogdanović 2017, 2019), although this depends on the surrounding gas environment (Toyouchi et al. 2020). This can lengthen the inspiral time of MBHs and reduce the MBH pairing probability (Li et al. 2020a). The suppression of MBH pairing is most severe in galaxies with MBH pairs with mass $< 10^8 \, M_\odot$ and low mass ratio, which are direct progenitors of the merging binaries targeted by LISA. See Sect. 2.2.1.2 for additional details.

Secondly, both hydrodynamic cosmological simulations with a physical model for light seed MBH formation (Habouzit et al. 2017) and semi-analytical models (Barausse et al. 2020b) converge on the fact that the number of MBHs growing enough to enter the LISA band depends on the strength of SN feedback. In case of strong feedback, SN winds can expel gas from the nuclear region of relatively low-mass galaxies ($M_\star \lesssim 10^{10} \, M_\odot$), depleting the gas reservoir of the MBHs (Dubois et al. 2015). This prevents the MBHs to grow in mass until the gravitational potential well of their host galaxies is deep enough to confine again the cold gas close to the central region. The MBHs may remain too light to be detected by LISA.

In addition to affecting the merger rates, strong feedback generated by the MBHs themselves can significantly slow down the growth of MBH seeds. As shown, e.g. in Regan et al. (2019) the strong outflows generated by the jets are able to deplete a region of ~ 0.1 pc around the seed. Although the outflow generally does not reach the escape velocity from the host galaxy, it does suppress the growth for a time-scale comparable to the dynamical time. A super-Eddington ($\dot{M}_{\rm BH} > \dot{M}_{\rm Edd} = L_{\rm Edd}/c^2$) accretion rate would then translate into a time-weighted, effective accretion rate of 0.1–0.5 the Eddington rate, significantly slowing down the growth of the MBH over ~ 0.5 Gyr by factors $\sim 30 - 3000$, when compared to the growth required to match the observations of $z \sim 7$ quasars. While this is potentially an issue to explain the brightest high-z quasars, it could act to increase event rates in the LISA band at the highest redshifts as heavy BH seeds could remain longer within the mass range where LISA is most sensitive.

Finally, galaxies can also experience external radiative feedback due to the heating background created by reionization photo-evaporating gas from the outskirts of low-mass galaxies in ionized regions (van Wassenhove et al. 2010; Dayal and Ferrara 2018). However, this feedback has almost no effect on the mass build-up of MBHs in the early Universe since the MBHs of such reionization feedback affected galaxies are already accretion-starved due to SN feedback (Dayal et al. 2019).

The variety of astrophysical processes involved in modelling MBH growth, described in this section, highlights that one of the challenges ahead of us to prepare for LISA is to assess degeneracies that can affect the interpretation of LISA's data. Overall, the large number of parameters and scales involved makes this a complex problem—at the same level of galaxy formation. Progress in delivering realistic

models that can be compared to LISA's detection will require on the one hand more detailed investigations in all the subfields, and on the other hand a way to consolidate these results into coherent models.

2.3.2.4 Spin evolution of MBHs under accretion and mergers   LISA has a unique potential in providing measurements of the spins of merging MBHs: this means a theoretical understanding of how MBH spins evolve is necessary in order to be able to interpret LISA's results. Accretion and mergers establish profound links between the spin and the mass of the MBHs, which therefore have to be studied jointly. In the accretion process, the spin is a critical physical parameter, as it determines the radiative efficiency. For a geometrically thin accretion disc, the efficiency of converting mass into light varies from 0.057 for a non-spinning MBH to 0.43 for a maximally spinning MBH (e.g. Novikov and Thorne 1973). This has a direct impact on the rate of MBH mass growth, on the amount of radiated energy, and on the spin magnitude and orientation at the end of an accretion episode. Also, a key manifestation of the spin when an MBH is accreting from a magnetized plasma is the launch of a collimated jet of matter and radiation which directly tracks its orientation (Blandford and Znajek 1977). The link between spin, accretion and jet power/efficiency has started being compared to observations (Unal and Loeb 2020) and being used to set lower bounds on AGN spins (Ünal et al. 2021).

Spins determine how efficiently the accreted matter is transformed into energy, but in turn the way in which MBHs accrete gas has a crucial bearing on their spins: depending on the accretion geometry, the resulting MBH spin's magnitude and direction can vary widely. Taking the limiting case of prolonged coherent accretion from a viscous disc, the spin can increase up to its limiting value of 0.998 (Thorne 1974; see also Popham and Gammie 1998; Gammie et al. 2004) after the MBH has accreted an amount of gas comparable to its initial mass, regardless of the flow being initially prograde or retrograde (Bardeen 1970). The spin in this case gets aligned with the angular momentum of the disc from which it is fed (Bardeen and Petterson 1975), and the time-scale for the alignment is short (10^5 year) compared to the typical time for mass growth. At the other extreme, chaotic accretion, made up of randomly oriented small-mass accretion events, results instead in an erratic orientation of the spin and, in general, in a spun-down MBH (King and Pringle 2006; King et al. 2008). Several semi-analytical models of MBH evolution have included either one (e.g. Volonteri et al. 2005) or both (e.g. Volonteri et al. 2007; Berti and Volonteri 2008; Barausse 2012) of these two limiting cases. More recent semi-analytical models (Sesana et al. 2014) have included accretion flows that are neither perfectly coherent nor perfectly isotropic depending on the fuelling geometry (Dotti et al. 2013). These studies, together with numerical works that follow the evolution of the spin in relation to the dynamics of the accreting gas (e.g. Maio et al. 2013; Dubois et al. 2014b, 2015, 2021; Sayeb et al. 2021), have shown that the distribution of MBH spins depends on several quantities, such as host morphology, MBH mass, mass ratios, and redshift.

In principle in a binary all spin orientations and all spin magnitudes allowed by GR are possible. However, when an MBH binary, in its latest stages of evolution, is

surrounded by a circumbinary disc, the interaction with the external gas leads both the binary orbital axis and the individual MBH spins to reorient their directions into a configuration of minimum energy where the two spins are aligned to a large degree with the orbital angular momentum axis, as discussed in Bogdanović et al. (2007) (see also Dotti et al. 2010; Miller and Krolik 2013). This has a strong impact on the final spin of the new MBH and on the magnitude of the velocity acquired by gravitational recoil, which depends sensibly not only on the mass ratio, but also on the magnitudes and orientations of the spins (Kesden et al. 2010b; Lousto et al. 2012; Berti et al. 2012). Extrapolation of MBH coalescences with large initial spins (larger than ~ 0.9) exactly aligned with the orbital angular momentum yields a final spin as large as ~ 0.95 (Marronetti et al. 2008; Berti and Volonteri 2008; Kesden et al. 2010a; Lovelace et al. 2011).

In gas-poor conditions, the potential lack of a massive circumbinary disc leads MBH binaries to have spins randomly oriented at the time of their coalescence relative to the orbital plane, with magnitudes determined by the previous accretion history. Statistically, when spins are equally distributed in all directions relative to the orbital axis, the remnant MBH spin depends on the binary's mass ratio: if an MBH merges with many lower-mass MBHs it tends to spin down, as the final spin is dominated by the orbit at plunge and retrograde accretion at larger radii reduces (on average) the spin of the larger MBH (Hughes and Blandford 2003). If instead the mergers involve MBHs of comparable mass, on average the remant will have a spin ~ 0.7 (Berti and Volonteri 2008), consistent with the value of the final spin resulting from the merger of two equal-mass, nonspinning MBHs (Scheel et al. 2009).

Berti and Volonteri (2008) studied the co-evolution of MBH masses and spins in a cosmological context, showing that in general accretion dominates over mergers in determining the spin evolution of the whole MBH population. While in prolonged accretion episodes spin-up is very efficient, with a large fraction of MBHs having individual spins in excess of 0.9, isotropic mergers reduce the fraction of high-spin MBHs and create a roughly uniform distribution. If accretion is chaotic, most MBHs have spins below 0.1 prior to merging. This demonstrates how spins offer the best diagnostics on whether MBHs before coalescence have experienced either coherent or chaotic accretion. These studies are important preparation for LISA as they provide insight for modelling realistic spin distributions to be used as priors during the analysis of waveforms to extract source parameters.

Indeed, LISA will measure not only the MBH individual masses, but also a mass-weighted combination of the individual spins projected along the orbital angular momentum (the so-called "effective spin" $\chi_{\rm eff} = (M_1\chi_{1z} + M_2\chi_{2z})/(M_1 + M_2)$, where M_1 and M_2 are the MBH masses, χ_{1z} and χ_{2z} are the components of the spins along the orbital angular momentum) and possibly their precessional dynamics, which is encoded in the amplitude and phase of the waveform. A measurement of $\chi_{\rm eff}$ alone does not constrain the individual spins. For example, a small $\chi_{\rm eff}$ could result from both MBHs having small spins; from each MBH having significant spins in the angular momentum direction, but anti-aligned with each other; or from nonzero spins oriented along the orbital plane. Through parameter estimation of precessing binaries, however, it is possible to infer posterior distributions for both

spins. Preliminary work on simulated MBH populations has shown that the spin of the primary MBH can be measured by LISA with an exquisite accuracy ($\sim 1-10\%$) for nearby, loud events. This precision in the measurement mirrors the fact that the primary MBH leaves a bigger imprint in the waveform through the mass-weighted χ_{eff}. The measurement is more problematic for the spin of the secondary, that can be either determined to an accuracy of 0.1, or can remain completely undetermined, depending on the mass ratio and spin magnitude (Klein et al. 2016).

If LISA's detection rates will be at the high end of current estimates, it may be possible to learn about the statistical distribution of the spins, and therefore constrain the relative importance of mergers and accretion in shaping the MBH spin population in the mass range below $10^6 \, M_{\odot}$, which is poorly constrained by EM observations (see Sect. 2.6). Having a comparison between spin measurements from LISA and EM observations, which are tracing different populations, will be of paramount importance (Sesana et al. 2014).

In preparation for LISA, further improvements in numerical simulations are needed to make use of novel techniques to model physical processes below the resolution limits (e.g. Dubois et al. 2014b; Fiacconi et al. 2018), and to include changes in the spin directions that affect feedback (Bustamante and Springel 2019; Cenci et al. 2020; Sala et al. 2021; Dubois et al. 2021). Semi-analytical models are also needed to understand whether the interaction between MBHs and their accretion discs can lead to spin alignment (see e.g. Miller and Krolik 2013; Lodato and Gerosa 2013; Gerosa et al. 2015b; Gerosa et al. 2020). Finally, an interesting possible outcome of MBH mergers is that in non-aligned conditions, the direction of the remnant's spin can flip with respect to those of the progenitors: this would leave an observed imprint in the surrounding medium in the form of a particular shape (X-shaped radio galaxies; Gergely et al. 2010), and observational searches for such systems (Roberts et al. 2015) can provide information on the spin properties of merging MBHBs complementary to those obtained from theoretical models.

2.4 Statistics on MBH mergers

Coordinators: Silvia Bonoli, Alessandro Lupi

Contributors: Monica Colpi, Pratika Dayal, Massimo Gaspari, Melanie Habouzit, Chung-Pei Ma, Lucio Mayer, Sean McGee, Hugo Pfister, Raffaella Schneider, Alberto Sesana, Rosa Valiante, Marta Volonteri

MBHs are not born nor evolve in isolation. The physical properties of the host galaxies are key not only to set the MBH initial mass (see Sect. 2.3), but also to modulate the subsequent growth and mergers. Indeed, most of the mass of today's MBHs is likely the result of multiple accretion episodes throughout their entire lifetime (Soltan 1982), likely triggered by secular processes or during violent events, such as galaxy interactions. For this reason there are various aspects of galaxy formation and evolution that are indirectly very relevant to LISA, and which need to

be well understood in order to enable predictions for observable MBH merger event rates as a function of key parameters, such as masses, mass ratios and spins of the MBHs, as well as their dependence on redshift. Likewise, the same deep understanding is required for post-launch interpretation of the LISA datastream. In the currently accepted cosmological framework, the ΛCDM model, galaxies are expected to experience a large number of interactions and mergers during their lifetimes (Lacey and Cole 1993). Galaxy interactions not only likely foster the activation of accretion episodes (e.g. Kauffmann and Haehnelt 2000; Di Matteo et al. 2005; Capelo et al. 2015), but also lead to the formation of binary MBH systems (Mayer et al. 2007; Tremmel et al. 2017; Volonteri et al. 2020). The creation of triplets and multiple MBH systems is also possible (Bonetti et al. 2019), in particular for galaxies in dense environments which generally experience more frequent mergers. The formation time-scale of an MBHB is, however, dependent on the properties of the host galaxies. As discussed in Sect. 2.3.1, the formation of a bound system is subject to the ability of the secondary MBH to sink towards the centre of the merger remnant, where the primary MBH is expected to reside. A substantial amount of orbital angular momentum needs to be transported away, with the distance between the two MBHs having to decrease by several orders of magnitude (from kpc to pc scales, see Fig. 16). The sinking process, driven by dynamical friction and global torques, depends non-trivially on the properties of the host, such as the overall galaxy structure, the gas fraction, the presence of clumps or stellar clusters and structures such as discs or bars (see Sect. 2.2). Once a bound binary forms, its ability to harden still depends on the properties of the surrounding medium (e.g. Sesana and Khan 2015; Biava et al. 2019). The hardening time-scale is shorter in galaxies with a large amount of stars that can cross the binary "loss-cone" and/or with enough gas in the centre to create a circumnuclear disc (e.g. Merritt and Poon 2004; Dotti et al. 2007).

Given that galaxy properties are tightly connected to the large-scale environment, the frequency of MBH mergers that LISA will detect depends on the global cosmological evolution of the host galaxies. All these physical processes, highly non-linear, can only be studied via sophisticated theoretical models, either analytical, semi-analytical, or fully numerical. The main difficulty resides in the extremely wide range of physical processes and scales that need to be resolved simultaneously, from the Mpc cosmological scales to the sub-pc scales where GWs become dominant (see Fig. 16). We are currently unable to resolve the full dynamical range that would be required to predict the number and properties of MBH mergers for LISA.

Despite such modelling difficulties, building the infrastructure for interpreting the LISA data-stream in the context of structure formation and evolution is one of the key tasks for the LISA Consortium and the astrophysical community at large. In fact, LISA will provide a catalogue of MBHBs with posterior distribution of the parameters of each source, including masses, sky localization, distance, magnitude and orientation of individual MBH spins, and eccentricity of the orbit. The degree of precision of these measurements will obviously depend on the specific source.

Individual binary parameters and parameter distribution across the detected population encode important information about the physics underlying MBHB formation. For example, the mass function and redshift distribution of detected

events strongly depend on the nature and efficiency of the seeding mechanism. The spins of individual MBHBs are strongly affected by their main accretion channel, whether this is accretion of cold gas, tidal disruptions of stars or capture of compact objects, or previous mergers with other MBHs.

The information encoded in LISA's catalogue of events has the potential to revolutionize our understanding of MBH formation and evolution, and the degree to which such potential can be exploited depends on the sophistication of the astrophysical inference models and pipelines at hand. Sesana et al. (2011a) conducted a pilot study demonstrating the power of inference on LISA data. They considered a number of different MBH cosmic evolution scenarios, encompassing different seeding models (Pop III versus direct collapse), accretion efficiency (Eddington versus sub-Eddington) and geometry (coherent versus chaotic), demonstrating that LISA will be able to discriminate among them with just a handful of detections. They also considered mixed models in which, for example, different seed populations were combined, and found that LISA could correctly recover the presence of multiple sub-populations and their relative abundance.

Although this was a successful first step, ideally, the community should employ all the arsenal of analytical and numerical models to distill a meaningful mapping of key astrophysical processes into MBHB parameter distributions. The LISA catalogue can then be used to tackle the 'inverse problem' of reconstructing the cosmic history of MBHs from GW observations. A proof of concept example of such process can be found in Padmanabhan and Loeb (2020). They used a parametric toy model connecting the MBH properties to the host DM haloes, to demonstrate that LISA would be able to constrain the halo occupation fraction and the MBH-halo relation.

As we summarized above, the properties of MBHs are shaped by a number of physical ingredients that go beyond the host DM halo and involve a number of gas and stellar dynamical processes, and likely involve a non-negligible degree of stochasticity. In this respect, exascale numerical simulations combined with neural network techniques for model emulation, as we outline below, can be used to anchor and inform flexible semi-analytical models that can efficiently map a vast physical parameter space into a likelihood function of the MBHB population. Ideally, those models would be flexible enough to include information coming from future observations across the EM spectrum, including Rubin, JWST, Athena, and SKA, to name few notable examples, to enhance their constraining power (see Sect. 2.6). Last but not least, the ultimate LISA MBHB astrophysical inference pipeline will also take advantage of any EM counterpart to individual LISA sources, which will provide additional information about the environment of the merging binary.

In this section, we first review the state of the art of the models that attempt to connect the small-scale processes of MBH formation, growth, and dynamics with the broader cosmological context of galaxy evolution. We then discuss the current estimates for the number of events that LISA will be able to detect as predicted by both numerical and semi-analytical models. At the end of the section, we provide an outlook on the need of pushing these models to be progressively more and more accurate and flexible, taking advantage of both the progress in computational power and new computational and statistical techniques. The theoretical framework

connecting MBH mergers with the broader cosmological picture will play a fundamental role in the data analysis and the physical interpretation of LISA events.

2.4.1 Modelling MBH evolution in a cosmological context

MBH assembly is considered an essential component of galaxy formation (e.g. Kormendy and Ho 2013). As anticipated, while not specific to LISA science, this is a central topic to enable pre-launch studies, such as to inform models of LISA event rates, as well as instruct post-launch studies by setting the framework for the interpretation of the data, allowing to generate astrophysical inference work. The inclusion of physical processes related to MBH growth into simulations of galaxy formation has been initially driven by the need of understanding the role of MBHs in shaping the host galaxies via processes such as AGN feedback. In particular, feedback from AGN has been invoked to explain the observed quenching of massive galaxies, which could not be explained by stellar feedback alone (e.g. Springel et al. 2005a; Croton et al. 2006; Bower et al. 2006).

Models of galaxy formation and MBH assembly can be grouped into two categories: cosmological hydrodynamical simulations and semi-analytical models. In the former, the DM and baryonic components of the Universe are followed simultaneously, starting from given initial conditions set by the chosen cosmological model. These simulations are computationally expensive and, in their set-up, a trade-off has to be made between the size of the cosmological volume that needs to be probed and the mass and spatial resolution desired. Thanks to the fast advance of computational power, state-of-the-art simulations are able to encompass large volumes of $\sim 100^3 \, \mathrm{cMpc}^3$ with kpc resolution (e.g. Dubois et al. 2014a; Vogelsberger et al. 2014; Hirschmann et al. 2014; Schaye et al. 2015; Pillepich et al. 2019; Davé et al. 2019). While allowing to study the evolution of DM and baryons in a self-consistent way down to the resolved physical scales, astrophysical processes that act at smaller scales (e.g. gas cooling, star formation, stellar feedback, MBH seeding, MBH accretion, MBH feedback) need to be included via sub-grid recipes.

Semi-analytical models, instead, follow the evolution of the baryonic component of the Universe through a series of differential equations which link the time-evolution of the baryons to that of the underlying DM haloes. While losing some level of self-consistency, this approach has the advantage of being able to statistically explore how different physical assumptions affect the global galaxy population or targeted sub-samples (see, e.g. the seminal paper by Kauffmann et al. 1993). The merger trees can either be derived via the Press-Schechter formalism (Press and Schechter 1974) or using the outputs of *N*-body simulations. While the first approach is computationally less expensive and merger trees with a broad range of masses can be resolved (e.g. down to the mass of the first star-forming haloes), *N*-body simulations offer the advantage that the 3D spatial distribution of galaxies is fully tracked, as the dynamical evolution of the underlying DM haloes is properly followed. This allows the modelling and studying of the complex link between physical non-linear processes and the large-scale environment.

Independently of the adopted technique, the models that track the evolution of the MBH population need to use sub-grid assumptions derived from higher-resolution simulations or analytical derivations, whose parameters are calibrated using observed properties of MBHs and their host galaxies. The local stellar mass function (e.g. Baldry et al. 2012), the distribution of galaxy colours (e.g. Baldry et al. 2004), and the evolution of the star formation rate density (e.g. Madau and Dickinson 2014) are some of the key observables used to calibrate the parameters regulating galaxy evolution, e.g., the galaxy and MBH sub-grid physics.

Models including the growth and evolution of MBHs are typically anchored to local relationships between the MBH masses and host properties, such as stellar mass and velocity dispersion (Kormendy and Richstone 1995; Magorrian et al. 1998; Ferrarese and Merritt 2000; Gebhardt et al. 2000; Tremaine et al. 2002; Graham and Scott 2015; Sahu et al. 2019a). Besides the calibration, the validation of the models is done by comparing the resulting MBH population to observational constraints. Typically, the AGN luminosity function from the local Universe to high redshifts (up to $z \sim 4$, Hopkins et al. 2007; Lacy et al. 2015; Shen et al. 2020), which constrains MBH accretion rates over cosmic time, is often used as diagnostics of the simulation or semi-analytical subgrid models. Additional diagnostics include the Eddington-ratio distribution of AGN (e.g. Hickox et al. 2009; Aird et al. 2018), the number density of the highest-redshift quasars (e.g. Fan et al. 2006; Mortlock et al. 2011; Decarli et al. 2018), and the clustering of active and luminous MBHs (e.g. Gilli et al. 2005; Ross et al. 2009).

Here, we briefly review the different modelling aspects of MBHs—seeding, fuelling, feedback, and dynamics—and discuss different implementations and uncertainties among models, highlighting in particular those that are relevant for LISA.

2.4.1.1 MBH seeding   The first aspect that is crucial to determine the MBH occupation fraction in galaxies, and therefore MBH formation efficiency, is MBH seeding. Despite the strong effort by the community and the variety of proposed models (see Sect. 2.3 for a detailed review), MBH seeding mechanisms are still unconstrained. As in Sect. 2.3, we consider models assuming "heavy" seeding, resulting in massive ($10^{4-6} M_\odot$) but rare seeds, as well as models assuming "light" seeding, which results in less massive ($\leqslant 10^3 M_\odot$) but more abundant seeds. LISA, by being sensitive to the mass of the merging MBHs that generate the GW signal, has the potential to constrain these models at statistical level through Bayesian analysis, because detection rates in the various mass intervals depend upon the seeding mechanism (Sesana et al. 2011a; Klein et al. 2016; Bonetti et al. 2019; Barausse et al. 2020b). Of course, right after their emergence, the mass growth of the seeds through various mechanisms will also affect that MBH merger mass distribution that LISA can detect at any given time, which may complicate the interpretation of the statistics (see next section).

In state-of-the-art cosmological hydrodynamical simulations of $\sim 100^3$ cMpc^3, the typical mass of DM particles is $M_{\mathrm{DM}} \sim 10^{6-8}$ M$_\odot$. This is not enough to resolve the haloes where we expect MBH formation to happen, for example the atomic

cooling haloes where we expect direct-collapse MBH seeds to form. These simulations also do not have enough resolution to model self-consistently some key physical processes required by the different channels of MBH formation described in Sect. 2.3. Instead, MBHs are commonly inserted as sink particles "by hand", either in massive haloes of $M_h \geqslant 10^{10} M_\odot$ (e.g. Springel et al. 2005a; Hirschmann et al. 2014; Sijacki et al. 2015; Schaye et al. 2015; Davé et al. 2019), or in regions of the volume depending on the local properties of the medium, such as gas density (e.g. Taylor and Kobayashi 2014; Bonoli et al. 2016; Habouzit et al. 2017; Dubois et al. 2014a, 2021).

In smaller-volume cosmological simulations with higher resolution, it has become possible to start implementing more physical MBH formation recipes. For example, several simulations formed heavy seeds according to the local gas properties in high-redshift haloes (Tremmel et al. 2017; Bellovary et al. 2019). A model by Dunn et al. (2018) additionally includes Lyman–Werner flux as a seed formation criterion, most closely mimicking the direct collapse model. Other realistic seed formation mechanisms forming lighter MBHs in cosmological simulations were explored in Habouzit et al. (2017): seed MBHs were formed in dense metal-free collapsing regions to mimic the collapse of the first generation of stars or of dense nuclear star clusters.

Leveraging the ability to efficiently probe larger effective volumes and smaller halo masses, semi-analytical models remain valuable for testing seeding models and statistically exploring the impact of seeding on multiple observables across cosmic times. Using a model connecting heavy MBH seeding to halo properties, Lodato and Natarajan (2006), Volonteri et al. (2008b), Volonteri and Natarajan (2009) explore, for example, the observational consequences of light seeding models compared to direct collapse models with varying efficiencies. These and other works (e.g. Bonoli et al. 2014) provided novel quantitative predictions on how seeding reflects on the galaxy-MBH correlation, e.g., $M_{BH} - \sigma$, with σ the galaxy velocity dispersion. Other works have instead focused on the high-redshift universe, analyzing the ability of different seeding scenarios to lead to a population of $z > 6$ quasars consistent with current observational data (see the review of Valiante et al. 2017). As discussed in subsequent sections, semi-analytical models also predict clear seeding signatures in the mass function of GW event rates detectable by LISA.

However, our current knowledge of the MBH population and their hosts across redshift is not sufficient to put tight constraints on seeding models, leaving predictions for the signatures of seeding on LISA events largely degenerate with other physical assumptions on MBH growth and dynamical evolution. This underlines on the one hand the importance of improving observational constraints of the key measurements in the seed mass regime to constrain models. This is needed to create reliable models to compare with LISA's event properties. On the other hand, LISA's results will likely provide the most stringent constraints on MBH seeds, since it can explore redshifts closer to seed formation ($z \gtrsim 10$) than any EM facility can do.

2.4.1.2 MBH fuelling After MBHs have formed, their growth is mainly driven by gas accretion, whose rate is determined by the efficiency of the fuelling process onto

the MBH from galactic (kpc) scales down to the nuclear region. Because of the limited resolution, and the inability to properly track the angular momentum evolution of the inflowing gas and the formation of the accretion disc, cosmological simulations almost always describe the accretion process through some version of Bondi–Hoyle–Lyttleton accretion (hereafter Bondi; Hoyle and Lyttleton 1939; Bondi and Hoyle 1944; Bondi 1952, accretion rate $\propto M_{\rm BH}^2$), which assumes spherical symmetry and can be inaccurate in most realistic physical scenarios (e.g. Levine et al. 2010; Hobbs et al. 2012; Gaspari et al. 2017; Negri and Volonteri 2017). In case of significant angular momentum of the MBH accreting material, the accretion rate may not be well represented by the Bondi model. As such, the EAGLE simulation employs a modified Bondi model that takes into account the circularization and subsequent viscous transport of the infalling material (Rosas-Guevara et al. 2015, 2016). The gravitational torque-driven model (Hopkins and Quataert 2010), implemented in some recent cosmological simulations (e.g. Anglés-Alcázar et al. 2017; Davé et al. 2019), takes a different approach and since the accretion rate $\propto M_{\rm BH}^{1/6}$, low-mass MBHs initially grow more than in the Bondi model (e.g. Çatmabacak et al. 2022). This emphasizes the need for progress in bridging the gap between galactic and accretion disc scales. Indeed, zoom-in high-resolution simulations (from galactic down to sub-pc scales) show that the actual accretion flow often proceeds in the form of chaotic cold accretion (Gaspari et al. 2013, 2015), in which fractal clouds condense out of the turbulent hot halo, rain on to the nuclear region and, via frequent inelastic collisions, boost the accretion rate by $100\times$ over the simple Bondi rate (see also Sect. 2.6.1.2).

Semi-analytical models often tie the growth of MBHs to galaxy mergers (e.g. Kauffmann and Haehnelt 2000; Marulli et al. 2008), or events of starbursts or bulge growth, assuming some form of MBH-galaxy co-evolution model (e.g. Somerville et al. 2008; Shirakata et al. 2019). Models which do not track the full evolution of the galaxy population, have modelled similar co-evolution with the velocity dispersion derived directly from the DM halo (Volonteri et al. 2003a) or estimating the velocity dispersion of the galaxy based on empirical relations (Ricarte and Natarajan 2018a). In this way, it is assumed that some combination of fuelling and feedback produces $M_{\rm BH}$-host relations. Other models directly relate the growth of MBHs to the evolution of different gas phases or different dynamical processes, such as disc instabilities (Gaspari et al. 2017; Dayal et al. 2019; Izquierdo-Villalba et al. 2020). The gravitational torque-driven model introduced by Hopkins and Quataert (2010) has also been implemented in semi-analytical models, together with analytic models for disc instabilities (Menci et al. 2014; Gatti et al. 2015).

On accretion disc scales, one of the most important physical ingredients is the Eddington limit, the accretion rate at which radiation pressure balances gravity for a spherical accretor (as defined in Sect. 2.3.2.3). Typically, MBH accretion rates are capped at Eddington, and indeed the overall quasar population appears to obey this limit (e.g. Wu et al. 2015). However, there are several theoretical motivations to consider relaxing this assumption. First, MBH accretion does not occur spherically, but rather through an accretion disc. State-of-the-art radiative MHD simulations have demonstrated that Super-Eddington flow regimes can be sustained for many disc

orbits (Jiang et al. 2014; McKinney et al. 2015; Sądowski and Narayan 2016; Dai et al. 2018). In addition, the existence of $10^{9-10}\,M_{\odot}$ quasars at $z \sim 6$ requires optimistic duty cycles to grow from the seed mass if an Eddington rate cap is assumed, even under a heavy seeding scenario (see the discussion in Sect. 2.3.2).

Being able to resolve the full journey of the gas inflow from galaxy scales down to the nuclear region is essential not only to properly address MBH accretion, but also to study formation of circumbinary discs (see Sect. 2.2.2.2, and below). Spin evolution is also connected to the frequency and properties of the accretion process. We refer the reader to Sect. 2.3.2.4 for a discussion of the physical approaches, and we only recall here that coherent accretion leads to maximally spinning MBHs, whereas randomly oriented accretion can spin MBHs down. MBH spins also evolve during coalescence, depending on the combination of the orbital angular momentum and the two initial spins. The latter part of the evolution is included in cosmological simulations by adopting fitting formulae to GR simulations (Rezzolla et al. 2008; Lousto et al. 2010; Barausse and Rezzolla 2009; Hofmann et al. 2016). Only few semi-analytical models (e.g. Volonteri et al. 2005; Barausse 2012; Volonteri et al. 2013; Izquierdo-Villalba et al. 2020) and cosmological simulations (Dubois et al. 2014b; Bustamante and Springel 2019; Trebitsch et al. 2021; Dubois et al. 2021) follow MBH spin self-consistently with a sub-grid model.

Improvements on the modelling of MBH fuelling, tighter observational constraints on MBH accretion rates across a wide range of masses and redshift, and direct estimates of MBH spins (see the review of Reynolds 2019) will help discriminating between different spin evolution models on the run up to LISA to sharpen predictions. The spin of MBHs also bears a relation to the energy that can be released through AGN feedback. MBHs with high spins are predicted to release more specific energy than MBHs that have low spins or are non rotating (Dubois et al. 2014b; Bustamante and Springel 2019). Constraining the spin distribution of MBHs with LISA could help us to better constrain AGN feedback models, which we discuss below.

2.4.1.3 MBH feedback   Feedback from AGN is arguably one of the most important and still open aspects of MBH-galaxy co-evolution. AGN are short-lived phases of MBHs evolution, and release substantial amounts of energy in their surroundings. The feedback drives winds, outflows, and jets, which create large-scale X-ray cavities in clusters and groups of galaxies. However, even if there is observational evidence for the role of AGN in quenching star formation and cooling flows in the host haloes, the exact mechanisms of such energetic processes are still unclear today (e.g. Fabian 2012; Gaspari et al. 2020). Indeed, the range of physical scales (~ 9 orders of magnitude) tied to gas inflows and negative/positive feedback processes in the host make this a very challenging problem to solve (see also Sect. 2.6.1.2).

Cosmological simulations often partition feedback into two modes, depending on the efficiency of the accretion on to the MBHs (e.g. Merloni and Heinz 2008). During accretion phases characterized by high Eddington ratios and thin accretion discs, often called 'quasar' mode, AGN feedback is strongly ejective and radiatively driven, whereas during phases of lower accretion rates, often called 'radio' mode and

characterized by a thick disc or chaotic cold accretion, AGN feedback is mostly driven via radio jets or sub-relativistic outflows that maintain the macro-scale gaseous haloes in quasi-thermal equilibrium for several billion years. The transition between the two states likely occurs around an Eddington ratio of ~ 0.01–0.1 (Yuan and Narayan 2014). Based on analytic arguments, the MBH mass-velocity dispersion scaling relation (M_{BH}-σ) may be a direct consequence of how these wind powers ought to scale with the host properties to curtail further accretion (Haehnelt et al. 1998; King 2003; Zubovas and King 2012).

The modelling of AGN feedback is one of the aspects that needs to be improved in cosmological simulations. Bridging the scale gap is unfeasible, and thus many sub-grid models often invoke simple direct heating mechanisms (either central or as pairs of hot bubbles) to quench local star formation (e.g. Springel et al. 2005b; Sijacki et al. 2007; Vogelsberger et al. 2014; Dubois et al. 2015; Schaye et al. 2015). Other approaches have included injection of kinetic energy via jets or winds (Dubois et al. 2012; Choi et al. 2012; Gaspari et al. 2012; Barai et al. 2016; Bourne and Sijacki 2017; Weinberger et al. 2017; Wittor and Gaspari 2020) instead of or jointly with heating.

While sub-grid models are rooted in physical insight, they are still not able to follow the full range of processes related to MBH accretion and star formation in the interstellar/circumgalactic medium. Therefore, future improvements should take into account magnetic fields, employ at least some approximate radiative transfer, and consider more realistic models of stellar feedback and of the clumpy, multi-phase interstellar medium (e.g. Hopkins et al. 2018; Marinacci et al. 2019). One key aspect is the connection between AGN feedback and the spin of MBHs. Given that LISA will provide us with spin distribution of the merging systems, this is a direction that we need to address in the coming years. The strength of AGN feedback scales with the radiative efficiency, which is closely tied to MBH spin. Therefore, a self-consistent treatment of AGN feedback should account for the effect of spin on radiative efficiency (as in Trebitsch et al. 2021; Dubois et al. 2021, for example), which could become feasible if the spin distribution will be robustly constrained by future GW datasets.

2.4.1.4 MBH dynamics   MBH dynamics is key to model LISA's MBH mergers. Between when a galaxy merger begins and the final MBHs coalesce, an MBH must complete a journey of many orders of magnitude in spatial scales. We refer the reader to Sect. 2.2 for a detailed account of the orbital decay mechanisms acting on different scales, and in varying astrophysical environments. However, most cosmological simulations are unable to follow the dynamics of the infalling MBH down to the scale where the MBH binary system can form, because of the trade-off between the maximum resolution achievable and the simulation volume. For example, large-scale cosmological simulations like Horizon-AGN (Dubois et al. 2014a; Volonteri et al. 2016), Illustris (Sijacki et al. 2015), and Eagle (Schaye et al. 2015), with spatial resolutions of about 1 kpc, cannot follow MBH dynamics down to the centre of galaxies. The kpc-scale regime can now be directly probed with smaller volume cosmological simulations, in which multiple MBHs are allowed to co-exist within the

same galaxy, although reaching the required resolution is very challenging. Taking care to correct the dynamical friction force onto MBHs lost due to gravitational softening, Tremmel et al. (2018b) find a wide range of delay times between galaxy merger and MBH pairing in the ROMULUS cosmological simulation, which can impact GW event rates (Barausse et al. 2020b). Even higher resolutions can be instead achieved by means of zoom-in simulations or isolated galaxy mergers, that allow to resolve the dynamics down to a few tens of pc (Van Wassenhove et al. 2014; Bellovary et al. 2019; Pfister et al. 2019b).

When MBHs become gravitationally bound, their orbit must still shrink, the hardening phase, before GWs can act to bring about coalescence (see Sect. 2.2.2 for a description of the physical processes). The binary hardening phase can not be resolved in cosmological simulations, thus assumptions for the estimate of the hardening time-scale need to be adopted in the post-processing analysis of hydro-simulations or in semi-analytical models. Delay times can be assumed to be fixed (DeGraf et al. 2021) or to depend on some simplified way on the properties of the host galaxy (e.g. Izquierdo-Villalba et al. 2020) and/or of the circumbinary disc (e.g. Kelley et al. 2017b; Volonteri et al. 2020; Sayeb et al. 2021). Finally, in any situation characterised by moderately long binary hardening times, triple or even multiple MBH systems are also likely to form in galaxies experiencing frequent mergers, and cosmological models should also take those into account (see, e.g. Rantala et al. 2017; Ryu et al. 2018; Bonetti et al. 2019). It is clear that in preparation for LISA, significant developments are needed to both semi-analytical models and simulations to improve how dynamics is treated and obtain convergence in the predicted rates and MBHB properties.

2.4.2 State of the art on MBH merger rates from cosmological simulations

In what follows, we discuss how the modelling and assumptions for the processes mentioned above affect the predicted rate and properties of LISA events. The range of predictions for the merger rate of MBHs that LISA can detect currently spans a wide range, from about one to several hundreds per year. The reason for this large span lies both in different physical assumptions and in the different techniques used. To give a rapid overview, in terms of physical modelling the merger rate is high when MBHs are abundant in galaxies, hinging on the efficiency of the MBH formation model adopted, and when the dynamical evolution is fast. Then, the rate decreases as one or the other of these assumptions is relaxed. The rate of mass growth also is important, as it determines the redshift at which MBHBs enter and exit the frequency range accessible by LISA. There are also other subtleties that enter the models. For instance, the spins and mass ratios of the binaries at the time of coalescence, which are determined by formation, growth, and dynamical evolution all together, influence the speed of recoil kicks (e.g. Peres 1962; Damour and Gopakumar 2006), which in turn modulate further the merger rate by ejecting MBHs from galaxies. Thus, not only the merger rates but also mass and spin distributions of merging MBHs depend sensitively on the specific assumptions of the models in terms of seeding, accretion, feedback, and spin evolution, which are largely unconstrained by available observational data-sets. The details of these physical aspects are described in

Sects. 2.2 and 2.3 of this paper and below we discuss how they influence the statistics of LISA's merging MBHs also in dependence of the technique used.

The techniques adopted also have a bearing on the resulting merger rate. The main parameter in this context is the mass resolution of the cosmological simulation or the DM merger tree used to build a model Universe. LISA's MBHs have masses in the range 10^3–$10^7 \, M_\odot$ and can be hosted in haloes with stellar masses as low as $10^6 \, M_\odot$ (Bellovary et al. 2019; Volonteri et al. 2020). If the resolution of the model does not allow to resolve low-mass haloes, the merger history of MBHs in these haloes cannot be tracked and therefore the MBH merger rate obtained will be a lower limit to the real merger rate. The volume of the simulation also matters, and ideally a large diversity of environments is needed to accurately derive reliable MBH merger rates that can provide sensible predictions in preparation for LISA. Obviously, both high resolution and large volume requirements increase the computational cost. Therefore, models are currently a compromise and not an ideal set-up.

In the next two sections, we review the existing predictions for LISA and critically discuss their physical assumptions and technical approaches.

2.4.2.1 Cosmological hydrodynamical simulations   Cosmological simulations are a recent addition to predictions for LISA's merger rates and properties of merging MBHs, which started with analytical and semi-analytical models about 15–20 years ago (Haehnelt 1994; Sesana et al. 2005). For LISA, these simulations are, in principle, the best tool, since they incorporate, to some extent, all the processes regarding MBH formation and evolution, and this in the context of an evolving population of host galaxies computed from high to low redshift. As a result, cosmological hydrodynamical simulations have the advantage over isolated merger simulations in that they naturally include a variety of mass ratios, orbital configurations, and galaxy structures. For instance, in isolated merger simulations the minimum mass ratio of a galaxy for MBHs to bind within ~ 1 Gyr seems to be > 0.25 (Callegari et al. 2009; Van Wassenhove et al. 2014; Capelo et al. 2015), but cosmological simulations show (i) that also galaxy mergers with lower mass ratio contribute to the MBH merger rate (Tremmel et al. 2018b; Volonteri et al. 2020) and also (ii) the effect of irregular potentials in high-redshift and dwarf galaxies (Pfister et al. 2019b; Bellovary et al. 2019; Bortolas et al. 2020).

Cosmological hydrodynamical simulations have for the most part focused on the merger rates and mass ratio distributions of the merging events (Salcido et al. 2016; Katz et al. 2020; DeGraf and Sijacki 2020; Volonteri et al. 2020). Spin has been for now included in post-processing in GW-related studies (Sayeb et al. 2021): although some simulations with spin evolution exist (Dubois et al. 2014b; Bustamante and Springel 2019; Trebitsch et al. 2021; Dubois et al. 2021), for the moment the spins of merging MBHs has only been investigated in post-processing (Sayeb et al. 2021).

Most cosmological simulations used to investigate statistically merging MBHs are large-volume ($\geq 100^3$ Mpc^3), low-resolution (DM particle mass $\sim 10^7$–$10^8 M_\odot$, with the proviso that ~ 50–100 particles are required to identify a halo; star particle mass $\sim 10^6 M_\odot$, spatial resolution 0.4–1 kpc) simulations (Salcido et al. 2016; Katz et al. 2020; DeGraf and Sijacki 2020; Volonteri et al. 2020). However, such simulations
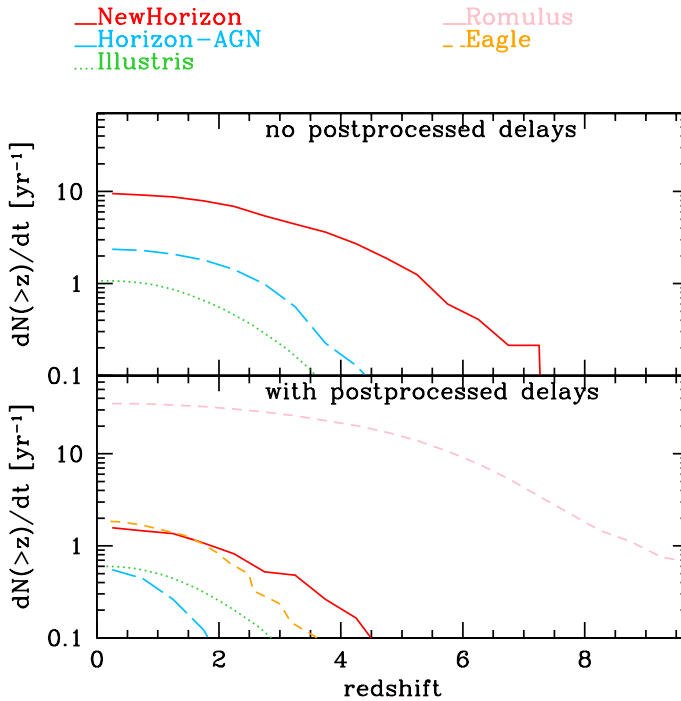
Fig. 24 Comparison of merger rates from different cosmological hydrodynamical simulations, with (bottom) and without (top) the addition of a delay in post-processing. No SNR LISA cut has been applied: this is the merger rate of all MBHs independent of whether LISA can detect them or not, e.g. most MBHs in low-resolution simulations are too massive to enter the LISA band. NewHorizon and Horizon-AGN (Volonteri et al. 2020) include intrinsic delays from dynamical friction from gas, and additional below-resolution delays (bottom panels), and model MBHs above 10^4 and $10^5 M_\odot$, respectively. Illustris (Katz et al. 2020), with $M_{BH} \sim 10^5 M_\odot$, does not implement any intrinsic delay and adds (bottom panel) physically motivated delays in post-processing. Romulus (Tremmel et al. 2018b), where $M_{BH} > 10^6 M_\odot$, includes intrinsic delays from dynamical friction from particles, and a fixed 0.1 Gyr below-resolution delay. Eagle (Salcido et al. 2016) seeds MBHs with $M_{BH} \sim 10^5 M_\odot$ and does not include any intrinsic delay, adding in post-processing fixed delays of 0.1 Gyr for gas-rich galaxies and 5 Gyr for gas-poor galaxies. Image credit: Marta Volonteri

are not suited for studying MBHs in the LISA mass range. Large volume is a positive aspect, improving statistics and capturing various environments in the large-scale structure. Mass resolution, as noted above, is a key point. LISA's MBHs have masses in the range 10^3–$10^7 M_\odot$, with some MBH formation models predicting MBHs with mass $\sim 10^4 M_\odot$ in haloes with mass as low as $10^8 M_\odot$ (see Sect. 2.3.2). Therefore, such low-mass haloes must be resolved in order to capture the full merger rate of LISA's MBHs. Most of the MBHs in well-resolved galaxies in low-resolution simulations are simply *too massive* and therefore merge outside the LISA band, at lower frequencies (they are better suited for PTA experiments, Kelley et al. 2017b). This means that we have to be aware that the merger rates predicted by current simulations—generally <1 per year—could be a lower limit.

Volonteri et al. ([2020](#)) present the first analysis of the merger rate and merging MBH properties in a high-resolution simulation ("NewHorizon", DM particle mass $\sim 10^6 M_\odot$, star particle mass $\sim 10^4 M_\odot$, spatial resolution 0.04 kpc) with a sufficiently large volume (a sphere of radius ~ 10 cMpc) to have some statistics, while Bellovary et al. ([2019](#)) simulate a number of isolated dwarf galaxies at somewhat lower spatial resolution but higher mass resolution and Khan et al. ([2016](#)) simulate one single galaxy at similar resolution in a sphere with radius 13.5 kpc (they then extract and resimulate further the central nucleus of the galaxy at higher resolution, but without hydrodynamics). Volonteri et al. ([2020](#)) analyze in the same way a high-resolution, small-volume simulation and a low-resolution large-volume simulation and show explicitly that indeed the merger rate of the former is higher. This is because dwarf galaxies are resolved, and there are more dwarf galaxies than high-mass galaxies in the Universe. Furthermore, a significant fraction of dwarf galaxies host MBHs: in NewHorizon at $z \sim 0.5$, about 10 per cent of galaxies with mass $10^6 M_\odot$ host an MBH, increasing to 100 per cent at $10^9 M_\odot$. Observationally, between 10 and 100 per cent of galaxies with mass $\sim 10^9$–$10^{10} M_\odot$ at $z = 0$ appear to host an MBH (Greene et al. [2020](#)), implying that MBH mergers in dwarf galaxies are indeed crucial for the low-mass MBHs relevant for LISA. Similar results have also been found by Bellovary et al. ([2019](#)), where, in addition, MBHs typically appear off-centred relative to the host.

Besides mass resolution, how MBH dynamics is treated in simulations is also important, and this circles back to spatial resolution. Typically, large-scale cosmological simulations do not have the sub-pc resolution needed to resolve MBH dynamics. Two approaches have been used in the literature.

The first is to not treat explicitly MBH dynamics: MBHs are repositioned at each timestep at the position of the lowest potential (gas) particle near the MBH. In a merger, an MBH would very rapidly be moved to the centre of the potential well, on time-scales much shorter than in reality. As a consequence, the merger rate of MBHs is increased. Some studies do not consider delays (DeGraf and Sijacki [2020](#)), in others delays have been added in post-processing, either using a fixed value (Salcido et al. [2016](#)) or adopting a physical approach (Katz et al. [2020](#)). (Salcido et al. [2016](#); Katz et al. [2020](#)).

The second approach is to include sub-grid dynamical friction from gas (Dubois et al. [2013](#)), from stars and DM (Tremmel et al. [2015](#)), or all of the above (Pfister et al. [2019b](#)). Adding dynamical friction in the code, however, poses an additional challenge: the ratio of MBH mass to the mass of star particles (or unsmoothed DM particles) must be > 10 to avoid spurious oscillations. This means a very challenging computational task when MBHs have mass $< 10^5 M_\odot$. On-the-fly dynamical friction helps in having realistic dynamics down to the resolution of the simulations: the force acting on the MBHs captures the inhomogeneous, time-varying density distribution and irregular potential wells where MBHs, especially at high redshift, evolve. Still, this approach operates only down to the spatial resolution of the simulation, which is ~ 10–50 pc in high-resolution cosmological simulations and 0.3–1 kpc in low-resolution simulations. Below this scale, statistical studies of MBH mergers can only rely on adding additional time-scales of binary evolution
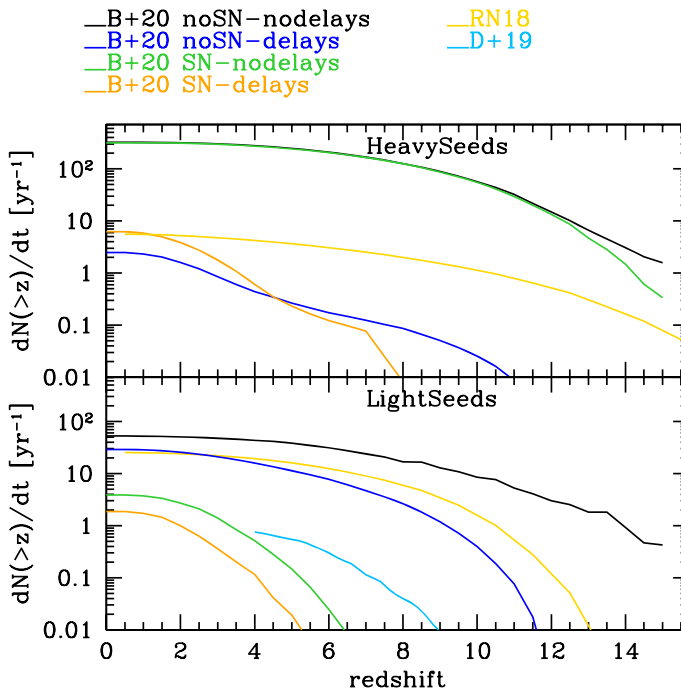
Fig. 25 Comparison of merger rates from different semi-analytical models, assuming heavy seeds (top panel) and light seeds (bottom panel). For all models, we employed the Science Requirement curve (Babak et al. 2021) applying an SNR cut of 8. Different assumptions for models by Barausse et al. (2020b) are shown, with or without SN feedback, and including or not delays. Dayal et al. (2019) include reionisation feedback and delays, whereas Ricarte and Natarajan (2018b) do not include delays. The still large uncertainties in the modelling result in significant variations, up to two orders of magnitude, with mergers between light seeds typically dominating the event rate, but for the case when SN feedback is included, as in Barausse et al. (2020b). Image credit: Marta Volonteri

(stellar hardening, torques in circumnuclear discs and circumbinary discs; see Sect. 2.3.1) in post-processing (Katz et al. 2020; Volonteri et al. 2020; Sayeb et al. 2021), although there are prospects for a full on-the-fly treatment (Rantala et al. 2017).

An important point is that for the moment the mass ratio of merging binaries is based either on information obtained long before the MBH mergers (before including the dynamical delays) or on specific choices applied in post-processing (Sayeb et al. 2021), which may or may not capture how each of the MBHs grows in mass during the final phase of dynamical friction and during the hardening and circumbinary disc phase. Moreover, the limited resolution limits the ability to self-consistently follow the tidal stripping of the galaxy nucleus during the dynamical friction phase, and this affects the orbital decay. A comparison of the predictions obtained by different state-of-the-art simulations is reported in Fig. 24, with (bottom panel) and without (top panel) the inclusion of a post-processed delay between the time when MBHs merge in the simulation and the estimate of the coalescence time taking into account the expected, but unresolved, physical processes.

2.4.2.2 Analytical and semi-analytical models   Several studies have developed analytical and semi-analytical models to predict merger rates and chirp masses for LISA, with various assumptions on the main seeding mechanism for MBHs. Most of these studies pre-date the use of cosmological hydrodynamical simulations in the context of LISA, and have paved the ground for the latter. The predictions of these models can vary significantly, mostly because the physics of the formation and of the orbital shrinking of the MBHBs are thus far loosely constrained, although some advancements have been recently put forward. Analytical and semi-analytical models suggest that different seed populations have a different impact on the total number and mass distribution of potential LISA sources at different cosmic epochs (see, e.g. Volonteri et al. 2003a; Sesana et al. 2011a; Barausse 2012; Klein et al. 2016; Bonetti et al. 2019; Dayal et al. 2019; Barausse et al. 2020b; Katz et al. 2020; Valiante et al. 2021). Generally speaking, all the models converge on predicting that the merger rates are significantly higher if seeding occurs mainly with light seeding mechanisms, e.g. MBHs are formed as remnants of Pop III stars, with a typical mass $\lesssim 10^3 \, M_\odot$ (see, e.g. Ferrara et al. 2014; Valiante et al. 2016; Pacucci et al. 2018, for a description of initial mass functions for light and heavy seeds). Specifically, Ricarte and Natarajan (2018b) predict that LISA will observe ~ 20 times more events if seeding occurred mainly from light seeds, with an upper limit of ~ 300 events (over a 4-year mission duration) with a typical mass $\sim 10^3 \, M_\odot$ in the most optimistic scenario. Similarly, Dayal et al. (2019) predict that light-seeding scenarios will drive the merger rates up, ending with a more conservative prediction of 12–20 mergers during a 4-year mission duration. Even when light and heavy seeds are combined in the same cosmological evolution history, as in Dayal et al. (2019) and Valiante et al. (2021), the number of predicted LISA events is dominated by (growing) light seed binary mergers, although the impact of feedback (reionization, SNae, AGN) by suppressing MBH growth or hindering dynamical friction, reduces the importance of the mergers of light and heavy seeds (Dayal et al. 2019; Barausse et al. 2020b; Li et al. 2020b). Notably, what drives significant differences in predictions is the probability that MBHs actually coalesce, once their host galaxies have merged (see a broad description of the issue in, e.g. Inayoshi et al. 2020 and in Sect. 2.2). Bonetti et al. (2019) predict a rate of ~ 25 and ~ 75 LISA events per year, respectively, in heavy and light seeding models, which is reduced to ~ 10–20 year^{-1} if MBHB mergers are efficiently driven only via triple interactions (i.e. if gas/stellar-driven shrinking mechanisms were to fail in driving the binary to coalescence). In addition, as the GWs emitted during the coalescence phase carry linear momentum, also the inclusion of gravitational recoil can impact the halo occupation fraction, hence the merger rates (see, e.g. Haiman 2004; Tanaka and Haiman 2009; Inayoshi et al. 2020; Izquierdo-Villalba et al. 2020).

A comparison of the prediction by different semi-analytical models is reported in Fig. 25, for light seeds (bottom panel) and heavy seeds (top panel). In general, the predicted event rates span a wide range, from no detection to a few hundred events, depending on the adopted description of the multi-scale and complex processes regulating seed MBH formation, mergers, accretion, and dynamics, which are far from being fully understood. It is therefore important, to reliably predict the rate of

MBH coalescences alongside the hierarchical assembly of galaxies, to get full control of the assumptions made to describe these processes, on different scales/times (see, e. g. Enoki et al. 2005; Sesana et al. 2011a; Klein et al. 2016; Tamanini et al. 2016; Ricarte and Natarajan 2018a, b; Bonetti et al. 2019; Dayal et al. 2019; Volonteri et al. 2020; Barausse et al. 2020b; Valiante et al. 2021, and Sects. 2.2 and 2.4).

From a statistical point of view, LISA detections (or non-detections) may reflect more the dynamical properties and evolution of binary MBHs (i.e. their ability to form and merge) rather than their origin. For instance, heavy seeds are expected to form binaries more efficiently than the more common light seeds. Therefore, a low number (or even the lack) of detections of high-redshift sources in the LISA band may indicate that heavy seeds are very rare and/or that they are not able to merge, after binding in binaries (because of inefficient hardening mechanisms in their host galaxies).

2.4.3 How to advance and optimize the scientific return of LISA

As we have seen above, predictions for LISA events depend in a complicated way on a large number of assumptions, from the seed mass to spin evolution and the dynamics of binary systems. In turn, these aspects are tightly linked to the properties of the host galaxies and of the environment.

The interplay between all these different non-linear physical processes leads to predictions for the merger rates that are highly degenerate.

Learning about spin evolution, merger time-scales, accretion physics, and seed masses from the merger rates of LISA requires a data analysis process where the multi-dimensional parameter space can be quickly explored. By the time LISA launches, the community needs to be ready with a comprehensive and flexible set of theoretical models that can be efficiently confronted with the data.

Numerical simulations of small-scale physical processes will need to be connected to simulations that trace the full cosmological evolution of structures and they will need to inform analytical or semi-anaytical models, that can scan and test the parameter space efficiently. This is central to quantify robustly the mapping between galaxy mergers and MBH mergers. Furthermore, we will need to understand which classes of galaxies, and in which environment, LISA events are most likely hosted. This aspect will be vital if an EM counterpart of a GW merger is to be discovered. Given the current capabilities of LISA to localize nearby sources (Mangiagli et al. 2020, and Sect. 2.5.2), from a few to a few hundreds of galaxies could be in the field of view of, e.g. X-ray telescopes, depending on the loudness of the source. Thus, anticipating the characteristic properties of the host galaxies from simulations will help identifying the host and its redshift.

In the remaining of this section, we will give a brief outlook on the expected advances in "traditional" techniques and on the possibility of using new statistical methods, and how those will be used to inform the LISA data processing.

2.4.3.1 Improvements on current techniques   An important role in building the theoretical framework will be played by the transition to the exascale computing, that

will allow us to develop simulations of much larger portions of the observable Universe, of order comoving Gpc^3 (either as single simulations or as several smaller-volume ones targeting different environments), compared to the current ones (limited to a few hundreds of comoving Mpc), and to further increase the resolution in order to resolve ever smaller scales currently achieved only via dedicated idealised studies. The combination of ultra-large simulated cosmological volumes and very high resolution is the best strategy to enable astrophysical inference studies with the LISA datastream because the properties of the MBH binaries that enter the LISA band are determined by both large scale and small scale processes, which demands both large volumes and high resolution, and because LISA is an all-sky instrument that probes the Universe from low to very high redshift, which again calls for very large volumes. However, exascale computing is not a guaranteed solution, since even the best cosmological hydrodynamic codes available today are far from being able to scale on the billion-core platforms that will characterize such a computing phase over the next decade, when the resolution is increased beyond a certain threshold. This is because in simulations with very high resolution, reaching below tens of parsecs, load balancing on large core counts becomes a computational bottleneck which, unfortunately, gets worse as the number of computing cores is increased. This is an intrinsic challenge with modelling the non-linear process of gravitational collapse. Thus, unless a quantum leap occurs in the parallel architecture of simulation codes, for example owing to improvements in task-based parallelism, the larger cosmological volumes will still be limited in their ability to capture the small-scale stellar and gaseous processes (at sub-pc scales) that drive the hardening phase. This is why simulations will always need to be complemented by other techniques. Different techniques will also require different improvements, and should be combined together to exploit the respective advantages, i.e. the speed and the easy parameter exploration of semi-analytical models and the spatial information of hydrodynamic simulations.

On the side of semi-analytical models, more sophisticated and comprehensive assumptions for MBH seeding and the dynamics of binaries and multiplets will have to be included. High-resolution small-scale numerical simulations covering a wide range in the parameter space will be needed to create new parametric prescriptions for these physical processes. Moreover, semi-analytical models can be combined together to offer a wide dynamic range: Press-Schechter-based models can be combined with models based on N-body simulations. Also, N-body simulations of different mass resolution and cosmological volume can be combined together.

For hydrodynamic simulations—including the so-called "zoom-in" cosmological simulations which probe small volumes, often a single galaxy—the larger computational power will also allow to increase the resolution, reaching scales currently achievable only by dedicated simulations with idealized boundary conditions (down to sub-pc and AU scales). Since it is already clear from the vendors' strategic plans that exascale platforms will have "fat nodes" with at least 128 cores, these simulations, which are much smaller for number of compute elements compared to cosmological volumes, could fit on just a few nodes, partially resolving the load balancing issue mainly caused by communication *between* nodes.

This also means that, with exascale computing, many more zoom-in simulations could be run with significantly less resources than today, allowing to probe a larger fraction of the parameter space.

For these improvements to be effective, a strong effort aimed at improving current sub-grid models of MBH formation, growth, and dynamics, and including new physical processes (e.g. magnetic fields, cosmic rays, non-equilibrium chemistry, radiation transport, and GR effects) is required. Furthermore, increasing resolution would ease the need for simplified prescriptions or post-processing models, but resolution cannot be increased *ad libitum* and a treatment of small-scale phases needs nevertheless to be added to simulations, based on the detailed results of smaller-scale simulations. This combination of different scales will be key to properly estimate the MBH spins, masses, and dynamics of MBHBs, and therefore the subsequent cosmic evolution of MBHs and sharpen predictions for, and intepretation of, LISA detections.

2.4.3.2 New methodologies: artificial intelligence integrated with simulations

Despite the foreseen progress in simulations with the advent of exascale computing, the parameter space potentially probed by LISA will always be too large to be explored at the resolution needed to capture all the effects that determine the time-scales and occurrence rate of MBH mergers. Such effects represent a truly daunting computational challenge of global models. Stochastic processes play a role throughout, which implies that to derive truly robust quantitative models for LISA predictions, e.g. on the mapping between galaxy and MBH mergers, one would need to run a very large sample of simulations. Stochasticity applies both to scales that might be directly resolved in the next generation of cosmological hydrodynamic simulations (10–100 pc) and to scales that will not be resolved for long (parsec scales and below, into the circumbinary disc regime). While semi-analytical models could be used in complement, the complex dependencies of torques/drag regimes on the interstellar medium properties and the stochastic nature of the processes themselves conceptually speak against the use of deterministic phenomenological recipes, which is instead the standard approach of semi-analytical models.

An alternative, promising avenue, which is gaining increasing momentum in observational cosmology and in the analysis of large-scale structure statistics, is artificial intelligence (e.g. Fluri et al. 2019; Tsizh et al. 2020; Li et al. 2021). This often entails using neural networks of varying complexity to recognize correlations and patterns, and subsequently produce many realizations of a given model (model emulator technique). One particular interesting class of such neural networks are generative adversarial networks. Such networks are at the base of modern facial recognition algorithms, which are becoming increasingly sophisticated, and are thus designed to work with an extremely large parameter space (each facial feature can be cast as a parameter, essentially). The networks are designed in such a way that they can be continuously updated to recognize deeper features and patterns without retraining, thus essentially allowing to tune the response based on the needs (namely based on the target, which would be determined by the scientific application). One can imagine training such algorithms to identify complex interstellar medium

patterns and to correlate them with orbital decay regimes/time-scales for MBHs. Training would of course have to be done on small-scale simulations (non-cosmological, galactic and nuclear scale). For example, a first application of such techniques to galaxy dynamics is the morphological identification of merging versus isolated galaxies (Goulding et al. 2018; Nevin et al. 2019; Snyder et al. 2019; Pfister et al. 2020), which is becoming increasingly common in these years. An emulator of the "small-scale dynamics" could be then be designed by integrating the sub-grid model computed via neural networks within a large-scale simulation, using a zoom-in simulation as intermediate step, to encapsulate their trends and results, and implant them in simulations of large cosmological volumes.

2.4.3.3 Summary of LISA measurable quantities and how it will inform us on MBH physics

- LISA can determine the mass of merging MBHs at any time. We expect LISA to discover MBHs closest to the redshift of their formation. At such high redshift, the emitted radiation of these MBHs (that are likely low-mass objects) is too faint to be detected by current EM missions. On single events, the detection of MBHs with $M_{\mathrm{MBH}} \leqslant 10^5 \, \mathrm{M_\odot}$ would confirm the existence of light MBH seeds, while not ruling out the existence of heavy ones (see Sect. 2.3.1 for a description of MBH formation channels). The detections of MBHs with $M_{\mathrm{MBH}} \geqslant 10^5 \, \mathrm{M_\odot}$ cannot, however, validate the existence of heavy seeds as the MBHs could be grown light seeds (except if many of these detections take place at very high redshift). In case of a sufficiently large number of events, LISA will provide us with constraints on the most likely dominant MBH formation channels, as well as the first constraints on the low-mass end of the MBH mass function from low to high redshift.

- LISA can measure the effective spin of merging MBHs (see Sect. 2.3.2.4). Posterior distributions of the spins will be used to determine the spins of the two merging MBHs. For single events, it provides us with information on the dominant nature of the growth of these MBHs, i.e. whether their accretion histories were chaotic or coherent (in other words, whether MBH growth is accretion- or merger-dominated). Spin distributions for the population of MBHs detected by LISA will constrain the relative contributions of MBH growth channels as a function of MBH mass and redshift (see Sects. 2.3.2.2, 2.3.2.3, and 2.3.2.4). In particular, spin measurements are likely going to be possible up to very high redshift ($z \sim 10$) with per-cent precision for nearly a third of the detections (Klein et al. 2016).

- LISA will measure on the full sky the merger rate of MBHs in the mass range 10^4–$10^7 \, M_\odot$. First, the observations of MBH mergers would be the evidence that these BHs dynamically pair and merge within relatively short time-scales, especially if observed at high redshift. Second, the merger rate of LISA will constrain a combination of MBH physical characteristics (MBH seeding, MBH

---

[10] https://sci.esa.int/web/athena.

dynamics, efficiency of MBHs to sink to galaxy centers, MBH growth) and characteristics of their host galaxies (Sect. 2.4.2). LISA will constrain the number density of merging MBHs, independently of their activity. As such, LISA could enable new investigations of the fraction of obscured AGN (by e.g. comparing LISA results to current and future AGN surveys).

- Localization of the LISA events on the sky will be crucial to enable multi-messenger science towards a full characterization of MBH physics and demographic evolution of MBHs. Among many new potential directions, LISA could open a new window on the origins of gamma-ray bursts (Sect. 2.5.1.3), jet (Sects. 2.5.1.3 and 2.5.1.4) and cosmic ray astrophysics (Sect. 2.5.1.4), and MBH accretion (Sect. 2.4.1.2). Localization of the events in space and time could also help linking merging MBHs to their galactic and larger-scale environments and further disentangle MBH formation and growth channels as well as MBH and galaxy co-evolution (e.g. Sect. 2.6.1.2).

2.5 Multimessenger on single events: what do we learn about BH physics from the multimessenger view of the coalescence of MBHs?

Coordinators: **Ioana Duțan, Delphine Porquet**

Contributors: **Imre Bartos, Tamara Bogdanovic, Federico Cattorini, Maria Charisi, Monica Colpi, Alessandra De Rosa, Daniel D'Orazio, Massimo Dotti, Massimo Gaspari, Alberto Mangiagli, Sean McGee, Vasileios Paschalidis, John Quenby, Milton Ruiz, Jessie Runnoe, Antonios Tsokaros, Rosa Valiante, Maurice van Putten, Silvia Zane**

The scientific exploitation of the LISA mission would be greatly increased by performing synergistic, multimessenger observations; that is, combining low-frequency GW observations by LISA with contemporary, prior, or follow-up observations of the same source by EM and astroparticle messengers. The overall goal of this section is to highlight the multimessenger view of single collisions between MBHs detected by LISA in the astrophysical environment posed by their host galaxies. We start this section by presenting the expected multimessenger signatures of coalescing MBHs (precursor, coincident, and afterglows observations). We then elaborate on the best observational strategies to maximize the multimes-senger observations. Moreover, we present different inputs on what we need to prepare to improve estimations of the source parameters (e.g. sky position, luminosity distance, chirp mass, and mass ratio). Finally, at the end of this section, we present what is needed in the near future to maximize the scientific returns of LISA. In this section, particular attention is also given to the synergy between the LISA and Athena[10] missions, both of which will operate at the same time.

2.5.1 The expected multimessenger signatures

The stages which precede and follow the merger of an MBHB feature different spacetime geometries, and the ability to simultaneously detect both the GW and EM signals during each step differs as well. We distinguish between the *pre-merger* (late inspiral) phase, that could lead to the detection of an *X-ray precursor signal*, and the *post-merger* phase, that could lead to *disc rebrightening,* the formation of an *X-ray corona*, and that of an *incipient jet*. This subsection covers first *pre-merger* signatures, and subsequently possible signatures *during merger* and *post-merger*. There are then additional opportunities of multi-messenger observations associated with potential precursor objects of MBHs themselves, such as SMSs.

2.5.1.1 Expected EM signatures of MBHB in-spirals at sub-pc scales In order to maximize the synergy between contemporaneous LISA and EM observations on single MBHB coalescence events, an understanding of the pre-merger population of MBHBs at sub-pc scales using EM observations is crucial. This section focuses on searches for MBHBs that are being carried out at the present time, and that can inform us of the expected LISA merger rate and possibly the expected orbital parameter distributions at merger time. The power of these predictions, however, will rely on how close to merger we can probe an EM identifiable MBHB population. After LISA detects MBHBs, interpretation of formation and evolution channels will rely on the characterization of EM identified populations. In such a case, population samples over the widest possible range of MBHB orbital parameters will be useful in piecing together the entire life stories of MBHBs.

While multiple methods for EM identification of a population of MBHBs have been proposed and practiced over the last two decades (for more details, see Sect. 2.6), there is currently no definitive observational evidence for MBHBs with separations of order one parsec or smaller. Hydrodynamical simulations of circumbinary accretion show that the accretion rate onto an MBHB can be strongly modulated at multiples of the orbital periods (Haiman et al. 2009; MacFadyen and Milosavljević 2008; D'Orazio et al. 2013). This has led to searches for sub-pc separation MBHBs manifesting as $\mathcal{O}(yr)$ time-scale periodicity in quasar light curves. Of order 100 such candidates exist to date (Graham et al. 2015; Charisi et al. 2016; Liu et al. 2019b). However, distinguishing the periodicities from the noise processes intrinsic to AGN variability remains a significant challenge (e.g. Vaughan et al. 2016; Zhu and Thrane 2020). Signatures unique to MBHBs, with which to vet these periodic quasar candidates, have been proposed through the relativistic Doppler boost and binary self-lensing models for periodic variability and flares (D'Orazio et al. 2015; D'Orazio and Di Stefano 2018; Hu et al. 2020; Charisi et al. 2018).

Most of the effort has been focused on the exploration of large optical spectroscopic surveys (e.g. SDSS) using several approaches, searching for:

– large velocity differences between the narrow and broad emission lines, tracing the host galaxy and at least one of the two MBHs, respectively (Tsalmantza et al. 2011; Eracleous et al. 2012; Decarli et al. 2013; Liu et al. 2014; Runnoe et al. 2015, 2017),

- a time varying shift of the broad emission lines, tracing the highly accelerated motion of one of the two MBHs in a binary (Ju et al. 2013; Shen et al. 2013; Wang et al. 2017; Guo et al. 2019), or
- peculiar ratios between broad emission lines with different ionizing potentials due to the tidal effect of the other component of the candidate binary (Montuori et al. 2011, 2012).

If any of these systems are true MBHBs, then the modelling of their broad optical emission lines can in principle yield the properties of the binary, such as the minimum mass, separation, and mass ratio (e.g. Nguyen and Bogdanović 2016; Bon et al. 2016; Runnoe et al. 2017; Nguyen et al. 2019, 2020). It is important to mention, however, that emission-line features mentioned above are not unique to MBHBs. As a consequence, searches like this can generate relatively large samples of MBHB *candidates* whose nature must be tested through continued follow-up or with help of other complementary observational techniques. For example, in the case of SDSS J0927+2943, multi-wavelength follow-up observations disproved both the binary and recoiling-MBH hypotheses (Decarli et al. 2014).

Because they rely on the existing EM spectroscopic surveys, searches of this type are generally biased toward active MBHB candidates with masses $\gtrsim 10^{6-7} M_\odot$ and orbital separations $\gtrsim 0.01$ pc (Pflueger et al. 2018; Xin and Haiman 2021). Similarly, they are sensitive to MBHBs at redshifts $z \lesssim 1$–2 (Montuori et al. 2011, 2012; Nguyen and Bogdanović 2016). Therefore, because of the observational selection effects, these widely used techniques may uncover a fraction of MBHB systems that are *progenitors* to binaries in the LISA frequency band but will not be detected by LISA because the coalescence time-scale is too long. These same techniques will miss low-mass and high-redshift systems, as well as the systems that do not show AGN activity intense enough to allow for a proper modelling of the broad emission lines.

More promising from the standpoint of the coincidental multimessenger detections are MBHBs with smaller orbital separations than those discovered by optical spectroscopic searches (the latter provides signatures too weak to detect if separation distances are smaller than the typical scales of the broad line regions). One can in principle search for such MBHBs using the broad iron fluorescence emission lines, observed at about 6.4 keV in the X-ray spectra of many individual AGN with masses as low as $\sim 10^6 M_\odot$ (e.g. Reynolds 2014). The broad iron emission lines are emitted by the parts of the accretion flow in the close proximity of the MBH (within ~ 10–1000 gravitational radii). They can therefore trace the relative motion of the two MBHs even when they are well within the LISA band (Sesana et al. 2012; McKernan and Ford 2015; Severgnini et al. 2018), as long as at least one of the MBHs exhibits observable AGN activity (see the discussion in Sect. 2.2). However, their current observations are limited to redshifts significantly smaller than those of the expected bulk of LISA MBHB coalescences, indicating a need for a high-sensitivity X-ray detector that will be able to measure broad iron emission lines in the spectra of AGN at higher redshift, such as the Athena mission. Additional signatures include modification of the disc emission caused by the presence of a gap, "suppressing" emission from an annulus in the multi-colour black-body model, and

shocks caused by matter hitting the minidiscs detectable in X-rays (Sesana et al. 2012; Roedig et al. 2014). In all cases, large enough signal-to-noise ratios (necessary in order to discriminate between single and double MBHs) will require long integration times, comparable to or longer than the orbital period of binaries in the LISA band.

What about directly imaging and tracking the orbits of many MBHBs at sub-pc separation in the near future? Advances in Very Long Base Inteferometry (VLBI) at mm-wavelengths should make the direct imaging possible, and this would definitely be very complementary to the indirect methods described above. For example, the Event Horizon Telescope (EHT; Event Horizon Telescope Collaboration et al. 2019) has the angular resolution and sensitivity to astrometrically track the orbits of MBHBs separated by 0.01 pc at Gpc distances. Simple MBHB population models suggest that near-future mm-VLBI experiments could directly image and track the orbits of many such MBHB in, and possibly before, the LISA era (Johnson et al. 2019; D'Orazio and Loeb 2018).

The next generation Very Large Array (ngVLA) will be added to this effort, with the ability to resolve MBHB pairs down to sub-10 pc separations and also track binary orbits through changing pc-scale jet morphology (Burke-Spolaor et al. 2018).

In summary, to prepare for LISA we must invest in theoretical understanding of accretion flows around MBHBs:

- to better understand what drives MBHB orbital evolution, and hence generate more accurate predictions for MBHB populations,
- to more accurately predict observational signatures generated before, during, and after merger, that we can reliably disentangle from AGN variability associated with single MBHs—this partly requires understanding such intrinsic variability better as well,
- to better model mm-wavelength emission from MBHB accretion for direct EM detection prospects.

On the observational side, we must:

- continue to extend time-domain surveys to longer baselines, in order to mitigate false-periodicity detections due to AGN red noise,
- improve our understanding of intrinsic AGN noise processes and quasi-periodic oscillations,
- improve methods for detecting non-standard periodicity (e.g. variable accretion and self-lensing induced periodic flares),
- advance MBHB-related science goals for VLBI experiments that could directly image MBHB orbits.

2.5.1.2 Expected EM counterparts during the late inspiral and merger stages   The multimessenger detection of MBHB inspirals and mergers will certainly establish unique breakthroughs in various fields of physics and astrophysics; yet, one shall be

mindful of a series of caveats that make the concurrent observation of this class of events uncertain. Besides lacking firm predictions on the EM light-curves and spectra of coalescing MBHBs under a variety of conditions (see Sect. 2.5.1.2), the structure and properties of the astrophysical environment around MBHBs are uncertain as well and largely depend on the supply of gas for accretion in the aftermath of a galactic merger.

Generically, MBHBs can be surrounded by a circumbinary disc, and mini-discs can form around the two black holes (see Sect. 2.2.2.2). The accretion of mini-disc gas onto each MBH is expected to produce copious amounts of X-ray radiation. Analogously to what was discussed in Sect. 2.5.1.1, the orbital motion of the binary may imprint a modulation to the expected X-ray emission thanks to Doppler boosting or modulations in the accretion rate. The modulation is expected to be in phase with the GW incoming signal, allowing the correct identification of the host galaxy in the relatively large area provided by LISA (Haiman 2017; Tang et al. 2018; Dal Canton et al. 2019). After the identification, alerts could be sent to other facilities in order to observe the very prompt emission.

Dynamical GR simulations of MBHBs in the force-free limit, which assumes that the plasma around the BHs is tenuous, suggest that two separate jets during the inspiral, one around each BH, could emerge from these systems (Palenzuela et al. 2010c; Mösta et al. 2012), providing a complementary way to search for MBHBs in the late inspiral phase.

What happens at the time of merger is an active subject of research. The natal kick imparted by the GW recoil affects the properties of the accretion disc leading to modifications in the spectrum and light curve that can be non-universal depending on the orientations of the kick relative to the orbital plane pre-merger (Schnittman and Krolik 2008; Rossi et al. 2010). The birth or rebrightening of a jet (Gold et al. 2014b; Khan et al. 2018a) are also possible outcomes. These studies have revealed new possibilities for EM counterparts from binary BHs that arise from jets in binary AGN. As a result, both non-thermal X-ray and gamma-ray signatures from these systems are expected, which would be of interest to Athena as well as other X-ray and gamma-ray satellites.

2.5.1.3 Possible GW and EM signatures of MBH formation from the collapse of supermassive stars   A widely accepted model of long gamma-ray bursts, with a typical duration of ~ 30 s, is the so-called collapsar scenario. In this model, a BH accretion disc system forms after the core-collapse of a massive low-metallicity star, and launches a relativistic jet. The jet breaks through the stellar debris producing gamma-rays (Narayan et al. 1992; Paczynski 1986; Woosley 1993).

Supermassive stars can be responsible for the formation of MBH seeds (see Sect. 2.3.1), hence they could have played a crucial role in generating the population of MBH binaries that LISA can detect out to very high redshift. If they were common at $z > 10$, then a direct-collapse population of high-redshift MBH binaries would have been prominent, leading to a very different population of GW sources detectable with LISA at high redshift relative to the case of light MBH seeds originating from Pop III stars (see Sect. 2.3.1). Hydrodynamic simulations in Shibata
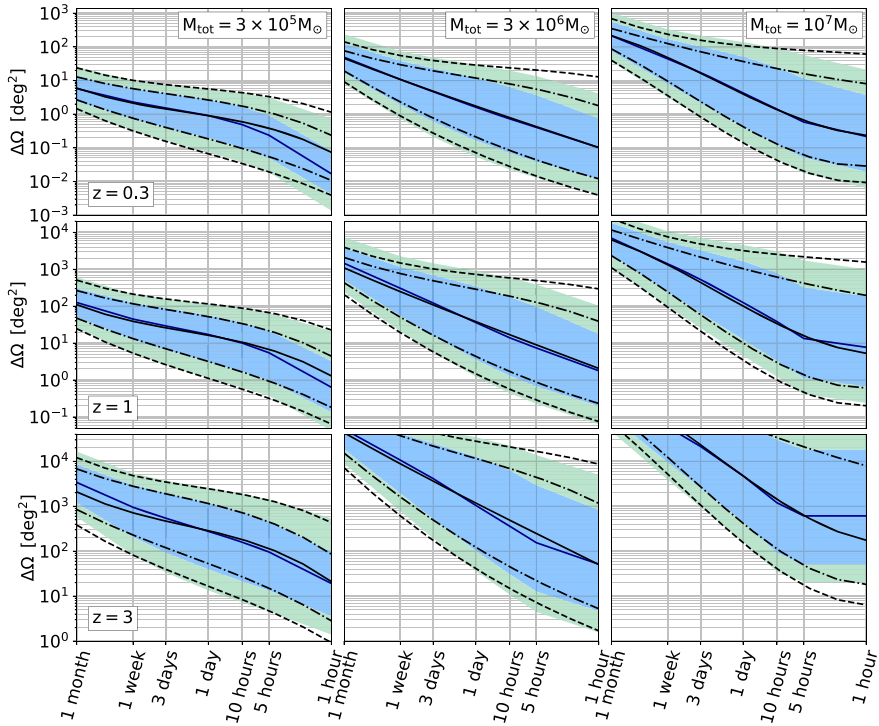
Fig. 26 Time evolution of sky position uncertainties from Fisher Matrix simulations, from Mangiagli et al. (2020), for different source-frame MBHB total mass and redshift. Blue lines correspond to the median of distribution, whereas blue and green areas correspond to the 68 and 95 percentiles, respectively. Overall, lower-mass systems are localized better than more massive MBHBs. At $z = 1$, systems with total mass of $3 \times 10^5 \, M_\odot$ are localized within $10 \, \mathrm{deg}^2$ 10 h before merger. The same accuracy is reached for MBHB with $10^7 \, M_\odot$ total mass only 1 h before merger

et al. (2016) found that the collapse of a $\gtrsim 10^5 \, \mathrm{M_\odot}$ massive star at redshift $z = 3$ emits GWs, with a peak amplitude of 5×10^{-21} at a frequency of $\sim 5 \, \mathrm{mHz}$. These GWs may be detectable by LISA (see also Liu et al. 2007; Sun et al. 2017, 2018). Simulations also found that after $\Delta t \approx 2000 (M_{\mathrm{MBH}}/10^6 \, \mathrm{M_\odot})$ s following the MBH formation a magnetically-driven jet is launched. The jet has a lifetime $\Delta t \sim 10^5 (M_{\mathrm{MBH}}/10^6 \, \mathrm{M_\odot})$ s, and the outgoing Poynting luminosity is $L_{\mathrm{EM}} \sim 10^{51-52} \, \mathrm{erg \, s^{-1}}$ (Sun et al. 2017, 2018). These engines can shine for very long times compared to standard gamma-ray bursts and could be detected as ultra long gamma-ray bursts. The combination of GW and EM signals could help us constrain the origins of GRBs and MBHs.

2.5.1.4 Expectations from astroparticle observations

The most likely origin of cosmic rays of energy above 10^{15} eV is in the jets of AGN. Shock acceleration is the popular explanation of the power law relativistic proton and electron energy spectra. A number of phenomena occurring in the dense hot plasma surrounding an MBH

binary can affect the jet production and evolution, hence opening the possibility to use LISA sources, specifically merging MBH binaries, as novel laboratories for jet and cosmic ray astrophysics. A favourable observational window would seem to be during a merger where the separate MBH jets tend to co-align. The possibility of a spin flip turning two misaligned jets into one where a single enhanced jet is pointing close to the direction of the spin axis of the more massive of the two MBHs has been discussed in Gregely and Biermann (2009) and applies to mass ratios ≥ 0.1. X-rays from the accretion disc relate to the seed particles for the accelerator and the source of p-nucleon or pγ neutrino production. The emergence of a gap in the circumbinary disc or lack of stars to be swallowed in the MBH could cause observable EM emission to cease. This situation is suggested from the lack of EM emission in the observation of the merger of stellar mass BHs. Correlated observation of GWs with those of the Athena X-ray mission and the Square Kilometer Array (SKA) in the radio bands could help in understanding cosmic ray origin. Specifically, data from Athena would reveal the amount of accreted gas available during the merger to power the jet, while simultaneous radio information would both yield the strength of the magnetic field associated with the jet and determine the spectrum of the accelerated relativistic electrons, which could then be directly related to the acceleration of protons.

For IceCube to detect neutrinos from p-nucleon collision, in the favourable case of a jet boosted flux and if 3 per cent of the accretion energy is available, requires that $M_8 m_e \gamma_{10}^4 D_4^{-2} \geq 3$ where M_8 is mass in units of $10^8 M_\odot$, m_e is the ratio of the accretion rate to the Eddington rate, γ_{10} is the jet Lorentz factor in units of 10 and D_4 is luminosity distance in units of 10^4 Mpc. However, the chance of seeing such a favourable geometry for the dominant jet in a merger is only $10^{-3} \gamma_{10}^{-2}$. Successful co-observation of neutrinos and GWs is yet to occur (Adrián-Martínez et al. 2016).

2.5.2 Multimessenger observation strategy for MBHB mergers with LISA

Mangiagli et al. (2020) recently demonstrated that overall the parameter estimation *on the fly* of light systems at $z \sim 1$ and with total intrinsic mass $\sim 10^5 M_\odot$ shows smaller uncertainties than in heavy systems ($10^7 M_\odot$). The chirp mass and mass ratio are well constrained prior to the merger proper, with errors at the per cent level. In Fig. 26, we report LISA's abilities to constrain the sky position of the source. At $z \approx 1$, MBHBs with a total mass of $3 \times 10^5 M_\odot$ can be localized with a median precision of ~ 100 deg^2 (1 deg^2) at 1 month (1 h) before merger, whereas the sky position of $10^7 M_\odot$ MBHBs can be determined to within 10 deg^2 only 1 h before merger. Thus, only light and nearby sources can be traced during the inspiral phase. If the MBHs are embedded in a circumbinary disc, optical emission is predicted from the inner ring of the circumbinary disc and soft and hard X-rays from the mini-discs and the shock heated cavity (Tang et al. 2018; d'Ascoli et al. 2018). Modulation of the light curve is expected at frequencies commensurate to the fluid patterns (Bowen et al. 2017; d'Ascoli et al. 2018; Tang et al. 2018). Thus, observatories such as the Vera Rubin large synoptic telescope could detect the optical signal when the sky

localization uncertainty falls below ~ 10 deg^2. Athena can strategically tile the optical field of view and then narrow down the sky position to detect a potential modulated X-ray chirp. This is possible for MBHBs in the near Universe ($z \lesssim 0.3$).

At merger, the sky localization improves down to $\sim 10^{-1}$ deg^2 for all masses, giving us the chance to detect the post-merger emission by staring at the source for a sufficiently long time, from weeks to months, and witness a re-brightening of an AGN. Again, no definite spectral template exists to identify the source within the narrower error box indicated by LISA (but see Schnittman and Krolik 2008; Rossi et al. 2010), and work in this direction should be performed before LISA flies. These multimessenger observations will be unique as for the first time and *in real time* it will be possible to correlate the masses and spins of the merging BHs with the EM emission by the surrounding gas to give quantitative estimates on the efficiency of the emission under extraordinary conditions, such as during the violence of a merger and from gas bound to a moving BH.

The exposure time needed to detect an Eddington-limited system varies with MBH mass, redshift, and can be more efficient in the soft or hard X-ray band depending on the obscuration of the source. For example, unobscured systems with $M \sim 10^{6-7} M_\odot$ require an Athena exposure time of less than 1 kilosecond (i.e., a single pointing) up to $z = 1.5$ in the soft band, whereas systems of $M \approx 10^5 M_\odot$ can be detected in a kilosecond up to $z = 0.4$. Similarly, systems of $M > 10^7 M_\odot$ require less than kilosecond exposures at redshifts of $z < 4.5$ (McGee et al. 2020; Piro et al.
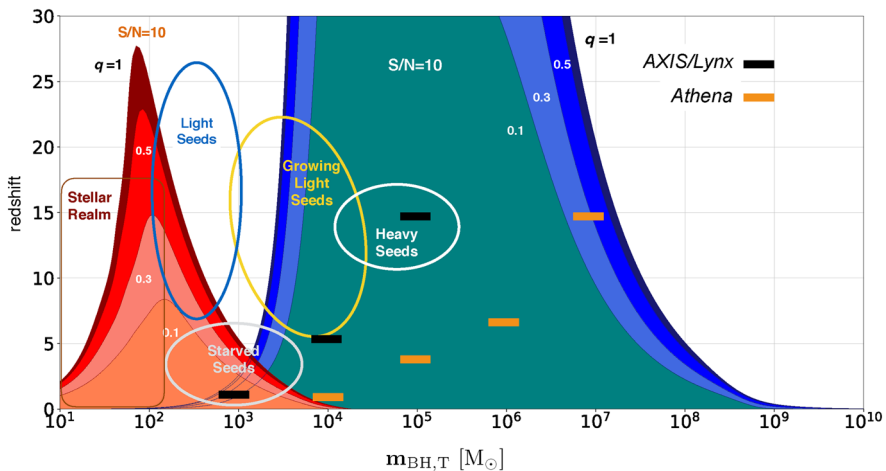
Fig. 27 LISA will be complemented by the X-ray mission Athena (launch expected in the early 2030s), and potentially by the NASA concept missions LynX and AXIS. These missions are shown in orange and black horizontal symbols, which indicate the sensitivity of the deepest pointing, in the [0.5–2] keV observed band, by *Athena* (orange) and *LynX/AXIS* (black). Waterfall plots show the average GW horizon computed for signal-to-noise ratio SNR = 10 and different BH mass ratios for the Einstein Telescope (red) and LISA (blue/green) bandwidth (Santamaría et al. 2010; Hild et al. 2011; Robson et al. 2019). For reference, main MBH formation mechanisms are shown with ellipses. The growth of some of MBH seeds could be stunted by several processes and could be detectable only at late times when merging with other MBHs at $z \leq 5$ ("starved MBHs" in the white bottom ellipse, Valiante et al. 2021). Image reproduced by permissions from Valiante et al. (2021), copyright by the authors

2022). For super-Eddington sources, shorter exposure times are expected, possibly through gas squeezing (Armitage and Natarajan 2002; Cerioli et al. 2016). However, in the case of obscured sources (Gilli et al. 2022, whose fraction remains poorly constrained, and could increase with redshift), whose detections would be more efficient in the hard X-ray band, or objects accreting at low rates below the Eddington limit, the required exposure time of Athena can increase significantly, as described in McGee et al. (2020), Piro et al. (2022). A system with $\sim 10^6 \, M_\odot$ and a luminosity of $L = 0.1 L_{\mathrm{Edd}}$ at $z \sim 1$ would require an exposure of more than 100 ks, against less than 10 ks for the same system with $L = L_{\mathrm{Edd}}$.

Identifying the best observational strategies to maximize the synergy between LISA and other missions such as Athena is a very recent and active field of research. Besides the detectability of the emission, in fact, matching the GW source to its EM counterpart requires the ability of identifying the host among a large number of potential candidates within the LISA error box. This aspect has recently been investigated by Lops et al. (2022), who considered the synergy between LISA and the future X-ray observatories LynX (The Lynx Team 2018) and Athena (see below for the description of the missions). Assuming an active binary at merger, they found that most LISA sources with masses in the range $10^5 - 10^7 \, M_\odot$ at $z < 2$ will be detectable by those instruments within kiloseconds in a single pointing. However, the number of contaminating AGN unrelated to the GW event can be up to thousands for high-redshift signals, making it hard to pinpoint the correct host. Identification strategies need to be developed but require a better theoretical understanding of the peculiar features associated with the EM counterpart. For example, Tang et al. (2018) find that the EM luminosity of a merging binary is suppressed in the last cycles prior to merger and enhanced after coalescence; if this is the case, a viable identification strategy would be to perform sequential pointings and search for a source displaying a monotonically increasing flux; in this case, the exposure time for each pointing might depend on the sky localization posterior distribution provided by LISA with longer exposure times for regions with higher probability to host the MBHB event. Identification of newborn jets powered by an highly spinning merger remnant (mentioned in Sect. 2.5.1.2) might offer another possibility for unambiguous counterpart identification. The best way to suppress the number of contaminants would be to improve the GW localization, which would be possible if LISA is joined by a second space-borne detector such as Taiji (Ruan et al. 2020) or TianQin (Luo et al. 2016). In particular, several works (Ruan et al. 2021; Wang et al. 2021b; Shuman and Cornish 2022) showed that LISA-Taiji joint observations would improve the precision of the sky localization by three orders of magnitude. With this assumption, Lops et al. (2022) demonstrated that unambiguous identification of the active AGN related to the binary would be possible up to $z = 2$.

In the context of sources identification, it is also important to mention that the astrophysical uncertainties on the population of merging MBHBs and on the type of EM emission strongly affect the number of expected EM counterparts. Recently, Mangiagli et al. (2022) computed the number of expected EM counterparts, starting from catalogs of merging MBHBs. Combining the information from radio, optical, and X-ray emission with the information from LISA sky localization, they estimated

between 7 and 20 counterparts in 4 year of LISA time mission. However, in the case of obscuration or collimated radio emission, the number of EM counterparts reduces to 2 or 3. This implies that a better understanding and modeling of the galaxies hosting MBHBs mergers are necessary to be ready for the LISA mission.

In general, it is clear that, in order to best prepare for LISA, we need to investigate better these multimessenger aspects, especially in view of forthcoming missions that could be operational when LISA will fly. AXIS (Mushotzky 2018) and LynX (The Lynx Team 2018) are two NASA concept X-ray observatories that could also fly simultaneously with LISA. Their flux sensitivity will be at least one order of magnitude better than Athena (while having smaller fields of view, see Sect. 2.6), making it possible to observe the X-ray emission from fainter AGN than achievable by current missions or Athena. Compared to the 5–10 arcsecond angular resolution of Athena, the high angular resolution of AXIS (sub-arcsecond resolution compared to the 5–10 arcsecond resolution of Athena), its fast slew rate and ToO response could be key for monitoring MBH binaries until coalescence. As mentioned above, further investigations are required in the near future to determine whether the sky position uncertainties of merging MBHB systems would be compatible with the characteristics of AXIS and LynX, and particularly their small fields of view.

We show in Fig. 27 how these X-ray missions will complement LISA by partially covering the same MBH mass and redshift ranges. The figure also illustrates the possible synergy between LISA and the Einstein Telescope (ET). As developed in Sect. 2.3, there are a lot of hurdles to grow light seeds efficiently in the high redshift Universe, and a population of long-living "starved" (i.e., ungrown) merging MBH seeds could exist (Valiante et al. 2021). In this mass range coordinated multi-band GW observations are possible, with LISA having the capability to first follow the early inspiral of MBHBs, and tracking the merger phase. This unique combination will revolutionise our ability to carry out precise measurements of the source parameters also at $z \sim 5$ (Jani et al. 2019). This mass and redshift range would also be covered by the X-ray missions LynX and AXIS.

In this section, we mainly discussed multimessenger observations with X-ray observatories. However, multimessenger observations with LISA span a large range of wavelengths. For example, we can learn about the physics of jets using radio and optical observations on LISA systems. Radio astronomy, for instance ngVLA as well as SKA, will allow us to observe MBH jets turning on. SKA should also be capable of detecting very luminous flares in the radio emitted by an equal mass MBH binary at merger time, and, through that, help with their sky localization (Tamanini et al. 2016). This can be complemented by observations of optical flares from, e.g., the Roman Space Telescope or the Rubin Observatory (see Sect. 2.6 for a more complete descriptions of relevant instruments and space missions). Observational and theoretical constraints on these EM flares are still very poor, e.g., on the frequency of the peak emissions.

2.5.3 The path towards LISA

In this subsection, we present several ideas for what we need to prepare to exploit the unique characteristics of LISA in the context of multimessenger study of MBHBs from the perspectives of theory, observations, and artificial intelligence.

2.5.3.1 Theoretical and observational improvements in the multimessenger study of MBHBs
On the theoretical front, work is necessary to understand accretion on to binary MBHs and their EM signatures at various wavelengths; on the observational front, efforts are necessary to find and understand more MBHB candidates. Strengthening the collaborative studies between the EM and GW scientific communities is thus very important for scientific utilization of LISA data products.

• **Numerical simulations of EM counterparts to MBHB inspirals and mergers**
Over the last decade, several theoretical groups studied MBHBs in a circumbinary disc or more tenuous gas clouds (see Sect. 2.5.1.2), systematically adding the layers of physics necessary to investigate potential mechanisms for EM counterpart signals emerging during MBHB inspiral and merger. Newtonian viscous hydrodynamics (Farris et al. 2015b; Tang et al. 2017) and MHD (Shi and Krolik 2016) simulations investigated the dynamics of the gas streams being stripped off the inner edge of circumbinary discs. MHD simulations over a post-Newtonian background spacetime explored the first stages of the strongly relativistic behaviour of MBHBs in circumbinary discs in the form of the disc's response to binary orbital evolution by GW emission (Noble et al. 2012) and, more recently, examined the mass-feeding mechanisms onto the individual mini-discs around the BHs (Bowen et al. 2017, 2018) and the systems' radiative properties in the stage immediately prior to merger adopting ray-tracing techniques (d'Ascoli et al. 2018).

The first simulations in full, dynamical GR with resolved BH horizons and the MHD plasma from a circumbinary disc were performed in Farris et al. (2012) and Gold et al. (2014a), modelling the binary-disc pre-decoupling epoch, and in Gold et al. (2014b), modelling the post-decoupling, merger, and post-merger epochs. The inclusion of the BH horizons in these studies showed that powerful outflows and jets are launched from these systems even when the BHs are non-spinning. The more recent study in Khan et al. (2018a) found that accretion rates, temperatures, and jet launching from the interactions of the horizons with the magnetized medium exhibit modest dependence on the initial disc thickness. Jets in binary AGN would produce both non-thermal X-ray and gamma-ray signatures, which would be of interest to Athena as well as other X-ray and gamma-ray satellites. However, modelling from first principles of such EM signals is currently absent. Therefore, efforts must be

---

[11] Any machine learning algorithm aims to learn from data. The data is divided in a *training* data set used for the algorithm learning process, a *validation* data set (optional) to evaluate the progress of learning, and a *test* data set to evaluate the algorithm performance. The level of accuracy of an algorithm depends on the available data, its complexity, and more specifically on the size of the training data.

[12] Neural networks were inspired by the structure and the function of the brain, and they can be thought of as networks of neurons organised in layers: predictors (or inputs) form the bottom layer, forecasts (or outputs) form the top layer, and there may also be intermediate layers containing hidden neurons.
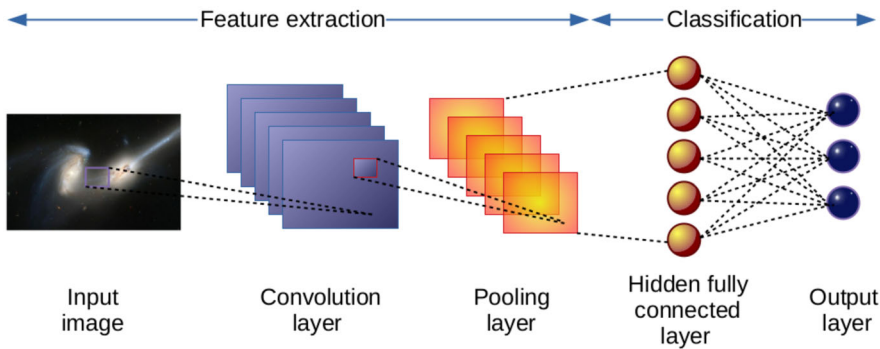
Fig. 28 Schematic representation of a basic convolutional neural network architecture. Such numerical network can be trained on simulations, and later apply to observations to systematically identify MBHB candidates. Image credit: Ioana Dutan

made towards adding radiation transport in dynamical-spacetime general relativistic MHD (GRMHD) simulations of accreting MBHBs.

In addition to GRMHD simulations in dynamical spacetime, dynamical GR simulations of MBHBs have been performed in the force-free limit, which assumes that the plasma around the BHs is tenuous (Palenzuela et al. 2009, 2010b, a, c; Mösta et al. 2010, 2012). These studies showed how the orbital motion of the BHs alters magnetic and electric fields and leads to possible EM emissions. In particular, it was suggested that two separate jets during the inspiral, one around each BH, could emerge from these systems (Palenzuela et al. 2010c; Mösta et al. 2012).

Dynamical-spacetime simulations of MBHBs have also been performed in moderately magnetized clouds in Giacomazzo et al. (2012), showing a rapid amplification of the magnetic field over the last few orbits, leading to the creation of a post-merger magnetically dominated funnel aligned with the spin axis of the final BH, with properties relatively insensitive to aspects of the initial configuration (Kelly et al. 2017)

The future of numerical simulations will require an improved insight into the fuelling rate and the MHD properties of plasma accreting on to the BHs to sharpen the EM predictions. Furthermore, it will be necessary to match a range of different spatial scales in order to more properly address the evolution of the accreting gas during the early inspiral up to merger. These simulations will also need to account for radiation processes in order to correctly estimate EM light curves/spectra, as well as other modes of accretions (such as chaotic cold accretion Gaspari et al. 2013, 2015, Sect. 2.6.1.2) and radiation feedback (e.g., Sądowski and Gaspari 2017). The development of reliable radiation transport schemes in dynamical spacetime is therefore a high priority.

2.5.3.2 Artificial intelligence: Deep learning methods to identify GW source candidates and to estimate LISA source parameters In recent years, artificial intelligence has been intensively applied in astronomy for a wide variety of tasks. As a sub-field of artificial intelligence, machine learning[11] has gained increasing

popularity among astronomers, especially through utilization of one of its sub-sets, namely deep learning, when big data is involved. The most widely used deep learning algorithms are neural networks[12] containing multiple hidden layers that progressively extract higher-level features from input data.

• **Deep learning methods to identify GW source candidates from EM observations** An important issue in astronomy is to find astronomical sources in survey images in order to build source catalogues. These catalogues are valuable tools used for testing theories and numerical simulations against observational data. Convolutional neural networks are deep learning neural networks designed for processing structured arrays of data such as images (see Fig. 28). Convolutional neural networks are very good at learning features from images by hierarchical convolutional and pooling operations.

More precisely, convolutional neural networks algorithms have been already applied for image classification in order to find sources/objects in different EM wavebands. Among the uses in relation to LISA science we can mention detection and classification of quasars from light curves and identification of galaxy mergers (e.g., Pearson et al. 2019; Ackermann et al. 2018). Image classification employed in observational cosmology and in the analysis of large-scale structure statistics can set the stage for improving the estimations of time-scales and occurrence rate of MBH mergers via integration of artificial intelligence with simulations (see discussions in Sect. 2.4.3.2).

More importantly, the time spent to generate catalogues decreases dramatically when using deep learning algorithms instead of standard approaches. However, to reach a desired level of accuracy in image classification, training a deep learning algorithm can be costly in terms of duration and computational resources. Nevertheless, once properly trained, the algorithm can quickly classify thousands of GW source candidates (e.g., Pearson et al. 2019). Here, the training and validation/ test samples can be either observational data from ongoing and upcoming galaxy imaging surveys or simulated data. Using such an approach, some possible biases in observations or additional requirements in simulations might be identified. In spite of current achievements, we need to further design algorithms that are able to learn representative features faster and achieve higher performance in image classification in order to better understand the AGN population and to find binarity signatures in the observational data.

• **Deep learning algorithms for estimation of LISA source parameters** Standard algorithms used for estimation of the physical parameters that govern GW signals are effective, but the computations are time-consuming and they can take up to a few days. For example, in the case of synergistic observations with both LISA and Athena, a poor sky localisation of the source during the inspiral phase limits the possibility of performing concurrent observations. Moreover, the Athena capability of carrying out a *target of opportunity* is about 4 h; that is, a low-latency alert should be released in less than 4 h in order for Athena to be able to watch the merger phase. Therefore, reducing the computational time of source parameters is crucial for multimessenger studies. Over the past few years, deep learning algorithms have been employed for classification of glitches (non-Gaussian noise transients) in Advanced LIGO data (data referring here to the "BH coalescence signal + noises", e.g., George
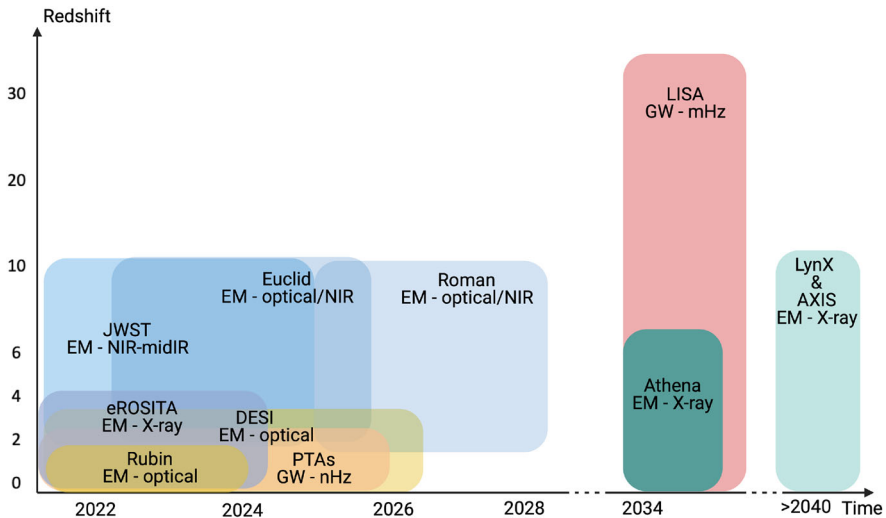
Fig. 29 Landscape of the upcoming and concept missions aiming at constraining the population of MBHs and their host galaxies, from the local to the high-redshift Universe. These missions will significantly increase current EM detections towards high redshifts ($z \sim 10$), while LISA will reach redshifts (e.g., $z \geqslant 30$) that will not be available with EM observations. We caution that the timelines reported in the figure are only indicative as delays in the launch of any of the missions, especially those a few years away from the time of writing, are always possible. In addition, at the time of writing the likely launch time-frame for ATHENA is set to slightly earlier than that of LISA. Characteristics of these and other missions are listed in Table 7. Image credit: Melanie Habouzit

et al. 2018; Razzano and Cuoco 2018). This allowed the identification of signals in Advanced LIGO data, where the training of the algorithm is performed on simulated stellar-mass BH merger signals in synthetic Gaussian noise representative to LIGO sensitivity (e.g., Gabbard et al. 2018), and for estimation of source parameters (e.g., Chua and Vallisneri 2020; Green and Gair 2020). Such models may have limited capacity as they do not currently account for an holistic approach to a quasi-realistic GW data analysis specific to LISA, where tens of thousands of signals overlap with many gaps and glitches. Nevertheless, the current models represent a starting point from which novel architectures can be trained on non-stationary, non-Gaussian noise LISA-like data to conduct parameter estimation. Such development can allow us to perform time-sensitive multimessenger searches to greatly increase the science return of the LISA and other (future) experiments and observatories.

2.6 Multimessenger view of MBH populations

Coordinators: **Maria Charisi, Alessandra De Rosa**

Contributors: **Stefano Bianchi, Tamara Bogdanovic, Monica Colpi, Pratika Dayal, Ioana Dutan, Saavik Ford, Massimo Gaspari, Melanie Habouzit, Albert Kong, Sean McGee, Barry McKernan, Francesca Panessa, Delphine Porquet,**

Raffaella Schneider, Stuart Shapiro, Rosa Valiante, Maurice van Putten, Cristian Vignali, Marta Volonteri, Silvia Zane

LISA will bring crucial constraints on mass, redshift, and spin of merging BHs in the mass range $\sim 10^4$–$10^7\,M_\odot$. To achieve a complete understanding of the population of MBHs, from high redshift to the local Universe, from low to high mass, single and in binaries, the synergy of LISA with other missions will be key. In this section, we provide a global view on the facilities that complement LISA, or will complement it in the near future. We discuss how these missions will address different aspects of MBH physics and populations, but also how they will help us to understand the galactic and large-scale environments in which MBHs assemble, which is a major question in modern astrophysics.

2.6.1 A landscape of new missions to understand MBH formation, growth, and environment

2.6.1.1 A diversity of missions to complement LISA   By exploring the "light" MBHs (the low end of the mass distribution), LISA will open a new window on the GW spectrum, bridging the gap between high-frequency ground-based GW observations (e.g. by LIGO and Virgo), and the nano-hertz frequency observations by PTAs (Desvignes et al. 2016; Ransom et al. 2019; Perera et al. 2019; Kerr et al. 2020). PTAs are currently building up constraints on the GW background, generated by tight binaries of MBHs at the high-mass end ($M_{\mathrm{BH}} \sim 10^{7-9}\,M_\odot$) in the low-redshift Universe (Burke-Spolaor et al. 2019). LISA will be deaf to the population of even lower-mass seed mergers with 10^2–$10^3\,M_\odot$, whose signal falls below the detection threshold (although some portion of the in-spiral might be accessible). These are potential sources for ground-based GW observatories, such as the Einstein Telescope (ET) and Cosmic Explorer. Space- and ground-based missions together will provide a complete census of MBHs, from the earliest seed BH mergers to the largest MBHs today.

The GW detections will be complemented by new observations of MBHBs from space- and ground-based facilities across the EM spectrum, as shown in Fig. 29. The ESA L2 mission Athena (Barcons et al. 2015), the proposed NASA missions AXIS (Mushotzky et al. 2019) and LynX (Lynx Team 2018; Gaskin et al. 2019), and the ongoing eROSITA mission (Predehl et al. 2010) will probe the accretion properties of AGN in X-rays, while surveys like the Dark Energy Spectroscopic Instrument (DESI; DESI Collaboration et al. 2016), the James Webb Space Telescope (JWST; Gardner et al. 2006), the Nancy Grace Roman Space Telescope (Green et al. 2012) and Euclid (Amendola et al. 2013) in the optical and IR band will investigate galaxy hosts up to the highest redshifts. The next-generation ground-based optical telescopes, like the Extremely Large Telescope (ELT; Tamai et al. 2016) and the Thirty-Meter Telescope (TMT; Sanders 2013), will reveal the assembly of the first galaxies, and large-area photometric and spectroscopic surveys, like the Rubin

Observatory Legacy Survey of Space and Time (LSST; Ivezić et al. 2019) and the Sloan Digital Sky Survey-V (SDSS-V; Kollmeier et al. 2017), are expected to discover a treasure trove of binary candidates. Wide-area and deep radio surveys will be available with radio interferometry provided by the Square Kilometre Array (SKA, Dewdney et al. 2009).

In Table 7, we summarize some of the existing and upcoming space- and ground-based telescopes, with their sky coverage and key science that they will address both leading up to LISA's launch and concurrently with LISA. We discuss in detail the role of all these missions in the following.

2.6.1.2 The synergy of LISA and EM missions to answer major questions on MBHs and their host galaxies
In the next decades, EM and GW messengers will work in concert, providing new knowledge of the galaxy and MBH assembly processes, as well as of the interplay between dynamic gravity and the relativistic plasma. Multimessenger observations are an emerging research domain of modern astrophysics. In the following, we detail how several missions can work in synergy with LISA to answer key scientific questions.

• **The formation of the first MBHs**

Thanks to its distant horizon and vast volume probed, LISA will be able to detect the first coalescing massive seeds of 10^4–$10^5\,M_\odot$, witnessing the dawn of MBHBs at redshifts that are not reachable with EM observations. LISA will not, however, detect all the first MBHs, but only those that form binaries and merge, or those that form from the collapse of SMSs that provide a sufficiently high GW signal. EM observations, targeting a complementary population, supplement LISA's detections to provide an improved understanding of the fundamental question of MBH formation.

Currently, the only EM observational insights on low-mass MBHs can be obtained from relatively local (up to $z \sim 2$) dwarf galaxies of total stellar mass $M_\star = 10^7 - 10^{9.5}\,M_\odot$ (e.g. Reines and Volonteri 2015; Baldassare et al. 2015; Mezcua et al. 2016, 2018). Unlike massive local galaxies, which have experienced significant mass growth, local dwarfs have experienced less growth through cosmic history (Habouzit et al. 2017). Their MBHs are also expected to have experienced a similar limited growth. Properties of MBH formation could have been preserved in local low-mass galaxies (Volonteri et al. 2008b; Greene 2012).

To directly probe the properties of seed MBHs, before they grow significantly in mass via gas accretion (Valiante et al. 2018a), it is necessary to search for such sources at high redshifts ($z > 10$). Theoretical models, including spectral-synthesis, predict that the emission from accreting heavy seeds (e.g., direct collapse MBH seeds), will be strong mainly in the IR-submm and X-ray bands, and thus could be detected by JWST up to $z \sim 15$ and Athena up to $z > 6$. By contrast, the emission from lighter accreting seeds ($\sim 10^4\,M_\odot$) is expected to be weaker and difficult to observe with EM facilities at high redshifts (Pacucci et al. 2015; Natarajan et al. 2017; Valiante et al. 2018b; Barrow et al. 2018). The NASA concept mission Lynx, and to a lesser extend AXIS, which has lower sensitivity, directly aim at detecting these young, faint and faraway AGN.

Table 7 Landscape of the upcoming and concept missions that will be complementary to LISA, and will provide us with crucial constraints on the population of MBHs and their host galaxies

Missions	Wavelength	Types	Sky coverage	Launch	Goals
LISA	GW mHz	Laser interferometry	All sky	Mid 2030s	MBH mergers with $M_{BH} =$ up to $z = 20$, constraints on BH mass, redshift, spin
PTAs	GW nHz	Pulsed radio emission	All sky	Current	GW background powered by low-redshift MBHs of $M_{BH} \sim 10^{7-9} M_\odot$
eROSITA	X-ray (0.3– 10 keV)	Spectroscopy imaging	All sky	2019	3 million AGN, of which several tens of thousands at $z \geq 3$
Athena	X-ray (0.3– 10 keV)	Spectroscopy imaging	2.4/30 deg^2 WFI deep/ shallow	2030s	AGN with $L_{2-10\,keV} \geqslant 10^{41-43}$ erg/s depending on redshift
AXIS	X-ray (0.3– 10 keV)	Spectroscopy imaging	2.5/50 deg^2 Medium/ Wide	Concept mission	AGN with $L_{2-10\,keV} \geqslant 10^{40-43}$ erg/s depending on redshift
Lynx	X-ray (0.3– 10 keV)	Spectroscopy imaging	2 deg^2	Concept mission	AGN with $L_{2-10\,keV} \geqslant 10^{39-41}$ erg/s depending on redshift, potentially reaching MBHs of $M_{BH} \sim 2 \times 10^4 M_\odot$ at $z = 7-10$
IXPE/ XL-Calibur/ eXTP	X-ray (2– 8 keV)	Polarimetry	Pointed observations, limited survey capability	2022	MBH accretion in star forming galaxies MBH spin and mass, astrophysical environments of the MBHs, AGN outflows
JWST	NIR-midIR (0.6– 28 μm)	Spectroscopy imaging	46/190 arcmin^2 Deep/ Medium	2021	High-redshift galaxies up to $z \sim 10$, high-redshift quasars, spectrum of young MBHs, constraints on MBH formation mechanisms
Roman	Optical/ NIR (0.5– 2 μm)	Imaging	2000 deg^2 WFI HLS	~ 2025	Mapping high-redshift galaxies, detection of massive quasars of $\sim 10^9 M_\odot$ up to $z \sim 10$
Euclid	Optical/ NIR (550– 2000 nm)	Spectroscopy imaging	40/15000 deg^2 Deep/Wide	~ 2022	Mapping high-redshift galaxies, detection of massive quasars of $\sim 10^9 M_\odot$ up to $z \sim 10$
DESI	360– 980 nm	Spectroscopy	14,000 deg^2	2021	Mapping high-redshift galaxies and quasars
E-ELT	0.35–14μm	Imaging spectroscopy		2025	Confirmation of high-redshift quasar candidates

Table 7 continued

Missions	Wavelength	Types	Sky coverage	Launch	Goals
SKA	0.01–4 m	Radio interferometry	10–20 deg^2 SKA1-MID deep	2027	Duty cycle of jet launching in AGN provide detailed insights on feedback/feeding loop in AGN
Rubin LSST	320–1050 nm	Photometry	18,000 deg^2	2023	Detection of sub-pc MBHBs through photometry variability study on 10^{4-5} AGN
SDSS-V	380–920 nm	Spectroscopy	All sky	2020	Detection of sub-pc MBHBs through spectroscopy spectroscopic identification and redshift of quasar/AGN MBH mass at $z = 0.1$–4.5

See the text for references

Given the small fraction of the sky that EM missions such as JWST, Athena, and Lynx will cover (see Table 7), an optimized observational strategy is crucial to detect as many low-mass MBHs as possible. The MBH community is currently leading an effort to build up target selection criteria designed on the basis of the combined analysis of IR colours (colour-colour cuts), X-rays-to-optical flux ratios (rest frame), IR excess, and UV continuum slopes to efficiently detect and distinguish candidates (Natarajan et al. 2017; Valiante et al. 2018b).

• **The growth of MBHs**

MBH growth is one of the major open questions in astrophysics, and because of this, constraining it is one of the main goals for several of the upcoming EM surveys. Understanding the processes that determine the growth of MBHs from low-mass seeds to MBHs with mass 10^8–$10^{10}\,M_\odot$ requires observations of MBHs at different evolutionary stages over cosmic history. With the large samples of AGN/quasars discovered by these surveys, we expect significant developments before LISA flies. Having a better understanding of MBH growth will help us refine the theoretical models that will be confronted with LISA data and sharpen the astrophysical interpretation of LISA's detections.

The current population of rare bright high-redshift quasars ($z \sim 6$–7, Mortlock et al. 2011; Bañados et al. 2016, 2018a; Matsuoka et al. 2019; Yang et al. 2020a) powered by MBHs of 10^8–$10^{10}\,M_\odot$ will be extended in the coming decade by several EM space and ground-based missions, and will provide us with a unique snapshot in the MBH growth timeline, offering a complementary view to LISA probing the low-mass end of the MBH mass spectrum. The Nancy Grace Roman Space Telescope (Fan et al. 2019) and the Euclid space telescope (Euclid Collaboration et al. 2019) are set to increase tenfold the number of high-redshift quasars discovered in the near-IR. By mapping large fractions of the sky, these surveys will identify quasar candidates, which will be confirmed with spectroscopic follow-up. At lower redshift, the SDSS-

V Black Hole mapper program will deliver MBH mass measurements for about 1000–1500 quasars/AGN between redshift 0.1 and 4.5 (Kollmeier et al. 2017).

X-ray observatories will also greatly enlarge the population of known AGN, in particular at high redshift. eROSITA, an all sky survey strong of an expected sample of about 3 million AGN, will study the accretion history of MBHs by measuring the luminosity-dependent fraction of obscured objects; studying the clustering properties of X-ray selected AGN at least up to $z \sim 2$; and identifying rare AGN sub-populations such as high redshift, possibly highly obscured nuclei. Athena, with higher sensitivity than current missions, aims at detecting over 400,000 AGN, several hundred of which at $z \geq 6$. With even higher sensitivity, the concept missions Lynx and AXIS aim to push the quest for faint AGN by two orders of magnitude in intrinsic luminosity. Besides probing high-redshift quasars, X-ray telescopes will complement the census of MBHs by discovering obscured AGN at the peak of the accreting MBH activity ($z \sim 2-4$), which are inaccessible with optical/near-IR facilities but are crucial in order to obtain a complete census of MBH growth. We will be able to build the mass and spin distributions of a large population of MBHs that will provide crucial information on the growth process (e.g. merger versus accretion, Berti and Volonteri 2008, see also Sect. 2.3.2.4).

• **The co-evolution of MBHs and cosmic structures**

Over 20 years of observations have unveiled fundamental correlations between the properties of galaxies and the mass of their central MBH. This promoted important advancements in extragalactic astronomy, suggesting that the central MBHs and the host galaxies co-evolve from high to low redshift. Notable correlations are the $M_{\mathrm{BH}}-\sigma$ and $M_{\mathrm{BH}}-M_{\mathrm{bulge}}$ relations, which link the stellar velocity dispersion σ and the mass of the stellar bulge M_{bulge} with the mass of the MBH (see Kormendy and Ho 2013, Graham 2016b for reviews). The correlation extends to haloes of galaxies, relating the MBH mass to the hot plasma halo temperature or luminosity (Gaspari et al. 2019; Bassini et al. 2019). These correlations indicate that the MBH, albeit tiny compared to the entire galaxy, is linked to the stellar component and the surrounding intracluster/intragroup medium (up to ~ 10 per cent of the virial radius). The co-evolution between MBHs and galaxies/haloes is possible due to the self-regulation between feeding and feedback processes, from near the MBHs' horizon to the edge of the bound stellar and dark matter structure (see Gaspari et al. 2020 for a review). One way LISA will contribute to investigating the link between MBHs and their hosts is by offering completely independent mass measurements, allowing us to better calibrate the known correlations with galaxy host properties since currently mass measurements suffer from biases introduced by EM observations. Advanced optical/IR facilities will be instrumental in constraining the related stellar properties and evolution of the hosts, both for LISA sources and for MBHs with more uncertain mass measurements. Future galaxy surveys of JWST, Euclid, and Roman will include the host galaxies of LISA-band MBHs, i.e., lower-mass galaxies than possible to detect today. Respectively, these telescopes should uncover galaxies with stellar mass of $\geqslant 10^7, 10^{9.5}, 10^8 \, M_\odot$ at high redshift. Among others, the PRIMER JWST Treasury Program should detect about 120 000 galaxies out to $z \sim 12$ (Dunlop et al. 2021), the FRESCO Program ~ 1200 galaxies at $z \sim 5$–6.5 (Oesch et al. 2021) and ~ 300

galaxies at $z \sim 7$–9), and the WDEEP Program $\geqslant 1000$ mostly low-mass galaxies with $10^{6-7} \, M_\odot$ (Finkelstein et al. 2021). Further investigations in the community are required to assess whether the galaxies of these surveys could be later matched to LISA events. To connect MBH and galaxy mass with the feeding and feedback physics expected to establish their self-regulation, next-generation X-ray telescopes (Athena, LynX and XRISM; Tashiro et al. 2018) will constrain the inner hot accretion flows and surrounding plasma haloes, in particular by leveraging IFU instruments with high spectral and spatial resolution. Radio-mm telescopes (such as ALMA and LOFAR/SKA) will provide constraints on relativistic jets (especially at low frequencies), their launching mode, and duty cycle of AGN kinetic feedback, thus providing us with a comprehensive view of the role of feeding, feedback and self-regulation in the co-evolution of galaxies and MBHs.

• **The impact of the cosmic large-scale structure on the MBH merger rate**

Observational studies of MBH scaling relations (e.g., M_{BH}–σ and M_{BH}–M_{bulge}) have shown evidence for a dependence on large scale environment. Both central and satellite galaxies in galaxy groups and brightest cluster galaxies appear to have larger MBH masses given their galaxy velocity dispersion (McConnell and Ma 2013; McGee 2013; Dullo 2019; Bogdán et al. 2012; McGee 2013). These departures in the scaling relations remain controversial and could be due to selection effects in the observational samples. If the results are confirmed, the cause could be an enhanced galaxy and MBH merger rate in dense environment, but alternatively tidal effects from the host group/cluster could strip stellar material from the host galaxy (Volonteri et al. 2008a; Graham and Soria 2019; van Son et al. 2019) or an additional channel of MBH growth could result from the host galaxy's interaction with the hot intragroup/cluster medium (Poggianti et al. 2017; Ricarte et al. 2020).

In group/cluster environments it is difficult to disentangle mergers and interactions from the abundant projection effects, so observational results on their relative rate are not firmly established (Edwards and Patton 2012; Pipino et al. 2014). The low-surface brightness and wide-field capabilities of the Rubin Observatory will enable the identification of diffuse merger and tidal features which should narrow the observational uncertainty (Brough et al. 2020). The identification of large samples of stripped galaxies (e.g., Yagi et al. 2010) combined with AGN measures from time-varying photometric analysis or X-ray measurements will allow a robust quantification of this growth channel. The improvements in the understanding of this physics prior to the launch of LISA should enable stronger predictions for the environmental dependence of the MBH merger rate. If MBH mergers are more common in biased overdense regions , this will also help focusing the efforts for finding the EM counterpart of LISA sources.

• **Matter behaviour in the strong field gravity regime**

Astrophysical BHs span 10 orders of magnitude in mass, allowing for unique tests of the scale invariance of gravitational effects. LISA will detect in-spiraling and merging MBHs. LISA's ability to perform tests of gravity through BH coalescences and EMRIs as well as to provide spin measurements will be complemented by EM and GW observations that probe the behaviour of matter in different gravity regimes. Electromagnetic signatures of the inspiral and merger phases in the X-ray domain are

produced so close to BHs that relativity enters into modelling their production. Spin measurements using EM observations include relativistic effects in modelling and data analysis.

The motion of accreting plasma near BHs provides a powerful diagnostic to study the very deep potential well generated by the central object. The infalling matter forms an accretion disc that may extend down to the ISCO, in the vicinity of which the bulk of the X-ray radiation is emitted. X-ray timing, spectroscopic and polarimetric techniques for probing matter flows into the strong gravity regime have been developed and, the first two have already been applied to real data, allowing us to infer the mass and spin of MBHs (Fabian et al. 2000; Remillard and McClintock 2006; McClintock et al. 2011; Reynolds 2014). Moreover, observations of matter orbiting a BH can be used to verify some of the key predictions of GR in a stationary spacetime metric, i.e., a very different—and complementary—setting to that probed using GW measurements of merging BHs.

The relativistically broadened Fe lines observed in accreting BHs are direct diagnostics of matter behaviour in the strong-field gravity regime. In the standard scenario, the hot gas in the 'corona' produces thermal Comptonized emission that is reflected by the inner regions of the accretion disc, resulting in the Fe Kα emission line. Special relativity (Doppler boost and relativistic aberration) and GR (gravitational redshift, light bending) affect the shape of the Fe line (Fabian et al. 2000). When line profile templates are fit to real data in both stellar mass BHs and MBHs, the disc inner radius and inclination can be measured. If the inner disc radius is assumed to be the ISCO, then the spin of BHs, which depends directly on the spin magnitude and whether the accretion disc is prograde or retrograde with respect to the BH rotation, can be inferred (Brenneman and Reynolds 2006; Miller 2007; Reynolds 2014). In the near future, the X-ray polarimetry mission IXPE (launched in December 2021, Weisskopf et al. 2016) will offer an independent method to measure inclinations and BH spins, mainly in stellar mass BH (Connors et al. 1980; Li et al. 2009; Schnittman and Krolik 2009). Larger effective area X-ray polarimetry missions, such as eXTP (Zhang et al. 2019), will extend the technique to the weakest AGN.

In order to further advance our understanding of the behaviour of matter around BHs, we need higher sensitivity (i.e. large effective area) and higher energy resolution, allowing a better characterization of the BH environment through the study of the narrow emission/absorption features in the X-ray spectrum. This will be achieved with the next generation of X-ray telescopes such as Athena, AXIS, Lynx, STROBE-X (Ray et al. 2018), eXTP, and XRISM, which are expected to produce unprecedented quality spectra with short exposures. Observations with such telescopes will minimize the modelling uncertainties (e.g., due to disc inclination, absorption properties, geometry), since these facilities will use different techniques (combining spectral-timing, and spectral-timing-polarimetry information) to measure the distinct physical quantities such as BH spin, accretion geometry, and BH mass (Dovčiak et al. 2008; Dovciak et al. 2013; De Rosa et al. 2019a). The sample of EM-measured MBH spins will also be enlarged.

● **Signatures of MBHB arising from circumbinary discs**

In contrast to earlier studies, recent simulations of GW-driven, nearly equal-mass binaries all the way to coalescence (Farris et al. 2015a; Tang et al. 2018; Bowen et al. 2018, 2019; Roedig et al. 2014) have shown that the gas is able to accrete on to the BHs all the way to the merger, despite the rapid contraction of the binary orbit and the formation of a central cavity (see Sect. 2.2.2.2). In the case of an optically thick flow, coronal emission around the two MBHs may give rise to hard X-ray emission at the mini-disc scales and soft X-ray emission from the inner rim of the circumbinary disc. Simulations suggest that the binaries can be very bright in hard X-rays when the spatial separation of the two MBHs is below about 100 gravitational radii, with thermal emission from the minidiscs dominating. The modulation of the X-ray emission might depend on the orientation of the binary orbital plane relative to the line of sight, Doppler beaming, and gravitational lensing (see Sects. 2.2.2.2 and 2.5.1.2).

eROSITA can detect candidates through the hard X-ray binary signature of shocks in mini-discs (Krolik et al. 2019), while notch signatures (i.e., the lower thermal output at the frequencies that would have been radiated from the radii in the cavity) can be detected in optical surveys. For instance, the plan for SDSS-V is to acquire spectra for eROSITA's AGN, then joint signatures (notch and shock) can be looked for in the same sources. eROSITA and SDSS-V, however, have relatively shallow flux limits, therefore only rapidly accreting MBHs at the upper end of the masses of interest for LISA can be detected.

As discussed in Sect. 2.5.2, for sources with mass $\sim 3 \times 10^5 \, M_\odot$ at $z < 0.5$ LISA's sky localization can be of a few square degrees weeks to months prior to merger. This will allow wide-field X-ray (and possibly optical) instruments to observe the EM precursor signal. Such sources, however, are expected to be few. For most sources a few square degrees in the sky localization uncertainty can be generally obtained only days/h prior to merger, making pre-merger EM observations extremely challenging (if not impossible). In the post-merger phase (with ~ 0.1–10 square degrees sky localization) we will have the chance to observe the disc re-brightening, the formation of an X-ray corona, and that of an incipient jet. In fact, in the post-merger phase, a relativistic jet may be launched by the newly born MBH, with production of gamma-ray emission and afterglow emission in its impact with the interstellar medium (Gold et al. 2014b).

● **Astrophysical neutrinos from MBHBs**

Astrophysical neutrinos may originate in AGN jets, as supported by the detection of 10^{15} eV neutrinos possibly associated with the blazar TXS 0506+056 (Aartsen et al. 2018). Since MBHBs are also likely associated with AGN, they may be promising sources for GWs+neutrinos observations. Coincident detections of GWs+neutrinos may be facilitated by the fact that neutrino observatories are all-sky detectors (like LISA) and do not need to be pointed towards a specific direction. If neutrinos are detected from a sizeable sample of LISA MBHBs, this will provide invaluable insights on the currently unexplored mechanisms of jet launching and acceleration in the presence of an MBHB.

2.6.2 Preparing LISA using prior knowledge on MBHBs from current and upcoming missions

LISA detection rates are uncertain, varying between several to few hundreds over the planned 4-year mission lifetime. Although the bulk of these events will involve MBHBs with $M_{BH} < 10^5 M_\odot$ at $z > 5$, more massive sources with $M_{BH} > 10^6 M_\odot$ at lower redshift ($z < 3$) might be detected at a rate of a few per year (see Sect. 2.4). A number of EM and GW facilities (already operating or upcoming) are expected to deliver significant results even before LISA flies, allowing us to tackle a number of key questions that will prepare the way for LISA. Detections by LISA will then complement these findings either through multimessenger observations or by opening a new window in the GW spectrum. Some of the main questions are as follows: *How do MBHs pair following a galaxy merger? What role does the gas play during the MBH mergers and on which time-scale does coalescence occur? Can the merging MBHs shine down to the final coalescence?* In this section, we summarize the EM and GW facilities that will operate before LISA, and discuss their main contribution to understanding MBHBs. LISA will bring unique and invaluable insights on this topic, enhancing the importance of the upcoming discoveries.

2.6.2.1 Multi-band gravitational waves

● **Exploring the nHz GW band with Pulsar Timing Arrays to uncover the most massive MBH binaries in the local Universe**

The detection of GWs with LISA will expand the GW spectrum in the mHz regime, thus enhancing the discoveries of PTAs in the nHz window. PTAs systematically monitor stable milli-second pulsars over a long period of time, currently spanning almost two decades. GWs passing between a pulsar and the Earth change the time required by successive pulses to travel the path from the pulsar to the Earth. If such deviations in the travel time pulses are correlated over multiple pulsars in the array showing a characteristic quadrupolar correlation signature (Hellings & Downs curve; Hellings and Downs 1983), then GWs can be detected. PTAs are sensitive to nHz GWs and thus target MBHBs with masses of 10^8–$10^{10} M_\odot$ at $z \sim 1 - 2$. PTAs are expected to detect primarily two signals: (1) the stochastic GW background from the superposition of many unresolved signals, and (2) continuous (monochromatic) GWs from individual sources that stand above the background. The former is expected to be detectable within the next few years, whereas GWs from individual binaries likely will follow soon after (Rosado et al. 2015; Taylor et al. 2016; Mingarelli et al. 2017; Kelley et al. 2018; Arzoumanian et al. 2020a). Recently, the North American Nanohertz Observatory for Gravitational Waves (NANOgrav) collaboration, based on their 12.5 years data release with a total of 47 pulsars studied with the Arecibo Observatory and Green Bank Telescope, showed that the stochastic GW background is consistent with predictions for the spectrum produced by SMBHs in the accessible frequency bands (Arzoumanian et al. 2020). However uncertainties remain large, and admit alternative explanations such as cosmic strings. which result in a slightly

different spectral slope. Using a larger number of pulsars, longer observations time, and reducing systematic errors, will be needed to improve upon this latest result.

Because of large theoretical uncertainties in binary evolution, models with similar amplitudes for the GW background predict different merger rates for LISA. The amplitude of the GW background depends on how often galaxy mergers deliver sub-pc binaries, which in turn depends on how often galaxies merge and on how rapidly bound binaries to reach the GW regime. It further depends on the mass of the MBHBs in galaxies (Sahu et al. 2019a), with recent upper limits placing constraints on the MBH scaling relationships (Simon and Burke-Spolaor 2016). It is expected that, prior to LISA's launch, PTAs will constrain not only the GW background amplitude, but also the shape of the background spectrum, which encodes information about the binary eccentricities and/or environmental coupling (Sesana et al. 2009; Taylor et al. 2017; Kelley et al. 2017b; Taylor et al. 2019).

Connecting the binary population at two cosmic epochs (i.e. the lower-mass binaries at higher redshifts observed with LISA and the higher-mass local binaries that dominate the GW background in the PTA band) will constrain the processes that drive the binary evolution following a galaxy merger, which have remained highly uncertain for several decades (Begelman et al. 1980), significantly improving our understanding of galaxy evolution, one of the most fundamental open questions in astronomy. Last but not least, individual MBHBs in the nHz band are candidates for multimessenger observations (Kelley et al. 2019; Arzoumanian et al. 2020b): the sky localization for PTA detections will be very poor (of order $\sim 100 \deg^2$), making the identification of the host galaxy challenging. Therefore, PTAs will develop and refine strategies for follow-up observations that will be invaluable for LISA.

● **Prospects from astrometry to reduce the gap between PTAs and LISA**

Low-frequency GWs can also be detected with precise astrometry. GWs passing through the MW can alter the apparent position of the stars on the sky, resulting in a characteristic oscillatory pattern. This requires long-term monitoring of the precise position of a large sample of stars. Fortunately, this can be achieved in the near future by Gaia, which at the end of its planned 5-year mission will provide precise astrometric measurements for billions of stars. It has been suggested that Gaia observations will provide high-quality data that would complement data from PTAs. This because, while the frequency domain is similar to that of PTAs, sensitivity is somewhat higher towards the high frequency tail accessible of the latter, around 300 nHz (Moore et al. 2017). The sensitivity of Gaia at those frequencies, which corresponds to a strain of order 10^{-14}, could perhaps allow to detect individual loud sources, such as a supermassive black hole binary with a mass of a few $10^8 M_\odot$, namely straddling between the typical PTA and typical LISA range, provided that the source is very nearby. Yet, even if detections would mainly occur for supermassive black hole binaries in the same range of masses of PTAs, the fact that the detection technique is completely different will, by itself, represent an important step forward. The three experiments (PTAs, Gaia, and LISA) together will consolidate our knowledge of the evolution of MBHBs through cosmic time.

2.6.2.2 Multimessenger astrophysics

• **The Legacy Survey of Space and Time of Vera Rubin Observatory to detect AGN binaries through photometric variability**

The Vera C. Rubin Observatory will perform the Legacy Survey of Space and Time (LSST), which will provide time-domain observations of unprecedented quality and quantity (LSST Science Collaboration et al. 2009). This is particularly significant for EM searches of MBHBs, since they can be detected as AGN with periodic variability. LSST will monitor a large number of quasars (of order one million) providing multi-band observations with high cadence, and long baselines, extending up to 10 year. Therefore, it is perfectly suited to detect the relatively short-lived and short-period MBHBs emitting GWs in the LISA band.

Already large numbers of binary candidates are identified in existing photometric datasets from the Catalina Real-time Transient Survey (CRTS; Graham et al. 2015), the Palomar Transient Factory (Charisi et al. 2016), the Panoramic Survey Telescope and Rapid Response System (PanSTARRS; Liu et al. 2019b), and the Dark Energy Survey (DES; Chen et al. 2020c). However, currently it is extremely challenging to distinguish the sources with genuinely periodic variability from the typical AGN that show intrinsic red noise variability (Vaughan et al. 2016). LSST will also facilitate binary searches from that perspective. The vast sample of AGN will allow an improved statistical description of the red noise properties of AGN, thus minimizing the false periodic detections.

The upcoming detections with LSST , along with the current candidates, will illuminate the accretion processes in the presence of a binary, paving the way for multimessenger observations with LISA. More importantly, LSST will constrain the demographics of the population of GW-emitting binaries, the distribution of periods, masses, and mass ratios. Additionally, LISA will provide independent measurements for the binary parameters, allowing us to examine potential biases in EM searches for binaries.

Another exciting possibility arises from the expectation that LSST will detect thousands of tidal disruption events (TDEs). The rate of TDEs depends on *(i)* the dynamics of stars surrounding MBHs; and *(ii)* the density surrounding MBHs. As orbits of stars can be perturbed by MBHB, it is expected that bound MBHB have a different rate than single MBHs, and N-body simulations actually find that galaxies hosting an MBHB should have a significantly higher rate of TDEs (Li et al. 2017). Therefore this is a possible explanation to the over-representation of TDEs in galaxies which undergone a starburst ~ 1 Gyr ago but currently exhibit no sign of star formation (E+A galaxies; French et al. 2016). However, theoretical works have not converged on the origin of these post-starburst galaxies: galaxy mergers triggering nuclear star formation and enhancing the central stellar density (Stone and van Velzen 2016; Pfister et al. 2019a, 2021) provides a possible explanation, but the higher TDE rate could also be due anisotropy in the nuclear star cluster produced caused by the starburst (Lezhnin and Vasiliev 2016) or a merger (Stone et al. 2018). In any case, the galaxies in which TDEs are detected may be more promising hosts of MBHBs or MBH pairs, and may serve as signposts for binary follow-up observations.

● **Spectroscopic search of MBHBs with the fifth Sloan Digital Sky Survey (SDDS-V)**

Spectroscopic surveys, like SDSS, provide another potential route to detect sub-pc MBHBs with EM observations. If one of the MBHs in a binary system is surrounded by enough gas to produce a prominent broad line region, the motion of the MBH will result in detectable Doppler shifts in the broad emission lines (Nguyen et al. 2020 and references therein). The spectroscopic database of SDSS has already provided significant samples for spectroscopic searches of MBHBs and dozens of binary candidates have been identified from their large broad-line offsets (Eracleous et al. 2012). However, these are not unique signatures for binaries, and long-term spectroscopic follow-up is necessary in order to observe coherent changes in the broad emission lines and confirm the binary nature of the sources (Runnoe et al. 2017).

SDSS-V will provide a promising sample for this type of search, since the BH mapper program will spectroscopically monitor thousands of AGN over multiple epochs (Kollmeier et al. 2017). This time-domain component to the spectroscopic survey will allow the detection of several more candidates. These candidates are likely progenitors of LISA sources before entering the GW-dominated phase of their evolution, since at mpc separations, the broad line region around individual MBHs cannot be that prominent. However, they can bridge the gap in our understanding of binary evolution in the sub-pc regime.

● **Identifying MBHBs through morphological and spectral investigations at radio wavelength**

Radio emission in galaxies can directly mark the location of the MBH, since it is typically associated with active MBHs. In case of binary systems, if both nuclei are active, then a double radio core can be resolved. However, such systems are rarely found (Rodriguez et al. 2006). Sometimes, jets are produced and their associated synchrotron emission can help in tracing the past and current dynamics of MBHs in a merging system. Radio observations are crucial in identifying pairs via a morphological, spectral, and variability investigation.

Nowadays the highest spatial resolutions on ground are achieved by Global VLBI (Very Long Baseline Interferometry) network observations, that combine radio telescopes all over the world to synthesize an equivalent Earth size instrument, being able to reach angular resolution at milli-arcsec scales, allowing to map the nuclear sub-pc scales for nearby sources (Venturi et al. 2020).

Future radio observatories such as Next Generation Very Large Array (ngVLA) and Square Kilometre Array (SKA) will work in excellent synergy with LISA on several grounds. On the one hand, they will be able to identify the radio EM counterparts to GWs due to MBHBs mergers, thanks to their high-resolution, sensitivity, and fast-mapping capabilities. On the other hand, the large-scale surveys on wide areas and with nearly μJy/beam sensitivity will significantly increase the dual AGN population at sub-kpc separation, by several orders of magnitude (see Paragi et al. 2015). For instance, SKA1-MID is expected to detect a few hundreds of dual AGN per square degree and probe scales of 1–100 kpc (Deane et al. 2014). In addition, precise measurements of AGN core positions will allow the investigation of offset MBH predicted by gravitational recoil. A combination of long baselines and high frequencies can ideally map and identify cores from MBHBs at sub-pc

separations. The ngVLA and SKA with a VLBI expansion will allow to resolve the sub-mJy source population, tracking the orbital motions of radio cores for the most nearby GW candidates (Bansal et al. 2017; Burke-Spolaor et al. 2018). Jet precession might be due to the presence of an MBHB, potentially producing an X-shape morphology (Horton et al. 2020) that can be traced by high-sensitivity low surface brightness observations as offered by SKA. In addition, radio light curves of AGN can show periodic activity that can be associated to orbital precession. Candidate binaries, dual and offset MBH can be cross-matched with multi-frequency observations to confirm their nature (redshifts from the optical spectra, X-ray emission, e.g. from Athena, etc.).

2.6.3 The path towards LISA

In the following, we inventory the different steps, studies, surveys, and developments, which to us seem crucial in view of LISA, and which are based on current and upcoming observational facilities.

– In the near future, the eROSITA X-ray survey will dramatically improve constraints on the MBH population at the upper end of the LISA band and beyond, up to high redshift. While waiting for the new X-ray missions with better sensitivity and spatial resolution, such as Athena, AXIS, and Lynx, we should aim at exploiting the best capabilities of Chandra and XMM in order to characterize and confirm the candidate MBHB selected through optical variability (photometric variability). Moreover, we should improve modelling of intrinsic emission related to disc-corona in AGN, in order to reduce systematic uncertainties on the estimates of MBH spin and mass. This goal requires the use of spectral-timing (and spectral polarimetry in the future with, e.g. the eXTP mission) techniques that need deep observations of specific targets to investigate the variability properties.

– The upcoming surveys from DESI, JWST, Euclid, ROMAN, and the next phase of SDSS will provide massive catalogues of galaxies. It is imperative to enhance these catalogues with measurements of their MBHs (e.g. MBH mass) which will facilitate the identification of host galaxies for a large sample of LISA MBHB coalescences.

– The optical photometric surveys offer the possibility to select large samples of MBHB candidates (see previous section). These candidates should be further monitored with highly rewarding, albeit risky, X-ray observations in order to confirm or reject their binary nature. This will constrain the expected event rate for LISA. Moreover, X-ray observations with their ability to arbitrate between genuine MBHs and false positives will allow us to validate and refine the selection techniques. Such techniques will be widely used and improved in future facilities such as LSST.

– It is also crucial to improve the numerical simulations of inspiralling MBHBs embedded in gaseous discs, considering accretion properties and detailed thermodynamics of single MBHs and including radiative feedback. These studies will provide more reliable EM signatures that will allow the detection of

LISA EM counterparts. They will also facilitate the efficient discovery (with low contamination of false detections) of binary candidates populations with current and future EM facilities.

3 Extreme and intermediate mass-ratio inspirals

Coordinators: **Pau Amaro Seoane, Saavik Ford, Alejandro Torres-Orjuela, Martina Toscani, Lorenz Zwick**

3.1 Introduction

Coordinators: **Pau Amaro Seoane, Saavik Ford and Cole Miller**

Contributors: **Pau Amaro Seoane, Christopher Berry, Alvin Chua, Saavik Ford, Barry McKernan, Cole Miller, Carlos F. Sopuerta, Alejandro Torres-Orjuela and Verónica Vázquez-Aceves**

Thanks to high-resolution observations of the kinematics of stars and gas we know that most nearby bright galaxies host a dark, massive, compact object (e.g., Kormendy 2004; Genzel et al. 2010; Kormendy and Ho 2013; Graham 2016b). One of the most impressive cases is our own Galactic Centre. The stellar dynamics of the central cluster of stars (the S-stars, or S0-stars), provides compelling evidence for the existence of a massive BH (MBH) of mass $\sim 4 \times 10^6\,M_\odot$, Sgr A* (see Genzel et al. 2010, for a review). In particular, the star S4714 in this cluster has an orbital eccentricity of 0.985 and moves at about 8% the speed of light at pericentre, with an orbital period of 9.9 years around the MBH in our Galactic centre. Another extreme case, S62, comes within 16 AU of Sgr A* (Peißker et al. 2020). Also very recently, Abuter et al. (2020) have presented the detection of pericentre precession in the orbit of the star S2. The best fit to a relativistic orbit yields a precession rate between 0.196 and 0.272 degrees per orbit, which is consistent with GR predictions at the $\sim 17\%$ level. Further compelling evidence for a MBH comes from the Event Horizon Telescope (EHT) observations of the centre of the galaxy M87. EHT measured the mass of its central MBH to be $\sim 6.5 \times 10^9\,M_\odot$, with an event horizon diameter of about 0.0013 pc (Akiyama et al. 2019).

More generally, it is believed that most large galaxies host a MBH. The currently highest inferred mass is $6.6 \times 10^{10}\,M_\odot$ (Shemmer et al. 2004). The stars in the centres of such galaxies have the potential to interact with MBHs, but only if their pericentres are small enough. These orbits typically lead to the tidal disruption of an extended star; when these orbits are represented in phase-space by their energy and angular momentum, the section of phase space that leads to tidally disrupted systems is called the loss cone (Frank and Rees 1976).

The range of frequencies that LISA will cover is ideally matched to the inspiral of a compact object such as a stellar-mass BH, a NS or a WD on to a (light) MBH; i.e., one with a mass between $\sim 10^4\,M_\odot$ and $\sim 10^7\,M_\odot$. Because of the difference in

mass between the MBH and the $\sim$ few–tens of solar masses of the compact object, we call these EMRIs—where the mass ratio q is $10^{-8} < q < 10^{-5}$. There is also a potential population of BHs with masses between $10^2 M_\odot$ and $10^4 M_\odot$, which are called intermediate-mass BHs (IMBHs). In principle, such BHs can be involved in intermediate mass-ratio inspiral (IMRI; $10^{-5} < q < 10^{-2}$) systems, either with a compact object inspiralling into them, or with them inspiralling into a MBH. These would fill the gap between EMRIs and comparable-mass binaries. IMRI observations are naturally complementary to EMRI observations, providing further insight into the development of MBHs and their surroundings and the possible evolutionary link between IMBHs and MBHs. Table 8 introduces the different acronyms used throughout this chapter, their meaning, mass ratio ranges, and configurations.

The frequencies of EMRIs are inaccessible to ground-based GW observatories, as are all but the lightest ($\lesssim 10^3 M_\odot$) IMRIs (Gair et al. 2011; Konstantinidis et al. 2013; Haster et al. 2016b; Amaro-Seoane 2018a), yet their astrophysical production may be related to stellar-mass binary BHs (BH+BHs). Indeed, astrophysical mechanisms for generating EMRIs and IMRIs touch on an extremely diverse range of topics (see below), and LISA will lead the way in distinguishing between various formation channels, and furthering our knowledge in all of these areas. Both EMRIs and IMRIs have been reviewed in Amaro-Seoane et al. (2007) and more recently in Amaro-Seoane (2021, 2018b), Berry et al. (2019). Substellar objects, in particular brown dwarfs, with masses around $10^{-2} M_\odot$ form a third class of inspirals potentially observable in the LISA frequency range. These objects can last as many as 10^8 cycles before crossing the event horizon, due to their extremely large mass ratio, which is why they have been dubbed extremely large mass-ratio inspirals (XMRIs; $q < 10^{-8}$). XMRIs are particularly important in our own Galactic Centre, where a few of them should be present when LISA observations begin (Rubbo et al. 2006; Amaro-Seoane 2019).

Ordinary stars that are similar to our Sun would only complete a single periapsis cycle around a MBH before being tidally disrupted (for a close enough passage to enter the LISA frequency range). In contrast, compact stars can revolve around an MBH thousands or even hundreds of thousands of times, with the number of cycles roughly inversely proportional to the mass ratio.[13] Although the system is constantly emitting GWs, it is at the periapsis when the EMRI emits a strong burst of gravitational radiation. Since the orbit shrinks and precesses, we can envisage this as a probe taking pictures of spacetime around a MBH in the strong regime.

Observing the large number of cycles of gravitational radiation emitted before disappearing into the event horizon has three main benefits:

– As an EMRI can spend up to hundreds of thousands of orbits within a few gravitational radii of the MBH, careful analysis promises to provide exceptionally precise tests of the nature of strong-field gravity and the Kerr nature of MBHs.
– Tracking the complicated orbit through many thousands of cycles yields outstanding measurements of parameters including the redshifted mass and spin of the MBH,

---

[13] Even compact objects may not always avoid tidal disruptions during the inspiral process; for example, a WD could be disrupted outside the event horizon of an IMBH (e.g., Menou et al. 2008; Sesana et al. 2008b; Rosswog et al. 2008; Rossi et al. 2021; Maguire et al. 2020).

without any modelling other than general relativity. In turn, this will give us hints about the evolution of MBHs, in a population that is typically inaccessible to EM observations, except, perhaps, for a limited number of local MBHs, e.g., with the Next Generation Event Horizon Telescope, but nevertheless with much less precision on mass and spin measurements compared to what LISA will do.

– If there is a correlation between the environment and the parameters of the EMRI or IMRI, we could reverse-engineer these to extract unique astrophysical information.

However, these exciting prospects must be earned: the weakness of the signal from individual EMRI orbits means that detection, let alone parameter estimation, will require highly accurate computation of thousands of waveform cycles. EMRI waveform templates are challenging to model. Traditional computation techniques are not suitable because the post-Newtonian (PN) approximation (Blanchet 2014) is inapplicable to these highly relativistic systems and numerical relativity calculations (Duez and Zlochower 2019) are infeasibly computationally expensive because of the large difference in scales between the two binary components. Instead, templates can be calculated by treating the effects of the compact object as a perturbation to the background spacetime of the more massive MBH (Poisson et al. 2011; Barack and Pound 2019). For IMRIs, the systems lie at the boundary of where perturbative methods may apply, where PN approximations may be used for the inspiral, and where numerical relativity simulations may be possible. Therefore, a combination of techniques will be needed to simulate IMRI templates. For EMRI and IMRI science, it will be essential to accurately compute these long waveforms in order to sift out these multi-year signals from the LISA data stream.

In this chapter we first give a summary about the formation mechanisms for EMRIs, which have received more detailed study than IMRIs or XMRIs, as well as the many different physical scenarios that play a crucial role in their event rate estimation. The fundamental theory on which these estimates rely, relaxation theory, is robustly understood and has yielded theoretical results which have been corroborated observationally. There remain astrophysical uncertainties which impact the EMRI rate, and there may be subtle effects that leave the theory incomplete. However, the theory has received extensive and detailed investigation in the context of EMRI formation and evolution in galactic nuclei over the last few decades. The narrative is complex. Here we will briefly summarise EMRI formation in the context of relaxation theory; for a detailed review see Amaro-Seoane (2021, 2018b). *Assuming* that at least one EMRI will be detected during the LISA mission, we lay out the anticipated science that is guaranteed, plausible, and speculative.

3.1.1 Guaranteed science with the detection of EMRIs

EMRIs are essentially guaranteed to happen in our Universe. The expected rates span a wide enough range that we cannot absolutely guarantee an observed EMRI in a 5-year mission (Mapelli et al. 2012). However, the uncertainties are such that LISA might also see multiple EMRIs—and if even one is observed, it is guaranteed to be a direct probe of the MBH spin. Currently our best measurements of MBH spin comes from studies of

the broad component of the FeKα line in X-rays. The FeKα line is broadened due to relativistic effects (special and general) within a few $10r_g$ (here $r_g = GM_{MBH}/c^2$, the gravitational radius) from the MBH. By assuming a compact X-ray illumination source close to the MBH, the FeKα line shape strongly constrains MBH spin (e.g. Reynolds and Nowak 2003; Brenneman et al. 2011), but only for $O(20)$ nearby AGN at present (Vasudevan et al. 2016), and both the statistical uncertainties and the possible systematic errors on the spin measurements are substantial. If we assume the Blandford–Znajek mechanism powers jets in radio-loud sources, it may also be possible to put constraints on MBH spin in a larger number of radio galaxies by measuring jet power (Daly 2011). MBH spins have the power to reveal their growth history: what is the contribution due to mergers with other MBH versus gas accretion? The answers have implications for our understanding of galaxy assembly and evolution. In particular, near maximal spin would indicate that the most recent significant mass increase occurred via gas accretion, predominantly from a thin disc with coherent direction of the angular momentum; other individual spin measurements lead to less clear-cut conclusions but can permit constraints on the accretion history (see Sect. 2.3.2.4 for details). If many EMRIs are observed, we will have the opportunity to probe the distribution of MBH spins. Ideally, this would also enable us to probe a couple of decades in MBH mass, informing the underlying astrophysics of the M_{BH}–σ relation. Second, GW inferences of MBH spin will allow us to test the assumptions underpinning EM measurements inferring spins (Daly 2011; Vasudevan et al. 2016).

EMRIs (and IMRIs) are also unique sources of GWs for studying fundamental physics with LISA—see more details in the white paper of the Fundamental Physics Working Group (Barausse et al. 2020a)—mainly because the small body spends a relatively high number of cycles (that scales with the inverse of the small mass ratio q) very close to the horizon of the MBH, where precessional effects (periastron shift and orbital plane precession) become as strong as they can be (Babak et al. 2017; Berry et al. 2019). The orbital dynamics get imprinted in the GW signal by introducing the associated fundamental frequencies and their harmonics (Drasco 2009). In the case of IMRIs there are extra timescales due to coupling of the small object spin with the orbital angular momentum and also with the MBH spin. These timescales evolve slowly due to gravitational backreaction of the small body gravitational field on its own trajectory. The orbital timescales depend on the MBH spacetime geometry (the Kerr geometry according to general relativity) and their evolution due to gravitational backreaction depends on the gravitational dynamics, which can be very sensitive to modifications to Einstein's equations of general relativity, such as modified gravity, extra fields, extra dimensions, etc.

It is expected (Babak et al. 2017) that EMRI and IMRI waveforms will be sensitive to both the parameters that describe the MBH geometry (mass, spin, and other gravitational multipole moments) and the parameters that describe deviations from the general relativity paradigm (coupling constants, extra dimension length scales, etc.). Therefore, they are unique probes of the geometry of the MBHs in galactic centres and of the particular details of the gravitational theory (and other non-gravitational fields that may affect the dynamics of EMRI/IMRIs) responsible for GW generation (Barack and Pound 2019).

However, in order to extract meaningful constraints from an EMRI (or IMRI) detection, it is essential to have reliable astrophysical predictions for the *distribution* of the key parameters of these systems. The values of such parameters determine to what level we can test the no-hair conjecture and general relativity, and what kind of fundamental physics we can expect to carry out with LISA observations of EMRI/ IMRIs. This leads us to discuss important plausible science, especially involving EMRIs in gas-rich environments.

3.1.2 Plausible science with the detection of EMRIs

Identifying EMRIs in gas-rich environments could be an important observational result, as the effects of gas could in some cases mimic the effect of alternative theories of gravity. For AGN-driven EMRIs, we expect the gas to circularize prograde orbiters, and for the merger to occur in the equatorial plane of the MBH. For retrograde orbiters, however, the eccentricity could be driven to extremely large values (Secunda et al. 2019), and the interplay of gas- and GW-driven decay may be challenging to disentangle. By isolating the gas-driven mergers, we may also be able to directly probe important parameters of the gas, notably the density and viscosity— however, the detectability of the gas-driven phase shift requires substantial gas densities (Barausse and Rezzolla 2008; Kocsis et al. 2011; Yunes et al. 2011a; Barausse et al. 2014; Derdzinski et al. 2019, 2021).

Although there are no known IMRI systems, there are multiple plausible channels for their formation. In particular:

- Dwarf galaxies may contain an IMBH that could interact with stellar mass BHs (Koliopanos et al. 2017; Graham and Soria 2019; Graham et al. 2019),
- Mergers of IMBH-bearing dwarf galaxies with larger MBH-bearing galaxies can produce systems with the relevant mass ratios;
- Globular clusters may contain IMBH that could (similar to dwarf galaxies) interact with stellar mass BH or decay into an MBH-bearing galactic nucleus;
- Finally, IMBHs could form through hierarchical mergers in a galactic nucleus— in particular in an AGN—which would continue to accrete stellar mass BH, while simultaneously creating a natural IMBH–MBH system.

We will discuss each of these formation scenarios in more detail in Sect. 3.2, and we further separate IMRIs into 2 classes: *light* IMRIs, where the primary mass is an IMBH and *heavy* IMRIs, where the primary mass is an MBH. Broadly, in the scenarios where we have the most theoretical confidence, the expected rates are small enough that there is a low probability of an event in the lifetime of a LISA mission (though as with EMRI rates, some uncertainties remain). In other scenarios, our uncertainty on many input parameters is such that the rate per galactic nucleus within the LISA observational horizon could be anywhere from zero to one per few years. However, this provides an excellent opportunity, even in the case of non-detections, to place important constraints on nuclear star clusters (NSCs) and their formation mechanisms, as well as on the structure and lifetime of AGN discs. In effect, LISA

will enable us to reverse engineer important properties of AGN discs, including their radial surface density profiles and lifetimes.

One theoretical concern regarding IMRIs has recently been addressed: IMBH $(10^2 - 10^5 M_\odot)$ *do* exist in the relatively nearby universe. GW190521 demonstrated the formation of an IMBH ($> 100 M_\odot$) at $z < 1$ (Abbott et al. 2020d). At the other end, some dwarf galaxies may host central IMBHs, at least at the lower end of their mass estimates (Moran et al. 2014; Koliopanos et al. 2017) and some of these may correspond to an extrapolation of the mass function and scaling relations towards low MBH mass $(10^5–10^6 M_\odot)$ (Reines et al. 2013; Graham and Scott 2015).

XMRIs, with $q < 10^{-8}$ are systems containing brown dwarfs (Amaro-Seoane 2019). On account of their mass ratio, XMRIs would not evolve appreciably over the course of the LISA mission (Gourgoulhon et al. 2019). XMRIs are the GW event mostly likely to permit LISA to probe the Milky Way MBH and its nuclear star cluster. However, XMRI GWs would only be detectable from the Milky Way, or perhaps a few nearby galaxies. Nevertheless, given their expected rate from Sgr A*, and their possible interactions with the stellar cusp as they inspiral, XMRIs are an exciting probe of our nearest MBH and its environs.

In addition to the direct effects of fundamental physics on waveform generation, there are other effects that are accumulated during the propagation of the GWs from the source to the detector, such as those due to possible high-energy effects beyond general relativity: breaking of Lorentz invariance or of the weak equivalence principle, extra polarizations, gravitational parity violation, etc. (Barausse et al. 2020a). We can in principle detect those effects in EMRI/IMRI waveforms, but in the case of LISA, sources that are detectable at higher redshift, i.e. MBH binary coalescence, are more competitive in this regard. The test of the no-hair conjecture that EMRI/IMRIs provide are complementary to those that can be performed using quasinormal models excited in the ringdown of the final MBH after a MBH binary merger (Berti et al. 2018).

3.1.3 Speculative science with the detection of EMRIs

EMRI/IMRI observations can also have impact on two other important subjects in fundamental physics. The first is the search for primordial BHs (Carr et al. 2021). Given the high precision expected for EMRI mass estimates, a detection would determine with confidence when the small compact object has a mass below what is reasonable from any astrophysical channel. This would be a strong indication of the primordial origin of that object. The other subject where EMRI/IMRIs can have an impact is in the understanding of dark matter. This is not independent from the previous subject since primordial BHs have been proposed to constitute all the dark matter in the observable universe (Carr and Kühnel 2020). An example of how EMRI/IMRIs may probe the nature of dark matter is in the case where it is made by bosons that can form clouds around MBHs (see for our Galactic Centre Amaro-Seoane et al. 2010a), which would affect the orbital dynamics of EMRI/IMRIs and hence would leave an imprint in the waveforms (see, e.g. Hannuksela et al. 2019). Moreover, EMRI/IMRIs could also contribute to the understanding of dark energy by

adding significantly to the knowledge of the expansion history of the universe, assuming that we are able to determine their redshift, either from direct EM counterparts or via correlation with galaxy surveys (MacLeod and Hogan 2008).

Finally, the fundamental physics (also the cosmology) that we can investigate using some IMRI systems may be enhanced if we can do multiband GW astronomy, that is, by combining the information obtained with LISA with the information from detections with ground-based detectors, provided that the IMRI masses are such the system can enter the frequency band of the ground-detectors at a later time (Amaro-Seoane 2018a; Datta et al. 2021).

3.1.4 Data analysis & waveform modelling

To unlock the rich scientific potential of EMRI and IMRI observations, we must be able to extract these signals from the LISA data stream. EMRI detection and characterisation is one of the most challenging problems in LISA data analysis (Amaro-Seoane et al. 2007, 2015; Amaro-Seoane 2018b, 2021). There are three main sources of challenge:

– The complexity of EMRI signals—EMRI orbits are generically eccentric and precessing over a large number of cycles. The waveforms are thus extremely sensitive to the source parameters, and there is a gargantuan space of potential signals to be searched.
– The length of EMRI signals—EMRIs need to be tracked for an extended time in order to accumulate sufficient signal-to-noise ratio (SNR) to be detectable. If the phase cannot be accurately tracked, either due to hard-to-model effects, like transient resonances (Flanagan and Hinderer 2012; Berry et al. 2016) or higher-order corrections due to nonlinear interactions of the compact object's gravitational field (Barack and Pound 2019), or unaccounted for environmental effects, such as viscous drag (Barausse and Rezzolla 2008; Kocsis et al. 2011; Barausse et al. 2014) or perturbations from a nearby object (Amaro-Seoane et al. 2012; Bonga et al. 2019), this will impact detectability.
– The number of EMRI signals—EMRIs are long-lived and possibly numerous. Thus there may be many EMRI signals in the LISA data stream at any given time, overlapping with one another as well as with signals from the multitude of other sources. This means that any data analysis strategy for EMRIs must be part of a global fit that analyzes all signals concurrently.

The first challenge means that, unlike when searching for LIGO–Virgo signals (e.g., Allen et al. 2012; Abbott et al. 2016b), it is computationally infeasible to perform a matched-filter search with a regular grid of templates: it has been estimated that $\sim 10^{40}$ templates may be needed for this goal (Gair et al. 2004). Instead, we must trade search sensitivity for computational expediency. Multiple data analysis approaches have been explored following the initiation of the Mock LISA Data Challenges (Babak et al. 2008a, b, 2010). Techniques include identifying time–frequency tracks (Wen and Gair 2005; Gair and Jones 2007; Gair et al. 2008b, a), although this can be difficult in the presence of multiple signals, or using Monte

Carlo techniques to stochastically search for signals, either using EMRI templates (Stroeer et al. 2006; Gair et al. 2008c; Babak et al. 2009; Cornish 2011; Ali et al. 2012) or phenomenological waveforms (Wang et al. 2012). These techniques still do not extend to the full scope of global EMRI search, which must ultimately be conducted in a hierarchical fashion (Gair et al. 2004; Chua et al. 2017). Stochastically searching parameter space to fit for EMRI signals is especially challenging as there may be many regions in parameter space where there are good matches to the data, aside from the vicinity of the true parameters (Babak et al. 2008b, 2010), the full extent and severity of such parameter degeneracy is difficult to determine due to the size of the parameter space and the lack of tractable waveforms, and is currently being investigated (Chua and Cutler 2021). Design of EMRI analyses hence remains an open area of research. IMRI detection is less well studied, but should be possible with a combination of the techniques designed for EMRIs and equal-mass binaries.

Essential to measuring the properties of EMRIs and IMRIs is the modelling of the gravitational waveforms. Only with accurate models can the source properties be inferred. For EMRI waveforms, the highest accuracy waveforms are calculated using the self-force formalism (Poisson et al. 2011; Blanchet 2019): the compact object's gravitational field is treated as a perturbation to the background spacetime of the larger black hole. For full characterisation of EMRI signals, we will require calculation of self-force effects to second order in the mass ratio for generic orbits in Kerr spacetime (Rosenthal 2006). The self-force program is now well advanced (Barack and Pound 2019), the self-force has been calculated to first order for a generic orbit in Kerr spacetime (van de Meent 2018), and the foundations have been laid for a second-order calculation (Pound and Miller 2014; Pound 2014; Miller et al. 2016; Pound 2017; Moxon and Flanagan 2018; Pound et al. 2020). It is expected that concerted waveform development will lead to successful computation of EMRI waveforms ahead of LISA's launch. In the meantime, less accurate approximate waveforms are used for developing LISA data analysis. The most common approximations are the analytic kludge (Barack and Cutler 2004b; Chua et al. 2017), based upon a Keplerian orbit augmented with relativistic corrections, and the numerical kludge (Babak et al. 2007), based upon Kerr geodesics mapped to flat spacetime for waveform generation. The low computational cost of these models makes them suitable for early stages of LISA data analysis, where we are looking for EMRI-like signals, but are not concerned about the precise parameter values. IMRI waveforms present a challenge as they lie at the boundary of different techniques for waveform generation (Hinderer and Flanagan 2008; Blanchet 2014). The self-force calculations may cover a large range of IMRI parameter space (van de Meent and Pfeiffer 2020). These can be supplemented with calculations from PN theory (Blanchet 2014; Buonanno et al. 2009) and effective one-body theory used for more equal mass binaries (Buonanno and Damour 1999, 2000; Taracchini et al. 2014; Ossokine et al. 2020). Finally, numerical relativity can model IMRIs. Numerical relativity should give exact numerical solutions to the Einstein equations (Sperhake 2015), but IMRIs require extremely high spatial and temporal resolution. Therefore, computation of high fidelity numerical relativity IMRI waveforms for LISA may require the development of a new generation of codes. The best IMRI waveform models should be produced through combining the strengths of each of these

formalisms. Both EMRIs and IMRIs provide a valuable chance to validate our waveform calculation theory in new regions of parameter space.

3.2 Formation channels

Coordinators: **Manuel Arca Sedda, Xian Chen, and Andrea Derdzinski**

Contributors: **Pau Amaro Seoane, Manuel Arca Sedda, Jillian Bellovary, Elisa Bortolas, Pedro R. Capelo, Xian Chen, Andrea Derdzinksi, Gaia Fabj, Saavik Ford, Jean-Baptiste Fouvry, Zoltan Haiman, Wen-Biao Han, Giuseppe Lodato, Barry McKernan, Syeda Nasim, Amy Secunda and Martina Toscani**

3.2.1 Gas-poor dynamics: Galactic nuclei including dwarfs, and globular clusters

Observations of galaxies and their nuclei have revealed close relationships between several galactic properties and the masses of their central MBHs (Seigar et al. 2008; Gültekin et al. 2009; Kormendy and Ho 2013; Berrier et al. 2013; Reines and Volonteri 2015; Graham 2016b; Davis et al. 2017, 2018, 2019a; Sahu et al. 2019a, b; Davis et al. 2019b; Sahu et al. 2020). Extrapolating these relations to the lower mass end, one would expect 10^3–$10^5 M_\odot$ IMBHs to exist in the centres of dwarf galaxies (Mezcua 2017; Greene et al. 2020), as suggested by X-ray observations of low-mass AGN (Koliopanos et al. 2017; Mezcua et al. 2018; Graham and Soria 2019; Graham et al. 2019; Reines et al. 2020). IMBHs may also form via collisions and mergers of stars and stellar-mass BHs in dense clusters (Portegies Zwart and McMillan 2000; Miller and Hamilton 2002b; Giersz et al. 2015; Mapelli 2016; Di Carlo et al. 2021; Rizzuto et al. 2021; Arca-Sedda et al. 2021; González et al. 2021; Rizzuto et al. 2022). Dynamical friction can subsequently lead to the orbital decay of globular clusters into a galactic nucleus (Tremaine et al. 1975; Tremaine 1976; Capuzzo-Dolcetta 1993), allowing the formation of an IMBH–MBH system (Ebisuzaki et al. 2001; Matsubayashi et al. 2004; Portegies Zwart et al. 2006; Matsubayashi et al. 2007; Gualandris and Merritt 2009; Arca-Sedda and Gualandris 2018). Depending on the populations of stars and BHs in these environments, galactic nuclei (including dwarf nuclei) and globular clusters each provide plausible formation channels for

Table 8 Nomenclature for the different types of mass ratio inspirals used in this chapter

Acronym	Meaning	Mass ratio	Constituents
light IMRI	Light intermediate mass-ratio inspiral	10^{-5}–10^{-2}	IMBH and stellar-mass compact object
heavy IMRI	Heavy intermediate mass-ratio inspiral	10^{-5}–10^{-2}	MBH and IMBH
EMRI	Extreme mass-ratio inspiral	10^{-8}–10^{-5}	MBH and stellar-mass compact object
b-EMRI	Binary-extreme mass-ratio inspiral	10^{-8}–10^{-5}	MBH and binary stellar-mass compact object
XMRI	Extremely large mass-ratio inspiral	$\lesssim 10^{-8}$	MBH and sub-stellar object

EMRIs and IMRIs. We group these channels together because the underlying physical mechanisms for EMRI and IMRI formation is similar for all (gravitational interactions alone); in addition, these channels interact with one another astrophysically through mergers. There remain major astrophysical uncertainties in each formation channel, meaning that LISA observations (perhaps including non-detections) can crucially constrain the astrophysics that lead to their formation.

3.2.2 Formation of EMRIs in gas-poor galactic nuclei

3.2.2.1 Physics of EMRI formation I. Relaxation processes   MBHs, often surrounded by nuclear star clusters, seem ubiquitous in the centre of nearby galaxies (Graham and Spitler 2009; Genzel et al. 2010; Kormendy and Ho 2013; Neumayer et al. 2020). Yet, the details of MBH formation, and their impact on both their surrounding NSC and their host galaxy, remain uncertain (Heckman and Best 2014). Owing to the overwhelming mass of the central MBH and the steep potential well that it generates, NSCs encompass a wide range of dynamical processes that act on radically different timescales (Rauch and Tremaine 1996; Hopman and Alexander 2006; Alexander 2017). The key dynamical processes that can generate an EMRI around a MBH hosted in an NSC are briefly illustrated in Fig. 30. Of these processes, the two-body relaxation time is the slowest, but also the main mechanism for producing EMRIs. We now discuss each timescale and their relevance for studying EMRIs with LISA. After that, we will give a description of how our understanding of EMRI formation has evolved in the last decades, and how LISA can help in that respect.

(1)   **Dynamical time** On account of its mass, the central MBH dominates the nucleus's mean potential, and imposes, at leading order, a Keplerian motion to any object orbiting within the MBH's sphere of influence. These motions take to leading order the form of closed ellipses, for example as currently monitored for the S cluster around Sgr A* (see, e.g., Fig. 31). A Keplerian orbit can be described by its orbital elements (Murray and Dermott 1999), which we denote with $(M, \omega, \Omega, L_c, L, L_z)$. Here, M stands for the mean anomaly, ω is the argument of the pericentre, and Ω the longitude of the ascending node. An orbit is also characterised by three actions $(L_c, L, L_z) = (\sqrt{GM_\bullet a}, L_c\sqrt{1-e^2}, L\cos(I))$. Here, $M_\bullet$ is the mass of the central MBH, a the ellipse's semi major axis, e its eccentricity, I its inclination, L the norm of the angular momentum, L_z its projection along a given axis, and finally L_c the circular angular momentum. Describing dynamics in NSCs amounts then to describing the dynamics of these particular orbital elements. The dynamical time is associated with the motion $\dot{M} = \sqrt{GM_\bullet/a^3}$. This dynamical time being so short, one is naturally led to performing an orbit-average over it, i.e. smearing out the orbiting objects along their Keplerian ellipses (see, e.g., Touma et al. 2009).
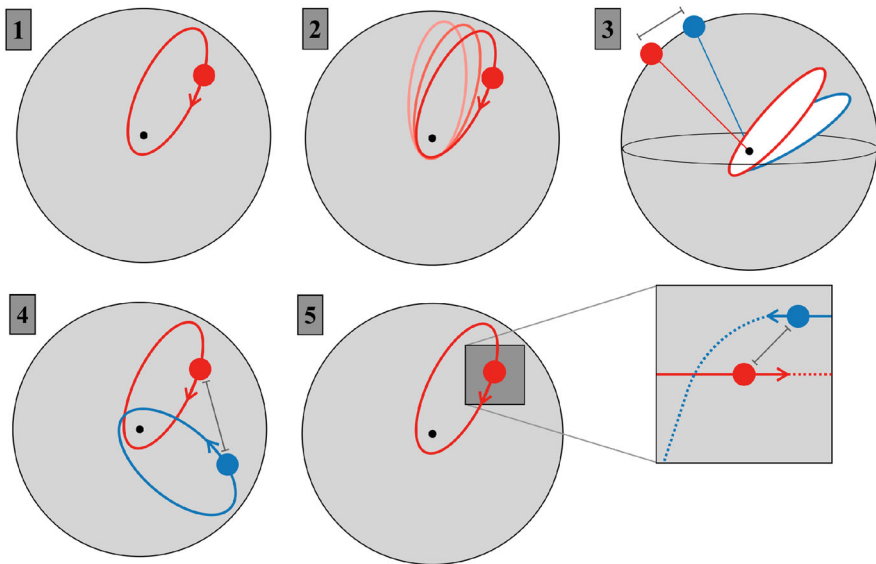
Fig. 30 Illustration of the hierarchy of timescales in a NSC: (1) the dynamical time; (2) the precession time; (3) the vector resonant relaxation time; (4) the scalar resonant relaxation time; (5) the two-body relaxation time

(2) **Precession time** On longer timescales, the gravitational potential self-consistently generated by the stellar cluster, as well as the relativistic corrections imposed by the MBH, namely the Schwarzschild precession (Merritt 2013) cause the ellipses to precess in their planes. This drives the evolution of ω. Importantly, one can note that the relativistic precession frequency diverges as orbits get more and more eccentric, which ultimately leads to the breakdown of the orbit-averaged assumption. Such a relativistic precession has recently been observed for the S2 star around Sgr A* by the Gravity interferometer (Abuter et al. 2018). This is presently the best direct observational constraint on the metric in the vicinity of Sgr A*.

(3) **Vector resonant relaxation** Subsequently, because of the non-spherical stellar fluctuations in the NSC, as well as the relativistic corrections induced by a spinning MBH, the Lense-Thirring precession (Merritt 2013), the ellipses' orbital orientations get reshuffled. This process is called vector resonant relaxation (Kocsis and Tremaine 2015). In that limit, the orbits' angular momenta change in their orientations, $\widehat{\mathbf{L}} = \mathbf{L}/|\mathbf{L}|$, without changing in magnitude $|\mathbf{L}|$ (equivalently in e), nor in energy L_c (equivalently in a).

The process of vector resonant relaxation has been studied, among others, through numerical simulations (Eilon et al. 2009), orbit-averaged simulations (Kocsis and Tremaine 2015), as well as thermodynamical (Roupas et al. 2017; Takács and Kocsis 2018) and kinetic theories (Fouvry et al. 2019). Vector resonant relaxation is essential to describe the warping of accretion (Bregman and Alexander 2012) and stellar discs (Kocsis and Tremaine 2015), and can
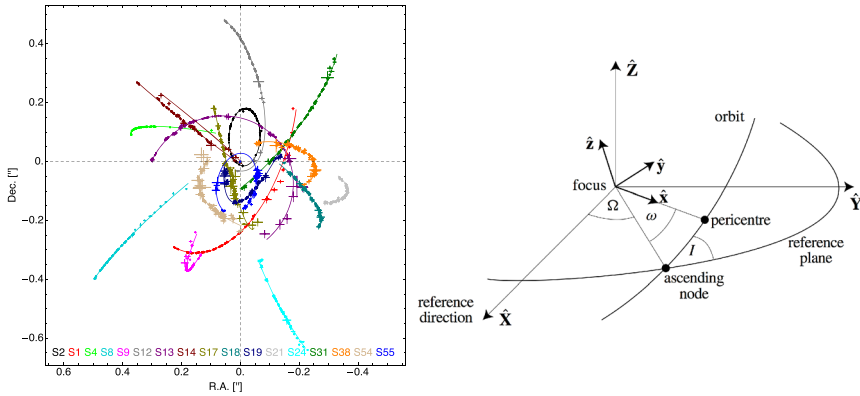
Fig. 31 Keplerian orbits around an MBH. Left: Detailed observations of the Keplerian dynamics of the S-stars in the vicinity of Sgr A* (~ 10 mpc) from Gillessen et al. (2017). At leading order, orbits take the form of closed ellipses, because the central MBH dominates the gravitational potential. Right: Illustration of the Keplerian orbital elements from Murray and Dermott (1999)

enhance the rate of binary mergers in NSCs (which could naturally produce an IMBH–MBH binary). Furthermore, it can also explain the possible presence of stellar discs (Bartko et al. 2009; Yelda et al. 2014), or even strong anisotropic mass segregation of IMBHs discs (Szölgyén and Kocsis 2018).

(4) **Scalar resonant relaxation**

On longer timescales, resonant torques between in-plane precessing orbits lead to an efficient diffusion of the ellipses' eccentricity. This process is called scalar resonant relaxation (Rauch and Tremaine 1996) as the quantity that diffuses is the norm of the orbit's angular momentum. It is also said to be resonant, as only orbits that precess with matching in-plane precession frequencies will effectively and constructively interact with one another.

This relaxation process has been investigated through ad hoc methods (Hopman and Alexander 2006; Eilon et al. 2009; Madigan et al. 2011; Antonini and Merritt 2013; Merritt 2015), as well as N-body simulations (Perets et al. 2009; Merritt et al. 2011; Antonini and Merritt 2013; Hamers et al. 2014), and kinetic theories (Bar-Or and Alexander 2014; Sridhar and Touma 2016; Bar-Or and Fouvry 2018). Scalar resonant relaxation may be paramount to explain the thermal distribution of stellar eccentricities around Sgr A* (Generozov and Madigan 2020), while not necessarily mandatory (Chen and Amaro-Seoane 2014). However, its efficiency drastically damps as orbits get very eccentric, an effect called the Schwarzschild barrier (Merritt et al. 2011). This particular problem has been addressed in detail by Bar-Or and Alexander (2014). They have shown that the divergence of the relativistic precession frequency as orbits get more and more eccentric is responsible for a drastic dampening of the efficiency of resonant relaxation. As such, the Schwarzschild barrier corresponds to the abrupt transition from a relaxation dominated by resonant interactions (for not too eccentric orbits) to a relaxation dominated by non-resonant two-body scatterings (for eccentric

enough orbits). Given that mainly highly eccentric stellar orbits undergo EMRIs, the total contribution of scalar resonant relaxation to EMRI event rates is small (Bar-Or and Alexander 2016).

(5) **Two-body relaxation**

Finally, on even longer timescales, rather than being driven by the interaction between Keplerian ellipses, an object will start to see its evolution being driven by nearby pairwise interactions, as a result of close two-body encounters. It is only through the cumulative contributions from these localised scatterings that objects can ultimately relax in their Keplerian energy (i.e. in a), through a process called two-body relaxation (Bahcall and Wolf 1976; Cohn and Kulsrud 1978; Shapiro and Marchant 1978; Bar-Or and Alexander 2016; Bar-Or et al. 2013; Vasiliev 2017; Amaro-Seoane 2018b, 2021). It is generically the slowest relaxation timescale in NSCs. The main mechanism for producing EMRI in NSCs is two-body relaxation. This is because it allows for the orbits to become highly eccentric, where other resonant processes significantly damp eccentricity (Bar-Or and Alexander 2014), the expected EMRI rates depend on the spin of the central MBH (Amaro-Seoane et al. 2013). We will elaborate on this later.

One of the first attempts to understand how to produce a successful orbit in a galactic nucleus that will lead to the formation of an EMRI goes back to the work of Sigurdsson and Rees (1997). By using standard relaxation and loss-cone theory (see Sect. 3.2), the authors derived the event rate for compact objects to merge with a MBH in a galactic nucleus. It is important to note that for MBHs above about a few $10^7 \, M_\odot$, the timescales for relaxation exceed a Hubble time; LISA is going to observe MBHs below this threshold, down to $10^5 \, M_\odot$. For lower masses, i.e. for IMBHs and hence IMRIs, we cannot further assume that the MBH is fixed at the centre of the stellar system and any analytical derivation becomes more difficult.

We define now a standard EMRI to consist of a stellar mass object of mass $10 \, M_\odot$ and a MBH with a mass such as that of Sgr A*, the MBH in our own Galaxy. The event rate for this kind of EMRI, we obtain of the order of 10^{-5}–$10^{-6} \, \mathrm{year}^{-1}$ (see e. g. Amaro-Seoane 2018b, 2021, and references therein). This analytical result has been reproduced using numerical algorithms such as in the work of Freitag (2001). The properties of EMRIs formed via relaxation are such that they have large eccentricities at semi-major axis of about 0.1–1 pc. They describe a random-walk-like evolution in phase-space, in particular in angular momentum, until one of two things happens: (i) the small mass deviates off the orbit which would evolved into an EMRI that inspirals into the MBH, or (ii) they cross a threshold in phase-space which separates orbital evolution dominated by dynamics into a regime where orbital evolution is driven only by the emission of GWs. When systems cross this line, which can be roughly derived by equating the relaxation timescale at pericenter to the associated timescale due to the emission of gravitational radiation, as derived by Peters (1964a), we can ignore any dynamical perturbation.

The increase in eccentricity during the EMRI formation can lead to a situation in which the eccentricity is so high that the smaller BH falls radially on to the MBH,

and there is only one or a handful of gravitational radiation bursts before the source is lost. This can be regarded as a head-on collision. This is what is commonly referred to as a direct plunge in the related literature (not to be confused with the plunge when the EMRI crosses the event horizon after hundreds of thousands of orbits). Direct plunge sources are basically lost, because we can extract little or no information from it (but see Hopman et al. 2007; Berry and Gair 2013c, a). It has been shown that the ratio between successful EMRIs and direct plunges could be of about 1:200 respectively (Amaro-Seoane 2018b, 2021, and references therein).

This result led to an interesting new avenue in investigating the role of other types of relaxation. By getting closer and closer to the MBH, the stellar density drops, so that the danger of producing direct plunges due to the accumulation of gravitational tugs of the orbit at apocentre is accordingly reduced. At the same time, the usual two-body relaxation time increases more and more. In addition, the process of scalar resonant relaxation was found to be inefficient in this region of phase-space.

However, as we explain later in this section, direct plunges mostly occur in Schwarzschild MBHs. If the MBH has a spin, any direct-plunging orbit turns out to be a successful EMRI, meaning that it spends tens and up to hundreds of thousands of cycles in the LISA band, depending on the inclination and the spin of the MBH, as shown in Amaro-Seoane et al. (2013). This has an impact on the event rate, because the ratio of 1:200 that we mentioned before increases in favour of successful EMRI orbits.

We note that recently, Zwick et al. (2020) derived an improvement to the pioneering work of Peters (1964a), extending the timescale to be accurate to first post-Newtonian order. By taking into account this modification, the EMRI rates drop by at least one order of magnitude per nucleus. But then the role of the spin has another impact on the inspiraling timescale that might again enhance the event rate (Zwick et al. 2021; Vazquez-Aceves et al in prep 2020b).

To sum up, relaxation is a robust theory which has been tested in observations in dense stellar systems. In particular, recent results show that theory, numerical simulations and observational data agree on the existence of a segregated stellar cusp at our Galactic Centre (Baumgardt et al. 2018; Schödel et al. 2018; Gallego-Cano et al. 2018; Panamarev et al. 2019). This theory has been used in numerical simulations along with relativistic corrections (both PN and geodesic ones) to derive the event rate of EMRIs for a Milky Way-like nucleus (Amaro-Seoane and Preto 2011; Brem et al. 2014; Arca-Sedda and Capuzzo-Dolcetta 2019).

3.2.2.2 Physics of EMRI formation II. Formation and disruption of binaries around a massive black hole
Besides stellar relaxation, binary separation is another way of delivering stellar BHs to the vicinity of a MBH and forming EMRIs (Miller et al. 2005). In this model, a binary containing a stellar-mass BH could form relatively far away from the MBH and later be scattered by other stars to the vicinity of the MBH. If the periastron distance is smaller than the tidal-disruption radius of the binary, the most likely outcome is that the binary gets tidally disrupted, leaving the stellar-mass BH gravitationally bound to the MBH and the other binary component ejected from the system. The event rate is difficult to estimate because of the uncertainties in the

physical properties of nuclear star clusters, but given the large cross section for tidal separation of binaries, it is considered that this channel could make a significant contribution to the total EMRI population. Unlike the EMRIs formed via stellar relaxation, the EMRIs produced by tidal separation have a much lower eccentricity in the LISA band because the captured stellar-mass BHs initially have a larger binding energy. As a result, these low-eccentricity EMRIs are less susceptible to the perturbation by the stars around the MBHs and hence are more stable.

3.2.2.3 The contribution of LISA to the physics of EMRI formation   As we have tried to convey in this section, there are a number of different processes that leave the expected EMRI event rate detectable by LISA substantially uncertain. It seems likely that many competing effects produce unique signatures in the LISA observables—either for individual events or in the distribution of their properties over multiple events. Theory work in advance of launch will help determine which effects may be dominant, and what observables are correlated with which effects. Hence, with detections in hand, we can hope to observe these phenomena and therefore address many open questions related to astrophysics, in addition to fundamental physics.

- LISA can determine the ratio of plunges (coalescence that involve tens or fewer orbits) to insprials (coalescence involving thousands or more orbits), since it can distinguish the waveforms of the two types of coalescences. Such a number can be used to test the predictions of stellar-dynamics models (Amaro-Seoane 2018b, 2021, and references therein).

- LISA can measure the eccentricity of an EMRI to a precession of 10^{-6} (Babak et al. 2017). Such a measurement can reveal those EMRIs formed by the binary-separation channel, since they have relatively mild eccentricities (~ 0.1, Miller et al. 2005), while those produced by stellar relaxation preferentially have extreme eccentricities (>0.9).

- LISA can identify those EMRIs with zero eccentricities, and they are most likely produced in AGN accretion disks. Moreover, the small sky-localization error (on average smaller than 1 $\deg^2$, Babak et al. 2017) of LISA may help us identify the host AGN of the EMRI and understand the condition faverable to the formation of such *wet* EMRIs.

3.2.3 Physics of IMRI formation: Dwarf galaxies, galactic nuclei and globular clusters

3.2.3.1 Heavy IMRIs from galaxy mergers   By providing the first access to the GW universe in the millihertz band, LISA will reveal the population of high-redshift MBHs co-evolving with their host galaxies to ultimately assemble the galaxies of today's Universe. While much of our astrophysical understanding of BHs and galaxies through the cosmic dawn era, say $5 < z < 20$, has so far focused on the largest structures including massive high-z quasars and their hosts, these are not the ancestors of today's typical galaxies. Galaxies like the MW were assembled from smaller, mainly dwarf, galaxies, and our galaxy's MBH grew through some combination of accretion and merger of smaller BHs hosted in these dwarfs, provided

that orbital decay is efficient (see Sect. 2.2.1). EM observations of the smaller systems through this epoch will remain extremely challenging, making LISA's data crucial for understanding our cosmic history.

Regardless of how IMBH seeds do form, it is likely that they form in low-mass ($\sim 10^8$–$10^9 M_\odot$) galaxies at high redshifts. These galaxies merge over time to build up more massive galaxies, and any BHs they host will likely merge as well. Further evidence in the local universe supports this hypothesis: dwarf galaxies possibly hosting IMBHs/MBHs have been discovered recently, lending further support that low-mass galaxies can be IMBH hosts (Reines et al. 2013; Moran et al. 2014; Pardo et al. 2016; Ahn et al. 2017; Chilingarian et al. 2018). When these low-mass galaxies merge with larger halos, they are tidally stripped and disrupted, with their remnants joining the greater halo population. An IMBH orbiting in the halo will eventually spiral to the centre due to dynamical friction, and merge with the central MBH.

Cosmological simulations have shown that when dwarf galaxies hosting IMBHs merge with larger halos, they are tidally disrupted, leaving the IMBH to wander within the larger galaxy halo (Bellovary et al. 2010; Tremmel et al. 2017; Bellovary et al. 2019). Depending on their orbits and dynamical timescales, these IMBHs may spiral into the galactic centre and merge with the existing MBH. Bellovary et al. (2019) have shown that this event has a characteristic mass ratio of ~ 20:1, which is reflected in the large peak at low mass ratios in Fig. 32.

Dwarf galaxies are the most numerous in the Universe, and while the occupation fraction of BHs in dwarfs may be less than 1, because dwarf mergers with larger halos are common, this case cannot be ignored. This type of BH–BH merger is the most common interaction in low-mass galaxy environments.

3.2.3.2 Heavy IMRIs from galactic nuclei assembly As discussed in the previous section, the mergers between dwarf satellites and their main galaxies can lead to the formation of IMBH–MBH pairs (corresponding to heavy IMRIs) in galactic nuclei. However, the corresponding merger timescale is long due to the large mass ratio between the merging galaxies, leaving this scenario unfavorable for the formation of IMRIs (Amaro-Seoane et al. 2007). For example, theoretical models show that hierarchical galaxy mergers produce $< 10\%$ of binary BHs with $q < 0.01$ (Volonteri

Fig. 32 Peak in IMBH/MBH mergers at mass ratios ~ 20 : 1 (Bellovary et al. 2019)
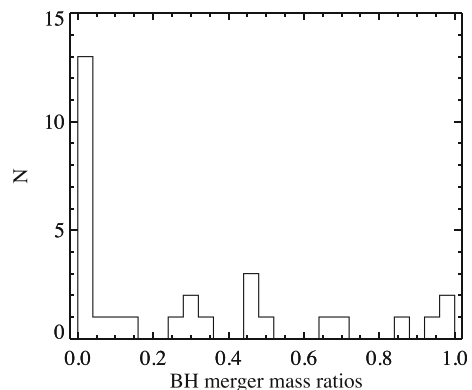
et al. 2003a, 2020). For those IMRIs whose primary MBHs fall in the mass range of 10^5–$10^7 \, M_\odot$ so that they can be detected by LISA, the event rate may be low because the host galaxies are relatively small, and low-mass galaxies merge much less frequently than those heavier ones.

Another viable route to the formation of an IMBH–MBH binary is related to the possible formation of IMBHs via stellar collisions and accretion onto stellar-mass BHs in the nuclei of dense stellar clusters, i.e. globular clusters (Portegies Zwart and McMillan 2002; Giersz et al. 2015; Mapelli 2016; Arca Sedda et al. 2019a; Rizzuto et al. 2020).

Clusters forming sufficiently close to the centre of their host galaxy can migrate toward the galactic centre via dynamical friction (Tremaine et al. 1975; Capuzzo-Dolcetta 1993). This mechanism is thought to contribute to the growth of galactic nuclei (Tremaine et al. 1975; Capuzzo-Dolcetta 1993; Gnedin et al. 2014; Arca-Sedda and Capuzzo-Dolcetta 2014; Antonini 2013). Clusters harboring an IMBH can bring the black hole to the galactic innermost regions and release it in the galactic centre. Such a mechanism might contribute to the seeding and growth of MBHs (Ebisuzaki et al. 2001; Portegies Zwart et al. 2006; Arca-Sedda et al. 2015; Arca-Sedda and Capuzzo-Dolcetta 2017; Askar et al. 2021). If one or more IMBHs reach the galactic centre after the MBH is fully grown, the subsequent interaction between the MBH and the IMBH can trigger the formation of a massive binary that might undergo coalescence within a Hubble time. Given the typical range of mass of IMBHs (10^2–$10^5 M_\odot$) and MBHs (10^5–$10^{10} M_\odot$) these merging binaries would have mass ratios in the range of 10^{-2}–10^{-5}, typical of IMRIs. In massive elliptical galaxies, this mechanism can drive the formation of several IMRIs over a Hubble time, with an inferred rate of around $0.003 - 0.03 \, \mathrm{Gpc}^{-3} \mathrm{year}^{-1}$ (e.g. Arca-Sedda and Gualandris 2018; Arca-Sedda and Capuzzo-Dolcetta 2019). Upon the simplest assumption that these mergers are distributed uniformly through space and are all detectable with LISA within a redshift $z < 1$ (Sesana et al. 2021), we can derive an upper limit to the number of LISA detections of $2 - 20 \, \mathrm{year}^{-1}$.

Massive ellipticals are not the only suitable nurseries for IMBH–MBH binaries. A number of IMBHs might be hiding in plain sight in our own Galaxy. The possible mass and location of such IMBHs can be constrained by the proper motion of Sgr A* and the kinematics of the S-stars close to it (Yu and Tremaine 2003; Hansen and Milosavljević 2003; Reid and Brunthaler 2004), as well as the TDE rate in the Galactic Centre (Chen and Liu 2013). According to these earlier studies, the possibility of an IMBH with a mass of $\lesssim 2000 \, M_\odot$ and residing at a distance of $\lesssim 10^{-3}$ pc from Sgr A* is not excluded. However, the motion of S-stars orbiting Sgr A* suggests that if the MW MBH has a companion IMBH, its mass should be most likely smaller than $10^3 M_\odot$ if the IMBH–MBH binary orbital period exceeds 5 year, or up to $10^5 M_\odot$ if the binary separation falls in the range 0.1–1 mpc (Gualandris and Merritt 2009; Arca-Sedda and Gualandris 2018). The recent measurements of relativistic precession in the S2 star (Abuter et al. 2018) helped in further constraining the phase space allowed for an IMBH, ruling out companions with a mass $10^5 M_\odot$ orbiting within 170 AU (0.8 mpc) from Sgr A* (Naoz et al. 2020). Nonetheless, there is growing suspicion of IMBH candidates orbiting farther

away, around 1–10 pc from the MBH. These putative IMBHs are supposedly harboured in a handful of compact gaseous clouds, whose measured velocity dispersion is so high to suggest the presence in their centres of point-like objects with masses in the range 10^4–$10^5 M_\odot$ (Oka et al. 2017; Takekawa et al. 2019, 2020). However, depending on their orbital properties, a population of IMBHs lurking at the Galactic Centre would affect significantly the motion of S-stars (Deme et al. 2020b) and the structure of the nuclear star cluster (Mastrobuono-Battisti et al. 2014).

The detection of such heavy IMRIs by LISA would have huge implications for our understandings of IMBH formation and evolution.

3.2.3.3 Light IMRIs in stellar clusters and dwarf nuclei   We can also imagine the formation of light IMRIs, where the IMBH is the more massive partner in a merger with a stellar mass BH. At first glance, one might expect these to be simply scaled down versions of the EMRI problem with a central MBH. However, the challenge of understanding stellar dynamics with an IMBH is that we cannot assume that the IMBH is fixed at the centre of the system, as we do with MBH in galactic nuclei. The wandering of the IMBH makes it demanding, to say the least, to attempt an analytical study, and hence we have to resort to numerical simulations to get an idea of what could be the IMRI event rate and the characteristic properties. Globular clusters and dwarf nuclei may also present quite different dynamical scenarios (higher escape velocities due to dark matter but lower stellar densities in dwarf galaxies, for example).

The first dynamical simulation addressing the evolution of a globular cluster harbouring an IMBH which successfully led to the formation of an IMRI was done by Konstantinidis et al. (2013). In this work they employed a direct-summation $N-$body code with relativistic corrections as presented by and a live treatment of the relativistic recoil. They find that IMBHs with masses 500–1000 $M_\odot$ merge with stellar-mass BHs and escape the host globular cluster due to the low escape velocity of the system. The IMBH is in a binary in almost all cases. The companion is a stellar-mass BH of mass ~ 20–$26 M_\odot$, and semi-major axis of about 5–7 AU. Later, Leigh et al. (2014) found similar results for this mass range. In their simulations, the heaviest stellar-mass BH forms a tight binary with the IMBH in the system. The work of Haster et al. (2016a) is basically a reproduction of Konstantinidis et al. (2013), but using a different numerical scheme. This is interesting because it validates of the findings of Konstantinidis et al. (2013). Later, MacLeod et al. (2016b) explore lighter mass ranges for the IMBH, with masses at most of $150 M_\odot$. They confirm that the IMBH has a bound companion most of the time, with the probability distribution function for the semi-major axis maximised at 2 AU.

Recently, Pestoni et al. (2021) performed a series of Fokker-Planck simulations to explore the occurrence of light IMRIs around IMBHs of $10^5 M_\odot$ residing at the centre of massive star-forming clumps in high-redshift galaxies, finding event rates of 10^{-8}–$10^{-7} \, \text{year}^{-1}$, depending on the assumptions for the initial inner density profile.

The IMRI rate from globular clusters and detectable by LISA depends intrinsically on a number of unknown quantities, namely the fraction of clusters capable of nursing the IMBH seed and growth (Portegies Zwart and McMillan 2002; Giersz

et al. 2015), the amount of stellar-mass BHs and other compact objects lurking in the IMBH closest vicinity (MacLeod et al. 2016b; Arca Sedda et al. 2019a), the number of times the same IMBH can pair in an IMRI (MacLeod et al. 2016b), and the probability that upon merger an IMBH is ejected from the parent cluster due to anisotropic GW emission (Holley-Bockelmann et al. 2008; Fragione et al. 2018; Arca Sedda et al. 2021a). Depending on all these quantities, LISA might be able to detect 0.01–60 IMRIs from globular clusters per year out to redshift $z \sim 2$ (Arca Sedda et al. 2020a, 2021a). The number of light IMRIs from massive star-forming clumps detectable by LISA falls in the same ballpark: by integrating their computed IMRI event rate over $z = 1$–3, when clumpy galaxies are more numerous, Pestoni et al. (2021) computed that LISA should be able to detect ~ 2 IMRIs per year, conservatively assuming that one star-forming clump per clumpy galaxy hosts a central IMBH. IMRIs with IMBHs in the mass range between $10^2 M_\odot$ and a few $10^3 M_\odot$ might be detected with LISA and provide advanced warning to ground-based detectors with a precision up to a second (Amaro-Seoane 2018a).

3.2.3.4 The contribution of LISA to the physics of heavy- and light-IMRI formation in gas-poor environments   In the processes we have just described with regard to the formation and evolution of heavy- and light IMRIs in gas-poor scenarios, our astrophysical theory so far only provides loose guidance about how the physics of the assembly process connects to the characteristics of this population. Current models suggest, though, that understanding heavy IMRIs will be an important discriminator between hierarchical formation models.

IMRIs provoke more open questions than EMRIs, as the theoretical frameworks required to address IMRI formation are even more complex, due to the mobility of an IMBH, as compared to an MBH. Thus, many approximations used in relaxation theory to predict the gas-poor dynamics of EMRI formation cannot be applied to an otherwise similar IMBH system. In addition, there are several plausible channels of IMRI formation that involve theoretical frameworks that have far larger uncertainties than relaxation theory.

As for galactic nuclei assembly, several uncertainties might affect the formation of such heavy IMRIs, namely the number of clusters capable of reaching the galactic centre, the probability of IMBH formation, the relation between IMBH formation and the host cluster properties. Theoretical models suggest that star cluster infall and dispersal could bring 1-50 IMBHs in the MBH vicinity (Portegies Zwart et al. 2006; Mastrobuono-Battisti et al. 2014; Arca-Sedda and Gualandris 2018; Arca-Sedda and Capuzzo-Dolcetta 2019; Leveque et al. 2022; Fragione 2022). If these models prove right, the delivery of IMBHs can give rise to up to 0.001–0.03 $Gpc^{-3} \, year^{-1}$ (Arca-Sedda and Capuzzo-Dolcetta 2019; Fragione 2022), corresponding roughly to 1 event per year within redshift 0.5-3 (Fragione 2022). Interestingly, the possible ejection of the IMRI product from the parent nucleus owing to GW radiation could account for up to $10^5 \, Gpc^{-3}$ MBH wandering outside their host galaxies at redshift < 1 (Arca-Sedda and Capuzzo-Dolcetta 2019).

Finally, less consideration has been given to possible light IMRI rates in dwarf nuclei, although the presence of at least some IMBH in dwarf galaxies is more secure

than in globular clusters. This is an important open question, especially since IMRI detection in dwarf nuclei could enable us to probe IMBH in *quiescent* dwarf galaxies. This in turn leads to a better understanding of the formation of seed MBHs. The detection of even a single light IMRI with LISA would incredibly improve our knowledge of how and where IMBHs form and grow.

3.2.4 Formation of EMRIs and IMRIs in gas-rich galactic nuclei: AGN discs

3.2.4.1 Gas-rich dynamics: active galactic nuclei   As discussed above, many galactic nuclei harbor a dense nuclear cluster of stellar-origin objects surrounding an MBH. Above we considered the state of the NSC as a result of stellar evolution, dynamical friction, secular evolution and minor mergers (Morris 1993; Antonini 2014; Generozov et al. 2018). Further complicating our picture, however, are the existence of AGN, which occur when low angular momentum gas forms a disc that accretes onto the MBH. As a result, a fraction of the nuclear cluster will end up embedded in the AGN disc via coincident orbits or capture (Syer et al. 1991; Artymowicz et al. 1993). While one might anticipate that AGN would be a subdominant mechanism for producing EMRIs or IMRIs, given that AGN represent only a fraction of all galactic nuclei (or, more likely, a relatively brief episode or series of episodes in the life of any given galactic nucleus), the presence of gas qualitatively changes the dynamics in the NSC.

Prograde orbiters embedded in a disc are expected to have their eccentricities rapidly damped (Ward 1988; Tanaka and Ward 2004; Cresswell et al. 2007; Bitsch and Kley 2010), although there is a strong dependence on the details and resolution of gas-flow on horse-shoe orbits (Bitsch and Kley 2010). For plausible AGN disc densities, gas dynamical cooling dominates over spherical component dynamical heating, so prograde orbiters should experience very rapid (< 0.1 Myr) eccentricity damping (McKernan et al. 2012; Kennedy et al. 2016; MacLeod and Lin 2020).

The majority of NSC objects begin as inclined orbiters not coincident with the disc. Stars experience geometric drag and BHs experience dynamical drag as they pass through the disc, causing a significant portion to be captured within a plausible range of AGN disc lifetimes (0.1–100 Myr). Stellar and BH orbiters not coincident with the disc experience geometric and dynamical drag forces, damping first the orbital eccentricity, followed by orbital inclination (Bitsch and Kley 2011; Just et al. 2012; Kennedy et al. 2016; Panamarev et al. 2018; MacLeod and Lin 2020; Fabj et al. 2020). Fabj et al. (2020) find $O(10\%)$ of prograde NSC BH are captured within a Sirko and Goodman (2003) type disc, for typical disc lifetimes, ignoring accretion. A much smaller fraction are captured by lower-density type Thompson et al. (2005) AGN discs. Stellar objects are primarily captured by the disc at small radii, losing around an order of magnitude in semi-major axis, whereas BHs are captured across the full range of disc radii but rapidly get delivered to the innermost disc (Fabj et al. 2020). The possibility of the accumulation of BHs at small radii across disc models has significant implications for the LIGO–Virgo merger detection rate (Fabj et al. 2020), but also for the possible EMRI/IMRI production rate.

The accumulation of prograde BH from the NSC in the inner disc leads to high interaction cross sections at low relative velocity. All embedded stellar-origin objects

on prograde orbits should undergo mass-dependent Type I migration due to torques from gas at Lindblad resonances and co-rotating gas (Tanaka et al. 2002), enhancing pile-up of BHs in inner AGN discs, leading to a high merger rate (McKernan et al. 2012, 2014; Bartos et al. 2017; Stone et al. 2017b).

3.2.4.2 Heavy IMRIs in AGN   The rate of change of surface density in AGN disc models implies that we should expect the occurrence of locations in the discs where the outward and inward migration torques cancel (Bellovary et al. 2016). At such so-called migration traps, the local merger rate is significantly enhanced and IMBHs with masses $\sim 10^3 \, M_\odot$ can quickly (1 Myr) be produced (Secunda et al. 2019, 2020; Yang et al. 2019; McKernan et al. 2020b). The IMBH-formation merger GW190521 detected by LIGO–Virgo (Abbott et al. 2020d) consisted of two BHs in the upper mass gap with mis-aligned spins, suggestive of a merger in a dynamically rich, deep gravitational potential well. If we assume this merger happened at a migration trap then the rate of such mergers inferred by LIGO–Virgo is $\sim 0.7 \, \mathrm{Gpc}^{-3} \, \mathrm{year}^{-1}$ The LIGO Scientific Collaboration et al. (2020). From McKernan et al. (2020a), assuming $O(15)$ mergers at migration traps over a Myr disc lifetime, and an AGN fraction of $O(1\%)$ of galactic nuclei (quasars and the brightest Seyfert nuclei), we find $\sim 1 \, \mathrm{Gpc}^{-3} \, \mathrm{year}^{-1}$ mergers at migration traps, consistent with the observed rate of GW190521-like events. All of these effects taken together enhance stellar BH merger rates and encourage the formation of IMBH in AGN discs. IMBH formed in this manner automatically create an IMBH–MBH binary, which will typically decay due to GW emission on timescales of a few hundred Myr (Bellovary et al. 2016).

3.2.4.3 Light IMRIs in AGN   A large IMBH sitting in an AGN disc migration trap is an excellent site for the creation of light IMRIs—less massive BH will be delivered to the IMBH from more distant regions of the disc via disc migration torques, with an approximate merger rate of $O(1) \, \mathrm{Gpc}^{-3} \, \mathrm{year}^{-1}$ (McKernan et al. 2020a), assuming Sirko and Goodman (2003) type AGN disc models. LISA can detect IMBHs of several hundred $M_\odot$ out to $\sim 10 \, \mathrm{Gpc}$. So for migration trap mergers with an IMBH of few hundred $M_\odot$, this suggests LISA can detect $O(10^3) \, \mathrm{year}^{-1}$ light IMRI mergers from AGN discs. If migration traps are less common in AGN discs, the maximum IMBH masses from bulk disc mergers are much smaller $\sim 10^2 \, M_\odot$—and migration torques could drive objects rapidly onto the MBH, typically creating EMRIs with small eccentricities and inclination angles.[14]

3.2.4.4 EMRIs in AGN   One likely exception to the small (e, i) expectation due to AGN gas damping comes from retrograde orbiters. Approximately half of the initial (NSC) population that is geometrically coincident with the disc, should lie on retrograde orbits (Ivanov et al. 2015). Migration torques on retrograde orbiters in AGN discs are a small fraction of that on prograde orbiters (McKernan et al. 2014). However, retrograde orbiters experience eccentricity pumping at apocenter which

---

[14] In providing fuel to the MBH, this process may contribute to explaining the $M_{\mathrm{bh}}-\sigma$ relation (Miralda-Escudé and Kollmeier 2005).

rapidly drives them to very high eccentricities (Dunhill et al. 2013; Teyssandier and Ogilvie 2016, 2019; MacLeod and Lin 2020) and increases the decay rate of the semi-major axis (Secunda et al. 2021). As a result we expect a significant population of retrograde orbiters in the innermost AGN disc. This population could yield a very high EMRI rate. The eccentricities of EMRIs from this population depend on the masses of the retrograde orbiters, since the GW circularization rate increases with mass (Peters 1964a) and the eccentricity driving of the gas decreases with mass (Secunda et al. 2021). For example, a $10\,M_\odot$ retrograde orbiter will likely have an eccentricity over 0.9 when it inspirals, whereas a $50\,M_\odot$ orbiter will circularize before inspiraling, making it much easier for LISA to detect over many cycles. However, the higher rate of eccentricity driving of lower mass retrograde orbiters also implies that their EMRI rates will be higher. Therefore, unlike prograde orbiters whose orbits tend to be circularized by the gas disc, retrograde orbiters could commonly produce highly eccentric EMRIs, though this effect is strongest at high (AGN disc) gas density and for low mass BH.

There may also be observable EM signals associated with smaller BHs in AGN discs. Stellar-mass BH binaries (BH+BHs) can merge at high rates in AGN discs (McKernan et al. 2012, 2014; Bartos et al. 2017). Under these circumstances, since the BH+BH is surrounded by gas, there will always be an EM counterpart. Indeed, a candidate EM counterpart to GW190521 has recently been suggested in an AGN (Graham et al. 2020). Several key questions underpin the search for EM counterparts to BH+BH mergers in AGN discs: Is the EM counterpart detectable through a potentially large optical depth? Is the emission completely outshined by the AGN emission, and on what timescale? Does the radiation from the BH reduce the EM emission?

At merger, a remnant stellar-mass BH formed from the BH+BHs recoils with a kick velocity v_k depending on the mass asymmetry and spin orientations of the progenitors. In an AGN disc, gas at distance $R_{\rm bound} < GM_{\rm BH+BH}/v_k^2$ is bound to the merged BH+BH and attempts to follow the kicked merger product. In doing so, it collides with surrounding disc gas and a shock luminosity emerges on a time-scale of ~ 20 days, with a bound gas energy of about 10^{45} erg (depending on the BH+BH and gas properties). After the kicked stellar-mass BH has shed the bound gas, the passage of the stellar-mass BH through the gas in the accretion disc produces a shocked Bondi drag tail (e.g. Ostriker 1999). This tail both decelerates the stellar-mass BH and accretes onto it, generating a potentially high luminosity. In order for enough radiation to escape to make for a bright flare against the AGN, a jet or collimated outflow is required. Such jets may also produce detectable X-ray or gamma-ray signatures.

Alternatively, stellar-mass BHs in AGN discs may undergo substantial accretion even prior to merger (Yang et al. 2020b), which can lead to e.g., longer term X-ray emission. This scenario largely depends on the poorly understood accretion efficiency and gap opening by stellar-mass BHs in AGN discs. We recommend that future simulations of hyper-Eddington accretion establish whether there is an upper limit to accretion which can choke off jet formation and launching. This will help establish luminosity upper limits on any flares that originate from kicked stellar-

mass BH mergers in AGN discs and can guide searches for EM counterparts from AGN discs. We also recommend simulations of lightcurves from false-positive flaring events such as SNe and TDEs breaking out from within the AGN disc, or lightcurves of micro-lensing events.

3.2.4.5 In situ formation of stars in AGN discs: a special population of EMRIs   AGN

discs are known to be prone to gravitational (Toomre) instability in the outer regions, and expected to form stars vigorously (Shlosman and Begelman 1989; Goodman 2003; Levin 2007; Nayakshin et al. 2007). This expectation is supported by observations of nearby stellar discs in the nucleus of the MW (Levin and Beloborodov 2003) and M31 (Bender et al. 2005) which, due to their large masses and orbital configurations, can be interpreted as remnants of a prior accretion episode from a gaseous disc (Levin 2007). Numerous observational studies also suggest a broader connection between AGN activity and nuclear starbursts (e.g., Davies et al. 2007; Wild et al. 2010; Ishibashi and Fabian 2016), although whether this connection is causal remains uncertain, given that AGN feeding occurs on scales difficult to resolve ($\lesssim$ parsecs) and is often obscured (Alexander and Hickox 2012). Theoretically, the stars formed in the outskirts of AGN discs are expected to be unusually massive because the disc material is much hotter and denser than star-forming regions in the galactic ISM. Once formed, a population of stars embedded in a gas disc will undergo a stellar evolution that is notably altered by their environment (Cantiello et al. 2021). Throughout their lifetime stars can grow by accretion, becoming even more massive (Goodman and Tan 2004; Davies and Lin 2020). In addition to experiencing drag and dynamical friction, they will excite perturbations in the disc that will exert torques on their orbit, typically causing inward migration (as discussed above). Furthermore, we expect an increased number of binaries within the stellar population in the AGN disc (e.g., Alexander et al. 2008), which can become harder due to disc-satellite interactions (e.g., Baruteau et al. 2011; Arca Sedda 2020a). All this makes fertile ground for forming BH remnants in the disc, which can subsequently encounter each other in migration traps (described above) or migrate to the inner regions of the disc where their evolution becomes GW dominated. Initial estimates show that this process may be an efficient method for feeding MBHs at early times in a way that is not Eddington-limited (Dittmann and Miller 2020).

Future numerical studies can help us narrow down the vast parameter space of accretion disc structures as a function of relevant parameters such as MBH mass, accretion rate, gas supply or redshift. As we improve our understanding of AGN discs, more investigations are needed to fully understand how embedded stars and BHs evolve over a range of system parameters and disc properties. Including more detailed physics (such as disc instabilities and stochastic torques, radiation transport or feedback from accretion, to name a few) may change the evolutionary outcome of these sources, the predicted rates and characteristic properties, as well as the precise waveform signatures and whether or not they are distinguishable amongst formation channels. At the same time, gas-embedded EMRIs/IMRIs also present a powerful opportunity to probe AGN properties in regions that are historically electromagnet-ically unresolvable, either with deviations in the GW waveforms that correlate with

properties of the gas (see Sect. 3.4) or with populations statistics, if multiple events are detected. This is in addition to the possibility for multimessenger astrophysics with associated EM counterparts (e.g., variability in emission, see Sect. 3.3).

As a distinguishing characteristic between various formation channels, here we quote approximate expectations of eccentricity and inclination at late stages of the inspiral, which we define as approaching the central MBH ISCO. Gas-driven, prograde EMRIs are expected to have low e ($e \lesssim 0.01$) given that circularization by gas and GWs is efficient, but there remains a possibility of disc-driven eccentricity pumping for relatively massive secondaries or IMRIs (e.g., D'Angelo et al. 2006). These sources are also likely fully embedded in the disc with low inclination—hence if the orientation of the disc aligns with the spin of the central MBH (which may be true to varying degrees, see Volonteri et al. 2013), we expect the spins of the binary components to be closely aligned. Gas driven, *retro*-grade EMRIs, on the other hand, may reach very high eccentricities even at the ISCO ($e \lesssim 0.9$, Secunda et al. 2021). They should also retain a low inclination, although the spin alignment of the BHs will depend on the accretion history of the embedded BH which remains to be investigated across the full range of parameter space. These estimates will be further constrained with future work that includes more realistic disc modelling and treatment of gas dynamics and accretion onto embedded BHs.

3.2.4.6 The contribution of LISA to the physics of formation of EMRIs and IMRIs in gas-rich galactic nuclei From what we have presented, we can derive that depending on the (highly uncertain) duty cycle of AGN, an IMBH–MBH binary could correspond to a heavy IMRI in nearly every galactic nucleus. However, the absence of any such detection with LISA would seriously constrain the existence of a migration trap in a generic AGN disc. The absence of a migration trap implies the absence of strong changes in the disc surface density gradient and thus tightly constrains the transition between the radiation pressure and gas pressure dominated regions of AGN discs.

As we have mentioned, there is a clear correlation between the dynamical parameters of EMRIs formed in AGN discs and their detection. Thus the rate of EMRIs detected by LISA can put strong constraints on the populations and dynamics we expect to live in innermost AGN discs, a system lurking in a region inaccessible to spatially resolved EM observations.

Prediction of rates and precise characteristics of disc-embedded EMRIs/IMRIs is a multi-faceted problem that relies on details of gravitational instability, stellar evolution, nonlinear gas dynamics, and accretion physics. Given that MBHs spend 1–10% of their evolution in an AGN phase (Shankar et al. 2013; Pardo et al. 2016) we expect at minimum the same fraction of EMRIs to occur in gas-rich environments. In-situ star formation likely leads to a population of compact remnants *in addition* to those that are captured from the nucleus. Thus we expect that dense accretion discs in near-Eddington AGN may not only boost EMRI rates, but also produce a population that is uniquely characteristic: with low eccentricity and (some degree of) spin alignment with the central MBH. These (e, i) expectations are strongest for EMRIs from objects formed in-situ. A single EMRI with low

eccentricity will indicate a current (or recent) interaction with gas, showing that the host galaxy harbors an active (or recently active) MBH. The precise parameters (e.g. eccentricity, secondary BH mass) are intimately connected to prior evolution of the accretion disk, and thus these measurements will give constraints on the efficiency of gas-driven circularization and accretion disk structure. If a larger population of such EMRIs is detected, the distribution of orbital characteristics will tell us about the diversity of AGN disks. Rates and orbital characteristics will constrain various aspects of accretion onto MBHs—for example, the number of detected events will inform how many nearby AGN host disk-embedded BHs. If the number is high, it will challenge accretion models. Just as the migration rates of stars and compact remnants depend sensitively on characteristics of the disk (Baruteau and Masset 2013; Duffell 2015), the secondary masses will be a consequence of BH accretion or hierarchical mergers, all of which are tied to disk models. Overall, measurements that shed light on accretion disk structure and prevalence will improve our constraints on AGN duty cycles and MBH growth.

3.2.5 Alternative formation scenarios

3.2.5.1 XMRIs   The possibility of observing an EMRI at our own galactic centre when LISA flies is basically zero, since the rates for an EMRI formed via relaxation in a MW-like galaxy are at most about $10^{-6}\,\mathrm{year}^{-1}$ (e.g., Amaro-Seoane 2018b, 2021). This means that about once every million years a stellar-mass BH plunges through the event horizon of our central MBH. Since the lifetime of LISA will be only a few years, the probability of detecting one at our galactic centre is negligible.

We can however find another class of EMRIs at our galactic centre. It has been recently put forward (Amaro-Seoane 2019) that substellar objects, in particular brown dwarfs, stand very high chances of being in band of the detector when it is launched. The reason for this is very simple: these substellar objects have mass ratios of about $q \sim 10^{-8}$ as compared to the central MBH, Sgr A*. Such XMRIs (extremely large mass ratio inspirals) can therefore cover up to $\sim 10^8$ cycles before crossing the event horizon, since the number of cycles is roughly inversely proportional to the mass ratio. This means that they stay in band for millions of years. About 2×10^6 year before merger they have an SNR at the galactic centre of 10. Later, $\sim 10^4$ year before merger, the SNR reaches several thousands, i.e. they are at the level of the loudest MBH mergers. At the last stages of their evolution, some $\sim 10^3$ year before the merger, they can reach SNR as high as a few 10^4 (Amaro-Seoane 2019; Gourgoulhon et al. 2019; Barack and Cutler 2004b).

The work of Amaro-Seoane (2019) predicts that at any given moment there should be of the order of $\gtrsim 5$ XMRI that are highly eccentric and are located at higher frequencies, and about $\gtrsim 15$ are circular and are at lower frequencies. The mass ratio for an XMRI is about three orders of magnitude smaller than that of stellar-mass BH EMRIs. Since backreaction depends on q, the orbit closely follows a standard geodesic, which means that many approximations work better in the calculation of

the orbit. XMRIs can be sufficiently loud so as to track the systematic growth of their SNR, which can be high enough to bury that of MBH binaries.

In addition, there are also plunge events during the formation of inspiralling sources. The GWs from low mass objects (brown dwarfs, primordial BHs, etc.) plunging into the central MBH are burst signals. For LISA, the SNRs of these bursts are quite high if they happen in our Galaxy. However, the event rates are estimated as ~ 0.01 year^{-1} for the Galaxy. If we are lucky, this kind of very extreme mass-ratio burst will offer a unique chance to reveal the nearest MBH and nucleus dynamics. The event rate could be as large as 4–8 year^{-1} within 10 Mpc, and because the signal is strong enough for observations by space-borne detectors, there is a good chance of being able to use these events to probe the nature of neighbouring BHs (Berry and Gair 2013b). This kind of burst sources are called XMRBs (extreme mass ratio bursts) (Han et al. 2020).

3.2.5.2 Binary and multiple EMRIs

Recent theoretical studies pointed out the existence of a new type of EMRI in which the small body is a stellar-mass BH+BH. Such a triple system could form either due to tidal capture of a BH+BH by a MBH (Addison et al. 2019; Chen and Han 2018) or the formation and migration of a BH+BH in the accretion disc of an AGN (Chen et al. 2019a). While the latter channel is considered to be more effective than the former one, both channels could deliver BH+BHs to a distance as small as tens of gravitational radii of the central MBH. As a result, the binary, as a single entity, spirals into the MBH due to GW radiation. For this reason, the source is referred to as a binary-EMRI, or b-EMRI.

The uniqueness of the b-EMRI lies in the fact that it simultaneously emits two kinds of GWs. One in the LISA band, due to the orbital motion of the BH+BH around the MBH, and the other in the ground-based detector band, when the BH+BH coalesces due to the tidal perturbation by the MBH. A coordinated observation by LISA and ground-based detectors would allow us to identify such interesting sources and, more importantly, constrain several aspects of fundamental physics to a precision more than one order of magnitude better than the current limit, including the loss of rest mass due to GW radiation, the recoil velocity of the merging BH+BH, and the dispersion of GWs of difference frequencies (Han and Chen 2019). Due to the merger of the BH+BH, the remnant will obtain a recoil velocity which may be up to a few thousand km s^{-1}. This sudden kick will induce a glitch on the waveform of a b-EMRI (see Fig. 33).

3.2.5.3 Supernova-driven EMRIs

In addition to the aforementioned mechanisms, an EMRI can also be generated via the supernova explosion that accompanies the formation of a CO. When this happens, the velocity of the compact object gets almost instantaneously significantly perturbed, so that the compact object settles on a brand new trajectory: the timescale for the CO to coalesce with the MBH via GWs on this new orbit may be shorter than the timescale for two-body relaxation to perturb it, so that the CO is bound to evolve into an EMRI. Focusing on the Galactic Centre environment, Bortolas and Mapelli (2019) showed that one supernova out of 10^4–10^5 occurring within the star forming structures present about the MW MBH will give
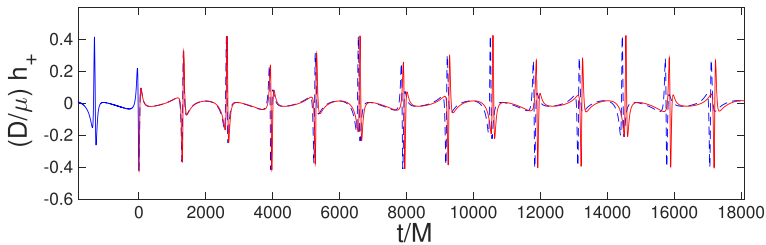
Fig. 33 Comparing the waveforms of the EMRIs with (red, solid) and without (blue, dashed) a glitch. The MBH has a mass of $M = 10^6 \, M_\odot$ and a spin parameter of 0.9. The total mass of the BH+BH is $m = 20 \, M_\odot$, and D refers to the luminosity distance. In this example, the centre of mass of the stellar-mass BH+BH initially is moving inside the equatorial plane of the MBH with an orbital eccentricity of $e = 0.7$ and a semilatus rectum of $p = R(1 - e^2) = 17 r_g$. At the time $t = 0$ a kick to the centre-of-mass velocity of the binary happens, in the polar direction and with a magnitude of $1500 \, \text{km s}^{-1}$. As a result, the orbital parameters change to $p = 16.9990 r_g$ and $e = 0.7019$, and the orbital plane of the EMRI becomes inclined by $\iota = 0.5233°$ relative to the equatorial plane of the MBH

rise to a supernova-driven EMRI. This result, coupled with the expected frequency of core-collapse supernovae explosions occurring in the Galactic Centre, implies a frequency of supernova-driven EMRIs up to $10^{-8} \, \text{year}^{-1}$, i.e., an EMRI rate that is comparable or only mildly lower than the one associated to the standard two-body relaxation process (Bortolas and Mapelli 2019).

3.2.5.4 The contribution of LISA to relativistic stellar dynamics and supernovae rates
What we have described about XMRIs allows us to understand that these might be envisaged as a double-edged sword. From the one side we have a promising and strong source of GWs from an extreme-mass ratio which is easy to model. On the other hand they might pose a problem because their SNRs (as high as 10^4 for 1-year observation if one resides in the Galactic Center) are such that can bury binaries of MBHs. Also, if they are present in most nuclei harbouring MBHs in the range of LISA, they might interact with EMRIs or even scatter them off from their inspiraling orbit. The detection of XMRIs will allow us to infer information on relativistic astrodynamics impossible to obtain otherwise.

LISA can distinguish b-EMRIs from normal EMRIs by detecting the GWs from the small binary black hole months to years prior to its coalescence around the SMBH. If the frequency of the GWs from the small binary matches a fundamental frequency of the SMBH, the SMBH could be resonantly excited and the EMRI waveform could contain an enhanced quasi-normal mode (Cardoso et al. 2021). Moreover, the binarity of the small body also induces an addititional phase shift to the EMRI waveform, which can be used to identify b-EMRIs as well (Chen and Zhang 2022).

Regarding the detection of EMRIs formed via supernova, this result calls for a more extended analysis, in order to investigate this process in a wider range of galaxy environments and star-formation rates, and exploring in more detail the waveform signatures associated to this kind of EMRI compared to other EMRI formation

mechanisms. In this framework, LISA will thus help us shed light on the rates of supernovae near MBHs via the detection of EMRIs.

3.3 Multimessenger prospects

Coordinators: **Giuseppe Lodato and Martina Toscani**

Contributors: **Pau Amaro Seoane, Jillian Bellovary, Stefano Bianchi, Saavik Ford, Barry McKernan, Giuseppe Lodato, Tom Kimpson, Scott Noble, Martina Toscani, Kinwah Wu, Ziri Younsi and Silvia Zane**

We outline a variety of proposed EM counterparts of EMRIs and IMRIs, including TDE (in multiple configurations), AGN-related signatures, and pulsar EMRIs.

3.3.1 Tidal disruption events

TDEs (Carter and Luminet 1983; Rees 1988; Phinney 1989; Rossi et al. 2021, for a recent review) can be considered a particular type of EMRI, where the star is disrupted by the MBH tides during the first passage at the pericenter. For this to happen, the pericenter radius should be smaller (cf. Ryu et al. 2020) than the *tidal radius*

$$r_{\mathrm{t}} \approx R_* \left(\frac{M_\bullet}{M_*} \right)^{1/3}, \tag{18}$$

where R_* and M_* are the stellar radius and stellar mass respectively, while $M_\bullet$ is the BH mass; r_{t} is usually a factor of 10–20 times the MBH Schwarzshild radius. For MBH masses larger than $\sim 10^8 \, M_\odot$ ($10^9 \, M_\odot$ for rapidly spinning BHs), the tidal radius is within the event horizon and no TDEs can happen.

TDEs are very luminous events over a broad range of EM bands. The first EM observations occurred in 1990s thanks to the ROSAT survey (Bade et al. 1996; Komossa and Greiner 1999; Grupe et al. 1999; Greiner et al. 2000), which detected some bright flares from the cores of non-AGN galaxies. Since then, the number of X-ray detections has increased. These observations seem to be in agreement with the theoretical expectation of X-ray emission from an accretion disc (e.g., Ulmer 1999; Auchettl et al. 2017; Lodato and Rossi 2011). Initially these flares are powered by a near-Eddington accretion, then the luminosity decreases over a period from months to years (Saxton et al. 2020, and references therein). Over the last decade, also a growing number of optical TDEs has been detected. It remains unclear what processes are at the origin of this optical emission. Some hypotheses concern the shocks from self-crossing debris (Piran et al. 2015; Shiokawa et al. 2015) or reprocessing in an outflow (e.g., Strubbe and Quataert 2009; Lodato and Rossi 2011; Metzger and Stone 2016). Detailed reviews of optical TDEs are found in Wevers et al. (2019) and van Velzen et al. (2020). A small fraction of these jetted events has also shown significant radio emission (Alexander et al. 2020, and references therein).

Furthermore, TDEs emit GWs. Their GW emission is produced by three different varying quadrupoles: (a) the star–BH quadrupole (Kobayashi et al. 2004; Toscani et al. 2022; b) the stellar internal quadrupole (Guillochon et al. 2009; Stone et al. 2013) and (c) the quadrupole of the compact torus formed after disruption (e.g., van Putten 2001, 2002; Kiuchi et al. 2011; Toscani et al. 2019; van Putten et al. 2019). The dominant contribution is the first term, that could be well described as a GW burst with strain (Kobayashi et al. 2004; Toscani et al. 2022)

$$
h \approx \beta \times \frac{r_{\mathrm{s}} r_{\mathrm{s}*}}{r_{\mathrm{t}} d} \approx \beta \times 2 \times 10^{-22} \left(\frac{M_*}{\mathrm{M}_\odot} \right)^{4/3} \left(\frac{M_\bullet}{10^6 M_\odot} \right)^{2/3} \left(\frac{R_*}{R_\odot} \right)^{-1} \left(\frac{d}{16\,\mathrm{Mpc}} \right)^{-1},
$$
(19)

and an associated Keplerian frequency of

$$
f \approx \frac{\beta^{3/2}}{2\pi} \left(\frac{GM_\bullet}{r_{\mathrm{t}}^3} \right)^{1/2} \approx \beta^{3/2} \times 10^{-4}\,\mathrm{Hz} \times \left(\frac{M_*}{M_\odot} \right)^{1/2} \left(\frac{R_*}{R_\odot} \right)^{-3/2}.
$$
(20)

In the above formulas we have introduced the Schwarzschild radius of the BH, $r_{\mathrm{S}} = 2r_{\mathrm{g}}$, the Schwarzschild radius of the star, $r_{\mathrm{s}*}$, and the penetration factor

$$
\beta = \frac{r_{\mathrm{t}}}{r_{\mathrm{p}}},
$$
(21)

where r_{p} is the pericentre distance. A library of gravitational waveforms from TDEs has been presented in Toscani et al. (2022), generated using a general relativistic smoothed particle hydrodynamic code, PHANTOM (Liptai and Price 2019). To date, this numerical study models the star as a polytropic sphere with index $\gamma = 5/3$, but we expect the strain to have a dependence on the internal structure of the star. This dependence needs to be further investigated.

The expected strain for a Sun-like star being disrupted by a $10^6\,M_\odot$ MBH at 15 Mpc distance (assuming $\beta = 1$) is $h \sim 10^{-22}$, with a frequency $f \sim 10^{-4}\,\mathrm{Hz}$. The two other contributions are expected to have similar frequency but are scaled down by some (two-five) orders of magnitude.

Pfister et al. (2022) estimate the rate of TDEs which could be observed with different instruments. They find for LISA it is unlikely to detect GWs from TDEs, unless BHs are surrounded by particularly massive stars. The next generation of detectors beyond LISA should however be able to detect GW from TDEs up to cosmological redshifts $z \gtrsim 1$.

An interesting signal to study is the GW background from the entire cosmic population of TDEs. Details on this signal and its derivation may be found in Sect. 3.5.1.

3.3.1.1 TDEs outside galactic nuclei

In the majority of TDE studies the MBH that disrupts a star is implicitly taken to be the nuclear BH of the galaxy. The Swift transient source AT2018cow has many characteristics resembling a TDE (Kuin et al. 2019), but peculiarly the source is not located at the nuclear region of its suspected

host galaxy Z 137-068. This leads to consideration of whether it is a TDE, with an MBH disrupting a WD, i.e. WD-TDE (Han and Fan 2018), or alternatively a violent stellar explosion. The question is now: Can TDE involving a wandering[15] MBH occur? This question would be answered if there are mechanisms to populate a galaxy with massive BHs of non-stellar nature. Stellar systems are not stationary structures. A stellar cluster can dissolve on timescales of 10–100 Myr (e.g., Gieles and Bastian 2008). Globular clusters can survive longer but they can also be disrupted (e.g., Belokurov et al. 2006; Wan et al. 2020) or dissolved (see Baumgardt 2009). Similarly, dwarf galaxies can be disrupted and dissolved (e.g., Li et al. 2018; Sanders et al. 2018) when they encounter and are accreted by a larger galaxy. The nuclear BHs, if present in these stellar systems, would be dispersed into the interstellar space of the cannibal galaxy. Stars are also carried along into the interstellar space by these BHs, and some of them will eventually spiral into their carrier BH and become a TDE.

3.3.2 Electromagnetic counterparts of light IMRIs in AGN discs

Most BHs that merge in AGN discs (including IMBH–BH mergers) are expected to experience a GW recoil kick at the moment of merger with speeds v_k of up to a few hundred $km\,s^{-1}$. Such merger kicks would happen for any comparable system, with or without gas; however, the consequences of such kicks for a gas-embedded merger may include a detectable EM counterpart. In an AGN disc, gas within

$$R_{bound} < \frac{GM_{BH+BH}}{v_k^2} \qquad (22)$$

is bound to the merged BH+BH and attempts to follow the kicked merger product. In doing so, it collides with surrounding disc gas and, as long as the disc is geometrically thin or optically thin, a shock luminosity can emerge on a timescale $t_{bound} = R_{bound}/v_k = GM_{BH+BH}/v_k^3$ (McKernan et al. 2019) or

$$t_{bound} \sim 20 \left(\frac{M_{BH+BH}}{100\,M_\odot}\right)\left(\frac{v_k}{200\,km\,s^{-1}}\right)^{-3} \text{ day.} \qquad (23)$$

The total energy delivered to the bound gas is $E_{bound} = (1/2)M_{bound}v_k^2 = (3/2)Nk_BT_{bound}$ where $M_{bound} = Nm_H$ is the mass of the bound gas expressed as N atoms of Hydrogen (mass m_H), k_B is the Boltzmann constant, and T_{bound} is the average temperature of the post-shock gas. This energy is

$$E_{bound} = 3 \times 10^{45} \left(\frac{\rho}{10^{-10}\,g\,cm^{-3}}\right)\left(\frac{M_{BH+BH}}{100\,M_\odot}\right)^3\left(\frac{v_k}{200\,km\,s^{-1}}\right)^{-4} \text{ erg,} \qquad (24)$$

and the resulting average hot spot temperature is

---

[15] See Sects. 2.2.1.1, 2.2.2.4 and 2.2.3.

$$T_{\text{bound}} \sim 1.8 \times 10^6 \left(\frac{v_k}{200\,\text{km s}^{-1}}\right)^2 \text{K}. \qquad (25)$$

The resulting UV/optical flare occurs between $t = [0, t_{\text{ram}}]$, has an average (low) luminosity $E_{\text{bound}}/t_{\text{ram}}$ and a shape given by $\sin^2(\pi t/2 t_{\text{ram}})$.

Once the kicked BH leaves behind originally bound gas, the disc gas it passes through is accelerated around the BH, producing an asymmetric low angular momentum Bondi tail inside the stagnation point (e.g., Ostriker 1999; Antoni et al. 2019). This tail both acts as a drag on the BH and accretes onto it. The Bondi–Hoyle–Lyttleton luminosity is $L_{\text{BHL}} = \eta \dot{M}_{\text{BHL}} c^2$ where η is the radiative efficiency and

$$\dot{M}_{\text{BHL}} = \frac{4\pi G^2 M_{\text{BH+BH}}^2 \rho}{v_{\text{rel}}^3}, \qquad (26)$$

with $v_{\text{rel}} = v_k + c_s$ and c_s is the gas sound speed. In principle, hyper-Eddington accretion is allowed by this process. This should cause trapping of emergent radiation, unless a collimated outflow allows radiation to escape. However, if the kicked merger product travels out of the dense disc midplane into a more tenuous disc atmosphere, such signatures may be bright enough to be detected even against bright AGN hosts (Graham et al. 2020).

3.3.3 FeKα lines (or other EM signatures) as probes of small separation MBH–IMBH binaries

The relativistically broadened component of the fluorescent FeKα line (centered around 6.4–7 keV source-frame) is believed to be a probe of material in the innermost accretion disc (Nandra et al. 1997; Fabian et al. 2000; Reynolds and Nowak 2003). EMRIs and heavy IMRIs pre-merger will disrupt the flow of gas in the innermost disc, yielding flicker in the innermost disc (EMRIs) or carving gaps or a central cavity (MBH–MBH, MBH–IMBH binaries) with minidiscs. The resulting re-arrangement of gas yields signatures prior to GW merger events which may be detectable in the broad FeKα with high-throughput X-ray telescopes like Athena. A gap-opening secondary IMBH close to the primary MBH will leave an imprint in the broad component of the FeKα emission line, which varies in a unique and predictable manner (McKernan et al. 2013).

3.3.4 EMRIs containing a pulsar

Pulsars are spinning NSs, mainly identified by their radio observations. To date there are about 2800 known pulsars in the Galaxy (Cameron et al. 2020), of which about 160 are found to be associated with globular clusters (see the ATNF pulsar catalogue, Manchester et al. 2005). Among these radio pulsars, more than 170 are MSPs (e.g., Levin et al. 2013), and the majority of them actually reside in globular clusters. Although the number of known MSPs is growing, most MSPs are yet to be discovered. It has been suggested that the total population number of MSPs in the

MW could be about 100,000 or even more (Levin et al. 2013). Radio pulsar timing is a relatively mature technique in astronomy, as researchers have accumulated experience in pulsar research over decades. The current developments in instrumentation and search techniques will enable us to detect radio pulsars outside the MW (Keane et al. 2015), and the detection range will be further extended by the time LISA is operating.

EMRIs containing a radio pulsar are a special class of GW sources with a guaranteed EM counterpart, if they are close enough. The presence of a MSP provides researchers with several advantages to study these EMRI systems and their associated physics. NSs have a small mass range centred around $1.4\,M_\odot$. Knowing the mass and the spin of one component in the EMRI system reduces the parameter space, hence easing the computational demands in the template matching and searching for establishing their GW properties, whereas other EMRI systems would require the determination of the system parameters simultaneously, relying solely on the GW signals. The availability of the EM signals with measurements at high precision will give another advantage. Both pulsar timing observations and GW experiments can obtain measurements to high precision; the accuracy and precision of pulsar timing is among the highest achievable in astrophysical time-domain analysis (Hartnett and Luiten 2011). Radio pulsar timing and GW experiments employ different analysis techniques. As such, the orbital and spin dynamics, as well as the system parameters which they determine, will be independent, thereby giving us a means to understand certain systematic properties in the statistical and data analyses.

3.3.4.1 The contribution of LISA to multimessenger science   The event rate of the potential emission of GWs by extended stars approaching a MBH will provide us with additional information about tidal disruption events. This combined with EM detections will deliver much more precise catalogues of disruptions and, within some limits, information about the star and MBH which is inaccessible via traditional telescopes.

Regarding TDEs outside galactic nuclei, a WD-TDE system would emit GWs (Han and Fan 2018) as well as bursts of EM radiation (Kuin et al. 2019). With the additional constraints provided by the GW observations, it would easily resolve the dispute about certain candidate TDE sources, such as AT 2018cow (Kuin et al. 2019; Perley et al. 2019).

From what we have explained about EM counterparts of light IMRIs, we can conclude that a population of stellar-origin BH+BH in the LISA band that harden into the ground-based GW detector band in AGN discs can yield potentially detectable optical/UV counterparts. IMBH–BH and IMBH–IMBH binary mergers in AGN discs are likely to occur at migration traps in the inner disc (Bellovary et al. 2016), so kicked merger products remain bound to the MBH. The kicked BH must splash back down into the AGN disc possibly yielding a repeat flare on half the orbital timescale. An off-center luminous flare should be detectable as an asymmetry in broad optical lines as the broad line region responds to non-central illumination (McKernan et al. 2019).

Double relativistic FeKα lines may be detectable from binary mini-disc emission, allowing us to localize LISA sources well before merger (Sesana et al. 2012). The barycenter of a MBH binary will lie outside the event horizon of the primary BH for modest values of mass ratio and binary separation. Analogous to the radial velocity method of planet detection, whereby the wobble of a star indicates the presence of a nearby Jupiter-sized planet, the radial velocity of the primary BH around the binary barycenter can leave a tell-tale oscillation in the broad component of FeKα emission (McKernan and Ford 2015). Such oscillations are detectable by Athena for binaries with mass ratios $q \geq 0.01$, at binary separations of up to $O(10^2 r_{\mathrm{g}})$. Both the general-relativistic and Lense–Thirring precession of the periape of the secondary orbit imprint a detectable modulation on these oscillations (McKernan and Ford 2015). Athena is likely to detect $O(30)$ FeKα broad lines at sufficient statistical significance in local AGN to carry out tests for ripples and oscillations of such binaries. $O(100)$ AGN may have broad FeKα components that will allow us to search for double components (McGee et al. 2020). Hence, the input from LISA and Athena can be compounded to extract information about the separation of heavy IMRIs.

LISA detection of EMRIs with a MSP will provide opportunities to investigate a variety of fundamental issues in gravitational physics. This is rooted in the extreme mass ratio between the MSP and the BH (the MSP being a test mass) and the ultra-fast rotation of the MSP (the MSP being an extreme gyro and a stable time-keeper). More specifically, the spin–spin, spin–orbit, and the spin–curvature interactions (Chicone et al. 2005; Iorio 2012; Remmen and Wu 2013; Singh et al. 2014) between the MSP and the BH will manifest in the spin and orbital dynamics of the MSP (Li et al. 2019; Kimpson et al. 2020b), which will in turn modify the pulsar timing signals via modification of the pulse period and the pulse arrival time (Kimpson et al. 2019a, 2020a). Together with the information extracted from the GWs generated by the EMRI, researchers will be able to investigate how EM waves propagate in a non-vacuum space time (Kimpson et al. 2019b) or in a slightly perturbed space time, as well as having the opportunity to gain some understanding of certain fundamental issues, such as the gravitational self-force (e.g., Barack and Pound 2019) in GW sources.

3.4 Environmental effects on waveforms

Coordinators: **Alvin Chua, Alejandro Torres-Orjuela and Lorenz Zwick**

Contributors: **Pau Amaro-Seoane, Manuel Arca Sedda, Emanuele Berti, Xian Chen, Alvin Chua, Andrea Derdzinski, Kyriakos Destounis, Wen-Biao Han, Kostas Kokkotas, Cole Miller, Scott Noble, Arthur Suvorov, Alejandro Torres-Orjuela and Lorenz Zwick**

We know that EMRI/IMRI events can form in a variety of interesting astrophysical environments. Some of these environments may leave detectable imprints on the waveforms measured by LISA (though detecting the imprints may be challenging).

We outline a wide variety of environmental effects, including gas-driven effects and many-body effects. Some effects may be degenerate with one another or with deviations from general relativity, even when an effect is detectable. Fortunately, complex dynamics sometimes lend themselves to breaking degeneracies through, e. g., Doppler effects. We also use this section to address the possibility of detecting (and extracting astrophysical information from) the EMRI background, and possibly detecting the signatures of chaotic systems. Finally, we specifically consider the degeneracies between environmental effects and PN/self-force effects.

3.4.1 Gas torques

For gas-embedded EMRIs/IMRIs, gas torques can speed up or slow down an inspiral while it is in the LISA band. The magnitude of the torques will scale with the disc density, and the precise value and direction of the torque will depend on the mass of the inspiralling CO and disc properties. The effect is several orders of magnitude weaker than GWs in this regime, but even a small dephasing over several thousand cycles may accumulate to a detectable phase shift (up to a few radians), depending on the density of the environment, as shown in analytic work (Yunes et al. 2011a; Kocsis et al. 2011; Barausse et al. 2014) as well as more recently in 2D hydrodynamical simulations (Derdzinski et al. 2019, 2021). Accretion discs in bright AGN are expected to be thin and dense, but their inner regions are hot and radiation pressure-dominated. Analytical estimates of densities in the inner regions of such discs from simple models predict surface densities varying from ~ 10–10^7 g cm^{-2} (Shakura and Sunyaev 1973; Frank et al. 2002). The wide range arises from our uncertainty on how viscosity scales with the (gas or total) pressure. State-of-the art 3D global magnetohydrodynamical disc simulations (Jiang et al. 2016, 2019; Jiang and Blaes 2020) suggest that densities are between these values, somewhat closer to the lower end, which could make gas dephasing too small to detect, but this may change as we continue to explore the parameter space of MBH masses.

Whether or not this effect is *detectable* will depend on the density of the environment as well as the SNR of the source. An EMRI embedded in a Shakura–Sunyaev alpha-disc with $\Sigma \sim 10^2$ g cm^{-2} can accumulate a phase shift up to $\lesssim 10^{-2}$ radians within 4 years, whereas if embedded in a beta-disc would dephase over 10^1–10^2 radians over 4 years (Derdzinski et al. 2021). IMRIs, due to their higher mass, accumulate higher SNR and also feel stronger torques (since they scale with secondary mass), making them ideal events for producing detectable gas signatures.

Whether or not this effect is *distinguishable* from other waveform deviations will depend on how well one can measure the phase shift and how this accumulates as the frequency evolves. Simulations suggest that the torque can be approximated by simple analytical formulae—torques are within an order of magnitude of the Type I torque derived by Tanaka et al. (2002), although variability in the torque can arise for sufficiently massive secondaries ($q \gtrsim 10^{-3}$). This means that one can estimate how the deviation accumulates with frequency, assuming we know the disc density profile, and if $\ddot{f}$ can be measured from the GW data, degeneracies between the GW waveform distortions due to disc torques versus parameter variations or other effects

can be disentangled in principle. In practice this may prove difficult given that the small mass ratio of these sources (and expected low eccentricity) means they will chirp slowly, and will more likely appear as near-continuous wave sources within a few year observation.

3.4.2 Many-body interactions

3.4.2.1 XMRIs and EMRIs   As explained above, we expect a handful of XMRIs to be present in our own Galactic Centre (Amaro-Seoane 2019). Since these systems are so loud, reaching SNRs of up to $\sim 20,000$, in principle we should be able to detect them in nearby galaxies harbouring MBHs in the mass range 10^5–$10^7\,M_\odot$ (i.e. nuclei for which the relaxation time is below a Hubble time Amaro-Seoane 2021, 2018b; Preto 2010). Farther away XMRI systems with much lower SNR will not be detected. However, XMRIs pose a problem for normal EMRI systems: Since XMRIs live in band for millions of years, and the estimated event rate for an EMRI is between 10^{-5}–$10^{-6}\,\mathrm{year}^{-1}$, the possibility that an EMRI encounters an XMRI on its way to the MBH is non-negligible.

3.4.2.2 EMRIs interacting with a perturbing star   Although unlikely, it is not ruled out that a star can be located close to an EMRI inspiraling towards the central MBH. In the work of Amaro-Seoane et al. (2012) the authors derive the shortest radius from the MBH within which one might expect to have at least one star. Then they run direct-summation $N-$body simulations with relativistic corrections following the first implementation as presented in Kupi et al. (2006) and find that periapsis shift along with gravitational-radiation effects induce non-determinism in the evolution of the EMRI. This means that for two identical dynamical setups of an EMRI system with a perturbing star located at a distance of about $\sim 5a_{\mathrm{EMRI}}$, with a_{EMRI} the semi-major axis of the EMRI, small changes of any dynamical parameter induces a different evolution of the EMRI. The presence of a perturbing star, therefore, can be misinterpreted as a deviation of general relativity, and this should be taken into account in the development of data analysis algorithms.

3.4.2.3 Binary-EMRIs   The formation rate of b-EMRIs for BH+BHs tidally captured by MBHs is equivalent to $(10^{-5}$–$10^{-4})\,\mathrm{Gpc}^{-3}\,\mathrm{year}^{-1}$ in the pessimistic case and 0.1 $\mathrm{Gpc}^{-3}\,\mathrm{year}^{-1}$ in the most optimistic one. However, due to the non-negligible lifetime of b-EMRIs, within a spherical volume of $1\,\mathrm{Gpc}^3$ (corresponding to a radial distance of about 600 Mpc), there are, on average, about 0.02–20 b-EMRIs expected during LISA's mission duration.

   The most exciting property of b-EMRIs is that they are multi-band GW sources, i.e., radiate low and high frequency GWs synchronously (Addison et al. 2019). Though the time scale of BH+BH merger is much shorter than the inspiral of binary into the MBH, LISA and the ground-based detectors (LIGO etc.) may observe the b-EMRI at the same time. The high-frequency GWs could be redshifted because they are generated close to a MBH (Chen et al. 2019a), providing an opportunity of studying the propagation of GWs in the regime of strong gravity.

3.4.3 Moving sources

Almost all astrophysical objects are moving relative to us and GWs sources are no exception. The motion of the centre of mass of a source is often related to the properties of its environment, e.g., the orbital motion induced by the interaction with other bodies (Wen 2003; McKernan et al. 2012; Antonini and Perets 2012; Naoz 2016; Arca Sedda 2020a; Stone et al. 2017b; Bartos et al. 2017; Tagawa et al. 2020a) and the motion of its host system like the peculiar velocity of galaxies (Zinn and West 1984; Bahcall 1988; Carlberg et al. 1996; Springel et al. 2001; Scrimgeour et al. 2016; Colin et al. 2017; Girardi et al. 1996; Ruel et al. 2014). Therefore, the detection of velocity can provide valuable and versatile information about the sources environment and its host system.

In the case of a constant velocity the Doppler effect changes the observed GW frequency f_{obs} by a factor (Chen et al. 2019a)

$$f_{obs} = f(1+z)^{-1}, \tag{27}$$

and its derivative, $\dot{f}_{obs}$, by the same factor squared

$$\dot{f}_{obs} = \dot{f}(1+z)^{-2}. \tag{28}$$

Here, f and $\dot{f}$ being, respectively, the GW frequency and its derivative in the source's rest frame. When only considering the dominant mode of GWs, these shifts lead to a wrong estimation for the sources actual chirp mass $\mathcal{M}$,

$$\mathcal{M}_{obs} = \mathcal{M}(1+z), \tag{29}$$

and actual luminosity distance, d_L,

$$d_{obs} = d_L(1+z), \tag{30}$$

thus fundamentally affecting our interpretation of the source. An analogous effect appears for the cosmological redshift of GWs. Although the latter one is considered in current GW models and detections, the same is in general not true for the effect of velocity (Abbott et al. 2019).

If the velocity of the source varies in time, the previous picture changes significantly. The Doppler effect induces a time-dependent phase shift, proportional to the velocity of the source along the line of sight, which can be detected when having accurate models of the evolution of the phase of the source and the velocity profile (Inayoshi et al. 2017b; Meiron et al. 2017; Wong et al. 2019a). For a LISA mission of 4 years probably no accelerated sources could be detected. However, the number of detections could be increased to up to 3 when conducting joint measurements with a ground-based detector. For a LISA mission of 10 years up to 40 accelerated sources could be detected by LISA alone and up to 103 when conducting joint measurements with an earth based detector (Tamanini et al. 2020). Moreover, the aberration of the GWs rays affects the line of sight thus inducing an additional phase shift (Torres-Orjuela et al. 2020). The magnitude of the aberrational phase shift

is of the same order as the Doppler phase shift but proportional to the components of the velocity perpendicular to the line-of-sight. Therefore, considering the total phase shift, i.e. Doppler effect plus aberrational phase shift, the SNR required for the detection of the acceleration could be reduced by a factor of up to 1.8, thus allowing the detection of up to 5.8 times more sources (Torres-Orjuela et al. 2020).

3.4.4 Dark matter as an environmental effect

The density profile of dark matter halos has a cusp at the centre of galaxies because of the large potential well there (Kuhlen et al. 2012). If a MBH resides at the centre of the galaxy, the strong gravity could lead to a significant increase of density in the central region and create a spike, which enhances the dark matter annihilation rate (Gondolo and Silk 1999; Sadeghian et al. 2013). Similarly, IMBHs may have a smaller dark matter spike (Zhao and Silk 2005; Bertone et al. 2005). The gravitational potential of the dark matter could impact the evolution of an EMRI/IMRI, particularly where enhancement of the density occurs due to spikes or a superradiant instability, leading to a detectable signature (Eda et al. 2013; Yue and Han 2018; Hannuksela et al. 2020). However, dynamical events such as mergers of host galaxies can weaken the dark matter cusp (Ullio et al. 2001; Merritt et al. 2002; Merritt 2004; Bertone and Merritt 2005), which makes its presence harder to detect.

3.4.5 Astrophysical chaos

Owing to the huge mass disparity for the objects involved in an EMRI, the dynamics of the companion body can be modelled as a point particle traversing the gravitational field of the (super-massive) primary to high accuracy. Characteristics of GWs emitted during the inspiral are therefore dominated by the particulars of the metric geometry of the primary. Fundamental symmetries, or the absence thereof, associated with the spacetime geometry can therefore be probed by LISA. For a primary which is both stationary and axisymmetric—properties expected of astrophysically stable BHs—the energy and one component of the angular momentum of a companion are both constants of motion with respect to the orbital dynamics. The companion's Hamiltonian, $H \sim g_{\mu\nu}p^{\mu}p^{\nu}$ for momentum $\boldsymbol{p}$, provides a third constant of motion. In *four* spacetime dimensions, however, having only *three* conserved quantities implies that the equations of motion are not Liouville integrable (Contopoulos 2002). In this context, a non-integrable system exhibits chaotic orbital phenomena, as is familiar from the three-body problem in (post-)Newtonian gravity (Huang and Wu 2014). The Kerr spacetime, which uniquely represents stable BHs in general relativity, also however admits a rank-two Killing tensor, which provides a fourth constant of motion in the form of the Carter constant (Carter 1968). This implies the absence of astrophysical chaos in EMRIs within general relativity, at least for companions which are not themselves spinning rapidly (Kiuchi and Maeda 2004; Lukes-Gerakopoulos et al. 2014; Piovano et al. 2020; Zelenka et al. 2020).

If, however, high-energy corrections to the field equations present themselves in nature, the particulars of gravitational collapse (e.g., Cembranos et al. 2012) and

accretion (e.g., Harko et al. 2010) may be such that a non-Kerr object resides within galactic centres or elsewhere. There are many ways in which a hypothetical departure from a Kerr description may manifest within the spacetime metric, such as those described in Johannsen (2013). One interesting possibility is that the Carter symmetry is broken, thereby giving rise to a non-Kerr object, as opposed to a deformed-Kerr body which still forbids chaotic phenomena even if the spacetime is not exactly Kerr (Papadopoulos and Kokkotas 2018; Destounis et al. 2020).

In general, sections of the inspiral that behave as bound orbits can be characterised by both radial (ω_r) and angular (ω_θ) libration frequencies, which describe the rate of transition from the periastron to the apastron of the orbit and longitudinal oscillations about the equatorial plane, respectively (Contopoulos 2002). On the other hand, classical results from dynamical systems theory infer that small islands of stability (Birkhoff islands) form around periodic orbits in the phase space of non-integrable dynamical systems (Arnold 1978). When an inspiralling orbit crosses an island, the ratio ω_r/ω_θ, which defines what is called the *rotation curve*, remains constant, while otherwise it behaves monotonically as a function of radius. Absence of islands therefore implies an everywhere monotonic rotation curve, while the dynamics display transient plateau features for non-Kerr spacetimes when orbits intersect with an island (Apostolatos et al. 2009).

Several studies have shown that these transient plateaus also introduce features into the gravitational waveforms which are, in principle, discernible from deformed-Kerr features (Apostolatos et al. 2009; Lukes-Gerakopoulos et al. 2010; Contopoulos et al. 2011; Cárdenas-Avendaño et al. 2018; Destounis et al. 2020; Lukes-Gerakopoulos and Witzany 2021). Figure 34 shows the fundamental frequency evolution of a gravitational waveform, associated with a particular non-Kerr spacetime (see Destounis et al. 2020, 2021; Destounis and Kokkotas 2021 for details). However, non-integrable perturbations in the Arnold (1978) sense of the particle Hamiltonian may also arise due to environmental effects within general relativity (Cardoso et al. 2022). For instance, $N > 2$-body interactions (as in the Newtonian case; see also Sect. 3.4.2) (Barausse et al. 2007; Amaro-Seoane et al. 2012) or significant internal spins in the companion (Kiuchi and Maeda 2004; Lukes-Gerakopoulos et al. 2014) can induce chaos.

3.4.6 Environment versus PN/self-force degeneracies

The secular evolution of EMRI orbital elements is intimately connected with the phase and the shape of the GWs that will be measured by LISA. In vacuum this evolution is fully described by general relativity, and it can in principle be computed to arbitrary precision with approximation schemes such as perturbation theory (an expansion in the small mass ratio q of the binary) or the PN expansion (an expansion in the small parameter v/c, where v is the orbital velocity and c is the speed of light). At leading order in perturbation theory, the system can be described as a point-like particle moving in a geodesic orbit around the large BH. The energy flux can be computed either numerically or analytically to varying degrees of accuracy. For example, Munna (2020) computed the energy radiated from eccentric orbits around nonrotating BHs up to 19PN order. Fujita (2015) computed the energy flux from a
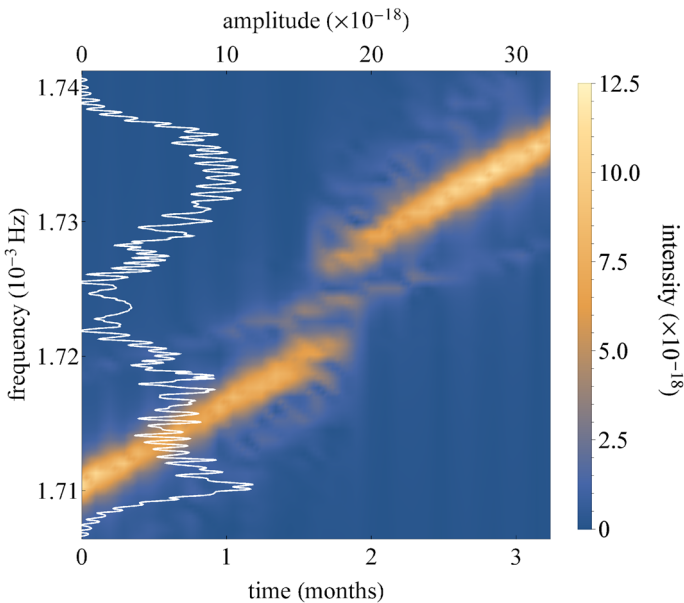
Fig. 34 Periodogram of the fundamental frequency of a gravitational waveform associated with an inspiral on a particular non-Kerr spacetime. A sudden jump in the frequency evolution appears when the inspiralling object crosses a Birkhoff island, which is associated with a valley in the amplitude of the signal's frequencies (white line)

particle in *circular* orbit around a rotating BH up to 11PN order. Sago and Fujita (2015) computed the expansion for *eccentric* orbits around rotating BHs up to 4PN, and up to order e^6 in a small-eccentricity expansion. The PN expansion is an asymptotic series, and it is known to converge quite slowly for EMRIs (Yunes and Berti 2008; Zhang et al. 2011). At higher orders in q, interaction of the particle with its own gravitational perturbation gives rise to gravitational self-force, which drives the radiative evolution of the orbit, and whose effects can be accounted for order by order in q (Barack and Pound 2019).

EMRIs are however by necessity embedded in astrophysical environments, and as such it is likely that their secular evolution will differ from the pure vacuum case. Of all the environmental factors, gravitational torques from accretion flows are likely to be most the significant (Cardoso and Maselli 2020). Obtaining realistic estimates for the influence of accreting gas on the orbital evolution and phase of the binary is difficult because accretion dynamics is a largely unexplored 3D magnetohydrodynamics problem over a large dynamic range. The best theoretical prediction for the impact of gas dynamics on IMRI/EMRI phase errors are from 2D viscous hydrodynamics (Derdzinski et al. 2019, 2021). Phase errors grow with the surface density of the accretion disc. The sign in the tidal torque, i.e. whether the separation increases or decreases, depends on the mass ratio, the strength of the viscosity (the α parameter), and the rate of inspiral (Derdzinski et al. 2021). Some parameters even experience stochastic variability in the sign of the tidal torque for EMRIs; such

variability would be in stark contrast with secular phase errors coming from truncating the PN expansion. Phase errors due to non-stochastic effects, however, will likely be comparable to PN errors for some disc configurations and orbital separations (Barausse et al. 2014; Cardoso and Maselli 2020; Annulli et al. 2020). Understanding whether these situations are likely requires a combination of results from 2D viscous simulations (cf. Derdzinski et al. 2019, 2021) with EM surveys of AGN discs, population synthesis modelling of AGN/binary discs (e.g., Krolik et al. 2019), and estimates of the distribution of the observed binary parameters for LISA. Since all EMRI/IMRI simulations have used 2D Newtonian viscous hydrodynamics, it will be interesting to see how these results change when using more realistic 3D general-relativistic magnetohydrodynamical simulations. Unfortunately, performing a series of simulations with $O(2000)$ orbits, which seems to be required to reach a steady-state in 2D simulations, is computationally prohibitive at present.

Another obvious effect that can spoil the vacuum evolution of an EMRI is the influence of a third gravitational body. In the case of a hierarchical triple, two effects can take place. First, the influence of the perturber can produce a shift in the binding energy of the inner binary. Will (2014) showed that this shift is constant even if the inner binary undergoes perihelion advance. Second, if the perturber is sufficiently inclined it can induce von Zeipel–Kozai–Lidov oscillations (von Zeipel 1910; Kozai 1962; Lidov 1962) in the inner binary. This can in principle cause an enhancement in the eccentricity of the inner binary. In the case of EMRIs, however, we can expect gravitational perturbations in a hierarchical triple to be very weak. The pull of the third body essentially acts as a tidal force between the components of the inner binary. Therefore, it scales as $\sim aR^{-3}$, where a is the typical separation of the inner binary and R is the distance of the perturber to its centre of mass. For EMRIs, a will generally be very small (10 to 10^3 Schwarzschild radii) and the third power of R will strongly suppress tidal forces. As an example, one can compare the von Zeipel–Kozai–Lidov oscillation timescale t_{KL} with the gravitational radiation reaction timescale t_{GW}:

$$t_{GW} \sim t_{KL} = 2\pi \frac{\sqrt{GM}}{Gm_3} \frac{R^3}{a^{3/2}}. \tag{31}$$

By using Peters' formula (Peters 1964a) one can find the typical orbital separation at which GW emission and von Zeipel–Kozai–Lidov oscillations change the orbital elements on the same timescale. For circular orbits, this yields

$$R_{KL/GW} \approx a \left(\frac{m_3}{qM}\right)^{1/3} \left(\frac{a}{r_S}\right)^{5/6}, \tag{32}$$

where q is the mass ratio and M the total mass of the inner binary, while r_S is the Schwarzschild radius of the central MBH and m_3 the mass of the perturber. For EMRIs, it is clear that the two timescales can be comparable only for very massive or very close perturbers. Nonetheless, recent works have used this result to compute event rates for binaries that are affected by the Kozai-Lidov eccentricity enhancement (Randall and Xianyu 2019b; Deme et al. 2020a), and Yunes et al. (2011b) showed

that a sufficiently large perturber ($\sim 10^6 \, M_\odot$) at sub-parsec distances can dephase the GW signal of an EMRI by a detectable amount.

The astrophysical community has mostly focused on understanding and modelling the influence of the environment on vacuum sources. Claims of detectability for any given effect are therefore often based on simple phenomenological criteria rather than complete signal injections and parameter inference methods. The simplest and most ubiquitous criterion is based on the concept of the SNR of a deviation from a vacuum waveform. While the SNR of a GW event can be estimated by the following formula:

$$\text{SNR} = \sqrt{2 \cdot 4 \int_{f_{\min}}^{f_{\max}} df' \, \frac{h_c^2(f')}{S_t(f')f'^2}}. \tag{33}$$

The SNR of a deviation can be found by replacing h_c with:

$$h_c \exp(i\phi) \rightarrow h_c \exp(i\phi) - h_c' \exp(i\phi'), \tag{34}$$

where the primes denote the waveform of a source that is modified through the action of some environmental effect. For GW sources in general, an SNR value of ~ 8 is chosen as a threshold required in order to claim detectability. The same is assumed to be true for a given deviation, δh_c which is deemed detectable whenever $\Delta\text{SNR} > 20$ (at least for EMRIs). While such criteria can serve as a first order approximation, they do not take into account many of the complications that will plague data analysis procedures required to extract signal from LISA's datastream. Effects such as degeneracies, the lack of appropriate waveforms and subtleties of Bayesian analysis in parameter spaces with many dimensions are only a few of the many considerations that should in principle be taken into account when considering the detectability of environmental effects. Degeneracies are especially important, since the influence of many environmental effects might be misinterpreted as sources with different intrinsic parameters. As a simple example, consider the evolution of a BH binary in gas. The primary effect of gas would be to change the rate at which the binary chirps, i.e. $\dot{f}$. However, in a blind waveform template search, the same variation in $\dot{f}$ could likely be accounted for by a slightly modified mass of the system, inducing a bias in parameter estimation. With sufficient SNR, it will be likely possible to break such degeneracies from leading order parameters such as chirp mass and distance, using e. g. the information contained in higher derivatives of the frequency, $\ddot{f}$. Further work should confirm that the same can be said for subtler GR vacuum effects, mainly the spin components and the eccentricity of the source. A possible way forward would be an increased collaboration between the data analysis and astrophysics working groups: the former can provide more sophisticated phenomenological detectability criteria, while the latter could direct the data analysis efforts towards those effects that are expected to be relevant.

3.4.6.1 The contribution of LISA to our understanding of the host environment

The variety of gas torques suggests that, if chirping, EMRIs in gaseous environments will exhibit characteristic signatures that may allow us to probe the inner regions of AGN discs. If a phase shift is detected and confirmed to be of gas

origin, its magnitude and evolution will be a direct consequence of interaction with local gas properties around the BHs. However, detecting such deviations will require improving models of environmental effects such that we can include them properly in parameter estimation. A critical step is to assess for which regions of parameter space these effects will be unique or degenerate with system parameters. In the latter case, neglecting them may induce biases in parameter estimation. We expect such signatures to arise in only a subset of systems, whereas deviations from general relativity would arise in all EMRIs (depending on the observed frequency). Gas effects can also lead to additional waveform implications: for example prograde, disc-embedded sources will likely have low eccentricity and some degree of spin/inclination alignment with the central MBH. If deep within the potential well of the MBH, these effects may be complemented by a phase-shifting from the Doppler effect (Sect. 3.4.3).

Elaborating on what we have presented here but also in the previous sections, the presence of an XMRI can alter the evolution of an EMRI on its way to cross the event horizon of the MBH. This can lead to extreme situations in which the orbital dynamics of the EMRI is not just affected by the presence of the XMRI, but to the point of scattering off the EMRI from its inspiraling orbit towards the MBH (Vretinaris and Amaro Seoane, in prep.). Since our Galactic Centre and MBH might be envisaged as a typical target for LISA, this means that many, if not all nuclei in the LISA observational volume are prone to this problem.

Our theory of how stars distribute around MBHs is more than four decades old and seems to be robust. However, at distances very close to the MBH, the power-law distribution of the stellar system (the "cusp") is ill-defined, because the number density drops significantly. If a star happened to be close to an EMRI, in principle one could reverse-engineer the modulation induced in the waveform, in particular in the phase, to recover information about such perturbing stars from a region which is too obscured to be accessible to EM telescopes.

The merger in a b-EMRI system induces a kick to the BH remnant (Centrella et al. 2010). This kick causes a glitch in the EMRI waveform, which, through a careful analysis, is discernible in the data stream (Han and Chen 2019). The b-EMRI can hence accurately weigh the mass loss due to the BH+BH merger, and offer an opportunity to test general-relativistic effects (in particular the dispersion relation of GWs and the weak equivalence principle).

Since a significant fraction of EMRIs can be hosted in galaxies which move relative to us at very high speeds, the imprint of the aberration and beaming effects on the waveform can be crucial. A constant drift of the centre of mass of a source also can affect the higher multipoles of the gravitational waveform. This, in turn, affects the frequency and amplitude of the wave as seen by a distant observer (Gualtieri et al. 2008; Torres-Orjuela et al. 2021b). Therefore, higher modes can be used to break the aforementioned degeneracy between a constant velocity and the mass/distance of the source. Considering the change of the modes for EMRIs, LISA should be able to detect constant velocities of just $1000\,\mathrm{km\,s^{-1}}$ for an SNR of around 70 (Torres-Orjuela et al. 2021a). Moreover, as mentioned in that work, we could use

this information to obtain a detailed map of the relative speed distribution of galactic clusters out to distances unaccessible to EM observations.

Another interesting possibility is that dark matter minispikes could impact the gravitational waveform, inducing dephasings that could be detected by LISA (Eda et al. 2013; Yue and Han 2018; Hannuksela et al. 2020; Kavanagh et al. 2020). Furthermore, the existence of dark matter halos around IMBHs could accelerate the formation of IMRIs (Yue and Han 2018). Therefore, the event rates of IMRIs may be much higher than previous estimates, which did not include a DM halo (Yue et al. 2019).

As for astrophysical chaos, we can deduce that the detectability of the plateau scales with the magnitude of the non-Kerr parameters and the mass ratio of the EMRI: the "islands" presented above become larger for greater non-Kerr parameters, and the system requires more time to cross an island for greater mass disparity (Lukes-Gerakopoulos et al. 2010). Crossing into an island leads to a period of frequency modulation, which can, in principle, be detected by LISA (Destounis et al. 2020). More careful data analysis (using, e.g., a Fisher matrix study) is therefore required to determine whether chaotic phenomena have a non-general-relativistic origin, since the frequency jumps described in Fig. 34 may be mimicked by environmental effects.

The research carried out so far demonstrates the difficulty of distinguishing gas-driven environmental effects from poorly modelled GR effects. Work to date has explored a relatively narrow range of parameter space for possible environmental effects, and more work should be done to understand the dominant effects, even within currently available 2D Newtonian hydrodynamical models. As computational resources increase, closer to launch, it would also be helpful to expand theoretical efforts to include at least some 3D general relativistic magnetohydrodynamical simulations. Though challenging, further work must also be done to examine the degeneracies between, e.g., additional PN terms and gas-driven departures from GR. The most important efforts are finding effects that share the same frequency or mass dependence—for effects that do not share dependencies, we can hope to distinguish the source from the GW observations themselves. Gas-driven sources should be a subset of all sources (and should have eccentricities and inclinations which help to distinguish them), while higher-order corrections should apply to every system (though the corrections may be mass- or frequency-dependent). Assuming we overcome the challenges listed here, disentangling various environmental signatures from GWs will give us access to unique measurements of MBH environments purely through GWs. Such measurements are inaccessible via EM observations. Characteristic deviations (or even a lack thereof) will provide constraints on gas densities, dark matter profiles, or the presence of external perturbers.

3.5 EMRI background

Coordinators: **Pau Amaro-Seoane, Andrea Derdzinski**

Contributors: **Pau Amaro-Seoane, Andrea Derdzinski, Giuseppe Lodato, Martina Toscani**

While the majority of this chapter describes resolvable sources (as they are certainly the most interesting for guaranteed science), most EMRIs/IMRIs throughout the Universe will not be individually detectable, particularly if they are too distant, at earlier stages of their inspiral, or their GWs are too weak (which is moreso an issue for inspirals of WDs or NSs). The combined signal from the population of faint, unresolved sources will constitute a stochastic background.

The EMRI background may lie well below the LISA sensitivity or exceed it, contributing an additional confusion noise. Its amplitude scales with the EMRI rate, although not necessarily linearly (Barack and Cutler 2004a), and its precise spectral shape will depend on the efficiency of various formation channels over cosmic time. Seminal predictions find that the background signal will only become comparable to the LISA noise if the EMRI rate is substantial: e.g., if the detection rate is as high as $\mathcal{O}(10^2)$ detections per year, the corresponding background may increase the LISA noise by a factor of nearly ~ 2 (Barack and Cutler 2004a). More recent estimates based on EMRI catalogues by Babak et al. (2017) use an updated version of the LISA sensitivity curve and find that, for a range of EMRI rates, the background may add considerable noise (attaining an SNR of a few to few-hundred) within the LISA sensitivity bucket around $f \sim 3\,\mathrm{mHz}$ (Bonetti and Sesana 2020). Higher levels of confusion noise may compromise our ability to detect faint sources that fall into this frequency range, such as high redshift, low mass MBH mergers–although one could argue that this would be compensated for by the generous resolvable EMRI rate.

A detectable background may provide additional information on the cosmological EMRI population and the efficiency of various formation mechanisms, if there exists robust differences in the spectrum between formation channels. The trick to detecting (and then hopefully characterizing) a background signal is to distinguish it from the instrumental noise as well as other confusion sources (see Romano and Cornish 2017 for a comprehensive review). For LISA, the main contributor to confusion noise is expected to arise from Galactic binaries: while many will be individually resolvable, the rest will form a confusion foreground (e.g., Nissanke et al. 2012, but see Chapter 1) that may overwhelm any extragalactic stochastic signal. Fortunately, LISA's orbital motion around the Sun introduces an annual modulation in the anisotropic galactic foreground, and this makes it possible to distinguish the astrophysical signal from the instrument noise. With a prior understanding of the LISA noise, knowing the distinct spectral shape of an astrophysical foreground further helps us separate the two, so there is hope for detecting an underlying stochastic background (Adams and Cornish 2014). Such techniques were successfully applied in the LISA mock data challenge (Robinson et al. 2008). At the moment, predictions for the EMRI background signal suffer from the same

Table 9 Rates and SNRs for inspirals. Note that the rates for XMRIs are at any given moment in the MW and, possibly, nearby galaxies (see reference)

Inspiral type	Rate (year^{-1})	SNR	References
EMRI	10–10^3	~ 100	Amaro-Seoane (2018b, 2021), Babak et al. (2017)
light IMRI	6–60	10–10^3	Arca Sedda et al. (2021a), Amaro-Seoane (2021)
heavy IMRI	2–20	10–100	Miller (2005), Arca-Sedda and Gualandris (2018)
			Arca-Sedda and Capuzzo-Dolcetta (2019)
XMRI	$\sim$ few tens (at any given moment)	10–10^4	Amaro-Seoane (2019, 2021)

uncertainties as detection rates (see Table 9), but these can be improved as we increase our understanding of formation mechanisms. Improving waveform modelling or finding other methods of accurate signal extraction will also be critical if we hope to detect an underlying signal.

An important step in this analysis would be to distinguish the EMRI background from other possible background sources. In addition to EMRIs, there may be characteristic background signals from extra-galactic WD, NS, or BH binaries (e.g., Chen et al. 2019b; D'Orazio and Samsing 2018), TDEs (discussed below), phase transitions in the early universe (Maggiore 2000; Giblin et al. 2012; Leitao et al. 2012), or cosmic strings (Siemens et al. 2007). If the spectrum is sufficiently constrained, then it is likely that the origin of the signal, whether from a large number of unresolved EMRIs or other extragalactic sources, can be determined (Barausse et al. 2020a).

3.5.1 TDE background

A particular type of EMRI background is the one generated by the unresolvale GW signal from the cosmic TDE population. The calculation of such background has been performed by Toscani et al. (2020) for both main-sequence stars being disrupted by MBHs in galactic nuclei and WDs being disrupted by IMBHs in globular clusters. The signal has a characteristic spectral shape $h_c \propto f^{-1/2}$, due to the specific impulsive nature of these events. The predicted amplitude of the background is generally low, with WDs on IMBHs providing typical strains of $\approx 10^{-23}$–10^{-21} and main-sequence stars on MBHs providing $\approx 10^{-22}$.

3.5.1.1 The contribution of LISA to our understanding of backgrounds of inspirals In summary, LISA will have the capability to detect a stochastic background signal, once the galactic foreground is subtracted. This measurement will improve throughout the mission lifetime as we constrain the instrument noise

and resolve individual sources (Adams and Cornish 2014). If EMRIs provide the dominant contribution within some frequency range—e.g., around 3 mHz, as predicted by Bonetti and Sesana (2020)—a measurement of the background spectrum can serve as an additional measurement of dynamics in galactic nuclei. For example, the amplitude and spectrum of the background are related to the number of EMRIs that are either at earlier inspiral stages or at higher redshifts, as well as the MBH mass function. If the background is above the LISA sensitivity and not well-characterised, it will contribute to the noise budget, possibly complicating the detection of other weak signals. To avoid this, it is important that we improve our predictions on the EMRI rate. Further work is also needed to constrain the expected spectrum of various background signals, in order to determine which will be dominant, distinguishable, and removable from the LISA data. If the EMRI rate is low enough such that the background falls below the LISA sensitivity, then it becomes possible to detect other stochastic signals, such as those predicted from extragalactic binaries or signatures from the early Universe.

As for the background from TDEs, its detection could provide interesting insights both on the distribution of quiescent MBHs (for main sequence stars tidally disrupted) and on the occupation fraction of IMBHs in globular clusters (for TDEs of WDs), up to redshift ≈ 3. Yet, this detection seems to be very difficult. Indeed, the background produced by WD TDEs will lie in a high part of the frequency window (deciHertz to a few Hertz), where LISA will be less sensitive (yet, more sensitive interferometers in this frequency interval are planned for the future). Instead, the background from MS TDEs is expected at lower frequency (10^{-4}–10^{-2} Hz), but will be still below the threshold LISA sensitivity. Hence, this detection seems unlikely (although some background signal below the strain sensitivity might still be visible in some cases; see Sesana 2016 for more details).

3.6 Conclusions

***Contributors:* Saavik Ford**

To summarise: the basic physics of EMRI mergers has been known for a long time. We can expect to find EMRIs in NSCs harboring an MBH, and can predict the dynamics of their formation and evolution using relaxation theory. The waveform modelling for EMRIs is also reasonably advanced, such that the path to detectability of such signals is understood (if challenging). However, there are substantial uncertainties in the astrophysical parameters that govern the *rates* of EMRI production, notably the spins of MBHs and, most critically, the radial mass distribution of NSCs. These astrophysical unknowns will change the ratio of plunging extreme mass ratio mergers to bona fide EMRIs—in the case of plunging mergers, an extreme mass ratio merger does occur, but the interactions of the merging object with the inner edge of the stellar cusp alters the trajectory of the low mass object after only a few orbits, and produce a rapid merger. Since LISA detection of EMRIs will depend on the buildup of a sufficient SNR over many orbits, plunges are rendered undetectable.

However, assuming the inner edge of an NSC is typically sufficiently far from the MBH, and if MBH spins are typically non-zero, EMRIs can occur at a high enough rate that LISA would detect one or more over the lifetime of the mission. If an EMRI is detected, we will immediately obtain a wide variety of both fundamental physical and astrophysical information (including, implicitly, information about the mass distribution in NSCs and MBH spins). Because of the many-orbit nature of an EMRI, such events can provide a detailed map of the gravitational field in the vicintiy of the MBH, yielding exquisite measurements of the mass and spin of that MBH, and providing an opportunity to probe fundamental physics by testing for subtle departures from GR.

Given the current uncertainties on EMRI rates, it is most useful to proceed along multiple fronts:

– Theoretical work to understand higher-order dynamical effects which may preserve more EMRIs for sufficient cycles to allow detection by LISA (i.e. preventing plunges)
– Observational work constraining the inner edge of the NSC cusp in nuclei other than the MW (M32 would be notably useful)
– Theoretical and observational work constraining the binary fraction in typical NSCs (enabling better estimates of the EMRI rate due to binary tidal separation)
– Theoretical work to develop non-standard EMRI channels, especially AGN and SNe routes, to constrain rates and parameter distributions, and permit reverse engineering of astrophysical parameters

In addition, there is groundwork to be done on the waveform, data analysis and coordination front:

– Self-force calculations to second order in mass ratio for generic orbits in a Kerr metric to enable high precision waveform calculations
– Further data analysis work with updated waveforms to improve EMRI extraction from the LISA datastream
– Coordination of data analysis with radio and ground-based GW observatories in case of pulsar or b-EMRI detection

IMRIs provide still more exciting science opportunities, but correspondingly more challenging uncertainties. Due to their larger mass ratio, IMRIs cannot be treated using the same theoretical mechanisms as EMRIs (i.e. as small perturbations), yet they are also not sufficiently large to be treated using the mechanisms that apply to near-equal-mass binaries. This reality provokes difficulties in several directions—we cannot generally apply the same relaxation theory strategies to predict IMRI formation dynamics, nor can we readily produce IMRI waveform models using numerical relativity without changing computational strategy. In addition, there are at least 2 types of IMRIs to be considered: (1) light IMRIs, where the more massive partner is an IMBH and the less massive partner is a stellar mass BH; and (2) heavy IMRIs, where the more massive partner is an MBH and the less massive partner is an IMBH. There are multiple formation channels for each, and thus large astrophysical uncertainties in predicting their rates. One substantial uncertainty has recently been

removed: with the announcement of GW190521, we are certain that low-mass IMBHs do exist. Though their formation environment remains uncertain, work thus far points to some kind of dynamical origin, encouraging expectations that there may be environments conducive to the formation of at least some light IMRIs.

Broadly, the channels for light IMRIs include: (1) formation in globular clusters (assuming the presence of an IMBH in the cluster); (2) formation in dwarf galaxies (assuming the presence of an IMBH in the galaxy); (3) formation in an AGN disc (assuming the formation of an IMBH at a disc migration trap). In each of these cases, the first uncertainty is the presence of an IMBH in the relevant environment. There are no universally accepted detections of IMBH in globular clusters. While there are some IMBH known in dwarf galaxies, their occupation fraction is not well-measured and depends on the still unknown physics of BH seed formation at high redshift. IMBH formation in AGN discs is expected to be nearly universal if such discs contain a migration trap and are sufficiently long-lived. Unfortunately neither condition is sufficiently theoretically or observationally well-constrained to make a confident statement on the rate of IMBH formation in AGN discs.

Sadly that is not the end of our uncertainties for the formation of these systems—the dynamics in each case are difficult to model, as noted above, and as with EMRIs, the systems might produce a beautiful, detectable inspiral, or a rapid plunge. Among the important open questions are the observational presence or absence of IMBH in each formation environment, and observations and theoretical investigation of the (extremely different) dynamical environment around each IMBH.

For heavy IMRIs, we have a similar diversity of formation channels: (1) globular clusters containing an IMBH infalling into a galactic nucleus containing a MBH; (2) dwarf galaxies infalling into a galactic nucleus containing a MBH; (3) AGN-produced IMBH falling into their host MBH (likely in the post-AGN phase). Globular clusters, being denser than dwarf galaxies, will deposit their IMBHs in galactic nuclei more rapidly than dwarf galaxies, and in general, are expected to dominate the rate in this formation channel. However, if globulars do not contain IMBHs, we should consider dwarf galaxy mergers quite carefully, since at least some dwarfs are known to harbor IMBHs. For low-mass galaxy groups, dwarf mergers will be the most common type of merger and do lead to the formation of bound IMBH-MBH systems in less than a Hubble time. However, theoretical astrophysical rate calculations for resulting IMRIs, over the volume probed by LISA, remain an important open question. Observations of dwarf galaxies and their evolution over cosmic time, as well as observations that inform the occupation fraction of globular clusters and dwarf galaxies are, consequently, critical unknowns. AGN production of IMBHs provide a potentially extremely high rate of IMRIs, given the formation location and expected GW inspiral time; such IMRI systems will not likely be disrupted by interactions with the NSC. However, as with the light IMRI channel, substantial uncertainties in the structure of AGN discs and their lifetimes lead to orders-of-magnitude uncertainties in the rate estimates for this channel.

IMRIs have received less attention in the literature to date, and consequently the tasks to complete before LISA launches tend to be larger. These include:

–   Determining the occupation fraction of globular clusters and dwarf galaxies

– Determining the contribution to the heavy IMRI rate from low mass galactic environments
– Determining the formation environment of GW190521-like sources
– IMRI waveform modelling and extraction (may require expensive numerical relativity modelling)
– Modelling of IMRI formation (and rates) in both gas-poor and gas-rich environments

Finally, we consider the open questions related to the relatively new class of unequal mass ratio inspirals, XMRIs. Here, the physics of their formation and evolution is similar to that of EMRIs, but they are labelled eXtreme due to the very small mass of the secondary—for LISA frequencies, the secondary would typically be a brown dwarf. Similar to the situation for EMRIs, the uncertainties largely relate to our astrophysical ignorance; however, we are able to limit the locations we must investigate. Due to their low mass and consequently small strains, XMRIs will only be detectable within roughly our Local Group, meaning either from the MW or M31. In addition to the relevant questions for EMRIs (especially NSC radial mass distribution), we must understand the mass function of those NSCs. How many brown dwarfs are there in the galactic centre? If the IMF is top heavy, there may be very few—however, if we assume a more standard IMF, and the radial mass distribution and MBH spin are favorable, LISA can expect to detect one or more XMRIs from Sgr A* over the mission lifetime.

For XMRIs there are several useful items to work on as we proceed towards launch:

– Determine the low end mass function in the galactic centre
– Investigate possible interactions between XMRIs and EMRIs (and find distinguishing observables between interacting EMRI-XMRI systems and departures from GR such as the chaotic behaviour introduced by non-Kerr objects)
– Data analysis work to properly characterize potential loud XMRIs

As we have discussed, various mechanisms for producing EMRIs and IMRIs may have EM counterparts—this may enable independent rate constraints either prior to or concurrent with LISA; further, if specific counterparts are reliably identified, we can use the complementary information provided by each messenger to learn more about the astrophysics of the emitting system. Notable work to be done includes:

– Detailed hydrodynamical models of EM emission mechanisms for GW events in AGN discs
– Athena observations of candidate IMRI systems if Athena will not be flying simultaneously with LISA (or coordination if missions are concurrent)

Each of these types of inspirals present a large parameter-space of possible waveforms, making detection itself a notable challenge. Narrowing the theoretical uncertainties for each channel, in advance of LISA, therefore also has implications for the detectability of their signals. However, work may also be done on the signal processing side to find new strategies for extracting the signals, and doing reliable

parameter estimation on them, from the LISA data stream. In this context, there is currently substantial concern over possible degeneracies between gas-induced phase shifts and departures from general relativity; fortunately, if we have multiple events from multiple populations, departures from general relativity should be universal, while gas effects will impact only a subset of events. On the other hand, some signals containing environmental effects will be clearly identifiable (e.g., b-EMRIs). All of these channels may contribute to a detectable EMRI background; however, disentangling multiple populations from such an unresolved background will be extremely challenging and fundamentally requires more theoretical development from each contributing channel. From these areas, we would especially like to highlight the need for a thorough parameter space exploration with at least 3d Newtonian hydrodynamical simulations of the impact of gas on the inspiral waveforms.

Substantially unequal mass ratio inspirals of all types represent an important class of sources, uniquely detectable by LISA. In order to best exploit the astrophysical and fundamental physical science achievable by LISA using these types of events, in the years preceding launch, we will need to work primarily on developing more detailed models for each formation channel, and on observationally constraining the parameters used as inputs of those models, along the lines we have outlined above.

4 General summary

The decade prior to LISA's launch will be an exciting one for the astrophysics community, presenting unique challenges and opportunities in preparing for LISA's first observations. This review outlines the extensive landscape of astrophysical theory, numerical simulations, and current astronomical observations that will influence preparations for the pipelines that will deliver LISA data, and guide our interpretations of the first LISA observations and catalogues.

This review describes the current state of knowledge regarding three main source classes for LISA: ultra-compact stellar-mass binaries, massive black hole binaries, and extreme or intermediate mass ratio inspirals. For each of these three source classes, our current understanding of the astrophysical processes that create them and guide their ongoing evolution is a rich tapestry formed from extant observations (usually electromagnetic), numerical simulations and modelling, and theoretical considerations. LISA data will be added to this, providing new independent information that will help constrain the physics governing these systems, and opening up new avenues of investigation for future observations, theory, and simulations.

Astronomy observations will continue to evolve and alter the scientific landscape prior to LISA's launch, and theory and modelling will become more refined. Such advances will inform our understanding of the ways in which LISA data can be used, and they can also sharpen the focus on the important ways in which gravitational wave data will expand and enhance our ability to understand astrophysical phenomena in many different environments and scales. This review endeavours to provide a framework within which to consider these possibilities, and should be a

good starting point for those interested in using LISA as a new observational tool for understanding the Universe.

References

Aarseth SJ (2012) Mergers and ejections of black holes in globular clusters. MNRAS 422(1):841–848. https://doi.org/10.1111/j.1365-2966.2012.20666.x. arXiv:1202.4688 [astro-ph.SR]

Aartsen M et al (2018) Neutrino emission from the direction of the blazar TXS 0506+056 prior to the IceCube-170922a alert. Science 361(6398):147–151. https://doi.org/10.1126/science.aat2890

Aasi J, Abbott BP, Abbott R, Abbott T, Abernathy MR, Ackley K, Adams C, Adams T, Addesso P et al (2015) Advanced LIGO. Class Quantum Grav 32(7):074001. https://doi.org/10.1088/0264-9381/32/7/074001. arXiv:1411.4547 [gr-qc]

Abadie J, Abbott BP, Abbott R, Abernathy M, Accadia T, Acernese F, Adams C, Adhikari R, Ajith P, Allen B et al (2010) Predictions for the rates of compact binary coalescences observable by ground-based gravitational-wave detectors. Class Quantum Grav 27(17):173001. https://doi.org/10.1088/0264-9381/27/17/173001. arXiv:1003.2480 [astro-ph.HE]

Abbott BP, Abbott R, Abbott TD, Abernathy MR, Acernese F, Ackley K, Adams C, Adams T, Addesso P, Adhikari RX et al (2016a) GW150914: implications for the stochastic gravitational-wave background from binary black holes. Phys Rev Lett 116(13):131102. https://doi.org/10.1103/PhysRevLett.116.131102. arXiv:1602.03847 [gr-qc]

Abbott BP, Abbott R, Abbott TD, Abernathy MR, Acernese F, Ackley K, Adams C, Adams T, Addesso P, Adhikari RX et al (2016b) GW150914: first results from the search for binary black hole coalescence with advanced LIGO. Phys Rev D 93(12):122003. https://doi.org/10.1103/PhysRevD.93.122003. arXiv:1602.03839 [gr-qc]

Abbott BP, Abbott R, Abbott TD, Abernathy MR, Acernese F, Ackley K, Adams C, Adams T, Addesso P, Adhikari RX et al (2016c) Observation of gravitational waves from a binary black hole merger. Phys Rev Lett 116(6):061102. https://doi.org/10.1103/PhysRevLett.116.061102. arXiv:1602.03837 [gr-qc]

Abbott BP, Abbott R, Abbott TD, Abernathy MR, Ackley K, Adams C, Addesso P, Adhikari RX, Adya VB, Affeldt C et al (2017a) Exploring the sensitivity of next generation gravitational wave detectors. Class Quantum Grav 34(4):044001. https://doi.org/10.1088/1361-6382/aa51f4. arXiv:1607.08697 [astro-ph.IM]

Abbott BP, Abbott R, Abbott TD, Acernese F, Ackley K, Adams C, Adams T, Addesso P, Adhikari RX, Adya VB et al (2017b) Multi-messenger observations of a binary neutron star merger. ApJ 848(2):L12. https://doi.org/10.3847/2041-8213/aa91c9. arXiv:1710.05833 [astro-ph.HE]

Abbott BP, Abbott R, Abbott TD, Acernese F, Ackley K, Adams C, Adams T, Addesso P, Adhikari RX, Adya VB et al (2018a) GW170817: measurements of neutron star radii and equation of state. Phys Rev Lett 121(16):161101. https://doi.org/10.1103/PhysRevLett.121.161101. arXiv:1805.11581 [gr-qc]

Abbott BP, Abbott R, Abbott TD, Acernese F, Ackley K et al (2018b) GW170817: implications for the stochastic gravitational-wave background from compact binary coalescences. Phys Rev Lett 120(9):091101. https://doi.org/10.1103/PhysRevLett.120.091101. arXiv:1710.05837 [gr-qc]

Abbott BP, Abbott R, Abbott TD, Abraham S, Acernese F, Ackley K, Adams C, Adhikari RX, Adya VB, Affeldt C et al (2019) GWTC-1: a gravitational-wave transient catalog of compact binary mergers observed by LIGO and Virgo during the first and second observing runs. Phys Rev X 9(3):031040. https://doi.org/10.1103/PhysRevX.9.031040. arXiv:1811.12907 [astro-ph.HE]

Abbott BP, Abbott R, Abbott TD, Abraham S, Acernese F, Ackley K, Adams C, Adhikari RX, Adya VB, Affeldt C et al (2020a) GW190425: observation of a compact binary coalescence with total mass $\sim$ 3.4 $M_{\odot}$. ApJ 892(1):L3. https://doi.org/10.3847/2041-8213/ab75f5. arXiv:2001.01761 [astro-ph.HE]

Abbott R, Abbott TD, Abraham S, Acernese F, Ackley K, Adams C, Adhikari RX, Adya VB, Affeldt C, Agathos M et al (2020b) GW190814: gravitational waves from the coalescence of a 23 solar mass black hole with a 2.6 solar mass compact object. ApJ 896(2):L44. https://doi.org/10.3847/2041-8213/ab960f. arXiv:2006.12611 [astro-ph.HE]

Abbott R, Abbott TD, Abraham S, Acernese F, Ackley K, Adams C, Adhikari RX, Adya VB, Affeldt C, Agathos M et al (2020c) GW190521: a binary black hole merger with a total mass of 150 $M_{\odot}$. Phys Rev Lett 125(10):101102. https://doi.org/10.1103/PhysRevLett.125.101102

Abbott R, Abbott TD, Abraham S, Acernese F, Ackley K, Adams C, Adhikari RX, Adya VB, Affeldt C, Agathos M et al (2020d) Properties and astrophysical implications of the 150 $M_{\odot}$ binary black hole merger GW190521. ApJ 900(1):L13. https://doi.org/10.3847/2041-8213/aba493

Abbott R, Abbott TD, Abraham S, Acernese F, Ackley K, Adams A, Adams C, Adhikari RX, Adya VB, Affeldt C et al (2021a) GWTC-2: compact binary coalescences observed by LIGO and Virgo during the first half of the third observing run. Phys Rev X 11(2):021053. https://doi.org/10.1103/PhysRevX.11.021053. arXiv:2010.14527 [gr-qc]

Abbott R, Abbott TD, Abraham S, Acernese F, Ackley K, Adams A, Adams C, Adhikari RX, Adya VB, Affeldt C et al (2021b) Population properties of compact objects from the Second LIGO–Virgo Gravitational-Wave Transient Catalog. ApJL 913:L7. https://doi.org/10.3847/2041-8213/abe949. arXiv:2010.14533 [astro-ph.HE]

Abel T, Bryan GL, Norman ML (2002) The formation of the first star in the universe. Science 295:93–98. https://doi.org/10.1126/science.1063991. arXiv:astro-ph/0112088

Abuter R, Amorim A, Anugu N, Bauböck M, Benisty M, Berger JP, Blind N, Bonnet H, Brandner W, Buron A et al (2018) Detection of the gravitational redshift in the orbit of the star S2 near the Galactic

centre massive black hole. A&A 615:L15. https://doi.org/10.1051/0004-6361/201833718. arXiv:1807.09409 [astro-ph.GA]

Abuter R, Amorim A, Bauböck M, Berger JP, Bonnet H, Brandner W, Cardoso V, Clénet Y, de Zeeuw PT, Dexter J et al (2020) Detection of the Schwarzschild precession in the orbit of the star S2 near the Galactic centre massive black hole. A&A 636:L5. https://doi.org/10.1051/0004-6361/202037813. arXiv:2004.07187 [astro-ph.GA]

Acernese F et al (2015) Advanced Virgo: a second-generation interferometric gravitational wave detector. Class Quant Grav 32(2):024001. https://doi.org/10.1088/0264-9381/32/2/024001. arXiv:1408.3978 [gr-qc]

Ackermann S, Schawinski K, Zhang C, Weigel AK, Turp MD (2018) Using transfer learning to detect galaxy mergers. MNRAS 479(1):415–425. https://doi.org/10.1093/mnras/sty1398. arXiv:1805.10289 [astro-ph.IM]

Adams MR, Cornish NJ (2014) Detecting a stochastic gravitational wave background in the presence of a galactic foreground and instrument noise. Phys Rev D 89(2):022001. https://doi.org/10.1103/PhysRevD.89.022001. arXiv:1307.4116 [gr-qc]

Adams MR, Cornish NJ, Littenberg TB (2012) Astrophysical model selection in gravitational wave astronomy. Phys Rev D 86(12):124032. https://doi.org/10.1103/PhysRevD.86.124032. arXiv:1209.6286 [gr-qc]

Addison E, Gracia-Linares M, Laguna P, Larson SL (2019) Busting up binaries: encounters between compact binaries and a supermassive black hole. Gen Relativ Gravit 51(3):38. https://doi.org/10.1007/s10714-019-2523-4

Adrián-Martínez S et al (2016) High-energy neutrino follow-up search of gravitational wave event gw150914 with antares and icecube. Phys Rev D 93:122010. https://doi.org/10.1103/PhysRevD.93.122010

Agarwal B, Khochfar S, Johnson JL, Neistein E, Dalla Vecchia C, Livio M (2012) Ubiquitous seeding of supermassive black holes by direct collapse. MNRAS 425(4):2854–2871. https://doi.org/10.1111/j.1365-2966.2012.21651.x. arXiv:1205.6464 [astro-ph.CO]

Agarwal B, Dalla Vecchia C, Johnson JL, Khochfar S, Paardekooper JP (2014) The First Billion Years project: birthplaces of direct collapse black holes. MNRAS 443(1):648–657. https://doi.org/10.1093/mnras/stu1112. arXiv:1403.5267 [astro-ph.CO]

Ahn CP, Seth AC, den Brok M, Strader J, Baumgardt H, van den Bosch R, Chilingarian I, Frank M, Hilker M, McDermid R (2017) Detection of supermassive black holes in two Virgo ultracompact dwarf galaxies. ApJ 839:72. https://doi.org/10.3847/1538-4357/aa6972. arXiv:1703.09221 [astro-ph.GA]

Aird J, Coil AL, Georgakakis A (2018) X-rays across the galaxy population—II. The distribution of AGN accretion rates as a function of stellar mass and redshift. MNRAS 474:1225–1249. https://doi.org/10.1093/mnras/stx2700. arXiv:1705.01132 [astro-ph.HE]

Akiyama K, Alberdi A, Alef W, Asada K, Azulay R, Baczko AK, Ball D, Baloković M, Barrett J, Bintley D et al (2019) First M87 event horizon telescope results. I. The shadow of the supermassive black hole. ApJ 875(1):L1. https://doi.org/10.3847/2041-8213/ab0ec7. arXiv:1906.11238 [astro-ph.GA]

Alexander DM, Hickox RC (2012) What drives the growth of black holes? New A Rev 56(4):93–121. https://doi.org/10.1016/j.newar.2011.11.003. arXiv:1112.1949 [astro-ph.GA]

Alexander KD, van Velzen S, Horesh A, Zauderer BA (2020) Radio properties of tidal disruption events. Space Sci Rev 216(5):81. https://doi.org/10.1007/s11214-020-00702-w. arXiv:2006.01159 [astro-ph.HE]

Alexander RD, Armitage PJ, Cuadra J (2008) Binary formation and mass function variations in fragmenting discs with short cooling times. MNRAS 389(4):1655–1664. https://doi.org/10.1111/j.1365-2966.2008.13706.x. arXiv:0807.1731 [astro-ph]

Alexander T (2017) Stellar dynamics and stellar phenomena near a massive black hole. ARA&A 55(1):17–57. https://doi.org/10.1146/annurev-astro-091916-055306. arXiv:1701.04762 [astro-ph.GA]

Alexander T, Bar-Or B (2017) A universal minimal mass scale for present-day central black holes. Nat Astron 1:0147. https://doi.org/10.1038/s41550-017-0147. arXiv:1701.00415 [astro-ph.GA]

Alexander T, Natarajan P (2014) Rapid growth of seed black holes in the early universe by supra-exponential accretion. Science 345(6202):1330–1333. https://doi.org/10.1126/science.1251053. arXiv:1408.1718 [astro-ph.GA]

Ali A, Christensen N, Meyer R, Röver C (2012) Bayesian inference on EMRI signals using low frequency approximations. Class Quantum Grav 29(14):145014. https://doi.org/10.1088/0264-9381/29/14/145014. arXiv:1301.0455 [gr-qc]

Ali-Haïmoud Y, Kamionkowski M (2017) Cosmic microwave background limits on accreting primordial black holes. Phys Rev D 95(4):043534. https://doi.org/10.1103/PhysRevD.95.043534. arXiv:1612.05644 [astro-ph.CO]

Ali-Haïmoud Y, Kovetz ED, Kamionkowski M (2017) Merger rate of primordial black-hole binaries. Phys Rev D 96(12):123523. https://doi.org/10.1103/PhysRevD.96.123523. arXiv:1709.06576 [astro-ph.CO]

Allen B, Anderson WG, Brady PR, Brown DA, Creighton JDE (2012) FINDCHIRP: an algorithm for detection of gravitational waves from inspiraling compact binaries. Phys Rev D 85(12):122006. https://doi.org/10.1103/PhysRevD.85.122006. arXiv:gr-qc/0509116 [gr-qc]

Almeida LA, de Almeida L, Damineli A, Rodrigues CV, Castro M, Ferreira Lopes CE, Jablonski F, do Nascimento J J-D, Pereira MG (2019) Orbital period variation of KIC 10544976: applegate mechanism versus light travel time effect. AJ 157(4):150. https://doi.org/10.3847/1538-3881/ab0963. arXiv:1903.09637 [astro-ph.SR]

Aloni D, Blum K, Flauger R (2017) Cosmic microwave background constraints on primordial black hole dark matter. J Cosmol Astropart Phys 05:017. https://doi.org/10.1088/1475-7516/2017/05/017. arXiv:1612.06811 [astro-ph.CO]

Amaro-Seoane P (2018) Detecting intermediate-mass ratio inspirals from the ground and space. Phys Rev D 98(6):063018. https://doi.org/10.1103/PhysRevD.98.063018. arXiv:1807.03824 [astro-ph.HE]

Amaro-Seoane P (2018) Relativistic dynamics and extreme mass ratio inspirals. Living Rev Relativ 21:4. https://doi.org/10.1007/s41114-018-0013-8. arXiv:1205.5240 [astro-ph.CO]

Amaro-Seoane P (2019) Extremely large mass-ratio inspirals. Phys Rev D 99(12):123025. https://doi.org/10.1103/PhysRevD.99.123025. arXiv:1903.10871 [astro-ph.GA]

Amaro-Seoane P (2021) The gravitational capture of compact objects by massive black holes. In: Bambi C, Katsanevas S, Kokkotas K (eds) Handbook of gravitational wave astronomy. Springer, Singapore. https://doi.org/10.1007/978-981-15-4702-7_17-1. arXiv:2011.03059 [gr-qc]

Amaro-Seoane P, Freitag M (2006) Intermediate-mass black holes in colliding clusters: implications for lower frequency gravitational-wave astronomy. ApJ 653:L53–L56. https://doi.org/10.1086/510405. arXiv:astro-ph/0610478

Amaro-Seoane P, Preto M (2011) The impact of realistic models of mass segregation on the event rate of extreme-mass ratio inspirals and cusp re-growth. Class Quantum Grav 28(9):094017. https://doi.org/10.1088/0264-9381/28/9/094017. arXiv:1010.5781 [astro-ph.CO]

Amaro-Seoane P, Santamaría L (2010) Detection of IMBHs with ground-based gravitational wave observatories: a biography of a binary of black holes, from birth to death. ApJ 722(2):1197–1206. https://doi.org/10.1088/0004-637X/722/2/1197. arXiv:0910.0254 [astro-ph.CO]

Amaro-Seoane P, Gair JR, Freitag M, Miller MC, Mandel I, Cutler CJ, Babak S (2007) TOPICAL REVIEW: intermediate and extreme mass-ratio inspirals-astrophysics, science applications and detection using LISA. Class Quantum Grav 24(17):R113–R169. https://doi.org/10.1088/0264-9381/24/17/R01. arXiv:astro-ph/0703495 [astro-ph]

Amaro-Seoane P, Barranco J, Bernal A, Rezzolla L (2010) Constraining scalar fields with stellar kinematics and collisional dark matter. J Cosmol Astropart Phys 11:002. https://doi.org/10.1088/1475-7516/2010/11/002. arXiv:1009.0019 [astro-ph.CO]

Amaro-Seoane P, Sesana A, Hoffman L, Benacquista M, Eichhorn C, Makino J, Spurzem R (2010) Triplets of supermassive black holes: astrophysics, gravitational waves and detection. MNRAS 402(4):2308–2320. https://doi.org/10.1111/j.1365-2966.2009.16104.x. arXiv:0910.1587 [astro-ph.CO]

Amaro-Seoane P, Brem P, Cuadra J, Armitage PJ (2012) The butterfly effect in the extreme-mass ratio inspiral problem. ApJ 744(2):L20. https://doi.org/10.1088/2041-8205/744/2/L20. arXiv:1108.5174 [astro-ph.CO]

Amaro-Seoane P, Sopuerta CF, Freitag MD (2013) The role of the supermassive black hole spin in the estimation of the EMRI event rate. MNRAS 429(4):3155–3165. https://doi.org/10.1093/mnras/sts572. arXiv:1205.4713 [astro-ph.CO]

Amaro-Seoane P, Gair JR, Pound A, Hughes SA, Sopuerta CF (2015) Research update on extreme-mass-ratio inspirals. J Phys Conf Ser 610:012002. https://doi.org/10.1088/1742-6596/610/1/012002. arXiv:1410.0958 [astro-ph.CO]

Amaro-Seoane P, Audley H, Babak S, Baker J, Barausse E, Bender P, Berti E, Binetruy P, Born M, Bortoluzzi D et al (2017) Laser Interferometer Space Antenna. arXiv e-prints arXiv:1702.00786 [astro-ph.IM]

Amendola L, Appleby S, Bacon D, Baker T, Baldi M, Bartolo N, Blanchard A, Bonvin C, Borgani S, Branchini E et al (2013) Cosmology and fundamental physics with the Euclid satellite. Living Rev Relativ 16:6. https://doi.org/10.12942/lrr-2013-6. arXiv:1206.1225 [astro-ph.CO]

Anderson SF, Haggard D, Homer L, Joshi NR, Margon B, Silvestri NM, Szkody P et al (2005) Ultracompact AM Canum Venaticorum binaries from the Sloan digital sky survey: three candidates plus the first confirmed eclipsing system. AJ 130(5):2230–2236. https://doi.org/10.1086/491587. arXiv:astro-ph/0506730 [astro-ph]

Andersson N (2019) Gravitational-wave astronomy: exploring the dark side of the universe. Oxford University Press, Oxford. https://doi.org/10.1093/oso/9780198568032.001.0001

Andrews JJ, Zezas A (2019) Double neutron star formation: merger times, systemic velocities, and travel distances. MNRAS 486(3):3213–3227. https://doi.org/10.1093/mnras/stz1066. arXiv:1904.06137 [astro-ph.HE]

Andrews JJ, Breivik K, Pankow C, D'Orazio DJ, Safarzadeh M (2020) LISA and the existence of a fast-merging double neutron star formation channel. ApJ 892(1):L9. https://doi.org/10.3847/2041-8213/ab5b9a. arXiv:1910.13436 [astro-ph.HE]

Anglés-Alcázar D, Davé R, Faucher-Giguère CA, Özel F, Hopkins PF (2017) Gravitational torque-driven black hole growth and feedback in cosmological simulations. MNRAS 464(3):2840–2853. https://doi.org/10.1093/mnras/stw2565. arXiv:1603.08007 [astro-ph.GA]

Annulli L, Cardoso V, Vicente R (2020) Stirred and shaken: dynamical behavior of boson stars and dark matter cores. Phys Lett B 811:135944. https://doi.org/10.1016/j.physletb.2020.135944. arXiv:2007.03700 [astro-ph.HE]

Antoni A, MacLeod M, Ramirez-Ruiz E (2019) The evolution of binaries in a gaseous medium: three-dimensional simulations of binary Bondi-Hoyle-Lyttleton accretion. ApJ 884(1):22. https://doi.org/10.3847/1538-4357/ab3466. arXiv:1901.07572 [astro-ph.HE]

Antonini F (2013) Origin and growth of nuclear star clusters around massive black holes. ApJ 763(1):62. https://doi.org/10.1088/0004-637X/763/1/62. arXiv:1207.6589 [astro-ph.GA]

Antonini F (2014) On the distribution of stellar remnants around massive black holes: slow mass segregation, star cluster inspirals, and correlated orbits. ApJ 794(2):106. https://doi.org/10.1088/0004-637X/794/2/106. arXiv:1402.4865 [astro-ph.GA]

Antonini F, Gieles M (2020) Population synthesis of black hole binary mergers from star clusters. MNRAS 492(2):2936–2954. https://doi.org/10.1093/mnras/stz3584. arXiv:1906.11855 [astro-ph.HE]

Antonini F, Merritt D (2012) Dynamical friction around supermassive black holes. ApJ 745(1):83. https://doi.org/10.1088/0004-637X/745/1/83. arXiv:1108.1163 [astro-ph.GA]

Antonini F, Merritt D (2013) Relativity and the evolution of the galactic center S-star orbits. ApJ 763(1):L10. https://doi.org/10.1088/2041-8205/763/1/L10. arXiv:1211.4594 [astro-ph.GA]

Antonini F, Perets HB (2012) Secular evolution of compact binaries near massive black holes: gravitational wave sources and other exotica. ApJ 757(1):27. https://doi.org/10.1088/0004-637X/757/1/27. arXiv:1203.2938 [astro-ph.GA]

Antonini F, Chatterjee S, Rodriguez CL, Morscher M, Pattabiraman B, Kalogera V, Rasio FA (2016) Black hole mergers and blue stragglers from hierarchical triples formed in globular clusters. ApJ 816(2):65. https://doi.org/10.3847/0004-637X/816/2/65. arXiv:1509.05080 [astro-ph.GA]

Antonini F, Toonen S, Hamers AS (2017) Binary black hole mergers from field triples: properties, rates, and the impact of stellar evolution. ApJ 841(2):77. https://doi.org/10.3847/1538-4357/aa6f5e. arXiv:1703.06614 [astro-ph.GA]

Antonini F, Rodriguez CL, Petrovich C, Fischer CL (2018) Precessional dynamics of black hole triples: binary mergers with near-zero effective spin. MNRAS 480(1):L58–L62. https://doi.org/10.1093/mnrasl/sly126. arXiv:1711.07142 [astro-ph.HE]

Antonini F, Gieles M, Gualandris A (2019) Black hole growth through hierarchical black hole mergers in dense star clusters: implications for gravitational wave detections. MNRAS 486(4):5008–5021. https://doi.org/10.1093/mnras/stz1149. arXiv:1811.03640 [astro-ph.HE]

Apostolatos TA, Cutler C, Sussman GJ, Thorne KS (1994) Spin-induced orbital precession and its modulation of the gravitational waveforms from merging binaries. Phys Rev D 49(12):6274–6297. https://doi.org/10.1103/PhysRevD.49.6274

Apostolatos TA, Lukes-Gerakopoulos G, Contopoulos G (2009) How to observe a non-Kerr spacetime using gravitational waves. Phys Rev Lett 103(11):111101. https://doi.org/10.1103/PhysRevLett.103.111101. arXiv:0906.0093 [gr-qc]

Applegate JH, Shaham J (1994) Orbital period variability in the eclipsing pulsar binary PSR B1957+20: evidence for a tidally powered star. ApJ 436:312. https://doi.org/10.1086/174906

Arca Sedda M (2020) Birth, life, and death of black hole binaries around supermassive black holes: dynamical evolution of gravitational wave sources. ApJ 891(1):47. https://doi.org/10.3847/1538-4357/ab723b. arXiv:2002.04037 [astro-ph.GA]

Arca Sedda M (2020) Dissecting the properties of neutron star-black hole mergers originating in dense star clusters. Commun Phys 3(1):43. https://doi.org/10.1038/s42005-020-0310-x. arXiv:2003.02279 [astro-ph.GA]

Arca-Sedda M, Capuzzo-Dolcetta R (2014) The globular cluster migratory origin of nuclear star clusters. MNRAS 444(4):3738–3755. https://doi.org/10.1093/mnras/stu1683. arXiv:1405.7593 [astro-ph.GA]

Arca-Sedda M, Capuzzo-Dolcetta R (2017) Lack of nuclear clusters in dwarf spheroidal galaxies: implications for massive black holes formation and the cusp/core problem. MNRAS 464(3):3060–3070. https://doi.org/10.1093/mnras/stw2483. arXiv:1611.01088 [astro-ph.GA]

Arca-Sedda M, Capuzzo-Dolcetta R (2019) The MEGaN project II. Gravitational waves from intermediate-mass and binary black holes around a supermassive black hole. MNRAS 483(1):152–171. https://doi.org/10.1093/mnras/sty3096. arXiv:1709.05567 [astro-ph.GA]

Arca-Sedda M, Gualandris A (2018) Gravitational wave sources from inspiralling globular clusters in the Galactic Centre and similar environments. MNRAS 477(4):4423–4442. https://doi.org/10.1093/mnras/sty922. arXiv:1804.06116 [astro-ph.GA]

Arca Sedda M, Mastrobuono-Battisti A (2019) Mergers of globular clusters in the Galactic disc: intermediate mass black hole coalescence and implications for gravitational waves detection. arXiv e-prints arXiv:1906.05864

Arca-Sedda M, Capuzzo-Dolcetta R, Antonini F, Seth A (2015) Henize 2–10: the ongoing formation of a nuclear star cluster around a massive black hole. ApJ 806(2):220. https://doi.org/10.1088/0004-637X/806/2/220. arXiv:1501.04567 [astro-ph.GA]

Arca Sedda M, Askar A, Giersz M (2018) MOCCA-survey database-I. Unravelling black hole subsystems in globular clusters. MNRAS 479(4):4652–4664. https://doi.org/10.1093/mnras/sty1859. arXiv:1801.00795 [astro-ph.GA]

Arca Sedda M, Askar A, Giersz M (2019a) MOCCA-SURVEY Database I. Intermediate mass black holes in Milky Way globular clusters and their connection to supermassive black holes. arXiv e-prints arXiv:1905.00902 [astro-ph.GA]

Arca Sedda M, Berczik P, Capuzzo-Dolcetta R, Fragione G, Sobolenko M, Spurzem R (2019) Supermassive black holes coalescence mediated by massive perturbers: implications for gravitational waves emission and nuclear cluster formation. MNRAS 484(1):520–542. https://doi.org/10.1093/mnras/sty3458. arXiv:1712.05810 [astro-ph.GA]

Arca Sedda M, Berry CPL, Jani K, Amaro-Seoane P, Auclair P, Baird J, Baker T, Berti E, Breivik K, Burrows A et al (2020) The missing link in gravitational-wave astronomy: discoveries waiting in the decihertz range. Class Quantum Grav 37(21):215011. https://doi.org/10.1088/1361-6382/abb5c1. arXiv:1908.11375 [gr-qc]

Arca Sedda M, Mapelli M, Spera M, Benacquista M, Giacobbo N (2020) Fingerprints of binary black hole formation channels encoded in the mass and spin of merger remnants. ApJ 894(2):133. https://doi.org/10.3847/1538-4357/ab88b2. arXiv:2003.07409 [astro-ph.GA]

Arca Sedda M, Amaro Seoane P, Chen X (2021) Merging stellar and intermediate-mass black holes in dense clusters: implications for LIGO, LISA, and the next generation of gravitational wave detectors. A&A 652:A54. https://doi.org/10.1051/0004-6361/202037785. arXiv:2007.13746 [astro-ph.GA]

Arca Sedda M, Li G, Kocsis B (2021b) Order in the chaos. Eccentric black hole binary mergers in triples formed via strong binary-binary scatterings. A&A 650:A189. https://doi.org/10.1051/0004-6361/202038795. arXiv:1805.06458 [astro-ph.HE]

Arca-Sedda M, Rizzuto FP, Naab T, Ostriker J, Giersz M, Spurzem R (2021) Breaching the limit: formation of GW190521-like and IMBH mergers in young massive clusters. ApJ 920(2):128. https://doi.org/10.3847/1538-4357/ac1419. arXiv:2105.07003 [astro-ph.GA]

Armano M et al (2022) Transient acceleration events in LISA Pathfinder: properties and possible physical origin. Phys Rev D 106:062001. https://doi.org/10.1103/PhysRevD.106.062001. arXiv:2205.11938 [astro-ph.IM]

Armitage PJ, Natarajan P (2002) Accretion during the merger of supermassive black holes. ApJ 567(1):L9–L12. https://doi.org/10.1086/339770. arXiv:astro-ph/0201318 [astro-ph]

Arnason RM, Papei H, Barmby P, Bahramian A, Gorski MD (2021) Distances to galactic X-ray binaries with Gaia DR2. MNRAS 502(4):5455–5470. https://doi.org/10.1093/mnras/stab345. arXiv:2102.02615 [astro-ph.HE]

Arnold VI (1978) Mathematical methods of classical mechanics. Springer, New York

Artale MC, Mapelli M, Giacobbo N, Sabha NB, Spera M, Santoliquido F, Bressan A (2019) Host galaxies of merging compact objects: mass, star formation rate, metallicity, and colours. MNRAS 487 (2):1675–1688. https://doi.org/10.1093/mnras/stz1382. arXiv:1903.00083 [astro-ph.GA]

Artymowicz P, Lin DNC, Wampler EJ (1993) Star trapping and metallicity enrichment in quasars and active galactic nuclei. ApJ 409:592. https://doi.org/10.1086/172690

Arzoumanian Z, Baker PT, Blumer H, Bécsy B, Brazier A, Brook PR, Burke-Spolaor S, Chatterjee S, Chen S, Cordes JM et al (2020) The NANOGrav 12.5 yr data set: search for an isotropic stochastic gravitational-wave background. ApJ 905(2):L34. https://doi.org/10.3847/2041-8213/abd401. arXiv:2009.04496 [astro-ph.HE]

Arzoumanian Z, Baker PT, Brazier A, Brook PR, Burke-Spolaor S, Bécsy B, Charisi M, Chatterjee S, Cordes JM, Cornish NJ et al (2020) Multimessenger gravitational-wave searches with pulsar timing arrays: application to 3C 66B using the NANOGrav 11-year data set. ApJ 900(2):102. https://doi.org/10.3847/1538-4357/ababa1. arXiv:2005.07123 [astro-ph.GA]

Arzoumanian Z et al (2020) The NANOGrav 12.5 yr data set: search for an isotropic stochastic gravitational-wave background. Astrophys J Lett 905(2):L34. https://doi.org/10.3847/2041-8213/abd401. arXiv:2009.04496 [astro-ph.HE]

Askar A, Arca Sedda M, Giersz M (2018) MOCCA-SURVEY database I: galactic globular clusters harbouring a black hole subsystem. MNRAS 478(2):1844–1854. https://doi.org/10.1093/mnras/sty1186. arXiv:1802.05284 [astro-ph.GA]

Askar A, Davies MB, Church RP (2021) Formation of supermassive black holes in galactic nuclei—I. Delivering seed intermediate-mass black holes in massive stellar clusters. MNRAS 502(2):2682–2700. https://doi.org/10.1093/mnras/stab113. arXiv:2006.04922 [astro-ph.GA]

Athanassoula E (2002) Formation and evolution of bars in disc galaxies. In: Athanassoula E, Bosma A, Mujica R (eds) Disks of galaxies: kinematics, dynamics and peturbations. Astronomical society of the pacific conference series, vol 275, pp 141–152. arXiv:astro-ph/0209438 [astro-ph]

Auchettl K, Guillochon J, Ramirez-Ruiz E (2017) New physical insights about tidal disruption events from a comprehensive observational inventory at X-ray wavelengths. ApJ 838(2):149. https://doi.org/10.3847/1538-4357/aa633b. arXiv:1611.02291 [astro-ph.HE]

Auclair P et al (2023) Cosmology with the Laser Interferometer Space Antenna. Living Rev Relativ

Bañados E, Venemans BP, Morganson E, Decarli R, Walter F, Chambers KC, Rix HW, Farina EP, Fan X, Jiang L et al (2014) Discovery of eight z ∼ 6 quasars from Pan-STARRS1. AJ 148(1):14. https://doi.org/10.1088/0004-6256/148/1/14. arXiv:1405.3986 [astro-ph.GA]

Bañados E, Venemans BP, Decarli R, Farina EP, Mazzucchelli C, Walter F, Fan X, Stern D, Schlafly E, Chambers KC et al (2016) The pan-STARRS1 distant z > 5.6 quasar survey: more than 100 quasars within the first Gyr of the universe. ApJS 227(1):11. https://doi.org/10.3847/0067-0049/227/1/11. arXiv:1608.03279 [astro-ph.GA]

Bañados E, Connor T, Stern D, Mulchaey J, Fan X, Decarli R, Farina EP, Mazzucchelli C, Venemans BP, Walter F et al (2018) Chandra X-rays from the redshift 7.54 quasar ULAS J1342+0928. ApJ 856(2):L25. https://doi.org/10.3847/2041-8213/aab61e. arXiv:1803.08105 [astro-ph.GA]

Bañados E, Venemans BP, Mazzucchelli C, Farina EP, Walter F, Wang F, Decarli R, Stern D, Fan X, Davies FB et al (2018) An 800-million-solar-mass black hole in a significantly neutral Universe at a redshift of 7.5. Nature 553(7689):473–476. https://doi.org/10.1038/nature25180. arXiv:1712.01860 [astro-ph.GA]

Bañados E, Novak M, Neeleman M, Walter F, Decarli R, Venemans BP, Mazzucchelli C, Carilli C, Wang F, Fan X et al (2019) The z = 7.54 quasar ULAS J1342+0928 is hosted by a galaxy merger. ApJ 881 (1):L23. https://doi.org/10.3847/2041-8213/ab3659. arXiv:1909.00027 [astro-ph.GA]

Babak S, Fang H, Gair JR, Glampedakis K, Hughes SA (2007) "Kludge" gravitational waveforms for a test-body orbiting a Kerr black hole. Phys Rev D 75(2):024005. https://doi.org/10.1103/PhysRevD.75.024005. arXiv:gr-qc/0607007 [gr-qc]

Babak S, Baker JG, Benacquista MJ, Cornish NJ, Crowder J, Cutler C, Larson SL, Littenberg TB, Porter EK, Vallisneri M et al (2008) Report on the second Mock LISA data challenge. Class Quantum Grav 25(11):114037. https://doi.org/10.1088/0264-9381/25/11/114037. arXiv:0711.2667 [gr-qc]

Babak S, Baker JG, Benacquista MJ, Cornish NJ, Crowder J, Larson SL, Plagnol E, Porter EK, Vallisneri M, Vecchio A et al (2008) The mock LISA data challenges: from challenge 1B to challenge 3. Class Quantum Grav 25(18):184026. https://doi.org/10.1088/0264-9381/25/18/184026. arXiv:0806.2110 [gr-qc]

Babak S, Gair JR, Porter EK (2009) An algorithm for the detection of extreme mass ratio inspirals in LISA data. Class Quantum Grav 26(13):135004. https://doi.org/10.1088/0264-9381/26/13/135004. arXiv:0902.4133 [gr-qc]

Babak S, Baker JG, Benacquista MJ, Cornish NJ, Larson SL, Mandel I, McWilliams ST, Petiteau A, Porter EK, Robinson EL et al (2010) The mock LISA data challenges: from challenge 3 to challenge 4. Class Quantum Grav 27(8):084009. https://doi.org/10.1088/0264-9381/27/8/084009. arXiv:0912.0548 [gr-qc]

Babak S, Gair J, Sesana A, Barausse E, Sopuerta CF, Berry CPL, Berti E, Amaro-Seoane P, Petiteau A, Klein A (2017) Science with the space-based interferometer LISA. V. Extreme mass-ratio inspirals. Phys Rev D 95(10):103012. https://doi.org/10.1103/PhysRevD.95.103012. arXiv:1703.09722 [gr-qc]

Babak S, Hewitson M, Petiteau A (2021) LISA sensitivity and SNR calculations. arXiv e-prints arXiv:2108.01167 [astro-ph.IM]

Bade N, Komossa S, Dahlem M (1996) Detection of an extremely soft X-ray outburst in the HII-like nucleus of NGC 5905. A&A 309:L35–L38

Baghi Q, Thorpe JI, Slutsky J, Baker J, Canton TD, Korsakova N, Karnesis N (2019) Gravitational-wave parameter estimation with gaps in LISA: a Bayesian data augmentation method. Phys Rev D 100(2):022003. https://doi.org/10.1103/PhysRevD.100.022003. arXiv:1907.04747 [gr-qc]

Baghi Q, Korsakova N, Slutsky J, Castelli E, Karnesis N, Bayle JB (2022) Detection and characterization of instrumental transients in LISA Pathfinder and their projection to LISA. Phys Rev D 105(4):042002. https://doi.org/10.1103/PhysRevD.105.042002. arXiv:2112.07490 [gr-qc]

Bahcall JN, Wolf RA (1976) Star distribution around a massive black hole in a globular cluster. ApJ 209:214–232. https://doi.org/10.1086/154711

Bahcall NA (1988) Large-scale structure in the universe indicated by galaxy clusters. ARA&A 26:631–686. https://doi.org/10.1146/annurev.aa.26.090188.003215

Bahramian A, Heinke CO, Tudor V, Miller-Jones JCA, Bogdanov S, Maccarone TJ, Knigge C, Sivakoff GR, Chomiuk L, Strader J et al (2017) The ultracompact nature of the black hole candidate X-ray binary 47 Tuc X9. MNRAS 467(2):2199–2216. https://doi.org/10.1093/mnras/stx166. arXiv:1702.02167 [astro-ph.HE]

Baker JG, Centrella J, Choi DI, Koppitz M, van Meter J (2006) Gravitational-wave extraction from an inspiraling configuration of merging black holes. Phys Rev Lett 96(11):111102. https://doi.org/10.1103/PhysRevLett.96.111102. arXiv:gr-qc/0511103 [gr-qc]

Baldassare VF, Reines AE, Gallo E, Greene JE (2015) A $\sim 50,000$ M$_\odot$ solar mass black hole in the nucleus of RGG 118. ApJ 809(1):L14. https://doi.org/10.1088/2041-8205/809/1/L14. arXiv:1506.07531 [astro-ph.GA]

Baldassare VF, Dickey C, Geha M, Reines AE (2020) Populating the low-mass end of the $M_{BH} - \sigma_*$ relation. ApJ 898(1):L3. https://doi.org/10.3847/2041-8213/aba0c1. arXiv:2006.15150 [astro-ph.GA]

Baldry IK, Glazebrook K, Brinkmann J, Ivezić Ž, Lupton RH, Nichol RC, Szalay AS (2004) Quantifying the bimodal color-magnitude distribution of galaxies. ApJ 600(2):681–694. https://doi.org/10.1086/380092. arXiv:astro-ph/0309710 [astro-ph]

Baldry IK, Driver SP, Loveday J, Taylor EN, Kelvin LS, Liske J, Norberg P, Robotham ASG, Brough S, Hopkins AM et al (2012) Galaxy and Mass Assembly (GAMA): the galaxy stellar mass function at z < 0.06. MNRAS 421(1):621–634. https://doi.org/10.1111/j.1365-2966.2012.20340.x. arXiv:1111.5707 [astro-ph.CO]

Banerjee S (2017) Stellar-mass black holes in young massive and open stellar clusters and their role in gravitational-wave generation. MNRAS 467(1):524–539. https://doi.org/10.1093/mnras/stw3392. arXiv:1611.09357 [astro-ph.HE]

Banerjee S (2018) Stellar-mass black holes in young massive and open stellar clusters and their role in gravitational-wave generation—II. MNRAS 473(1):909–926. https://doi.org/10.1093/mnras/stx2347. arXiv:1707.00922 [astro-ph.HE]

Banerjee S (2020) LISA sources from young massive and open stellar clusters. Phys Rev D 102(10):103002. https://doi.org/10.1103/PhysRevD.102.103002. arXiv:2006.14587 [astro-ph.HE]

Banerjee S (2021) Stellar-mass black holes in young massive and open stellar clusters—IV. Updated stellar-evolutionary and black hole spin models and comparisons with the LIGO-Virgo O1/O2 merger-event data. MNRAS 500(3):3002–3026. https://doi.org/10.1093/mnras/staa2392. arXiv:2004.07382 [astro-ph.HE]

Banerjee S, Baumgardt H, Kroupa P (2010) Stellar-mass black holes in star clusters: implications for gravitational wave radiation. MNRAS 402(1):371–380. https://doi.org/10.1111/j.1365-2966.2009.15880.x. arXiv:0910.3954 [astro-ph.SR]

Banerjee S, Belczynski K, Fryer CL, Berczik P, Hurley JR, Spurzem R, Wang L (2020) BSE versus StarTrack: implementations of new wind, remnant-formation, and natal-kick schemes in NBODY7 and their astrophysical consequences. A&A 639:A41. https://doi.org/10.1051/0004-6361/201935332. arXiv:1902.07718 [astro-ph.SR]

Bansal K, Taylor GB, Peck AB, Zavala RT, Romani RW (2017) Constraining the orbit of the supermassive black hole binary 0402+379. ApJ 843(1):14. https://doi.org/10.3847/1538-4357/aa74e1. arXiv:1705.08556 [astro-ph.GA]

Bar-Or B, Alexander T (2014) The statistical mechanics of relativistic orbits around a massive black hole. Class Quantum Grav 31(24):244003. https://doi.org/10.1088/0264-9381/31/24/244003. arXiv:1404.0351 [astro-ph.GA]

Bar-Or B, Alexander T (2016) Steady-state relativistic stellar dynamics around a massive black hole. ApJ 820(2):129. https://doi.org/10.3847/0004-637X/820/2/129. arXiv:1508.01390 [astro-ph.GA]

Bar-Or B, Fouvry JB (2018) Scalar resonant relaxation of stars around a massive black hole. ApJ 860(2): L23. https://doi.org/10.3847/2041-8213/aac88e. arXiv:1802.08890 [astro-ph.GA]

Bar-Or B, Kupi G, Alexander T (2013) Stellar energy relaxation around a massive black hole. ApJ 764 (1):52. https://doi.org/10.1088/0004-637X/764/1/52. arXiv:1209.4594 [astro-ph.GA]

Barack L, Cutler C (2004) Confusion noise from LISA capture sources. Phys Rev D 70(12):122002. https://doi.org/10.1103/PhysRevD.70.122002. arXiv:gr-qc/0409010 [gr-qc]

Barack L, Cutler C (2004) LISA capture sources: approximate waveforms, signal-to-noise ratios, and parameter estimation accuracy. Phys Rev D 69(8):082005. https://doi.org/10.1103/PhysRevD.69.082005. arXiv:gr-qc/0310125 [gr-qc]

Barack L, Pound A (2019) Self-force and radiation reaction in general relativity. Rep Progress Phys 82 (1):016904. https://doi.org/10.1088/1361-6633/aae552. arXiv:1805.10385 [gr-qc]

Barai P, Murante G, Borgani S, Gaspari M, Granato GL, Monaco P, Ragone-Figueroa C (2016) Kinetic AGN feedback effects on cluster cool cores simulated using SPH. MNRAS 461(2):1548–1567. https://doi.org/10.1093/mnras/stw1389. arXiv:1605.08051 [astro-ph.GA]

Barausse E (2012) The evolution of massive black holes and their spins in their galactic hosts. MNRAS 423(3):2533–2557. https://doi.org/10.1111/j.1365-2966.2012.21057.x. arXiv:1201.5888 [astro-ph.CO]

Barausse E, Rezzolla L (2008) Influence of the hydrodynamic drag from an accretion torus on extreme mass-ratio inspirals. Phys Rev D 77(10):104027. https://doi.org/10.1103/PhysRevD.77.104027. arXiv:0711.4558 [gr-qc]

Barausse E, Rezzolla L (2009) Predicting the direction of the final spin from the coalescence of two black holes. ApJ 704(1):L40–L44. https://doi.org/10.1088/0004-637X/704/1/L40. arXiv:0904.2577 [gr-qc]

Barausse E, Rezzolla L, Petroff D, Ansorg M (2007) Gravitational waves from extreme mass ratio inspirals in nonpure Kerr spacetimes. Phys Rev D 75(6):064026. https://doi.org/10.1103/PhysRevD.75.064026. arXiv:gr-qc/0612123 [gr-qc]

Barausse E, Cardoso V, Pani P (2014) Can environmental effects spoil precision gravitational-wave astrophysics? Phys Rev D 89(10):104059. https://doi.org/10.1103/PhysRevD.89.104059. arXiv:1404.7149 [gr-qc]

Barausse E, Yunes N, Chamberlain K (2016) Theory-agnostic constraints on black-hole dipole radiation with multiband gravitational-wave astrophysics. Phys Rev Lett 116(24):241104. https://doi.org/10.1103/PhysRevLett.116.241104. arXiv:1603.04075 [gr-qc]

Barausse E, Berti E, Hertog T, Hughes SA, Jetzer P, Pani P, Sotiriou TP, Tamanini N, Witek H, Yagi K et al (2020) Prospects for fundamental physics with LISA. Gen Relat Gravit 52(8):81. https://doi.org/10.1007/s10714-020-02691-1. arXiv:2001.09793 [gr-qc]

Barausse E, Dvorkin I, Tremmel M, Volonteri M, Bonetti M (2020) Massive black hole merger rates: the effect of kiloparsec separation wandering and supernova feedback. ApJ 904(1):16. https://doi.org/10.3847/1538-4357/abba7f. arXiv:2006.03065 [astro-ph.GA]

Barclay T, Ramsay G, Hakala P, Napiwotzki R, Nelemans G, Potter S, Todd I (2011) Stellar variability on time-scales of minutes: results from the first 5 yr of the Rapid Temporal Survey. MNRAS 413 (4):2696–2708. https://doi.org/10.1111/j.1365-2966.2011.18345.x. arXiv:1101.2445 [astro-ph.GA]

Barcons X, Nandra K, Barret D, den Herder JW, Fabian AC, Piro L, Watson MG, the Athena Team (2015) Athena: the X-ray observatory to study the hot and energetic Universe. J Phys Conf Ser 610:012008. https://doi.org/10.1088/1742-6596/610/1/012008

Bardeen JM (1970) Kerr metric black holes. Nature 226(5240):64–65. https://doi.org/10.1038/226064a0

Bardeen JM, Petterson JA (1975) The Lense-Thirring effect and accretion disks around Kerr black holes. ApJ 195:L65. https://doi.org/10.1086/181711

Barrow KSS, Aykutalp A, Wise JH (2018) Observational signatures of massive black hole formation in the early Universe. Nat Astron 2:987–994. https://doi.org/10.1038/s41550-018-0569-y. arXiv:1809.03526 [astro-ph.GA]

Barstow MA, Casewell SL, Catalan S, Copperwheat C, Gaensicke B, Garcia-Berro E, Hambly N, Heber U, Holberg J, Isern J et al (2014) White paper: Gaia and the end states of stellar evolution. arXiv e-prints arXiv:1407.6163

Bartko H, Martins F, Fritz TK, Genzel R, Levin Y, Perets HB, Paumard T, Nayakshin S, Gerhard O, Alexander T et al (2009) Evidence for warped disks of young stars in the galactic center. ApJ 697 (2):1741–1763. https://doi.org/10.1088/0004-637X/697/2/1741. arXiv:0811.3903 [astro-ph]

Bartolo N, De Luca V, Franciolini G, Peloso M, Racco D, Riotto A (2019) Testing primordial black holes as dark matter with LISA. Phys Rev D 99(10):103521. https://doi.org/10.1103/PhysRevD.99.103521. arXiv:1810.12224 [astro-ph.CO]

Bartos I, Kocsis B, Haiman Z, Márka S (2017) Rapid and bright stellar-mass binary black hole mergers in active galactic nuclei. ApJ 835(2):165. https://doi.org/10.3847/1538-4357/835/2/165. arXiv:1602.03831 [astro-ph.HE]

Baruteau C, Masset F (2013) Recent developments in planet migration theory. In: Souchay J, Mathis S, Tokieda T (eds) Tides in astronomy and astrophysics. Lecture notes in physics, vol 861. Springer, Berlin, pp 201–253. https://doi.org/10.1007/978-3-642-32961-6_6

Baruteau C, Cuadra J, Lin DNC (2011) Binaries migrating in a gaseous disk: where are the galactic center binaries? ApJ 726(1):28. https://doi.org/10.1088/0004-637X/726/1/28. arXiv:1011.0360 [astro-ph. GA]

Bassini L, Rasia E, Borgani S, Ragone-Figueroa C, Biffi V, Dolag K, Gaspari M, Granato GL, Murante G, Taffoni G et al (2019) Black hole mass of central galaxies and cluster mass correlation in cosmological hydro-dynamical simulations. A&A 630:A144. https://doi.org/10.1051/0004-6361/201935383. arXiv:1903.03142 [astro-ph.GA]

Bastian N, Covey KR, Meyer MR (2010) A universal stellar initial mass function? A critical look at variations. ARA&A 48:339–389. https://doi.org/10.1146/annurev-astro-082708-101642. arXiv:1001.2965 [astro-ph.GA]

Baumgardt H (2009) Dissolution of globular clusters. In: Richtler T, Larsen S (eds) Globular clusters—guides to galaxies. Springer, pp 387–394. https://doi.org/10.1007/978-3-540-76961-3_89

Baumgardt H, Amaro-Seoane P, Schödel R (2018) The distribution of stars around the Milky Way's central black hole. III. Comparison with simulations. A&A 609:A28. https://doi.org/10.1051/0004-6361/201730462. arXiv:1701.03818 [astro-ph.GA]

Bavera SS, Fragos T, Qin Y, Zapartas E, Neijssel CJ, Mandel I, Batta A, Gaebel SM, Kimball C, Stevenson S (2020) The origin of spin in binary black holes. Predicting the distributions of the main observables of Advanced LIGO. A&A 635:A97. https://doi.org/10.1051/0004-6361/201936204. arXiv:1906.12257 [astro-ph.HE]

Bavera SS, Fragos T, Zevin M, Berry CPL, Marchant P, Andrews JJ, Coughlin S, Dotter A, Kovlakas K, Misra D et al (2021) The impact of mass-transfer physics on the observable properties of field binary black hole populations. A&A 647:A153. https://doi.org/10.1051/0004-6361/202039804. arXiv:2010.16333 [astro-ph.HE]

Begelman MC, Blandford RD, Rees MJ (1980) Massive black hole binaries in active galactic nuclei. Nature 287(5780):307–309. https://doi.org/10.1038/287307a0

Bekenstein JD (1973) Gravitational-radiation recoil and runaway black holes. ApJ 183:657–664. https://doi.org/10.1086/152255

Belczynski K, Kalogera V, Bulik T (2002) A comprehensive study of binary compact objects as gravitational wave sources: evolutionary channels, rates, and physical properties. ApJ 572(1):407–431. https://doi.org/10.1086/340304. arXiv:astro-ph/0111452 [astro-ph]

Belczynski K, Kalogera V, Rasio FA, Taam RE, Zezas A, Bulik T, Maccarone TJ, Ivanova N (2008) Compact object modeling with the Startrack population synthesis code. ApJS 174(1):223–260. https://doi.org/10.1086/521026. arXiv:astro-ph/0511811 [astro-ph]

Belczynski K, Benacquista M, Bulik T (2010) Double compact objects as low-frequency gravitational wave sources. ApJ 725(1):816–823. https://doi.org/10.1088/0004-637X/725/1/816. arXiv:0811.1602 [astro-ph]

Belczynski K, Dominik M, Bulik T, O'Shaughnessy R, Fryer C, Holz DE (2010) The effect of metallicity on the detection prospects for gravitational waves. ApJ 715(2):L138–L141. https://doi.org/10.1088/2041-8205/715/2/L138. arXiv:1004.0386 [astro-ph.HE]

Belczynski K, Bulik T, Fryer CL (2012) High mass X-ray binaries: future evolution and fate. arXiv e-prints arXiv:1208.2422

Belczynski K, Bulik T, Mandel I, Sathyaprakash BS, Zdziarski AA, Mikołajewska J (2013) Cyg X-3: a galactic double black hole or black-hole-neutron-star progenitor. ApJ 764(1):96. https://doi.org/10.1088/0004-637X/764/1/96. arXiv:1209.2658 [astro-ph.HE]

Belczynski K, Buonanno A, Cantiello M, Fryer CL, Holz DE, Mandel I, Miller MC, Walczak M (2014) The formation and gravitational-wave detection of massive stellar black hole binaries. ApJ 789:120. https://doi.org/10.1088/0004-637X/789/2/120. arXiv:1403.0677 [astro-ph.HE]

Belczynski K, Holz DE, Bulik T, O'Shaughnessy R (2016) The first gravitational-wave source from the isolated evolution of two stars in the 40–100 solar mass range. Nature 534(7608):512–515. https://doi.org/10.1038/nature18322. arXiv:1602.04531 [astro-ph.HE]

Belczynski K, Repetto S, Holz DE, O'Shaughnessy R, Bulik T, Berti E, Fryer C, Dominik M (2016) Compact binary merger rates: comparison with LIGO/Virgo upper limits. ApJ 819(2):108. https://doi.org/10.3847/0004-637X/819/2/108. arXiv:1510.04615 [astro-ph.HE]

Belczynski K, Klencki J, Fields CE, Olejak A, Berti E, Meynet G, Fryer CL, Holz DE, O'Shaughnessy R, Brown DA et al (2020) Evolutionary roads leading to low effective spins, high black hole masses, and O1/O2 rates for LIGO/Virgo binary black holes. A&A 636:A104. https://doi.org/10.1051/0004-6361/201936528. arXiv:1706.07053 [astro-ph.HE]

Bell KJ, Gianninas A, Hermes JJ, Winget DE, Kilic M, Montgomery MH, Castanheira BG, Vanderbosch Z, Winget KI, Brown WR (2017) Pruning the ELM survey: characterizing candidate low-mass white dwarfs through photometric variability. ApJ 835(2):180. https://doi.org/10.3847/1538-4357/835/2/180. arXiv:1612.06390 [astro-ph.SR]

Bellm EC, Kulkarni SR, Graham MJ, Dekany R, Smith RM, Riddle R, Masci FJ et al (2019) The Zwicky transient facility: system overview, performance, and first results. PASP 131(995):018002. https://doi.org/10.1088/1538-3873/aaecbe. arXiv:1902.01932 [astro-ph.IM]

Belloni D, Giersz M, Askar A, Leigh N, Hypki A (2016) MOCCA-SURVEY database I. Accreting white dwarf binary systems in globular clusters—I. Cataclysmic variables—present-day population. MNRAS 462(3):2950–2969. https://doi.org/10.1093/mnras/stw1841. arXiv:1607.07619 [astro-ph.GA]

Bellovary JM, Governato F, Quinn TR, Wadsley J, Shen S, Volonteri M (2010) Wandering black holes in bright disk galaxy halos. ApJ 721(2):L148–L152. https://doi.org/10.1088/2041-8205/721/2/L148. arXiv:1008.5147 [astro-ph.CO]

Bellovary JM, Mac Low MM, McKernan B, Ford KES (2016) Migration traps in disks around supermassive black holes. ApJ 819(2):L17. https://doi.org/10.3847/2041-8205/819/2/L17. arXiv:1511.00005 [astro-ph.GA]

Bellovary JM, Cleary CE, Munshi F, Tremmel M, Christensen CR, Brooks A, Quinn TR (2019) Multimessenger signatures of massive black holes in dwarf galaxies. MNRAS 482(3):2913–2923. https://doi.org/10.1093/mnras/sty2842. arXiv:1806.00471 [astro-ph.GA]

Belokurov V, Evans NW, Irwin MJ, Hewett PC, Wilkinson MI (2006) The discovery of tidal tails around the globular cluster NGC 5466. ApJ 637(1):L29–L32. https://doi.org/10.1086/500362. arXiv:astro-ph/0511767 [astro-ph]

Belotsky KM, Dmitriev AE, Esipova EA, Gani VA, Grobov AV, Khlopov MY, Kirillov AA, Rubin SG, Svadkovsky IV (2014) Signatures of primordial black hole dark matter. Mod Phys Lett A 29(37):1440005. https://doi.org/10.1142/S0217732314400057. arXiv:1410.0203 [astro-ph.CO]

Benacquista M, Holley-Bockelmann K (2006) Consequences of disk scale height on LISA confusion noise from close white dwarf binaries. ApJ 645(1):589–596. https://doi.org/10.1086/504024. arXiv:astro-ph/0504135 [astro-ph]

Benacquista MJ (2011) Tidal perturbations to the gravitational Inspiral of J0651+2844. ApJ 740(2):L54. https://doi.org/10.1088/2041-8205/740/2/L54. arXiv:1109.2744 [astro-ph.SR]

Bender PL, Hils D (1997) Confusion noise level due to galactic and extragalactic binaries. Class Quantum Grav 14(6):1439–1444. https://doi.org/10.1088/0264-9381/14/6/008

Bender R, Kormendy J, Bower G, Green R, Thomas J, Danks AC, Gull T, Hutchings JB, Joseph CL, Kaiser ME et al (2005) HST STIS spectroscopy of the triple nucleus of M31: two nested disks in Keplerian rotation around a supermassive black hole. ApJ 631(1):280–300. https://doi.org/10.1086/432434. arXiv:astro-ph/0509839 [astro-ph]

Beniamini P, Piran T (2016) Formation of double neutron star systems as implied by observations. MNRAS 456(4):4089–4099. https://doi.org/10.1093/mnras/stv2903. arXiv:1510.03111 [astro-ph.HE]

Benvenuto OG, De Vito MA, Horvath JE (2014) Understanding the evolution of close binary systems with radio pulsars. ApJ 786(1):L7. https://doi.org/10.1088/2041-8205/786/1/L7. arXiv:1402.7338 [astro-ph.SR]

Berczik P, Merritt D, Spurzem R (2005) Long-term evolution of massive black hole binaries. II. Binary evolution in low-density galaxies. ApJ 633(2):680–687. https://doi.org/10.1086/491598. arXiv:astro-ph/0507260 [astro-ph]

Berczik P, Merritt D, Spurzem R, Bischof HP (2006) Efficient merger of binary supermassive black holes in nonaxisymmetric galaxies. ApJ 642(1):L21–L24. https://doi.org/10.1086/504426. arXiv:astro-ph/0601698 [astro-ph]

Berczik P, Nitadori K, Zhong S, Spurzem R, Hamada T, Wang X, Berentzen I, Veles A, Ge W (2011) High performance massively parallel direct N-body simulations on large GPU clusters. In: International conference on high performance computing, pp 8–18

Berczik P, Spurzem R, Wang L, Zhong S, Huang S (2013) Up to 700k GPU cores, Kepler, and the Exascale future for simulations of star clusters around black holes. In: Third international conference high performance computing, pp 52–59. arXiv:1312.1789 [astro-ph.IM]

Berrier JC, Davis BL, Kennefick D, Kennefick JD, Seigar MS, Barrows RS, Hartley M, Shields D, Bentz MC, Lacy CHS (2013) Further evidence for a supermassive black hole mass-pitch angle relation. ApJ 769(2):132. https://doi.org/10.1088/0004-637X/769/2/132. arXiv:1304.4937 [astro-ph.GA]

Berry C, Hughes S, Sopuerta C, Chua A, Heffernan A, Holley-Bockelmann K, Mihaylov D, Miller C, Sesana A (2019) The unique potential of extreme mass-ratio inspirals for gravitational-wave astronomy. BAAS 51(3):42 arXiv:1903.03686 [astro-ph.HE]

Berry CPL, Gair JR (2013) Expectations for extreme-mass-ratio bursts from the Galactic Centre. MNRAS 435(4):3521–3540. https://doi.org/10.1093/mnras/stt1543. arXiv:1307.7276 [astro-ph.HE]

Berry CPL, Gair JR (2013) Extreme-mass-ratio-bursts from extragalactic sources. MNRAS 433(4):3572–3583. https://doi.org/10.1093/mnras/stt990. arXiv:1306.0774 [astro-ph.HE]

Berry CPL, Gair JR (2013) Observing the Galaxy's massive black hole with gravitational wave bursts. MNRAS 429(1):589–612. https://doi.org/10.1093/mnras/sts360. arXiv:1210.2778 [astro-ph.HE]

Berry CPL, Cole RH, Cañizares P, Gair JR (2016) Importance of transient resonances in extreme-mass-ratio inspirals. Phys Rev D 94(12):124042. https://doi.org/10.1103/PhysRevD.94.124042. arXiv:1608.08951 [gr-qc]

Berti E, Volonteri M (2008) Cosmological black hole spin evolution by mergers and accretion. ApJ 684(2):822–828. https://doi.org/10.1086/590379. arXiv:0802.0025 [astro-ph]

Berti E, Kesden M, Sperhake U (2012) Effects of post-Newtonian spin alignment on the distribution of black-hole recoils. Phys Rev D 85(12):124049. https://doi.org/10.1103/PhysRevD.85.124049. arXiv:1203.2920 [astro-ph.HE]

Berti E, Yagi K, Yang H, Yunes N (2018) Extreme gravity tests with gravitational waves from compact binary coalescences: (II) ringdown. Gen Relativ Gravit 50(5):49. https://doi.org/10.1007/s10714-018-2372-6. arXiv:1801.03587 [gr-qc]

Bertone G, Merritt D (2005) Time-dependent models for dark matter at the galactic center. Phys Rev D 72(10):103502. https://doi.org/10.1103/PhysRevD.72.103502. arXiv:astro-ph/0501555 [astro-ph]

Bertone G, Zentner AR, Silk J (2005) New signature of dark matter annihilations: Gamma rays from intermediate-mass black holes. Phys Rev D 72(10):103517. https://doi.org/10.1103/PhysRevD.72.103517. arXiv:astro-ph/0509565 [astro-ph]

Beuermann K, Dreizler S, Hessman FV, Deller J (2012) The quest for companions to post-common envelope binaries. III. A reexamination of <ASTROBJ> HW Virginis </ASTROBJ> . A&A 543: A138. https://doi.org/10.1051/0004-6361/201219391. arXiv:1206.3080 [astro-ph.SR]

Bhattacharya D, van den Heuvel EPJ (1991) Formation and evolution of binary and millisecond radio pulsars. Phys Rep 203(1–2):1–124. https://doi.org/10.1016/0370-1573(91)90064-S

Biava N, Colpi M, Capelo PR, Bonetti M, Volonteri M, Tamfal T, Mayer L, Sesana A (2019) The lifetime of binary black holes in Sérsic galaxy models. MNRAS 487(4):4985–4994. https://doi.org/10.1093/mnras/stz1614. arXiv:1903.05682 [astro-ph.GA]

Bildsten L, Cutler C (1992) Tidal interactions of inspiraling compact binaries. ApJ 400:175. https://doi.org/10.1086/171983

Bildsten L, Salpeter EE, Wasserman I (1992) The fate of accreted CNO elements in neutron star atmospheres: X-ray bursts and gamma-ray lines. ApJ 384:143. https://doi.org/10.1086/170860

Bildsten L, Shen KJ, Weinberg NN, Nelemans G (2007) Faint thermonuclear supernovae from AM Canum Venaticorum binaries. ApJ 662(2):L95–L98. https://doi.org/10.1086/519489. arXiv:astro-ph/0703578 [astro-ph]

Binggeli B, Barazza F, Jerjen H (2000) Off-center nuclei in dwarf elliptical galaxies. A&A 359:447–456

Binney J, Tremaine S (1987) Galactic dynamics. Princeton University Press, Princeton

Bird S, Cholis I, Muñoz JB, Ali-Haïmoud Y, Kamionkowski M, Kovetz ED, Raccanelli A, Riess AG (2016) Did LIGO detect dark matter? Phys Rev Lett 116(20):201301. https://doi.org/10.1103/PhysRevLett.116.201301. arXiv:1603.00464 [astro-ph.CO]

Bitsch B, Kley W (2010) Orbital evolution of eccentric planets in radiative discs. A&A 523:A30. https://doi.org/10.1051/0004-6361/201014414. arXiv:1008.2656 [astro-ph.EP]

Bitsch B, Kley W (2011) Evolution of inclined planets in three-dimensional radiative discs. A&A 530:A41. https://doi.org/10.1051/0004-6361/201016179. arXiv:1104.2408 [astro-ph.EP]

Blaauw A (1961) On the origin of the O- and B-type stars with high velocities (the "run-away" stars), and some related problems. Bull Astron Inst Neth 15:265

Blaes O, Lee MH, Socrates A (2002) The Kozai mechanism and the evolution of binary supermassive black holes. ApJ 578(2):775–786. https://doi.org/10.1086/342655. arXiv:astro-ph/0203370 [astro-ph]

Blanchet L (2014) Gravitational radiation from post-Newtonian sources and inspiralling compact binaries. Living Rev Relativ 17:2. https://doi.org/10.12942/lrr-2014-2. arXiv:1310.1528 [gr-qc]

Blanchet L (2019) Analytic approximations in GR and gravitational waves. Int J Mod Phys D 28(6):1930011–144. https://doi.org/10.1142/S0218271819300118. arXiv:1812.07490 [gr-qc]

Blanchet L, Qusailah MSS, Will CM (2005) Gravitational recoil of inspiraling black hole binaries to second post-Newtonian order. ApJ 635(1):508–515. https://doi.org/10.1086/497332. arXiv:astro-ph/0507692 [astro-ph]

Blandford RD, Znajek RL (1977) Electromagnetic extraction of energy from Kerr black holes. MNRAS 179:433–456. https://doi.org/10.1093/mnras/179.3.433

Blecha L, Loeb A (2008) Effects of gravitational-wave recoil on the dynamics and growth of supermassive black holes. MNRAS 390(4):1311–1325. https://doi.org/10.1111/j.1365-2966.2008.13790.x. arXiv:0805.1420 [astro-ph]

Blecha L, Cox TJ, Loeb A, Hernquist L (2011) Recoiling black holes in merging galaxies: relationship to active galactic nucleus lifetimes, starbursts and the M_{BH}-σ_* relation. MNRAS 412(4):2154–2182. https://doi.org/10.1111/j.1365-2966.2010.18042.x. arXiv:1009.4940 [astro-ph.CO]

Blecha L, Sijacki D, Kelley LZ, Torrey P, Vogelsberger M, Nelson D, Springel V, Snyder G, Hernquist L (2016) Recoiling black holes: prospects for detection and implications of spin alignment. MNRAS 456(1):961–989. https://doi.org/10.1093/mnras/stv2646. arXiv:1508.01524 [astro-ph.GA]

Blelly A, Bobin J, Moutarde H (2022) Sparse data inpainting for the recovery of Galactic-binary gravitational wave signals from gapped data. MNRAS 509(4):5902–5917. https://doi.org/10.1093/mnras/stab3314. arXiv:2104.05250 [gr-qc]

Bloom JS, Sigurdsson S, Pols OR (1999) The spatial distribution of coalescing neutron star binaries: implications for gamma-ray bursts. MNRAS 305(4):763–769. https://doi.org/10.1046/j.1365-8711.1999.02437.x. arXiv:astro-ph/9805222 [astro-ph]

Bobrick A, Davies MB, Church RP (2017) Mass transfer in white dwarf-neutron star binaries. MNRAS 467(3):3556–3575. https://doi.org/10.1093/mnras/stx312. arXiv:1702.02377 [astro-ph.HE]

Boco L, Lapi A, Goswami S, Perrotta F, Baccigalupi C, Danese L (2019) Merging rates of compact binaries in galaxies: perspectives for gravitational wave detections. ApJ 881(2):157. https://doi.org/10.3847/1538-4357/ab328e. arXiv:1907.06841 [astro-ph.GA]

Boekholt TCN, Schleicher DRG, Fellhauer M, Klessen RS, Reinoso B, Stutz AM, Haemmerlé L (2018) Formation of massive seed black holes via collisions and accretion. MNRAS 476(1):366–380. https://doi.org/10.1093/mnras/sty208. arXiv:1801.05841 [astro-ph.GA]

Bogdán Á, Forman WR, Zhuravleva I, Mihos JC, Kraft RP, Harding P, Guo Q, Li Z, Churazov E, Vikhlinin A et al (2012) Exploring the unusually high black-hole-to-bulge mass ratios in NGC 4342 and NGC 4291: the asynchronous growth of bulges and black holes. ApJ 753(2):140. https://doi.org/10.1088/0004-637X/753/2/140. arXiv:1203.1641 [astro-ph.CO]

Bogdanović T, Reynolds CS, Miller MC (2007) Alignment of the spins of supermassive black holes prior to coalescence. ApJ 661(2):L147–L150. https://doi.org/10.1086/518769. arXiv:astro-ph/0703054 [astro-ph]

Bon E, Zucker S, Netzer H, Marziani P, Bon N, Jovanović P, Shapovalova AI, Komossa S, Gaskell CM, Popović LČ et al (2016) Evidence for periodicity in 43 year-long monitoring of NGC 5548. ApJS 225(2):29. https://doi.org/10.3847/0067-0049/225/2/29. arXiv:1606.04606 [astro-ph.HE]

Bondi H (1952) On spherically symmetrical accretion. MNRAS 112:195. https://doi.org/10.1093/mnras/112.2.195

Bondi H, Hoyle F (1944) On the mechanism of accretion by stars. MNRAS 104:273. https://doi.org/10.1093/mnras/104.5.273

Bonetti M, Sesana A (2020) Gravitational wave background from extreme mass ratio inspirals. Phys Rev D 102(10):103023. https://doi.org/10.1103/PhysRevD.102.103023. arXiv:2007.14403 [astro-ph.GA]

Bonetti M, Haardt F, Sesana A, Barausse E (2018) Post-Newtonian evolution of massive black hole triplets in galactic nuclei—II. Survey of the parameter space. MNRAS 477(3):3910–3926. https://doi.org/10.1093/mnras/sty896. arXiv:1709.06088 [astro-ph.GA]

Bonetti M, Sesana A, Haardt F, Barausse E, Colpi M (2019) Post-Newtonian evolution of massive black hole triplets in galactic nuclei—IV. Implications for LISA. MNRAS 486(3):4044–4060. https://doi.org/10.1093/mnras/stz903. arXiv:1812.01011 [astro-ph.GA]

Bonetti M, Bortolas E, Lupi A, Dotti M, Raimundo SI (2020) Dynamical friction-driven orbital circularization in rotating discs: a semi-analytical description. MNRAS 494(2):3053–3059. https://doi.org/10.1093/mnras/staa964. arXiv:2002.04621 [astro-ph.GA]

Bonetti M, Rasskazov A, Sesana A, Dotti M, Haardt F, Leigh NWC, Arca Sedda M, Fragione G, Rossi E (2020) On the eccentricity evolution of massive black hole binaries in stellar backgrounds. MNRAS 493(1):L114–L119. https://doi.org/10.1093/mnrasl/slaa018. arXiv:2001.02231 [astro-ph.GA]

Bonetti M, Bortolas E, Lupi A, Dotti M (2021) Dynamical evolution of massive perturbers in realistic multicomponent galaxy models I: implementation and validation. MNRAS 502(3):3554–3568. https://doi.org/10.1093/mnras/stab222. arXiv:2010.08555 [astro-ph.GA]

Bonfini P, Bitsakis T, Zezas A, Duc PA, Iodice E, González-Martín O, Bruzual G, González Sanoja AJ (2018) Connecting traces of galaxy evolution: the missing core mass-morphological fine structure relation. MNRAS 473(1):L94–L100. https://doi.org/10.1093/mnrasl/slx169. arXiv:1710.05025 [astro-ph.GA]

Bonga B, Yang H, Hughes SA (2019) Tidal resonance in extreme mass-ratio inspirals. Phys Rev Lett 123(10):101103. https://doi.org/10.1103/PhysRevLett.123.101103. arXiv:1905.00030 [gr-qc]

Bonnor WB, Rotenberg MA (1961) Transport of momentum by gravitational waves: the linear approximation. Proc R Soc Lond Ser A 265(1320):109–116. https://doi.org/10.1098/rspa.1961.0226

Bonoli S, Mayer L, Callegari S (2014) Massive black hole seeds born via direct gas collapse in galaxy mergers: their properties, statistics and environment. MNRAS 437(2):1576–1592. https://doi.org/10.1093/mnras/stt1990. arXiv:1211.3752 [astro-ph.CO]

Bonoli S, Mayer L, Kazantzidis S, Madau P, Bellovary J, Governato F (2016) Black hole starvation and bulge evolution in a Milky Way-like galaxy. MNRAS 459(3):2603–2617. https://doi.org/10.1093/mnras/stw694. arXiv:1508.07328 [astro-ph.GA]

Bortolas E, Mapelli M (2019) Can supernova kicks trigger EMRIs in the Galactic Centre? MNRAS 485(2):2125–2138. https://doi.org/10.1093/mnras/stz440. arXiv:1902.04581 [astro-ph.GA]

Bortolas E, Gualandris A, Dotti M, Spera M, Mapelli M (2016) Brownian motion of massive black hole binaries and the final parsec problem. MNRAS 461(1):1023–1031. https://doi.org/10.1093/mnras/stw1372. arXiv:1606.06728 [astro-ph.GA]

Bortolas E, Gualandris A, Dotti M, Read JI (2018) The influence of massive black hole binaries on the morphology of merger remnants. MNRAS 477(2):2310–2325. https://doi.org/10.1093/mnras/sty775. arXiv:1710.04658 [astro-ph.GA]

Bortolas E, Mapelli M, Spera M (2018) Star cluster disruption by a massive black hole binary. MNRAS 474(1):1054–1064. https://doi.org/10.1093/mnras/stx2795. arXiv:1710.09418 [astro-ph.GA]

Bortolas E, Capelo PR, Zana T, Mayer L, Bonetti M, Dotti M, Davies MB, Madau P (2020) Global torques and stochasticity as the drivers of massive black hole pairing in the young Universe. MNRAS 498(3):3601–3615. https://doi.org/10.1093/mnras/staa2628. arXiv:2005.02409 [astro-ph.GA]

Bortolas E, Franchini A, Bonetti M, Sesana A (2021) The competing effect of gas and stars in the evolution of massive black hole binaries. ApJ 918(1):L15. https://doi.org/10.3847/2041-8213/ac1c0c. arXiv:2108.13436 [astro-ph.HE]

Bortolas E, Bonetti M, Dotti M, Lupi A, Capelo PR, Mayer L, Sesana A (2022) The role of bars on the dynamical-friction-driven inspiral of massive objects. MNRAS 512(3):3365–3382. https://doi.org/10.1093/mnras/stac645. arXiv:2103.07486 [astro-ph.GA]

Bourne MA, Sijacki D (2017) AGN jet feedback on a moving mesh: cocoon inflation, gas flows and turbulence. MNRAS 472(4):4707–4735. https://doi.org/10.1093/mnras/stx2269. arXiv:1705.07900 [astro-ph.GA]

Bowen DB, Mewes V, Campanelli M, Noble SC, Krolik JH, Zilhão M (2018) Quasi-periodic behavior of mini-disks in binary black holes approaching merger. ApJ 853(1):L17. https://doi.org/10.3847/2041-8213/aaa756. arXiv:1712.05451 [astro-ph.HE]

Bowen DB, Mewes V, Noble SC, Avara M, Campanelli M, Krolik JH (2019) Quasi-periodicity of supermassive binary black hole accretion approaching merger. ApJ 879(2):76. https://doi.org/10.3847/1538-4357/ab2453. arXiv:1904.12048 [astro-ph.HE]

Bowen DB et al (2017) Relativistic dynamics and mass exchange in binary black hole mini-disks. ApJ 838 (1):42. https://doi.org/10.3847/1538-4357/aa63f3

Bower RG, Benson AJ, Malbon R, Helly JC, Frenk CS, Baugh CM, Cole S, Lacey CG (2006) Breaking the hierarchy of galaxy formation. MNRAS 370(2):645–655. https://doi.org/10.1111/j.1365-2966.2006.10519.x. arXiv:astro-ph/0511338 [astro-ph]

Boylan-Kolchin M, Ma CP, Quataert E (2004) Core formation in galactic nuclei due to recoiling black holes. ApJ 613(1):L37–L40. https://doi.org/10.1086/425073. arXiv:astro-ph/0407488 [astro-ph]

Bray JC, Eldridge JJ (2016) Neutron star kicks and their relationship to supernovae ejecta mass. MNRAS 461(4):3747–3759. https://doi.org/10.1093/mnras/stw1275. arXiv:1605.09529 [astro-ph.HE]

Breedt E, Steeghs D, Marsh TR, Gentile Fusillo NP, Tremblay PE, Green M, De Pasquale S, Hermes JJ, Gänsicke BT, Parsons SG et al (2017) Using large spectroscopic surveys to test the double degenerate model for Type Ia supernovae. MNRAS 468(3):2910–2922. https://doi.org/10.1093/mnras/stx430. arXiv:1702.05117 [astro-ph.SR]

Breen PG, Heggie DC (2013) Dynamical evolution of black hole subsystems in idealized star clusters. MNRAS 432(4):2779–2797. https://doi.org/10.1093/mnras/stt628. arXiv:1304.3401 [astro-ph.GA]

Bregman M, Alexander T (2012) The torquing of circumnuclear accretion disks by stars and the evolution of massive black holes. ApJ 748(1):63. https://doi.org/10.1088/0004-637X/748/1/63. arXiv:1109.5384 [astro-ph.GA]

Breivik K, Rodriguez CL, Larson SL, Kalogera V, Rasio FA (2016) Distinguishing between formation channels for binary black holes with LISA. ApJ 830(1):L18. https://doi.org/10.3847/2041-8205/830/1/L18. arXiv:1606.09558 [astro-ph.GA]

Breivik K, Chatterjee S, Larson SL (2017) Revealing black holes with Gaia. ApJ 850(1):L13. https://doi.org/10.3847/2041-8213/aa97d5. arXiv:1710.04657 [astro-ph.SR]

Breivik K, Kremer K, Bueno M, Larson SL, Coughlin S, Kalogera V (2018) Characterizing accreting double white dwarf binaries with the laser interferometer space antenna and Gaia. ApJ 854(1):L1. https://doi.org/10.3847/2041-8213/aaaa23. arXiv:1710.08370 [astro-ph.SR]

Breivik K, Coughlin S, Zevin M, Rodriguez CL, Kremer K, Ye CS, Andrews JJ, Kurkowski M, Digman MC, Larson SL et al (2020) COSMIC variance in binary population synthesis. ApJ 898(1):71. https://doi.org/10.3847/1538-4357/ab9d85. arXiv:1911.00903 [astro-ph.HE]

Breivik K, Mingarelli CMF, Larson SL (2020) Constraining galactic structure with the LISA white dwarf foreground. ApJ 901(1):4. https://doi.org/10.3847/1538-4357/abab99. arXiv:1912.02200 [astro-ph.GA]

Brem P, Amaro-Seoane P, Spurzem R (2013) Relativistic mergers of compact binaries in clusters: the fingerprint of the spin. MNRAS 434(4):2999–3007. https://doi.org/10.1093/mnras/stt1220. arXiv:1302.3135 [astro-ph.CO]

Brem P, Amaro-Seoane P, Sopuerta CF (2014) Blocking low-eccentricity EMRIs: a statistical direct-summation N-body study of the Schwarzschild barrier. MNRAS 437(2):1259–1267. https://doi.org/10.1093/mnras/stt1948. arXiv:1211.5601 [astro-ph.CO]

Brenneman LW, Reynolds CS (2006) Constraining black hole spin via X-ray spectroscopy. ApJ 652 (2):1028–1043. https://doi.org/10.1086/508146. arXiv:astro-ph/0608502 [astro-ph]

Brenneman LW, Reynolds CS, Nowak MA, Reis RC, Trippe M, Fabian AC, Iwasawa K, Lee JC, Miller JM, Mushotzky RF et al (2011) The spin of the supermassive black hole in NGC 3783. ApJ 736 (2):103. https://doi.org/10.1088/0004-637X/736/2/103. arXiv:1104.1172 [astro-ph.HE]

Brough S, Collins C, Demarco R, Ferguson HC, Galaz G, Holwerda B, Martinez-Lombilla C, Mihos C, Montes M (2020) The vera rubin observatory legacy survey of space and time and the low surface brightness universe. arXiv e-prints arXiv:2001.11067 [astro-ph.GA]

Brown WR, Kilic M, Allende Prieto C, Kenyon SJ (2010) The ELM survey. I. A complete sample of extremely low-mass white dwarfs. ApJ 723(2):1072–1081. https://doi.org/10.1088/0004-637X/723/2/1072. arXiv:1011.3050 [astro-ph.GA]

Brown WR, Kilic M, Hermes JJ, Allende Prieto C, Kenyon SJ, Winget DE (2011) A 12 minute orbital period detached white dwarf eclipsing binary. ApJ 737(1):L23. https://doi.org/10.1088/2041-8205/737/1/L23. arXiv:1107.2389 [astro-ph.GA]

Brown WR, Kilic M, Kenyon SJ, Gianninas A (2016) Most double degenerate low-mass white dwarf binaries merge. ApJ 824(1):46. https://doi.org/10.3847/0004-637X/824/1/46. arXiv:1604.04269 [astro-ph.SR]

Brown WR, Kilic M, Bédard A, Kosakowski A, Bergeron P (2020) A 1201 s orbital period detached binary: the first double helium core white dwarf LISA verification binary. ApJ 892(2):L35. https://doi.org/10.3847/2041-8213/ab8228. arXiv:2004.00641 [astro-ph.SR]

Brown WR, Kilic M, Kosakowski A, Andrews JJ, Heinke CO, Agüeros MA, Camilo F, Gianninas A, Hermes JJ, Kenyon SJ (2020) The ELM survey. VIII. Ninety-eight double white dwarf binaries. ApJ 889(1):49. https://doi.org/10.3847/1538-4357/ab63cd. arXiv:2002.00064 [astro-ph.SR]

Brügmann B, González JA, Hannam M, Husa S, Sperhake U (2008) Exploring black hole superkicks. Phys Rev D 77(12):124047. https://doi.org/10.1103/PhysRevD.77.124047. arXiv:0707.0135 [gr-qc]

Büning A, Ritter H (2004) Long-term evolution of compact binaries with irradiation feedback. A&A 423:281–299. https://doi.org/10.1051/0004-6361:20035678. arXiv:astro-ph/0403306 [astro-ph]

Buonanno A, Damour T (1999) Effective one-body approach to general relativistic two-body dynamics. Phys Rev D 59(8):084006. https://doi.org/10.1103/PhysRevD.59.084006. arXiv:gr-qc/9811091 [gr-qc]

Buonanno A, Damour T (2000) Transition from inspiral to plunge in binary black hole coalescences. Phys Rev D 62(6):064015. https://doi.org/10.1103/PhysRevD.62.064015. arXiv:gr-qc/0001013 [gr-qc]

Buonanno A, Iyer BR, Ochsner E, Pan Y, Sathyaprakash BS (2009) Comparison of post-Newtonian templates for compact binary inspiral signals in gravitational-wave detectors. Phys Rev D 80(8):084043. https://doi.org/10.1103/PhysRevD.80.084043. arXiv:0907.0700 [gr-qc]

Burdge KB, Coughlin MW, Fuller J, Kupfer T, Bellm EC, Bildsten L, Graham MJ et al (2019) General relativistic orbital decay in a seven-minute-orbital-period eclipsing binary system. Nature 571(7766):528–531. https://doi.org/10.1038/s41586-019-1403-0. arXiv:1907.11291 [astro-ph.SR]

Burdge KB, Fuller J, Phinney ES, van Roestel J, Claret A, Cukanovaite E, Gentile Fusillo NP, Coughlin MW, Kaplan DL, Kupfer T et al (2019) Orbital decay in a 20 minute orbital period detached binary with a hydrogen-poor low-mass white dwarf. ApJ 886(1):L12. https://doi.org/10.3847/2041-8213/ab53e5. arXiv:1910.11389 [astro-ph.SR]

Burdge KB, Coughlin MW, Fuller J, Kaplan DL, Kulkarni SR, Marsh TR, Bellm EC, Dekany RG, Duev DA, Graham MJ et al (2020) An 8.8 minute orbital period eclipsing detached double white dwarf binary. ApJ 905(1):L7. https://doi.org/10.3847/2041-8213/abca91. arXiv:2010.03555 [astro-ph.SR]

Burdge KB, Prince TA, Fuller J, Kaplan DL, Marsh TR et al (2020) A systematic search of Zwicky transient facility data for ultracompact binary LISA-detectable gravitational-wave sources. ApJ 905(1):32. https://doi.org/10.3847/1538-4357/abc261. arXiv:2009.02567 [astro-ph.SR]

Burke-Spolaor S, Blecha L, Bogdanovic T, Comerford JM, Lazio TJW, Liu X, Maccarone TJ, Pesce D, Shen Y, Taylor G (2018) The next-generation very large array: supermassive black hole pairs and binaries. arXiv e-prints arXiv:1808.04368 [astro-ph.GA]

Burke-Spolaor S, Taylor SR, Charisi M, Dolch T, Hazboun JS, Holgado AM, Kelley LZ, Lazio TJW, Madison DR, McMann N et al (2019) The astrophysics of nanohertz gravitational waves. A&A Rev 27(1):5. https://doi.org/10.1007/s00159-019-0115-7. arXiv:1811.08826 [astro-ph.HE]

Burningham B (2018) Large-scale searches for brown dwarfs and free-floating planets. In: Deeg HJ, Belmonte JA (eds) Handbook of exoplanets. Springer, New York, p 118. https://doi.org/10.1007/978-3-319-55333-7_118

Buscicchio R, Klein A, Roebber E, Moore CJ, Gerosa D, Finch E, Vecchio A (2021) Bayesian parameter estimation of stellar-mass black-hole binaries with LISA. Phys Rev D 104(4):044065. https://doi.org/10.1103/PhysRevD.104.044065. arXiv:2106.05259 [astro-ph.HE]

Bustamante S, Springel V (2019) Spin evolution and feedback of supermassive black holes in cosmological simulations. MNRAS 490(3):4133–4153. https://doi.org/10.1093/mnras/stz2836. arXiv:1902.04651 [astro-ph.GA]

Byrd GG, Valtonen MJ, Sundelius B, Valtaoja L (1986) Tidal triggering of Seyfert galaxies and quasars? Perturbed galaxy disk models versus observations. A&A 166:75–82

Byrnes CT, Cole PS, Patil SP (2019) Steepest growth of the power spectrum and primordial black holes. J Cosmol Astropart Phys 06:028. https://doi.org/10.1088/1475-7516/2019/06/028. arXiv:1811.11158 [astro-ph.CO]

Caballero JA (2009) Reaching the boundary between stellar kinematic groups and very wide binaries. The Washington double stars with the widest angular separations. A&A 507(1):251–259. https://doi.org/10.1051/0004-6361/200912596. arXiv:0908.2761 [astro-ph.SR]

Cai Rg, Pi S, Sasaki M (2019) Gravitational waves induced by non-Gaussian scalar perturbations. Phys Rev Lett 122(20):201101. https://doi.org/10.1103/PhysRevLett.122.201101. arXiv:1810.11000 [astro-ph.CO]

Calderón Bustillo J, Clark JA, Laguna P, Shoemaker D (2018) Tracking black hole kicks from gravitational-wave observations. Phys Rev Lett 121(19):191102. https://doi.org/10.1103/PhysRevLett.121.191102. arXiv:1806.11160 [gr-qc]

Callegari S, Mayer L, Kazantzidis S, Colpi M, Governato F, Quinn T, Wadsley J (2009) Pairing of supermassive black holes in unequal-mass galaxy mergers. ApJ 696(1):L89–L92. https://doi.org/10.1088/0004-637X/696/1/L89. arXiv:0811.0615 [astro-ph]

Callegari S, Kazantzidis S, Mayer L, Colpi M, Bellovary JM, Quinn T, Wadsley J (2011) Growing massive black hole pairs in minor mergers of disk galaxies. ApJ 729(2):85. https://doi.org/10.1088/0004-637X/729/2/85. arXiv:1002.1712 [astro-ph.CO]

Callister T, Sammut L, Qiu S, Mandel I, Thrane E (2016) Limits of astrophysics with gravitational-wave backgrounds. Phys Rev X 6(3):031018. https://doi.org/10.1103/PhysRevX.6.031018. arXiv:1604.02513 [gr-qc]

Cameron AD, Champion DJ, Bailes M, Balakrishnan V, Barr ED, Bassa CG, Bates S, Bhandari S, Bhat NDR, Burgay M et al (2020) The high time resolution universe pulsar survey—XVI. Discovery and timing of 40 pulsars from the southern Galactic plane. MNRAS 493(1):1063–1087. https://doi.org/10.1093/mnras/staa039. arXiv:2001.01823 [astro-ph.HE]

Campanelli M, Lousto CO, Marronetti P, Zlochower Y (2006) Accurate evolutions of orbiting black-hole binaries without excision. Phys Rev Lett 96(11):111101. https://doi.org/10.1103/PhysRevLett.96.111101. arXiv:gr-qc/0511048 [gr-qc]

Campanelli M, Lousto C, Zlochower Y, Merritt D (2007) Large merger recoils and spin flips from generic black hole binaries. ApJ 659(1):L5–L8. https://doi.org/10.1086/516712. arXiv:gr-qc/0701164 [gr-qc]

Campanelli M, Lousto CO, Zlochower Y, Merritt D (2007) Maximum gravitational recoil. Phys Rev Lett 98(23):231102. https://doi.org/10.1103/PhysRevLett.98.231102. arXiv:gr-qc/0702133 [gr-qc]

Cantiello M, Jermyn AS, Lin DNC (2021) Stellar evolution in AGN disks. ApJ 910(2):94. https://doi.org/10.3847/1538-4357/abdf4f. arXiv:2009.03936 [astro-ph.SR]

Capelo PR, Volonteri M, Dotti M, Bellovary JM, Mayer L, Governato F (2015) Growth and activity of black holes in galaxy mergers with varying mass ratios. MNRAS 447(3):2123–2143. https://doi.org/10.1093/mnras/stu2500. arXiv:1409.0004 [astro-ph.GA]

Cappelluti N, Hasinger G, Natarajan P (2022) Exploring the high-redshift PBH-ΛCDM universe: early black hole seeding, the first stars and cosmic radiation backgrounds. ApJ 926(2):205. https://doi.org/10.3847/1538-4357/ac332d. arXiv:2109.08701 [astro-ph.CO]

Caprini C, Figueroa DG, Flauger R, Nardini G, Peloso M, Pieroni M, Ricciardone A, Tasinato G (2019) Reconstructing the spectral shape of a stochastic gravitational wave background with LISA. J Cosmol Astropart Phys 11:017. https://doi.org/10.1088/1475-7516/2019/11/017. arXiv:1906.09244 [astro-ph.CO]

Capuzzo-Dolcetta R (1993) The evolution of the globular cluster system in a triaxial galaxy: can a galactic nucleus form by globular cluster capture? ApJ 415:616. https://doi.org/10.1086/173189. arXiv:astro-ph/9301006 [astro-ph]

Capuzzo-Dolcetta R, Spera M, Punzo D (2013) A fully parallel, high precision, N-body code running on hybrid computing platforms. J Comput Phys 236:580–593. https://doi.org/10.1016/j.jcp.2012.11.013. arXiv:1207.2367 [astro-ph.IM]

Cárdenas-Avendaño A, Gutierrez AF, Pachón LA, Yunes N (2018) The exact dynamical Chern–Simons metric for a spinning black hole possesses a fourth constant of motion: a dynamical-systems-based conjecture. Class Quantum Grav 35(16):165010. https://doi.org/10.1088/1361-6382/aad06f. arXiv:1804.04002 [gr-qc]

Cardoso V, Maselli A (2020) Constraints on the astrophysical environment of binaries with gravitational-wave observations. A&A 644:A147. https://doi.org/10.1051/0004-6361/202037654. arXiv:1909.05870 [astro-ph.HE]

Cardoso V, Duque F, Khanna G (2021) Gravitational tuning forks and hierarchical triple systems. Phys Rev D 103(8):L081501. https://doi.org/10.1103/PhysRevD.103.L081501. arXiv:2101.01186 [gr-qc]

Cardoso V, Destounis K, Duque F, Macedo RP, Maselli A (2022) Black holes in galaxies: environmental impact on gravitational-wave generation and propagation. Phys Rev D 105(6):L061501. https://doi.org/10.1103/PhysRevD.105.L061501. arXiv:2109.00005 [gr-qc]

Carlberg RG, Yee HKC, Ellingson E, Abraham R, Gravel P, Morris S, Pritchet CJ (1996) Galaxy cluster virial masses and omega. ApJ 462:32. https://doi.org/10.1086/177125. arXiv:astro-ph/9509034 [astro-ph]

Carr B, Kühnel F (2020) Primordial black holes as dark matter: recent developments. Annu Rev Nucl Part Sci 70(1):annurev. https://doi.org/10.1146/annurev-nucl-050520-125911. arXiv:2006.02838 [astro-ph.CO]

Carr B, Kohri K, Sendouda Y, Yokoyama J (2021) Constraints on primordial black holes. Rep Prog Phys 84(11):116902. https://doi.org/10.1088/1361-6633/ac1e31. arXiv:2002.12778 [astro-ph.CO]

Carson Z, Yagi K (2020) Multi-band gravitational wave tests of general relativity. Class Quantum Grav 37 (2):02LT01. https://doi.org/10.1088/1361-6382/ab5c9a. arXiv:1905.13155 [gr-qc]

Carter B (1968) Global structure of the Kerr family of gravitational fields. Phys Rev 174(5):1559–1571. https://doi.org/10.1103/PhysRev.174.1559

Carter B, Luminet JP (1983) Tidal compression of a star by a large black hole. I Mechanical evolution and nuclear energy release by proton capture. A&A 121(1):97–113 arXiv:1905.13155 [gr-qc]

Carter PJ, Marsh TR, Steeghs D, Groot PJ, Nelemans G, Levitan D, Rau A, Copperwheat CM, Kupfer T, Roelofs GHA (2013) A search for the hidden population of AM CVn binaries in the Sloan Digital Sky Survey. MNRAS 429(3):2143–2160. https://doi.org/10.1093/mnras/sts485. arXiv:1211.6439 [astro-ph.SR]

Çatmabacak O, Feldmann R, Anglés-Alcázar D, Faucher-Giguère CA, Hopkins PF, Kereš D (2022) Black hole-galaxy scaling relations in FIRE: the importance of black hole location and mergers. MNRAS 511(1):506–535. https://doi.org/10.1093/mnras/stac040

Cembranos JAR, de la Cruz-Dombriz A, Montes Núñez B (2012) Gravitational collapse in f(R) theories. JCAP 4:021. https://doi.org/10.1088/1475-7516/2012/04/021. arXiv:1201.1289 [gr-qc]

Cenci E, Sala L, Lupi A, Capelo PR, Dotti M (2020) Black hole spin evolution in warped accretion discs. MNRAS 500(3):3719–3727. https://doi.org/10.1093/mnras/staa3449. arXiv:2011.06596 [astro-ph.GA]

Centrella J, Baker JG, Kelly BJ, van Meter JR (2010) Black-hole binaries, gravitational waves, and numerical relativity. Rev Mod Phys 82(4):3069–3119. https://doi.org/10.1103/RevModPhys.82.3069. arXiv:1010.5260 [gr-qc]

Cerioli A, Lodato G, Price DJ (2016) Gas squeezing during the merger of a supermassive black hole binary. MNRAS 457(1):939–948. https://doi.org/10.1093/mnras/stw034. arXiv:1601.03776 [astro-ph.HE]

Ceverino D, Dekel A, Bournaud F (2010) High-redshift clumpy discs and bulges in cosmological simulations. MNRAS 404(4):2151–2169. https://doi.org/10.1111/j.1365-2966.2010.16433.x. arXiv:0907.3271 [astro-ph.CO]

Chabrier G (2003) Galactic stellar and substellar initial mass function. PASP 115(809):763–795. https://doi.org/10.1086/376392. arXiv:astro-ph/0304382 [astro-ph]

Chamandy L, Frank A, Blackman EG, Carroll-Nellenback J, Liu B, Tu Y, Nordhaus J, Chen Z, Peng B (2018) Accretion in common envelope evolution. MNRAS 480(2):1898–1911. https://doi.org/10.1093/mnras/sty1950. arXiv:1805.03607 [astro-ph.SR]

Chandrasekhar S (1943) Dynamical friction. I. General considerations: the coefficient of dynamical friction. ApJ 97:255. https://doi.org/10.1086/144517

Chang P, Strubbe LE, Menou K, Quataert E (2010) Fossil gas and the electromagnetic precursor of supermassive binary black hole mergers. MNRAS 407(3):2007–2016. https://doi.org/10.1111/j.1365-2966.2010.17056.x. arXiv:0906.0825 [astro-ph.HE]

Chapon D, Mayer L, Teyssier R (2013) Hydrodynamics of galaxy mergers with supermassive black holes: is there a last parsec problem? MNRAS 429(4):3114–3122. https://doi.org/10.1093/mnras/sts568. arXiv:1110.6086 [astro-ph.GA]

Charisi M, Bartos I, Haiman Z, Price-Whelan AM, Graham MJ, Bellm EC, Laher RR, Márka S (2016) A population of short-period variable quasars from PTF as supermassive black hole binary candidates. MNRAS 463(2):2145–2171. https://doi.org/10.1093/mnras/stw1838. arXiv:1604.01020 [astro-ph.GA]

Charisi M, Haiman Z, Schiminovich D, D'Orazio DJ (2018) Testing the relativistic Doppler boost hypothesis for supermassive black hole binary candidates. MNRAS 476(4):4617–4628. https://doi.org/10.1093/mnras/sty516. arXiv:1801.06189 [astro-ph.GA]

Chatterjee P, Hernquist L, Loeb A (2003) Effects of wandering on the coalescence of black hole binaries in galactic centers. ApJ 592(1):32–41. https://doi.org/10.1086/375552. arXiv:astro-ph/0302573 [astro-ph]

Chaty S (2022) Accreting binaries, pp 2514–3433. IOP Publishing. https://doi.org/10.1088/2514-3433/ac595f

Chen HL, Chen X, Tauris TM, Han Z (2013) Formation of black widows and redbacks-two distinct populations of eclipsing binary millisecond pulsars. ApJ 775(1):27. https://doi.org/10.1088/0004-637X/775/1/27. arXiv:1308.4107 [astro-ph.SR]

Chen WC, Liu DD, Wang B (2020) Detectability of ultra-compact X-ray binaries as LISA sources. ApJ 900(1):L8. https://doi.org/10.3847/2041-8213/abae66. arXiv:2008.05143 [astro-ph.HE]

Chen X, Amaro-Seoane P (2014) A rapidly evolving region in the galactic center: why S-stars thermalize and more massive stars are missing. ApJ 786(2):L14. https://doi.org/10.1088/2041-8205/786/2/L14. arXiv:1401.6456 [astro-ph.GA]

Chen X, Han WB (2018) Extreme-mass-ratio inspirals produced by tidal capture of binary black holes. Commun Phys 1(1):53. https://doi.org/10.1038/s42005-018-0053-0. arXiv:1801.05780 [astro-ph.HE]

Chen X, Han Z (2008) Mass transfer from a giant star to a main-sequence companion and its contribution to long-orbital-period blue stragglers. MNRAS 387(4):1416–1430. https://doi.org/10.1111/j.1365-2966.2008.13334.x. arXiv:0804.2294 [astro-ph]

Chen X, Liu FK (2013) Is there an intermediate massive black hole in the galactic center: imprints on the stellar tidal-disruption rate. ApJ 762(2):95. https://doi.org/10.1088/0004-637X/762/2/95. arXiv:1211.4609 [astro-ph.GA]

Chen X, Zhang Z (2022) Binaries wandering around supermassive black holes due to gravito-electromagnetism. arXiv e-prints arXiv:2206.08104 [astro-ph.HE]

Chen X, Li S, Cao Z (2019) Mass-redshift degeneracy for the gravitational-wave sources in the vicinity of supermassive black holes. MNRAS 485(1):L141–L145. https://doi.org/10.1093/mnrasl/slz046. arXiv:1703.10543 [astro-ph.HE]

Chen Y, Yu Q, Lu Y (2020) Dynamical evolution of cosmic supermassive binary black holes and their gravitational-wave radiation. ApJ 897(1):86. https://doi.org/10.3847/1538-4357/ab9594. arXiv:2005.10818 [astro-ph.HE]

Chen YC, Liu X, Liao WT, Holgado AM, Guo H, Gruendl RA, Morganson E, Shen Y, Zhang K, Abbott TMC et al (2020) Candidate periodically variable quasars from the Dark Energy Survey and the Sloan Digital Sky Survey. MNRAS 499(2):2245–2264. https://doi.org/10.1093/mnras/staa2957. arXiv:2008.12329 [astro-ph.HE]

Chen ZC, Huang F, Huang QG (2019) Stochastic gravitational-wave background from binary black holes and binary neutron stars and implications for LISA. ApJ 871(1):97. https://doi.org/10.3847/1538-4357/aaf581. arXiv:1809.10360 [gr-qc]

Chiaberge M, Ely JC, Meyer ET, Georganopoulos M, Marinucci A, Bianchi S, Tremblay GR, Hilbert B, Kotyla JP, Capetti A et al (2017) The puzzling case of the radio-loud QSO 3C 186: a gravitational wave recoiling black hole in a young radio source? A&A 600:A57. https://doi.org/10.1051/0004-6361/201629522. arXiv:1611.05501 [astro-ph.GA]

Chicone C, Mashhoon B, Punsly B (2005) Relativistic motion of spinning particles in a gravitational field. Phys Lett A 343(1–3):1–7. https://doi.org/10.1016/j.physleta.2005.05.072. arXiv:gr-qc/0504146 [gr-qc]

Chilingarian IV, Katkov IY, Zolotukhin IY, Grishin KA, Beletsky Y, Boutsia K, Osip DJ (2018) A population of bona fide intermediate-mass black holes identified as low-luminosity active galactic nuclei. ApJ 863(1):1. https://doi.org/10.3847/1538-4357/aad184. arXiv:1805.01467 [astro-ph.GA]

Chluba J, Erickcek AL, Ben-Dayan I (2012) Probing the inflaton: small-scale power spectrum constraints from measurements of the CMB energy spectrum. Astrophys J 758:76. https://doi.org/10.1088/0004-637X/758/2/76. arXiv:1203.2681 [astro-ph.CO]

Choi E, Ostriker JP, Naab T, Johansson PH (2012) Radiative and momentum-based mechanical active galactic nucleus feedback in a three-dimensional galaxy evolution code. ApJ 754(2):125. https://doi.org/10.1088/0004-637X/754/2/125. arXiv:1205.2082 [astro-ph.GA]

Chon S, Omukai K (2020) Supermassive star formation via super competitive accretion in slightly metal-enriched clouds. MNRAS https://doi.org/10.1093/mnras/staa863. arXiv:2001.06491 [astro-ph.GA]

Chon S, Hosokawa T, Yoshida N (2018) Radiation hydrodynamics simulations of the formation of direct-collapse supermassive stellar systems. MNRAS 475(3):4104–4121. https://doi.org/10.1093/mnras/sty086. arXiv:1711.05262 [astro-ph.GA]

Chruslinska M, Nelemans G (2019) Metallicity of stars formed throughout the cosmic history based on the observational properties of star-forming galaxies. MNRAS 488(4):5300–5326. https://doi.org/10.1093/mnras/stz2057. arXiv:1907.11243 [astro-ph.GA]

Chruslinska M, Belczynski K, Klencki J, Benacquista M (2018) Double neutron stars: merger rates revisited. MNRAS 474(3):2937–2958. https://doi.org/10.1093/mnras/stx2923. arXiv:1708.07885 [astro-ph.HE]

Chruslinska M, Nelemans G, Belczynski K (2019) The influence of the distribution of cosmic star formation at different metallicities on the properties of merging double compact objects. MNRAS 482 (4):5012–5017. https://doi.org/10.1093/mnras/sty3087. arXiv:1811.03565 [astro-ph.HE]

Chruślińska M, Jeřábková T, Nelemans G, Yan Z (2020) The effect of the environment-dependent IMF on the formation and metallicities of stars over the cosmic history. A&A 636:A10. https://doi.org/10.1051/0004-6361/202037688. arXiv:2002.11122 [astro-ph.GA]

Chua AJK, Cutler CJ (2021) Non-local parameter degeneracy in the intrinsic space of gravitational-wave signals from extreme-mass-ratio inspirals. arXiv e-prints arXiv:2109.14254 [gr-qc]

Chua AJK, Vallisneri M (2020) Learning Bayesian posteriors with neural networks for gravitational-wave inference. Phys Rev Lett 124(4):041102. https://doi.org/10.1103/PhysRevLett.124.041102. arXiv:1909.05966 [gr-qc]

Chua AJK, Moore CJ, Gair JR (2017) Augmented kludge waveforms for detecting extreme-mass-ratio inspirals. Phys Rev D 96(4):044005. https://doi.org/10.1103/PhysRevD.96.044005. arXiv:1705.04259 [gr-qc]

Church RP, Bush SJ, Tout CA, Davies MB (2006) Detailed models of the binary pulsars J1141–6545 and B2303+46. MNRAS 372(2):715–727. https://doi.org/10.1111/j.1365-2966.2006.10897.x

Church RP, Strader J, Davies MB, Bobrick A (2017) Formation constraints indicate a black hole accretor in 47 Tuc X9. ApJ 851(1):L4. https://doi.org/10.3847/2041-8213/aa9aeb. arXiv:1801.00796 [astro-ph.HE]

Civano F, Elvis M, Lanzuisi G, Aldcroft T, Trichas M, Bongiorno A, Brusa M, Blecha L, Comastri A, Loeb A et al (2012) Chandra high-resolution observations of CID-42, a candidate recoiling supermassive black hole. ApJ 752(1):49. https://doi.org/10.1088/0004-637X/752/1/49. arXiv:1205.0815 [astro-ph.CO]

Clark PC, Glover SCO, Klessen RS, Bromm V (2011) Gravitational fragmentation in turbulent primordial gas and the initial mass function of population III stars. ApJ 727:110. https://doi.org/10.1088/0004-637X/727/2/110. arXiv:1006.1508 [astro-ph.GA]

Clark PC, Glover SCO, Smith RJ, Greif TH, Klessen RS, Bromm V (2011) The formation and fragmentation of disks around primordial protostars. Science 331:1040. https://doi.org/10.1126/science.1198027. arXiv:1101.5284 [astro-ph.CO]

Clayton M, Podsiadlowski P, Ivanova N, Justham S (2017) Episodic mass ejections from common-envelope objects. MNRAS 470(2):1788–1808. https://doi.org/10.1093/mnras/stx1290. arXiv:1705.08457 [astro-ph.SR]

Clesse S, García-Bellido J (2015) Massive primordial black holes from hybrid inflation as dark matter and the seeds of galaxies. Phys Rev D 92(2):023524. https://doi.org/10.1103/PhysRevD.92.023524. arXiv:1501.07565 [astro-ph.CO]

Clesse S, García-Bellido J (2017) The clustering of massive Primordial Black Holes as Dark Matter: measuring their mass distribution with Advanced LIGO. Phys Dark Univ 15:142–147. https://doi.org/10.1016/j.dark.2016.10.002. arXiv:1603.05234 [astro-ph.CO]

Cohn H, Kulsrud RM (1978) The stellar distribution around a black hole: numerical integration of the Fokker-Planck equation. ApJ 226:1087–1108. https://doi.org/10.1086/156685

Colin J, Mohayaee R, Rameez M, Sarkar S (2017) High-redshift radio galaxies and divergence from the CMB dipole. MNRAS 471(1):1045–1055. https://doi.org/10.1093/mnras/stx1631. arXiv:1703.09376 [astro-ph.CO]

Colpi M (2014) Massive binary black holes in galactic nuclei and their path to coalescence. Space Sci Rev 183(1–4):189–221. https://doi.org/10.1007/s11214-014-0067-1. arXiv:1407.3102 [astro-ph.GA]

Comastri A, Gilli R, Marconi A, Risaliti G, Salvati M (2015) Mass without radiation: heavily obscured AGNs, the X-ray background, and the black hole mass density. A&A 574:L10. https://doi.org/10.1051/0004-6361/201425496. arXiv:1501.03620 [astro-ph.GA]

Comerford TAF, Izzard RG (2020) Estimating the outcomes of common envelope evolution in triple stellar systems. MNRAS 498(2):2957–2967. https://doi.org/10.1093/mnras/staa2539. arXiv:2008.09671 [astro-ph.SR]

Comerford TAF, Izzard RG, Booth RA, Rosotti G (2019) Bondi–Hoyle–Lyttleton accretion by binary stars. MNRAS 490(4):5196–5209. https://doi.org/10.1093/mnras/stz2977. arXiv:1910.13353 [astro-ph.SR]

Connors PA, Piran T, Stark RF (1980) Polarization features of X-ray radiation emitted near black holes. ApJ 235:224–244. https://doi.org/10.1086/157627

Consolandi G (2016) Automated bar detection in local disk galaxies from the SDSS. The colors of bars. A&A 595:A67. https://doi.org/10.1051/0004-6361/201629115. arXiv:1607.05563 [astro-ph.GA]

Contenta F, Balbinot E, Petts JA, Read JI, Gieles M, Collins MLM, Peñarrubia J, Delorme M, Gualandris A (2018) Probing dark matter with star clusters: a dark matter core in the ultra-faint dwarf Eridanus II. MNRAS 476(3):3124–3136. https://doi.org/10.1093/mnras/sty424. arXiv:1705.01820 [astro-ph.GA]

Contopoulos G (2002) Order and chaos in dynamical astronomy. Springer, New York

Contopoulos G, Lukes-Gerakopoulos G, Apostolatos TA (2011) Orbits in a non-Kerr dynamical system. Int J Bifurcat Chaos 21(8):2261. https://doi.org/10.1142/S0218127411029768. arXiv:1108.5057 [gr-qc]

Copperwheat CM, Marsh TR, Littlefair SP, Dhillon VS, Ramsay G, Drake AJ, Gänsicke BT, Groot PJ, Hakala P, Koester D et al (2011) SDSS J0926+3624: the shortest period eclipsing binary star. MNRAS 410(2):1113–1129. https://doi.org/10.1111/j.1365-2966.2010.17508.x. arXiv:1008.1907 [astro-ph.SR]

Cornish N, Robson T (2017) Galactic binary science with the new LISA design. J Phys Conf Ser 840:012024. https://doi.org/10.1088/1742-6596/840/1/012024. arXiv:1703.09858 [astro-ph.IM]

Cornish NJ (2011) Detection strategies for extreme mass ratio inspirals. Class Quantum Grav 28 (9):094016. https://doi.org/10.1088/0264-9381/28/9/094016. arXiv:0804.3323 [gr-qc]

Cornish NJ, Crowder J (2005) LISA data analysis using Markov chain Monte Carlo methods. Phys Rev D 72(4):043005. https://doi.org/10.1103/PhysRevD.72.043005. arXiv:gr-qc/0506059 [astro-ph]

Cornish NJ, Larson SL (2003) LISA data analysis: source identification and subtraction. Phys Rev D 67 (10):103001. https://doi.org/10.1103/PhysRevD.67.103001. arXiv:astro-ph/0301548 [astro-ph]

Cornish NJ, Littenberg TB (2007) Tests of Bayesian model selection techniques for gravitational wave astronomy. Phys Rev D 76(8):083006. https://doi.org/10.1103/PhysRevD.76.083006. arXiv:0704.1808 [gr-qc]

Cornish NJ, Shuman K (2020) Black hole hunting with LISA. Phys Rev D 101(12):124008. https://doi.org/10.1103/PhysRevD.101.124008. arXiv:2005.03610 [gr-qc]

Corrales L, Mills BS, Heinz S, Williger GM (2019) The X-ray variable sky as seen by MAXI: the future of dust-echo tomography with bright galactic X-ray bursts. ApJ 874(2):155. https://doi.org/10.3847/1538-4357/ab0c9b. arXiv:1903.08299 [astro-ph.HE]

Corrales LR, Haiman Z, MacFadyen A (2010) Hydrodynamical response of a circumbinary gas disc to black hole recoil and mass loss. MNRAS 404(2):947–962. https://doi.org/10.1111/j.1365-2966.2010.16324.x. arXiv:0910.0014 [astro-ph.HE]

Coughlin MW, Dietrich T, Doctor Z, Kasen D, Coughlin S, Jerkstrand A, Leloudas G, McBrien O, Metzger BD, O'Shaughnessy R et al (2018) Constraints on the neutron star equation of state from AT2017gfo using radiative transfer simulations. MNRAS 480(3):3871–3878. https://doi.org/10.1093/mnras/sty2174. arXiv:1805.09371 [astro-ph.HE]

Cresswell P, Dirksen G, Kley W, Nelson RP (2007) On the evolution of eccentric and inclined protoplanets embedded in protoplanetary disks. A&A 473(1):329–342. https://doi.org/10.1051/0004-6361:20077666. arXiv:0707.2225 [astro-ph]

Cromartie HT, Fonseca E, Ransom SM, Demorest PB, Arzoumanian Z, Blumer H, Brook PR, DeCesar ME, Dolch T, Ellis JA et al (2020) Relativistic Shapiro delay measurements of an extremely massive millisecond pulsar. Nat Astron 4:72–76. https://doi.org/10.1038/s41550-019-0880-2. arXiv:1904.06759 [astro-ph.HE]

Croton DJ, Springel V, White SDM, De Lucia G, Frenk CS, Gao L, Jenkins A, Kauffmann G, Navarro JF, Yoshida N (2006) The many lives of active galactic nuclei: cooling flows, black holes and the luminosities and colours of galaxies. MNRAS 365(1):11–28. https://doi.org/10.1111/j.1365-2966.2005.09675.x. arXiv:astro-ph/0508046 [astro-ph]

Cuadra J, Armitage PJ, Alexander RD, Begelman MC (2009) Massive black hole binary mergers within subparsec scale gas discs. MNRAS 393(4):1423–1432. https://doi.org/10.1111/j.1365-2966.2008.14147.x. arXiv:0809.0311 [astro-ph]

Cunningham EC, Garavito-Camargo N, Deason AJ, Johnston KV, Erkal D, Laporte CFP, Besla G, Luger R, Sanderson RE (2020) Quantifying the stellar Halo's response to the LMC's infall with spherical harmonics. ApJ 898(1):4. https://doi.org/10.3847/1538-4357/ab9b88. arXiv:2006.08621 [astro-ph.GA]

Cusin G, Dvorkin I, Pitrou C, Uzan JP (2020) Stochastic gravitational wave background anisotropies in the mHz band: astrophysical dependencies. MNRAS 493(1):L1–L5. https://doi.org/10.1093/mnrasl/slz182. arXiv:1904.07757 [astro-ph.CO]

Cutler C, Flanagan ÉÉ (1994) Gravitational waves from merging compact binaries: how accurately can one extract the binary's parameters from the inspiral waveform? Phys Rev D 49(6):2658–2697. https://doi.org/10.1103/PhysRevD.49.2658. arXiv:gr-qc/9402014 [gr-qc]

Cutler C, Berti E, Holley-Bockelmann K, Jani K, Kovetz ED, Larson SL, Littenberg T, McWilliams ST, Mueller G, Randall L et al (2019) What can we learn from multi-band observations of black hole binaries? BAAS 51(3):109 arXiv:1903.04069 [astro-ph.HE]

Dabringhausen J, Kroupa P, Baumgardt H (2009) A top-heavy stellar initial mass function in starbursts as an explanation for the high mass-to-light ratios of ultra-compact dwarf galaxies. MNRAS 394 (3):1529–1543. https://doi.org/10.1111/j.1365-2966.2009.14425.x. arXiv:0901.0915 [astro-ph.GA]

Dage KC, Zepf SE, Bahramian A, Strader J, Maccarone TJ, Peacock MB, Kundu A, Steele MM, Britt CT (2019) Slow decline and rise of the broad [O III] emission line in globular cluster black hole candidate RZ2109. MNRAS 489(4):4783–4790. https://doi.org/10.1093/mnras/stz2514. arXiv:1909. 02683 [astro-ph.HE]

Dai L, McKinney JC, Roth N, Ramirez-Ruiz E, Miller MC (2018) A unified model for tidal disruption events. ApJ 859(2):L20. https://doi.org/10.3847/2041-8213/aab429. arXiv:1803.03265 [astro-ph.HE]

Dal Canton T, Mangiagli A, Noble SC, Schnittman J, Ptak A, Klein A, Sesana A, Camp J (2019) Detectability of modulated x-rays from LISA's supermassive black hole mergers. ApJ 886(2):146. https://doi.org/10.3847/1538-4357/ab505a

Dall'Osso S, Rossi EM (2013) Tidal torque induced by orbital decay in compact object binaries. MNRAS 428(1):518–531. https://doi.org/10.1093/mnras/sts037. arXiv:1203.3440 [astro-ph.HE]

Dall'Osso S, Rossi EM (2014) Constraining white dwarf viscosity through tidal heating in detached binary systems. MNRAS 443(2):1057–1064. https://doi.org/10.1093/mnras/stu901. arXiv:1308.1664 [astro-ph.HE]

Daly RA (2011) Estimates of black hole spin properties of 55 sources. MNRAS 414(2):1253–1262. https://doi.org/10.1111/j.1365-2966.2011.18452.x. arXiv:1103.0940 [astro-ph.CO]

Damour T, Gopakumar A (2006) Gravitational recoil during binary black hole coalescence using the effective one body approach. Phys Rev D 73(12):124006. https://doi.org/10.1103/PhysRevD.73. 124006. arXiv:gr-qc/0602117 [gr-qc]

Dan M, Rosswog S, Guillochon J, Ramirez-Ruiz E (2011) Prelude to a double degenerate merger: the onset of mass transfer and its impact on gravitational waves and surface detonations. ApJ 737(2):89. https://doi.org/10.1088/0004-637X/737/2/89. arXiv:1101.5132 [astro-ph.HE]

D'Angelo G, Lubow SH, Bate MR (2006) Evolution of giant planets in eccentric disks. ApJ 652(2):1698–1714. https://doi.org/10.1086/508451. arXiv:astro-ph/0608355 [astro-ph]

Danielski C, Tamanini N (2020) Will gravitational waves discover the first extra-galactic planetary system? Int J Mod Phys D 29:2043007. https://doi.org/10.1142/S0218271820430075. arXiv:2007.07010 [astro-ph.IM]

Danielski C, Korol V, Tamanini N, Rossi EM (2019) Circumbinary exoplanets and brown dwarfs with the Laser Interferometer Space Antenna. A&A 632:A113. https://doi.org/10.1051/0004-6361/ 201936729. arXiv:1910.05414 [astro-ph.EP]

d'Ascoli S et al (2018) Electromagnetic emission from supermassive binary black holes approaching merger. ApJ 865:140. https://doi.org/10.3847/1538-4357/aad8b4. arXiv:1806.05697 [astro-ph.HE]

Datta S, Gupta A, Kastha S, Arun KG, Sathyaprakash BS (2021) Tests of general relativity using multiband observations of intermediate mass binary black hole mergers. Phys Rev D 103(2):024036. https://doi.org/10.1103/PhysRevD.103.024036. arXiv:2006.12137 [gr-qc]

Davé R, Anglés-Alcázar D, Narayanan D, Li Q, Rafieferantsoa MH, Appleby S (2019) SIMBA: cosmological simulations with black hole growth and feedback. MNRAS 486(2):2827–2849. https:// doi.org/10.1093/mnras/stz937. arXiv:1901.10203 [astro-ph.GA]

Davies MB, Lin DNC (2020) Making massive stars in the Galactic Centre via accretion onto low-mass stars within an accretion disc. MNRAS https://doi.org/10.1093/mnras/staa2590 [astro-ph.GA]

Davies MB, Miller MC, Bellovary JM (2011) Supermassive black hole formation via gas accretion in nuclear stellar clusters. ApJ 740(2):L42. https://doi.org/10.1088/2041-8205/740/2/L42. arXiv:1106. 5943 [astro-ph.CO]

Davies RI, Müller Sánchez F, Genzel R, Tacconi LJ, Hicks EKS, Friedrich S, Sternberg A (2007) A close look at star formation around active galactic nuclei. ApJ 671(2):1388–1412. https://doi.org/10.1086/ 523032. arXiv:0704.1374 [astro-ph]

Davis BL, Graham AW, Seigar MS (2017) Updating the (supermassive black hole mass)-(spiral arm pitch angle) relation: a strong correlation for galaxies with pseudobulges. MNRAS 471(2):2187–2203. https://doi.org/10.1093/mnras/stx1794. arXiv:1707.04001 [astro-ph.GA]

Davis BL, Graham AW, Cameron E (2018) Black hole mass scaling relations for spiral galaxies. II. M_{BH}-$M_{*,tot}$ and M_{BH}-$M_{*,disk}$. ApJ 869(2):113. https://doi.org/10.3847/1538-4357/aae820. arXiv:1810.04888 [astro-ph.GA]

Davis BL, Graham AW, Cameron E (2019) Black hole mass scaling relations for spiral galaxies. I. M_{BH}-$M_{*,sph}$. ApJ 873(1):85. https://doi.org/10.3847/1538-4357/aaf3b8. arXiv:1810.04887 [astro-ph.GA]

Davis BL, Graham AW, Combes F (2019) A consistent set of empirical scaling relations for spiral galaxies: the (v_{max}, M_{oM})-(σ_0, M_{BH}, ϕ) relations. ApJ 877(1):64. https://doi.org/10.3847/1538-4357/ab1aa4. arXiv:1901.06509 [astro-ph.GA]

Dayal P, Ferrara A (2018) Early galaxy formation and its large-scale effects. Phys Rep 780:1–64. https://doi.org/10.1016/j.physrep.2018.10.002. arXiv:1809.09136 [astro-ph.GA]

Dayal P, Rossi EM, Shiralilou B, Piana O, Choudhury TR, Volonteri M (2019) The hierarchical assembly of galaxies and black holes in the first billion years: predictions for the era of gravitational wave astronomy. MNRAS 486(2):2336–2350. https://doi.org/10.1093/mnras/stz897. arXiv:1810.11033 [astro-ph.GA]

De S, MacLeod M, Everson RW, Antoni A, Mandel I, Ramirez-Ruiz E (2020) Common envelope wind tunnel: the effects of binary mass ratio and implications for the accretion-driven growth of LIGO binary black holes. ApJ 897(2):130. https://doi.org/10.3847/1538-4357/ab9ac6. arXiv:1910.13333 [astro-ph.SR]

De Luca V, Franciolini G, Pani P, Riotto A (2020) Constraints on primordial black holes: the importance of accretion. Phys Rev D 102(4):043505. https://doi.org/10.1103/PhysRevD.102.043505. arXiv:2003.12589 [astro-ph.CO]

De Luca V, Franciolini G, Riotto A (2021) NANOGrav data hints at primordial black holes as dark matter. Phys Rev Lett 126(4):041303. https://doi.org/10.1103/PhysRevLett.126.041303. arXiv:2009.08268 [astro-ph.CO]

De Marco O, Passy JC, Moe M, Herwig F, Mac Low MM, Paxton B (2011) On the α formalism for the common envelope interaction. MNRAS 411(4):2277–2292. https://doi.org/10.1111/j.1365-2966.2010.17891.x. arXiv:1010.4374 [astro-ph.SR]

de Mink SE, Cantiello M, Langer N, Pols OR, Brott I, Yoon SC (2009) Rotational mixing in massive binaries. Detached short-period systems. A&A 497(1):243–253. https://doi.org/10.1051/0004-6361/200811439. arXiv:0902.1751 [astro-ph.SR]

De Rosa A, Uttley P, Gou L, Liu Y, Bambi C, Barret D, Belloni T, Berti E, Bianchi S, Caiazzo I et al (2019) Accretion in strong field gravity with eXTP. Sci China Phys Mech Astron 62(2):29504. https://doi.org/10.1007/s11433-018-9297-0. arXiv:1812.04022 [astro-ph.HE]

De Rosa A, Vignali C, Bogdanović T, Capelo PR, Charisi M, Dotti M, Husemann B, Lusso E, Mayer L, Paragi Z et al (2019) The quest for dual and binary supermassive black holes: a multi-messenger view. New A Rev 86:101525. https://doi.org/10.1016/j.newar.2020.101525. arXiv:2001.06293 [astro-ph.GA]

de Val-Borro M, Karovska M, Sasselov DD, Stone JM (2017) Three-dimensional hydrodynamical models of wind and outburst-related accretion in symbiotic systems. MNRAS 468(3):3408–3417. https://doi.org/10.1093/mnras/stx684. arXiv:1704.03460 [astro-ph.SR]

Deane RP, Paragi Z, Jarvis MJ, Coriat M, Bernardi G, Fender RP, Frey S, Heywood I, Klöckner HR, Grainge K et al (2014) A close-pair binary in a distant triple supermassive black hole system. Nature 511(7507):57–60. https://doi.org/10.1038/nature13454. arXiv:1406.6365 [astro-ph.GA]

Decarli R, Dotti M, Fumagalli M, Tsalmantza P, Montuori C, Lusso E, Hogg DW, Prochaska JX (2013) The nature of massive black hole binary candidates—I. Spectral properties and evolution. MNRAS 433(2):1492–1504. https://doi.org/10.1093/mnras/stt831. arXiv:1305.4941 [astro-ph.CO]

Decarli R, Dotti M, Mazzucchelli C, Montuori C, Volonteri M (2014) New insights on the recoiling/binary black hole candidate J0927+2943 via molecular gas observations. MNRAS 445(2):1558–1566. https://doi.org/10.1093/mnras/stu1810. arXiv:1409.1585 [astro-ph.GA]

Decarli R, Walter F, Venemans BP, Bañados E, Bertoldi F, Carilli C, Fan X, Farina EP, Mazzucchelli C, Riechers D et al (2018) An ALMA [C II] survey of 27 quasars at z > 5.94. ApJ 854(2):97. https://doi.org/10.3847/1538-4357/aaa5aa. arXiv:1801.02641 [astro-ph.GA]

Decarli R, Aravena M, Boogaard L, Carilli C, González-López J, Walter F, Cortes PC, Cox P, da Cunha E, Daddi E et al (2020) The ALMA spectroscopic survey in the hubble ultra deep field: multiband constraints on line-luminosity functions and the cosmic density of molecular gas. ApJ 902(2):110. https://doi.org/10.3847/1538-4357/abaa3b. arXiv:2009.10744 [astro-ph.GA]

DeGraf C, Sijacki D (2020) Cosmological simulations of massive black hole seeds: predictions for next-generation electromagnetic and gravitational wave observations. MNRAS 491(4):4973–4992. https://doi.org/10.1093/mnras/stz3309. arXiv:1906.11271 [astro-ph.GA]

DeGraf C, Sijacki D, Di Matteo T, Holley-Bockelmann K, Snyder G, Springel V (2021) Morphological evolution of supermassive black hole merger hosts and multimessenger signatures. MNRAS 503 (3):3629–3642. https://doi.org/10.1093/mnras/stab721. arXiv:2012.00775 [astro-ph.GA]

del Valle L, Volonteri M (2018) The effect of AGN feedback on the migration time-scale of supermassive black holes binaries. MNRAS 480(1):439–450. https://doi.org/10.1093/mnras/sty1815. arXiv:1807.03844 [astro-ph.GA]

del Valle L, Escala A, Maureira-Fredes C, Molina J, Cuadra J, Amaro-Seoane P (2015) Supermassive black holes in a star-forming gaseous circumnuclear disk. ApJ 811(1):59. https://doi.org/10.1088/0004-637X/811/1/59. arXiv:1503.01664 [astro-ph.GA]

Deloye CJ, Taam RE (2006) The turn-on of mass transfer in AM CVn binaries: implications for RX J0806+1527 and RX J1914+2456. ApJ 649(2):L99–L102. https://doi.org/10.1086/508372. arXiv:astro-ph/0608442 [astro-ph]

Deme B, Hoang BM, Naoz S, Kocsis B (2020) Detecting Kozai–Lidov imprints on the gravitational waves of intermediate-mass black holes in galactic nuclei. ApJ 901(2):125. https://doi.org/10.3847/1538-4357/abafa3. arXiv:2005.03677 [astro-ph.HE]

Deme B, Meiron Y, Kocsis B (2020) Intermediate-mass black holes' effects on compact object binaries. ApJ 892(2):130. https://doi.org/10.3847/1538-4357/ab7921. arXiv:1909.04678 [astro-ph.GA]

Derdzinski A, D'Orazio D, Duffell P, Haiman Z, MacFadyen A (2021) Evolution of gas disc-embedded intermediate mass ratio inspirals in the LISA band. MNRAS 501(3):3540–3557. https://doi.org/10.1093/mnras/staa3976. arXiv:2005.11333 [astro-ph.HE]

Derdzinski AM, D'Orazio D, Duffell P, Haiman Z, MacFadyen A (2019) Probing gas disc physics with LISA: simulations of an intermediate mass ratio inspiral in an accretion disc. MNRAS 486(2):2754–2765. https://doi.org/10.1093/mnras/stz1026. arXiv:1810.03623 [astro-ph.HE]

DESI Collaboration, Aghamousa A, Aguilar J, Ahlen S, Alam S, Allen LE, Allende Prieto C, Annis J, Bailey S, Balland C et al (2016) The DESI experiment part I: science, targeting, and survey design. arXiv e-prints arXiv:1611.00036 [astro-ph.IM]

Dessart L, Burrows A, Ott CD, Livne E, Yoon SC, Langer N (2006) Multidimensional simulations of the accretion-induced collapse of white dwarfs to neutron stars. ApJ 644(2):1063–1084. https://doi.org/10.1086/503626. arXiv:astro-ph/0601603 [astro-ph]

Destounis K, Kokkotas KD (2021) Gravitational-wave glitches: resonant islands and frequency jumps in nonintegrable extreme-mass-ratio inspirals. Phys Rev D 104(6):064023. https://doi.org/10.1103/PhysRevD.104.064023. arXiv:2108.02782 [gr-qc]

Destounis K, Suvorov AG, Kokkotas KD (2020) Testing spacetime symmetry through gravitational waves from extreme-mass-ratio inspirals. Phys Rev D 102:064041. https://doi.org/10.1103/PhysRevD.102.064041

Destounis K, Suvorov AG, Kokkotas KD (2021) Gravitational wave glitches in chaotic extreme-mass-ratio inspirals. Phys Rev Lett 126(14):141102. https://doi.org/10.1103/PhysRevLett.126.141102. arXiv:2103.05643 [gr-qc]

Desvignes G, Caballero RN, Lentati L, Verbiest JPW, Champion DJ, Stappers BW, Janssen GH, Lazarus P, Osłowski S, Babak S et al (2016) High-precision timing of 42 millisecond pulsars with the European Pulsar Timing Array. MNRAS 458(3):3341–3380. https://doi.org/10.1093/mnras/stw483. arXiv:1602.08511 [astro-ph.HE]

Devecchi B, Volonteri M (2009) Formation of the first nuclear clusters and massive black holes at high redshift. ApJ 694(1):302–313. https://doi.org/10.1088/0004-637X/694/1/302. arXiv:0810.1057 [astro-ph]

Dewdney PE, Hall PJ, Schilizzi RT, Lazio TJLW (2009) The square kilometre array. IEEE Proc 97 (8):1482–1496. https://doi.org/10.1109/JPROC.2009.2021005

Dewi JDM, Pols OR (2003) The late stages of evolution of helium star-neutron star binaries and the formation of double neutron star systems. MNRAS 344(2):629–643. https://doi.org/10.1046/j.1365-8711.2003.06844.x. arXiv:astro-ph/0306066 [astro-ph]

Dewi JDM, Podsiadlowski P, Pols OR (2005) The spin period-eccentricity relation of double neutron stars: evidence for weak supernova kicks? MNRAS 363(1):L71–L75. https://doi.org/10.1111/j.1745-3933.2005.00085.x. arXiv:astro-ph/0507628 [astro-ph]

Di Carlo UN, Giacobbo N, Mapelli M, Pasquato M, Spera M, Wang L, Haardt F (2019) Merging black holes in young star clusters. MNRAS 487(2):2947–2960. https://doi.org/10.1093/mnras/stz1453. arXiv:1901.00863 [astro-ph.HE]

Di Carlo UN, Mapelli M, Bouffanais Y, Giacobbo N, Santoliquido F, Bressan Ar, Spera M, Haardt F (2020) Binary black holes in the pair instability mass gap. MNRAS 497(1):1043–1049. https://doi.org/10.1093/mnras/staa1997. arXiv:1911.01434 [astro-ph.HE]

Di Carlo UN, Mapelli M, Giacobbo N, Spera M, Bouffanais Y, Rastello S, Santoliquido F, Pasquato M, Ballone Ar, Trani AA et al (2020) Binary black holes in young star clusters: the impact of metallicity. MNRAS 498(1):495–506. https://doi.org/10.1093/mnras/staa2286. arXiv:2004.09525 [astro-ph.HE]

Di Carlo UN, Mapelli M, Pasquato M, Rastello S, Ballone A, Dall'Amico M, Giacobbo N, Iorio G, Spera M, Torniamenti S et al (2021) Intermediate-mass black holes from stellar mergers in young star clusters. MNRAS 507(4):5132–5143. https://doi.org/10.1093/mnras/stab2390. arXiv:2105.01085 [astro-ph.GA]

Di Cintio A, Tremmel M, Governato F, Pontzen A, Zavala J, Fry Ae Bastidas, Brooks A, Vogelsberger M (2017) A rumble in the dark: signatures of self-interacting dark matter in supermassive black hole dynamics and galaxy density profiles. MNRAS 469(3):2845–2854. https://doi.org/10.1093/mnras/stx1043. arXiv:1701.04410 [astro-ph.GA]

Di Matteo T, Springel V, Hernquist L (2005) Energy input from quasars regulates the growth and activity of black holes and their host galaxies. Nature 433(7026):604–607. https://doi.org/10.1038/nature03335. arXiv:astro-ph/0502199 [astro-ph]

Dieball A, Knigge C, Zurek DR, Shara MM, Long KS, Charles PA, Hannikainen DC, van Zyl L (2005) An ultracompact X-ray binary in the globular cluster M15 (NGC 7078). ApJ 634(1):L105–L108. https://doi.org/10.1086/498712. arXiv:astro-ph/0510430 [astro-ph]

Dijkstra M, Haiman Z, Mesinger A, Wyithe JSB (2008) Fluctuations in the high-redshift Lyman-Werner background: close halo pairs as the origin of supermassive black holes. MNRAS 391:1961–1972. https://doi.org/10.1111/j.1365-2966.2008.14031.x. arXiv:0810.0014

Dijkstra M, Ferrara A, Mesinger A (2014) Feedback-regulated supermassive black hole seed formation. MNRAS 442(3):2036–2047. https://doi.org/10.1093/mnras/stu1007. arXiv:1405.6743 [astro-ph.GA]

Dittmann AJ, Miller MC (2020) Star formation in accretion discs and SMBH growth. MNRAS 493(3):3732–3743. https://doi.org/10.1093/mnras/staa463. arXiv:1911.08685 [astro-ph.HE]

Domcke V, Muia F, Pieroni M, Witkowski LT (2017) PBH dark matter from axion inflation. J Cosmol Astropart Phys 07:048. https://doi.org/10.1088/1475-7516/2017/07/048. arXiv:1704.03464 [astro-ph.CO]

Dominik M, Belczynski K, Fryer C, Holz DE, Berti E, Bulik T, el Mand I, O'Shaughnessy R (2013) Double compact objects. II. Cosmological merger rates. ApJ 779(1):72. https://doi.org/10.1088/0004-637X/779/1/72. arXiv:1308.1546 [astro-ph.HE]

D'Orazio DJ, Di Stefano R (2018) Periodic self-lensing from accreting massive black hole binaries. MNRAS 474(3):2975–2986. https://doi.org/10.1093/mnras/stx2936. arXiv:1707.02335 [astro-ph.HE]

D'Orazio DJ, Loeb A (2018) Repeated imaging of massive black hole binary orbits with millimeter interferometry: measuring black hole masses and the Hubble constant. ApJ 863(2):185. https://doi.org/10.3847/1538-4357/aad413. arXiv:1712.02362 [astro-ph.HE]

D'Orazio DJ, Samsing J (2018) Black hole mergers from globular clusters observable by LISA II. Resolved eccentric sources and the gravitational wave background. MNRAS 481(4):4775–4785. https://doi.org/10.1093/mnras/sty2568. arXiv:1805.06194 [astro-ph.HE]

D'Orazio DJ, Haiman Z, MacFadyen A (2013) Accretion into the central cavity of a circumbinary disc. MNRAS 436(4):2997–3020. https://doi.org/10.1093/mnras/stt1787. arXiv:1210.0536 [astro-ph.GA]

D'Orazio DJ, Haiman Z, Schiminovich D (2015) Relativistic boost as the cause of periodicity in a massive black-hole binary candidate. Nature 525(7569):351–353. https://doi.org/10.1038/nature15262. arXiv:1509.04301 [astro-ph.HE]

D'Orazio DJ, Haiman Z, Duffell P, MacFadyen A, Farris B (2016) A transition in circumbinary accretion discs at a binary mass ratio of 1:25. MNRAS 459(3):2379–2393. https://doi.org/10.1093/mnras/stw792. arXiv:1512.05788 [astro-ph.HE]

Dosopoulou F, Antonini F (2017) Dynamical friction and the evolution of supermassive black hole binaries: the final hundred-parsec problem. ApJ 840(1):31. https://doi.org/10.3847/1538-4357/aa6b58. arXiv:1611.06573 [astro-ph.GA]

Dotti M, Colpi M, Haardt F (2006) Laser interferometer space antenna double black holes: dynamics in gaseous nuclear discs. MNRAS 367(1):103–112. https://doi.org/10.1111/j.1365-2966.2005.09956.x. arXiv:astro-ph/0509813 [astro-ph]

Dotti M, Colpi M, Haardt F, Mayer L (2007) Supermassive black hole binaries in gaseous and stellar circumnuclear discs: orbital dynamics and gas accretion. MNRAS 379(3):956–962. https://doi.org/10.1111/j.1365-2966.2007.12010.x. arXiv:astro-ph/0612505 [astro-ph]

Dotti M, Volonteri M, Perego A, Colpi M, Ruszkowski M, Haardt F (2010) Dual black holes in merger remnants—II. Spin evolution and gravitational recoil. MNRAS 402(1):682–690. https://doi.org/10.1111/j.1365-2966.2009.15922.x. arXiv:0910.5729 [astro-ph.HE]

Dotti M, Sesana A, Decarli R (2012) Massive black hole binaries: dynamical evolution and observational signatures. Adv Astron 2012:940568. https://doi.org/10.1155/2012/940568. arXiv:1111.0664 [astro-ph.CO]

Dotti M, Colpi M, Pallini S, Perego A, Volonteri M (2013) On the orientation and magnitude of the black hole spin in galactic nuclei. ApJ 762(2):68. https://doi.org/10.1088/0004-637X/762/2/68. arXiv:1211.4871 [astro-ph.CO]

Dovciak M, Matt G, Bianchi S, Boller T, Brenneman L, Bursa M, D'Ai A, di Salvo T, de Marco B, Goosmann R et al (2013) The hot and energetic universe: the close environments of supermassive black holes. arXiv e-prints arXiv:1306.2331 [astro-ph.HE]

Dovčiak M, Muleri F, Goosmann RW, Karas V, Matt G (2008) Thermal disc emission from a rotating black hole: X-ray polarization signatures. MNRAS 391(1):32–38. https://doi.org/10.1111/j.1365-2966.2008.13872.x. arXiv:0809.0418 [astro-ph]

Drasco S (2009) Verifying black hole orbits with gravitational spectroscopy. Phys Rev D 79(10):104016. https://doi.org/10.1103/PhysRevD.79.104016. arXiv:0711.4644 [gr-qc]

du Buisson L, Marchant P, Podsiadlowski P, Kobayashi C, Abdalla FB, Taylor P, Mandel I, de Mink SE, Moriya TJ, Langer N (2020) Cosmic rates of black hole mergers and pair-instability supernovae from chemically homogeneous binary evolution. MNRAS 499:5941–5959. https://doi.org/10.1093/mnras/staa3225. arXiv:2002.11630 [astro-ph.HE]

Dubois Y, Devriendt J, Slyz A, Teyssier R (2012) Self-regulated growth of supermassive black holes by a dual jet-heating active galactic nucleus feedback mechanism: methods, tests and implications for cosmological simulations. MNRAS 420(3):2662–2683. https://doi.org/10.1111/j.1365-2966.2011.20236.x. arXiv:1108.0110 [astro-ph.CO]

Dubois Y, Pichon C, Devriendt J, Silk J, Haehnelt M, Kimm T, Slyz A (2013) Blowing cold flows away: the impact of early AGN activity on the formation of a brightest cluster galaxy progenitor. MNRAS 428(4):2885–2900. https://doi.org/10.1093/mnras/sts224. arXiv:1206.5838 [astro-ph.CO]

Dubois Y, Pichon C, Welker C, Le Borgne D, Devriendt J, Laigle C, Codis S, Pogosyan D, Arnouts S, Benabed K et al (2014) Dancing in the dark: galactic properties trace spin swings along the cosmic web. MNRAS 444(2):1453–1468. https://doi.org/10.1093/mnras/stu1227. arXiv:1402.1165 [astro-ph.CO]

Dubois Y, Volonteri M, Silk J (2014) Black hole evolution—III. Statistical properties of mass growth and spin evolution using large-scale hydrodynamical cosmological simulations. MNRAS 440(2):1590–1606. https://doi.org/10.1093/mnras/stu373. arXiv:1304.4583 [astro-ph.CO]

Dubois Y, Volonteri M, Silk J, Devriendt J, Slyz A, Teyssier R (2015) Black hole evolution—I. Supernova-regulated black hole growth. MNRAS 452(2):1502–1518. https://doi.org/10.1093/mnras/stv1416. arXiv:1504.00018 [astro-ph.GA]

Dubois Y, Beckmann R, Bournaud F, Choi H, Devriendt J, Jackson R, Kaviraj S, Kimm T, Kraljic K, Laigle C et al (2021) Introducing the NEWHORIZON simulation: galaxy properties with resolved internal dynamics across cosmic time. A&A 651:A109. https://doi.org/10.1051/0004-6361/202039429. arXiv:2009.10578 [astro-ph.GA]

Duechting N (2004) Supermassive black holes from primordial black hole seeds. Phys Rev D 70:064015. https://doi.org/10.1103/PhysRevD.70.064015. arXiv:astro-ph/0406260

Duez MD, Zlochower Y (2019) Numerical relativity of compact binaries in the 21st century. Rep Prog Phys 82(1):016902. https://doi.org/10.1088/1361-6633/aadb16. arXiv:1808.06011 [gr-qc]

Duffell PC (2015) Halting migration: numerical calculations of corotation torques in the weakly nonlinear regime. ApJ 806(2):182. https://doi.org/10.1088/0004-637X/806/2/182. arXiv:1412.8092 [astro-ph.EP]

Duffell PC, D'Orazio D, Derdzinski A, Haiman Z, MacFadyen A, Rosen AL, Zrake J (2020) Circumbinary disks: accretion and torque as a function of mass ratio and disk viscosity. ApJ 901(1):25. https://doi.org/10.3847/1538-4357/abab95. arXiv:1911.05506 [astro-ph.SR]

Dullo BT (2019) The most massive galaxies with large depleted cores: structural parameter relations and black hole masses. ApJ 886(2):80. https://doi.org/10.3847/1538-4357/ab4d4f. arXiv:1910.10240 [astro-ph.GA]

Dullo BT, Graham AW (2013) Central stellar mass deficits in the bulges of local lenticular galaxies, and the connection with compact z −1.5 galaxies. ApJ 768(1):36. https://doi.org/10.1088/0004-637X/768/1/36. arXiv:1303.1273 [astro-ph.CO]

Dullo BT, Graham AW (2014) Depleted cores, multicomponent fits, and structural parameter relations for luminous early-type galaxies. MNRAS 444(3):2700–2722. https://doi.org/10.1093/mnras/stu1590. arXiv:1310.5867 [astro-ph.CO]

Duncan MJ, Lissauer JJ (1998) The effects of post-main-sequence solar mass loss on the stability of our planetary system. Icarus 134(2):303–310. https://doi.org/10.1006/icar.1998.5962

Dunhill AC, Alexander RD, Armitage PJ (2013) A limit on eccentricity growth from global 3D simulations of disc-planet interactions. MNRAS 428(4):3072–3082. https://doi.org/10.1093/mnras/sts254. arXiv:1210.6035 [astro-ph.EP]

Dunlop JS, Abraham RG, Ashby MLN, Bagley M, Best PN, Bongiorno A, Bouwens R, Bowler RAA, Brammer G, Bremer M, et al (2021) PRIMER: public release IMaging for extragalactic research. JWST proposal. Cycle 1, ID. #1837

Dunn G, Bellovary J, Holley-Bockelmann K, Christensen C, Quinn T (2018) Sowing black hole seeds: direct collapse black hole formation with realistic Lyman–Werner radiation in cosmological simulations. ApJ 861(1):39. https://doi.org/10.3847/1538-4357/aac7c2. arXiv:1803.01007 [astro-ph.GA]

Dunn G, Holley-Bockelmann K, Bellovary J (2020) The role of gravitational recoil in the assembly of massive black hole seeds. ApJ 896(1):72. https://doi.org/10.3847/1538-4357/ab7cd2. arXiv:2002.04740 [astro-ph.GA]

Dvorkin I, Uzan JP, Vangioni E, Silk J (2016) Synthetic model of the gravitational wave background from evolving binary compact objects. Phys Rev D 94(10):103011. https://doi.org/10.1103/PhysRevD.94.103011. arXiv:1607.06818 [astro-ph.HE]

Dvorkin I, Vangioni E, Silk J, Uzan JP, Olive KA (2016) Metallicity-constrained merger rates of binary black holes and the stochastic gravitational wave background. MNRAS 461(4):3877–3885. https://doi.org/10.1093/mnras/stw1477. arXiv:1604.04288 [astro-ph.HE]

Eatough RP, Kramer M, Lyne AG, Keith MJ (2013) A coherent acceleration search of the Parkes multibeam pulsar survey—techniques and the discovery and timing of 16 pulsars. MNRAS 431(1):292–307. https://doi.org/10.1093/mnras/stt161. arXiv:1301.6346 [astro-ph.IM]

Ebisuzaki T, Makino J, Okumura SK (1991) Merging of two galaxies with central black holes. Nature 354(6350):212–214. https://doi.org/10.1038/354212a0

Ebisuzaki T, Makino J, Tsuru TG, Funato Y, Portegies Zwart S, Hut P, McMillan S, Matsushita S, Matsumoto H, Kawabe R (2001) Missing link found? The "runaway" path to supermassive black holes. ApJ 562(1):L19–L22. https://doi.org/10.1086/338118. arXiv:astro-ph/0106252 [astro-ph]

Eda K, Itoh Y, Kuroyanagi S, Silk J (2013) New probe of dark-matter properties: gravitational waves from an intermediate-mass black hole embedded in a dark-matter minispike. Phys Rev Lett 110(22):221101. https://doi.org/10.1103/PhysRevLett.110.221101. arXiv:1301.5971 [gr-qc]

Edlund JA, Tinto M, Królak A, Nelemans G (2005) White-dwarf white-dwarf galactic background in the LISA data. Phys Rev D 71(12):122003. https://doi.org/10.1103/PhysRevD.71.122003. arXiv:gr-qc/0504112 [gr-qc]

Edwards LOV, Patton DR (2012) Close companions to brightest cluster galaxies: support for minor mergers and downsizing. MNRAS 425(1):287–295. https://doi.org/10.1111/j.1365-2966.2012.21457.x. arXiv:1206.1612 [astro-ph.CO]

Eggleton P (2006) Evolutionary processes in binary and multiple stars. Cambridge University Press, Cambridge

Eggleton PP (1983) Aproximations to the radii of Roche lobes. ApJ 268:368–369. https://doi.org/10.1086/160960

Eilon E, Kupi G, Alexander T (2009) The efficiency of resonant relaxation around a massive black hole. ApJ 698(1):641–647. https://doi.org/10.1088/0004-637X/698/1/641. arXiv:0807.1430 [astro-ph]

Elbert OD, Bullock JS, Kaplinghat M (2018) Counting black holes: the cosmic stellar remnant population and implications for LIGO. MNRAS 473(1):1186–1194. https://doi.org/10.1093/mnras/stx1959. arXiv:1703.02551 [astro-ph.GA]

Eldridge JJ, Stanway ER (2016) BPASS predictions for binary black hole mergers. MNRAS 462(3):3302–3313. https://doi.org/10.1093/mnras/stw1772. arXiv:1602.03790 [astro-ph.HE]

Enoki M, Inoue KT, Nagashima M, Sugiyama N (2005) Gravitational waves from coalescing supermassive black hole binaries in a hierarchical galaxy formation model. Annu Rep Natl Astron Observ Jpn 7:34 arXiv:astro-ph/0502529 [astro-ph]

Eracleous M, Boroson TA, Halpern JP, Liu J (2012) A large systematic search for close supermassive binary and rapidly recoiling black holes. ApJS 201(2):23. https://doi.org/10.1088/0067-0049/201/2/23. arXiv:1106.2952 [astro-ph.CO]

Espaillat C, Patterson J, Warner B, Woudt P (2005) The helium-rich cataclysmic variable ES Ceti. PASP 117(828):189–198. https://doi.org/10.1086/427959. arXiv:astro-ph/0412068 [astro-ph]

Euclid Collaboration, Barnett R, Warren SJ, Mortlock DJ, Cuby JG, Conselice C, Hewett PC, Willott CJ, Auricchio N, Balaguera-Antolínez A et al (2019) Euclid preparation. V. Predicted yield of redshift $7 < z < 9$ quasars from the wide survey. A&A 631:A85. https://doi.org/10.1051/0004-6361/201936427. arXiv:1908.04310 [astro-ph.GA]

Everson RW, MacLeod M, De S, Macias P, Ramirez-Ruiz E (2020) Common envelope wind tunnel: range of applicability and self-similarity in realistic stellar envelopes. ApJ 899(1):77. https://doi.org/10.3847/1538-4357/aba75c. arXiv:2006.07471 [astro-ph.SR]

Fabian AC (2012) Observational evidence of active galactic nuclei feedback. ARA&A 50:455–489. https://doi.org/10.1146/annurev-astro-081811-125521. arXiv:1204.4114 [astro-ph.CO]

Fabian AC, Pringle JE, Rees MJ (1975) Tidal capture formation of binary systems and X-ray sources in globular clusters. MNRAS 172:15. https://doi.org/10.1093/mnras/172.1.15P

Fabian AC, Iwasawa K, Reynolds CS, Young AJ (2000) Broad iron lines in active galactic nuclei. PASP 112(775):1145–1161. https://doi.org/10.1086/316610. arXiv:astro-ph/0004366 [astro-ph]

Fabj G, Nasim SS, Caban F, Ford KES, McKernan B, Bellovary JM (2020) Aligning nuclear cluster orbits with an active galactic nucleus accretion disk. MNRAS 499(2). https://doi.org/10.1093/mnras/staa3004. arXiv:2006.11229 [astro-ph.GA]

Fabrycky D, Tremaine S (2007) Shrinking binary and planetary orbits by Kozai cycles with tidal friction. ApJ 669(2):1298–1315. https://doi.org/10.1086/521702. arXiv:0705.4285 [astro-ph]

Fairhurst S (2009) Triangulation of gravitational wave sources with a network of detectors. New J Phys 11:123006

Fakhouri O, Ma CP, Boylan-Kolchin M (2010) The merger rates and mass assembly histories of dark matter haloes in the two Millennium simulations. MNRAS 406(4):2267–2278. https://doi.org/10.1111/j.1365-2966.2010.16859.x. arXiv:1001.2304 [astro-ph.CO]

Falta D, Fisher R, Khanna G (2011) Gravitational wave emission from the single-degenerate channel of type Ia supernovae. Phys Rev Lett 106(20):201103. https://doi.org/10.1103/PhysRevLett.106.201103. arXiv:1011.6387 [astro-ph.HE]

Fan X, Strauss MA, Schneider DP, Becker RH, White RL, Haiman Z, Gregg M, Pentericci L, Grebel EK, Narayanan VK et al (2003) A survey of z > 5.7 quasars in the Sloan digital sky survey. II. Discovery of three additional quasars at z > 6. AJ 125(4):1649–1659. https://doi.org/10.1086/368246. arXiv:astro-ph/0301135 [astro-ph]

Fan X, Carilli CL, Keating B (2006) Observational constraints on cosmic reionization. ARA&A 44(1):415–462. https://doi.org/10.1146/annurev.astro.44.051905.092514. arXiv:astro-ph/0602375 [astro-ph]

Fan X, Barth A, Banados E, De Rosa G, Decarli R, Eilers AC, Farina EP, Greene J, Habouzit M, Jiang L et al (2019) The first luminous quasars and their host galaxies. BAAS 51(3):121 arXiv:1903.04078 [astro-ph.GA]

Farihi J, Becklin EE, Zuckerman B (2005) Low-luminosity companions to white dwarfs. ApJS 161(2):394–428. https://doi.org/10.1086/444362. arXiv:astro-ph/0506017 [astro-ph]

Farihi J, Jura M, Zuckerman B (2009) Infrared signatures of disrupted minor planets at white dwarfs. ApJ 694(2):805–819. https://doi.org/10.1088/0004-637X/694/2/805. arXiv:0901.0973 [astro-ph.EP]

Farmer AJ, Phinney ES (2003) The gravitational wave background from cosmological compact binaries. MNRAS 346(4):1197–1214. https://doi.org/10.1111/j.1365-2966.2003.07176.x. arXiv:astro-ph/0304393 [astro-ph]

Farmer R, Renzo M, de Mink SE, Marchant P, Justham S (2019) Mind the gap: the location of the lower edge of the pair-instability supernova black hole mass gap. ApJ 887(1):53. https://doi.org/10.3847/1538-4357/ab518b. arXiv:1910.12874 [astro-ph.SR]

Farr WM, Stevenson S, Miller MC, Mandel I, Farr B, Vecchio A (2017) Distinguishing spin-aligned and isotropic black hole populations with gravitational waves. Nature 548:426–429. https://doi.org/10.1038/nature23453. arXiv:1706.01385 [astro-ph.HE]

Farris BD, Liu YT, Shapiro SL (2010) Binary black hole mergers in gaseous environments: "Binary Bondi" and "binary Bondi–Hoyle–Lyttleton" accretion. Phys Rev D 81(8):084008. https://doi.org/10.1103/PhysRevD.81.084008. arXiv:0912.2096 [astro-ph.HE]

Farris BD, Gold R, Paschalidis V, Etienne ZB, Shapiro SL (2012) Binary black-hole mergers in magnetized disks: simulations in full general relativity. Phys Rev Lett 109(22):221102. https://doi.org/10.1103/PhysRevLett.109.221102. arXiv:1207.3354 [astro-ph.HE]

Farris BD, Duffell P, MacFadyen AI, Haiman Z (2015) Binary black hole accretion during inspiral and merger. MNRAS 447:L80–L84. https://doi.org/10.1093/mnrasl/slu184. arXiv:1409.5124 [astro-ph.HE]

Farris BD, Duffell P, MacFadyen AI, Haiman Z (2015) Characteristic signatures in the thermal emission from accreting binary black holes. MNRAS 446:L36–L40. https://doi.org/10.1093/mnrasl/slu160. arXiv:1406.0007 [astro-ph.HE]

Farrow N, Zhu XJ, Thrane E (2019) The mass distribution of galactic double neutron stars. ApJ 876(1):18. https://doi.org/10.3847/1538-4357/ab12e3. arXiv:1902.03300 [astro-ph.HE]

Faulkner J (1971) Ultrashort-period binaries, gravitational radiation, and mass transfer. I. The standard model, with applications to WZ Sagittae and Z camelopardalis. ApJ 170:L99. https://doi.org/10.1086/180848

Feng H, Soria R (2011) Ultraluminous X-ray sources in the Chandra and XMM-Newton era. New A Rev 55(5):166–183. https://doi.org/10.1016/j.newar.2011.08.002. arXiv:1109.1610 [astro-ph.HE]

Fernández R, Metzger BD (2013) Nuclear dominated accretion flows in two dimensions. I. Torus evolution with parametric microphysics. ApJ 763(2):108. https://doi.org/10.1088/0004-637X/763/2/108. arXiv:1209.2712 [astro-ph.HE]

Fernandez R, Bryan GL, Haiman Z, Li M (2014) H_2 suppression with shocking inflows: testing a pathway for supermassive black hole formation. MNRAS 439:3798–3807. https://doi.org/10.1093/mnras/stu230. arXiv:1401.5803 [astro-ph.CO]

Ferrara A, Salvadori S, Yue B, Schleicher D (2014) Initial mass function of intermediate-mass black hole seeds. MNRAS 443(3):2410–2425. https://doi.org/10.1093/mnras/stu1280. arXiv:1406.6685 [astro-ph.GA]

Ferrarese L, Merritt D (2000) A fundamental relation between supermassive black holes and their host galaxies. ApJ 539(1):L9–L12. https://doi.org/10.1086/312838. arXiv:astro-ph/0006053 [astro-ph]

Ferrario L, de Martino D, Gänsicke BT (2015) Magnetic white dwarfs. Space Sci Rev 191(1–4):111–169. https://doi.org/10.1007/s11214-015-0152-0. arXiv:1504.08072 [astro-ph.SR]

Fiacconi D, Mayer L, Roškar R, Colpi M (2013) Massive black hole pairs in clumpy, self-gravitating circumnuclear disks: stochastic orbital decay. ApJ 777(1):L14. https://doi.org/10.1088/2041-8205/777/1/L14. arXiv:1307.0822 [astro-ph.CO]

Fiacconi D, Mayer L, Madau P, Lupi A, Dotti M, Haardt F (2017) Young and turbulent: the early life of massive galaxy progenitors. MNRAS 467(4):4080–4100. https://doi.org/10.1093/mnras/stx335. arXiv:1609.09499 [astro-ph.GA]

Fiacconi D, Sijacki D, Pringle JE (2018) Galactic nuclei evolution with spinning black holes: method and implementation. MNRAS 477(3):3807–3835. https://doi.org/10.1093/mnras/sty893. arXiv:1712.00023 [astro-ph.GA]

Fink M, Röpke FK, Hillebrandt W, Seitenzahl IR, Sim SA, Kromer M (2010) Double-detonation sub-Chandrasekhar supernovae: can minimum helium shell masses detonate the core? A&A 514:A53. https://doi.org/10.1051/0004-6361/200913892. arXiv:1002.2173 [astro-ph.SR]

Finkelstein SL, Papovich C, Pirzkal N, Bagley M, Berg D, Castellano M, Chavez Ortiz OA, Chworowsky K, Dave R, Dickinson M et al (2021) The Webb deep extragalactic exploratory public (WDEEP) survey: feedback in low-mass galaxies from cosmic dawn to dusk. JWST proposal. Cycle 1, ID. #2079

Fiore F, Puccetti S, Brusa M, Salvato M, Zamorani G, Aldcroft T, Aussel H, Brunner H, Capak P, Cappelluti N et al (2009) Chasing highly obscured QSOs in the COSMOS field. ApJ 693(1):447–462. https://doi.org/10.1088/0004-637X/693/1/447. arXiv:0810.0720 [astro-ph]

Fitchett MJ (1983) The influence of gravitational wave momentum losses on the centre of mass motion of a Newtonian binay system. MNRAS 203:1049–1062. https://doi.org/10.1093/mnras/203.4.1049

Flanagan ÉÉ, Hinderer T (2008) Constraining neutron-star tidal Love numbers with gravitational-wave detectors. Phys Rev D 77(2):021502. https://doi.org/10.1103/PhysRevD.77.021502. arXiv:0709.1915 [astro-ph]

Flanagan ÉÉ, Hinderer T (2012) Transient resonances in the inspirals of point particles into black holes. Phys Rev Lett 109(7):071102. https://doi.org/10.1103/PhysRevLett.109.071102. arXiv:1009.4923 [gr-qc]

Fluri J, Kacprzak T, Lucchi A, Refregier A, Amara A, Hofmann T, Schneider A (2019) Cosmological constraints with deep learning from KiDS-450 weak lensing maps. Phys Rev D 100(6):063514. https://doi.org/10.1103/PhysRevD.100.063514. arXiv:1906.03156 [astro-ph.CO]

Fontaine G, Brassard P, Green EM, Charpinet S, Dufour P, Hubeny I, Steeghs D, Aerts C, Randall SK, Bergeron P et al (2011) Discovery of a new AM CVn system with the Kepler satellite. ApJ 726(2):92. https://doi.org/10.1088/0004-637X/726/2/92

Fontecilla C, Chen X, Cuadra J (2017) A second decoupling between merging binary black holes and the inner disc—impact on the electromagnetic counterpart. MNRAS 468(1):L50–L54. https://doi.org/10.1093/mnrasl/slw258. arXiv:1610.09382 [astro-ph.HE]

Ford EB, Kozinsky B, Rasio FA (2000) Secular evolution of hierarchical triple star systems. ApJ 535 (1):385–401. https://doi.org/10.1086/308815

Fouvry JB, Bar-Or B, Chavanis PH (2019) Vector resonant relaxation of stars around a massive black hole. ApJ 883(2):161. https://doi.org/10.3847/1538-4357/ab2f78. arXiv:1812.07053 [astro-ph.GA]

Fragione G (2022) Mergers of supermassive and intermediate-mass black holes in galactic nuclei from disruptions of star clusters. ApJ 939:97. https://doi.org/10.3847/1538-4357/ac98b6. arXiv:2202.05618 [astro-ph.HE]

Fragione G, Kocsis B (2019) Black hole mergers from quadruples. MNRAS 486(4):4781–4789. https://doi.org/10.1093/mnras/stz1175. arXiv:1903.03112 [astro-ph.GA]

Fragione G, Loeb A (2019) Black hole-neutron star mergers from triples. MNRAS 486(3):4443–4450. https://doi.org/10.1093/mnras/stz1131. arXiv:1903.10511 [astro-ph.GA]

Fragione G, Silk J (2020) Repeated mergers and ejection of black holes within nuclear star clusters. MNRAS https://doi.org/10.1093/mnras/staa2629. arXiv:2006.01867 [astro-ph.GA]

Fragione G, Ginsburg I, Kocsis B (2018) Gravitational waves and intermediate-mass black hole retention in globular clusters. ApJ 856(2):92. https://doi.org/10.3847/1538-4357/aab368. arXiv:1711.00483 [astro-ph.GA]

Fragione G, Grishin E, Leigh NWC, Perets HB, Perna R (2019) Black hole and neutron star mergers in galactic nuclei. MNRAS 488(1):47–63. https://doi.org/10.1093/mnras/stz1651. arXiv:1811.10627 [astro-ph.GA]

Fragione G, Martinez MAS, Kremer K, Chatterjee S, Rodriguez CL, Ye CS, Weatherford NC, Naoz S, Rasio FA (2020) Demographics of triple systems in dense star clusters. ApJ 900(1):16. https://doi.org/10.3847/1538-4357/aba89b. arXiv:2007.11605 [astro-ph.GA]

Fragos T, Andrews JJ, Ramirez-Ruiz E, Meynet G, Kalogera V, Taam RE, Zezas A (2019) The complete evolution of a neutron-star binary through a common envelope phase using 1D hydrodynamic simulations. ApJ 883(2):L45. https://doi.org/10.3847/2041-8213/ab40d1. arXiv:1907.12573 [astro-ph.HE]

Fragos T, Andrews JJ, Bavera SS, Berry CPL, Coughlin S, Dotter A, Giri P, Kalogera V, Katsaggelos A, Kovlakas K et al (2022) POSYDON: a general-purpose population synthesis code with detailed binary-evolution simulations. arXiv e-prints arXiv:2202.05892 [astro-ph.SR]

Franchini A, Sesana A, Dotti M (2021) Circumbinary disc self-gravity governing supermassive black hole binary mergers. MNRAS 507(1):1458–1467. https://doi.org/10.1093/mnras/stab2234. arXiv:2106.13253 [astro-ph.HE]

Franchini A, Lupi A, Sesana A (2022) Resolving massive black hole binary evolution via adaptive particle splitting. ApJ 929(1):L13. https://doi.org/10.3847/2041-8213/ac63a2. arXiv:2201.05619 [astro-ph.HE]

Frank J, Rees MJ (1976) Effects of massive black holes on dense stellar systems. MNRAS 176:633–647. https://doi.org/10.1093/mnras/176.3.633

Frank J, King A, Raine DJ (2002) Accretion power in astrophysics, 3rd edn. Cambridge University Press, Cambridge

Freitag M (2001) Monte Carlo cluster simulations to determine the rate of compact star inspiralling to a central galactic black hole. Class Quantum Grav 18(19):4033–4038. https://doi.org/10.1088/0264-9381/18/19/309. arXiv:astro-ph/0107193 [astro-ph]

Freitag M, Gürkan MA, Rasio FA (2006) Runaway collisions in young star clusters—II. Numerical results. MNRAS 368(1):141–161. https://doi.org/10.1111/j.1365-2966.2006.10096.x. arXiv:astro-ph/0503130 [astro-ph]

Freitag M, Rasio FA, Baumgardt H (2006) Runaway collisions in young star clusters—I. Methods and tests. MNRAS 368(1):121–140. https://doi.org/10.1111/j.1365-2966.2006.10095.x. arXiv:astro-ph/0503129 [astro-ph]

French KD, Arcavi I, Zabludoff A (2016) Tidal disruption events prefer unusual host galaxies. ApJ 818(1):L21. https://doi.org/10.3847/2041-8205/818/1/L21. arXiv:1601.04705 [astro-ph.GA]

Fruchter AS, Stinebring DR, Taylor JH (1988) A millisecond pulsar in an eclipsing binary. Nature 333(6170):237–239. https://doi.org/10.1038/333237a0

Fryer CL, Belczynski K, Wiktorowicz G, Dominik M, Kalogera V, Holz DE (2012) Compact remnant mass function: dependence on the explosion mechanism and metallicity. ApJ 749(1):91. https://doi.org/10.1088/0004-637X/749/1/91. arXiv:1110.1726 [astro-ph.SR]

Fujita R (2015) Gravitational waves from a particle in circular orbits around a rotating black hole to the 11th post-Newtonian order. Prog Theor Exp Phys 2015(3):033E01. https://doi.org/10.1093/ptep/ptv012. arXiv:1412.5689 [gr-qc]

Fuller J, Lai D (2012) Dynamical tides in compact white dwarf binaries: tidal synchronization and dissipation. MNRAS 421(1):426–445. https://doi.org/10.1111/j.1365-2966.2011.20320.x. arXiv:1108.4910 [astro-ph.SR]

Gabbard H, Williams M, Hayes F, Messenger C (2018) Matching matched filtering with deep networks for gravitational-wave astronomy. Phys Rev Lett 120(14):141103. https://doi.org/10.1103/PhysRevLett.120.141103. arXiv:1712.06041 [astro-ph.IM]

Gaia Collaboration, Brown AGA, Vallenari A, Prusti T, de Bruijne JHJ, Babusiaux C, Bailer-Jones CAL, Biermann M, Evans DW, Eyer L et al (2018) Gaia data release 2. Summary of the contents and survey properties. A&A 616:A1. https://doi.org/10.1051/0004-6361/201833051. arXiv:1804.09365 [astro-ph.GA]

Gaia Collaboration, Katz D, Antoja T, Romero-Gómez M, Drimmel R, Reylé C, Seabroke GM, Soubiran C, Babusiaux C, Di Matteo P et al (2018) Gaia data release 2. Mapping the milky way disc kinematics. A&A 616:A11. https://doi.org/10.1051/0004-6361/201832865. arXiv:1804.09380 [astro-ph.GA]

Gaia Collaboration, Brown AGA, Vallenari A, Prusti T, de Bruijne JHJ, Babusiaux C, Biermann M (2021) Gaia early data release 3: summary of the contents and survey properties. A&A 649:A1. https://doi.org/10.1051/0004-6361/202039657. arXiv:2012.01533 [astro-ph.GA]

Gair J, Jones G (2007) Detecting extreme mass ratio inspiral events in LISA data using the hierarchical algorithm for clusters and ridges (HACR). Class Quantum Grav 24(5):1145–1168. https://doi.org/10.1088/0264-9381/24/5/007. arXiv:gr-qc/0610046 [gr-qc]

Gair JR, Barack L, Creighton T, Cutler C, Larson SL, Phinney ES, Vallisneri M (2004) Event rate estimates for LISA extreme mass ratio capture sources. Class Quantum Grav 21(20):S1595–S1606. https://doi.org/10.1088/0264-9381/21/20/003. arXiv:gr-qc/0405137 [gr-qc]

Gair JR, Mandel I, Wen L (2008) Improved time frequency analysis of extreme-mass-ratio inspiral signals in mock LISA data. Class Quantum Grav 25(18):184031. https://doi.org/10.1088/0264-9381/25/18/184031. arXiv:0804.1084 [gr-qc]

Gair JR, Mandel I, Wen L (2008) Time-frequency analysis of extreme-mass-ratio inspiral signals in mock LISA data. J Phys Conf Ser 122:012037. https://doi.org/10.1088/1742-6596/122/1/012037. arXiv:0710.5250 [gr-qc]

Gair JR, Porter E, Babak S, Barack L (2008) A constrained metropolis Hastings search for EMRIs in the mock LISA data challenge 1B. Class Quantum Grav 25(18):184030. https://doi.org/10.1088/0264-9381/25/18/184030. arXiv:0804.3322 [gr-qc]

Gair JR, Mandel I, Miller MC, Volonteri M (2011) Exploring intermediate and massive black-hole binaries with the Einstein Telescope. Gen Relativ Gravit 43(2):485–518. https://doi.org/10.1007/s10714-010-1104-3. arXiv:0907.5450 [astro-ph.CO]

Galaudage S, Adamcewicz C, Zhu XJ, Stevenson S, Thrane E (2021) Heavy double neutron stars: birth, midlife, and death. ApJ 909(2):L19. https://doi.org/10.3847/2041-8213/abe7f6. arXiv:2011.01495 [astro-ph.HE]

Gallego-Cano E, Schödel R, Dong H, Nogueras-Lara F, Gallego-Calvente AT, Amaro-Seoane P, Baumgardt H (2018) The distribution of stars around the Milky Way's central black hole. I. Deep star counts. A&A 609:A26. https://doi.org/10.1051/0004-6361/201730451. arXiv:1701.03816 [astro-ph.GA]

Gammie CF, Shapiro SL, McKinney JC (2004) Black hole spin evolution. ApJ 602(1):312–319. https://doi.org/10.1086/380996. arXiv:astro-ph/0310886 [astro-ph]

Gandhi P, Rao A, Johnson MAC, Paice JA, Maccarone TJ (2019) Gaia Data Release 2 distances and peculiar velocities for Galactic black hole transients. MNRAS 485(2):2642–2655. https://doi.org/10.1093/mnras/stz438. arXiv:1804.11349 [astro-ph.HE]

Gänsicke BT, Marsh TR, Southworth J, Rebassa-Mansergas A (2006) A gaseous metal disk around a white dwarf. Science 314(5807):1908. https://doi.org/10.1126/science.1135033. arXiv:astro-ph/0612697 [astro-ph]

Gänsicke BT, Schreiber MR, Toloza O, Gentile Fusillo NP, Koester D, Manser CJ (2019) Accretion of a giant planet onto a white dwarf star. Nature 576(7785):61–64. https://doi.org/10.1038/s41586-019-1789-8. arXiv:1912.01611 [astro-ph.EP]

Garavito-Camargo N, Besla G, Laporte CFP, Johnston KV, Gómez FA, Watkins LL (2019) Hunting for the dark matter wake induced by the large magellanic cloud. ApJ 884(1):51. https://doi.org/10.3847/1538-4357/ab32eb. arXiv:1902.05089 [astro-ph.GA]

Garavito-Camargo N, Besla G, Laporte CFP, Price-Whelan AM, Cunningham EC, Johnston KV, Weinberg M, Gómez FA (2021) Quantifying the impact of the large magellanic cloud on the structure of the milky way's dark matter halo using basis function expansions. ApJ 919(2):109. https://doi.org/10.3847/1538-4357/ac0b44. arXiv:2010.00816 [astro-ph.GA]

García JA, Fabian AC, Kallman TR, Dauser T, Parker ML, McClintock JE, Steiner JF, Wilms J (2016) The effects of high density on the X-ray spectrum reflected from accretion discs around black holes. MNRAS 462(1):751–760. https://doi.org/10.1093/mnras/stw1696. arXiv:1603.05259 [astro-ph.HE]

Garcia-Bellido J, Peloso M, Unal C (2016) Gravitational waves at interferometer scales and primordial black holes in axion inflation. J Cosmol Astropart Phys 12:031. https://doi.org/10.1088/1475-7516/2016/12/031. arXiv:1610.03763 [astro-ph.CO]

Garcia-Bellido J, Peloso M, Unal C (2017) Gravitational Wave signatures of inflationary models from Primordial Black Hole Dark Matter. J Cosmol Astropart Phys 09:013. https://doi.org/10.1088/1475-7516/2017/09/013. arXiv:1707.02441 [astro-ph.CO]

Gardner JP, Mather JC, Clampin M, Doyon R, Greenhouse MA, Hammel HB, Hutchings JB, Jakobsen P, Lilly SJ, Long KS et al (2006) The James Webb space telescope. Space Sci Rev 123(4):485–606. https://doi.org/10.1007/s11214-006-8315-7. arXiv:astro-ph/0606175 [astro-ph]

Gaskin JA, Swartz DA, Vikhlinin A, Özel F, Gelmis KE, Arenberg JW, Bandler SR, Bautz MW, Civitani MM, Dominguez A et al (2019) Lynx X-ray observatory: an overview. J Astron Telesc Instr Syst 5:021001. https://doi.org/10.1117/1.JATIS.5.2.021001

Gaspari M, Ruszkowski M, Sharma P (2012) Cause and effect of feedback: multiphase gas in cluster cores heated by AGN jets. ApJ 746(1):94. https://doi.org/10.1088/0004-637X/746/1/94. arXiv:1110.6063 [astro-ph.CO]

Gaspari M, Ruszkowski M, Oh SP (2013) Chaotic cold accretion on to black holes. MNRAS 432(4):3401–3422. https://doi.org/10.1093/mnras/stt692. arXiv:1301.3130 [astro-ph.CO]

Gaspari M, Brighenti F, Temi P (2015) Chaotic cold accretion on to black holes in rotating atmospheres. A&A 579:A62. https://doi.org/10.1051/0004-6361/201526151. arXiv:1407.7531 [astro-ph.GA]

Gaspari M, Temi P, Brighenti F (2017) Raining on black holes and massive galaxies: the top-down multiphase condensation model. MNRAS 466(1):677–704. https://doi.org/10.1093/mnras/stw3108. arXiv:1608.08216 [astro-ph.GA]

Gaspari M, Eckert D, Ettori S, Tozzi P, Bassini L, Rasia E, Brighenti F, Sun M, Borgani S, Johnson SD et al (2019) The X-ray halo scaling relations of supermassive black holes. ApJ 884(2):169. https://doi.org/10.3847/1538-4357/ab3c5d. arXiv:1904.10972 [astro-ph.GA]

Gaspari M, Tombesi F, Cappi M (2020) Linking macro-, meso- and microscales in multiphase AGN feeding and feedback. Nat Astron 4:10–13. https://doi.org/10.1038/s41550-019-0970-1. arXiv:2001.04985 [astro-ph.GA]

Gatti M, Lamastra A, Menci N, Bongiorno A, Fiore F (2015) Physical properties of AGN host galaxies as a probe of supermassive black hole feeding mechanisms. A&A 576:A32. https://doi.org/10.1051/0004-6361/201425094. arXiv:1412.7660 [astro-ph.GA]

Gavazzi G, Consolandi G, Dotti M, Fanali R, Fossati M, Fumagalli M, Viscardi E, Savorgnan G, Boselli A, Gutiérrez L et al (2015) Hα3: an Hα imaging survey of HI selected galaxies from ALFALFA. VI. The role of bars in quenching star formation from z = 3 to the present epoch. A&A 580:A116. https://doi.org/10.1051/0004-6361/201425351. arXiv:1505.07836 [astro-ph.GA]

Ge H, Webbink RF, Han Z (2020) The thermal equilibrium mass-loss model and its applications in binary evolution. ApJS 249(1):9. https://doi.org/10.3847/1538-4365/ab98f6. arXiv:2006.00774 [astro-ph.SR]

Gebhardt K, Bender R, Bower G, Dressler A, Faber SM, Filippenko AV, Green R, Grillmair C, Ho LC, Kormendy J et al (2000) A relationship between nuclear black hole mass and galaxy velocity dispersion. ApJ 539(1):L13–L16. https://doi.org/10.1086/312840. arXiv:astro-ph/0006289 [astro-ph]

Geha M, Brown TM, Tumlinson J, Kalirai JS, Simon JD, Kirby EN, Vand enBerg DA, Muñoz RR, Avila RJ, Guhathakurta P et al (2013) The stellar initial mass function of ultra-faint dwarf galaxies: evidence for IMF variations with galactic environment. ApJ 771(1):29. https://doi.org/10.1088/0004-637X/771/1/29. arXiv:1304.7769 [astro-ph.CO]

Geier S, Marsh TR, Wang B, Dunlap B, Barlow BN, Schaffenroth V, Chen X, Irrgang A, Maxted PFL et al (2013) A progenitor binary and an ejected mass donor remnant of faint type Ia supernovae. A&A 554:A54. https://doi.org/10.1051/0004-6361/201321395. arXiv:1304.4452 [astro-ph.SR]

Gendreau KC, Arzoumanian Z, Adkins PW, Albert CL, Anders JF, Aylward AT, Baker CL, Balsamo ER, Bamford WA, Benegalrao SS et al (2016) The neutron star interior composition explorer (NICER): design and development. In: den Herder JWA, Takahashi T, Bautz M (eds) Space telescopes and instrumentation 2016: ultraviolet to gamma ray. Society of photo-optical instrumentation engineers (SPIE) conference series, vol 9905. p 99051H. https://doi.org/10.1117/12.2231304

Generozov A, Madigan AM (2020) The hills mechanism and the galactic center S-stars. ApJ 896(2):137. https://doi.org/10.3847/1538-4357/ab94bc. arXiv:2002.10547 [astro-ph.GA]

Generozov A, Stone NC, Metzger BD, Ostriker JP (2018) An overabundance of black hole X-ray binaries in the Galactic Centre from tidal captures. MNRAS 478(3):4030–4051. https://doi.org/10.1093/mnras/sty1262. arXiv:1804.01543 [astro-ph.HE]

Genzel R, Eisenhauer F, Gillessen S (2010) The Galactic Center massive black hole and nuclear star cluster. Rev Mod Phys 82(4):3121–3195. https://doi.org/10.1103/RevModPhys.82.3121. arXiv:1006.0064 [astro-ph.GA]

Georgakarakos N (2008) Stability criteria for hierarchical triple systems. Celest Mech Dyn Astron 100 (2):151–168. https://doi.org/10.1007/s10569-007-9109-2. arXiv:1408.5431 [astro-ph.EP]

George D, Shen H, Huerta EA (2018) Classification and unsupervised clustering of LIGO data with Deep Transfer Learning. Phys Rev D 97(10):101501. https://doi.org/10.1103/PhysRevD.97.101501. arXiv:1706.07446 [gr-qc]

Gergely LÁ, Biermann PL, Caramete LI (2010) Supermassive black hole spin-flip during the inspiral. Class Quantum Grav 27(19):194009. https://doi.org/10.1088/0264-9381/27/19/194009. arXiv:1005.2287 [astro-ph.CO]

Gerosa D, Kesden M (2016) Precession: dynamics of spinning black-hole binaries with python. Phys Rev D 93(12):124066. https://doi.org/10.1103/PhysRevD.93.124066. arXiv:1605.01067 [astro-ph.HE]

Gerosa D, Moore CJ (2016) Black hole kicks as new gravitational wave observables. Phys Rev Lett 117 (1):011101. https://doi.org/10.1103/PhysRevLett.117.011101. arXiv:1606.04226 [gr-qc]

Gerosa D, Sesana A (2015) Missing black holes in brightest cluster galaxies as evidence for the occurrence of superkicks in nature. MNRAS 446(1):38–55. https://doi.org/10.1093/mnras/stu2049. arXiv:1405.2072 [astro-ph.GA]

Gerosa D, Kesden M, Berti E, O'Shaughnessy R, Sperhake U (2013) Resonant-plane locking and spin alignment in stellar-mass black-hole binaries: a diagnostic of compact-binary formation. Phys Rev D 87(10):104028. https://doi.org/10.1103/PhysRevD.87.104028. arXiv:1302.4442 [gr-qc]

Gerosa D, Kesden M, Sperhake U, Berti E, O'Shaughnessy R (2015) Multi-timescale analysis of phase transitions in precessing black-hole binaries. Phys Rev D 92(6):064016. https://doi.org/10.1103/PhysRevD.92.064016. arXiv:1506.03492 [gr-qc]

Gerosa D, Veronesi B, Lodato G, Rosotti G (2015) Spin alignment and differential accretion in merging black hole binaries. MNRAS 451(4):3941–3954. https://doi.org/10.1093/mnras/stv1214. arXiv:1503.06807 [astro-ph.GA]

Gerosa D, Berti E, O'Shaughnessy R, Belczynski K, Kesden M, Wysocki D, Gladysz W (2018) Spin orientations of merging black holes formed from the evolution of stellar binaries. Phys Rev D 98 (8):084036. https://doi.org/10.1103/PhysRevD.98.084036. arXiv:1808.02491 [astro-ph.HE]

Gerosa D, Hébert F, Stein LC (2018) Black-hole kicks from numerical-relativity surrogate models. Phys Rev D 97(10):104049. https://doi.org/10.1103/PhysRevD.97.104049. arXiv:1802.04276 [gr-qc]

Gerosa D, Ma S, Wong KWK, Berti E, O'Shaughnessy R, Chen Y, Belczynski K (2019) Multiband gravitational-wave event rates and stellar physics. Phys Rev D 99(10):103004. https://doi.org/10.1103/PhysRevD.99.103004. arXiv:1902.00021 [astro-ph.HE]

Gerosa D, Rosotti G, Barbieri R (2020) The Bardeen–Petterson effect in accreting supermassive black hole binaries: a systematic approach. MNRAS 496(3):3060–3075. https://doi.org/10.1093/mnras/staa1693. arXiv:2004.02894 [astro-ph.GA]

Giacobbo N, Mapelli M (2018) The progenitors of compact-object binaries: impact of metallicity, common envelope and natal kicks. MNRAS 480(2):2011–2030. https://doi.org/10.1093/mnras/sty1999. arXiv:1806.00001 [astro-ph.HE]

Giacobbo N, Mapelli M (2020) Revising natal kick prescriptions in population synthesis simulations. ApJ 891(2):141. https://doi.org/10.3847/1538-4357/ab7335. arXiv:1909.06385 [astro-ph.HE]

Giacobbo N, Mapelli M, Spera M (2018) Merging black hole binaries: the effects of progenitor's metallicity, mass-loss rate and Eddington factor. MNRAS 474(3):2959–2974. https://doi.org/10.1093/mnras/stx2933. arXiv:1711.03556 [astro-ph.SR]

Giacomazzo B, Baker JG, Miller MC, Reynolds CS, van Meter JR (2012) General relativistic simulations of magnetized plasmas around merging supermassive black holes. ApJ 752(1):L15. https://doi.org/10.1088/2041-8205/752/1/L15. arXiv:1203.6108 [astro-ph.HE]

Giammichele N, Bergeron P, Dufour P (2012) Know your neighborhood: a detailed model atmosphere analysis of nearby white dwarfs. ApJS 199(2):29. https://doi.org/10.1088/0067-0049/199/2/29. arXiv:1202.5581 [astro-ph.SR]

Giblin J, John T, Price LR, Siemens X, Vlcek B (2012) Gravitational waves from global second order phase transitions. J Cosmol Astropart Phys 11:006. https://doi.org/10.1088/1475-7516/2012/11/006. arXiv:1111.4014 [astro-ph.CO]

Gieles M, Bastian N (2008) An alternative method to study star cluster disruption. A&A 482(1):165–171. https://doi.org/10.1051/0004-6361:20078909. arXiv:0802.3387 [astro-ph]

Giersz M, Heggie DC, Hurley JR, Hypki A (2013) MOCCA code for star cluster simulations—II. Comparison with N-body simulations. MNRAS 431(3):2184–2199. https://doi.org/10.1093/mnras/stt307. arXiv:1112.6246 [astro-ph.GA]

Giersz M, Leigh N, Hypki A, Lützgendorf N, Askar A (2015) MOCCA code for star cluster simulations—IV. A new scenario for intermediate mass black hole formation in globular clusters. MNRAS 454(3):3150–3165. https://doi.org/10.1093/mnras/stv2162. arXiv:1506.05234 [astro-ph.GA]

Giersz M, Askar A, Wang L, Hypki A, Leveque A, Spurzem R (2019) MOCCA survey data base-I. Dissolution of tidally filling star clusters harbouring black hole subsystems. MNRAS 487(2):2412–2423. https://doi.org/10.1093/mnras/stz1460. arXiv:1904.01227 [astro-ph.GA]

Gillessen S, Plewa PM, Eisenhauer F, Sari R, Waisberg I, Habibi M, Pfuhl O, George E, Dexter J, von Fellenberg S et al (2017) An update on monitoring stellar orbits in the galactic center. ApJ 837(1):30. https://doi.org/10.3847/1538-4357/aa5c41. arXiv:1611.09144 [astro-ph.GA]

Gilli R, Daddi E, Zamorani G, Tozzi P, Borgani S, Bergeron J, Giacconi R, Hasinger G, Mainieri V, Norman C et al (2005) The spatial clustering of X-ray selected AGN and galaxies in the Chandra Deep Field South and North. A&A 430:811–825. https://doi.org/10.1051/0004-6361:20041375. arXiv:astro-ph/0409759 [astro-ph]

Gilli R, Norman C, Calura F, Vito F, Decarli R, Marchesi S, Iwasawa K, Comastri A, Lanzuisi G, Pozzi F et al (2022) Supermassive black holes at high redshift are expected to be obscured by their massive host galaxies interstellar medium. A&A 666:A17. https://doi.org/10.1051/0004-6361/202243708. arXiv:2206.03508 [astro-ph.GA]

Ginat YB, Glanz H, Perets HB, Grishin E, Desjacques V (2020) Gravitational waves from in-spirals of compact objects in binary common-envelope evolution. MNRAS 493(4):4861–4867. https://doi.org/10.1093/mnras/staa465. arXiv:1903.11072 [astro-ph.SR]

Girardi M, Fadda D, Giuricin G, Mardirossian F, Mezzetti M, Biviano A (1996) Velocity dispersions and X-ray temperatures of galaxy clusters. ApJ 457:61. https://doi.org/10.1086/176711. arXiv:astro-ph/9507031 [astro-ph]

Glanz H, Perets HB (2021) Simulations of common envelope evolution in triple systems: circumstellar case. MNRAS 500(2):1921–1932. https://doi.org/10.1093/mnras/staa3242. arXiv:2004.00020 [astro-ph.SR]

Gnedin OY, Ostriker JP, Tremaine S (2014) Co-evolution of galactic nuclei and globular cluster systems. ApJ 785(1):71. https://doi.org/10.1088/0004-637X/785/1/71. arXiv:1308.0021 [astro-ph.CO]

Gnocchi G, Maselli A, Abdelsalhin T, Giacobbo N, Mapelli M (2019) Bounding alternative theories of gravity with multiband GW observations. Phys Rev D 100(6):064024. https://doi.org/10.1103/PhysRevD.100.064024. arXiv:1905.13460 [gr-qc]

Goicovic FG, Cuadra J, Sesana A, Stasyszyn F, Amaro-Seoane P, Tanaka TL (2016) Infalling clouds on to supermassive black hole binaries—I. Formation of discs, accretion and gas dynamics. MNRAS 455(2):1989–2003. https://doi.org/10.1093/mnras/stv2470. arXiv:1507.05596 [astro-ph.HE]

Goicovic FG, Sesana A, Cuadra J, Stasyszyn F (2017) Infalling clouds on to supermassive black hole binaries—II. Binary evolution and the final parsec problem. MNRAS 472(1):514–531. https://doi.org/10.1093/mnras/stx1996. arXiv:1602.01966 [astro-ph.HE]

Goicovic FG, Maureira-Fredes C, Sesana A, Amaro-Seoane P, Cuadra J (2018) Accretion of clumpy cold gas onto massive black hole binaries: a possible fast route to binary coalescence. MNRAS 479 (3):3438–3455. https://doi.org/10.1093/mnras/sty1709. arXiv:1801.04937 [astro-ph.HE]

Gokhale V, Peng Xa, Frank J (2007) Evolution of close white dwarf binaries. ApJ 655(2):1010–1024. https://doi.org/10.1086/510119. arXiv:astro-ph/0610919 [astro-ph]

Gold R, Paschalidis V, Etienne ZB, Shapiro SL, Pfeiffer HP (2014) Accretion disks around binary black holes of unequal mass: general relativistic magnetohydrodynamic simulations near decoupling. Phys Rev D 89(6):064060. https://doi.org/10.1103/PhysRevD.89.064060. arXiv:1312.0600 [astro-ph.HE]

Gold R, Paschalidis V, Ruiz M, Shapiro SL, Etienne ZB, Pfeiffer HP (2014) Accretion disks around binary black holes of unequal mass: general relativistic MHD simulations of postdecoupling and merger. Phys Rev D 90(10):104030. https://doi.org/10.1103/PhysRevD.90.104030. arXiv:1410.1543 [astro-ph.GA]

Gondolo P, Silk J (1999) Dark matter annihilation at the galactic center. Phys Rev Lett 83(9):1719–1722. https://doi.org/10.1103/PhysRevLett.83.1719. arXiv:astro-ph/9906391 [astro-ph]

González E, Kremer K, Chatterjee S, Fragione G, Rodriguez CL, Weatherford NC, Ye CS, Rasio FA (2021) Intermediate-mass black holes from high massive-star binary fractions in young star clusters. ApJ 908(2):L29. https://doi.org/10.3847/2041-8213/abdf5b. arXiv:2012.10497 [astro-ph.HE]

González JA, Hannam M, Sperhake U, Brügmann B, Husa S (2007) Supermassive recoil velocities for binary black-hole mergers with antialigned spins. Phys Rev Lett 98(23):231101. https://doi.org/10.1103/PhysRevLett.98.231101. arXiv:gr-qc/0702052 [gr-qc]

González JA, Sperhake U, Brügmann B, Hannam M, Husa S (2007) Maximum kick from nonspinning black-hole binary inspiral. Phys Rev Lett 98(9):091101. https://doi.org/10.1103/PhysRevLett.98.091101. arXiv:gr-qc/0610154 [gr-qc]

González Delgado RM, Pérez E, Cid Fernandes R, Schmitt H (2008) HST/WFPC2 imaging of the circumnuclear structure of low-luminosity active galactic nuclei. I. Data and nuclear morphology. AJ 135(3):747–765. https://doi.org/10.1088/0004-6256/135/3/747. arXiv:0710.4450 [astro-ph]

Goodman J (2003) Self-gravity and quasi-stellar object discs. MNRAS 339(4):937–948. https://doi.org/10.1046/j.1365-8711.2003.06241.x. arXiv:astro-ph/0201001 [astro-ph]

Goodman J, Hut P (1993) Binary-single-star scattering. V. Steady state binary distribution in a homogeneous static background of single stars. ApJ 403:271. https://doi.org/10.1086/172200. arXiv:astro-ph/0201001 [astro-ph]

Goodman J, Tan JC (2004) Supermassive stars in quasar disks. ApJ 608(1):108–118. https://doi.org/10.1086/386360. arXiv:astro-ph/0307361 [astro-ph]

Götberg Y, Korol V, Lamberts A, Kupfer T, Breivik K, Ludwig B, Drout MR (2020) Stars stripped in binaries—the living gravitational wave sources. ApJ 904:56. https://doi.org/10.3847/1538-4357/abbda5. arXiv:2006.07382 [astro-ph.SR]

Goulding AD, Greene JE, Bezanson R, Greco J, Johnson S, Leauthaud A, Matsuoka Y, Medezinski E, Price-Whelan AM (2018) Galaxy interactions trigger rapid black hole growth: an unprecedented view from the Hyper Suprime-Cam survey. PASJ 70:S37. https://doi.org/10.1093/pasj/psx135. arXiv:1706.07436 [astro-ph.GA]

Gourgoulhon E, Le Tiec A, Vincent FH, Warburton N (2019) Gravitational waves from bodies orbiting the Galactic center black hole and their detectability by LISA. A&A 627:A92. https://doi.org/10.1051/0004-6361/201935406. arXiv:1903.02049 [gr-qc]

Governato F, Brook C, Mayer L, Brooks A, Rhee G, Wadsley J, Jonsson P, Willman B, Stinson G, Quinn T et al (2010) Bulgeless dwarf galaxies and dark matter cores from supernova-driven outflows. Nature 463(7278):203–206. https://doi.org/10.1038/nature08640. arXiv:0911.2237 [astro-ph.CO]

Gow AD, Byrnes CT, Cole PS, Young S (2021) The power spectrum on small scales: robust constraints and comparing PBH methodologies. J Cosmol Astropart Phys 2:002. https://doi.org/10.1088/1475-7516/2021/02/002. arXiv:2008.03289 [astro-ph.CO]

Goździewski K, Słowikowska A, Dimitrov D, Krzeszowski K, Zejmo M, Kanbach G, Burwitz V, Rau A, Irawati P, Richichi A et al (2015) The HU Aqr planetary system hypothesis revisited. MNRAS 448 (2):1118–1136. https://doi.org/10.1093/mnras/stu2728. arXiv:1412.5899 [astro-ph.EP]

Graham AW (2004) Core depletion from coalescing supermassive black holes. ApJ 613(1):L33–L36. https://doi.org/10.1086/424928. arXiv:astro-ph/0503177 [astro-ph]

Graham AW (2016a) Black hole and nuclear cluster scaling relations: $M_{bh} - M_{nc}^{2.7+/-0.7}$. Proc Int Astron Union 10(S312):269–273. https://doi.org/10.1017/S1743921315008017. arXiv:1412.5715 [astro-ph. GA]

Graham AW (2016b) Galaxy bulges and their massive black holes: a review. In: Laurikainen E, Peletier R, Gadotti D (eds) Galactic bulges. Astrophysics and Space Science Library, vol 418. Springer, pp 263–313. https://doi.org/10.1007/978-3-319-19378-6_11

Graham AW, Driver SP (2007) A log-quadratic relation for predicting supermassive black hole masses from the host bulge Sérsic index. ApJ 655(1):77–87. https://doi.org/10.1086/509758. arXiv:astro-ph/0607378 [astro-ph]

Graham AW, Scott N (2015) The (black hole)-bulge mass scaling relation at low masses. ApJ 798(1):54. https://doi.org/10.1088/0004-637X/798/1/54. arXiv:1412.3091 [astro-ph.GA]

Graham AW, Soria R (2019) Expected intermediate-mass black holes in the Virgo cluster—I. Early-type galaxies. MNRAS 484(1):794–813. https://doi.org/10.1093/mnras/sty3398. arXiv:1812.01231 [astro-ph.HE]

Graham AW, Spitler LR (2009) Quantifying the coexistence of massive black holes and dense nuclear star clusters. MNRAS 397(4):2148–2162. https://doi.org/10.1111/j.1365-2966.2009.15118.x. arXiv:0907.5250 [astro-ph.CO]

Graham AW, Erwin P, Trujillo I, Asensio Ramos A (2003) A new empirical model for the structural analysis of early-type galaxies, and a critical review of the Nuker model. AJ 125(6):2951–2963. https://doi.org/10.1086/375320. arXiv:astro-ph/0306023 [astro-ph]

Graham AW, Driver SP, Allen PD, Liske J (2007) The Millennium Galaxy Catalogue: the local supermassive black hole mass function in early- and late-type galaxies. MNRAS 378(1):198–210. https://doi.org/10.1111/j.1365-2966.2007.11770.x. arXiv:0704.0316 [astro-ph]

Graham AW, Soria R, Davis BL (2019) Expected intermediate-mass black holes in the Virgo cluster—II. Late-type galaxies. MNRAS 484(1):814–831. https://doi.org/10.1093/mnras/sty3068. arXiv:1811.03232 [astro-ph.GA]

Graham MJ, Djorgovski SG, Stern D, Drake AJ, Mahabal AA, Donalek C, Glikman E, Larson S, Christensen E (2015) A systematic search for close supermassive black hole binaries in the Catalina Real-time Transient Survey. MNRAS 453(2):1562–1576. https://doi.org/10.1093/mnras/stv1726. arXiv:1507.07603 [astro-ph.GA]

Graham MJ, Ford KES, McKernan B, Ross NP, Stern D, Burdge K, Coughlin M, Djorgovski SG, Drake AJ, Duev D et al (2020) Candidate electromagnetic counterpart to the binary black hole merger gravitational-wave event S190521g*. Phys Rev Lett 124(25):251102. https://doi.org/10.1103/PhysRevLett.124.251102. arXiv:2006.14122 [astro-ph.HE]

Graziani L (2019) Hunting for dwarf galaxies hosting the formation and coalescence of compact binaries. Physics 1(3):412–429. https://doi.org/10.3390/physics1030030

Graziani L, Salvadori S, Schneider R, Kawata D, de Bennassuti M, Maselli A (2015) Galaxy formation with radiative and chemical feedback. MNRAS 449(3):3137–3148. https://doi.org/10.1093/mnras/stv494. arXiv:1502.07344 [astro-ph.GA]

Graziani L, de Bennassuti M, Schneider R, Kawata D, Salvadori S (2017) The history of the dark and luminous side of Milky Way-like progenitors. MNRAS 469(1):1101–1116. https://doi.org/10.1093/mnras/stx900. arXiv:1704.02983 [astro-ph.GA]

Graziani L, Schneider R, Marassi S, Del Pozzo W, Mapelli M, Giacobbo N (2020) Cosmic archaeology with massive stellar black hole binaries. MNRAS 495(1):L81–L85. https://doi.org/10.1093/mnrasl/slaa063. arXiv:2004.03603 [astro-ph.GA]

Green J, Schechter P, Baltay C, Bean R, Bennett D, Brown R, Conselice C, Donahue M, Fan X, Gaudi BS et al (2012) Wide-field infrared survey telescope (WFIRST) final report. arXiv e-prints arXiv:1208.4012 [astro-ph.IM]

Green MJ, Hermes JJ, Marsh TR, Steeghs DTH, Bell KJ, Littlefair SP, Parsons SG, Dennihy E, Fuchs JT, Reding JS et al (2018) A 15.7-minAM CVn binary discovered in K2. MNRAS 477(4):5646–5656. https://doi.org/10.1093/mnras/sty1032. arXiv:1804.07138 [astro-ph.SR]

Green MJ, Marsh TR, Steeghs DTH, Kupfer T, Ashley RP, Bloemen S et al (2018) High-speed photometry of Gaia14aae: an eclipsing AM CVn that challenges formation models. MNRAS 476(2):1663–1679. https://doi.org/10.1093/mnras/sty299. arXiv:1802.00499 [astro-ph.SR]

Green SR, Gair J (2020) Complete parameter inference for GW150914 using deep learning. arXiv e-prints arXiv:2008.03312 [astro-ph.IM]

Greene JE (2012) Low-mass black holes as the remnants of primordial black hole formation. Nat Commun 3:1304. https://doi.org/10.1038/ncomms2314. arXiv:1211.7082 [astro-ph.CO]

Greene JE, Strader J, Ho LC (2020) Intermediate-mass black holes. ARA&A 58:257–312. https://doi.org/10.1146/annurev-astro-032620-021835. arXiv:1911.09678 [astro-ph.GA]

Grefenstette BW, Harrison FA, Boggs SE, Reynolds SP, Fryer CL, Madsen KK, Wik DR et al (2014) Asymmetries in core-collapse supernovae from maps of radioactive ^{44}Ti in CassiopeiaA. Nature 506 (7488):339–342. https://doi.org/10.1038/nature12997. arXiv:1403.4978 [astro-ph.HE]

Gregely LA, Biermann PL (2009) The spin flip phenomenon and supermassive black hole binary systems. ApJ 697:1621–1633. https://doi.org/10.1088/0004-637X/697/2/1621

Greiner J, Schwarz R, Zharikov S, Orio M (2000) RX J1420.4+5334—another tidal disruption event? A&A 362:L25–L28 arXiv:astro-ph/0009430 [astro-ph]

Grindlay JE, Cool AM, Callanan PJ, Bailyn CD, Cohn HN, Lugger PM (1995) Spectroscopic identification of probable cataclysmic variables in the globular cluster NGC 6397. ApJ 455:L47. https://doi.org/10.1086/309806

Grover K, Fairhurst S, Farr BF et al (2014) Comparison of gravitational wave detector network sky localization approximations. Phys Rev D 89(4):042004. https://doi.org/10.1103/PhysRevD.89.042004. arXiv:1310.7454 [gr-qc]

Grupe D, Thomas HC, Leighly KM (1999) RX J1624.9+7554: a new X-ray transient AGN. A&A 350: L31–L34 arXiv:astro-ph/9909101 [astro-ph]

Gruzinov A, Levin Y, Matzner CD (2020) Negative dynamical friction on compact objects moving through dense gas. MNRAS 492(2):2755–2761. https://doi.org/10.1093/mnras/staa013. arXiv:1906.01186 [astro-ph.HE]

Gualandris A, Merritt D (2008) Ejection of supermassive black holes from galaxy cores. ApJ 678(2):780–797. https://doi.org/10.1086/586877. arXiv:0708.0771 [astro-ph]

Gualandris A, Merritt D (2009) Perturbations of intermediate-mass black holes on stellar orbits in the galactic center. ApJ 705(1):361–371. https://doi.org/10.1088/0004-637X/705/1/361. arXiv:0905.4514 [astro-ph.GA]

Gualandris A, Dotti M, Sesana A (2012) Massive black hole binary plane reorientation in rotating stellar systems. MNRAS 420(1):L38–L42. https://doi.org/10.1111/j.1745-3933.2011.01188.x. arXiv:1109.3707 [astro-ph.GA]

Gualandris A, Read JI, Dehnen W, Bortolas E (2017) Collisionless loss-cone refilling: there is no final parsec problem. MNRAS 464(2):2301–2310. https://doi.org/10.1093/mnras/stw2528. arXiv:1609.09383 [astro-ph.GA]

Gualtieri L, Berti E, Cardoso V, Sperhake U (2008) Transformation of the multipolar components of gravitational radiation under rotations and boosts. Phys Rev D 78(4):044024. https://doi.org/10.1103/PhysRevD.78.044024. arXiv:0805.1017 [gr-qc]

Guillochon J, Ramirez-Ruiz E, Rosswog S, Kasen D (2009) Three-dimensional simulations of tidally disrupted solar-type stars and the observational signatures of shock breakout. ApJ 705(1):844–853. https://doi.org/10.1088/0004-637X/705/1/844. arXiv:0811.1370 [astro-ph]

Guillochon J, Dan M, Ramirez-Ruiz E, Rosswog S (2010) Surface detonations in double degenerate binary systems triggered by accretion stream instabilities. ApJ 709(1):L64–L69. https://doi.org/10.1088/2041-8205/709/1/L64. arXiv:0911.0416 [astro-ph.HE]

Gültekin K, Richstone DO, Gebhardt K, Lauer TR, Tremaine S, Aller MC, Bender R, Dressler A, Faber SM, Filippenko AV et al (2009) The M-σ and M-L relations in galactic bulges, and determinations of their intrinsic scatter. ApJ 698(1):198–221. https://doi.org/10.1088/0004-637X/698/1/198. arXiv:0903.4897 [astro-ph.GA]

Gunn JE, Ostriker JP (1970) On the nature of pulsars. III. Analysis of observations. ApJ 160:979. https://doi.org/10.1086/150487

Guo H, Liu X, Shen Y, Loeb A, Monroe T, Prochaska JX (2019) Constraining sub-parsec binary supermassive black holes in quasars with multi-epoch spectroscopy—III. Candidates from continued radial velocity tests. MNRAS 482(3):3288–3307. https://doi.org/10.1093/mnras/sty2920. arXiv:1809.04610 [astro-ph.GA]

Gürkan MA, Freitag M, Rasio FA (2004) Formation of massive black holes in dense star clusters. I. Mass segregation and core collapse. ApJ 604(2):632–652. https://doi.org/10.1086/381968. arXiv:astro-ph/0308449 [astro-ph]

Gürkan MA, Fregeau JM, Rasio FA (2006) Massive black hole binaries from collisional runaways. ApJ 640(1):L39–L42. https://doi.org/10.1086/503295. arXiv:astro-ph/0512642 [astro-ph]

Habets GMHJ (1986) The evolution of a single and a binary helium star of 2.5 solar mass up to neon ignition. A&A 165:95–109

Habouzit M, Volonteri M, Latif M, Dubois Y, Peirani S (2016) On the number density of 'direct collapse' black hole seeds. MNRAS 463(1):529–540. https://doi.org/10.1093/mnras/stw1924. arXiv:1601.00557 [astro-ph.GA]

Habouzit M, Volonteri M, Dubois Y (2017) Blossoms from black hole seeds: properties and early growth regulated by supernova feedback. MNRAS 468(4):3935–3948. https://doi.org/10.1093/mnras/stx666. arXiv:1605.09394 [astro-ph.GA]

Hachisu I, Kato M, Nomoto K (1999) A wide symbiotic channel to type IA supernovae. ApJ 522(1):487–503. https://doi.org/10.1086/307608. arXiv:astro-ph/9902304 [astro-ph]

Haehnelt MG (1994) Low-frequency gravitational waves from supermassive black-holes. MNRAS 269:199. https://doi.org/10.1093/mnras/269.1.199. arXiv:astro-ph/9405032 [astro-ph]

Haehnelt MG, Natarajan P, Rees MJ (1998) High-redshift galaxies, their active nuclei and central black holes. MNRAS 300(3):817–827. https://doi.org/10.1046/j.1365-8711.1998.01951.x. arXiv:astro-ph/9712259 [astro-ph]

Haemmerlé L, Woods TE, Klessen RS, Heger A, Whalen DJ (2018) The evolution of supermassive Population III stars. MNRAS 474(2):2757–2773. https://doi.org/10.1093/mnras/stx2919. arXiv:1705.09301 [astro-ph.SR]

Haemmerlé L, Klessen RS, Mayer L, Zwick L (2021) Maximum accretion rate of supermassive stars. A&A 652(L7):L7–L11. https://doi.org/10.1051/0004-6361/202141376. arXiv:arXiv:2105.13373 [astro-ph.SR]

Haiman Z (2004) Constraints from gravitational recoil on the growth of supermassive black holes at high redshift. ApJ 613(1):36–40. https://doi.org/10.1086/422910. arXiv:astro-ph/0404196 [astro-ph]

Haiman Z (2017) Electromagnetic chirp of a compact binary black hole: A phase template for the gravitational wave inspiral. Phys Rev D 96(2):023004. https://doi.org/10.1103/PhysRevD.96.023004. arXiv:1705.06765 [astro-ph.HE]

Haiman Z, Loeb A (2001) What is the highest plausible redshift of luminous quasars? ApJ 552(2):459–463. https://doi.org/10.1086/320586. arXiv:astro-ph/0011529 [astro-ph]

Haiman Z, Kocsis B, Menou K (2009) The population of viscosity- and gravitational wave-driven supermassive black hole binaries among luminous active galactic nuclei. ApJ 700(2):1952–1969. https://doi.org/10.1088/0004-637X/700/2/1952. arXiv:0904.1383 [astro-ph.CO]

Halpern JP, Holt SS (1992) Discovery of soft X-ray pulsations from the γ-ray source Geminga. Nature 357(6375):222–224. https://doi.org/10.1038/357222a0

Hamers AS (2017) On the formation of hot and warm Jupiters via secular high-eccentricity migration in stellar triples. MNRAS 466(4):4107–4120. https://doi.org/10.1093/mnras/stx035. arXiv:1701.01733 [astro-ph.EP]

Hamers AS, Portegies Zwart SF (2016) White dwarf pollution by planets in stellar binaries. MNRAS 462(1):L84–L87. https://doi.org/10.1093/mnrasl/slw134. arXiv:1607.01397 [astro-ph.EP]

Hamers AS, Safarzadeh M (2020) Was GW190412 born from a hierarchical 3 + 1 quadruple configuration? ApJ 898(2):99. https://doi.org/10.3847/1538-4357/ab9b27. arXiv:2005.03045 [astro-ph.HE]

Hamers AS, Pols OR, Claeys JSW, Nelemans G (2013) Population synthesis of triple systems in the context of mergers of carbon-oxygen white dwarfs. MNRAS 430(3):2262–2280. https://doi.org/10.1093/mnras/stt046. arXiv:1301.1469 [astro-ph.SR]

Hamers AS, Portegies Zwart SF, Merritt D (2014) Relativistic dynamics of stars near a supermassive black hole. MNRAS 443(1):355–387. https://doi.org/10.1093/mnras/stu1126. arXiv:1406.2846 [astro-ph.GA]

Hamilton C, Heinemann T (2020) Noise and waves: a unified kinetic theory for stellar systems. arXiv e-prints arXiv:2011.14812 [astro-ph.GA]

Hamilton C, Rafikov RR (2019) Compact object binary mergers driven by cluster tides: a new channel for LIGO/Virgo gravitational-wave events. ApJ 881(1):L13. https://doi.org/10.3847/2041-8213/ab3468. arXiv:1907.00994 [astro-ph.GA]

Hamilton C, Rafikov RR (2019) Secular dynamics of binaries in stellar clusters—I. General formulation and dependence on cluster potential. MNRAS 488(4):5489–5511. https://doi.org/10.1093/mnras/stz1730. arXiv:1902.01344 [astro-ph.GA]

Han WB, Chen X (2019) Testing general relativity using binary extreme-mass-ratio inspirals. MNRAS 485(1):L29–L33. https://doi.org/10.1093/mnrasl/slz021. arXiv:1801.07060 [gr-qc]

Han WB, Fan XL (2018) Determining the nature of white dwarfs from low-frequency gravitational waves. ApJ 856(1):82. https://doi.org/10.3847/1538-4357/aab03c. arXiv:1711.08628 [astro-ph.HE]

Han WB, Zhong XY, Chen X, Xin S (2020) Very extreme mass-ratio bursts in the Galaxy and neighbouring galaxies in relation to space-borne detectors. MNRAS 498(1):L61–L65. https://doi.org/10.1093/mnrasl/slaa115. arXiv:2004.04016 [gr-qc]

Hannuksela OA, Wong KW, Brito R, Berti E, Li TG (2019) Probing the existence of ultralight bosons with a single gravitational-wave measurement. Nat Astron 3(5):447–451. https://doi.org/10.1038/s41550-019-0712-4. arXiv:1804.09659 [astro-ph.HE]

Hannuksela OA, Ng KCY, Li TGF (2020) Extreme dark matter tests with extreme mass ratio inspirals. Phys Rev D 102(10):103022. https://doi.org/10.1103/PhysRevD.102.103022. arXiv:1906.11845 [astro-ph.CO]

Hansen BMS, Milosavljević M (2003) The need for a second black hole at the galactic center. ApJ 593(2):L77–L80. https://doi.org/10.1086/378182. arXiv:astro-ph/0306074 [astro-ph]

Hansen RO (1972) Post-Newtonian gravitational radiation from point masses in a hyperbolic kepler orbit. Phys Rev D 5(4):1021–1023. https://doi.org/10.1103/PhysRevD.5.1021

Harko T, Kovács Z, Lobo FSN (2010) Thin accretion disk signatures in dynamical Chern–Simons-modified gravity. Class Quantum Grav 27(10):105010. https://doi.org/10.1088/0264-9381/27/10/105010. arXiv:0909.1267 [gr-qc]

Hartnett JG, Luiten AN (2011) Colloquium: comparison of astrophysical and terrestrial frequency standards. Rev Mod Phys 83(1):1–9. https://doi.org/10.1103/RevModPhys.83.1. arXiv:1004.0115 [astro-ph.IM]

Haster CJ, Antonini F, Kalogera V, el Mand I (2016) N-body dynamics of intermediate mass-ratio inspirals in star clusters. ApJ 832(2):192. https://doi.org/10.3847/0004-637X/832/2/192. arXiv:1606.07097 [astro-ph.HE]

Haster CJ, Wang Z, Berry CPL, Stevenson S, Veitch J, Mandel I (2016) Inference on gravitational waves from coalescences of stellar-mass compact objects and intermediate-mass black holes. MNRAS 457(4):4499–4506. https://doi.org/10.1093/mnras/stw233. arXiv:1511.01431 [astro-ph.HE]

He MY, Petrovich C (2018) On the stability and collisions in triple stellar systems. MNRAS 474(1):20–31. https://doi.org/10.1093/mnras/stx2718. arXiv:1710.04698 [astro-ph.SR]

Heath RM, Nixon CJ (2020) On the orbital evolution of binaries with circumbinary discs. A&A 641:A64. https://doi.org/10.1051/0004-6361/202038548. arXiv:2007.11592 [astro-ph.HE]

Heber U (2016) Hot subluminous stars. PASP 128(966):082001. https://doi.org/10.1088/1538-3873/128/966/082001. arXiv:1604.07749 [astro-ph.SR]

Heckman TM, Best PN (2014) The coevolution of galaxies and supermassive black holes: insights from surveys of the contemporary universe. ARA&A 52:589–660. https://doi.org/10.1146/annurev-astro-081913-035722. arXiv:1403.4620 [astro-ph.GA]

Heger A, Fryer CL, Woosley SE, Langer N, Hartmann DH (2003) How massive single stars end their life. ApJ 591:288–300. https://doi.org/10.1086/375341. arXiv:astro-ph/0212469

Heggie D, Hut P (2003) The gravitational million-body problem: a multidisciplinary approach to star cluster dynamics. Cambridge University Press, Cambridge

Heggie DC (1975) Binary evolution in stellar dynamics. MNRAS 173:729–787. https://doi.org/10.1093/mnras/173.3.729

Heinämäki P (2001) Symmetry of black hole ejections in mergers of galaxies. A&A 371:795–805. https://doi.org/10.1051/0004-6361:20010460

Heinke CO, Grindlay JE, Lugger PM, Cohn HN, Edmonds PD, Lloyd DA, Cool AM (2003) Analysis of the quiescent low-mass X-ray binary population in galactic globular clusters. ApJ 598(1):501–515. https://doi.org/10.1086/378885. arXiv:astro-ph/0305445 [astro-ph]

Heinke CO, Ivanova N, Engel MC, Pavlovskii K, Sivakoff GR, Cartwright TF, Gladstone JC (2013) Galactic ultracompact X-ray binaries: disk stability and evolution. ApJ 768(2):184. https://doi.org/10.1088/0004-637X/768/2/184. arXiv:1303.5864 [astro-ph.HE]

Hellings RW, Downs GS (1983) Upper limits on the isotopic gravitational radiation background frompulsar timing analysis. ApJ 265:L39–L42. https://doi.org/10.1086/183954

Hennawi JF, Prochaska JX, Cantalupo S, Arrigoni-Battaia F (2015) Quasar quartet embedded in giant nebula reveals rare massive structure in distant universe. Science 348(6236):779–783. https://doi.org/10.1126/science.aaa5397. arXiv:1505.03786 [astro-ph.GA]

Hermes JJ, Kilic M, Brown WR, Winget DE, Allende Prieto C, Gianninas A, Mukadam AS, Cabrera-Lavers A, Kenyon SJ (2012) Rapid orbital decay in the 12.75-minute binary white dwarf J0651+2844. ApJ 757(2):L21. https://doi.org/10.1088/2041-8205/757/2/L21. arXiv:1208.5051 [astro-ph.SR]

Hickox RC, Jones C, Forman WR, Murray SS, Kochanek CS, Eisenstein D, Jannuzi BT, Dey A, Brown MJI, Stern D et al (2009) Host galaxies, clustering, Eddington ratios, and evolution of radio, X-ray, and infrared-selected AGNs. ApJ 696(1):891–919. https://doi.org/10.1088/0004-637X/696/1/891. arXiv:0901.4121 [astro-ph.GA]

Hicks WM, Wells A, Norman ML, Wise JH, Smith BD, O'Shea BW (2021) External enrichment of mini halos by the first supernovae. ApJ 909(1):70. https://doi.org/10.3847/1538-4357/abda3a. arXiv:2009. 05499 [astro-ph.GA]

Hild S et al (2011) Sensitivity studies for third-generation gravitational wave observatories. Class Quantum Grav 28(9):094013. https://doi.org/10.1088/0264-9381/28/9/094013. arXiv:1012.0908 [gr-qc]

Hilditch RW (2001) An introduction to close binary stars. Cambridge University Press, Cambridge

Hills JG (1976) The formation of binaries containing black holes by the exchange of companions and the X-ray sources in globular clusters. MNRAS 175:1P-4P. https://doi.org/10.1093/mnras/175.1.1P

Hills JG, Fullerton LW (1980) Computer simulations of close encounters between single stars and hard binaries. AJ 85:1281–1291. https://doi.org/10.1086/112798

Hils D, Bender PL, Webbink RF (1990) Gravitational radiation from the galaxy. ApJ 360:75. https://doi.org/10.1086/169098

Hinderer T, Flanagan ÉÉ (2008) Two-timescale analysis of extreme mass ratio inspirals in Kerr spacetime: orbital motion. Phys Rev D 78(6):064028. https://doi.org/10.1103/PhysRevD.78.064028. arXiv: 0805.3337 [gr-qc]

Hirano S, Hosokawa T, Yoshida N, Umeda H, Omukai K, Chiaki G, Yorke HW (2014) One hundred first stars: protostellar evolution and the final masses. ApJ 781(2):60. https://doi.org/10.1088/0004-637X/781/2/60. arXiv:1308.4456 [astro-ph.CO]

Hirschmann M, Dolag K, Saro A, Bachmann L, Borgani S, Burkert A (2014) Cosmological simulations of black hole growth: AGN luminosities and downsizing. MNRAS 442(3):2304–2324. https://doi.org/10.1093/mnras/stu1023. arXiv:1308.0333 [astro-ph.CO]

Hjellming MS, Webbink RF (1987) Thresholds for rapid mass transfer in binary system. I. Polytropic models. ApJ 318:794. https://doi.org/10.1086/165412

Hoang BM, Naoz S, Kocsis B, Rasio FA, Dosopoulou F (2018) Black hole mergers in galactic nuclei induced by the eccentric Kozai–Lidov effect. ApJ 856(2):140. https://doi.org/10.3847/1538-4357/aaafce. arXiv:1706.09896 [astro-ph.HE]

Hoang BM, Naoz S, Kocsis B, Farr WM, McIver J (2019) Detecting supermassive black hole-induced binary eccentricity oscillations with LISA. ApJ 875(2):L31. https://doi.org/10.3847/2041-8213/ab14f7. arXiv:1903.00134 [astro-ph.HE]

Hobbs A, Power C, Nayakshin S, King AR (2012) Modelling supermassive black hole growth: towards an improved sub-grid prescription. MNRAS 421(4):3443–3449. https://doi.org/10.1111/j.1365-2966. 2012.20563.x. arXiv:1202.4725 [astro-ph.IM]

Hobbs G, Lorimer DR, Lyne AG, Kramer M (2005) A statistical study of 233 pulsar proper motions. MNRAS 360(3):974–992. https://doi.org/10.1111/j.1365-2966.2005.09087.x. arXiv:astro-ph/0504584 [astro-ph]

Hoffman L, Loeb A (2007) Dynamics of triple black hole systems in hierarchically merging massive galaxies. MNRAS 377(3):957–976. https://doi.org/10.1111/j.1365-2966.2007.11694.x. arXiv:astro-ph/0612517 [astro-ph]

Hofmann F, Barausse E, Rezzolla L (2016) The final spin from binary black holes in quasi-circular orbits. ApJ 825(2):L19. https://doi.org/10.3847/2041-8205/825/2/L19. arXiv:1605.01938 [gr-qc]

Holley-Bockelmann K, Khan FM (2015) Galaxy rotation and rapid supermassive binary coalescence. ApJ 810(2):139. https://doi.org/10.1088/0004-637X/810/2/139. arXiv:1505.06203 [astro-ph.GA]

Holley-Bockelmann K, Gültekin K, Shoemaker D, Yunes N (2008) Gravitational wave recoil and the retention of intermediate-mass black holes. ApJ 686(2):829–837. https://doi.org/10.1086/591218. arXiv:0707.1334 [astro-ph]

Hong J, Lee HM (2015) Black hole binaries in galactic nuclei and gravitational wave sources. MNRAS 448(1):754–770. https://doi.org/10.1093/mnras/stv035. arXiv:1501.02717 [astro-ph.GA]

Hong J, Askar A, Giersz M, Hypki A, Yoon SJ (2020) MOCCA-SURVEY database I: binary black hole mergers from globular clusters with intermediate mass black holes. MNRAS. https://doi.org/10.1093/mnras/staa2677. arXiv:2008.10823 [astro-ph.HE]

Hopkins PF, Quataert E (2010) How do massive black holes get their gas? MNRAS 407(3):1529–1564. https://doi.org/10.1111/j.1365-2966.2010.17064.x. arXiv:0912.3257 [astro-ph.CO]

Hopkins PF, Richards GT, Hernquist L (2007) An observational determination of the bolometric quasar luminosity function. ApJ 654(2):731–753. https://doi.org/10.1086/509629. arXiv:astro-ph/0605678 [astro-ph]

Hopkins PF, Kereš D, Oñorbe J, Faucher-Giguère CA, Quataert E, Murray N, Bullock JS (2014) Galaxies on FIRE (Feedback In Realistic Environments): stellar feedback explains cosmologically inefficient star formation. MNRAS 445(1):581–603. https://doi.org/10.1093/mnras/stu1738. arXiv:1311.2073 [astro-ph.CO]

Hopkins PF, Wetzel A, Kereš D, Faucher-Giguère CA, Quataert E, Boylan-Kolchin M, Murray N, Hayward CC, Garrison-Kimmel S, Hummels C et al (2018) FIRE-2 simulations: physics versus numerics in galaxy formation. MNRAS 480(1):800–863. https://doi.org/10.1093/mnras/sty1690. arXiv:1702.06148 [astro-ph.GA]

Hopman C, Alexander T (2006) Resonant relaxation near a massive black hole: the stellar distribution and gravitational wave sources. ApJ 645(2):1152–1163. https://doi.org/10.1086/504400. arXiv:astro-ph/0601161 [astro-ph]

Hopman C, Freitag M, Larson SL (2007) Gravitational wave bursts from the Galactic massive black hole. MNRAS 378(1):129–136. https://doi.org/10.1111/j.1365-2966.2007.11758.x. arXiv:astro-ph/0612337 [astro-ph]

Horton MA, Hardcastle MJ, Read SC, Krause MGH (2020) A Markov chain Monte Carlo approach for measurement of jet precession in radio-loud active galactic nuclei. MNRAS 493(3):3911–3919. https://doi.org/10.1093/mnras/staa429. arXiv:2002.04966 [astro-ph.GA]

Howitt G, Stevenson S, Vigna-Gómez Ar, Justham S, Ivanova N, Woods TE, Neijssel CJ, Mandel I (2020) Luminous Red Novae: population models and future prospects. MNRAS 492(3):3229–3240. https://doi.org/10.1093/mnras/stz3542. arXiv:1912.07771 [astro-ph.HE]

Hoyle F, Lyttleton RA (1939) The effect of interstellar matter on climatic variation. Proc Camb Philos Soc 35(3):405. https://doi.org/10.1017/S0305004100021150

Hu BX, D'Orazio DJ, Haiman Z, Smith KL, Snios B, Charisi M, Di Stefano R (2020) Spikey: self-lensing flares from eccentric SMBH binaries. MNRAS 495(4):4061–4070. https://doi.org/10.1093/mnras/staa1312. arXiv:1910.05348 [astro-ph.HE]

Hu XC, Li XH, Wang Y, Feng WF, Zhou MY, Hu YM, Hu SC, Mei JW, Shao CG (2018) Fundamentals of the orbit and response for TianQin. Class Quantum Grav 35(9):095008. https://doi.org/10.1088/1361-6382/aab52f. arXiv:1803.03368 [gr-qc]

Huang G, Wu X (2014) Dynamics of the post-Newtonian circular restricted three-body problem with compact objects. Phys Rev D 89(12):124034. https://doi.org/10.1103/PhysRevD.89.124034

Huang SJ, Hu YM, Korol V, Li PC, Liang ZC, Lu Y, Wang HT, Yu S, Mei J (2020) Science with the TianQin Observatory: Preliminary results on Galactic double white dwarf binaries. Phys Rev D 102:063021. https://doi.org/10.1103/PhysRevD.102.063021. arXiv:2005.07889 [astro-ph.HE]

Hughes SA, Blandford RD (2003) Black hole mass and spin coevolution by mergers. ApJ 585(2):L101–L104. https://doi.org/10.1086/375495. arXiv:astro-ph/0208484 [astro-ph]

Hui CY, Wu K, Han Q, Kong AKH, Tam PHT (2018) On the orbital properties of millisecond pulsar binaries. ApJ 864(1):30. https://doi.org/10.3847/1538-4357/aad5ec. arXiv:1807.09001 [astro-ph.HE]

Hui L, Ostriker JP, Tremaine S, Witten E (2017) Ultralight scalars as cosmological dark matter. Phys Rev D 95(4):043541. https://doi.org/10.1103/PhysRevD.95.043541. arXiv:1610.08297 [astro-ph.CO]

Hulse RA, Taylor JH (1975) Discovery of a pulsar in a binary system. ApJ 195:L51–L53. https://doi.org/10.1086/181708

Hurley JR, Tout CA, Pols OR (2002) Evolution of binary stars and the effect of tides on binary populations. MNRAS 329(4):897–928. https://doi.org/10.1046/j.1365-8711.2002.05038.x. arXiv:astro-ph/0201220 [astro-ph]

Hut P (1981) Tidal evolution in close binary systems. A&A 99:126–140

Hut P, Bahcall JN (1983) Binary-single star scattering. I—Numerical experiments for equal masses. ApJ 268:319–341. https://doi.org/10.1086/160956

Hut P, Paczynski B (1984) Effects of encounters with field stars on the evolution of low-mass semidetached binaries. ApJ 284:675–684. https://doi.org/10.1086/162450

Hut P, McMillan S, Goodman J, Mateo M, Phinney ES, Pryor C, Richer HB, Verbunt F, Weinberg M (1992) Binaries in globular clusters. PASP 104:981. https://doi.org/10.1086/133085

Hypki A, Giersz M (2013) MOCCA code for star cluster simulations—I. Blue stragglers, first results. MNRAS 429(2):1221–1243. https://doi.org/10.1093/mnras/sts415. arXiv:1207.6700 [astro-ph.GA]

Iaconi R, De Marco O, Passy JC, Staff J (2018) The effect of binding energy and resolution in simulations of the common envelope binary interaction. MNRAS 477(2):2349–2365. https://doi.org/10.1093/mnras/sty794. arXiv:1706.09786 [astro-ph.SR]

Iben J Icko, Webbink RF (1987) On the formation and properties of close binary white dwarfs. In: Philip AGD, Hayes DF, Liebert JW (eds) The second conference on faint blue stars. IAU colloquia, vol 95. L. Davis Press, Schenectady, NY, p 401

Icko Iben J, Tutukov AV, Fedorova ArV (1998) On the luminosity of white dwarfs in close binaries merging under the influence of gravitational wave radiation. ApJ 503(1):344–349. https://doi.org/10.1086/305972

Inayoshi K, Haiman Z, Ostriker JP (2016) Hyper-Eddington accretion flows on to massive black holes. MNRAS 459:3738–3755. https://doi.org/10.1093/mnras/stw836. arXiv:1511.02116 [astro-ph.HE]

Inayoshi K, Hirai R, Kinugawa T, Hotokezaka K (2017) Formation pathway of Population III coalescing binary black holes through stable mass transfer. MNRAS 468(4):5020–5032. https://doi.org/10.1093/mnras/stx757. arXiv:1701.04823 [astro-ph.HE]

Inayoshi K, Tamanini N, Caprini C, Haiman Z (2017) Probing stellar binary black hole formation in galactic nuclei via the imprint of their center of mass acceleration on their gravitational wave signal. Phys Rev D 96(6):063014. https://doi.org/10.1103/PhysRevD.96.063014. arXiv:1702.06529 [astro-ph.HE]

Inayoshi K, Visbal E, Haiman Z (2020) The assembly of the first massive black holes. ARA&A 58:27–97. https://doi.org/10.1146/annurev-astro-120419-014455. arXiv:1911.05791 [astro-ph.GA]

Inman D, Ali-Haïmoud Y (2019) Early structure formation in primordial black hole cosmologies. Phys Rev D 100(8):083528. https://doi.org/10.1103/PhysRevD.100.083528. arXiv:1907.08129 [astro-ph.CO]

Inomata K, Nakama T (2019) Gravitational waves induced by scalar perturbations as probes of the small-scale primordial spectrum. Phys Rev D 99(4):043511. https://doi.org/10.1103/PhysRevD.99.043511. arXiv:1812.00674 [astro-ph.CO]

Inomata K, Kawasaki M, Mukaida K, Tada Y, Yanagida TT (2017) Inflationary primordial black holes for the LIGO gravitational wave events and pulsar timing array experiments. Phys Rev D 95(12):123510. https://doi.org/10.1103/PhysRevD.95.123510. arXiv:1611.06130 [astro-ph.CO]

in't Zand JJM, Cumming A, van der Sluys MV, Verbunt F, Pols OR (2005) On the possibility of a helium white dwarf donor in the presumed ultracompact binary 2S 0918–549. A&A 441(2):675–684. https://doi.org/10.1051/0004-6361:20053002. arXiv:astro-ph/0506666 [astro-ph]

Iorio L (2012) General relativistic spin-orbit and spin-spin effects on the motion of rotating particles in an external gravitational field. Gen Relativ Gravit 44(3):719–736. https://doi.org/10.1007/s10714-011-1302-7. arXiv:1012.5622 [gr-qc]

Ishibashi W, Fabian AC (2016) AGN-starburst evolutionary connection: a physical interpretation based on radiative feedback. MNRAS 463(2):1291–1296. https://doi.org/10.1093/mnras/stw2063. arXiv:1609.08963 [astro-ph.GA]

Isoyama S, Nakano H, Nakamura T (2018) Multiband gravitational-wave astronomy: observing binary inspirals with a decihertz detector, B-DECIGO. PTEP 2018(7):073E01. https://doi.org/10.1093/ptep/pty078. arXiv:1802.06977 [gr-qc]

Istrate AG, Tauris TM, Langer N (2014) The formation of low-mass helium white dwarfs orbiting pulsars. Evolution of low-mass X-ray binaries below the bifurcation period. A&A 571:A45. https://doi.org/10.1051/0004-6361/201424680

Istrate AG, Tauris TM, Langer N, Antoniadis J (2014) The timescale of low-mass proto-helium white dwarf evolution. A&A 571:L3. https://doi.org/10.1051/0004-6361/201424681. arXiv:1410.5471 [astro-ph.SR]

Istrate AG, Marchant P, Tauris TM, Langer N, Stancliffe RJ, Grassitelli L (2016) Models of low-mass helium white dwarfs including gravitational settling, thermal and chemical diffusion, and rotational mixing. A&A 595:A35. https://doi.org/10.1051/0004-6361/201628874. arXiv:1606.04947 [astro-ph.SR]

Ivanov PB, Papaloizou JCB, Paardekooper SJ, Polnarev AG (2015) The evolution of a binary in a retrograde circular orbit embedded in an accretion disk. A&A 576:A29. https://doi.org/10.1051/0004-6361/201424359. arXiv:1410.3250 [astro-ph.HE]

Ivanova N, Belczynski K, Kalogera V, Rasio FA, Taam RE (2003) The role of helium stars in the formation of double neutron stars. ApJ 592(1):475–485. https://doi.org/10.1086/375578. arXiv:astro-ph/0210267 [astro-ph]

Ivanova N, Heinke CO, Rasio FA, Taam RE, Belczynski K, Fregeau J (2006) Formation and evolution of compact binaries in globular clusters—I. Binaries with white dwarfs. MNRAS 372(3):1043–1059. https://doi.org/10.1111/j.1365-2966.2006.10876.x. arXiv:astro-ph/0604085 [astro-ph]

Ivanova N, Justham S, Chen X, De Marco O, Fryer CL, Gaburov E, Ge H, Glebbeek E, Han Z, Li XD et al (2013) Common envelope evolution: where we stand and how we can move forward. A&A Rev 21:59. https://doi.org/10.1007/s00159-013-0059-2. arXiv:1209.4302 [astro-ph.HE]

Ivanova N, Justham S, Ricker P (2020) Common envelope evolution. IOP Publishing. https://doi.org/10.1088/2514-3433/abb6f0

Ivezić Ž, Kahn SM, Tyson JA, Abel B, Acosta E, Allsman R, Alonso D, AlSayyad Y, Anderson SF, Andrew J et al (2019) LSST: from science drivers to reference design and anticipated data products. ApJ 873(2):111. https://doi.org/10.3847/1538-4357/ab042c. arXiv:0805.2366 [astro-ph]

Izquierdo-Villalba D, Bonoli S, Dotti M, Sesana A, Rosas-Guevara Y, Spinoso D (2020) From galactic nuclei to the halo outskirts: tracing supermassive black holes across cosmic history and environments. MNRAS 495(4):4681–4706. https://doi.org/10.1093/mnras/staa1399. arXiv:2001.10548 [astro-ph.GA]

Izzard RG (2004) Nucleosynthesis in binary stars. PhD thesis, University of Cambridge

Izzard RG, Dray LM, Karakas AI, Lugaro M, Tout CA (2006) Population nucleosynthesis in single and binary stars. I. Model. A&A 460(2):565–572. https://doi.org/10.1051/0004-6361:20066129

Izzard RG, Glebbeek E, Stancliffe RJ, Pols OR (2009) Population synthesis of binary carbon-enhanced metal-poor stars. A&A 508(3):1359–1374. https://doi.org/10.1051/0004-6361/200912827. arXiv:0910.2158 [astro-ph.SR]

Jani K, Shoemaker D, Cutler C (2019) Detectability of intermediate-mass black holes in multiband gravitational wave astronomy. Nat Astron 4:260–265. https://doi.org/10.1038/s41550-019-0932-7. arXiv:1908.04985 [gr-qc]

Janka HT (2012) Explosion mechanisms of core-collapse supernovae. Annu Rev Nucl Part Sci 62(1):407–451. https://doi.org/10.1146/annurev-nucl-102711-094901. arXiv:1206.2503 [astro-ph.SR]

Janka HT (2017) Neutron star kicks by the gravitational tug-boat mechanism in asymmetric supernova explosions: progenitor and explosion dependence. ApJ 837(1):84. https://doi.org/10.3847/1538-4357/aa618e. arXiv:1611.07562 [astro-ph.HE]

Jha SW, Maguire K, Sullivan M (2019) Observational properties of thermonuclear supernovae. Nat Astron 3:706–716. https://doi.org/10.1038/s41550-019-0858-0. arXiv:1908.02303 [astro-ph.HE]

Jia K, Li XD (2016) Evolution of low-mass X-ray binaries: the effect of donor evaporation. ApJ 830(2):153. https://doi.org/10.3847/0004-637X/830/2/153. arXiv:1608.01076 [astro-ph.HE]

Jiang YF, Blaes O (2020) Opacity-driven convection and variability in accretion disks around supermassive black holes. ApJ 900(1):25. https://doi.org/10.3847/1538-4357/aba4b7. arXiv:2006.08657 [astro-ph.HE]

Jiang YF, Stone JM, Davis SW (2014) A global three-dimensional radiation magneto-hydrodynamic simulation of super-eddington accretion disks. ApJ 796(2):106. https://doi.org/10.1088/0004-637X/796/2/106. arXiv:1410.0678 [astro-ph.HE]

Jiang YF, Davis SW, Stone JM (2016) Iron opacity bump changes the stability and structure of accretion disks in active galactic nuclei. ApJ 827(1):10. https://doi.org/10.3847/0004-637X/827/1/10. arXiv:1601.06836 [astro-ph.HE]

Jiang YF, Blaes O, Stone JM, Davis SW (2019) Global radiation magnetohydrodynamic simulations of sub-Eddington accretion disks around supermassive black holes. ApJ 885(2):144. https://doi.org/10.3847/1538-4357/ab4a00. arXiv:1904.01674 [astro-ph.HE]

Johannsen T (2013) Regular black hole metric with three constants of motion. Phys Rev D 88(4):044002. https://doi.org/10.1103/PhysRevD.88.044002. arXiv:1501.02809 [gr-qc]

Johnson JL, Haardt F (2016) The early growth of the first black holes. PASA 33:e007. https://doi.org/10.1017/pasa.2016.4. arXiv:1601.05473 [astro-ph.GA]

Johnson M, Haworth K, Pesce DW, Palumbo DCM, Blackburn L, Akiyama K, Boroson D, Bouman KL, Farah JR, Fish VL et al (2019) Studying black holes on horizon scales with space-VLBI. In: Bulletin of the American Astronomical Society, vol 51, p 235. arXiv:1909.01405 [astro-ph.IM]

Jones S, Hirschi R, Nomoto K, Fischer T, Timmes FX, Herwig F, Paxton B, Toki H, Suzuki T, Martínez-Pinedo G et al (2013) Advanced burning stages and fate of 8–10 $M_\odot$ stars. ApJ 772(2):150. https://doi.org/10.1088/0004-637X/772/2/150. arXiv:1306.2030 [astro-ph.SR]

Ju W, Greene JE, Rafikov RR, Bickerton SJ, Badenes C (2013) Search for supermassive black hole binaries in the Sloan digital sky survey spectroscopic sample. ApJ 777(1):44. https://doi.org/10.1088/0004-637X/777/1/44. arXiv:1306.4987 [astro-ph.CO]

Juett AM, Psaltis D, Chakrabarty D (2001) Ultracompact X-ray binaries with neon-rich degenerate donors. ApJ 560(1):L59–L63. https://doi.org/10.1086/324225. arXiv:astro-ph/0108102 [astro-ph]

Just A, Yurin D, Makukov M, Berczik P, Omarov C, Spurzem R, Vilkoviskij EY (2012) Enhanced accretion rates of stars on supermassive black holes by star-disk interactions in galactic nuclei. ApJ 758(1):51. https://doi.org/10.1088/0004-637X/758/1/51. arXiv:1208.4954 [astro-ph.CO]

Kahabka P, van den Heuvel EPJ (1997) Luminous supersoft X-ray sources. ARA&A 35:69–100. https://doi.org/10.1146/annurev.astro.35.1.69

Kalaja A, Bellomo N, Bartolo N, Bertacca D, Matarrese S, Musco I, Raccanelli A, Verde L (2019) From primordial black holes abundance to primordial curvature power spectrum (and back). J Cosmol Astropart Phys 10:031. https://doi.org/10.1088/1475-7516/2019/10/031. arXiv:1908.03596 [astro-ph. CO]

Kalfountzou E, Santos Lleo M, Trichas M (2017) SDSS J1056+5516: a triple AGN or an SMBH recoil candidate? ApJ 851(1):L15. https://doi.org/10.3847/2041-8213/aa9b2d. arXiv:1712.03909 [astro-ph. GA]

Kalogera V, Belczynski K, Kim C, O'Shaughnessy R, Willems B (2007) Formation of double compact objects. Phys Rep 442(1–6):75–108. https://doi.org/10.1016/j.physrep.2007.02.008. arXiv:astro-ph/0612144 [astro-ph]

Karnesis N, Lilley M, Petiteau A (2020) Assessing the detectability of a Stochastic Gravitational Wave Background with LISA, using an excess of power approach. Class Quantum Grav 37:215017. https://doi.org/10.1088/1361-6382/abb637. arXiv:1906.09027 [astro-ph.IM]

Karnesis N, Babak S, Pieroni M, Cornish N, Littenberg T (2021) Characterization of the stochastic signal originating from compact binary populations as measured by LISA. Phys Rev D 104(4):043019. https://doi.org/10.1103/PhysRevD.104.043019. arXiv:2103.14598 [astro-ph.IM]

Kato M, Hachisu I (1999) A new estimation of mass accumulation efficiency in helium shell flashestoward type IA supernova explosions. ApJ 513(1):L41–L44. https://doi.org/10.1086/311893. arXiv:astro-ph/9901080 [astro-ph]

Katz H, Sijacki D, Haehnelt MG (2015) Seeding high-redshift QSOs by collisional runaway in primordial star clusters. MNRAS 451(3):2352–2369. https://doi.org/10.1093/mnras/stv1048. arXiv:1502.03448 [astro-ph.GA]

Katz ML, Kelley LZ, Dosopoulou F, Berry S, Blecha L, Larson SL (2020) Probing massive black hole binary populations with LISA. MNRAS 491(2):2301–2317. https://doi.org/10.1093/mnras/stz3102. arXiv:1908.05779 [astro-ph.HE]

Kauffmann G, Haehnelt M (2000) A unified model for the evolution of galaxies and quasars. MNRAS 311 (3):576–588. https://doi.org/10.1046/j.1365-8711.2000.03077.x. arXiv:astro-ph/9906493 [astro-ph]

Kauffmann G, White SDM, Guiderdoni B (1993) The formation and evolution of galaxies within merging dark matter haloes. MNRAS 264:201–218. https://doi.org/10.1093/mnras/264.1.201

Kavanagh BJ, Nichols DA, Bertone G, Gaggero D (2020) Detecting dark matter around black holes with gravitational waves: effects of dark-matter dynamics on the gravitational waveform. Phys Rev D 102 (8):083006. https://doi.org/10.1103/PhysRevD.102.083006. arXiv:2002.12811 [gr-qc]

Kawamura S, Ando M, Seto N, Sato S, Nakamura T, Tsubono K, Kand AN, Tanaka T, Yokoyama J, Funaki I, et al (2011) The Japanese space gravitational wave antenna: DECIGO. CQGra 28 (9):094011. https://doi.org/10.1088/0264-9381/28/9/094011

Kawamura S, Ando M, Seto N, Sato S, Musha M, Kawano I, Yokoyama J, Tanaka T, Ioka K, Akutsu T et al (2020) Current status of space gravitational wave antenna DECIGO and B-DECIGO. arXiv e-prints arXiv:2006.13545 [gr-qc]

Kawanaka N, Yamaguchi M, Piran T, Bulik T (2017) Prospects for the discovery of black hole binaries without mass accretion with Gaia. In: Gomboc A (ed) New frontiers in black hole astrophysics. IAU symposium, vol 324, pp 41–42. https://doi.org/10.1017/S1743921316012606

Kawka A, Vennes S, Ferrario L (2020) An ancient double degenerate merger in the Milky Way halo. MNRAS 491(1):L40–L45. https://doi.org/10.1093/mnrasl/slz165. arXiv:1910.13053 [astro-ph.SR]

Keane E, Bhattacharyya B, Kramer M, Stappers B, Keane EF, Bhattacharyya B, Kramer M, Stappers BW et al (2015) A cosmic census of radio pulsars with the SKA. In: Advancing astrophysics with the square kilometre array (AASKA14), p 40. arXiv:1501.00056 [astro-ph.IM]

Kelley L, Charisi M, Burke-Spolaor S, Simon J, Blecha L, Bogdanovic T, Colpi M, Comerford J, D'Orazio D, Dotti M et al (2019) Multi-messenger astrophysics with pulsar timing arrays. BAAS 51(3):490 arXiv:1903.07644 [astro-ph.HE]

Kelley LZ, Blecha L, Hernquist L (2017) Massive black hole binary mergers in dynamical galactic environments. MNRAS 464(3):3131–3157. https://doi.org/10.1093/mnras/stw2452. arXiv:1606.01900 [astro-ph.HE]

Kelley LZ, Blecha L, Hernquist L, Sesana A, Taylor SR (2017) The gravitational wave background from massive black hole binaries in Illustris: spectral features and time to detection with pulsar timing arrays. MNRAS 471(4):4508–4526. https://doi.org/10.1093/mnras/stx1638. arXiv:1702.02180 [astro-ph.HE]

Kelley LZ, Blecha L, Hernquist L, Sesana A, Taylor SR (2018) Single sources in the low-frequency gravitational wave sky: properties and time to detection by pulsar timing arrays. MNRAS 477(1):964–976. https://doi.org/10.1093/mnras/sty689. arXiv:1711.00075 [astro-ph.HE]

Kelly BJ, Baker JG, Etienne ZB, Giacomazzo B, Schnittman J (2017) Prompt electromagnetic transients from binary black hole mergers. Phys Rev D 96(12):123003. https://doi.org/10.1103/PhysRevD.96.123003. arXiv:1710.02132 [astro-ph.HE]

Kennedy GF, Meiron Y, Shukirgaliyev B, Panamarev T, Berczik P, Just A, Spurzem R (2016) Star-disc interaction in galactic nuclei: orbits and rates of accreted stars. MNRAS 460(1):240–255. https://doi.org/10.1093/mnras/stw908. arXiv:1604.05309 [astro-ph.GA]

Kerr M, Reardon DJ, Hobbs G, Shannon RM, Manchester RN, Dai S, Russell CJ, Zhang S, van Straten W, Osłowski S et al (2020) The Parkes Pulsar Timing Array project: second data release. PASA 37:e020. https://doi.org/10.1017/pasa.2020.11. arXiv:2003.09780 [astro-ph.IM]

Kesden M, Sperhake U, Berti E (2010) Final spins from the merger of precessing binary black holes. Phys Rev D 81(8):084054. https://doi.org/10.1103/PhysRevD.81.084054. arXiv:1002.2643 [astro-ph.GA]

Kesden M, Sperhake U, Berti E (2010) Relativistic suppression of black hole recoils. ApJ 715(2):1006–1011. https://doi.org/10.1088/0004-637X/715/2/1006. arXiv:1003.4993 [astro-ph.CO]

Kesden M, Gerosa D, O'Shaughnessy R, Berti E, Sperhake U (2015) Effective potentials and morphological transitions for binary black hole spin precession. Phys Rev Lett 114(8):081103. https://doi.org/10.1103/PhysRevLett.114.081103. arXiv:1411.0674 [gr-qc]

Khan A, Paschalidis V, Ruiz M, Shapiro SL (2018) Disks around merging binary black holes: from GW150914 to supermassive black holes. Phys Rev D 97(4):044036. https://doi.org/10.1103/PhysRevD.97.044036. arXiv:1801.02624 [astro-ph.HE]

Khan FM, Just A, Merritt D (2011) Efficient merger of binary supermassive black holes in merging galaxies. ApJ 732(2):89. https://doi.org/10.1088/0004-637X/732/2/89. arXiv:1103.0272 [astro-ph.CO]

Khan FM, Preto M, Berczik P, Berentzen I, Just A, Spurzem R (2012) Mergers of unequal-mass galaxies: supermassive black hole binary evolution and structure of merger remnants. ApJ 749(2):147. https://doi.org/10.1088/0004-637X/749/2/147. arXiv:1202.2124 [astro-ph.CO]

Khan FM, Fiacconi D, Mayer L, Berczik P, Just A (2016) Swift coalescence of supermassive black holes in cosmological mergers of massive galaxies. ApJ 828(2):73. https://doi.org/10.3847/0004-637X/828/2/73. arXiv:1604.00015 [astro-ph.GA]

Khan FM, Berczik P, Just A (2018) Gravitational wave driven mergers and coalescence time of supermassive black holes. A&A 615:A71. https://doi.org/10.1051/0004-6361/201730489. arXiv:1803.11394 [astro-ph.GA]

Khan FM, Capelo PR, Mayer L, Berczik P (2018) Dynamical evolution and merger timescales of LISA massive black hole binaries in disk galaxy mergers. ApJ 868(2):97. https://doi.org/10.3847/1538-4357/aae77b. arXiv:1807.11004 [astro-ph.GA]

Khan FM, Mirza MA, Holley-Bockelmann K (2020) Inward bound: the incredible journey of massive black holes as they pair and merge—I. The effect of mass ratio in flattened rotating galactic nuclei. MNRAS 492(1):256–267. https://doi.org/10.1093/mnras/stz3360. arXiv:1911.07946 [astro-ph.GA]

Kidder LE (1995) Coalescing binary systems of compact objects to (post)$^{5/2}$-Newtonian order. V. Spin effects. Phys Rev D 52(2):821–847. https://doi.org/10.1103/PhysRevD.52.821. arXiv:gr-qc/9506022 [gr-qc]

Kilic M, Brown WR, Hermes JJ, Allende Prieto C, Kenyon SJ, Winget DE, Winget KI (2011) SDSS J163030.58+423305.8: a 40-min orbital period detached white dwarf binary. MNRAS 418(1):L157–L161. https://doi.org/10.1111/j.1745-3933.2011.01165.x. arXiv:1109.6339 [astro-ph.GA]

Kilic M, Brown WR, Allende Prieto C, Kenyon SJ, Heinke CO, Agüeros MA, Kleinman SJ (2012) The ELM survey. IV. 24 white dwarf merger systems. ApJ 751(2):141. https://doi.org/10.1088/0004-637X/751/2/141. arXiv:1204.0028 [astro-ph.GA]

Kilic M, Brown WR, Gianninas A, Hermes JJ, Allende Prieto C, Kenyon SJ (2014) A new gravitational wave verification source. MNRAS 444:L1–L5. https://doi.org/10.1093/mnrasl/slu093. arXiv:1406.3346 [astro-ph.SR]

Kilic M, Brown WR, Gianninas A, Curd B, Bell KJ, Allende Prieto C (2017) A Gemini snapshot survey for double degenerates. MNRAS 471(4):4218–4227. https://doi.org/10.1093/mnras/stx1886. arXiv:1707.08948 [astro-ph.SR]

Kim C, Kalogera V, Lorimer DR (2003) The probability distribution of binary pulsar coalescence rates. I. Double neutron star systems in the galactic field. ApJ 584(2):985–995. https://doi.org/10.1086/345740. arXiv:astro-ph/0207408 [astro-ph]

Kim DC, Yoon I, Privon GC, Evans AS, Harvey D, Stierwalt S, Kim JH (2017) A potential recoiling supermassive black hole, CXO J101527.2+625911. ApJ 840(2):71. https://doi.org/10.3847/1538-4357/aa6030. arXiv:1704.05549 [astro-ph.GA]

Kimpson T, Wu K, Zane S (2019) Pulsar timing in extreme mass ratio binaries: a general relativistic approach. MNRAS 486(1):360–377. https://doi.org/10.1093/mnras/stz845. arXiv:1903.08258 [astro-ph.HE]

Kimpson T, Wu K, Zane S (2019) Spatial dispersion of light rays propagating through a plasma in Kerr space-time. MNRAS 484(2):2411–2419. https://doi.org/10.1093/mnras/stz138. arXiv:1901.03733 [astro-ph.HE]

Kimpson T, Wu K, Zane S (2020) Gravitational burst radiation from pulsars in the Galactic centre and stellar clusters. MNRAS 495(1):600–613. https://doi.org/10.1093/mnras/staa1259. arXiv:2005.02053 [astro-ph.HE]

Kimpson T, Wu K, Zane S (2020) Orbital spin dynamics of a millisecond pulsar around a massive BH with a general mass quadrupole. MNRAS 497(4):5421–5431. https://doi.org/10.1093/mnras/staa2103. arXiv:2007.05219 [astro-ph.HE]

King A (2003) Black holes, galaxy formation, and the M_{BH}-σ relation. ApJ 596(1):L27–L29. https://doi.org/10.1086/379143. arXiv:astro-ph/0308342 [astro-ph]

King AR, Pringle JE (2006) Growing supermassive black holes by chaotic accretion. MNRAS 373(1):L90–L92. https://doi.org/10.1111/j.1745-3933.2006.00249.x. arXiv:astro-ph/0609598 [astro-ph]

King AR, Frank J, Whitehurst R (1990) Synchronous rotation in AM Herculis systems-I. Equilibrium configurations. MNRAS 244:731

King AR, Pringle JE, Hofmann JA (2008) The evolution of black hole mass and spin in active galactic nuclei. MNRAS 385(3):1621–1627. https://doi.org/10.1111/j.1365-2966.2008.12943.x. arXiv:0801.1564 [astro-ph]

Kiseleva LG, Eggleton PP, Orlov VV (1994) Instability of close triple systems with coplanar initial doubly circular motion. MNRAS 270:936–946. https://doi.org/10.1093/mnras/270.4.936

Kiseleva LG, Eggleton PP, Mikkola S (1998) Tidal friction in triple stars. MNRAS 300(1):292–302. https://doi.org/10.1046/j.1365-8711.1998.01903.x

Kiuchi K, Maeda KI (2004) Gravitational waves from a chaotic dynamical system. Phys Rev D 70(6):064036. https://doi.org/10.1103/PhysRevD.70.064036. arXiv:gr-qc/0404124 [gr-qc]

Kiuchi K, Shibata M, Montero PJ, Font JA (2011) Gravitational waves from the Papaloizou-Pringle instability in black-hole-torus systems. Phys Rev Lett 106(25):251102. https://doi.org/10.1103/PhysRevLett.106.251102. arXiv:1105.5035 [astro-ph.HE]

Klein A, Barausse E, Sesana A, Petiteau A, Berti E, Babak S, Gair J, Aoudia S, Hinder I, Ohme F et al (2016) Science with the space-based interferometer eLISA: supermassive black hole binaries. Phys Rev D 93(2):024003. https://doi.org/10.1103/PhysRevD.93.024003. arXiv:1511.05581 [gr-qc]

Klencki J, Moe M, Gladysz W, Chruslinska M, Holz DE, Belczynski K (2018) Impact of inter-correlated initial binary parameters on double black hole and neutron star mergers. A&A 619:A77. https://doi.org/10.1051/0004-6361/201833025. arXiv:1808.07889 [astro-ph.HE]

Knigge C, Baraffe I, Patterson J (2011) The evolution of cataclysmic variables as revealed by their donor stars. ApJS 194(2):28. https://doi.org/10.1088/0067-0049/194/2/28. arXiv:1102.2440 [astro-ph.SR]

Kobayashi S, Laguna P, Phinney ES, Mészáros P (2004) Gravitational waves and X-ray signals from stellar disruption by a massive black hole. ApJ 615(2):855–865. https://doi.org/10.1086/424684. arXiv:astro-ph/0404173 [astro-ph]

Kochanek CS (1992) Coalescing binary neutron stars. ApJ 398:234. https://doi.org/10.1086/171851

Kochanek CS, Shapiro SL, Teukolsky SA, Chernoff DF (1990) Gravitational radiation from colliding clusters: Newtonian simulations in three dimensions. ApJ 358:81. https://doi.org/10.1086/168964

Kocsis B, Tremaine S (2015) A numerical study of vector resonant relaxation. MNRAS 448(4):3265–3296. https://doi.org/10.1093/mnras/stv057. arXiv:1406.1178 [astro-ph.GA]

Kocsis B, Gáspár ME, Márka S (2006) Detection rate estimates of gravity waves emitted during parabolic encounters of stellar black holes in globular clusters. ApJ 648(1):411–429. https://doi.org/10.1086/505641. arXiv:astro-ph/0603441 [astro-ph]

Kocsis B, Yunes N, Loeb A (2011) Observable signatures of extreme mass-ratio inspiral black hole binaries embedded in thin accretion disks. Phys Rev D 84(2):024032. https://doi.org/10.1103/PhysRevD.84.024032. arXiv:1104.2322 [astro-ph.GA]

Koester D, Gänsicke BT, Farihi J (2014) The frequency of planetary debris around young white dwarfs. A&A 566:A34. https://doi.org/10.1051/0004-6361/201423691. arXiv:1404.2617 [astro-ph.SR]

Kohri K, Terada T (2021) Solar-mass primordial black holes explain NANOGrav hint of gravitational waves. Phys Lett B 813:136040. https://doi.org/10.1016/j.physletb.2020.136040. arXiv:2009.11853 [astro-ph.CO]

Kolb U (1993) A model for the intrinsic population of cataclysmic variables. A&A 271:149

Koliopanos F, Ciambur BC, Graham AW, Webb NA, Coriat M, Mutlu-Pakdil B, Davis BL, Godet O, Barret D, Seigar MS (2017) Searching for intermediate-mass black holes in galaxies with low-luminosity AGN: a multiple-method approach. A&A 601:A20. https://doi.org/10.1051/0004-6361/201630061. arXiv:1612.06794 [astro-ph.GA]

Koliopanos F, Peault M, Vasilopoulos G, Webb N (2020) The chemical composition of the accretion disk and donor star in Ultra Compact X-ray Binaries: a comprehensive X-ray analysis. MNRAS 501:548–563. https://doi.org/10.1093/mnras/staa3474. arXiv:2001.00716 [astro-ph.HE]

Kollmeier JA, Zasowski G, Rix HW, Johns M, Anderson SF, Drory N, Johnson JA, Pogge RW, Bird JC, Blanc GA et al (2017) SDSS-V: pioneering panoptic spectroscopy. arXiv e-prints arXiv:1711.03234 [astro-ph.GA]

Komossa S (2012) Recoiling black holes: electromagnetic signatures, candidates, and astrophysical implications. Adv Astron 2012:364973. https://doi.org/10.1155/2012/364973. arXiv:1202.1977 [astro-ph.CO]

Komossa S, Greiner J (1999) Discovery of a giant and luminous X-ray outburst from the optically inactive galaxy pair RX J1242.6-1119. A&A 349:L45–L48 arXiv:astro-ph/9908216 [astro-ph]

Komossa S, Zhou H, Lu H (2008) A recoiling supermassive black hole in the quasar SDSS J092712.65+294344.0? ApJ 678(2):L81. https://doi.org/10.1086/588656. arXiv:0804.4585 [astro-ph]

Konstantinidis S, Amaro-Seoane P, Kokkotas KD (2013) Investigating the retention of intermediate-mass black holes in star clusters using N-body simulations. A&A 557:A135. https://doi.org/10.1051/0004-6361/201219620. arXiv:1108.5175 [astro-ph.CO]

Kormendy J (2004) The stellar-dynamical search for supermassive black holes in galactic nuclei. In: Ho LC (ed) Coevolution of black holes and galaxies, p 1. arXiv:astro-ph/0306353 [astro-ph]

Kormendy J, Ho LC (2013) Coevolution (or not) of supermassive black holes and host galaxies. ARA&A 51(1):511–653. https://doi.org/10.1146/annurev-astro-082708-101811. arXiv:1304.7762 [astro-ph.CO]

Kormendy J, Richstone D (1995) Inward bound-the search for supermassive black holes in galactic nuclei. ARA&A 33:581. https://doi.org/10.1146/annurev.aa.33.090195.003053

Korol V, Safarzadeh M (2021) How can LISA probe a population of GW190425-like binary neutron stars in the Milky Way? MNRAS 502(4):5576–5583. https://doi.org/10.1093/mnras/stab310. arXiv:2012.03070 [astro-ph.HE]

Korol V, Rossi EM, Groot PJ, Nelemans G, Toonen S, Brown AGA (2017) Prospects for detection of detached double white dwarf binaries with Gaia, LSST and LISA. MNRAS 470(2):1894–1910. https://doi.org/10.1093/mnras/stx1285. arXiv:1703.02555 [astro-ph.HE]

Korol V, Koop O, Rossi EM (2018) Detectability of double white dwarfs in the local group with LISA. ApJ 866(2):L20. https://doi.org/10.3847/2041-8213/aae587. arXiv:1808.05959 [astro-ph.HE]

Korol V, Rossi EM, Barausse E (2019) A multimessenger study of the Milky Way's stellar disc and bulge with LISA, Gaia, and LSST. MNRAS 483(4):5518–5533. https://doi.org/10.1093/mnras/sty3440. arXiv:1806.03306 [astro-ph.GA]

Korol V, Toonen S, Klein A, Belokurov V, Vincenzo F, Buscicchio R, Gerosa D, Moore CJ, Roebber E, Rossi EM et al (2020) Populations of double white dwarfs in Milky Way satellites and their detectability with LISA. A&A 638:A153. https://doi.org/10.1051/0004-6361/202037764. arXiv:2002.10462 [astro-ph.GA]

Korol V, Belokurov V, Moore CJ, Toonen S (2021) Weighing Milky Way satellites with LISA. MNRAS 502(1):L55–L60. https://doi.org/10.1093/mnrasl/slab003. arXiv:2010.05918 [astro-ph.GA]

Koss M, Blecha L, Mushotzky R, Hung CL, Veilleux S, Trakhtenbrot B, Schawinski K, Stern D, Smith N, Li Y et al (2014) SDSS1133: an unusually persistent transient in a nearby dwarf galaxy. MNRAS 445 (1):515–527. https://doi.org/10.1093/mnras/stu1673. arXiv:1401.6798 [astro-ph.GA]

Kostov VB, Moore K, Tamayo D, Jayawardhana R, Rinehart SA (2016) Tatooine's future: the eccentric response of Kepler's circumbinary planets to common-envelope evolution of their host stars. ApJ 832 (2):183. https://doi.org/10.3847/0004-637X/832/2/183. arXiv:1610.03436 [astro-ph.EP]

Kozai Y (1962) Secular perturbations of asteroids with high inclination and eccentricity. AJ 67:591–598. https://doi.org/10.1086/108790

Kramer M, Schneider FRN, Ohlmann ST, Geier S, Schaffenroth V, Pakmor R, Röpke FK (2020) Formation of sdB-stars via common envelope ejection by substellar companions. A&A 642:A97. https://doi.org/10.1051/0004-6361/202038702. arXiv:2007.00019 [astro-ph.SR]

Kremer K, Breivik K, Larson SL, Kalogera V (2017) Accreting double white dwarf binaries: implications for LISA. ApJ 846(2):95. https://doi.org/10.3847/1538-4357/aa8557. arXiv:1707.01104 [astro-ph. HE]

Kremer K, Chatterjee S, Breivik K, Rodriguez CL, Larson SL, Rasio FA (2018) LISA sources in milky way globular clusters. Phys Rev Lett 120(19):191103. https://doi.org/10.1103/PhysRevLett.120.191103. arXiv:1802.05661 [astro-ph.HE]

Kremer K, Chatterjee S, Rodriguez CL, Rasio FA (2018) Accreting black hole binaries in globular clusters. ApJ 852(1):29. https://doi.org/10.3847/1538-4357/aa99df. arXiv:1709.05444 [astro-ph.HE]

Kremer K, Chatterjee S, Ye CS, Rodriguez CL, Rasio FA (2019) How initial size governs core collapse in globular clusters. ApJ 871(1):38. https://doi.org/10.3847/1538-4357/aaf646. arXiv:1808.02204 [astro-ph.GA]

Kremer K, Rodriguez CL, Amaro-Seoane P, Breivik K, Chatterjee S, Katz ML, Larson SL, Rasio FA, Samsing J, Ye CS et al (2019) Post-Newtonian dynamics in dense star clusters: binary black holes in the LISA band. Phys Rev D 99(6):063003. https://doi.org/10.1103/PhysRevD.99.063003. arXiv:1811.11812 [astro-ph.HE]

Kremer K, Spera M, Becker D, Chatterjee S, Di Carlo UN, Fragione G, Rodriguez CL, Ye CS, Rasio FA (2020a) Populating the upper black hole mass gap through stellar collisions in dense star clusters. ApJ 903:45. https://doi.org/10.3847/1538-4357/abb945. arXiv:2006.10771 [astro-ph.HE]

Kremer K, Ye CS, Rui NZ, Weatherford NC, Chatterjee S, Fragione G, Rodriguez CL, Spera M, Rasio FA (2020b) Modeling dense star clusters in the milky way and beyond with the CMC cluster catalog. ApJS 247(2):48. https://doi.org/10.3847/1538-4365/ab7919. arXiv:1911.00018 [astro-ph.HE]

Krolik JH, Volonteri M, Dubois Y, Devriendt J (2019) Population estimates for electromagnetically distinguishable supermassive binary black holes. ApJ 879(2):110. https://doi.org/10.3847/1538-4357/ab24c9. arXiv:1905.10450 [astro-ph.GA]

Kroupa P (2001) On the variation of the initial mass function. MNRAS 322(2):231–246. https://doi.org/10.1046/j.1365-8711.2001.04022.x. arXiv:astro-ph/0009005 [astro-ph]

Kruckow MU, Tauris TM, Langer N, Szécsi D, Marchant P, Podsiadlowski P (2016) Common-envelope ejection in massive binary stars. Implications for the progenitors of GW150914 and GW151226. A&A 596:A58. https://doi.org/10.1051/0004-6361/201629420. arXiv:1610.04417 [astro-ph.SR]

Kruckow MU, Tauris TM, Langer N, Kramer M, Izzard RG (2018) Progenitors of gravitational wave mergers: binary evolution with the stellar grid-based code COMBINE. MNRAS 481(2):1908–1949. https://doi.org/10.1093/mnras/sty2190. arXiv:1801.05433 [astro-ph.SR]

Krumholz MR (2014) The big problems in star formation: the star formation rate, stellar clustering, and the initial mass function. Phys Rep 539:49–134. https://doi.org/10.1016/j.physrep.2014.02.001. arXiv:1402.0867 [astro-ph.GA]

Kuhlen M, Vogelsberger M, Angulo R (2012) Numerical simulations of the dark universe: state of the art and the next decade. Phys Dark Universe 1(1–2):50–93. https://doi.org/10.1016/j.dark.2012.10.002. arXiv:1209.5745 [astro-ph.CO]

Kuin NPM, Wu K, Oates S, Lien A, Emery S, Kennea JA, de Pasquale M, Han Q, Brown PJ, Tohuvavohu A et al (2019) Swift spectra of AT2018cow: a white dwarf tidal disruption event? MNRAS 487 (2):2505–2521. https://doi.org/10.1093/mnras/stz053. arXiv:1808.08492 [astro-ph.HE]

Kulkarni G, Loeb A (2012) Formation of galactic nuclei with multiple supermassive black holes at high redshifts. MNRAS 422(2):1306–1323. https://doi.org/10.1111/j.1365-2966.2012.20699.x. arXiv:1107.0517 [astro-ph.CO]

Kulkarni SR, Ofek EO, Rau A, Cenko SB, Soderberg AM, Fox DB, Gal-Yam A, Capak PL, Moon DS, Li W et al (2007) An unusually brilliant transient in the galaxy M85. Nature 447(7143):458–460. https://doi.org/10.1038/nature05822. arXiv:0705.3668 [astro-ph]

Kumamoto J, Fujii MS, Tanikawa A (2019) Gravitational-wave emission from binary black holes formed in open clusters. MNRAS 486(3):3942–3950. https://doi.org/10.1093/mnras/stz1068. arXiv:1811.06726 [astro-ph.HE]

Kumamoto J, Fujii MS, Tanikawa A (2020) Merger rate density of binary black holes formed in open clusters. MNRAS 495(4):4268–4278. https://doi.org/10.1093/mnras/staa1440. arXiv:2001.10690 [astro-ph.HE]

Kupfer T, Groot PJ, Bloemen S, Levitan D, Steeghs D, Marsh TR, Rutten RGM, Nelemans G, Prince TA, Fürst F et al (2015) Phase-resolved spectroscopy and Kepler photometry of the ultracompact AM CVn binary SDSS J190817.07+394036.4. MNRAS 453(1):483–496. https://doi.org/10.1093/mnras/stv1609. arXiv:1507.03926 [astro-ph.SR]

Kupfer T, Ramsay G, van Roestel J, Brooks J, MacFarlane SA, Toma R, Groot PJ, Woudt PA, Bildsten L et al (2017) The OmegaWhite survey for short-period variable stars. V. Discovery of an ultracompact hot subdwarf binary with a compact companion in a 44-minute orbit. ApJ 851(1):28. https://doi.org/10.3847/1538-4357/aa9522. arXiv:1710.07287 [astro-ph.SR]

Kupfer T, Korol V, Shah S, Nelemans G, Marsh TR, Ramsay G, Groot PJ, Steeghs DTH, Rossi EM (2018) LISA verification binaries with updated distances from Gaia Data Release 2. MNRAS 480(1):302–309. https://doi.org/10.1093/mnras/sty1545. arXiv:1805.00482 [astro-ph.SR]

Kupfer T, Bauer EB, Burdge KB, Roestel Jv, Bellm EC, Fuller J, Hermes J, Marsh TR et al (2020) A new class of Roche lobe-filling hot subdwarf binaries. ApJ 898(1):L25. https://doi.org/10.3847/2041-8213/aba3c2. arXiv:2007.05349 [astro-ph.SR]

Kupfer T, Bauer EB, Marsh TR, van Roestel J, Bellm EC, Burdge KB, Coughlin MW, Fuller J et al (2020) The first ultracompact Roche lobe-filling hot subdwarf binary. ApJ 891(1):45. https://doi.org/10.3847/1538-4357/ab72ff. arXiv:2002.01485 [astro-ph.SR]

Kupfer T, Prince TA, van Roestel J, Bellm EC, Bildsten L, Coughlin MW, Drake AJ, Graham MJ, Klein C, Kulkarni SR et al (2021) Year 1 of the ZTF high-cadence Galactic plane survey: strategy, goals, and early results on new single-mode hot subdwarf B-star pulsators. MNRAS 505(1):1254–1267. https://doi.org/10.1093/mnras/stab1344. arXiv:2105.02758 [astro-ph.SR]

Kupi G, Amaro-Seoane P, Spurzem R (2006) Dynamics of compact object clusters: a post-Newtonian study. MNRAS 371(1):L45–L49. https://doi.org/10.1111/j.1745-3933.2006.00205.x. arXiv:astro-ph/0602125 [astro-ph]

Kuroda T, Arcones A, Takiwaki T, Kotake K (2020) Magnetorotational explosion of a massive star supported by neutrino heating in general relativistic three-dimensional simulations. ApJ 896(2):102. https://doi.org/10.3847/1538-4357/ab9308. arXiv:2003.02004 [astro-ph.HE]

Kuruwita RL, Staff J, De Marco O (2016) Considerations on the role of fall-back discs in the final stages of the common envelope binary interaction. MNRAS 461(1):486–496. https://doi.org/10.1093/mnras/stw1414. arXiv:1606.04635 [astro-ph.SR]

Kushnir D, Katz B, Dong S, Livne E, Fernández R (2013) Head-on collisions of white dwarfs in triple systems could explain type Ia supernovae. ApJ 778(2):L37. https://doi.org/10.1088/2041-8205/778/2/L37. arXiv:1303.1180 [astro-ph.HE]

Kuulkers E, den Hartog PR, in't Zand JJM, Verbunt FWM, Harris WE, Cocchi M (2003) Photospheric radius expansion X-ray bursts as standard candles. A&A 399:663–680. https://doi.org/10.1051/0004-6361:20021781. arXiv:astro-ph/0212028 [astro-ph]

Kyutoku K, Seto N (2016) Concise estimate of the expected number of detections for stellar-mass binary black holes by eLISA. MNRAS 462(2):2177–2183. https://doi.org/10.1093/mnras/stw1767. arXiv:1606.02298 [astro-ph.HE]

Kyutoku K, Nishino Y, Seto N (2019) How to detect the shortest period binary pulsars in the era of LISA. MNRAS 483(2):2615–2620. https://doi.org/10.1093/mnras/sty3322. arXiv:1812.02177 [astro-ph.HE]

Lacey C, Cole S (1993) Merger rates in hierarchical models of galaxy formation. MNRAS 262(3):627–649. https://doi.org/10.1093/mnras/262.3.627

Lacy M, Ridgway SE, Sajina A, Petric AO, Gates EL, Urrutia T, Storrie-Lombardi LJ (2015) The Spitzer mid-infrared AGN survey. II. The demographics and cosmic evolution of the AGN population. ApJ 802(2):102. https://doi.org/10.1088/0004-637X/802/2/102. arXiv:1501.04118 [astro-ph.GA]

Lai D, Shapiro SL (1995) Hydrodynamics of coalescing binary neutron stars: ellipsoidal treatment. ApJ 443:705. https://doi.org/10.1086/175562. arXiv:astro-ph/9408054 [astro-ph]

Lai D, Rasio FA, Shapiro SL (1994) Hydrodynamics of rotating stars and close binary interactions: compressible ellipsoid models. ApJ 437:742. https://doi.org/10.1086/175036. arXiv:astro-ph/9404031 [astro-ph]

Lai D, Chernoff DF, Cordes JM (2001) Pulsar jets: implications for neutron star kicks and initial spins. ApJ 549(2):1111–1118. https://doi.org/10.1086/319455. arXiv:astro-ph/0007272 [astro-ph]

Lamberts A, Garrison-Kimmel S, Clausen DR, Hopkins PF (2016) When and where did GW150914 form? MNRAS 463(1):L31–L35. https://doi.org/10.1093/mnrasl/slw152. arXiv:1605.08783 [astro-ph.HE]

Lamberts A, Garrison-Kimmel S, Hopkins PF, Quataert E, Bullock JS, Faucher-Giguère CA, Wetzel A, Kereš D, Drango K, Sand erson RE (2018) Predicting the binary black hole population of the Milky Way with cosmological simulations. MNRAS 480(2):2704–2718. https://doi.org/10.1093/mnras/sty2035. arXiv:1801.03099 [astro-ph.GA]

Lamberts A, Blunt S, Littenberg TB, Garrison-Kimmel S, Kupfer T, Sanderson RE (2019) Predicting the LISA white dwarf binary population in the Milky Way with cosmological simulations. MNRAS 490 (4):5888–5903. https://doi.org/10.1093/mnras/stz2834. arXiv:1907.00014 [astro-ph.HE]

Lasky PD, Mingarelli CMF, Smith TL et al (2016) Gravitational-wave cosmology across 29 decades in frequency. Phys Rev X 6(1):011035. https://doi.org/10.1103/PhysRevX.6.011035. arXiv:1511.05994

Lattimer JM, Prakash M (2016) The equation of state of hot, dense matter and neutron stars. Phys Rep 621:127–164. https://doi.org/10.1016/j.physrep.2015.12.005. arXiv:1512.07820 [astro-ph.SR]

Lau MYM, Mandel I, Vigna-Gómez A, Neijssel CJ, Stevenson S, Sesana A (2020) Detecting double neutron stars with LISA. MNRAS 492(3):3061–3072. https://doi.org/10.1093/mnras/staa002. arXiv:1910.12422 [astro-ph.HE]

Law-Smith JAP, Everson RW, Ramirez-Ruiz E, de Mink SE, van Son LAC, Götberg Y, Zellmann S, Vigna-Gómez A, Renzo M, Wu S et al (2020) Successful common envelope ejection and binary neutron star formation in 3D hydrodynamics. arXiv e-prints arXiv:2011.06630 [astro-ph.HE]

Lee HM (1995) Evolution of galactic nuclei with 10-M_ black holes. MNRAS 272(3):605–617. https://doi.org/10.1093/mnras/272.3.605. arXiv:astro-ph/9409073 [astro-ph]

Leigh NWC, Geller AM (2013) The dynamical significance of triple star systems in star clusters. MNRAS 432(3):2474–2479. https://doi.org/10.1093/mnras/stt617. arXiv:1304.2775 [astro-ph.SR]

Leigh NWC, Böker T, Maccarone TJ, Perets HB (2013) Gas depletion in primordial globular clusters due to accretion on to stellar-mass black holes. MNRAS 429(4):2997–3006. https://doi.org/10.1093/mnras/sts554. arXiv:1212.1461 [astro-ph.SR]

Leigh NWC, Lützgendorf N, Geller AM, Maccarone TJ, Heinke C, Sesana A (2014) On the coexistence of stellar-mass and intermediate-mass black holes in globular clusters. MNRAS 444(1):29–42. https://doi.org/10.1093/mnras/stu1437. arXiv:1407.4459 [astro-ph.SR]

Leitao L, Mégevand A, Sánchez AD (2012) Gravitational waves from the electroweak phase transition. J Cosmol Astropart Phys 10:024. https://doi.org/10.1088/1475-7516/2012/10/024. arXiv:1205.3070 [astro-ph.CO]

Lena D, Robinson A, Marconi A, Axon DJ, Capetti A, Merritt D, Batcheldor D (2014) Recoiling supermassive black holes: a search in the nearby universe. ApJ 795(2):146. https://doi.org/10.1088/0004-637X/795/2/146. arXiv:1409.3976 [astro-ph.GA]

Lenon AK, Nitz AH, Brown DA (2020) Measuring the eccentricity of GW170817 and GW190425. MNRAS 497(2):1966–1971. https://doi.org/10.1093/mnras/staa2120. arXiv:2005.14146 [astro-ph.HE]

Leung GYC, Leaman R, van de Ven G, Battaglia G (2020) A dwarf-dwarf merger and dark matter core as a solution to the globular cluster problems in the Fornax dSph. MNRAS 493(1):320–336. https://doi.org/10.1093/mnras/stz3017. arXiv:1911.09167 [astro-ph.GA]

Leveque A, Giersz M, Arca-Sedda M, Askar A (2022) MOCCA-survey data base: extra galactic globular clusters—II. Milky way and andromeda. MNRAS 514(4):5751–5766. https://doi.org/10.1093/mnras/stac1694

Levin L, Bailes M, Barsdell BR, Bates SD, Bhat NDR, Burgay M, Burke-Spolaor S, Champion DJ, Coster P, D'Amico N et al (2013) The high time resolution universe pulsar survey—VIII. The galactic millisecond pulsar population. MNRAS 434(2):1387–1397. https://doi.org/10.1093/mnras/stt1103. arXiv:1306.4190 [astro-ph.SR]

Levin Y (2007) Starbursts near supermassive black holes: young stars in the Galactic Centre, and gravitational waves in LISA band. MNRAS 374(2):515–524. https://doi.org/10.1111/j.1365-2966.2006.11155.x. arXiv:astro-ph/0603583 [astro-ph]

Levin Y, Beloborodov AM (2003) Stellar disk in the galactic center: a remnant of a dense accretion disk? ApJ 590(1):L33–L36. https://doi.org/10.1086/376675. arXiv:astro-ph/0303436 [astro-ph]

Levine R, Gnedin NY, Hamilton AJS (2010) Measuring gas accretion and angular momentum near simulated supermassive black holes. ApJ 716(2):1386–1396. https://doi.org/10.1088/0004-637X/716/2/1386. arXiv:1004.3785 [astro-ph.CO]

Levitan D, Kupfer T, Groot PJ, Margon B, Prince TA, Kulkarni SR, Hallinan G, Harding LK, Kyne G, Laher R et al (2014) PTF1 J191905.19+481506.2—a partially eclipsing AM CVn system discovered in the Palomar transient factory. ApJ 785(2):114. https://doi.org/10.1088/0004-637X/785/2/114. arXiv:1402.7129 [astro-ph.SR]

Lezhnin K, Vasiliev E (2016) Tidal disruption rates in non-spherical galactic nuclei formed by galaxy mergers. ApJ 831(1):84. https://doi.org/10.3847/0004-637X/831/1/84. arXiv:1609.00009 [astro-ph.GA]

Li K, Bogdanović T, Ballantyne DR (2020) Pairing of massive black holes in merger galaxies driven by dynamical friction. ApJ 896(2):113. https://doi.org/10.3847/1538-4357/ab93c6. arXiv:2006.08520 [astro-ph.GA]

Li K, Bogdanović T, Ballantyne DR (2020) The pairing probability of massive black holes in merger galaxies in the presence of radiative feedback. ApJ 905(2):123. https://doi.org/10.3847/1538-4357/abc555. arXiv:2007.02051 [astro-ph.GA]

Li KJ, Wu K, Singh D (2019) Spin dynamics of a millisecond pulsar orbiting closely around a massive black hole. MNRAS 485(1):1053–1066. https://doi.org/10.1093/mnras/stz389. arXiv:1902.03146 [astro-ph.HE]

Li LX, Narayan R, McClintock JE (2009) Inferring the inclination of a black hole accretion disk from observations of its polarized continuum radiation. ApJ 691(1):847–865. https://doi.org/10.1088/0004-637X/691/1/847. arXiv:0809.0866 [astro-ph]

Li S, Liu FK, Berczik P, Spurzem R (2017) Boosted tidal disruption by massive black hole binaries during galaxy mergers from the view of N-body simulation. ApJ 834(2):195. https://doi.org/10.3847/1538-4357/834/2/195. arXiv:1509.00158 [astro-ph.GA]

Li TS, Simon JD, Kuehn K, Pace AB, Erkal D, Bechtol K, Yanny B, Drlica-Wagner A, Marshall JL, Lidman C et al (2018) The first tidally disrupted ultra-faint dwarf galaxy? A spectroscopic analysis of the Tucana III stream. ApJ 866(1):22. https://doi.org/10.3847/1538-4357/aadf91. arXiv:1804.07761 [astro-ph.GA]

Li Y, Ni Y, Croft RAC, Di Matteo T, Bird S, Feng Y (2021) AI-assisted superresolution cosmological simulations. Proc Natl Acad Sci 118(19):e2022038118. https://doi.org/10.1073/pnas.2022038118. arXiv:2010.06608 [astro-ph.CO]

Lidov ML (1962) The evolution of orbits of artificial satellites of planets under the action of gravitational perturbations of external bodies. Planet Space Sci 9(10):719–759. https://doi.org/10.1016/0032-0633(62)90129-0

Lim H, Rodriguez CL (2020) Relativistic three-body effects in hierarchical triples. Phys Rev D 102(6):064033. https://doi.org/10.1103/PhysRevD.102.064033. arXiv:2001.03654 [astro-ph.HE]

Lippai Z, Frei Z, Haiman Z (2008) Prompt shocks in the gas disk around a recoiling supermassive black hole binary. ApJ 676(1):L5. https://doi.org/10.1086/587034. arXiv:0801.0739 [astro-ph]

Liptai D, Price DJ (2019) General relativistic smoothed particle hydrodynamics. MNRAS 485(1):819–842. https://doi.org/10.1093/mnras/stz111. arXiv:1901.08064 [astro-ph.IM]

Lipunov VM, Postnov KA, Prokhorov ME (1996) The scenario machine: binary star population synthesis. Harwood Academic, Amsterdam

Lipunov VM, Postnov KA, Prokhorov ME, Bogomazov AI (2009) Description of the "scenario machine". Astron Rep 53(10):915–940. https://doi.org/10.1134/S1063772909100047. arXiv:0704.1387 [astro-ph]

Littenberg TB, Cornish NJ (2019) Prospects for gravitational wave measurement of ZTF J1539+5027. ApJ 881(2):L43. https://doi.org/10.3847/2041-8213/ab385f. arXiv:1908.00678 [astro-ph.IM]

Littenberg TB, Larson SL, Nelemans G, Cornish NJ (2013) Prospects for observing ultracompact binaries with space-based gravitational wave interferometers and optical telescopes. MNRAS 429(3):2361–2365. https://doi.org/10.1093/mnras/sts507. arXiv:1207.4848 [astro-ph.IM]

Littenberg TB, Cornish NJ, Lackeos K, Robson T (2020) Global analysis of the gravitational wave signal from Galactic binaries. Phys Rev D 101(12):123021. https://doi.org/10.1103/PhysRevD.101.123021. arXiv:2004.08464 [gr-qc]

Liu B, Lai D (2017) Spin-orbit misalignment of merging black hole binaries with tertiary companions. ApJ 846(1):L11. https://doi.org/10.3847/2041-8213/aa8727. arXiv:1706.02309 [astro-ph.HE]

Liu B, Lai D (2018) Black hole and neutron star binary mergers in triple systems: merger fraction and spin-orbit misalignment. ApJ 863(1):68. https://doi.org/10.3847/1538-4357/aad09f. arXiv:1805.03202 [astro-ph.HE]

Liu C, Shao L, Zhao J, Gao Y (2020) Multiband observation of LIGO/Virgo binary black hole mergers in the gravitational-wave transient catalog GWTC-1. MNRAS 496(1):182–196. https://doi.org/10.1093/mnras/staa1512. arXiv:2004.12096 [astro-ph.HE]

Liu J, Han Z, Zhang F, Zhang Y (2010) A comprehensive study of close double white dwarfs as gravitational wave sources: evolutionary channels, birth rates, and physical properties. ApJ 719 (2):1546–1552. https://doi.org/10.1088/0004-637X/719/2/1546

Liu J, Zhang H, Howard AW, Bai Z, Lu Y, Soria R, Justham S, Li X, Zheng Z (2019) A wide star-black-hole binary system from radial-velocity measurements. Nature 575(7784):618–621. https://doi.org/10.1038/s41586-019-1766-2. arXiv:1911.11989 [astro-ph.SR]

Liu T, Gezari S, Ayers M, Burgett W, Chambers K, Hodapp K, Huber ME, Kudritzki RP, Metcalfe N, Tonry J et al (2019) Supermassive black hole binary candidates from the pan-STARRS1 medium deep survey. ApJ 884(1):36. https://doi.org/10.3847/1538-4357/ab40cb. arXiv:1906.08315 [astro-ph.HE]

Liu X, Shen Y, Bian F, Loeb A, Tremaine S (2014) Constraining sub-parsec binary supermassive black holes in quasars with multi-epoch spectroscopy. II. The population with kinematically offset broad Balmer emission lines. ApJ 789(2):140. https://doi.org/10.1088/0004-637X/789/2/140. arXiv:1312.6694 [astro-ph.CO]

Liu YT, Shapiro SL, Stephens BC (2007) Magnetorotational collapse of very massive stars in full general relativity. Phys Rev D 76:084017. https://doi.org/10.1103/PhysRevD.76.084017. arXiv:0706.2360 [astro-ph]

Livio M, Soker N (1984) Star-planet systems as possible progenitors of cataclysmic binaries. MNRAS 208:763–781. https://doi.org/10.1093/mnras/208.4.763

Lodato G, Gerosa D (2013) Black hole mergers: do gas discs lead to spin alignment? MNRAS 429:L30–L34. https://doi.org/10.1093/mnrasl/sls018. arXiv:1211.0284 [astro-ph.CO]

Lodato G, Natarajan P (2006) Supermassive black hole formation during the assembly of pre-galactic discs. MNRAS 371(4):1813–1823. https://doi.org/10.1111/j.1365-2966.2006.10801.x. arXiv:astro-ph/0606159 [astro-ph]

Lodato G, Rossi EM (2011) Multiband light curves of tidal disruption events. MNRAS 410(1):359–367. https://doi.org/10.1111/j.1365-2966.2010.17448.x. arXiv:1008.4589 [astro-ph.CO]

Lodato G, Nayakshin S, King AR, Pringle JE (2009) Black hole mergers: can gas discs solve the 'final parsec' problem? MNRAS 398(3):1392–1402. https://doi.org/10.1111/j.1365-2966.2009.15179.x. arXiv:0906.0737 [astro-ph.CO]

Lops G, Izquierdo-Villalba D, Colpi M, Bonoli S, Sesana A, Mangiagli A (2022) Galaxy fields of LISA massive black hole mergers in a simulated universe. arXiv e-prints arXiv:2207.10683 [astro-ph.GA]

Lousto CO, Zlochower Y (2008) Further insight into gravitational recoil. Phys Rev D 77(4):044028. https://doi.org/10.1103/PhysRevD.77.044028. arXiv:0708.4048 [gr-qc]

Lousto CO, Zlochower Y (2011) Hangup kicks: still larger recoils by partial spin-orbit alignment of black-hole binaries. Phys Rev Lett 107(23):231102. https://doi.org/10.1103/PhysRevLett.107.231102. arXiv:1108.2009 [gr-qc]

Lousto CO, Zlochower Y (2013) Nonlinear gravitational recoil from the mergers of precessing black-hole binaries. Phys Rev D 87(8):084027. https://doi.org/10.1103/PhysRevD.87.084027. arXiv:1211.7099 [gr-qc]

Lousto CO, Campanelli M, Zlochower Y, Nakano H (2010) Remnant masses, spins and recoils from the merger of generic black hole binaries. Class Quantum Grav 27(11):114006. https://doi.org/10.1088/0264-9381/27/11/114006. arXiv:0904.3541 [gr-qc]

Lousto CO, Zlochower Y, Dotti M, Volonteri M (2012) Gravitational recoil from accretion-aligned black-hole binaries. Phys Rev D 85(8):084015. https://doi.org/10.1103/PhysRevD.85.084015. arXiv:1201.1923 [gr-qc]

Lovelace G, Scheel MA, Szilágyi B (2011) Simulating merging binary black holes with nearly extremal spins. Phys Rev D 83(2):024010. https://doi.org/10.1103/PhysRevD.83.024010. arXiv:1010.2777 [gr-qc]

Loveridge AJ, van der Sluys MV, Kalogera V (2011) Analytical expressions for the envelope binding energy of giants as a function of basic stellar parameters. ApJ 743(1):49. https://doi.org/10.1088/0004-637X/743/1/49. arXiv:1009.5400 [astro-ph.SR]

LSST Science Collaboration, Abell PA, Allison J, Anderson SF, Andrew JR, Angel JRP, Armus L, Arnett D, Asztalos SJ, Axelrod TS et al (2009) LSST science book, version 2.0. arXiv e-prints arXiv:0912.0201 [astro-ph.IM]

Lu W, Beniamini P, Bonnerot C (2020) On the formation of GW190814. MNRAS 500:1817–1832. https://doi.org/10.1093/mnras/staa3372. arXiv:2009.10082 [astro-ph.HE]

Lukes-Gerakopoulos G, Witzany V (2021) Nonlinear effects in EMRI dynamics and their imprints on gravitational waves. In: Bambi C, Katsanevas S, Kokkotas KD (eds) Handbook of gravitational wave astronomy. Springer, p 42. https://doi.org/10.1007/978-981-15-4702-7_42-1

Lukes-Gerakopoulos G, Apostolatos TA, Contopoulos G (2010) Observable signature of a background deviating from the Kerr metric. Phys Rev D 81(12):124005. https://doi.org/10.1103/PhysRevD.81.124005. arXiv:1003.3120 [gr-qc]

Lukes-Gerakopoulos G, Seyrich J, Kunst D (2014) Investigating spinning test particles: spin supplementary conditions and the Hamiltonian formalism. Phys Rev D 90(10):104019. https://doi.org/10.1103/PhysRevD.90.104019. arXiv:1409.4314 [gr-qc]

Luo J, Chen LS, Duan HZ, Gong YG, Hu S, Ji J, Liu Q, Mei J, Milyukov V, Sazhin M et al (2016) TianQin: a space-borne gravitational wave detector. Class Quantum Grav 33(3):035010. https://doi.org/10.1088/0264-9381/33/3/035010. arXiv:1512.02076 [astro-ph.IM]

Lupi A, Haardt F, Dotti M, Fiacconi D, Mayer L, Madau P (2016) Growing massive black holes through supercritical accretion of stellar-mass seeds. MNRAS 456:2993–3003. https://doi.org/10.1093/mnras/stv2877. arXiv:1512.02651

Luyten WJ (1949) An Atlas of identification charts of white dwarfs. ApJ 109:528. https://doi.org/10.1086/145156

Lyne AG, Burgay M, Kramer M, Possenti A, Manchester RN, Camilo F, McLaughlin MA, Lorimer DR, D'Amico N, Joshi BC et al (2004) A double-pulsar system: a rare laboratory for relativistic gravity and plasma physics. Science 303(5661):1153–1157. https://doi.org/10.1126/science.1094645. arXiv:astro-ph/0401086 [astro-ph]

Lynx Team (2018) The Lynx mission concept study interim report. arXiv e-prints arXiv:1809.09642 [astro-ph.IM]

Ma L, Hopkins PF, Ma X, Anglés-Alcázar D, Faucher-Giguère CA, Kelley LZ (2021) Seeds don't sink: even massive black hole "seeds" cannot migrate to galaxy centres efficiently. MNRAS 508(2):1973–1985. https://doi.org/10.1093/mnras/stab2713. arXiv:2101.02727 [astro-ph.GA]

Maccarone TJ, Kundu A, Zepf SE, Rhode KL (2007) A black hole in a globular cluster. Nature 445(7124):183–185. https://doi.org/10.1038/nature05434. arXiv:astro-ph/0701310 [astro-ph]

MacFadyen AI, Milosavljević M (2008) An eccentric circumbinary accretion disk and the detection of binary massive black holes. ApJ 672(1):83–93. https://doi.org/10.1086/523869. arXiv:astro-ph/0607467 [astro-ph]

Macfarlane SA, Toma R, Ramsay G, Groot PJ, Woudt PA, Drew JE, Barentsen G, Eislöffel J (2015) The OmegaWhite survey for short-period variable stars—I. Overview and first results. MNRAS 454(1):507–530. https://doi.org/10.1093/mnras/stv1989. arXiv:1508.06277 [astro-ph.SR]

Mack KJ, Ostriker JP, Ricotti M (2007) Growth of structure seeded by primordial black holes. Astrophys J 665:1277–1287. https://doi.org/10.1086/518998. arXiv:astro-ph/0608642

Mackey AD, Wilkinson MI, Davies MB, Gilmore GF (2007) The effect of stellar-mass black holes on the structural evolution of massive star clusters. MNRAS 379(1):L40–L44. https://doi.org/10.1111/j.1745-3933.2007.00330.x. arXiv:0704.2494 [astro-ph]

Mackey AD, Wilkinson MI, Davies MB, Gilmore GF (2008) Black holes and core expansion in massive star clusters. MNRAS 386(1):65–95. https://doi.org/10.1111/j.1365-2966.2008.13052.x. arXiv:0802.0513 [astro-ph]

MacLeod CL, Hogan CJ (2008) Precision of Hubble constant derived using black hole binary absolute distances and statistical redshift information. Phys Rev D 77:043512. https://doi.org/10.1103/PhysRevD.77.043512. arXiv:0712.0618 [astro-ph]

MacLeod M, Lin DNC (2020) The effect of star-disk interactions on highly eccentric stellar orbits in active galactic nuclei: a disk loss cone and implications for stellar tidal disruption events. ApJ 889(2):94. https://doi.org/10.3847/1538-4357/ab64db. arXiv:1909.09645 [astro-ph.SR]

MacLeod M, Ramirez-Ruiz E (2015) On the accretion-fed growth of neutron stars during common envelope. ApJ 798(1):L19. https://doi.org/10.1088/2041-8205/798/1/L19. arXiv:1410.5421 [astro-ph.SR]

MacLeod M, Guillochon J, Ramirez-Ruiz E, Kasen D, Rosswog S (2016) Optical thermonuclear transients from tidal compression of white dwarfs as tracers of the low end of the massive black hole mass function. ApJ 819(1):3. https://doi.org/10.3847/0004-637X/819/1/3. arXiv:1508.02399 [astro-ph.HE]

MacLeod M, Trenti M, Ramirez-Ruiz E (2016) The close stellar companions to intermediate-mass black holes. ApJ 819(1):70. https://doi.org/10.3847/0004-637X/819/1/70. arXiv:1508.07000 [astro-ph.HE]

MacLeod M, Antoni A, Murguia-Berthier A, Macias P, Ramirez-Ruiz E (2017) Common envelope wind tunnel: coefficients of drag and accretion in a simplified context for studying flows around objects embedded within stellar envelopes. ApJ 838(1):56. https://doi.org/10.3847/1538-4357/aa6117. arXiv:1704.02372 [astro-ph.SR]

Madau P, Dickinson M (2014) Cosmic star-formation history. ARA&A 52:415–486. https://doi.org/10.1146/annurev-astro-081811-125615. arXiv:1403.0007 [astro-ph.CO]

Madau P, Fragos T (2017) Radiation backgrounds at cosmic dawn: X-rays from compact binaries. ApJ 840(1):39. https://doi.org/10.3847/1538-4357/aa6af9. arXiv:1606.07887 [astro-ph.GA]

Madau P, Rees MJ (2001) Massive black holes as population III remnants. ApJ 551(1):L27–L30. https://doi.org/10.1086/319848. arXiv:astro-ph/0101223 [astro-ph]

Madej OK, Jonker PG, Groot PJ, van Haaften LM, Nelemans G, Maccarone TJ (2013) Time-resolved X-shooter spectra and RXTE light curves of the ultra-compact X-ray binary candidate 4U 0614+091. MNRAS 429(4):2986–2996. https://doi.org/10.1093/mnras/sts550. arXiv:1212.0862 [astro-ph.HE]

Madigan AM, Hopman C, Levin Y (2011) Secular stellar dynamics near a massive black hole. ApJ 738(1):99. https://doi.org/10.1088/0004-637X/738/1/99. arXiv:1010.1535 [astro-ph.GA]

Maggiore M (2000) Stochastic backgrounds of gravitational waves. arXiv e-prints arXiv:gr-qc/0008027 [astro-ph]

Magorrian J, Tremaine S, Richstone D, Bender R, Bower G, Dressler A, Faber SM, Gebhardt K, Green R, Grillmair C et al (1998) The demography of massive dark objects in galaxy centers. AJ 115(6):2285–2305. https://doi.org/10.1086/300353. arXiv:astro-ph/9708072 [astro-ph]

Maguire K, Eracleous M, Jonker PG, MacLeod M, Rosswog S (2020) Tidal disruptions of white dwarfs: theoretical models and observational prospects. Space Sci Rev 216(3):39. https://doi.org/10.1007/s11214-020-00661-2. arXiv:2004.00146 [astro-ph.HE]

Maio U, Dotti M, Petkova M, Perego A, Volonteri M (2013) Effects of circumnuclear disk gas evolution on the spin of central black holes. ApJ 767(1):37. https://doi.org/10.1088/0004-637X/767/1/37. arXiv:1203.1877 [astro-ph.HE]

Makino J, Funato Y (2004) Evolution of massive black hole binaries. ApJ 602(1):93–102. https://doi.org/10.1086/380917. arXiv:astro-ph/0307327 [astro-ph]

Manchester RN, Hobbs GB, Teoh A, Hobbs M (2005) The Australia telescope national facility pulsar catalogue. AJ 129(4):1993–2006. https://doi.org/10.1086/428488. arXiv:astro-ph/0412641 [astro-ph]

Mandel I (2016) Estimates of black hole natal kick velocities from observations of low-mass X-ray binaries. MNRAS 456(1):578–581. https://doi.org/10.1093/mnras/stv2733. arXiv:1510.03871 [astro-ph.HE]

Mandel I, de Mink SE (2016) Merging binary black holes formed through chemically homogeneous evolution in short-period stellar binaries. MNRAS 458(3):2634–2647. https://doi.org/10.1093/mnras/stw379. arXiv:1601.00007 [astro-ph.HE]

Mandel I, Müller B (2020) Simple recipes for compact remnant masses and natal kicks. MNRAS 499:3214–3221. https://doi.org/10.1093/mnras/staa3043. arXiv:2006.08360 [astro-ph.HE]

Mandel I, Brown DA, Gair JR, Miller MC (2008) Rates and characteristics of intermediate mass ratio Inspirals detectable by advanced LIGO. ApJ 681:1431–1447. https://doi.org/10.1086/588246. arXiv:0705.0285

Mandel I, Sesana A, Vecchio A (2018) The astrophysical science case for a decihertz gravitational-wave detector. Class Quantum Grav 35(5):054004. https://doi.org/10.1088/1361-6382/aaa7e0. arXiv:1710.11187 [astro-ph.HE]

Mandic V, Thrane E, Giampanis S, Regimbau T (2012) Parameter estimation in searches for the stochastic gravitational-wave background. Phys Rev Lett 109(17):171102. https://doi.org/10.1103/PhysRevLett.109.171102. arXiv:1209.3847 [astro-ph.CO]

Mangiagli A, Klein A, Sesana A, Barausse E, Colpi M (2019) Post-Newtonian phase accuracy requirements for stellar black hole binaries with LISA. Phys Rev D 99(6):064056. https://doi.org/10.1103/PhysRevD.99.064056. arXiv:1811.01805 [gr-qc]

Mangiagli A, Klein A, Bonetti M, Katz ML, Sesana A, Volonteri M, Colpi M, Marsat S, Babak S (2020) Observing the inspiral of coalescing massive black hole binaries with LISA in the era of multimessenger astrophysics. Phys Rev D 102(8):084056. https://doi.org/10.1103/PhysRevD.102.084056. arXiv:2006.12513 [astro-ph.HE]

Mangiagli A, Caprini C, Volonteri M, Marsat S, Vergani S, Tamanini N, Inchauspé H (2022) Massive black hole binaries in LISA: multimessenger prospects and electromagnetic counterparts. Phys Rev D 106:103017. https://doi.org/10.1103/PhysRevD.106.103017. arXiv:2207.10678 [astro-ph.HE]

Mannerkoski M, Johansson PH, Pihajoki P, Rantala A, Naab T (2019) Gravitational waves from the inspiral of supermassive black holes in galactic-scale simulations. ApJ 887(1):35. https://doi.org/10.3847/1538-4357/ab52f9. arXiv:1909.01373 [astro-ph.GA]

Mannerkoski M, Johansson PH, Rantala A, Naab T, Liao S (2021) Resolving the complex evolution of a supermassive black hole triplet in a cosmological simulation. ApJ 912(2):L20. https://doi.org/10.3847/2041-8213/abf9a5. arXiv:2103.16254 [astro-ph.GA]

Manser CJ, Gänsicke BT, Marsh TR, Veras D, Koester D, Breedt E, Pala AF, Parsons SG, Southworth J (2016) Doppler imaging of the planetary debris disc at the white dwarf SDSS J122859.93+104032.9. MNRAS 455(4):4467–4478. https://doi.org/10.1093/mnras/stv2603. arXiv:1511.02230 [astro-ph.SR]

Manser CJ, Gänsicke BT, Eggl S, Hollands M, Izquierdo P, Koester D, Landstreet JD, Lyra W, Marsh TR, Meru F et al (2019) A planetesimal orbiting within the debris disc around a white dwarf star. Science 364(6435):66–69. https://doi.org/10.1126/science.aat5330. arXiv:1904.02163 [astro-ph.EP]

Mapelli M (2016) Massive black hole binaries from runaway collisions: the impact of metallicity. MNRAS 459(4):3432–3446. https://doi.org/10.1093/mnras/stw869. arXiv:1604.03559 [astro-ph.GA]

Mapelli M, Giacobbo N (2018) The cosmic merger rate of neutron stars and black holes. MNRAS 479(4):4391–4398. https://doi.org/10.1093/mnras/sty1613. arXiv:1806.04866 [astro-ph.HE]

Mapelli M, Ripamonti E, Vecchio A, Graham AW, Gualandris A (2012) A cosmological view of extreme mass-ratio inspirals in nuclear star clusters. A&A 542:A102. https://doi.org/10.1051/0004-6361/201118444. arXiv:1205.2702 [astro-ph.CO]

Mapelli M, Giacobbo N, Ripamonti E, Spera M (2017) The cosmic merger rate of stellar black hole binaries from the Illustris simulation. MNRAS 472(2):2422–2435. https://doi.org/10.1093/mnras/stx2123. arXiv:1708.05722 [astro-ph.GA]

Mapelli M, Santoliquido F, Bouffanais Y, Arca Sedda M, Giacobbo N, Artale MC, Ballone A (2021) Mass and rate of hierarchical black hole mergers in young, globular and nuclear star clusters. Symmetry 13:1678. https://doi.org/10.3390/sym13091678. arXiv:2007.15022 [astro-ph.HE]

Marassi S, Schneider R, Corvino G, Ferrari V, Portegies Zwart S (2011) Imprint of the merger and ring-down on the gravitational wave background from black hole binaries coalescence. Phys Rev D 84(12):124037. https://doi.org/10.1103/PhysRevD.84.124037. arXiv:1111.6125 [astro-ph.CO]

Marassi S, Graziani L, Ginolfi M, Schneider R, Mapelli M, Spera M, Alparone M (2019) Evolution of dwarf galaxies hosting GW150914-like events. MNRAS 484(3):3219–3232. https://doi.org/10.1093/mnras/stz170. arXiv:1901.04494 [astro-ph.GA]

Marchant P, Langer N, Podsiadlowski P, Tauris TM, Moriya TJ (2016) A new route towards merging massive black holes. A&A 588:A50. https://doi.org/10.1051/0004-6361/201628133. arXiv:1601.03718 [astro-ph.SR]

Marconi A, Risaliti G, Gilli R, Hunt LK, Maiolino R, Salvati M (2004) Local supermassive black holes, relics of active galactic nuclei and the X-ray background. MNRAS 351(1):169–185. https://doi.org/10.1111/j.1365-2966.2004.07765.x. arXiv:astro-ph/0311619 [astro-ph]

Mardling R, Aarseth S (1999) Dynamics and stability of three-body systems. In: Steves BA, Roy AE (eds) The dynamics of small bodies in the solar system, a major key to solar system studies. NATO Advanced Study Institute (ASI) Series C, vol 522, p 385

Marelli M, Mignani RP, De Luca A, Saz Parkinson PM, Salvetti D, Den Hartog PR, Wolff MT (2015) Radio-quiet and radio-loud pulsars: similar in gamma-rays but different in X-rays. ApJ 802(2):78. https://doi.org/10.1088/0004-637X/802/2/78. arXiv:1501.06215 [astro-ph.HE]

Margalit B, Metzger BD (2019) The multi-messenger matrix: the future of neutron star merger constraints on the nuclear equation of state. ApJ 880(1):L15. https://doi.org/10.3847/2041-8213/ab2ae2. arXiv:1904.11995 [astro-ph.HE]

Marinacci F, Sales LV, Vogelsberger M, Torrey P, Springel V (2019) Simulating the interstellar medium and stellar feedback on a moving mesh: implementation and isolated galaxies. MNRAS 489(3):4233–4260. https://doi.org/10.1093/mnras/stz2391. arXiv:1905.08806 [astro-ph.GA]

Marronetti P, Tichy W, Brügmann B, González J, Sperhake U (2008) High-spin binary black hole mergers. Phys Rev D 77(6):064010. https://doi.org/10.1103/PhysRevD.77.064010. arXiv:0709.2160 [gr-qc]

Marsh TR, Steeghs D (2002) V407 Vul: a direct impact accretor. MNRAS 331(1):L7–L11. https://doi.org/10.1046/j.1365-8711.2002.05346.x. arXiv:astro-ph/0201309 [astro-ph]

Marsh TR, Dhillon VS, Duck SR (1995) Low-mass white dwarfs need friends—five new double-degenerate close binary stars. MNRAS 275:828. https://doi.org/10.1093/mnras/275.3.828

Marsh TR, Nelemans G, Steeghs D (2004) Mass transfer between double white dwarfs. MNRAS 350(1):113–128. https://doi.org/10.1111/j.1365-2966.2004.07564.x. arXiv:astro-ph/0312577 [astro-ph]

Martinez MAS, Fragione G, Kremer K, Chatterjee S, Rodriguez CL, Samsing J, Ye CS, Weatherford NC, Zevin M, Naoz S et al (2020) Black hole mergers from hierarchical triples in dense star clusters. ApJ 903:67. https://doi.org/10.3847/1538-4357/abba25. arXiv:2009.08468 [astro-ph.GA]

Martinez-Valpuesta I, Aguerri J, González-García C (2016) Characterization of bars induced by interactions. Galaxies 4(2):7. https://doi.org/10.3390/galaxies4020007

Marulli F, Bonoli S, Branchini E, Moscardini L, Springel V (2008) Modelling the cosmological co-evolution of supermassive black holes and galaxies—I. BH scaling relations and the AGN luminosity function. MNRAS 385(4):1846–1858. https://doi.org/10.1111/j.1365-2966.2008.12988.x. arXiv:0711.2053 [astro-ph]

Masci FJ, Laher RR, Rusholme B, Shupe DL, Groom S, Surace J, Jackson E, Monkewitz S, Beck R, Flynn D et al (2019) The Zwicky transient facility: data processing, products, and archive. PASP 131 (995):018003. https://doi.org/10.1088/1538-3873/aae8ac. arXiv:1902.01872 [astro-ph.IM]

Mashian N, Loeb A (2017) Hunting black holes with Gaia. MNRAS 470(3):2611–2616. https://doi.org/10.1093/mnras/stx1410. arXiv:1704.03455 [astro-ph.HE]

Mastrobuono-Battisti A, Perets HB, Loeb A (2014) Effects of intermediate mass black holes on nuclear star clusters. ApJ 796(1):40. https://doi.org/10.1088/0004-637X/796/1/40. arXiv:1403.3094 [astro-ph.GA]

Mathis S (2019) Tidal dissipation in stars and giant planets: Jean-Paul Zahn's pioneering work and legacy. In: EAS publications series. EAS Publications Series, vol 82, pp 5–33. https://doi.org/10.1051/eas/1982002

Matsubayashi T, Shinkai Ha, Ebisuzaki T (2004) Gravitational waves from merging intermediate-mass black holes. ApJ 614(2):864–868. https://doi.org/10.1086/423796

Matsubayashi T, Makino J, Ebisuzaki T (2007) Orbital evolution of an IMBH in the galactic nucleus with a massive central black hole. ApJ 656(2):879–896. https://doi.org/10.1086/510344. arXiv:astro-ph/0511782 [astro-ph]

Matsuoka Y, Iwasawa K, Onoue M, Kashikawa N, Strauss MA, Lee CH, Imanishi M, Nagao T, Akiyama M, Asami N et al (2019) Subaru high-z exploration of low-luminosity quasars (SHELLQs). X. Discovery of 35 quasars and luminous galaxies at $5.7 \leq z \leq 7.0$. ApJ 883(2):183. https://doi.org/10.3847/1538-4357/ab3c60. arXiv:1908.07910 [astro-ph.GA]

Maureira-Fredes C, Goicovic FG, Amaro-Seoane P, Sesana A (2018) Accretion of clumpy cold gas on to massive black hole binaries: the challenging formation of extended circumbinary structures. MNRAS 478(2):1726–1748. https://doi.org/10.1093/mnras/sty1105. arXiv:1801.06179 [astro-ph.HE]

Maxted PFL, Marsh TR, Moran CKJ (2000) Radial velocity measurements of white dwarfs. MNRAS 319 (1):305–317. https://doi.org/10.1046/j.1365-8711.2000.03840.x. arXiv:astro-ph/0007129 [astro-ph]

Maxted PFL, Marsh TR, Moran CKJ, Han Z (2000) The triple degenerate star WD 1704+481. MNRAS 314(2):334–337. https://doi.org/10.1046/j.1365-8711.2000.03343.x. arXiv:astro-ph/0001212 [astro-ph]

Maxted PFL, Marsh TR, Moran CKJ (2002) The mass ratio distribution of short-period double degenerate stars. MNRAS 332(3):745–753. https://doi.org/10.1046/j.1365-8711.2002.05368.x. arXiv:astro-ph/0201411 [astro-ph]

Maxted PFL, Napiwotzki R, Dobbie PD, Burleigh MR (2006) Survival of a brown dwarf after engulfment by a red giant star. Nature 442(7102):543–545. https://doi.org/10.1038/nature04987. arXiv:astro-ph/0608054 [astro-ph]

Mayer L (2013) Massive black hole binaries in gas-rich galaxy mergers; multiple regimes of orbital decay and interplay with gas inflows. Class Quantum Grav 30(24):244008. https://doi.org/10.1088/0264-9381/30/24/244008. arXiv:1308.0431 [astro-ph.CO]

Mayer L (2017) Multiple regimes and coalescence timescales for massive black hole pairs; the critical role of galaxy formation physics. J Phys Conf Ser 840:012025. https://doi.org/10.1088/1742-6596/840/1/012025. arXiv:1703.00661 [astro-ph.GA]

Mayer L, Wadsley J (2004) The formation and evolution of bars in low surface brightness galaxies with cold dark matter haloes. MNRAS 347(1):277–294. https://doi.org/10.1111/j.1365-2966.2004.07202.x. arXiv:astro-ph/0303239 [astro-ph]

Mayer L, Kazantzidis S, Madau P, Colpi M, Quinn T, Wadsley J (2007) Rapid formation of supermassive black hole binaries in galaxy mergers with gas. Science 316(5833):1874. https://doi.org/10.1126/science.1141858. arXiv:0706.1562 [astro-ph]

Mayer L, Kazantzidis S, Escala A, Callegari S (2010) Direct formation of supermassive black holes via multi-scale gas inflows in galaxy mergers. Nature 466(7310):1082–1084. https://doi.org/10.1038/nature09294. arXiv:0912.4262 [astro-ph.CO]

Mayer L, Fiaconni D, Bonoli S, Quinn T, Roškar R, Shen S, Wadsley J (2015) Direct formation of supermassive black holes in metal-enriched gas at the heart of high-redshift galaxy mergers. ApJ 810:51. https://doi.org/10.1088/0004-637X/810/1/51. arXiv:1411.5683

Mazeh T, Shaham J (1979) The orbital evolution of close triple systems: the binary eccentricity. A&A 77:145

McClintock JE, Remillard RA (2006) Black hole binaries. In: Compact stellar X-ray sources. Cambridge astrophysics series. Cambridge University Press, vol 39, pp 157–213. https://doi.org/10.1017/CBO9780511536281.005

McClintock JE, Narayan R, Davis SW, Gou L, Kulkarni A, Orosz JA, Penna RF, Remillard RA, Steiner JF (2011) Measuring the spins of accreting black holes. Class Quantum Grav 28(11):114009. https://doi.org/10.1088/0264-9381/28/11/114009. arXiv:1101.0811 [astro-ph.HE]

McConnell NJ, Ma CP (2013) Revisiting the scaling relations of black hole masses and host Galaxy properties. ApJ 764(2):184. https://doi.org/10.1088/0004-637X/764/2/184. arXiv:1211.2816 [astro-ph.CO]

McConnell NJ, Ma CP, Gebhardt K, Wright SA, Murphy JD, Lauer TR, Graham JR, Richstone DO (2011) Two ten-billion-solar-mass black holes at the centres of giant elliptical galaxies. Nature 480 (7376):215–218. https://doi.org/10.1038/nature10636. arXiv:1112.1078 [astro-ph.CO]

McGee S, Sesana A, Vecchio A (2020) Linking gravitational waves and X-ray phenomena with joint LISA and Athena observations. Nat Astron 4:26–31. https://doi.org/10.1038/s41550-019-0969-7. arXiv:1811.00050 [astro-ph.HE]

McGee SL (2013) The strong environmental dependence of black hole scaling relations. MNRAS 436 (3):2708–2721. https://doi.org/10.1093/mnras/stt1769. arXiv:1302.6237 [astro-ph.CO]

McKernan B, Ford KES (2015) Detection of radial velocity shifts due to black hole binaries near merger. MNRAS 452:L1–L5. https://doi.org/10.1093/mnrasl/slv076. arXiv:1505.04120 [astro-ph.HE]

McKernan B, Ford KES, Lyra W, Perets HB (2012) Intermediate mass black holes in AGN discs—I. Production and growth. MNRAS 425(1):460–469. https://doi.org/10.1111/j.1365-2966.2012.21486.x. arXiv:1206.2309 [astro-ph.GA]

McKernan B, Ford KES, Kocsis B, Haiman Z (2013) Ripple effects and oscillations in the broad Fe Kα line as a probe of massive black hole mergers. MNRAS 432(2):1468–1482. https://doi.org/10.1093/mnras/stt567. arXiv:1303.7206 [astro-ph.HE]

McKernan B, Ford KES, Kocsis B, Lyra W, Winter LM (2014) Intermediate-mass black holes in AGN discs—II. Model predictions and observational constraints. MNRAS 441(1):900–909. https://doi.org/10.1093/mnras/stu553. arXiv:1403.6433 [astro-ph.GA]

McKernan B, Ford KES, Bartos I, Graham MJ, Lyra W, Marka S, Marka Z, Ross NP, Stern D, Yang Y (2019) Ram-pressure stripping of a kicked hill sphere: prompt electromagnetic emission from the merger of stellar mass black holes in an AGN accretion disk. ApJ 884(2):L50. https://doi.org/10.3847/2041-8213/ab4886. arXiv:1907.03746 [astro-ph.HE]

McKernan B, Ford KES, O'Shaughnessy R (2020) Black hole, neutron star, and white dwarf merger rates in AGN discs. MNRAS 498(3):4088–4094. https://doi.org/10.1093/mnras/staa2681. arXiv:2002.00046 [astro-ph.HE]

McKernan B, Ford KES, O'Shaugnessy R, Wysocki D (2020) Monte Carlo simulations of black hole mergers in AGN discs: low χ_{eff} mergers and predictions for LIGO. MNRAS 494(1):1203–1216. https://doi.org/10.1093/mnras/staa740. arXiv:1907.04356 [astro-ph.HE]

McKinney JC, Dai L, Avara MJ (2015) Efficiency of super-Eddington magnetically-arrested accretion. MNRAS 454(1):L6–L10. https://doi.org/10.1093/mnrasl/slv115. arXiv:1508.02433 [astro-ph.HE]

McMillan S, Hut P, Makino J (1991) Star cluster evolution with primordial binaries. II. Detailed analysis. ApJ 372:111. https://doi.org/10.1086/169958

McNeill LO, Mardling RA, Müller B (2020) Gravitational waves from dynamical tides in white-dwarf binaries. MNRAS 491(2):3000–3012. https://doi.org/10.1093/mnras/stz3215. arXiv:1901.09045 [astro-ph.HE]

Mei J, Bai YZ, Bao J, Barausse E, Cai L, Canuto E, Cao B, Chen WM et al (2020) The TianQin project: current progress on science and technology. PTEP 2021:05A107. https://doi.org/10.1093/ptep/ptaa114. arXiv:2008.10332 [gr-qc]

Meiron Y, Kocsis B, Loeb A (2017) Detecting triple systems with gravitational wave observations. ApJ 834(2):200. https://doi.org/10.3847/1538-4357/834/2/200. arXiv:1604.02148 [astro-ph.HE]

Melvin T, Masters K, Lintott C, Nichol RC, Simmons B, Bamford SP, Casteels KRV, Cheung E, Edmondson EM, Fortson L et al (2014) Galaxy Zoo: an independent look at the evolution of the bar

fraction over the last eight billion years from HST-COSMOS. MNRAS 438(4):2882–2897. https://doi.org/10.1093/mnras/stt2397. arXiv:1401.3334 [astro-ph.GA]

Memmesheimer RM, Gopakumar A, Schäfer G (2004) Third post-Newtonian accurate generalized quasi-Keplerian parametrization for compact binaries in eccentric orbits. Phys Rev D 70(10):104011. https://doi.org/10.1103/PhysRevD.70.104011 (**gr-qc/0407049**)

Menci N, Gatti M, Fiore F, Lamastra A (2014) Triggering active galactic nuclei in hierarchical galaxy formation: disk instability vs. interactions. A&A 569:A37. https://doi.org/10.1051/0004-6361/201424217. arXiv:1406.7740 [astro-ph.GA]

Menou K, Haiman Z, Kocsis B (2008) Cosmological physics with black holes (and possibly white dwarfs). New A Rev 51(10–12):884–890. https://doi.org/10.1016/j.newar.2008.03.020. arXiv:0803.3627 [astro-ph]

Merloni A, Heinz S (2008) A synthesis model for AGN evolution: supermassive black holes growth and feedback modes. MNRAS 388(3):1011–1030. https://doi.org/10.1111/j.1365-2966.2008.13472.x. arXiv:0805.2499 [astro-ph]

Merritt D (2001) Brownian motion of a massive binary. ApJ 556(1):245–264. https://doi.org/10.1086/321550. arXiv:astro-ph/0012264 [astro-ph]

Merritt D (2004) Evolution of the dark matter distribution at the galactic center. Phys Rev Lett 92(20):201304. https://doi.org/10.1103/PhysRevLett.92.201304. arXiv:astro-ph/0311594 [astro-ph]

Merritt D (2013) Dynamics and evolution of galactic nuclei. Princeton University Press, Princeton

Merritt D (2015) Gravitational encounters and the evolution of galactic nuclei. I. Method. ApJ 804(1):52. https://doi.org/10.1088/0004-637X/804/1/52. arXiv:1505.07516 [astro-ph.GA]

Merritt D, Milosavljević M (2005) Massive black hole binary evolution. Living Rev Relativ 8:8. https://doi.org/10.12942/lrr-2005-8. arXiv:astro-ph/0410364 [astro-ph]

Merritt D, Poon MY (2004) Chaotic loss cones and black hole fueling. ApJ 606(2):788–798. https://doi.org/10.1086/382497. arXiv:astro-ph/0302296 [astro-ph]

Merritt D, Vasiliev E (2011) Orbits around black holes in triaxial nuclei. ApJ 726(2):61. https://doi.org/10.1088/0004-637X/726/2/61. arXiv:1005.0040 [astro-ph.GA]

Merritt D, Milosavljević M, Verde L, Jimenez R (2002) Dark matter spikes and annihilation radiation from the galactic center. Phys Rev Lett 88(19):191301. https://doi.org/10.1103/PhysRevLett.88.191301. arXiv:astro-ph/0201376 [astro-ph]

Merritt D, Milosavljević M, Favata M, Hughes SA, Holz DE (2004) Consequences of gravitational radiation recoil. ApJ 607(1):L9–L12. https://doi.org/10.1086/421551. arXiv:astro-ph/0402057 [astro-ph]

Merritt D, Alexander T, Mikkola S, Will CM (2011) Stellar dynamics of extreme-mass-ratio inspirals. Phys Rev D 84(4):044024. https://doi.org/10.1103/PhysRevD.84.044024. arXiv:1102.3180 [astro-ph.CO]

Metzger BD (2012) Nuclear-dominated accretion and subluminous supernovae from the merger of a white dwarf with a neutron star or black hole. MNRAS 419(1):827–840. https://doi.org/10.1111/j.1365-2966.2011.19747.x. arXiv:1105.6096 [astro-ph.HE]

Metzger BD (2019) Kilonovae. Living Rev Relativ 23:1. https://doi.org/10.1007/s41114-019-0024-0. arXiv:1910.01617 [astro-ph.HE]

Metzger BD, Stone NC (2016) A bright year for tidal disruptions. MNRAS 461(1):948–966. https://doi.org/10.1093/mnras/stw1394. arXiv:1506.03453 [astro-ph.HE]

Mezcua M (2017) Observational evidence for intermediate-mass black holes. Int J Mod Phys D 26(11):1730021. https://doi.org/10.1142/S021827181730021X. arXiv:1705.09667 [astro-ph.GA]

Mezcua M, Domínguez Sánchez H (2020) Hidden AGNs in dwarf galaxies revealed by MaNGA: light echoes, off-nuclear wanderers, and a new broad-line AGN. ApJ 898(2):L30. https://doi.org/10.3847/2041-8213/aba199. arXiv:2007.08527 [astro-ph.GA]

Mezcua M, Civano F, Fabbiano G, Miyaji T, Marchesi S (2016) A population of intermediate-mass black holes in dwarf starburst galaxies up to redshift=1.5. ApJ 817(1):20. https://doi.org/10.3847/0004-637X/817/1/20. arXiv:1511.05844 [astro-ph.GA]

Mezcua M, Civano F, Marchesi S, Suh H, Fabbiano G, Volonteri M (2018) Intermediate-mass black holes in dwarf galaxies out to redshift ~ 2.4 in the Chandra COSMOS-Legacy Survey. MNRAS 478(2):2576–2591. https://doi.org/10.1093/mnras/sty1163. arXiv:1802.01567 [astro-ph.GA]

Michaely E, Perets HB (2014) Secular dynamics in hierarchical three-body systems with mass loss and mass transfer. ApJ 794(2):122. https://doi.org/10.1088/0004-637X/794/2/122. arXiv:1406.3035 [astro-ph.SR]

Mikkola S (1983) Encounters of binaries. I—equal energies. MNRAS 203:1107–1121. https://doi.org/10.1093/mnras/203.4.1107

Mikkola S (1984) Encounters of binaries. II—unequal energies. MNRAS 207:115–126. https://doi.org/10.1093/mnras/207.1.115

Mikkola S, Valtonen MJ (1990) The slingshot ejections in merging galaxies. ApJ 348:412. https://doi.org/10.1086/168250

Mikkola S, Valtonen MJ (1992) Evolution of binaries in the field of light particles and the problem of two black holes. MNRAS 259(1):115–120. https://doi.org/10.1093/mnras/259.1.115

Miller J, Wardell B, Pound A (2016) Second-order perturbation theory: the problem of infinite mode coupling. Phys Rev D 94(10):104018. https://doi.org/10.1103/PhysRevD.94.104018. arXiv:1608.06783 [gr-qc]

Miller JM (2007) Relativistic X-ray lines from the inner accretion disks around black holes. ARA&A 45(1):441–479. https://doi.org/10.1146/annurev.astro.45.051806.110555. arXiv:0705.0540 [astro-ph]

Miller MC (2005) Probing general relativity with mergers of supermassive and intermediate-mass black holes. ApJ 618(1):426–431. https://doi.org/10.1086/425910. arXiv:astro-ph/0409331 [astro-ph]

Miller MC, Colbert EJM (2004) Intermediate-mass black holes. Int J Mod Phys D 13:1–64. https://doi.org/10.1142/S0218271804004426. arXiv:astro-ph/0308402

Miller MC, Davies MB (2012) An upper limit to the velocity dispersion of relaxed stellar systems without massive black holes. ApJ 755(1):81. https://doi.org/10.1088/0004-637X/755/1/81. arXiv:1206.6167 [astro-ph.GA]

Miller MC, Hamilton DP (2002) Four-body effects in globular cluster black hole coalescence. ApJ 576(2):894–898. https://doi.org/10.1086/341788. arXiv:astro-ph/0202298 [astro-ph]

Miller MC, Hamilton DP (2002) Production of intermediate-mass black holes in globular clusters. MNRAS 330(1):232–240. https://doi.org/10.1046/j.1365-8711.2002.05112.x. arXiv:astro-ph/0106188 [astro-ph]

Miller MC, Krolik JH (2013) Alignment of supermassive black hole binary orbits and spins. ApJ 774(1):43. https://doi.org/10.1088/0004-637X/774/1/43. arXiv:1307.6569 [astro-ph.HE]

Miller MC, Lauburg VM (2009) Mergers of stellar-mass black holes in nuclear star clusters. ApJ 692(1):917–923. https://doi.org/10.1088/0004-637X/692/1/917. arXiv:0804.2783 [astro-ph]

Miller MC, Freitag M, Hamilton DP, Lauburg VM (2005) Binary encounters with supermassive black holes: zero-eccentricity LISA events. ApJ 631(2):L117–L120. https://doi.org/10.1086/497335. arXiv:astro-ph/0507133 [astro-ph]

Miller MC, Lamb FK, Dittmann AJ, Bogdanov S, Arzoumanian Z, Gendreau KC, Guillot S, Harding AK, Ho WCG, Lattimer JM et al (2019) PSR J0030+0451 mass and radius from NICER data and implications for the properties of neutron star matter. ApJ 887(1):L24. https://doi.org/10.3847/2041-8213/ab50c5. arXiv:1912.05705 [astro-ph.HE]

Miller-Jones JCA, Strader J, Heinke CO, Maccarone TJ, van den Berg M, Knigge C, Chomiuk L, Noyola E, Russell TD, Seth AC et al (2015) Deep radio imaging of 47 Tuc identifies the peculiar X-ray source X9 as a new black hole candidate. MNRAS 453(4):3918–3931. https://doi.org/10.1093/mnras/stv1869. arXiv:1509.02579 [astro-ph.HE]

Miller-Jones JCA, Bahramian A, Orosz JA, Mandel I, Gou L, Maccarone TJ, Neijssel CJ, Zhao X, Ziółkowski J, Reid MJ et al (2021) Cygnus X-1 contains a 21-solar mass black hole—implications for massive star winds. Science 371(6533):1046–1049. https://doi.org/10.1126/science.abb3363. arXiv:2102.09091 [astro-ph.HE]

Milosavljević M, Merritt D (2001) Formation of galactic nuclei. ApJ 563(1):34–62. https://doi.org/10.1086/323830. arXiv:astro-ph/0103350 [astro-ph]

Milosavljević M, Merritt D (2003) Long-term evolution of massive black hole binaries. ApJ 596(2):860–878. https://doi.org/10.1086/378086. arXiv:astro-ph/0212459 [astro-ph]

Milosavljević M, Phinney ES (2005) The afterglow of massive black hole coalescence. ApJ 622(2):L93–L96. https://doi.org/10.1086/429618. arXiv:astro-ph/0410343 [astro-ph]

Mingarelli CMF, Lazio TJW, Sesana A, Greene JE, Ellis JA, Ma CP, Croft S, Burke-Spolaor S, Taylor SR (2017) The local nanohertz gravitational-wave landscape from supermassive black hole binaries. Nat Astron 1:886–892. https://doi.org/10.1038/s41550-017-0299-6. arXiv:1708.03491 [astro-ph.GA]

Mirabel F (2017) The formation of stellar black holes. New A Rev 78:1–15. https://doi.org/10.1016/j.newar.2017.04.002

Miralda-Escudé J, Kollmeier JA (2005) Star captures by quasar accretion disks: a possible explanation of the M-σ relation. ApJ 619(1):30–40. https://doi.org/10.1086/426467. arXiv:astro-ph/0310717 [astro-ph]

Mirza MA, Tahir A, Khan FM, Holley-Bockelmann H, Baig AM, Berczik P, Chishtie F (2017) Galaxy rotation and supermassive black hole binary evolution. MNRAS 470(1):940–947. https://doi.org/10.1093/mnras/stx1248. arXiv:1704.03490 [astro-ph.GA]

Misra D, Fragos T, Tauris TM, Zapartas E, Aguilera-Dena DR (2020) The origin of pulsating ultraluminous X-ray sources: low- and intermediate-mass X-ray binaries containing neutron star accretors. A&A 642:A174. https://doi.org/10.1051/0004-6361/202038070. arXiv:2004.01205 [astro-ph.HE]

Montuori C, Dotti M, Colpi M, Decarli R, Haardt F (2011) Search for sub-parsec massive binary black holes through line diagnosis. MNRAS 412(1):26–32. https://doi.org/10.1111/j.1365-2966.2010.17888.x. arXiv:1010.4303 [astro-ph.CO]

Montuori C, Dotti M, Haardt F, Colpi M, Decarli R (2012) Search for sub-parsec massive binary black holes through line diagnosis—II. MNRAS 425(3):1633–1639. https://doi.org/10.1111/j.1365-2966.2012.21530.x. arXiv:1207.0813 [astro-ph.CO]

Moody MSL, Shi JM, Stone JM (2019) Hydrodynamic torques in circumbinary accretion disks. ApJ 875(1):66. https://doi.org/10.3847/1538-4357/ab09ee. arXiv:1903.00008 [astro-ph.HE]

Moore B (1994) Evidence against dissipation-less dark matter from observations of galaxy haloes. Nature 370(6491):629–631. https://doi.org/10.1038/370629a0

Moore CJ, Cole RH, Berry CPL (2015) Gravitational-wave sensitivity curves. Class Quantum Grav 32(1):015014. https://doi.org/10.1088/0264-9381/32/1/015014. arXiv:1408.0740 [gr-qc]

Moore CJ, Mihaylov DP, Lasenby A, Gilmore G (2017) Astrometric search method for individually resolvable gravitational wave sources with Gaia. Phys Rev Lett 119(26):261102. https://doi.org/10.1103/PhysRevLett.119.261102. arXiv:1707.06239 [astro-ph.IM]

Moore CJ, Gerosa D, Klein A (2019) Are stellar-mass black-hole binaries too quiet for LISA? MNRAS 488(1):L94–L98. https://doi.org/10.1093/mnrasl/slz104. arXiv:1905.11998 [astro-ph.HE]

Moran EC, Shahinyan K, Sugarman HR, Vélez DO, Eracleous M (2014) Black holes at the centers of nearby dwarf galaxies. AJ 148(6):136. https://doi.org/10.1088/0004-6256/148/6/136. arXiv:1408.4451 [astro-ph.GA]

Morawski J, Giersz M, Askar A, Belczynski K (2018) MOCCA-SURVEY Database I: assessing GW kick retention fractions for BH-BH mergers in globular clusters. MNRAS 481(2):2168–2179. https://doi.org/10.1093/mnras/sty2401. arXiv:1802.01192 [astro-ph.GA]

Morris M (1993) Massive star formation near the galactic center and the fate of the stellar remnants. ApJ 408:496. https://doi.org/10.1086/172607

Morscher M, Umbreit S, Farr WM, Rasio FA (2013) Retention of Stellar-mass black holes in globular clusters. ApJ 763(1):L15. https://doi.org/10.1088/2041-8205/763/1/L15. arXiv:1211.3372 [astro-ph.GA]

Morscher M, Pattabiraman B, Rodriguez C, Rasio FA, Umbreit S (2015) The dynamical evolution of stellar black holes in globular clusters. ApJ 800(1):9. https://doi.org/10.1088/0004-637X/800/1/9. arXiv:1409.0866 [astro-ph.GA]

Mortlock DJ, Warren SJ, Venemans BP, Patel M, Hewett PC, McMahon RG, Simpson C, Theuns T, Gonzáles-Solares EA, Adamson A et al (2011) A luminous quasar at a redshift of z = 7.085. Nature 474(7353):616–619. https://doi.org/10.1038/nature10159. arXiv:1106.6088 [astro-ph.CO]

Mösta P et al (2010) Vacuum electromagnetic counterparts of binary black-hole mergers. Phys Rev D 81:064017. https://doi.org/10.1103/PhysRevD.81.064017

Mösta P et al (2012) On the detectability of dual jets from binary black holes. ApJ 749(2):L32. https://doi.org/10.1088/2041-8205/749/2/l32

Motl PM, Frank J, Tohline JE, D'Souza MCR (2007) The stability of double white dwarf binaries undergoing direct-impact accretion. ApJ 670(2):1314–1325. https://doi.org/10.1086/522076. arXiv:astro-ph/0702388 [astro-ph]

Moxon J, Flanagan É (2018) Radiation-reaction force on a small charged body to second order. Phys Rev D 97(10):105001. https://doi.org/10.1103/PhysRevD.97.105001. arXiv:1711.05212 [gr-qc]

Muñoz DJ, Miranda R, Lai D (2019) Hydrodynamics of circumbinary accretion: angular momentum transfer and binary orbital evolution. ApJ 871(1):84. https://doi.org/10.3847/1538-4357/aaf867. arXiv:1810.04676 [astro-ph.HE]

Muñoz DJ, Lai D, Kratter K, Mirand AR (2020) Circumbinary accretion from finite and infinite disks. ApJ 889(2):114. https://doi.org/10.3847/1538-4357/ab5d33. arXiv:1910.04763 [astro-ph.HE]

Müller B, Tauris TM, Heger A, Banerjee P, Qian YZ, Powell J, Chan C, Gay DW, Langer N (2019) Three-dimensional simulations of neutrino-driven core-collapse supernovae from low-mass single and binary star progenitors. MNRAS 484(3):3307–3324. https://doi.org/10.1093/mnras/stz216. arXiv:1811.05483 [astro-ph.SR]

Munna C (2020) Analytic post-Newtonian expansion of the energy and angular momentum radiated to infinity by eccentric-orbit nonspinning extreme-mass-ratio inspirals to the 19th order. Phys Rev D 102(12):124001. https://doi.org/10.1103/PhysRevD.102.124001. arXiv:2008.10622 [gr-qc]

Muratov AL, Gnedin OY (2010) Modeling the metallicity distribution of globular clusters. ApJ 718 (2):1266–1288. https://doi.org/10.1088/0004-637X/718/2/1266. arXiv:1002.1325 [astro-ph.GA]

Murguia-Berthier A, Batta A, Janiuk A, Ramirez-Ruiz E, Mandel I, Noble SC, Everson RW (2020) On the maximum stellar rotation to form a black hole without an accompanying luminous transient. ApJ 901 (2):L24. https://doi.org/10.3847/2041-8213/abb818. arXiv:2005.10212 [astro-ph.HE]

Murphy EJ, Bolatto A, Chatterjee S, Casey CM, Chomiuk L, Dale D, de Pater I, Dickinson M, Francesco JD, Hallinan G et al (2018) The ngVLA science case and associated science requirements. In: Murphy E (ed) Science with a next generation very large array. Astronomical society of the pacific conference series, vol 517, p 3. arXiv:1810.07524 [astro-ph.IM]

Murray CD, Dermott SF (1999) Solar system dynamics. Cambridge University Press, Cambridge

Mushotzky R (2018) AXIS: a probe class next generation high angular resolution x-ray imaging satellite. In: Space telescopes and instrumentation 2018: ultraviolet to gamma ray. Society of photo-optical instrumentation engineers (SPIE) conference series, vol 10699, p 1069929. https://doi.org/10.1117/12.2310003. arXiv:1807.02122 [astro-ph.HE]

Mushotzky R, Aird J, Barger AJ, Cappelluti N, Chartas G, Corrales L, Eufrasio R, Fabian AC, Falcone AD, Gallo E et al (2019) The advanced X-ray imaging satellite. In: Bulletin of the American astronomical society, vol 51, p 107. arXiv:1903.04083 [astro-ph.HE]

Nakama T, Suyama T, Yokoyama J (2016) Supermassive black holes formed by direct collapse of inflationary perturbations. Phys Rev D 94(10):103522. https://doi.org/10.1103/PhysRevD.94.103522. arXiv:1609.02245 [gr-qc]

Nakama T, Carr B, Silk J (2018) Limits on primordial black holes from μ distortions in cosmic microwave background. Phys Rev D 97(4):043525. https://doi.org/10.1103/PhysRevD.97.043525. arXiv:1710.06945 [astro-ph.CO]

Nandez JLA, Ivanova N (2016) Common envelope events with low-mass giants: understanding the energy budget. MNRAS 460(4):3992–4002. https://doi.org/10.1093/mnras/stw1266. arXiv:1606.04922 [astro-ph.SR]

Nandez JLA, Ivanova N, Lombardi JCJ (2015) Recombination energy in double white dwarf formation. MNRAS 450:L39–L43. https://doi.org/10.1093/mnrasl/slv043. arXiv:1503.02750 [astro-ph.SR]

Nandra K, George IM, Mushotzky RF, Turner TJ, Yaqoob T (1997) ASCA observations of Seyfert 1 galaxies. II. Relativistic iron Kα emission. ApJ 477(2):602–622. https://doi.org/10.1086/303721. arXiv:astro-ph/9606169 [astro-ph]

Nandra K, Barret D, Barcons X, Fabian A, den Herder JW, Piro L, Watson M, Adami C, Aird J, Afonso JM,et al (2013) The hot and energetic universe: a white paper presenting the science theme motivating the Athena+ mission. arXiv e-prints arXiv:1306.2307 [astro-ph.HE]

Naoz S (2016) The eccentric Kozai–Lidov effect and its applications. ARA&A 54:441–489. https://doi.org/10.1146/annurev-astro-081915-023315. arXiv:1601.07175 [astro-ph.EP]

Naoz S, Will CM, Ramirez-Ruiz E, Hees A, Ghez AM, Do T (2020) A hidden friend for the galactic center black hole, Sgr A*. ApJ 888(1):L8. https://doi.org/10.3847/2041-8213/ab5e3b. arXiv:1912.04910 [astro-ph.GA]

Napiwotzki R, Karl CA, Lisker T, Catalán S, Drechsel H, Heber U, Homeier D, Koester D, Leibundgut B, Marsh TR et al (2020) The ESO supernovae type Ia progenitor survey (SPY). The radial velocities of 643 DA white dwarfs. A&A 638:A131. https://doi.org/10.1051/0004-6361/201629648. arXiv:1906.10977 [astro-ph.SR]

Narayan R, Yi I (1994) Advection-dominated accretion: a self-similar solution. ApJ 428:L13. https://doi.org/10.1086/187381. arXiv:astro-ph/9403052 [astro-ph]

Narayan R, Paczynski B, Piran T (1992) Gamma-ray bursts as the death throes of massive binary stars. ApJ 395:L83. https://doi.org/10.1086/186493. arXiv:astro-ph/9204001 [astro-ph]

Natarajan P (2021) A new channel to form IMBHs throughout cosmic time. MNRAS 501(1):1413–1425. https://doi.org/10.1093/mnras/staa3724. arXiv:2009.09156 [astro-ph.GA]

Natarajan P, Pacucci F, Ferrara A, Agarwal B, Ricarte A, Zackrisson E, Cappelluti N (2017) Unveiling the first black holes with JWST: multi-wavelength spectral predictions. ApJ 838(2):117. https://doi.org/10.3847/1538-4357/aa6330. arXiv:1610.05312 [astro-ph.GA]

Nayakshin S, Cuadra J, Springel V (2007) Simulations of star formation in a gaseous disc around Sgr A*—a failed active galactic nucleus. MNRAS 379(1):21–33. https://doi.org/10.1111/j.1365-2966.2007.11938.x. arXiv:astro-ph/0701141 [astro-ph]

Negri A, Volonteri M (2017) Black hole feeding and feedback: the physics inside the 'sub-grid'. MNRAS 467(3):3475–3492. https://doi.org/10.1093/mnras/stx362. arXiv:1610.04753 [astro-ph.GA]

Neijssel CJ, Vigna-Gómez A, Stevenson S, Barrett JW, Gaebel SM, Broekgaarden FS, de Mink SE, Szécsi D, Vinciguerra S, Mandel I (2019) The effect of the metallicity-specific star formation history on double compact object mergers. MNRAS 490(3):3740–3759. https://doi.org/10.1093/mnras/stz2840. arXiv:1906.08136 [astro-ph.SR]

Nelemans G, Tauris TM (1998) Formation of undermassive single white dwarfs and the influence of planets on late stellar evolution. A&A 335:L85–L88 arXiv:astro-ph/9806011 [astro-ph]

Nelemans G, Verbunt F, Yungelson LR, Portegies Zwart SF (2000) Reconstructing the evolution of double helium white dwarfs: envelope loss without spiral-in. A&A 360:1011–1018 arXiv:astro-ph/0006216 [astro-ph]

Nelemans G, Portegies Zwart SF, Verbunt F, Yungelson LR (2001) Population synthesis for double white dwarfs. II. Semi-detached systems: AM CVn stars. A&A 368:939–949. https://doi.org/10.1051/0004-6361:20010049. arXiv:astro-ph/0101123 [astro-ph]

Nelemans G, Yungelson LR, Portegies Zwart SF (2001) The gravitational wave signal from the Galactic disk population of binaries containing two compact objects. A&A 375:890–898. https://doi.org/10.1051/0004-6361:20010683. arXiv:astro-ph/0105221 [astro-ph]

Nelemans G, Yungelson LR, Portegies Zwart SF, Verbunt F (2001) Population synthesis for double white dwarfs. I. Close detached systems. A&A 365:491–507. https://doi.org/10.1051/0004-6361:20000147. arXiv:astro-ph/0010457 [astro-ph]

Nelemans G, Jonker PG, Marsh TR, van der Klis M (2004) Optical spectra of the carbon-oxygen accretion discs in the ultra-compact X-ray binaries 4U 0614+09, 4U 1543–624 and 2S 0918–549. MNRAS 348(1):L7–L11. https://doi.org/10.1111/j.1365-2966.2004.07486.x. arXiv:astro-ph/0312008 [astro-ph]

Nelemans G, Yungelson LR, Portegies Zwart SF (2004) Short-period AM CVn systems as optical, X-ray and gravitational-wave sources. MNRAS 349(1):181–192. https://doi.org/10.1111/j.1365-2966.2004.07479.x. arXiv:astro-ph/0312193 [astro-ph]

Nelemans G, Napiwotzki R, Karl C, Marsh TR, Voss B, Roelofs G, Izzard RG, Montgomery M, Reerink T, Christlieb N et al (2005) Binaries discovered by the SPYproject. IV. Five single-lined DA double white dwarfs. A&A 440(3):1087–1095. https://doi.org/10.1051/0004-6361:20053174. arXiv:astro-ph/0506231 [astro-ph]

Nelemans G, Jonker PG, Steeghs D (2006) Optical spectroscopy of (candidate) ultracompact X-ray binaries: constraints on the composition of the donor stars. MNRAS 370(1):255–262. https://doi.org/10.1111/j.1365-2966.2006.10496.x. arXiv:astro-ph/0604597 [astro-ph]

Nelemans G, Yungelson LR, van der Sluys MV, Tout CA (2010) The chemical composition of donors in AM CVn stars and ultracompact X-ray binaries: observational tests of their formation. MNRAS 401(2):1347–1359. https://doi.org/10.1111/j.1365-2966.2009.15731.x. arXiv:0909.3376 [astro-ph.SR]

Nelson LA, Rappaport SA, Joss PC (1986) The evolution of ultrashort period binary systems. ApJ 304:231. https://doi.org/10.1086/164156

Neumayer N, Seth A, Böker T (2020) Nuclear star clusters. A&A Rev 28(1):4. https://doi.org/10.1007/s00159-020-00125-0. arXiv:2001.03626 [astro-ph.GA]

Nevin R, Blecha L, Comerford J, Greene J (2019) Accurate identification of galaxy mergers with imaging. ApJ 872(1):76. https://doi.org/10.3847/1538-4357/aafd34. arXiv:1901.01975 [astro-ph.GA]

Nguyen K, Bogdanović T (2016) Emission signatures from sub-parsec binary supermassive black holes. I. Diagnostic power of broad emission lines. ApJ 828(2):68. https://doi.org/10.3847/0004-637X/828/2/68. arXiv:1605.09389 [astro-ph.HE]

Nguyen K, Bogdanović T, Runnoe JC, Eracleous M, Sigurdsson S, Boroson T (2019) Emission signatures from sub-parsec binary supermassive black holes. II. Effect of accretion disk wind on broad emission lines. ApJ 870(1):16. https://doi.org/10.3847/1538-4357/aaeff0. arXiv:1807.09782 [astro-ph.HE]

Nguyen K, Bogdanović T, Runnoe JC, Eracleous M, Sigurdsson S, Boroson T (2020) Emission signatures from subparsec binary supermassive black holes. III. Comparison of models with observations. ApJ 894(2):105. https://doi.org/10.3847/1538-4357/ab88b5. arXiv:1908.01799 [astro-ph.HE]

Nishizawa A, Berti E, Klein A, Sesana A (2016) eLISA eccentricity measurements as tracers of binary black hole formation. Phys Rev D 94(6):064020. https://doi.org/10.1103/PhysRevD.94.064020. arXiv:1605.01341 [gr-qc]

Nishizawa A, Sesana A, Berti E, Klein A (2017) Constraining stellar binary black hole formation scenarios with eLISA eccentricity measurements. MNRAS 465(4):4375–4380. https://doi.org/10.1093/mnras/stw2993. arXiv:1606.09295 [astro-ph.HE]

Nissanke S, Vallisneri M, Nelemans G, Prince TA (2012) Gravitational-wave emission from compact galactic binaries. ApJ 758(2):131. https://doi.org/10.1088/0004-637X/758/2/131. arXiv:1201.4613 [astro-ph.GA]

Nitadori K, Aarseth SJ (2012) Accelerating NBODY6 with graphics processing units. MNRAS 424 (1):545–552. https://doi.org/10.1111/j.1365-2966.2012.21227.x. arXiv:1205.1222 [astro-ph.IM]

Noble SC, Mundim BC, Nakano H, Krolik JH, Campanelli M, Zlochower Y, Yunes N (2012) Circumbinary magnetohydrodynamic accretion into inspiraling binary black holes. ApJ 755(1):51. https://doi.org/10.1088/0004-637X/755/1/51. arXiv:1204.1073 [astro-ph.HE]

Nomoto K, Saio H, Kato M, Hachisu I (2007) Thermal stability of white dwarfs accreting hydrogen-rich matter and progenitors of type Ia supernovae. ApJ 663(2):1269–1276. https://doi.org/10.1086/518465. arXiv:astro-ph/0603351 [astro-ph]

Noutsos A, Kramer M, Carr P, Johnston S (2012) Pulsar spin-velocity alignment: further results and discussion. MNRAS 423(3):2736–2752. https://doi.org/10.1111/j.1365-2966.2012.21083.x. arXiv:1205.2305 [astro-ph.GA]

Novikov ID, Thorne KS (1973) Astrophysics of black holes. In: Black holes (Les Astres Occlus), pp 343–450

Obergaulinger M, Aloy MÁ (2020) Magnetorotational core collapse of possible GRB progenitors—I. Explosion mechanisms. MNRAS 492(4):4613–4634. https://doi.org/10.1093/mnras/staa096. arXiv:1909.01105 [astro-ph.HE]

Oesch P, Bouwens R, Brammer G, Chisholm J, Fudamoto Y, Illingworth GD, Kerutt J, Labbe I, Magee DK, Marchesini D et al (2021) FRESCO: the first reionization epoch spectroscopic complete survey. JWST proposal. Cycle 1, ID. #1895

Ogilvie GI (2013) Tides in rotating barotropic fluid bodies: the contribution of inertial waves and the role of internal structure. MNRAS 429(1):613–632. https://doi.org/10.1093/mnras/sts362. arXiv:1211.0837 [astro-ph.EP]

Ogilvie GI (2014) Tidal dissipation in stars and giant planets. ARA&A 52:171–210. https://doi.org/10.1146/annurev-astro-081913-035941. arXiv:1406.2207 [astro-ph.SR]

Ogiya G, Hahn O, Mingarelli CMF, Volonteri M (2020) Accelerated orbital decay of supermassive black hole binaries in merging nuclear star clusters. MNRAS 493(3):3676–3689. https://doi.org/10.1093/mnras/staa444. arXiv:1911.11526 [astro-ph.GA]

SH Oh, Hunter DA, Brinks E, Elmegreen BG, Schruba A, Walter F, Rupen MP, Young LM, Simpson CE, Johnson MC et al (2015) High-resolution mass models of dwarf galaxies from LITTLE THINGS. AJ 149(6):180. https://doi.org/10.1088/0004-6256/149/6/180. arXiv:1502.01281 [astro-ph.GA]

Oh SP, Haiman Z (2003) Fossil H II regions: self-limiting star formation at high redshift. MNRAS 346 (2):456–472. https://doi.org/10.1046/j.1365-2966.2003.07103.x. arXiv:astro-ph/0307135 [astro-ph]

Ohlmann ST (2016) Hydrodynamics of the common envelope phase in binary stellar evolution. PhD thesis

Ohlmann ST, Röpke FK, Pakmor R, Springel V (2016) Hydrodynamic moving-mesh simulations of the common envelope phase in binary stellar systems. ApJ 816(1):L9. https://doi.org/10.3847/2041-8205/816/1/L9. arXiv:1512.04529 [astro-ph.SR]

Ohlmann ST, Röpke FK, Pakmor R, Springel V, Müller E (2016) Magnetic field amplification during the common envelope phase. MNRAS 462(1):L121–L125. https://doi.org/10.1093/mnrasl/slw144. arXiv:1607.05996 [astro-ph.SR]

Oka T, Tsujimoto S, Iwata Y, Nomura M, Takekawa S (2017) Millimetre-wave emission from an intermediate-mass black hole candidate in the Milky Way. Nat Astron 1:709–712. https://doi.org/10.1038/s41550-017-0224-z. arXiv:1707.07603 [astro-ph.GA]

O'Leary JA, Moster BP, Naab T, Somerville RS (2021) EMERGE: empirical predictions of galaxy merger rates since z ∼ 6. MNRAS 501(3):3215–3237. https://doi.org/10.1093/mnras/staa3746. arXiv:2001.02687

Omukai K, Si Inutsuka (2002) An upper limit on the mass of a primordial star due to the formation of an Hii region: the effect of ionizing radiation force. MNRAS 332(1):59–64. https://doi.org/10.1046/j.1365-8711.2002.05276.x. arXiv:astro-ph/0112345 [astro-ph]

Omukai K, Palla F (2003) Formation of the first stars by accretion. ApJ 589(2):677–687. https://doi.org/10.1086/374810. arXiv:astro-ph/0302345 [astro-ph]

Omukai K, Schneider R, Haiman Z (2008) Can supermassive black holes form in metal-enriched high-redshift protogalaxies? ApJ 686(2):801–814. https://doi.org/10.1086/591636. arXiv:0804.3141 [astro-ph]

O'Shaughnessy R, Bellovary JM, Brooks A, Shen S, Governato F, Christensen CR (2017) The effects of host galaxy properties on merging compact binaries detectable by LIGO. MNRAS 464(3):2831–2839. https://doi.org/10.1093/mnras/stw2550. arXiv:1609.06715 [astro-ph.GA]

O'Shea BW, Wise JH, Xu H, Norman ML (2015) Probing the ultraviolet luminosity function of the earliest galaxies with the renaissance simulations. ApJ 807:L12. https://doi.org/10.1088/2041-8205/807/1/L12. arXiv:1503.01110

Ossokine S, Buonanno A, Marsat S, Cotesta R, Babak S, Dietrich T, Haas R, Hinder I, Pfeiffer HP, Pürrer M et al (2020) Multipolar effective-one-body waveforms for precessing binary black holes: construction and validation. Phys Rev D 102(4):044055. https://doi.org/10.1103/PhysRevD.102.044055. arXiv:2004.09442 [gr-qc]

Ostriker EC (1999) Dynamical friction in a gaseous medium. ApJ 513(1):252–258. https://doi.org/10.1086/306858. arXiv:astro-ph/9810324 [astro-ph]

Owen BJ (1996) Search templates for gravitational waves from inspiraling binaries: choice of template spacing. Phys Rev D 53(12):6749–6761. https://doi.org/10.1103/PhysRevD.53.6749. arXiv:gr-qc/9511032 [gr-qc]

Özel F, Freire P (2016) Masses, radii, and the equation of state of neutron stars. ARA&A 54:401–440. https://doi.org/10.1146/annurev-astro-081915-023322. arXiv:1603.02698 [astro-ph.HE]

Pacucci F, Loeb A (2020) Separating accretion and mergers in the cosmic growth of black holes with X-ray and gravitational-wave observations. ApJ 895(2):95. https://doi.org/10.3847/1538-4357/ab886e. arXiv:2004.07246 [astro-ph.GA]

Pacucci F, Ferrara A, Volonteri M, Dubus G (2015) Shining in the dark: the spectral evolution of the first black holes. MNRAS 454(4):3771–3777. https://doi.org/10.1093/mnras/stv2196. arXiv:1506.05299 [astro-ph.HE]

Pacucci F, Natarajan P, Volonteri M, Cappelluti N, Urry CM (2017) Conditions for optimal growth of black hole seeds. ApJ 850(2):L42. https://doi.org/10.3847/2041-8213/aa9aea. arXiv:1710.09375 [astro-ph.GA]

Pacucci F, Loeb A, Mezcua M, Martín-Navarro I (2018) Glimmering in the dark: modeling the low-mass end of the $M_\bullet$-σ relation and of the quasar luminosity function. ApJ 864(1):L6. https://doi.org/10.3847/2041-8213/aad8b2. arXiv:1808.09452 [astro-ph.GA]

Paczyński B (1967) Gravitational waves and the evolution of close binaries. Acta Astron 17:287

Paczynski B (1976) Common envelope binaries. In: Eggleton P, Mitton S, Whelan J (eds) Structure and evolution of close binary systems. IAUS, vol 73, p 75

Paczynski B (1986) Gamma-ray bursters at cosmological distances. ApJ 308:L43–L46. https://doi.org/10.1086/184740

Paczyński B, Sienkiewicz R (1972) Evolution of close binaries VIII. Mass exchange on the dynamical time scale. Acta Astron 22:73–91

Padmanabhan H, Loeb A (2020) Constraining the host galaxy halos of massive black holes from LISA event rates. J Cosmol Astropart Phys 11:055. https://doi.org/10.1088/1475-7516/2020/11/055. arXiv:2007.12710 [astro-ph.CO]

Pakmor R, Kromer M, Röpke FK, Sim SA, Ruiter AJ, Hillebrandt W (2010) Sub-luminous type Ia supernovae from the mergers of equal-mass white dwarfs with mass $\sim 0.9 M_{solar}$. Nature 463(7277):61–64. https://doi.org/10.1038/nature08642. arXiv:0911.0926 [astro-ph.HE]

Pakmor R, Kromer M, Taubenberger S, Sim SA, Röpke FK, Hillebrandt W (2012) Normal type Ia supernovae from violent mergers of white dwarf binaries. ApJ 747(1):L10. https://doi.org/10.1088/2041-8205/747/1/L10. arXiv:1201.5123 [astro-ph.HE]

Pala AF, Schmidtobreick L, Tappert C, Gänsicke BT, Mehner A (2018) The cataclysmic variable QZ Lib: a period bouncer. MNRAS 481(2):2523–2535. https://doi.org/10.1093/mnras/sty2434. arXiv:1809.02135 [astro-ph.SR]

Palenzuela C, Garrett T, Lehner L, Liebling SL (2010) Magnetospheres of black hole systems in force-free plasma. Phys Rev D 82:044045. https://doi.org/10.1103/PhysRevD.82.044045

Palenzuela C, Lehner L, Yoshida S (2010) Understanding possible electromagnetic counterparts to loud gravitational wave events: Binary black hole effects on electromagnetic fields. Phys Rev D 81:084007. https://doi.org/10.1103/PhysRevD.81.084007

Palenzuela C et al (2009) Binary black holes' effects on electromagnetic fields. Phys Rev Lett 103:081101. https://doi.org/10.1103/PhysRevLett.103.081101

Palenzuela C et al (2010) Dual jets from binary black holes. Science 329:927–930. https://doi.org/10.1126/science.1191766

Panamarev T, Shukirgaliyev B, Meiron Y (2018) Star–disc interaction in galactic nuclei: formation of a central stellar disc. MNRAS

Panamarev T, Just A, Spurzem R, Berczik P, Wang L, Arca Sedda M (2019) Direct N-body simulation of the Galactic centre. MNRAS 484(3):3279–3290. https://doi.org/10.1093/mnras/stz208. arXiv:1805.02153 [astro-ph.GA]

Papadopoulos GO, Kokkotas KD (2018) Preserving Kerr symmetries in deformed spacetimes. Class Quantum Grav 35(18):185014. https://doi.org/10.1088/1361-6382/aad7f4. arXiv:1807.08594 [gr-qc]

Paragi Z, Godfrey L, Reynolds C, Rioja MJ, Deller A, Zhang B, Gurvits L, Bietenholz M, Szomoru A, Bignall HE et al (2015) Very long baseline interferometry with the SKA. In: Advancing astrophysics with the square kilometre array (AASKA14), p 143. arXiv:1412.5971 [astro-ph.IM]

Pardo K, Goulding AD, Greene JE, Somerville RS, Gallo E, Hickox RC, Miller BP, Reines AE, Silverman JD (2016) X-ray detected active galactic nuclei in dwarf galaxies at $0 < z < 1$. ApJ 831(2):203. https://doi.org/10.3847/0004-637X/831/2/203. arXiv:1603.01622 [astro-ph.GA]

Park K, Bogdanović T (2017) Gaseous dynamical friction in presence of black hole radiative feedback. ApJ 838(2):103. https://doi.org/10.3847/1538-4357/aa65ce. arXiv:1701.00526 [astro-ph.GA]

Park K, Bogdanović T (2019) Erratum: "Gaseous dynamical friction in presence of black hole radiative feedback". ApJ 883(2):209. https://doi.org/10.3847/1538-4357/ab3f30

Paschalidis V, Stergioulas N (2017) Rotating stars in relativity. Living Rev Relativ 20:7. https://doi.org/10.1007/s41114-017-0008-x. arXiv:1612.03050 [astro-ph.HE]

Paschalidis V, MacLeod M, Baumgarte TW, Shapiro SL (2009) Merger of white dwarf-neutron star binaries: prelude to hydrodynamic simulations in general relativity. Phys Rev D 80(2):024006. https://doi.org/10.1103/PhysRevD.80.024006. arXiv:0910.5719 [astro-ph.HE]

Paschalidis V, Bright J, Ruiz M, Gold R (2021) Minidisk dynamics in accreting, spinning black hole binaries: simulations in full general relativity. ApJL 910:L26. https://doi.org/10.3847/2041-8213/abee21. arXiv:2102.06712 [astro-ph.HE]

Passy JC, De Marco O, Fryer CL, Herwig F, Diehl S, Oishi JS, Mac Low MM, Bryan GL, Rockefeller G (2012) Simulating the common envelope phase of a red giant using smoothed-particle hydrodynamics and uniform-grid codes. ApJ 744(1):52. https://doi.org/10.1088/0004-637X/744/1/52. arXiv:1107.5072 [astro-ph.SR]

Passy JC, Herwig F, Paxton B (2012) The response of giant stars to dynamical-timescale mass loss. ApJ 760(1):90. https://doi.org/10.1088/0004-637X/760/1/90. arXiv:1111.4202 [astro-ph.SR]

Pavlík V, Jeřábková T, Kroupa P, Baumgardt H (2018) The black hole retention fraction in star clusters. A&A 617:A69. https://doi.org/10.1051/0004-6361/201832919. arXiv:1806.05192 [astro-ph.GA]

Pavlovskii K, Ivanova N (2015) Mass transfer from giant donors. MNRAS 449(4):4415–4427. https://doi.org/10.1093/mnras/stv619. arXiv:1410.5109 [astro-ph.SR]

Pearson WJ, Wang L, Trayford JW, Petrillo CE, van der Tak FFS (2019) Identifying galaxy mergers in observations and simulations with deep learning. A&A 626:A49. https://doi.org/10.1051/0004-6361/201935355. arXiv:1902.10626 [astro-ph.GA]

Peißker F, Eckart A, Zajaček M, Ali B, Parsa M (2020) S62 and S4711: indications of a population of faint fast-moving stars inside the S2 Orbit–S4711 on a 7.6 yr Orbit around Sgr A*. ApJ 899(1):50. https://doi.org/10.3847/1538-4357/ab9c1c. arXiv:2008.04764 [astro-ph.GA]

Perera BBP, DeCesar ME, Demorest PB, Kerr M, Lentati L, Nice DJ, Osłowski S, Ransom SM, Keith MJ, Arzoumanian Z et al (2019) The international pulsar timing array: second data release. MNRAS 490(4):4666–4687. https://doi.org/10.1093/mnras/stz2857. arXiv:1909.04534 [astro-ph.HE]

Peres A (1962) Classical radiation recoil. Phys Rev 128(5):2471–2475. https://doi.org/10.1103/PhysRev.128.2471

Perets HB, Alexander T (2008) Massive perturbers and the efficient merger of binary massive black holes. ApJ 677(1):146–159. https://doi.org/10.1086/527525. arXiv:0705.2123 [astro-ph]

Perets HB, Hopman C, Alexander T (2007) Massive perturber-driven interactions between stars and a massive black hole. ApJ 656(2):709–720. https://doi.org/10.1086/510377. arXiv:astro-ph/0606443 [astro-ph]

Perets HB, Gualandris A, Kupi G, Merritt D, Alexander T (2009) Dynamical evolution of the young stars in the galactic center: N-body simulations of the S-stars. ApJ 702(2):884–889. https://doi.org/10.1088/0004-637X/702/2/884. arXiv:0903.2912 [astro-ph.GA]

Périgois C, Belczynski C, Bulik T, Regimbau T (2021) StarTrack predictions of the stochastic gravitational-wave background from compact binary mergers. Phys Rev D 103(4):043002. https://doi.org/10.1103/PhysRevD.103.043002. arXiv:2008.04890 [astro-ph.CO]

Perley DA, Mazzali PA, Yan L, Cenko SB, Gezari S, Taggart K, Blagorodnova N, Fremling C, Mockler B, Singh A et al (2019) The fast, luminous ultraviolet transient AT2018cow: extreme supernova, or disruption of a star by an intermediate-mass black hole? MNRAS 484(1):1031–1049. https://doi.org/10.1093/mnras/sty3420. arXiv:1808.00969 [astro-ph.HE]

Perpinyà-Vallès M, Rebassa-Mansergas A, Gänsicke BT, Toonen S, Hermes JJ, Gentile Fusillo NP, Tremblay PE (2019) Discovery of the first resolved triple white dwarf. MNRAS 483(1):901–907. https://doi.org/10.1093/mnras/sty3149. arXiv:1811.07752 [astro-ph.SR]

Peschken N, Łokas EL (2019) Tidally induced bars in Illustris galaxies. MNRAS 483(2):2721–2735. https://doi.org/10.1093/mnras/sty3277. arXiv:1804.06241 [astro-ph.GA]

Pestoni B, Bortolas E, Capelo PR, Mayer L (2021) Generation of gravitational waves and tidal disruptions in clumpy galaxies. MNRAS 500(4):4628–4638. https://doi.org/10.1093/mnras/staa3496. arXiv:2011.02488 [astro-ph.GA]

Peters PC (1964) Gravitational radiation and the motion of two point masses. Phys Rev 136(4B):1224–1232. https://doi.org/10.1103/PhysRev.136.B1224

Peters PC (1964b) Gravitational radiation and the motion of two point masses. PhD thesis, California Institute of Technology

Peters PC, Mathews J (1963) Gravitational radiation from point masses in a Keplerian orbit. Phys Rev 131(1):435–440. https://doi.org/10.1103/PhysRev.131.435

Petrovich C, Antonini F (2017) Greatly enhanced merger rates of compact-object binaries in non-spherical nuclear star clusters. ApJ 846(2):146. https://doi.org/10.3847/1538-4357/aa8628. arXiv:1705.05848 [astro-ph.HE]

Pezzulli E, Valiante R, Schneider R (2016) Super-Eddington growth of the first black holes. MNRAS 458(3):3047–3059. https://doi.org/10.1093/mnras/stw505. arXiv:1603.00475 [astro-ph.GA]

Pezzulli E, Volonteri M, Schneider R, Valiante R (2017) The sustainable growth of the first black holes. MNRAS 471(1):589–595. https://doi.org/10.1093/mnras/stx1640. arXiv:1706.06592 [astro-ph.GA]

Pfister H, Lupi A, Capelo PR, Volonteri M, Bellovary JM, Dotti M (2017) The birth of a supermassive black hole binary. MNRAS 471(3):3646–3656. https://doi.org/10.1093/mnras/stx1853. arXiv:1706.04010 [astro-ph.GA]

Pfister H, Bar-Or B, Volonteri M, Dubois Y, Capelo PR (2019) Tidal disruption event rates in galaxy merger remnants. MNRAS 488(1):L29–L34. https://doi.org/10.1093/mnrasl/slz091. arXiv:1903.09124 [astro-ph.GA]

Pfister H, Volonteri M, Dubois Y, Dotti M, Colpi M (2019) The erratic dynamical life of black hole seeds in high-redshift galaxies. MNRAS 486(1):101–111. https://doi.org/10.1093/mnras/stz822. arXiv:1902.01297 [astro-ph.GA]

Pfister H, Dotti M, Laigle C, Dubois Y, Volonteri M (2020) Real galaxy mergers from galaxy pair catalogues. MNRAS 493(1):922–929. https://doi.org/10.1093/mnras/staa227. arXiv:2001.02461 [astro-ph.GA]

Pfister H, Dai JL, Volonteri M, Auchettl K, Trebitsch M, Ramirez-Ruiz E (2021) Tidal disruption events in the first billion years of a galaxy. MNRAS 500(3):3944–3956. https://doi.org/10.1093/mnras/staa3471. arXiv:2006.06565 [astro-ph.GA]

Pfister H, Toscani M, Wong THT, Dai JL, Lodato G, Rossi EM (2022) Observable gravitational waves from tidal disruption events and their electromagnetic counterpart. MNRAS 510(2):2025–2040. https://doi.org/10.1093/mnras/stab3387. arXiv:2103.05883 [astro-ph.HE]

Pflueger BJ, Nguyen K, Bogdanović T, Eracleous M, Runnoe JC, Sigurdsson S, Boroson T (2018) Likelihood for detection of subparsec supermassive black hole binaries in spectroscopic surveys. ApJ 861(1):59. https://doi.org/10.3847/1538-4357/aaca2c. arXiv:1803.02368 [astro-ph.HE]

Phillips SN, Podsiadlowski P (2002) Irradiation pressure effects in close binary systems. MNRAS 337(2):431–444. https://doi.org/10.1046/j.1365-8711.2002.05886.x. arXiv:astro-ph/0109304 [astro-ph]

Phinney ES (1989) Manifestations of a massive black hole in the galactic center. In: Morris M (ed) The center of the galaxy. IAU Symposium, vol 136. p 543

Phinney ES (1991) The rate of neutron star binary mergers in the universe: minimal predictions for gravity wave detectors. ApJ 380:L17. https://doi.org/10.1086/186163

Piana O, Dayal P, Volonteri M, Choudhury TR (2021) The mass assembly of high-redshift black holes. MNRAS 500(2):2146–2158. https://doi.org/10.1093/mnras/staa3363

Pieroni M, Barausse E (2020) Foreground cleaning and template-free stochastic background extraction for LISA. J Cosmol Astropart Phys 7:021. https://doi.org/10.1088/1475-7516/2020/07/021. arXiv:2004.01135 [astro-ph.CO]

Pillepich A, Nelson D, Springel V, Pakmor R, Torrey P, Weinberger R, Vogelsberger M, Marinacci F, Genel S, van der Wel A et al (2019) First results from the TNG50 simulation: the evolution of stellar and gaseous discs across cosmic time. MNRAS 490(3):3196–3233. https://doi.org/10.1093/mnras/stz2338. arXiv:1902.05553 [astro-ph.GA]

Piovano GA, Maselli A, Pani P (2020) Extreme mass ratio inspirals with spinning secondary: a detailed study of equatorial circular motion. Phys Rev D 102(2):024041. https://doi.org/10.1103/PhysRevD.102.024041. arXiv:2004.02654 [gr-qc]

Pipino A, Cibinel A, Tacchella S, Carollo CM, Lilly SJ, Miniati F, Silverman JD, van Gorkom JH, Finoguenov A (2014) The Zurich environmental study (ZENS) of galaxies in groups along the cosmic web V properties and frequency of merging satellites and centrals in different environments. ApJ 797(2):127. https://doi.org/10.1088/0004-637X/797/2/127. arXiv:1409.8298 [astro-ph.GA]

Piran T, Svirski G, Krolik J, Cheng RM, Shiokawa H (2015) Disk formation versus disk accretion-what powers tidal disruption events? ApJ 806(2):164. https://doi.org/10.1088/0004-637X/806/2/164. arXiv:1502.05792 [astro-ph.HE]

Piro AL (2011) Tidal interactions in merging white dwarf binaries. ApJ 740(2):L53. https://doi.org/10.1088/2041-8205/740/2/L53. arXiv:1108.3110 [astro-ph.SR]

Piro AL (2012) Magnetic interactions in coalescing neutron star binaries. ApJ 755(1):80. https://doi.org/10.1088/0004-637X/755/1/80. arXiv:1205.6482 [astro-ph.HE]

Piro L, Ahlers M, Coleiro A, Colpi M, de Oña Wilhelmi E, Guainazzi M, Jonker PG, Namara PM, Nichols DA, O'Brien P et al (2022) Athena synergies in the multi-messenger and transient universe. Exp Astron. https://doi.org/10.1007/s10686-022-09865-6. arXiv:2110.15677 [astro-ph.HE]

Podsiadlowski P (1991) Irradiation-driven mass transfer in low-mass X-ray binaries. Nature 350(6314):136–138. https://doi.org/10.1038/350136a0

Podsiadlowski P, Rappaport S, Pfahl ED (2002) Evolutionary sequences for low- and intermediate-mass X-ray binaries. ApJ 565(2):1107–1133. https://doi.org/10.1086/324686. arXiv:astro-ph/0107261 [astro-ph]

Podsiadlowski P, Rappaport S, Han Z (2003) On the formation and evolution of black hole binaries. MNRAS 341(2):385–404. https://doi.org/10.1046/j.1365-8711.2003.06464.x. arXiv:astro-ph/0207153 [astro-ph]

Podsiadlowski P, Langer N, Poelarends AJT, Rappaport S, Heger A, Pfahl E (2004) The effects of binary evolution on the dynamics of core collapse and neutron star kicks. ApJ 612(2):1044–1051. https://doi.org/10.1086/421713. arXiv:astro-ph/0309588 [astro-ph]

Poggianti BM, Jaffé YL, Moretti A, Gullieuszik M, Radovich M, Tonnesen S, Fritz J, Bettoni D, Vulcani B, Fasano G et al (2017) Ram-pressure feeding of supermassive black holes. Nature 548(7667):304–309. https://doi.org/10.1038/nature23462. arXiv:1708.09036 [astro-ph.GA]

Poisson E, Will CM (1995) Gravitational waves from inspiraling compact binaries: parameter estimation using second-post-Newtonian waveforms. Phys Rev D 52:848–855 arXiv:gr-qc/9502040

Poisson E, Pound A, Vega I (2011) The motion of point particles in curved spacetime. Living Rev Relativ 14:7. https://doi.org/10.12942/lrr-2011-7. arXiv:1102.0529 [gr-qc]

Pol N, McLaughlin M, Lorimer DR, Garver-Daniels N (2021) On the detectability of ultra-compact binary pulsar systems. ApJ 912:22. https://doi.org/10.3847/1538-4357/abe9b7. arXiv:2010.04151 [astro-ph.HE]

Popham R, Gammie CF (1998) Advection-dominated accretion flows in the Kerr metric. II. Steady state global solutions. ApJ 504(1):419–430. https://doi.org/10.1086/306054. arXiv:astro-ph/9802321 [astro-ph]

Portegies Zwart S (2013) Planet-mediated precision reconstruction of the evolution of the cataclysmic variable HU Aquarii. MNRAS 429:L45–L49. https://doi.org/10.1093/mnrasl/sls022. arXiv:1210.5540 [astro-ph.EP]

Portegies Zwart SF, McMillan SLW (2000) Black hole mergers in the universe. ApJ 528(1):L17–L20. https://doi.org/10.1086/312422. arXiv:astro-ph/9910061 [astro-ph]

Portegies Zwart SF, McMillan SLW (2002) The runaway growth of intermediate-mass black holes in dense star clusters. ApJ 576(2):899–907. https://doi.org/10.1086/341798. arXiv:astro-ph/0201055 [astro-ph]

Portegies Zwart SF, Verbunt F (1996) Population synthesis of high-mass binaries. A&A 309:179–196

Portegies Zwart SF, Yungelson LR (1998) Formation and evolution of binary neutron stars. A&A 332:173–188 arXiv:astro-ph/9710347 [astro-ph]

Portegies Zwart SF, Baumgardt H, Hut P, Makino J, McMillan SLW (2004) Formation of massive black holes through runaway collisions in dense young star clusters. Nature 428(6984):724–726. https://doi.org/10.1038/nature02448. arXiv:astro-ph/0402622 [astro-ph]

Portegies Zwart SF, Baumgardt H, McMillan SLW, Makino J, Hut P, Ebisuzaki T (2006) The ecology of star clusters and intermediate-mass black holes in the galactic bulge. ApJ 641(1):319–326. https://doi.org/10.1086/500361. arXiv:astro-ph/0511397 [astro-ph]

Postnov KA, Yungelson LR (2014) The evolution of compact binary star systems. Living Rev Relativ 17:3. https://doi.org/10.12942/lrr-2014-3. arXiv:1403.4754 [astro-ph.HE]

Pound A (2014) Conservative effect of the second-order gravitational self-force on quasicircular orbits in Schwarzschild spacetime. Phys Rev D 90(8):084039. https://doi.org/10.1103/PhysRevD.90.084039. arXiv:1404.1543 [gr-qc]

Pound A (2017) Nonlinear gravitational self-force: second-order equation of motion. Phys Rev D 95(10):104056. https://doi.org/10.1103/PhysRevD.95.104056. arXiv:1703.02836 [gr-qc]

Pound A, Miller J (2014) Practical, covariant puncture for second-order self-force calculations. Phys Rev D 89(10):104020. https://doi.org/10.1103/PhysRevD.89.104020. arXiv:1403.1843 [gr-qc]

Pound A, Wardell B, Warburton N, Miller J (2020) Second-order self-force calculation of gravitational binding energy in compact binaries. Phys Rev Lett 124(2):021101. https://doi.org/10.1103/PhysRevLett.124.021101. arXiv:1908.07419 [gr-qc]

Poveda A, Herrera MA, Allen C, Cordero G, Lavalley C (1994) Statistical studies of visual double and multiple stars. II. A catalogue of nearby wide binary and multiple systems. Rev Mex Astron Astrof 28:43–89

Power C, Baugh CM, Lacey CG (2010) The redshift evolution of the mass function of cold gas in hierarchical galaxy formation models. MNRAS 406(1):43–59. https://doi.org/10.1111/j.1365-2966.2010.16481.x. arXiv:0908.1396 [astro-ph.CO]

Predehl P, Andritschke R, Böhringer H, Bornemann W, Bräuninger H, Brunner H, Brusa M, Burkert W, Burwitz V, Cappelluti N et al (2010) eROSITA on SRG. In: Arnaud M, Murray SS, Takahashi T (eds) Space telescopes and instrumentation 2010: ultraviolet to gamma ray. Society of photo-optical instrumentation engineers (SPIE) conference series, vol 7732, p 77320U. https://doi.org/10.1117/12.856577. arXiv:1001.2502 [astro-ph.CO]

Press WH, Schechter P (1974) Formation of galaxies and clusters of galaxies by self-similar gravitational condensation. ApJ 187:425–438. https://doi.org/10.1086/152650

Preto M (2010) Gravitational waves notes, issue #3 : "Stellar cusps in galactic nuclei—how stars distribute around a massive black hole". arXiv e-prints arXiv:1005.4048 [astro-ph.CO]

Preto M, Berentzen I, Berczik P, Spurzem R (2011) Fast coalescence of massive black hole binaries from mergers of galactic nuclei: implications for low-frequency gravitational-wave astrophysics. ApJ 732(2):L26. https://doi.org/10.1088/2041-8205/732/2/L26. arXiv:1102.4855 [astro-ph.GA]

Pretorius F (2005) Evolution of binary black-hole spacetimes. Phys Rev Lett 95(12):121101. https://doi.org/10.1103/PhysRevLett.95.121101. arXiv:gr-qc/0507014 [gr-qc]

Provencal JL, Winget DE, Nather RE, Robinson EL, Clemens JC, Bradley PA, Claver CF, Kleinman SJ, Grauer AD, Hine BP et al (1997) Whole earth telescope observations of the helium interacting binary PG 1346+082 (CR Bootis). ApJ 480(1):383–394. https://doi.org/10.1086/303971

Prust LJ, Chang P (2019) Common envelope evolution on a moving mesh. MNRAS 486(4):5809–5818. https://doi.org/10.1093/mnras/stz1219. arXiv:1904.09256 [astro-ph.SR]

Punturo M, Abernathy M, Acernese F, Allen B, Andersson N, Arun K, Barone F, Barr B, Barsuglia M, Beker M et al (2010) The third generation of gravitational wave observatories and their science reach. Class Quantum Grav 27(8):084007. https://doi.org/10.1088/0264-9381/27/8/084007

Qin Y, Fragos T, Meynet G, Andrews J, Sørensen M, Song HF (2018) The spin of the second-born black hole in coalescing binary black holes. A&A 616:A28. https://doi.org/10.1051/0004-6361/201832839. arXiv:1802.05738 [astro-ph.SR]

Quinlan GD (1996) The dynamical evolution of massive black hole binaries I. Hardening in a fixed stellar background. New A 1(1):35–56. https://doi.org/10.1016/S1384-1076(96)00003-6. arXiv:astro-ph/9601092 [astro-ph]

Quinlan GD, Hernquist L (1997) The dynamical evolution of massive black hole binaries—II. Self-consistent N-body integrations. New A 2(6):533–554. https://doi.org/10.1016/S1384-1076(97)00039-0. arXiv:astro-ph/9706298 [astro-ph]

Quinlan GD, Shapiro SL (1989) Dynamical evolution of dense clusters of compact stars. ApJ 343:725. https://doi.org/10.1086/167745

Raaijmakers G, Greif SK, Riley TE, Hinderer T, Hebeler K, Schwenk A, Watts AL, Nissanke S, Guillot S, Lattimer JM et al (2020) Constraining the dense matter equation of state with joint analysis of NICER and LIGO/Virgo measurements. ApJ 893(1):L21. https://doi.org/10.3847/2041-8213/ab822f. arXiv:1912.11031 [astro-ph.HE]

Raffai P, Haiman Z, Frei Z (2016) A statistical method to search for recoiling supermassive black holes in active galactic nuclei. MNRAS 455(1):484–492. https://doi.org/10.1093/mnras/stv2371. arXiv:1509.02075 [astro-ph.GA]

Ragusa E, Lodato G, Price DJ (2016) Suppression of the accretion rate in thin discs around binary black holes. MNRAS 460(2):1243–1253. https://doi.org/10.1093/mnras/stw1081. arXiv:1605.01730 [astro-ph.HE]

Raidal M, Spethmann C, Vaskonen V, Veermäe H (2019) Formation and evolution of primordial black hole binaries in the early universe. J Cosmol Astropart Phys 02:018. https://doi.org/10.1088/1475-7516/2019/02/018. arXiv:1812.01930 [astro-ph.CO]

Ramsay G, Hakala P (2005) RApid temporal survey (RATS)—I. Overview and first results. MNRAS 360(1):314–321. https://doi.org/10.1111/j.1365-2966.2005.09035.x. arXiv:astro-ph/0503138 [astro-ph]

Ramsay G, Hakala P, Marsh T, Nelemans G, Steeghs D, Cropper M (2005) XMM-Newton observations of AM CVn binaries. A&A 440(2):675–681. https://doi.org/10.1051/0004-6361:20052950. arXiv:astro-ph/0505549 [astro-ph]

Ramsay G, Groot PJ, Marsh T, Nelemans G, Steeghs D, Hakala P (2006) XMM-Newton observations of AM CVn binaries: V396 Hya and SDSS J1240–01. A&A 457(2):623–627. https://doi.org/10.1051/0004-6361:20065491. arXiv:astro-ph/0607178 [astro-ph]

Ramsay G, Green MJ, Marsh TR, Kupfer T, Breedt E, Korol V, Groot PJ, Knigge C, Nelemans G, Steeghs D et al (2018) Physical properties of AM CVn stars: new insights from Gaia DR2. A&A 620:A141. https://doi.org/10.1051/0004-6361/201834261. arXiv:1810.06548 [astro-ph.SR]

Randall L, Xianyu ZZ (2019a) Eccentricity without measuring eccentricity: discriminating among stellar mass black hole binary formation channels. arXiv e-prints arXiv:1907.02283 [astro-ph.HE]

Randall L, Xianyu ZZ (2019b) Observing eccentricity oscillations of binary black holes in LISA. arXiv e-prints arXiv:1902.08604 [astro-ph.HE]

Randall L, Shelest A, Xianyu ZZ (2021) An efficient signal to noise approximation for eccentric inspiraling binaries. arXiv e-prints arXiv:2103.16030 [astro-ph.HE]

Ransom S, Brazier A, Chatterjee S, Cohen T, Cordes JM, DeCesar ME, Demorest PB, Hazboun JS, Lam MT, Lynch RS et al (2019) The NANOGrav program for gravitational waves and fundamental physics. In: Bulletin of the American Astronomical Society, vol 51, p 195. arXiv:1908.05356 [astro-ph.IM]

Ransom SM, Stairs IH, Archibald AM, Hessels JWT, Kaplan DL, van Kerkwijk MH et al (2014) A millisecond pulsar in a stellar triple system. Nature 505(7484):520–524. https://doi.org/10.1038/nature12917. arXiv:1401.0535 [astro-ph.SR]

Rantala A, Pihajoki P, Johansson PH, Naab T, Lahén N, Sawala T (2017) Post-Newtonian dynamical modeling of supermassive black holes in galactic-scale simulations. ApJ 840(1):53. https://doi.org/10.3847/1538-4357/aa6d65. arXiv:1611.07028 [astro-ph.GA]

Rantala A, Johansson PH, Naab T, Thomas J, Frigo M (2018) The formation of extremely diffuse galaxy cores by merging supermassive black holes. ApJ 864(2):113. https://doi.org/10.3847/1538-4357/aada47. arXiv:1805.10295 [astro-ph.GA]

Rappaport S, Joss PC, Webbink RF (1982) The evolution of highly compact binary stellar systems. ApJ 254:616–640. https://doi.org/10.1086/159772

Rappaport S, Vanderburg A, Schwab J, Nelson L (2021) Minimum orbital periods of H-rich bodies. ApJ 913:118. https://doi.org/10.3847/1538-4357/abf7b0. arXiv:2104.12083 [astro-ph.SR]

Rasio FA, Livio M (1996) On the formation and evolution of common envelope systems. ApJ 471:366. https://doi.org/10.1086/177975. arXiv:astro-ph/9511054 [astro-ph]

Raskin C, Timmes FX, Scannapieco E, Diehl S, Fryer C (2009) On Type Ia supernovae from the collisions of two white dwarfs. MNRAS 399(1):L156–L159. https://doi.org/10.1111/j.1745-3933.2009.00743.x. arXiv:0907.3915 [astro-ph.SR]

Rasskazov A, Merritt D (2017) Evolution of binary supermassive black holes in rotating nuclei. ApJ 837(2):135. https://doi.org/10.3847/1538-4357/aa6188. arXiv:1610.08555 [astro-ph.GA]

Rasskazov A, Fragione G, Leigh NWC, Tagawa H, Sesana A, Price-Whelan A, Rossi EM (2019) Hypervelocity stars from a supermassive black hole-intermediate-mass black hole binary. ApJ 878(1):17. https://doi.org/10.3847/1538-4357/ab1c5d. arXiv:1810.12354 [astro-ph.GA]

Rastello S, Amaro-Seoane P, Arca-Sedda M, Capuzzo-Dolcetta R, Fragione G, Tosta e Melo I (2019) Stellar black hole binary mergers in open clusters. MNRAS 483(1):1233–1246. https://doi.org/10.1093/mnras/sty3193. arXiv:1811.10628 [astro-ph.GA]

Rastello S, Mapelli M, Di Carlo UN, Giacobbo N, Santoliquido F, Spera M, Ballone A, Iorio G (2020) Dynamics of black hole-neutron star binaries in young star clusters. MNRAS 497(2):1563–1570. https://doi.org/10.1093/mnras/staa2018. arXiv:2003.02277 [astro-ph.HE]

Rauch KP, Tremaine S (1996) Resonant relaxation in stellar systems. New A 1(2):149–170. https://doi.org/10.1016/S1384-1076(96)00012-7. arXiv:astro-ph/9603018 [astro-ph]

Ravenhall DG, Pethick CJ (1994) Neutron star moments of inertia. ApJ 424:846. https://doi.org/10.1086/173935

Ray PS, Arzoumanian Z, Brandt S, Burns E, Chakrabarty D, Feroci M, Gendreau KC, Gevin O, Hernanz M, Jenke P et al (2018) STROBE-X: a probe-class mission for X-ray spectroscopy and timing on timescales from microseconds to years. In: den Herder JWA, Nikzad S, Nakazawa K (eds) Space telescopes and instrumentation 2018: ultraviolet to gamma ray. Society of photo-optical instrumentation engineers (SPIE) conference series, vol 10699, p 1069919. https://doi.org/10.1117/12.2312257. arXiv:1807.01179 [astro-ph.IM]

Ray PS, Arzoumanian Z, Ballantyne D, Bozzo E, Brandt S, Brenneman L, Chakrabarty D, Christophersen M, DeRosa A, Feroci M et al (2019) STROBE-X: X-ray timing and spectroscopy on dynamical timescales from microseconds to years. arXiv e-prints arXiv:1903.03035 [astro-ph.IM]

Razzano M, Cuoco E (2018) Image-based deep learning for classification of noise transients in gravitational wave detectors. Class Quantum Grav 35(9):095016. https://doi.org/10.1088/1361-6382/aab793. arXiv:1803.09933 [gr-qc]

Rebassa-Mansergas A, Gänsicke BT, Rodríguez-Gil P, Schreiber MR, Koester D (2007) Post-common-envelope binaries from SDSS - I. 101 white dwarf main-sequence binaries with multiple Sloan Digital Sky Survey spectroscopy. MNRAS 382(4):1377–1393. https://doi.org/10.1111/j.1365-2966.2007.12288.x. arXiv:0707.4107 [astro-ph]

Rebassa-Mansergas A, Toonen S, Korol V, Torres S (2019) Where are the double-degenerate progenitors of Type Ia supernovae? MNRAS 482(3):3656–3668. https://doi.org/10.1093/mnras/sty2965. arXiv:1809.07158 [astro-ph.SR]

Redmount IH, Rees MJ (1989) Gravitational-radiation rocket effects and galactic structure. Comments Astrophys 14:165

Rees MJ (1988) Tidal disruption of stars by black holes of 10^6-10^8 solar masses in nearby galaxies. Nature 333(6173):523–528. https://doi.org/10.1038/333523a0

Regan JA, Visbal E, Wise JH, Haiman Z, Johansson PH, Bryan GL (2017) Rapid formation of massive black holes in close proximity to embryonic protogalaxies. Nat Astron 1:0075. https://doi.org/10.1038/s41550-017-0075

Regan JA, Downes TP, Volonteri M, Beckmann R, Lupi A, Trebitsch M, Dubois Y (2019) Super-Eddington accretion and feedback from the first massive seed black holes. MNRAS 486(3):3892–3906. https://doi.org/10.1093/mnras/stz1045. arXiv:1811.04953 [astro-ph.GA]

Regan JA, Haiman Z, Wise JH, O'Shea BW, Norman ML (2020a) Massive star formation in metal-enriched haloes at high redshift. Open J Astrophys 3:E9. https://doi.org/10.21105/astro.2006.14625. arXiv:2006.14625 [astro-ph.GA]

Regan JA, Wise JH, O'Shea BW, Norman ML (2020) The emergence of the first star-free atomic cooling haloes in the Universe. MNRAS 492(2):3021–3031. https://doi.org/10.1093/mnras/staa035. arXiv:1908.02823 [astro-ph.GA]

Regimbau T (2011) The astrophysical gravitational wave stochastic background. Res Astron Astrophys 11(4):369–390. https://doi.org/10.1088/1674-4527/11/4/001. arXiv:1101.2762 [astro-ph.CO]

Reichardt TA, De Marco O, Iaconi R, Tout CA, Price DJ (2019) Extending common envelope simulations from Roche lobe overflow to the nebular phase. MNRAS 484(1):631–647. https://doi.org/10.1093/mnras/sty3485. arXiv:1809.02297 [astro-ph.SR]

Reid MJ, Brunthaler A (2004) The proper motion of Sagittarius A*. II. The mass of Sagittarius A*. ApJ 616(2):872–884. https://doi.org/10.1086/424960. arXiv:astro-ph/0408107 [astro-ph]

Reines AE, Volonteri M (2015) Relations between central black hole mass and total galaxy stellar mass in the local universe. ApJ 813(2):82. https://doi.org/10.1088/0004-637X/813/2/82. arXiv:1508.06274 [astro-ph.GA]

Reines AE, Greene JE, Geha M (2013) Dwarf galaxies with optical signatures of active massive black holes. ApJ 775:116. https://doi.org/10.1088/0004-637X/775/2/116. arXiv:1308.0328 [astro-ph.CO]

Reines AE, Condon JJ, Darling J, Greene JE (2020) A new sample of (wandering) massive black holes in dwarf galaxies from high-resolution radio observations. ApJ 888(1):36. https://doi.org/10.3847/1538-4357/ab4999. arXiv:1909.04670 [astro-ph.GA]

Reinoso B, Schleicher DRG, Fellhauer M, Klessen RS, Boekholt TCN (2018) Collisions in primordial star clusters. Formation pathway for intermediate mass black holes. A&A 614:A14. https://doi.org/10.1051/0004-6361/201732224. arXiv:1801.05891 [astro-ph.GA]

Remillard RA, McClintock JE (2006) X-ray properties of black-hole binaries. ARA&A 44(1):49–92. https://doi.org/10.1146/annurev.astro.44.051905.092532. arXiv:astro-ph/0606352 [astro-ph]

Remmen GN, Wu K (2013) Complex orbital dynamics of a double neutron star system revolving around a massive black hole. MNRAS 430(3):1940–1955. https://doi.org/10.1093/mnras/stt023. arXiv:1301.2836 [astro-ph.HE]

Remus F, Mathis S, Zahn JP (2012) The equilibrium tide in stars and giant planets. I. The coplanar case. A&A 544:A132. https://doi.org/10.1051/0004-6361/201118160. arXiv:1205.3536 [astro-ph.SR]

Renzo M, Callister T, Chatziioannou K, van Son LAC, Mingarelli CMF, Cantiello M, Ford KES, McKernan B, Ashton G (2021) Prospects of gravitational-waves detections from common-envelope evolution with LISA. ApJ 919:128. https://doi.org/10.3847/1538-4357/ac1110. arXiv:2102.00078 [astro-ph.SR]

Reynolds CS (2014) Measuring black hole spin using X-ray reflection spectroscopy. Space Sci Rev 183(1–4):277–294. https://doi.org/10.1007/s11214-013-0006-6. arXiv:1302.3260 [astro-ph.HE]

Reynolds CS (2019) Observing black holes spin. Nat Astron 3:41–47. https://doi.org/10.1038/s41550-018-0665-z. arXiv:1903.11704 [astro-ph.HE]

Reynolds CS, Nowak MA (2003) Fluorescent iron lines as a probe of astrophysical black hole systems. Phys Rep 377(6):389–466. https://doi.org/10.1016/S0370-1573(02)00584-7. arXiv:astro-ph/0212065 [astro-ph]

Rezzolla L, Barausse E, Dorband EN, Pollney D, Reisswig C, Seiler J, Husa S (2008) Final spin from the coalescence of two black holes. Phys Rev D 78(4):044002. https://doi.org/10.1103/PhysRevD.78.044002. arXiv:0712.3541 [gr-qc]

Ricarte A, Natarajan P (2018) Exploring SMBH assembly with semi-analytic modelling. MNRAS 474(2):1995–2011. https://doi.org/10.1093/mnras/stx2851. arXiv:1710.11532 [astro-ph.HE]

Ricarte A, Natarajan P (2018) The observational signatures of supermassive black hole seeds. MNRAS 481(3):3278–3292. https://doi.org/10.1093/mnras/sty2448. arXiv:1809.01177 [astro-ph.GA]

Ricarte A, Tremmel M, Natarajan P, Quinn T (2020) A link between ram pressure stripping and active galactic nuclei. ApJ 895(1):L8. https://doi.org/10.3847/2041-8213/ab9022. arXiv:2003.05950 [astro-ph.GA]

Ricker PM, Taam RE (2012) An AMR study of the common-envelope phase of binary evolution. ApJ 746(1):74. https://doi.org/10.1088/0004-637X/746/1/74. arXiv:1107.3889 [astro-ph.SR]

Riley TE, Watts AL, Bogdanov S, Ray PS, Ludlam RM, Guillot S, Arzoumanian Z, Baker CL, Bilous AV, Chakrabarty D et al (2019) A NICER view of PSR J0030+0451: millisecond pulsar parameter estimation. ApJ 887(1):L21. https://doi.org/10.3847/2041-8213/ab481c. arXiv:1912.05702 [astro-ph.HE]

Rivera Sandoval LE, van den Berg M, Heinke CO, Cohn HN, Lugger PM, Anderson J, Cool AM, Edmonds PD, Wijnands R, Ivanova N et al (2018) New cataclysmic variables and other exotic binaries in the globular cluster 47 Tucanae*. MNRAS 475(4):4841–4867. https://doi.org/10.1093/mnras/sty058. arXiv:1705.07100 [astro-ph.SR]

Rizzuto FP, Naab T, Spurzem R, Giersz M, Ostriker JP, Stone NC, Wang L, Berczik P, Rampp M (2020) Intermediate mass black hole formation in compact young massive star clusters. MNRAS 501:5257–5273. https://doi.org/10.1093/mnras/staa3634. arXiv:2008.09571 [astro-ph.GA]

Rizzuto FP, Naab T, Spurzem R, Giersz M, Ostriker JP, Stone NC, Wang L, Berczik P, Rampp M (2021) Intermediate mass black hole formation in compact young massive star clusters. MNRAS 501(4):5257–5273. https://doi.org/10.1093/mnras/staa3634. arXiv:2008.09571 [astro-ph.GA]

Rizzuto FP, Naab T, Spurzem R, Arca-Sedda M, Giersz M, Ostriker JP, Banerjee S (2022) Black hole mergers in compact star clusters and massive black hole formation beyond the mass gap. MNRAS 512(1):884–898. https://doi.org/10.1093/mnras/stac231. arXiv:2108.11457 [astro-ph.GA]

Roberts DH, Saripalli L, Subrahmanyan R (2015) The abundance of X-shaped radio sources: implications for the gravitational wave background. ApJ 810(1):L6. https://doi.org/10.1088/2041-8205/810/1/L6. arXiv:1503.02021 [astro-ph.GA]

Roberts MSE (2013) Surrounded by spiders! New black widows and redbacks in the Galactic field. In: van Leeuwen J (ed) Neutron stars and pulsars: challenges and opportunities after 80 years. IAU

symposium, vol 291, pp 127–132. https://doi.org/10.1017/S174392131202337X. arXiv:1210.6903 [astro-ph.HE]

Robinson EL, Romano JD, Vecchio A (2008) Search for a stochastic gravitational-wave signal in the second round of the Mock LISA Data Challenges. Class Quantum Grav 25(18):184019. https://doi.org/10.1088/0264-9381/25/18/184019. arXiv:0804.4144 [gr-qc]

Robson T, Cornish NJ, Tamanini N, Toonen S (2018) Detecting hierarchical stellar systems with LISA. Phys Rev D 98(6):064012. https://doi.org/10.1103/PhysRevD.98.064012. arXiv:1806.00500 [gr-qc]

Robson T, Cornish NJ, Liu C (2019) The construction and use of LISA sensitivity curves. Class Quantum Grav 36(10):105011. https://doi.org/10.1088/1361-6382/ab1101. arXiv:1803.01944 [astro-ph.HE]

Rodriguez C, Taylor GB, Zavala RT, Peck AB, Pollack LK, Romani RW (2006) A compact supermassive binary black hole system. ApJ 646(1):49–60. https://doi.org/10.1086/504825. arXiv:astro-ph/0604042 [astro-ph]

Rodriguez CL, Antonini F (2018) A triple origin for the heavy and low-spin binary black holes detected by LIGO/VIRGO. ApJ 863(1):7. https://doi.org/10.3847/1538-4357/aacea4. arXiv:1805.08212 [astro-ph.HE]

Rodriguez CL, Zevin M, Amaro-Seoane P, Chatterjee S, Kremer K, Rasio FA, Ye CS (2019) Black holes: the next generation–repeated mergers in dense star clusters and their gravitational-wave properties. Phys Rev D 100(4):043027. https://doi.org/10.1103/PhysRevD.100.043027. arXiv:1906.10260 [astro-ph.HE]

Roebber E, Buscicchio R, Vecchio A, Moore CJ, Klein A, Korol V, Toonen S, Gerosa D, Goldstein J, Gaebel SM et al (2020) Milky way satellites shining bright in gravitational waves. ApJ 894(2):L15. https://doi.org/10.3847/2041-8213/ab8ac9. arXiv:2002.10465 [astro-ph.GA]

Roedig C, Sesana A (2014) Migration of massive black hole binaries in self-gravitating discs: retrograde versus prograde. MNRAS 439(4):3476–3489. https://doi.org/10.1093/mnras/stu194. arXiv:1307.6283 [astro-ph.HE]

Roedig C, Dotti M, Sesana A, Cuadra J, Colpi M (2011) Limiting eccentricity of subparsec massive black hole binaries surrounded by self-gravitating gas discs. MNRAS 415(4):3033–3041. https://doi.org/10.1111/j.1365-2966.2011.18927.x. arXiv:1104.3868 [astro-ph.CO]

Roedig C, Sesana A, Dotti M, Cuadra J, Amaro-Seoane P, Haardt F (2012) Evolution of binary black holes in self gravitating discs. Dissecting the torques. A&A 545:A127. https://doi.org/10.1051/0004-6361/201219986. arXiv:1202.6063 [astro-ph.CO]

Roedig C, Krolik JH, Miller MC (2014) Observational signatures of binary supermassive black holes. ApJ 785(2):115. https://doi.org/10.1088/0004-637X/785/2/115. arXiv:1402.7098 [astro-ph.HE]

Roelofs GHA, Groot PJ, Nelemans G, Marsh TR, Steeghs D (2006) Kinematics of the ultracompact helium accretor AM Canum Venaticorum. MNRAS 371(3):1231–1242. https://doi.org/10.1111/j.1365-2966.2006.10718.x. arXiv:astro-ph/0606327 [astro-ph]

Roelofs GHA, Groot PJ, Benedict GF, McArthur BE, Steeghs D, Morales-Rueda L, Marsh TR, Nelemans G (2007) Hubble space telescope parallaxes of AM CVn stars and astrophysical consequences. ApJ 666(2):1174–1188. https://doi.org/10.1086/520491. arXiv:0705.3855 [astro-ph]

Roelofs GHA, Groot PJ, Nelemans G, Marsh TR, Steeghs D (2007) On the orbital periods of the AM CVn stars HP Librae and V803 Centauri. MNRAS 379(1):176–182. https://doi.org/10.1111/j.1365-2966.2007.11931.x. arXiv:0705.0402 [astro-ph]

Roelofs GHA, Nelemans G, Groot PJ (2007) The population of AM CVn stars from the Sloan Digital Sky Survey. MNRAS 382(2):685–692. https://doi.org/10.1111/j.1365-2966.2007.12451.x. arXiv:0709.2951 [astro-ph]

Roelofs GHA, Rau A, Marsh TR, Steeghs D, Groot PJ, Nelemans G (2010) Spectroscopic evidence for a 5.4 minute orbital period in HM Cancri. ApJ 711(2):L138–L142. https://doi.org/10.1088/2041-8205/711/2/L138. arXiv:1003.0658 [astro-ph.SR]

Romano JD, Cornish NJ (2017) Detection methods for stochastic gravitational-wave backgrounds: a unified treatment. Living Rev Relativ 20:2. https://doi.org/10.1007/s41114-017-0004-1. arXiv:1608.06889 [gr-qc]

Romano-Díaz E, Shlosman I, Heller C, Hoffman Y (2008) Disk evolution and bar triggering driven by interactions with dark matter substructure. ApJ 687(1):L13. https://doi.org/10.1086/593168. arXiv:0809.2785 [astro-ph]

Romero-Shaw IM, Lasky PD, Thrane E (2019) Searching for eccentricity: signatures of dynamical formation in the first gravitational-wave transient catalogue of LIGO and Virgo. MNRAS 490 (4):5210–5216. https://doi.org/10.1093/mnras/stz2996. arXiv:1909.05466 [astro-ph.HE]

Rosado PA, Sesana A, Gair J (2015) Expected properties of the first gravitational wave signal detected with pulsar timing arrays. MNRAS 451(3):2417–2433. https://doi.org/10.1093/mnras/stv1098. arXiv:1503.04803 [astro-ph.HE]

Rosas-Guevara Y, Bower RG, Schaye J, McAlpine S, Dalla Vecchia C, Frenk CS, Schaller M, Theuns T (2016) Supermassive black holes in the EAGLE. Universe revealing the observables of their growth. MNRAS 462(1):190–205. https://doi.org/10.1093/mnras/stw1679. arXiv:1604.00020 [astro-ph.GA]

Rosas-Guevara YM, Bower RG, Schaye J, Furlong M, Frenk CS, Booth CM, Crain RA, Dalla Vecchia C, Schaller M, Theuns T (2015) The impact of angular momentum on black hole accretion rates in simulations of galaxy formation. MNRAS 454(1):1038–1057. https://doi.org/10.1093/mnras/stv2056. arXiv:1312.0598 [astro-ph.CO]

Rosenthal E (2006) Construction of the second-order gravitational perturbations produced by a compact object. Phys Rev D 73(4):044034. https://doi.org/10.1103/PhysRevD.73.044034. arXiv:gr-qc/0602066 [gr-qc]

Ross NP, Shen Y, Strauss MA, Vanden Berk DE, Connolly AJ, Richards GT, Schneider DP, Weinberg DH, Hall PB, Bahcall NA et al (2009) Clustering of low-redshift ($z < = 2.2$) quasars from the sloan digital sky survey. ApJ 697(2):1634–1655. https://doi.org/10.1088/0004-637X/697/2/1634. arXiv:0903.3230 [astro-ph.CO]

Rossi EM, Lodato G, Armitage PJ, Pringle JE, King AR (2010) Black hole mergers: the first light. MNRAS 401(3):2021–2035. https://doi.org/10.1111/j.1365-2966.2009.15802.x. arXiv:0910.0002 [astro-ph.HE]

Rossi EM, Stone NC, Law-Smith JAP, Macleod M, Lodato G, Dai JL, Mandel I (2021) The process of stellar tidal disruption by supermassive black holes. Space Sci Rev 217(3):40. https://doi.org/10.1007/s11214-021-00818-7. arXiv:2005.12528 [astro-ph.HE]

Rosswog S, Ramirez-Ruiz E, Hix WR (2008) Atypical thermonuclear supernovae from tidally crushed white dwarfs. ApJ 679(2):1385–1389. https://doi.org/10.1086/528738. arXiv:0712.2513 [astro-ph]

Rosswog S, Kasen D, Guillochon J, Ramirez-Ruiz E (2009) Collisions of white dwarfs as a new progenitor channel for type Ia supernovae. ApJ 705(2):L128–L132. https://doi.org/10.1088/0004-637X/705/2/L128. arXiv:0907.3196 [astro-ph.HE]

Rosswog S, Ramirez-Ruiz E, Hix WR (2009) Tidal disruption and ignition of white dwarfs by moderately massive black holes. ApJ 695(1):404–419. https://doi.org/10.1088/0004-637X/695/1/404. arXiv:0808.2143 [astro-ph]

Roupas Z, Kocsis B, Tremaine S (2017) Isotropic-nematic phase transitions in gravitational systems. ApJ 842(2):90. https://doi.org/10.3847/1538-4357/aa7141. arXiv:1701.03271 [astro-ph.GA]

Roškar R, Fiacconi D, Mayer L, Kazantzidis S, Quinn TR, Wadsley J (2015) Orbital decay of supermassive black hole binaries in clumpy multiphase merger remnants. MNRAS 449(1):494–505. https://doi.org/10.1093/mnras/stv312. arXiv:1406.4505 [astro-ph.GA]

Ruan WH, Guo ZK, Cai RG, Zhang YZ (2020) Taiji program: gravitational-wave sources. Int J Mod Phys A 35(17):2050075. https://doi.org/10.1142/S0217751X2050075X. arXiv:1807.09495 [gr-qc]

Ruan WH, Liu C, Guo ZK, Wu YL, Cai RG (2021) The LISA-Taiji network: precision localization of coalescing massive black hole binaries. Research 2021:6014164. https://doi.org/10.34133/2021/6014164

Rubbo LJ, Holley-Bockelmann K, Finn LS (2006) Event rate for extreme mass ratio burst signals in the laser interferometer space antenna band. ApJ 649(1):L25–L28. https://doi.org/10.1086/508326

Rueda JA, Ruffini R, Wang Y, Bianco CL, Blanco-Iglesias JM, Karlica M, Lorén-Aguilar P, Moradi R, Sahakyan N (2019) Electromagnetic emission of white dwarf binary mergers. J Cosmol Astropart Phys 3:044. https://doi.org/10.1088/1475-7516/2019/03/044. arXiv:1807.07905 [astro-ph.HE]

Ruel J, Bazin G, Bayliss M, Brodwin M, Foley RJ, Stalder B, Aird KA, Armstrong R, Ashby MLN, Bautz M et al (2014) Optical spectroscopy and velocity dispersions of galaxy clusters from the SPT-SZ survey. ApJ 792(1):45. https://doi.org/10.1088/0004-637X/792/1/45. arXiv:1311.4953 [astro-ph.CO]

Ruiter AJ (2020) Type Ia supernova sub-classes and progenitor origin. IAU Symp 357:1–15. https://doi.org/10.1017/S1743921320000587. arXiv:2001.02947 [astro-ph.SR]

Ruiter AJ, Belczynski K, Benacquista M, Holley-Bockelmann K (2009) The contribution of halo white dwarf binaries to the laser interferometer space antenna signal. ApJ 693(1):383–387. https://doi.org/10.1088/0004-637X/693/1/383

Ruiter AJ, Belczynski K, Benacquista M, Larson SL, Williams G (2010) The LISA gravitational wave foreground: a study of double white dwarfs. ApJ 717(2):1006–1021. https://doi.org/10.1088/0004-637X/717/2/1006. arXiv:0705.3272 [astro-ph]

Ruiter AJ, Ferrario L, Belczynski K, Seitenzahl IR, Crocker RM, Karakas AI (2019) On the formation of neutron stars via accretion-induced collapse in binaries. MNRAS 484(1):698–711. https://doi.org/10.1093/mnras/stz001. arXiv:1802.02437 [astro-ph.SR]

Runnoe JC, Eracleous M, Mathes G, Pennell A, Boroson T, Sigurdsson S, Bogdanović T, Halpern JP, Liu J (2015) A large systematic search for close supermassive binary and rapidly recoiling black holes. II. Continued spectroscopic monitoring and optical flux variability. ApJS 221(1):7. https://doi.org/10.1088/0067-0049/221/1/7. arXiv:1509.02575 [astro-ph.GA]

Runnoe JC, Eracleous M, Pennell A, Mathes G, Boroson T, Sigurdsson S, Bogdanović T, Halpern JP, Liu J, Brown S (2017) A large systematic search for close supermassive binary and rapidly recoiling black holes—III. Radial velocity variations. MNRAS 468(2):1683–1702. https://doi.org/10.1093/mnras/stx452. arXiv:1702.05465 [astro-ph.GA]

Ryu T, Perna R, Haiman Z, Ostriker JP, Stone NC (2018) Interactions between multiple supermassive black holes in galactic nuclei: a solution to the final parsec problem. MNRAS 473(3):3410–3433. https://doi.org/10.1093/mnras/stx2524. arXiv:1709.06501 [astro-ph.GA]

Ryu T, Krolik J, Piran T, Noble SC (2020) Tidal disruptions of main-sequence stars. II. Simulation methodology and stellar mass dependence of the character of full tidal disruptions. ApJ 904(2):99. https://doi.org/10.3847/1538-4357/abb3cd. arXiv:2001.03502 [astro-ph.HE]

Sadeghian L, Ferrer F, Will CM (2013) Dark-matter distributions around massive black holes: a general relativistic analysis. Phys Rev D 88(6):063522. https://doi.org/10.1103/PhysRevD.88.063522. arXiv:1305.2619 [astro-ph.GA]

Safarzadeh M, Ramirez-Ruiz E, Andrews JJ, Macias P, Fragos T, Scannapieco E (2019) r-Process enrichment of the ultra-faint dwarf galaxies by fast-merging double-neutron stars. ApJ 872(1):105. https://doi.org/10.3847/1538-4357/aafe0e. arXiv:1810.04176 [astro-ph.HE]

Safarzadeh M, Hamers AS, Loeb A, Berger E (2020) Formation and merging of mass gap black holes in gravitational-wave merger events from wide hierarchical quadruple systems. ApJ 888(1):L3. https://doi.org/10.3847/2041-8213/ab5dc8. arXiv:1911.04495 [astro-ph.HE]

Safarzadeh M, Ramirez-Ruiz E, Berger E (2020) Does GW190425 require an alternative formation pathway than a fast-merging channel? ApJ 900(1):13. https://doi.org/10.3847/1538-4357/aba596. arXiv:2001.04502 [astro-ph.HE]

Saffer RA, Livio M, Yungelson LR (1998) Close binary white dwarf systems: numerous new detections and their interpretation. ApJ 502(1):394–407. https://doi.org/10.1086/305907. arXiv:astro-ph/9802356 [astro-ph]

Sago N, Fujita R (2015) Calculation of radiation reaction effect on orbital parameters in Kerr spacetime. Prog Theor Exp Phys 2015(7):073E03. https://doi.org/10.1093/ptep/ptv092. arXiv:1505.01600 [gr-qc]

Sahu N, Graham AW, Davis BL (2019) Black hole mass scaling relations for early-type galaxies. I. M_{BH}-$M_{*,sph}$ and M_{BH}-$M_{*,gal}$. ApJ 876(2):155. https://doi.org/10.3847/1538-4357/ab0f32. arXiv:1903.04738 [astro-ph.GA]

Sahu N, Graham AW, Davis BL (2019) Revealing hidden substructures in the M_{BH}-σ diagram, and refining the bend in the L-σ relation. ApJ 887(1):10. https://doi.org/10.3847/1538-4357/ab50b7. arXiv:1908.06838 [astro-ph.GA]

Sahu N, Graham AW, Davis BL (2020) Defining the (black hole)-spheroid connection with the discovery of morphology-dependent substructure in the M_{BH}-n_{sph} and M_{BH}-$R_{e,sph}$ diagrams: new tests for advanced theories and realistic simulations. ApJ 903(2):97. https://doi.org/10.3847/1538-4357/abb675. arXiv:2101.04895 [astro-ph.GA]

Saito R, Yokoyama J (2009) Gravitational wave background as a probe of the primordial black hole abundance. Phys Rev Lett 102:161101. https://doi.org/10.1103/PhysRevLett.102.161101 [Erratum: Phys Rev Lett 107, 069901 (2011)] arXiv:0812.4339 [astro-ph]

Sakurai Y, Vorobyov EI, Hosokawa T, Yoshida N, Omukai K, Yorke HW (2016) Supermassive star formation via episodic accretion: protostellar disc instability and radiative feedback efficiency. MNRAS 459:1137–1145. https://doi.org/10.1093/mnras/stw637. arXiv:1511.06080 [astro-ph.SR]

Sakurai Y, Yoshida N, Fujii MS, Hirano S (2017) Formation of intermediate-mass black holes through runaway collisions in the first star clusters. MNRAS 472(2):1677–1684. https://doi.org/10.1093/mnras/stx2044. arXiv:1704.06130 [astro-ph.GA]

Sakurai Y, Yoshida N, Fujii MS (2019) Growth of intermediate mass black holes by tidal disruption events in the first star clusters. MNRAS 484(4):4665–4677. https://doi.org/10.1093/mnras/stz315. arXiv:1810.01985 [astro-ph.GA]

Sakurai Y, Haiman Z, Inayoshi K (2020) Radiative feedback for supermassive star formation in a massive cloud with H_2 molecules in an atomic-cooling halo. MNRAS 499(4):5960–5971. https://doi.org/10.1093/mnras/staa3227. arXiv:2009.02629 [astro-ph.GA]

Sala L, Cenci E, Capelo PR, Lupi A, Dotti M (2021) Non-isotropic feedback from accreting spinning black holes. MNRAS 500(4):4788–4800. https://doi.org/10.1093/mnras/staa3552. arXiv:2011.06606 [astro-ph.GA]

Saladino MI, Pols OR, van der Helm E, Pelupessy I, Portegies Zwart S (2018) Gone with the wind: the impact of wind mass transfer on the orbital evolution of AGB binary systems. A&A 618:A50. https://doi.org/10.1051/0004-6361/201832967. arXiv:1805.03208 [astro-ph.SR]

Saladino MI, Pols OR, Abate C (2019) Slowly, slowly in the wind. 3D hydrodynamical simulations of wind mass transfer and angular-momentum loss in AGB binary systems. A&A 626:A68. https://doi.org/10.1051/0004-6361/201834598. arXiv:1903.04515 [astro-ph.SR]

Salcido J, Bower RG, Theuns T, McAlpine S, Schaller M, Crain RA, Schaye J, Regan J (2016) Music from the heavens—gravitational waves from supermassive black hole mergers in the EAGLE simulations. MNRAS 463(1):870–885. https://doi.org/10.1093/mnras/stw2048. arXiv:1601.06156 [astro-ph.GA]

Samsing J (2018) Eccentric black hole mergers forming in globular clusters. Phys Rev D 97(10):103014. https://doi.org/10.1103/PhysRevD.97.103014. arXiv:1711.07452 [astro-ph.HE]

Samsing J, D'Orazio DJ (2018) Black hole mergers from globular clusters observable by LISA I: eccentric sources originating from relativistic n-body dynamics. MNRAS 481(4):5445–5450. https://doi.org/10.1093/mnras/sty2334. arXiv:1804.06519 [astro-ph.HE]

Samsing J, D'Orazio DJ (2019) How post-Newtonian dynamics shape the distribution of stationary binary black hole LISA sources in nearby globular clusters. Phys Rev D 99(6):063006. https://doi.org/10.1103/PhysRevD.99.063006. arXiv:1807.08864 [astro-ph.HE]

Samsing J, Hotokezaka K (2021) Populating the black hole mass gaps in stellar clusters: general relations and upper limits. ApJ 923:126. https://doi.org/10.3847/1538-4357/ac2b27. arXiv:2006.09744 [astro-ph.HE]

Samsing J, MacLeod M, Ramirez-Ruiz E (2014) The formation of eccentric compact binary inspirals and the role of gravitational wave emission in binary-single stellar encounters. ApJ 784(1):71. https://doi.org/10.1088/0004-637X/784/1/71. arXiv:1308.2964 [astro-ph.HE]

Sand C, Ohlmann ST, Schneider FRN, Pakmor R, Röpke FK (2020) Common-envelope evolution with an asymptotic giant branch star. A&A 644:A60. https://doi.org/10.1051/0004-6361/202038992. arXiv:2007.11000 [astro-ph.SR]

Sanders GH (2013) The thirty meter telescope (TMT): an international observatory. J Astrophys Astron 34(2):81–86. https://doi.org/10.1007/s12036-013-9169-5

Sanders JL, Evans NW, Dehnen W (2018) Tidal disruption of dwarf spheroidal galaxies: the strange case of Crater II. MNRAS 478(3):3879–3889. https://doi.org/10.1093/mnras/sty1278. arXiv:1802.09537 [astro-ph.GA]

Sandquist EL, Taam RE, Burkert A (2000) On the formation of helium double degenerate stars and pre-cataclysmic variables. ApJ 533(2):984–997. https://doi.org/10.1086/308687. arXiv:astro-ph/9912243 [astro-ph]

Santamaría L, Ohme F, Ajith P, Brügmann B, Dorband N, Hannam M, Husa S, Mösta P, Pollney D, Reisswig C et al (2010) Matching post-Newtonian and numerical relativity waveforms: systematic errors and a new phenomenological model for nonprecessing black hole binaries. Phys Rev D 82(6):064016. https://doi.org/10.1103/PhysRevD.82.064016. arXiv:1005.3306 [gr-qc]

Santoliquido F, Mapelli M, Bouffanais Y, Giacobbo N, Di Carlo UN, Rastello S, Artale MC, Ballone A (2020) The cosmic merger rate density evolution of compact binaries formed in young star clusters and in isolated binaries. ApJ 898(2):152. https://doi.org/10.3847/1538-4357/ab9b78. arXiv:2004.09533 [astro-ph.HE]

Santoliquido F, Mapelli M, Giacobbo N, Bouffanais Y, Artale MC (2021) The cosmic merger rate density of compact objects: impact of star formation, metallicity, initial mass function and binary evolution. MNRAS 502:4877–4889. https://doi.org/10.1093/mnras/stab280. arXiv:2009.03911 [astro-ph.HE]

Sanyal D, Grassitelli L, Langer N, Bestenlehner JM (2015) Massive main-sequence stars evolving at the Eddington limit. A&A 580:A20. https://doi.org/10.1051/0004-6361/201525945. arXiv:1506.02997 [astro-ph.SR]

Sasaki M, Suyama T, Tanaka T, Yokoyama S (2016) Primordial black hole scenario for the gravitational-wave event GW150914. Phys Rev Lett 117(6):061101. https://doi.org/10.1103/PhysRevLett.117.061101 [Erratum: Phys Rev Lett 121, 059901 (2018)] arXiv:1603.08338 [astro-ph.CO]

Sato S, Kawamura S, Ando M, Nakamura T, Tsubono K, Araya A, et al (2017) The status of DECIGO. J Phys Conf Ser 840:012010. https://doi.org/10.1088/1742-6596/840/1/012010

Sawai H, Kotake K, Yamada S (2008) Numerical simulations of equatorially asymmetric magnetized supernovae: formation of magnetars and their kicks. ApJ 672(1):465–478. https://doi.org/10.1086/523624. arXiv:0709.1795 [astro-ph]

Saxton R, Komossa S, Auchettl K, Jonker PG (2020) X-ray properties of TDEs. Space Sci Rev 216(5):85. https://doi.org/10.1007/s11214-020-00708-4

Sayeb M, Blecha L, Kelley LZ, Gerosa D, Kesden M, Thomas J (2021) Massive black hole binary inspiral and spin evolution in a cosmological framework. MNRAS 501(2):2531–2546. https://doi.org/10.1093/mnras/staa3826. arXiv:2006.06647 [astro-ph.GA]

Sberna L, Toubiana A, Miller MC (2021) Golden galactic binaries for LISA: mass-transferring white dwarf black hole binaries. ApJ 908:1. https://doi.org/10.3847/1538-4357/abccc7. arXiv:2010.05974 [astro-ph.SR]

Schaye J, Crain RA, Bower RG, Furlong M, Schaller M, Theuns T, Dalla Vecchia C, Frenk CS, McCarthy IG, Helly JC et al (2015) The EAGLE project: simulating the evolution and assembly of galaxies and their environments. MNRAS 446(1):521–554. https://doi.org/10.1093/mnras/stu2058. arXiv:1407.7040 [astro-ph.GA]

Scheck L, Kifonidis K, Janka HT, Müller E (2006) Multidimensional supernova simulations with approximative neutrino transport. I. Neutron star kicks and the anisotropy of neutrino-driven explosions in two spatial dimensions. A&A 457(3):963–986. https://doi.org/10.1051/0004-6361:20064855. arXiv:astro-ph/0601302 [astro-ph]

Scheel MA, Boyle M, Chu T, Kidder LE, Matthews KD, Pfeiffer HP (2009) High-accuracy waveforms for binary black hole inspiral, merger, and ringdown. Phys Rev D 79(2):024003. https://doi.org/10.1103/PhysRevD.79.024003. arXiv:0810.1767 [gr-qc]

Schleicher DRG, Dreizler S (2014) Planet formation from the ejecta of common envelopes. A&A 563:A61. https://doi.org/10.1051/0004-6361/201322860. arXiv:1312.3479 [astro-ph.EP]

Schleicher DRG, Reinoso B, Latif M, Klessen RS, Vergara MZC, Das A, Alister P, Díaz VB, Solar PA (2022) Origin of supermassive black holes in massive metal-poor protoclusters. MNRAS 512(4):6192–6200. https://doi.org/10.1093/mnras/stac926. arXiv:2204.02361 [astro-ph.GA]

Schneider R, Ferrari V, Matarrese S, Portegies Zwart SF (2001) Low-frequency gravitational waves from cosmological compact binaries. MNRAS 324(4):797–810. https://doi.org/10.1046/j.1365-8711.2001.04217.x. arXiv:astro-ph/0002055 [astro-ph]

Schneider R, Graziani L, Marassi S, Spera M, Mapelli M, Alparone M, Bennassuti Md (2017) The formation and coalescence sites of the first gravitational wave events. MNRAS 471(1):L105–L109. https://doi.org/10.1093/mnrasl/slx118. arXiv:1705.06781 [astro-ph.GA]

Schnittman JD (2007) Retaining black holes with very large recoil velocities. ApJ 667(2):L133–L136. https://doi.org/10.1086/522203. arXiv:0706.1548 [astro-ph]

Schnittman JD, Buonanno A (2007) The distribution of recoil velocities from merging black holes. ApJ 662(2):L63–L66. https://doi.org/10.1086/519309. arXiv:astro-ph/0702641 [astro-ph]

Schnittman JD, Krolik JH (2008) The infrared afterglow of supermassive black hole mergers. ApJ 684(2):835–844. https://doi.org/10.1086/590363. arXiv:0802.3556 [astro-ph]

Schnittman JD, Krolik JH (2009) X-ray polarization from accreting black holes: the thermal state. ApJ 701(2):1175–1187. https://doi.org/10.1088/0004-637X/701/2/1175. arXiv:0902.3982 [astro-ph.HE]

Schödel R, Gallego-Cano E, Dong H, Nogueras-Lara F, Gallego-Calvente AT, Amaro-Seoane P, Baumgardt H (2018) The distribution of stars around the Milky Way's central black hole. II. Diffuse light from sub-giants and dwarfs. A&A 609:A27. https://doi.org/10.1051/0004-6361/201730452. arXiv:1701.03817 [astro-ph.GA]

Schröder KP, Smith RC (2008) Distant future of the Sun and Earth revisited. MNRAS 386(1):155–163. https://doi.org/10.1111/j.1365-2966.2008.13022.x. arXiv:0801.4031 [astro-ph]

Scott N, Graham AW (2013) Updated mass scaling relations for nuclear star clusters and a comparison to supermassive black holes. ApJ 763(2):76. https://doi.org/10.1088/0004-637X/763/2/76. arXiv:1205.5338 [astro-ph.CO]

Scrimgeour MI, Davis TM, Blake C, Staveley-Smith L, Magoulas C, Springob CM, Beutler F, Colless M, Johnson A, Jones DH et al (2016) The 6dF galaxy survey: bulk flows on 50–70 h^{-1} Mpc scales. MNRAS 455(1):386–401. https://doi.org/10.1093/mnras/stv2146. arXiv:1511.06930 [astro-ph.CO]

Secunda A, Bellovary J, Mac Low MM, Ford KES, McKernan B, Leigh NWC, Lyra W, Sándor Z (2019) Orbital migration of interacting stellar mass black holes in disks around supermassive black holes. ApJ 878(2):85. https://doi.org/10.3847/1538-4357/ab20ca. arXiv:1807.02859 [astro-ph.HE]

Secunda A, Bellovary J, Mac Low MM, Ford KES, McKernan B, Leigh NWC, Lyra W, Sándor Z, Adorno JI (2020) Orbital migration of interacting stellar mass black holes in disks around supermassive black holes. II. Spins and incoming objects. ApJ 903(2):133. https://doi.org/10.3847/1538-4357/abbc1d. arXiv:2004.11936 [astro-ph.HE]

Secunda A, Hernandez B, Goodman J, Leigh NWC, McKernan B, Ford KES, Adorno JI (2021) Evolution of retrograde orbiters in an active galactic nucleus disk. ApJ 908(2):L27. https://doi.org/10.3847/2041-8213/abe11d. arXiv:2009.03910 [astro-ph.HE]

Seigar MS, Kennefick D, Kennefick J, Lacy CHS (2008) Discovery of a relationship between spiral arm morphology and supermassive black hole mass in disk galaxies. ApJ 678(2):L93. https://doi.org/10.1086/588727. arXiv:0804.0773 [astro-ph]

Seitenzahl IR, Cescutti G, Röpke FK, Ruiter AJ, Pakmor R (2013) Solar abundance of manganese: a case for near Chandrasekhar-mass Type Ia supernova progenitors. A&A 559:L5. https://doi.org/10.1051/0004-6361/201322599. arXiv:1309.2397 [astro-ph.SR]

Seitenzahl IR, Herzog M, Ruiter AJ, Marquardt K, Ohlmann ST, Röpke FK (2015) Neutrino and gravitational wave signal of a delayed-detonation model of type Ia supernovae. Phys Rev D 92(12):124013. https://doi.org/10.1103/PhysRevD.92.124013. arXiv:1511.02542 [astro-ph.SR]

Sellwood JA (2014) Secular evolution in disk galaxies. Rev Mod Phys 86(1):1–46. https://doi.org/10.1103/RevModPhys.86.1. arXiv:1310.0403 [astro-ph.GA]

Sengar R, Tauris TM, Langer N, Istrate AG (2017) Novel modelling of ultracompact X-ray binary evolution—stable mass transfer from white dwarfs to neutron stars. MNRAS 470(1):L6–L10. https://doi.org/10.1093/mnrasl/slx064. arXiv:1704.08260 [astro-ph.SR]

Serpico PD, Poulin V, Inman D, Kohri K (2020) Cosmic microwave background bounds on primordial black holes including dark matter halo accretion. Phys Rev Res 2(2):023204. https://doi.org/10.1103/PhysRevResearch.2.023204. arXiv:2002.10771 [astro-ph.CO]

Sesana A (2007) Extreme recoils: impact on the detection of gravitational waves from massive black hole binaries. MNRAS 382(1):L6–L10. https://doi.org/10.1111/j.1745-3933.2007.00375.x. arXiv:0707.4677 [astro-ph]

Sesana A (2016) Prospects for multiband gravitational-wave astronomy after GW150914. Phys Rev Lett 116(23):231102. https://doi.org/10.1103/PhysRevLett.116.231102. arXiv:1602.06951 [gr-qc]

Sesana A (2017) Multi-band gravitational wave astronomy: science with joint space- and ground-based observations of black hole binaries. J Phys Conf Ser 840:012018. https://doi.org/10.1088/1742-6596/840/1/012018. arXiv:1702.04356 [astro-ph.HE]

Sesana A, Khan FM (2015) Scattering experiments meet N-body—I. A practical recipe for the evolution of massive black hole binaries in stellar environments. MNRAS 454(1):L66–L70. https://doi.org/10.1093/mnrasl/slv131. arXiv:1505.02062 [astro-ph.GA]

Sesana A, Haardt F, Madau P, Volonteri M (2005) The gravitational wave signal from massive black hole binaries and its contribution to the LISA data stream. ApJ 623(1):23–30. https://doi.org/10.1086/428492. arXiv:astro-ph/0409255 [astro-ph]

Sesana A, Haardt F, Madau P (2006) Interaction of massive black hole binaries with their stellar environment. I. Ejection of hypervelocity stars. ApJ 651(1):392–400. https://doi.org/10.1086/507596. arXiv:astro-ph/0604299 [astro-ph]

Sesana A, Haardt F, Madau P (2008) Interaction of massive black hole binaries with their stellar environment. III. Scattering of bound stars. ApJ 686(1):432–447. https://doi.org/10.1086/590651. arXiv:0710.4301 [astro-ph]

Sesana A, Vecchio A, Eracleous M, Sigurdsson S (2008) Observing white dwarfs orbiting massive black holes in the gravitational wave and electro-magnetic window. MNRAS 391(2):718–726. https://doi.org/10.1111/j.1365-2966.2008.13904.x. arXiv:0806.0624 [astro-ph]

Sesana A, Vecchio A, Volonteri M (2009) Gravitational waves from resolvable massive black hole binary systems and observations with Pulsar Timing Arrays. MNRAS 394(4):2255–2265. https://doi.org/10.1111/j.1365-2966.2009.14499.x. arXiv:0809.3412 [astro-ph]

Sesana A, Gair J, Berti E, Volonteri M (2011) Reconstructing the massive black hole cosmic history through gravitational waves. Phys Rev D 83(4):044036. https://doi.org/10.1103/PhysRevD.83.044036. arXiv:1011.5893 [astro-ph.CO]

Sesana A, Gualandris A, Dotti M (2011) Massive black hole binary eccentricity in rotating stellar systems. MNRAS 415(1):L35–L39. https://doi.org/10.1111/j.1745-3933.2011.01073.x. arXiv:1105.0670 [astro-ph.GA]

Sesana A, Roedig C, Reynolds MT, Dotti M (2012) Multimessenger astronomy with pulsar timing and x-ray observations of massive black hole binaries. MNRAS 420(1):860–877. https://doi.org/10.1111/j.1365-2966.2011.20097.x. arXiv:1107.2927 [astro-ph.CO]

Sesana A, Barausse E, Dotti M, Rossi EM (2014) Linking the spin evolution of massive black holes to galaxy kinematics. ApJ 794(2):104. https://doi.org/10.1088/0004-637X/794/2/104. arXiv:1402.7088 [astro-ph.CO]

Sesana A, Lamberts A, Petiteau A (2020) Finding binary black holes in the Milky Way with LISA. MNRAS 494(1):L75–L80. https://doi.org/10.1093/mnrasl/slaa039. arXiv:1912.07627 [astro-ph.GA]

Sesana A, Korsakova N, Arca Sedda M, Baibhav V, Barausse E, Barke S, Berti E, Bonetti M, Capelo PR, Caprini C et al (2021) Unveiling the gravitational universe at μ-Hz frequencies. Exp Astron 51 (3):1333–1383. https://doi.org/10.1007/s10686-021-09709-9. arXiv:1908.11391 [astro-ph.IM]

Seto N (2016) Prospects of eLISA for detecting Galactic binary black holes similar to GW150914. MNRAS 460(1):L1–L4. https://doi.org/10.1093/mnrasl/slw060. arXiv:1602.04715 [astro-ph.HE]

Seto N (2019) Search for neutron star binaries in the Local Group galaxies using LISA. MNRAS 489 (4):4513–4519. https://doi.org/10.1093/mnras/stz2439. arXiv:1909.01471 [astro-ph.HE]

Severgnini P, Cicone C, Della Ceca R, Braito V, Caccianiga A, Ballo L, Campana S, Moretti A, La Parola V, Vignali C et al (2018) Swift data hint at a binary supermassive black hole candidate at sub-parsec separation. MNRAS 479(3):3804–3813. https://doi.org/10.1093/mnras/sty1699. arXiv:1806.10150 [astro-ph.HE]

Shah S, Nelemans G (2014) Constraining parameters of white-dwarf binaries using gravitational-wave and electromagnetic observations. ApJ 790(2):161. https://doi.org/10.1088/0004-637X/790/2/161. arXiv:1406.3599 [astro-ph.SR]

Shah S, Nelemans G (2014) Measuring tides and binary parameters from gravitational wave data and eclipsing timings of detached white dwarf binaries. ApJ 791(2):76. https://doi.org/10.1088/0004-637X/791/2/76. arXiv:1406.3603 [astro-ph.SR]

Shah S, van der Sluys M, Nelemans G (2012) Using electromagnetic observations to aid gravitational-wave parameter estimation of compact binaries observed with LISA. A&A 544:A153. https://doi.org/10.1051/0004-6361/201219309. arXiv:1207.6770 [astro-ph.IM]

Shah S, Nelemans G, van der Sluys M (2013) Using electromagnetic observations to aid gravitational-wave parameter estimation of compact binaries observed with LISA. II. The effect of knowing the sky position. A&A 553:A82. https://doi.org/10.1051/0004-6361/201321123. arXiv:1303.6116 [astro-ph.IM]

Shakura NI, Sunyaev RA (1973) Reprint of 1973A&A....24.337S. Black holes in binary systems. Observational appearance. A&A 500:33–51

Shakura NI, Sunyaev RA (1976) A theory of the instability of disk accretion on to black holes and the variability of binary X-ray sources, galactic nuclei and quasars. MNRAS 175:613–632. https://doi.org/10.1093/mnras/175.3.613

Shankar F (2009) The demography of supermassive black holes: growing monsters at the heart of galaxies. New A Rev 53(4–6):57–77. https://doi.org/10.1016/j.newar.2009.07.006. arXiv:0907.5213 [astro-ph.CO]

Shankar F, Weinberg DH, Miralda-Escudé J (2009) Self-consistent models of the AGN and black hole populations: duty cycles, accretion rates, and the mean radiative efficiency. ApJ 690(1):20–41. https://doi.org/10.1088/0004-637X/690/1/20. arXiv:0710.4488 [astro-ph]

Shankar F, Weinberg DH, Miralda-Escudé J (2013) Accretion-driven evolution of black holes: Eddington ratios, duty cycles and active galaxy fractions. MNRAS 428(1):421–446. https://doi.org/10.1093/mnras/sts026. arXiv:1111.3574 [astro-ph.CO]

Shannon RM, Ravi V, Lentati LT, Lasky PD, Hobbs G, Kerr M, Manchester RN, Coles WA, Levin Y, Bailes M et al (2015) Gravitational waves from binary supermassive black holes missing in pulsar observations. Science 349(6255):1522–1525. https://doi.org/10.1126/science.aab1910. arXiv:1509.07320 [astro-ph.CO]

Shao L, Sennett N, Buonanno A, Kramer M, Wex N (2017) Constraining nonperturbative strong-field effects in scalar-tensor gravity by combining pulsar timing and laser-interferometer gravitational-wave detectors. Phys Rev X 7(4):041025. https://doi.org/10.1103/PhysRevX.7.041025. arXiv:1704.07561 [gr-qc]

Shapiro SL, Marchant AB (1978) Star clusters containing massive, central black holes: Monte Carlo simulations in two-dimensional phase space. ApJ 225:603–624. https://doi.org/10.1086/156521

Shappee BJ, Thompson TA (2013) The mass-loss-induced eccentric Kozai mechanism: a new channel for the production of close compact object-stellar binaries. ApJ 766(1):64. https://doi.org/10.1088/0004-637X/766/1/64. arXiv:1204.1053 [astro-ph.SR]

Shemmer O, Netzer H, Maiolino R, Oliva E, Croom S, Corbett E, di Fabrizio L (2004) Near-infrared spectroscopy of high-redshift active galactic nuclei. I. A metallicity-accretion rate relationship. ApJ 614(2):547–557. https://doi.org/10.1086/423607. arXiv:astro-ph/0406559 [astro-ph]

Shen KJ (2015) Every interacting double white dwarf binary may merge. ApJ 805(1):L6. https://doi.org/10.1088/2041-8205/805/1/L6. arXiv:1502.05052 [astro-ph.SR]

Shen X, Hopkins PF, Faucher-Giguère CA, Alexander DM, Richards GT, Ross NP, Hickox RC (2020) The bolometric quasar luminosity function at z = 0–7. MNRAS 495(3):3252–3275. https://doi.org/10.1093/mnras/staa1381. arXiv:2001.02696 [astro-ph.GA]

Shen Y, Liu X, Loeb A, Tremaine S (2013) Constraining sub-parsec binary supermassive black holes in quasars with multi-epoch spectroscopy. I. The general quasar population. ApJ 775(1):49. https://doi.org/10.1088/0004-637X/775/1/49. arXiv:1306.4330 [astro-ph.CO]

Sheth K, Elmegreen DM, Elmegreen BG, Capak P, Abraham RG, Athanassoula E, Ellis RS, Mobasher B, Salvato M, Schinnerer E et al (2008) Evolution of the bar fraction in COSMOS: quantifying the assembly of the hubble sequence. ApJ 675(2):1141–1155. https://doi.org/10.1086/524980. arXiv:0710.4552 [astro-ph]

Shi JM, Krolik JH (2016) How bright are the gaps in circumbinary disk systems? ApJ 832(1):22. https://doi.org/10.3847/0004-637x/832/1/22

Shibata M, Taniguchi K (2011) Coalescence of black hole-neutron star binaries. Living Rev Relativ https://doi.org/10.12942/lrr-2011-6

Shibata M, Sekiguchi Y, Uchida H, Umeda H (2016) Gravitational waves from supermassive stars collapsing to a supermassive black hole. Phys Rev D 94(2):021501. https://doi.org/10.1103/PhysRevD.94.021501. arXiv:1606.07147 [astro-ph.HE]

Shiber S, Iaconi R, De Marco O, Soker N (2019) Companion-launched jets and their effect on the dynamics of common envelope interaction simulations. MNRAS 488(4):5615–5632. https://doi.org/10.1093/mnras/stz2013. arXiv:1902.03931 [astro-ph.SR]

Shibuya T, Ouchi M, Kubo M, Harikane Y (2016) Morphologies of ∼ 190,000 galaxies at z = 0–10 revealed with HST legacy data. II. Evolution of clumpy galaxies. ApJ 821(2):72. https://doi.org/10.3847/0004-637X/821/2/72. arXiv:1511.07054 [astro-ph.GA]

Shields GA, Bonning EW (2008) Powerful flares from recoiling black holes in quasars. ApJ 682(2):758–766. https://doi.org/10.1086/589427. arXiv:0802.3873 [astro-ph]

Shiokawa H, Krolik JH, Cheng RM, Piran T, Noble SC (2015) General relativistic hydrodynamic simulation of accretion flow around a stellar tidal disruption. ApJ 804(2):85. https://doi.org/10.1088/0004-637X/804/2/85. arXiv:1501.04365 [astro-ph.HE]

Shirakata H, Okamoto T, Kawaguchi T, Nagashima M, Ishiyama T, Makiya R, Kobayashi MAR, Enoki M, Oogi T, Okoshi K (2019) The new numerical galaxy catalogue (v^2GC): properties of active galactic nuclei and their host galaxies. MNRAS 482(4):4846–4873. https://doi.org/10.1093/mnras/sty2958. arXiv:1802.02169 [astro-ph.GA]

Shlosman I, Begelman MC (1989) Evolution of self-gravitating accretion disks in active galactic nuclei. ApJ 341:685. https://doi.org/10.1086/167526

Shore SN, Livio M, van den Heuvel EPJ (1994) Interacting binaries, Saas-Fee Advanced Course, vol 22. Springer. https://doi.org/10.1007/3-540-31626-4

Shuman KJ, Cornish NJ (2022) Massive black hole binaries and where to find them with dual detector networks. Phys Rev D 105(6):064055. https://doi.org/10.1103/PhysRevD.105.064055. arXiv:2105.02943 [gr-qc]

Siemens X, Mandic V, Creighton J (2007) Gravitational-wave stochastic background from cosmic strings. Phys Rev Lett 98(11):111101. https://doi.org/10.1103/PhysRevLett.98.111101. arXiv:astro-ph/0610920 [astro-ph]

Sigurdsson S, Phinney ES (1993) Binary-single star interactions in globular clusters. ApJ 415:631. https://doi.org/10.1086/173190

Sigurdsson S, Rees MJ (1997) Capture of stellar mass compact objects by massive black holes in galactic cusps. MNRAS 284(2):318–326. https://doi.org/10.1093/mnras/284.2.318. arXiv:astro-ph/9608093 [astro-ph]

Sigurdsson S, Richer HB, Hansen BM, Stairs IH, Thorsett SE (2003) A young white dwarf companion to pulsar B1620–26: evidence for early planet formation. Science 301(5630):193–196. https://doi.org/10.1126/science.1086326. arXiv:astro-ph/0307339 [astro-ph]

Sijacki D, Springel V, Di Matteo T, Hernquist L (2007) A unified model for AGN feedback in cosmological simulations of structure formation. MNRAS 380(3):877–900. https://doi.org/10.1111/j.1365-2966.2007.12153.x. arXiv:0705.2238 [astro-ph]

Sijacki D, Springel V, Haehnelt MG (2011) Gravitational recoils of supermassive black holes in hydrodynamical simulations of gas-rich galaxies. MNRAS 414:3656–3670. https://doi.org/10.1111/j.1365-2966.2011.18666.x. arXiv:1008.3313

Sijacki D, Vogelsberger M, Genel S, Springel V, Torrey P, Snyder GF, Nelson D, Hernquist L (2015) The Illustris simulation: the evolving population of black holes across cosmic time. MNRAS 452(1):575–596. https://doi.org/10.1093/mnras/stv1340. arXiv:1408.6842 [astro-ph.GA]

Silsbee K, Tremaine S (2017) Lidov–Kozai cycles with gravitational radiation: merging black holes in isolated triple systems. ApJ 836(1):39. https://doi.org/10.3847/1538-4357/aa5729. arXiv:1608.07642 [astro-ph.HE]

Simmons BD, Melvin T, Lintott C, Masters KL, Willett KW, Keel WC, Smethurst RJ, Cheung E, Nichol RC, Schawinski K et al (2014) Galaxy Zoo: CANDELS barred discs and bar fractions. MNRAS 445(4):3466–3474. https://doi.org/10.1093/mnras/stu1817. arXiv:1409.1214 [astro-ph.GA]

Simon J, Burke-Spolaor S (2016) Constraints on black hole/host galaxy co-evolution and binary stalling using pulsar timing arrays. ApJ 826(1):11. https://doi.org/10.3847/0004-637X/826/1/11. arXiv:1603.06577 [astro-ph.GA]

Singh D, Wu K, Sarty GE (2014) Fast spinning pulsars as probes of massive black holes' gravity. MNRAS 441(1):800–808. https://doi.org/10.1093/mnras/stu614. arXiv:1403.7171 [astro-ph.HE]

Sippel AC, Hurley JR (2013) Multiple stellar-mass black holes in globular clusters: theoretical confirmation. MNRAS 430:L30–L34. https://doi.org/10.1093/mnrasl/sls044. arXiv:1211.6608 [astro-ph.GA]

Sirko E, Goodman J (2003) Spectral energy distributions of marginally self-gravitating quasi-stellar object discs. MNRAS 341(2):501–508. https://doi.org/10.1046/j.1365-8711.2003.06431.x

Sądowski A, Gaspari M (2017) Kinetic and radiative power from optically thin accretion flows. MNRAS 468(2):1398–1404. https://doi.org/10.1093/mnras/stx543. arXiv:1701.07033 [astro-ph.HE]

Sądowski A, Narayan R (2016) Three-dimensional simulations of supercritical black hole accretion discs —luminosities, photon trapping and variability. MNRAS 456(4):3929–3947. https://doi.org/10.1093/mnras/stv2941. arXiv:1509.03168 [astro-ph.HE]

Skillman DR, Patterson J, Kemp J, Harvey DA, Fried RE, Retter A, Lipkin Y, Vanmunster T (1999) Superhumps in cataclysmic binaries. XVII. AM Canum Venaticorum. PASP 111(764):1281–1291. https://doi.org/10.1086/316437

Smarr LL, Blandford R (1976) The binary pulsar: physical processes, possible companions, and evolutionary histories. ApJ 207:574–588. https://doi.org/10.1086/154524

Smith BD, Wise JH, O'Shea BW, Norman ML, Khochfar S (2015) The first Population II stars formed in externally enriched mini-haloes. MNRAS 452:2822–2836. https://doi.org/10.1093/mnras/stv1509. arXiv:1504.07639

Smith BD, Regan JA, Downes TP, Norman ML, O'Shea BW, Wise JH (2018) The growth of black holes from Population III remnants in the Renaissance simulations. MNRAS 480(3):3762–3773. https://doi.org/10.1093/mnras/sty2103. arXiv:1804.06477 [astro-ph.GA]

Smith TL, Caldwell RR (2019) LISA for cosmologists: calculating the signal-to-noise ratio for stochastic and deterministic sources. Phys Rev D 100(10):104055. https://doi.org/10.1103/PhysRevD.100.104055. arXiv:1908.00546 [astro-ph.CO]

Snyder GF, Rodriguez-Gomez V, Lotz JM, Torrey P, Quirk ACN, Hernquist L, Vogelsberger M, Freeman PE (2019) Automated distant galaxy merger classifications from Space Telescope images using the Illustris simulation. MNRAS 486(3):3702–3720. https://doi.org/10.1093/mnras/stz1059. arXiv:1809.02136 [astro-ph.GA]

Soberman GE, Phinney ES, van den Heuvel EPJ (1997) Stability criteria for mass transfer in binary stellar evolution. A&A 327:620–635 arXiv:astro-ph/9703016 [astro-ph]

Soker N, Tylenda R (2003) Main-sequence stellar eruption model for V838 monocerotis. ApJ 582(2): L105–L108. https://doi.org/10.1086/367759. arXiv:astro-ph/0210463 [astro-ph]

Solanki S, Kupfer T, Blaes O, Breedt E, Scaringi S (2021) Periodicities in the K2 light curve of HP Librae. MNRAS 500(1):1222–1230. https://doi.org/10.1093/mnras/staa3240. arXiv:2010.09754 [astro-ph.HE]

Solheim JE (2010) AM CVn stars: status and challenges. PASP 122(896):1133. https://doi.org/10.1086/656680

Soltan A (1982) Masses of quasars. MNRAS 200:115–122. https://doi.org/10.1093/mnras/200.1.115

Somerville RS, Hopkins PF, Cox TJ, Robertson BE, Hernquist L (2008) A semi-analytic model for the co-evolution of galaxies, black holes and active galactic nuclei. MNRAS 391(2):481–506. https://doi.org/10.1111/j.1365-2966.2008.13805.x. arXiv:0808.1227 [astro-ph]

Souza Lima R, Mayer L, Capelo PR, Bellovary JM (2017) The pairing of accreting massive black holes in multiphase circumnuclear disks: the interplay between radiative cooling, star formation, and feedback processes. ApJ 838(1):13. https://doi.org/10.3847/1538-4357/aa5d19. arXiv:1610.01600 [astro-ph.GA]

Souza Lima R, Mayer L, Capelo PR, Bortolas E, Quinn TR (2020) The erratic path to coalescence of Lisa massive black hole binaries in subparsec-resolution simulations of smooth circumnuclear gas disks. ApJ 899(2):126. https://doi.org/10.3847/1538-4357/aba624. arXiv:2003.13789 [astro-ph.GA]

Spera M, Mapelli M (2017) Very massive stars, pair-instability supernovae and intermediate-mass black holes with the sevn code. MNRAS 470(4):4739–4749. https://doi.org/10.1093/mnras/stx1576. arXiv:1706.06109 [astro-ph.SR]

Spera M, Mapelli M, Bressan A (2015) The mass spectrum of compact remnants from the PARSEC stellar evolution tracks. MNRAS 451(4):4086–4103. https://doi.org/10.1093/mnras/stv1161. arXiv:1505.05201 [astro-ph.SR]

Spergel D, Gehrels N, Baltay C, Bennett D, Breckinridge J, Donahue M, Dressler A, Gaudi BS, Greene T, Guyon O et al (2015) Wide-field InfraRed survey telescope-astrophysics focused telescope assets WFIRST-AFTA 2015 report. arXiv e-prints arXiv:1503.03757 [astro-ph.IM]

Sperhake U (2015) The numerical relativity breakthrough for binary black holes. Class Quantum Grav 32(12):124011. https://doi.org/10.1088/0264-9381/32/12/124011. arXiv:1411.3997 [gr-qc]

Spitzer L (1969) Equipartition and the formation of compact nuclei in spherical stellar systems. ApJ 158:L139. https://doi.org/10.1086/180451

Spitzer L, Schwarzschild M (1951) The possible influence of interstellar clouds on stellar velocities. ApJ 114:385. https://doi.org/10.1086/145478

Spitzer L (1987) Dynamical evolution of globular clusters. Princeton University Press, Princeton

Springel V, White SDM, Tormen G, Kauffmann G (2001) Populating a cluster of galaxies—I. Results at [formmu2]z=0. MNRAS 328(3):726–750. https://doi.org/10.1046/j.1365-8711.2001.04912.x. arXiv:astro-ph/0012055 [astro-ph]

Springel V, Di Matteo T, Hernquist L (2005) Black holes in galaxy mergers: the formation of red elliptical galaxies. ApJ 620(2):L79–L82. https://doi.org/10.1086/428772. arXiv:astro-ph/0409436 [astro-ph]

Springel V, Di Matteo T, Hernquist L (2005) Modelling feedback from stars and black holes in galaxy mergers. MNRAS 361(3):776–794. https://doi.org/10.1111/j.1365-2966.2005.09238.x. arXiv:astro-ph/0411108 [astro-ph]

Sridhar S, Touma JR (2016) Stellar dynamics around a massive black hole—II. Resonant relaxation. MNRAS 458(4):4143–4161. https://doi.org/10.1093/mnras/stw543. arXiv:1509.02401 [astro-ph.GA]

Stadel JG (2001) Cosmological N-body simulations and their analysis. PhD thesis, University of Washington

Stanway ER, Eldridge JJ (2018) Re-evaluating old stellar populations. MNRAS 479(1):75–93. https://doi.org/10.1093/mnras/sty1353. arXiv:1805.08784 [astro-ph.GA]

Steele MM, Zepf SE, Maccarone TJ, Kundu A, Rhode KL, Salzer JJ (2014) Composition of an emission line system in black hole host globular cluster RZ2109. ApJ 785(2):147. https://doi.org/10.1088/0004-637X/785/2/147. arXiv:1403.2784 [astro-ph.GA]

Stella L (1987) A 685 second orbital period from the X-ray source 4U 1820-30 in the globular cluster NGC 6624. In: Variability of galactic and extragalactic X-ray sources, pp 157–164

Stella L, Priedhorsky W, White NE (1987) The discovery of a second orbital period from the X-ray source 4U 1820–30 in the globular cluster NGC 6624. ApJ 312:L17. https://doi.org/10.1086/184811

Stephan AP, Naoz S, Ghez AM, Witzel G, Sitarski BN, Do T, Kocsis B (2016) Merging binaries in the Galactic Center: the eccentric Kozai–Lidov mechanism with stellar evolution. MNRAS 460(4):3494–3504. https://doi.org/10.1093/mnras/stw1220. arXiv:1603.02709 [astro-ph.SR]

Stephan AP, Naoz S, Gaudi BS (2018) A-type stars, the destroyers of worlds: the lives and deaths of jupiters in evolving stellar binaries. AJ 156(3):128. https://doi.org/10.3847/1538-3881/aad6e5. arXiv:1806.04145 [astro-ph.SR]

Stephan AP, Naoz S, Ghez AM, Morris MR, Ciurlo A, Do T, Breivik K, Coughlin S, Rodriguez CL (2019) The fate of binaries in the galactic center: the mundane and the exotic. ApJ 878(1):58. https://doi.org/10.3847/1538-4357/ab1e4d. arXiv:1903.00010 [astro-ph.SR]

Stephan AP, Naoz S, Gaudi BS, Salas JM (2020) Eating planets for lunch and dinner: signatures of planet consumption by evolving stars. ApJ 889(1):45. https://doi.org/10.3847/1538-4357/ab5b00. arXiv:1909.05259 [astro-ph.SR]

Stevenson S, Berry CPL, Mandel I (2017) Hierarchical analysis of gravitational-wave measurements of binary black hole spin-orbit misalignments. MNRAS 471:2801–2811. https://doi.org/10.1093/mnras/stx1764. arXiv:1703.06873 [astro-ph.HE]

Stevenson S, Vigna-Gómez A, Mandel I, Barrett JW, Neijssel CJ, Perkins D, de Mink SE (2017) Formation of the first three gravitational-wave observations through isolated binary evolution. Nat Commun 8:14906. https://doi.org/10.1038/ncomms14906. arXiv:1704.01352 [astro-ph.HE]

Stone N, Sari R, Loeb A (2013) Consequences of strong compression in tidal disruption events. MNRAS 435(3):1809–1824. https://doi.org/10.1093/mnras/stt1270. arXiv:1210.3374 [astro-ph.HE]

Stone NC, van Velzen S (2016) An enhanced rate of tidal disruptions in the centrally overdense E+A Galaxy NGC 3156. ApJ 825(1):L14. https://doi.org/10.3847/2041-8205/825/1/L14. arXiv:1604.02056 [astro-ph.GA]

Stone NC, Küpper AHW, Ostriker JP (2017) Formation of massive black holes in galactic nuclei: runaway tidal encounters. MNRAS 467(4):4180–4199. https://doi.org/10.1093/mnras/stx097. arXiv:1606.01909 [astro-ph.GA]

Stone NC, Metzger BD, Haiman Z (2017) Assisted inspirals of stellar mass black holes embedded in AGN discs: solving the 'final au problem'. MNRAS 464(1):946–954. https://doi.org/10.1093/mnras/stw2260. arXiv:1602.04226 [astro-ph.GA]

Stone NC, Generozov A, Vasiliev E, Metzger BD (2018) The delay time distribution of tidal disruption flares. MNRAS 480(4):5060–5077. https://doi.org/10.1093/mnras/sty2045. arXiv:1709.00423 [astro-ph.GA]

Strader J, Chomiuk L, Maccarone TJ, Miller-Jones JCA, Seth AC (2012) Two stellar-mass black holes in the globular cluster M22. Nature 490(7418):71–73. https://doi.org/10.1038/nature11490. arXiv:1210.0901 [astro-ph.HE]

Stritzinger MD, Taddia F, Fraser M, Tauris TM, Contreras C, Drybye S, Galbany L, Holmbo S, Morrell N, Pastorello A et al (2020) The Carnegie Supernova Project II Observations of the luminous red nova AT 2014ej. A&A 639:A104. https://doi.org/10.1051/0004-6361/202038019. arXiv:2005.00076 [astro-ph.HE]

Stroeer A, Vecchio A (2006) The LISA verification binaries. Class Quantum Grav 23(19):S809–S817. https://doi.org/10.1088/0264-9381/23/19/S19. arXiv:astro-ph/0605227 [astro-ph]

Stroeer A, Gair J, Vecchio A (2006) Automatic Bayesian inference for LISA data analysis strategies. In: Merkovitz SM, Livas JC (eds) Laser interferometer space antenna: 6th international LISA symposium. American institute of physics conference series, vol 873, pp 444–451. https://doi.org/10.1063/1.2405082. arXiv:gr-qc/0609010 [gr-qc]

Strohmayer TE (2004) Chandra detection of the AM Canum Venaticorum binary ES Ceti (KUV 01584–0939). ApJ 614(1):358–362. https://doi.org/10.1086/423615. arXiv:astro-ph/0405203 [astro-ph]

Strohmayer TE (2005) Precision X-ray timing of RX J0806.3+1527 with Chandra: evidence for gravitational radiation from an ultracompact binary. ApJ 627(2):920–925. https://doi.org/10.1086/430439. arXiv:astro-ph/0504150 [astro-ph]

Strubbe LE, Quataert E (2009) Optical flares from the tidal disruption of stars by massive black holes. MNRAS 400(4):2070–2084. https://doi.org/10.1111/j.1365-2966.2009.15599.x. arXiv:0905.3735 [astro-ph.CO]

Sun L, Paschalidis V, Ruiz M, Shapiro SL (2017) Magnetorotational collapse of supermassive stars: black hole formation, gravitational waves and jets. Phys Rev D 96(4):043006. https://doi.org/10.1103/PhysRevD.96.043006. arXiv:1704.04502 [astro-ph.HE]

Sun L, Ruiz M, Shapiro SL (2018) Simulating the magnetorotational collapse of supermassive stars: incorporating gas pressure perturbations and different rotation profiles. Phys Rev D 98(10):103008. https://doi.org/10.1103/PhysRevD.98.103008. arXiv:1807.07970 [astro-ph.HE]

Sutantyo W (1975) The formation of globular cluster X-ray sources through neutron star—giant collisions. A&A 44:227–230

Suvorov AG (2021) Ultra-compact X-ray binaries as dual-line gravitational-wave sources. MNRAS 503(4):5495–5503. https://doi.org/10.1093/mnras/stab825. arXiv:2103.09858 [astro-ph.HE]

Syer D, Clarke CJ, Rees MJ (1991) Star-disc interactions near a massive black hole. MNRAS 250:505–512. https://doi.org/10.1093/mnras/250.3.505

Szölgyén Á, Kocsis B (2018) Black hole disks in galactic nuclei. Phys Rev Lett 121(10):101101. https://doi.org/10.1103/PhysRevLett.121.101101. arXiv:1803.07090 [astro-ph.GA]

Tacconi LJ, Genzel R, Saintonge A, Combes F, García-Burillo S, Neri R, Bolatto A, Contini T, Förster Schreiber NM, Lilly S et al (2018) PHIBSS: unified scaling relations of gas depletion time and molecular gas fractions. ApJ 853(2):179. https://doi.org/10.3847/1538-4357/aaa4b4. arXiv:1702.01140 [astro-ph.GA]

Tagawa H, Haiman Z, Kocsis B (2020) Formation and evolution of compact-object binaries in AGN disks. ApJ 898(1):25. https://doi.org/10.3847/1538-4357/ab9b8c. arXiv:1912.08218 [astro-ph.GA]

Tagawa H, Haiman Z, Kocsis B (2020) Making a supermassive star by stellar bombardment. ApJ 892(1):36. https://doi.org/10.3847/1538-4357/ab7922. arXiv:1909.10517 [astro-ph.GA]

Takács Á, Kocsis B (2018) Isotropic-nematic phase transitions in gravitational systems. II. Higher order multipoles. ApJ 856(2):113. https://doi.org/10.3847/1538-4357/aab268. arXiv:1712.04449 [astro-ph.GA]

Takekawa S, Oka T, Iwata Y, Tsujimoto S, Nomura M (2019) Indication of another intermediate-mass black hole in the galactic center. ApJ 871(1):L1. https://doi.org/10.3847/2041-8213/aafb07. arXiv:1812.10733 [astro-ph.GA]

Takekawa S, Oka T, Iwata Y, Tsujimoto S, Nomura M (2020) The fifth candidate for an intermediate-mass black hole in the galactic center. ApJ 890(2):167. https://doi.org/10.3847/1538-4357/ab6f6f. arXiv:2002.05173 [astro-ph.GA]

Tamai R, Cirasuolo M, González JC, Koehler B, Tuti M (2016) The E-ELT program status. In: Hall HJ, Gilmozzi R, Marshall HK (eds) Ground-based and airborne telescopes VI. Society of photo-optical instrumentation engineers (SPIE) conference series, vol 9906, p 99060W. https://doi.org/10.1117/12.2232690

Tamanini N, Danielski C (2019) The gravitational-wave detection of exoplanets orbiting white dwarf binaries using LISA. Nat Astron 3:858–866. https://doi.org/10.1038/s41550-019-0807-y. arXiv:1812.04330 [astro-ph.EP]

Tamanini N, Caprini C, Barausse E, Sesana A, Klein A, Petiteau A (2016) Science with the space-based interferometer eLISA. III: probing the expansion of the universe using gravitational wave standard sirens. J Cosmol Astropart Phys 4:002. https://doi.org/10.1088/1475-7516/2016/04/002. arXiv:1601.07112 [astro-ph.CO]

Tamanini N, Klein A, Bonvin C, Barausse E, Caprini C (2020) Peculiar acceleration of stellar-origin black hole binaries: measurement and biases with LISA. Phys Rev D 101(6):063002. https://doi.org/10.1103/PhysRevD.101.063002. arXiv:1907.02018 [astro-ph.IM]

Tamburello V, Mayer L, Shen S, Wadsley J (2015) A lower fragmentation mass scale in high-redshift galaxies and its implications on giant clumps: a systematic numerical study. MNRAS 453(3):2490–2514. https://doi.org/10.1093/mnras/stv1695. arXiv:1412.3319 [astro-ph.GA]

Tamburello V, Capelo PR, Mayer L, Bellovary JM, Wadsley JW (2017) Supermassive black hole pairs in clumpy galaxies at high redshift: delayed binary formation and concurrent mass growth. MNRAS 464(3):2952–2962. https://doi.org/10.1093/mnras/stw2561. arXiv:1603.00021 [astro-ph.GA]

Tamburello V, Rahmati A, Mayer L, Cava A, Dessauges-Zavadsky M, Schaerer D (2017) Clumpy galaxies seen in H α: inflated observed clump properties due to limited spatial resolution and sensitivity. MNRAS 468(4):4792–4800. https://doi.org/10.1093/mnras/stx784. arXiv:1610.05304 [astro-ph.GA]

Tamfal T, Capelo PR, Kazantzidis S, Mayer L, Potter D, Stadel J, Widrow LM (2018) Formation of LISA black hole binaries in merging dwarf galaxies: the imprint of dark matter. ApJ 864(1):L19. https://doi.org/10.3847/2041-8213/aada4b. arXiv:1806.11112 [astro-ph.GA]

Tamfal T, Mayer L, Quinn TR, Capelo PR, Kazantzidis S, Babul A, Potter D (2021) Revisiting dynamical friction: the role of global modes and local wakes. ApJ 916(1):55. https://doi.org/10.3847/1538-4357/ac0627. arXiv:2007.13763 [astro-ph.GA]

Tan J, Morgan E, Lewin WHG, Penninx W, van der Klis M, van Paradijs J, Makishima K, Inoue H, Dotani T, Mitsuda K (1991) Changes in the 11 minute period of 4U 1820–30. ApJ 374:291. https://doi.org/10.1086/170118

Tanaka H, Ward WR (2004) Three-dimensional interaction between a planet and an isothermal gaseous disk. II. Eccentricity waves and bending waves. ApJ 602(1):388–395. https://doi.org/10.1086/380992

Tanaka H, Takeuchi T, Ward WR (2002) Three-dimensional interaction between a planet and an isothermal gaseous disk. I. Corotation and Lindblad torques and planet migration. ApJ 565(2):1257–1274. https://doi.org/10.1086/324713

Tanaka T, Haiman Z (2009) The assembly of supermassive black holes at high redshifts. ApJ 696(2):1798–1822. https://doi.org/10.1088/0004-637X/696/2/1798. arXiv:0807.4702 [astro-ph]

Tang Y, MacFadyen A, Haiman Z (2017) On the orbital evolution of supermassive black hole binaries with circumbinary accretion discs. MNRAS 469(4):4258–4267. https://doi.org/10.1093/mnras/stx1130. arXiv:1703.03913 [astro-ph.HE]

Tang Y et al (2018) The late inspiral of supermassive black hole binaries with circumbinary gas discs in the Lisa band. MNRAS 476(2):2249–2257. https://doi.org/10.1093/mnras/sty423

Taracchini A, Buonanno A, Pan Y, Hinderer T, Boyle M, Hemberger DA, Kidder LE, Lovelace G, Mroué AH, Pfeiffer HP et al (2014) Effective-one-body model for black-hole binaries with generic mass ratios and spins. Phys Rev D 89(6):061502. https://doi.org/10.1103/PhysRevD.89.061502. arXiv:1311.2544 [gr-qc]

Tashiro M, Maejima H, Toda K, Kelley R, Reichenthal L, Lobell J, Petre R, Guainazzi M, Costantini E, Edison M et al (2018) Concept of the X-ray astronomy recovery mission. In: den Herder JWA, Nikzad S, Nakazawa K (eds) Space telescopes and instrumentation 2018: ultraviolet to gamma ray. Society of photo-optical instrumentation engineers (SPIE) conference series, vol 10699, p 1069922. https://doi.org/10.1117/12.2309455

Tauris (2018) Disentangling coalescing neutron-star-white-dwarf binaries for LISA. Phys Rev Lett 121 (13):131105. https://doi.org/10.1103/PhysRevLett.121.131105. arXiv:1809.03504 [astro-ph.SR]

Tauris TM, Dewi JDM (2001) Research note on the binding energy parameter of common envelope evolution. Dependency on the definition of the stellar core boundary during spiral-in. A&A 369:170–173. https://doi.org/10.1051/0004-6361:20010099. arXiv:astro-ph/0101530 [astro-ph]

Tauris TM, Savonije GJ (1999) Formation of millisecond pulsars. I. Evolution of low-mass X-ray binaries with $P\_orb > 2$ days. A&A 350:928–944 arXiv:astro-ph/9909147 [astro-ph]

Tauris TM, Sennels T (2000) Formation of the binary pulsars PSR B2303+46 and PSR J1141−6545. Young neutron stars with old white dwarf companions. A&A 355:236–244 arXiv:astro-ph/9909149 [astro-ph]

Tauris TM, van den Heuvel EPJ (2014) Formation of the galactic millisecond pulsar triple system PSR J0337+1715—a neutron star with two orbiting white dwarfs. ApJ 781(1):L13. https://doi.org/10.1088/2041-8205/781/1/L13. arXiv:1401.0941 [astro-ph.SR]

Tauris TM, van den Heuvel EPJ (2023) Physics of binary star evolution. From stars to X-ray binaries and gravitational wave sources. Princeton University Press, Princeton

Tauris TM, van den Heuvel EPJ, Savonije GJ (2000) Formation of millisecond pulsars with heavy white dwarf companions: extreme mass transfer on subthermal timescales. ApJ 530(2):L93–L96. https://doi.org/10.1086/312496. arXiv:astro-ph/0001013 [astro-ph]

Tauris TM, Langer N, Kramer M (2012) Formation of millisecond pulsars with CO white dwarf companions—II. Accretion, spin-up, true ages and comparison to MSPs with He white dwarf companions. MNRAS 425(3):1601–1627. https://doi.org/10.1111/j.1365-2966.2012.21446.x. arXiv:1206.1862 [astro-ph.SR]

Tauris TM, Langer N, Moriya TJ, Podsiadlowski P, Yoon SC, Blinnikov SI (2013) Ultra-stripped type Ic supernovae from close binary evolution. ApJ 778(2):L23. https://doi.org/10.1088/2041-8205/778/2/L23. arXiv:1310.6356 [astro-ph.SR]

Tauris TM, Langer N, Podsiadlowski P (2015) Ultra-stripped supernovae: progenitors and fate. MNRAS 451(2):2123–2144. https://doi.org/10.1093/mnras/stv990. arXiv:1505.00270 [astro-ph.SR]

Tauris TM, Kramer M, Freire PCC, Wex N, Janka HT, Langer N, Podsiadlowski P, Bozzo E, Chaty S, Kruckow MU et al (2017) Formation of double neutron star systems. ApJ 846(2):170. https://doi.org/10.3847/1538-4357/aa7e89. arXiv:1706.09438 [astro-ph.HE]

Tavani M, Brookshaw L (1992) The origin of planets orbiting millisecond pulsars. Nature 356(6367):320–322. https://doi.org/10.1038/356320a0

Taylor P, Kobayashi C (2014) Seeding black holes in cosmological simulations. MNRAS 442(3):2751–2767. https://doi.org/10.1093/mnras/stu983. arXiv:1405.4194 [astro-ph.GA]

Taylor S, Burke-Spolaor S, Baker PT, Charisi M, Islo K, Kelley LZ, Madison DR, Simon J, Vigeland S, Nanograv Collaboration (2019) Supermassive black-hole demographics & environments with pulsar timing arrays. BAAS 51(3):336 arXiv:1903.08183 [astro-ph.GA]

Taylor SR, Vallisneri M, Ellis JA, Mingarelli CMF, Lazio TJW, van Haasteren R (2016) Are we there yet? Time to detection of nanohertz gravitational waves based on pulsar-timing array limits. ApJ 819(1):L6. https://doi.org/10.3847/2041-8205/819/1/L6. arXiv:1511.05564 [astro-ph.IM]

Taylor SR, Simon J, Sampson L (2017) Constraints on the dynamical environments of supermassive black-hole binaries using pulsar-timing arrays. Phys Rev Lett 118(18):181102. https://doi.org/10.1103/PhysRevLett.118.181102. arXiv:1612.02817 [astro-ph.GA]

Tazzari M, Lodato G (2015) Estimating the fossil disc mass during supermassive black hole mergers: the importance of torque implementation. MNRAS 449(1):1118–1128. https://doi.org/10.1093/mnras/stv352. arXiv:1502.05046 [astro-ph.HE]

Telescope Collaboration Event Horizon, Akiyama K, Alberdi A, Alef W, Asada K, Azulay R, Baczko AK, Ball D, Baloković M, Barrett J et al (2019) First M87 event horizon telescope results. II. Array and instrumentation. ApJ 875(1):L2. https://doi.org/10.3847/2041-8213/ab0c96. arXiv:1906.11239 [astro-ph.IM]

Terrazas BA, Bell EF, Henriques BMB, White SDM, Cattaneo A, Woo J (2016) Quiescence correlates strongly with directly measured black hole mass in central galaxies. ApJ 830(1):L12. https://doi.org/10.3847/2041-8205/830/1/L12. arXiv:1609.07141 [astro-ph.GA]

Teyssandier J, Ogilvie G (2019) Growth of eccentricity in planet-disc interactions. In: EAS publications series. EAS Publications Series, vol 82, pp 415–422. https://doi.org/10.1051/eas/1982036

Teyssandier J, Ogilvie GI (2016) Growth of eccentric modes in disc-planet interactions. MNRAS 458(3):3221–3247. https://doi.org/10.1093/mnras/stw521. arXiv:1603.00653 [astro-ph.EP]

Thompson TA (2011) Accelerating compact object mergers in triple systems with the Kozai resonance: a mechanism for "prompt" type ia supernovae, gamma-ray bursts, and other exotica. ApJ 741(2):82. https://doi.org/10.1088/0004-637X/741/2/82. arXiv:1011.4322 [astro-ph.HE]

Thompson TA, Quataert E, Murray N (2005) Radiation pressure-supported starburst disks and active galactic nucleus fueling. ApJ 630(1):167–185. https://doi.org/10.1086/431923

Thompson TA, Kochanek CS, Stanek KZ, Badenes C, Post RS, Jayasinghe T, Latham DW, Bieryla A, Esquerdo GA, Berlind P et al (2019) A noninteracting low-mass black hole-giant star binary system. Science 366(6465):637–640. https://doi.org/10.1126/science.aau4005. arXiv:1806.02751 [astro-ph.HE]

Thorne KS (1974) Disk-accretion onto a black hole. II. Evolution of the hole. ApJ 191:507–520. https://doi.org/10.1086/152991

Thorsett SE, Arzoumanian Z, Camilo F, Lyne AG (1999) The triple pulsar system PSR B1620–26 in M4. ApJ 523(2):763–770. https://doi.org/10.1086/307771. arXiv:astro-ph/9903227 [astro-ph]

Thrane E, Osłowski S, Lasky PD (2020) Ultrarelativistic astrophysics using multimessenger observations of double neutron stars with LISA and the SKA. MNRAS 493(4):5408–5412. https://doi.org/10.1093/mnras/staa593. arXiv:1910.12330 [astro-ph.HE]

Tichy W, Marronetti P (2007) Binary black hole mergers: large kicks for generic spin orientations. Phys Rev D 76(6):061502. https://doi.org/10.1103/PhysRevD.76.061502. arXiv:gr-qc/0703075 [gr-qc]

Tiede C, Zrake J, MacFadyen A, Haiman Z (2020) Gas-driven inspiral of binaries in thin accretion disks. ApJ 900(1):43. https://doi.org/10.3847/1538-4357/aba432. arXiv:2005.09555 [astro-ph.GA]

Timpano SE, Rubbo LJ, Cornish NJ (2006) Characterizing the galactic gravitational wave background with LISA. Phys Rev D 73(12):122001. https://doi.org/10.1103/PhysRevD.73.122001. arXiv:gr-qc/0504071 [gr-qc]

Tisserand P, Clayton GC, Bessell MS, Welch DL, Kamath D, Wood PR, Wils P, Wyrzykowski Ł, Mróz P, Udalski A (2020) A plethora of new R Coronae Borealis stars discovered from a dedicated spectroscopic follow-up survey. A&A 635:A14. https://doi.org/10.1051/0004-6361/201834410. arXiv:1809.01743 [astro-ph.SR]

Tomsick JA, Parker ML, García JA, Yamaoka K, Barret D, Chiu JL, Clavel M, Fabian A, Fürst F, Gandhi P et al (2018) Alternative explanations for extreme supersolar iron abundances inferred from the energy spectrum of cygnus X-1. ApJ 855(1):3. https://doi.org/10.3847/1538-4357/aaaab1. arXiv:1801.07267 [astro-ph.HE]

Toonen S, Nelemans G (2013) The effect of common-envelope evolution on the visible population of post-common-envelope binaries. A&A 557:A87. https://doi.org/10.1051/0004-6361/201321753. arXiv:1309.0327 [astro-ph.SR]

Toonen S, Nelemans G, Portegies Zwart S (2012) Supernova Type Ia progenitors from merging double white dwarfs. Using a new population synthesis model. A&A 546:A70. https://doi.org/10.1051/0004-6361/201218966. arXiv:1208.6446 [astro-ph.HE]

Toonen S, Claeys JSW, Mennekens N, Ruiter AJ (2014) PopCORN: hunting down the differences between binary population synthesis codes. A&A 562:A14. https://doi.org/10.1051/0004-6361/201321576. arXiv:1311.6503 [astro-ph.SR]

Toonen S, Hamers A, Portegies Zwart S (2016) The evolution of hierarchical triple star-systems. Comput Astrophys Cosmol 3(1):6. https://doi.org/10.1186/s40668-016-0019-0. arXiv:1612.06172 [astro-ph.SR]

Toonen S, Hollands M, Gänsicke BT, Boekholt T (2017) The binarity of the local white dwarf population. A&A 602:A16. https://doi.org/10.1051/0004-6361/201629978. arXiv:1703.06893 [astro-ph.SR]

Toonen S, Perets HB, Hamers AS (2018) Rate of WD-WD head-on collisions in isolated triples is too low to explain standard type Ia supernovae. A&A 610:A22. https://doi.org/10.1051/0004-6361/201731874. arXiv:1709.00422 [astro-ph.HE]

Toonen S, Portegies Zwart S, Hamers AS, Band opadhyay D (2020) The evolution of stellar triples. The most common evolutionary pathways. A&A 640:A16. https://doi.org/10.1051/0004-6361/201936835. arXiv:2004.07848 [astro-ph.SR]

Torres-Orjuela A, Chen X, Amaro-Seoane P (2020) Phase shift of gravitational waves induced by aberration. Phys Rev D 101(8):083028. https://doi.org/10.1103/PhysRevD.101.083028. arXiv:2001.00721 [astro-ph.HE]

Torres-Orjuela A, Amaro Seoane P, Xuan Z, Chua AJK, Rosell MJB, Chen X (2021) Exciting modes due to the aberration of gravitational waves: measurability for extreme-mass-ratio inspirals. Phys Rev Lett 127(4):041102. https://doi.org/10.1103/PhysRevLett.127.041102. arXiv:2010.15842 [gr-qc]

Torres-Orjuela A, Chen X, Amaro Seoane P (2021) Excitation of gravitational wave modes by a center-of-mass velocity of the source. Phys Rev D 104(12):123025. https://doi.org/10.1103/PhysRevD.104.123025. arXiv:2010.15856 [astro-ph.CO]

Toscani M, Lodato G, Nealon R (2019) Gravitational wave emission from unstable accretion discs in tidal disruption events. MNRAS 489(1):699–706. https://doi.org/10.1093/mnras/stz2201. arXiv:1908.02969 [astro-ph.HE]

Toscani M, Rossi EM, Lodato G (2020) The gravitational wave background signal from tidal disruption events. MNRAS 498(1):507–516. https://doi.org/10.1093/mnras/staa2290. arXiv:2007.13225 [astro-ph.HE]

Toscani M, Lodato G, Price DJ, Liptai D (2022) Gravitational waves from tidal disruption events: an open and comprehensive catalog. MNRAS 510(1):992–1001. https://doi.org/10.1093/mnras/stab3384. arXiv:2111.05145 [astro-ph.HE]

Toubiana A, Marsat S, Babak S, Barausse E, Baker J (2020) Tests of general relativity with stellar-mass black hole binaries observed by LISA. Phys Rev D 101(10):104038. https://doi.org/10.1103/PhysRevD.101.104038. arXiv:2004.03626 [gr-qc]

Toubiana A, Sberna L, Caputo A, Cusin G, Marsat S, Jani K, Babak S, Barausse E, Caprini C, Pani P et al (2021) Detectable environmental effects in GW190521-like black-hole binaries with LISA. Phys Rev Lett 126:101105. https://doi.org/10.1103/PhysRevLett.126.101105. arXiv:2010.06056 [astro-ph.HE]

Touma JR, Tremaine S, Kazandjian MV (2009) Gauss's method for secular dynamics, softened. MNRAS 394(2):1085–1108. https://doi.org/10.1111/j.1365-2966.2009.14409.x. arXiv:0811.2812 [astro-ph]

Toyouchi D, Hosokawa T, Sugimura K, Kuiper R (2020) Gaseous dynamical friction under radiative feedback: do intermediate-mass black holes speed up or down? MNRAS 496(2):1909–1921. https://doi.org/10.1093/mnras/staa1338. arXiv:2002.08017 [astro-ph.GA]

Trebitsch M, Dubois Y, Volonteri M, Pfister H, Cadiou C, Katz H, Rosdahl J, Kimm T, Pichon C, Beckmann RS et al (2021) The OBELISK simulation: galaxies contribute more than AGN to H I reionization of protoclusters. A&A 653:A154. https://doi.org/10.1051/0004-6361/202037698. arXiv:2002.04045 [astro-ph.GA]

Tremaine S, Weinberg MD (1984) Dynamical friction in spherical systems. MNRAS 209:729–757. https://doi.org/10.1093/mnras/209.4.729

Tremaine S, Gebhardt K, Bender R, Bower G, Dressler A, Faber SM, Filippenko AV, Green R, Grillmair C, Ho LC et al (2002) The slope of the black hole mass versus velocity dispersion correlation. ApJ 574(2):740–753. https://doi.org/10.1086/341002. arXiv:astro-ph/0203468 [astro-ph]

Tremaine SD (1976) The formation of the nuclei of galaxies. II. The local group. ApJ 203:345–351. https://doi.org/10.1086/154085

Tremaine SD, Ostriker JP, Spitzer JL (1975) The formation of the nuclei of galaxies. I. M31. ApJ 196:407–411. https://doi.org/10.1086/153422

Tremmel M, Governato F, Volonteri M, Quinn TR (2015) Off the beaten path: a new approach to realistically model the orbital decay of supermassive black holes in galaxy formation simulations. MNRAS 451(2):1868–1874. https://doi.org/10.1093/mnras/stv1060. arXiv:1501.07609 [astro-ph.GA]

Tremmel M, Karcher M, Governato F, Volonteri M, Quinn TR, Pontzen A, Anderson L, Bellovary J (2017) The Romulus cosmological simulations: a physical approach to the formation, dynamics and accretion models of SMBHs. MNRAS 470(1):1121–1139. https://doi.org/10.1093/mnras/stx1160. arXiv:1607.02151 [astro-ph.GA]

Tremmel M, Governato F, Volonteri M, Pontzen A, Quinn TR (2018) Wandering supermassive black holes in milky-way-mass halos. ApJ 857(2):L22. https://doi.org/10.3847/2041-8213/aabc0a. arXiv:1802.06783 [astro-ph.GA]

Tremmel M, Governato F, Volonteri M, Quinn TR, Pontzen A (2018) Dancing to CHANGA: a self-consistent prediction for close SMBH pair formation time-scales following galaxy mergers. MNRAS 475(4):4967–4977. https://doi.org/10.1093/mnras/sty139. arXiv:1708.07126 [astro-ph.GA]

Trümper J, Schönfelder V (1973) Distance determination of variable X-ray sources. A&A 25:445

Tsalmantza P, Decarli R, Dotti M, Hogg DW (2011) A systematic search for massive black hole binaries in the Sloan digital sky survey spectroscopic sample. ApJ 738(1):20. https://doi.org/10.1088/0004-637X/738/1/20. arXiv:1106.1180 [astro-ph.CO]

Tsizh M, Novosyadlyj B, Holovatch Y, Libeskind NI (2020) Large-scale structures in the ΛCDM Universe: network analysis and machine learning. MNRAS 495(1):1311–1320. https://doi.org/10.1093/mnras/staa1030. arXiv:1910.07868 [astro-ph.CO]

Tso R, Gerosa D, Chen Y (2019) Optimizing LIGO with LISA forewarnings to improve black-hole spectroscopy. Phys Rev D 99(12):124043. https://doi.org/10.1103/PhysRevD.99.124043. arXiv:1807.00075 [gr-qc]

Turk MJ, Abel T, O'Shea B (2009) The formation of population III binaries from cosmological initial conditions. Science 325:601. https://doi.org/10.1126/science.1173540. arXiv:0907.2919 [astro-ph.CO]

Tutukov AV, Yungelson LR (1993) The merger rate of neutron star and black hole binaries. MNRAS 260:675–678. https://doi.org/10.1093/mnras/260.3.675

Tylenda R, Hajduk M, Kamiński T, Udalski A, Soszyński I, Szymański MK, Kubiak M, Pietrzyński G, Poleski R, Wyrzykowski Ł et al (2011) V1309 Scorpii: merger of a contact binary. A&A 528:A114. https://doi.org/10.1051/0004-6361/201016221. arXiv:1012.0163 [astro-ph.SR]

Ullio P, Zhao H, Kamionkowski M (2001) Dark-matter spike at the galactic center? Phys Rev D 64(4):043504. https://doi.org/10.1103/PhysRevD.64.043504. arXiv:astro-ph/0101481 [astro-ph]

Ulmer A (1999) Flares from the tidal disruption of stars by massive black holes. ApJ 514(1):180–187. https://doi.org/10.1086/306909

Umstätter R, Christensen N, Hendry M, Meyer R, Simha V, Veitch J, Vigeland S, Woan G (2005) Bayesian modeling of source confusion in LISA data. Phys Rev D 72(2):022001. https://doi.org/10.1103/PhysRevD.72.022001. arXiv:gr-qc/0506055 [gr-qc]

Unal C (2019) Imprints of primordial non-Gaussianity on gravitational wave spectrum. Phys Rev D 99(4):041301. https://doi.org/10.1103/PhysRevD.99.041301. arXiv:1811.09151 [astro-ph.CO]

Unal C, Loeb A (2020) On spin dependence of the fundamental plane of black hole activity. MNRAS 495(1):278–284. https://doi.org/10.1093/mnras/staa1119. arXiv:2002.11778 [astro-ph.HE]

Ünal C, Pacucci F (2021) Properties of ultralight bosons from heavy quasar spins via superradiance. J Cosmol Astropart Phys 5:007. https://doi.org/10.1088/1475-7516/2021/05/007. arXiv:2012.12790 [hep-ph]

Valiante R, Schneider R, Volonteri M, Omukai K (2016) From the first stars to the first black holes. MNRAS 457(3):3356–3371. https://doi.org/10.1093/mnras/stw225. arXiv:1601.07915 [astro-ph.GA]

Valiante R, Agarwal B, Habouzit M, Pezzulli E (2017) On the formation of the first quasars. PASA 34: e031. https://doi.org/10.1017/pasa.2017.25. arXiv:1703.03808 [astro-ph.GA]

Valiante R, Schneider R, Graziani L, Zappacosta L (2018) Chasing the observational signatures of seed black holes at z > 7: candidate statistics. MNRAS 474(3):3825–3834. https://doi.org/10.1093/mnras/stx3028. arXiv:1801.08165 [astro-ph.GA]

Valiante R, Schneider R, Zappacosta L, Graziani L, Pezzulli E, Volonteri M (2018) Chasing the observational signatures of seed black holes at z > 7: candidate observability. MNRAS 476(1):407–420. https://doi.org/10.1093/mnras/sty213

Valiante R, Colpi M, Schneider R, Mangiagli A, Bonetti M, Cerini G, Fairhurst S, Haardt F, Mills C, Sesana A (2021) Unveiling early black hole growth with multifrequency gravitational wave observations. MNRAS 500(3):4095–4109. https://doi.org/10.1093/mnras/staa3395. arXiv:2010.15096 [astro-ph.GA]

van de Meent M (2018) Gravitational self-force on generic bound geodesics in Kerr spacetime. Phys Rev D 97(10):104033. https://doi.org/10.1103/PhysRevD.97.104033. arXiv:1711.09607 [gr-qc]

van de Meent M, Pfeiffer HP (2020) Intermediate mass-ratio black hole binaries: applicability of small mass-ratio perturbation theory. Phys Rev Lett 125(18):181101. https://doi.org/10.1103/PhysRevLett.125.181101. arXiv:2006.12036 [gr-qc]

van den Heuvel EPJ (1976) Late stages of close binary systems. In: Eggleton P, Mitton S, Whelan J (eds) Structure and evolution of close binary systems. IAU symposium, vol 73, p 35

van den Heuvel EPJ (2007) Double neutron stars: evidence for two different neutron-star formation mechanisms. In: di Salvo T, Israel GL, Piersant L, Burderi L, Matt G, Tornambe A, Menna MT (eds) The multicolored landscape of compact objects and their explosive origins. American Institute of Physics conference series, vol 924, pp 598–606. https://doi.org/10.1063/1.2774916. arXiv:0704.1215 [astro-ph]

van den Heuvel EPJ (2019) High-mass X-ray binaries: progenitors of double compact objects. In: Oskinova LM, Bozzo E, Bulik T, Gies DR (eds) IAU symposium. IAU Symposium, vol 346, pp 1–13. https://doi.org/10.1017/S1743921319001315. arXiv:1901.06939 [astro-ph.HE]

van den Heuvel EPJ, Tauris TM (2020) Comment on "A noninteracting low-mass black hole-giant star binary system". Science 368(6491):eaba3282. https://doi.org/10.1126/science.aba3282. arXiv:2005.04896 [astro-ph.SR]

van den Heuvel EPJ, Portegies Zwart SF, de Mink SE (2017) Forming short-period Wolf-Rayet X-ray binaries and double black holes through stable mass transfer. MNRAS 471(4):4256–4264. https://doi.org/10.1093/mnras/stx1430. arXiv:1701.02355 [astro-ph.SR]

van der Sluys MV, Verbunt F, Pols OR (2005) Reduced magnetic braking and the magnetic capture model for the formation of ultra-compact binaries. A&A 440(3):973–979. https://doi.org/10.1051/0004-6361:20052696. arXiv:astro-ph/0506375 [astro-ph]

van der Sluys MV, Verbunt F, Pols OR (2006) Modelling the formation of double white dwarfs. A&A 460(1):209–228. https://doi.org/10.1051/0004-6361:20065066. arXiv:astro-ph/0610492 [astro-ph]

van Haaften LM, Nelemans G, Voss R, Wood MA, Kuijpers J (2012) The evolution of ultracompact X-ray binaries. A&A 537:A104. https://doi.org/10.1051/0004-6361/201117880. arXiv:1111.5978 [astro-ph.SR]

van Meter JR, Miller MC, Baker JG, Boggs WD, Kelly BJ (2010) Test of a general formula for black hole gravitational wave kicks. ApJ 719(2):1427–1432. https://doi.org/10.1088/0004-637X/719/2/1427. arXiv:1003.3865 [astro-ph.HE]

van Oirschot P, Nelemans G, Toonen S, Pols O, Brown AGA, Helmi A, Portegies Zwart S (2014) Binary white dwarfs in the halo of the Milky Way. A&A 569:A42. https://doi.org/10.1051/0004-6361/201424195. arXiv:1407.2405 [astro-ph.GA]

van Putten MH (2001) Proposed source of gravitational radiation from a torus around a black hole. Phys Rev Lett 87(9):091101. https://doi.org/10.1103/PhysRevLett.87.091101. arXiv:astro-ph/0107007 [astro-ph]

van Putten MHPM (2002) LIGO/VIRGO searches for gravitational radiation in hypernovae. ApJ 575(2):L71–L74. https://doi.org/10.1086/342781. arXiv:astro-ph/0207242 [astro-ph]

van Putten MHPM, Levinson A, Frontera F, Guidorzi C, Amati L, Della Valle M (2019) Prospects for multi-messenger extended emission from core-collapse supernovae in the Local Universe. Eur Phys J Plus 134(10):537. https://doi.org/10.1140/epjp/i2019-12932-3. arXiv:1709.04455 [astro-ph.HE]

van Son LAC, Barber C, Bahé YM, Schaye J, Barnes DJ, Crain RA, Kay ST, Theuns T, Dalla Vecchia C (2019) Galaxies with monstrous black holes in galaxy cluster environments. MNRAS 485(1):396–407. https://doi.org/10.1093/mnras/stz399. arXiv:1901.03156 [astro-ph.GA]

van Velzen S, Holoien TWS, Onori F, Hung T, Arcavi I (2020) Optical-ultraviolet tidal disruption events. Space Sci Rev 216(8):124. https://doi.org/10.1007/s11214-020-00753-z. arXiv:2008.05461 [astro-ph.HE]

van Wassenhove S, Volonteri M, Walker MG, Gair JR (2010) Massive black holes lurking in Milky Way satellites. MNRAS 408(2):1139–1146. https://doi.org/10.1111/j.1365-2966.2010.17189.x. arXiv:1001.5451 [astro-ph.CO]

Van Wassenhove S, Capelo PR, Volonteri M, Dotti M, Bellovary JM, Mayer L, Governato F (2014) Nuclear coups: dynamics of black holes in galaxy mergers. MNRAS 439(1):474–487. https://doi.org/10.1093/mnras/stu024. arXiv:1310.7581 [astro-ph.CO]

Vanderburg A, Johnson JA, Rappaport S, Bieryla A, Irwin J, Lewis JA, Kipping D, Brown WR, Dufour P, Ciardi DR et al (2015) A disintegrating minor planet transiting a white dwarf. Nature 526(7574):546–549. https://doi.org/10.1038/nature15527. arXiv:1510.06387 [astro-ph.EP]

Vanderburg A, Rappaport SA, Xu S, Crossfield IJM, Becker JC, Gary B, Murgas F, Blouin S, Kaye TG, Palle E et al (2020) A giant planet candidate transiting a white dwarf. Nature 585(7825):363–367. https://doi.org/10.1038/s41586-020-2713-y. arXiv:2009.07282 [astro-ph.EP]

Varma V, Gerosa D, Stein LC, Hébert F, Zhang H (2019) High-accuracy mass, spin, and recoil predictions of generic black-hole merger remnants. Phys Rev Lett 122(1):011101. https://doi.org/10.1103/PhysRevLett.122.011101. arXiv:1809.09125 [gr-qc]

Varma V, Isi M, Biscoveanu S (2020) Extracting the gravitational recoil from black hole merger signals. Phys Rev Lett 124(10):101104. https://doi.org/10.1103/PhysRevLett.124.101104. arXiv:2002.00296 [gr-qc]

Vasiliev E (2017) A new Fokker-Planck approach for the relaxation-driven evolution of galactic nuclei. ApJ 848(1):10. https://doi.org/10.3847/1538-4357/aa8cc8. arXiv:1709.04467 [astro-ph.GA]

Vasiliev E, Antonini F, Merritt D (2015) The final-parsec problem in the collisionless limit. ApJ 810(1):49. https://doi.org/10.1088/0004-637X/810/1/49. arXiv:1505.05480 [astro-ph.GA]

Vaskonen V, Veermäe H (2021) Did NANOGrav see a signal from primordial black hole formation? Phys Rev Lett 126(5):051303. https://doi.org/10.1103/PhysRevLett.126.051303. arXiv:2009.07832 [astro-ph.CO]

Vasudevan RV, Fabian AC, Reynolds CS, Aird J, Dauser T, Gallo LC (2016) A selection effect boosting the contribution from rapidly spinning black holes to the cosmic X-ray background. MNRAS 458 (2):2012–2023. https://doi.org/10.1093/mnras/stw363. arXiv:1506.01027 [astro-ph.HE]

Vaughan S, Uttley P, Markowitz AG, Huppenkothen D, Middleton MJ, Alston WN, Scargle JD, Farr WM (2016) False periodicities in quasar time-domain surveys. MNRAS 461(3):3145–3152. https://doi.org/10.1093/mnras/stw1412. arXiv:1606.02620 [astro-ph.IM]

Vennes S, Kawka A, O'Toole SJ, Németh P, Burton D (2012) The shortest period sdB plus white dwarf binary CD-30 11223 (GALEX J1411–3053). ApJ 759(1):L25. https://doi.org/10.1088/2041-8205/759/1/L25. arXiv:1210.1512 [astro-ph.SR]

Venturi T, Paragi Z, Lindqvist M, Bartkiewicz A, Beswick R, Bogdanović T, Brisken W, Charlot P, Colomer F, Conway J et al (2020) VLBI20-30: a scientific roadmap for the next decade—the future of the European VLBI Network. arXiv e-prints arXiv:2007.02347 [astro-ph.IM]

Veras D, Georgakarakos N, Gänsicke BT, Dobbs-Dixon I (2018) Effects of non-Kozai mutual inclinations on two-planet system stability through all phases of stellar evolution. MNRAS 481(2):2180–2188. https://doi.org/10.1093/mnras/sty2409. arXiv:1809.01157 [astro-ph.EP]

Verbunt F, Igoshev A, Cator E (2017) The observed velocity distribution of young pulsars. A&A 608:A57. https://doi.org/10.1051/0004-6361/201731518. arXiv:1708.08281 [astro-ph.HE]

Vick M, Lai D (2019) Tidal effects in eccentric coalescing neutron star binaries. Phys Rev D 100 (6):063001. https://doi.org/10.1103/PhysRevD.100.063001. arXiv:1906.08780 [astro-ph.HE]

Vigna-Gómez A, Neijssel CJ, Stevenson S, Barrett JW, Belczynski K, Justham S, de Mink SE, Müller B, Podsiadlowski P, Renzo M et al (2018) On the formation history of Galactic double neutron stars. MNRAS 481(3):4009–4029. https://doi.org/10.1093/mnras/sty2463. arXiv:1805.07974 [astro-ph.SR]

Vigna-Gómez A, MacLeod M, Neijssel CJ, Broekgaarden FS, Justham S, Howitt G, de Mink SE, Vinciguerra S, Mandel I (2020) Common-envelope episodes that lead to double neutron star formation. PASA 37:E038. https://doi.org/10.1017/pasa.2020.31. arXiv:2001.09829 [astro-ph.SR]

Vila SC (1971) Late evolution of close binaries. ApJ 168:217. https://doi.org/10.1086/151076

Vinciguerra S, Neijssel CJ, Vigna-Gómez A, Mandel I, Podsiadlowski P, Maccarone TJ, Nicholl M, Kingdon S, Perry A, Salemi F (2020) Be X-ray binaries in the SMC as indicators of mass-transfer efficiency. MNRAS 498(4):4705–4720. https://doi.org/10.1093/mnras/staa2177. arXiv:2003.00195 [astro-ph.HE]

Visbal E, Haiman Z, Bryan GL (2014) Direct collapse black hole formation from synchronized pairs of atomic cooling haloes. MNRAS 445(1):1056–1063. https://doi.org/10.1093/mnras/stu1794. arXiv:1406.7020 [astro-ph.GA]

Vitale S (2016) Multiband gravitational-wave astronomy: parameter estimation and tests of general relativity with space- and ground-based detectors. Phys Rev Lett 117(5):051102. https://doi.org/10.1103/PhysRevLett.117.051102. arXiv:1605.01037 [gr-qc]

Vitale S, Lynch R, Sturani R, Graff P (2017) Use of gravitational waves to probe the formation channels of compact binaries. Class Quantum Grav 34(3):03LT01. https://doi.org/10.1088/1361-6382/aa552e. arXiv:1503.04307 [gr-qc]

Vitale S, Farr WM, Ng KKY, Rodriguez CL (2019) Measuring the star formation rate with gravitational waves from binary black holes. ApJ 886(1):L1. https://doi.org/10.3847/2041-8213/ab50c0. arXiv:1808.00901 [astro-ph.HE]

Vogelsberger M, Genel S, Springel V, Torrey P, Sijacki D, Xu D, Snyder G, Nelson D, Hernquist L (2014) Introducing the Illustris Project: simulating the coevolution of dark and visible matter in the Universe. MNRAS 444(2):1518–1547. https://doi.org/10.1093/mnras/stu1536. arXiv:1405.2921 [astro-ph.CO]

Voit GM, Meece G, Li Y, O'Shea BW, Bryan GL, Donahue M (2017) A global model for circumgalactic and cluster-core precipitation. ApJ 845(1):80. https://doi.org/10.3847/1538-4357/aa7d04. arXiv:1607.02212 [astro-ph.GA]

Volonteri M (2007) Gravitational recoil: signatures on the massive black hole population. ApJ 663(1):L5–L8. https://doi.org/10.1086/519525. arXiv:astro-ph/0703180 [astro-ph]

Volonteri M (2010) Formation of supermassive black holes. A&A Rev 18(3):279–315. https://doi.org/10.1007/s00159-010-0029-x. arXiv:1003.4404 [astro-ph.CO]

Volonteri M, Madau P (2008) Off-nuclear AGNs as a signature of recoiling massive black holes. ApJ 687(2):L57. https://doi.org/10.1086/593353. arXiv:0809.4007 [astro-ph]

Volonteri M, Natarajan P (2009) Journey to the M_{BH}-σ relation: the fate of low-mass black holes in the Universe. MNRAS 400(4):1911–1918. https://doi.org/10.1111/j.1365-2966.2009.15577.x. arXiv:0903.2262 [astro-ph.CO]

Volonteri M, Perna R (2005) Dynamical evolution of intermediate-mass black holes and their observable signatures in the nearby Universe. MNRAS 358(3):913–922. https://doi.org/10.1111/j.1365-2966.2005.08832.x. arXiv:astro-ph/0501345 [astro-ph]

Volonteri M, Haardt F, Madau P (2003) The assembly and merging history of supermassive black holes in hierarchical models of galaxy formation. ApJ 582(2):559–573. https://doi.org/10.1086/344675. arXiv:astro-ph/0207276 [astro-ph]

Volonteri M, Madau P, Haardt F (2003) The formation of galaxy stellar cores by the hierarchical merging of supermassive black holes. ApJ 593(2):661–666. https://doi.org/10.1086/376722. arXiv:astro-ph/0304389 [astro-ph]

Volonteri M, Madau P, Quataert E, Rees MJ (2005) The distribution and cosmic evolution of massive black hole spins. ApJ 620(1):69–77. https://doi.org/10.1086/426858. arXiv:astro-ph/0410342 [astro-ph]

Volonteri M, Sikora M, Lasota JP (2007) Black hole spin and galactic morphology. ApJ 667(2):704–713. https://doi.org/10.1086/521186. arXiv:0706.3900 [astro-ph]

Volonteri M, Haardt F, Gültekin K (2008) Compact massive objects in Virgo galaxies: the black hole population. MNRAS 384(4):1387–1392. https://doi.org/10.1111/j.1365-2966.2008.12911.x. arXiv:0710.5770 [astro-ph]

Volonteri M, Lodato G, Natarajan P (2008) The evolution of massive black hole seeds. MNRAS 383 (3):1079–1088. https://doi.org/10.1111/j.1365-2966.2007.12589.x. arXiv:0709.0529 [astro-ph]

Volonteri M, Sikora M, Lasota JP, Merloni A (2013) The evolution of active galactic nuclei and their spins. ApJ 775(2):94. https://doi.org/10.1088/0004-637X/775/2/94. arXiv:1210.1025 [astro-ph.HE]

Volonteri M, Dubois Y, Pichon C, Devriendt J (2016) The cosmic evolution of massive black holes in the Horizon-AGN simulation. MNRAS 460:2979–2996. https://doi.org/10.1093/mnras/stw1123. arXiv:1602.01941

Volonteri M, Pfister H, Beckmann RS, Dubois Y, Colpi M, Conselice CJ, Dotti M, Martin G, Jackson R, Kraljic K et al (2020) Black hole mergers from dwarf to massive galaxies with the NewHorizon and Horizon-AGN simulations. MNRAS 498:2219. https://doi.org/10.1093/mnras/staa2384. arXiv:2005.04902 [astro-ph.GA]

Volonteri M, Habouzit M, Colpi M (2021) The origins of massive black holes. Nat Rev Phys 3(11):732–743. https://doi.org/10.1038/s42254-021-00364-9. arXiv:2110.10175 [astro-ph.GA]

von Zeipel H (1910) Sur l'application des séries de M. Lindstedt à l'étude du mouvement des comètes périodiques. Astron Nachr 183(22):345. https://doi.org/10.1002/asna.19091832202

Voss R, Tauris TM (2003) Galactic distribution of merging neutron stars and black holes—prospects for short gamma-ray burst progenitors and LIGO/VIRGO. MNRAS 342(4):1169–1184. https://doi.org/10.1046/j.1365-8711.2003.06616.x. arXiv:astro-ph/0303227 [astro-ph]

Wadsley JW, Stadel J, Quinn T (2004) Gasoline: a flexible, parallel implementation of TreeSPH. New A 9 (2):137–158. https://doi.org/10.1016/j.newast.2003.08.004. arXiv:astro-ph/0303521 [astro-ph]

Wan Z, Lewis GF, Li TS, Simpson JD, Martell SL, Zucker DB, Mould JR, Erkal D, Pace AB, Mackey D et al (2020) The tidal remnant of an unusually metal-poor globular cluster. Nature 583(7818):768–770. https://doi.org/10.1038/s41586-020-2483-6. arXiv:2007.14577 [astro-ph.GA]

Wang B, Han Z (2012) Progenitors of type Ia supernovae. New A Rev 56(4):122–141. https://doi.org/10.1016/j.newar.2012.04.001. arXiv:1204.1155 [astro-ph.SR]

Wang C, Lai D, Han JL (2006) Neutron star kicks in isolated and binary pulsars: observational constraints and implications for kick mechanisms. ApJ 639(2):1007–1017. https://doi.org/10.1086/499397. arXiv:astro-ph/0509484 [astro-ph]

Wang C, Jia K, Li XD (2016) The binding energy parameter for common envelope evolution. Res Astron Astrophys 16(8):126. https://doi.org/10.1088/1674-4527/16/8/126. arXiv:1605.03668 [astro-ph.SR]

Wang F, Yang J, Fan X, Hennawi JF, Barth AJ, Banados E, Bian F, Boutsia K, Connor T, Davies FB et al (2021) A luminous quasar at redshift 7.642. ApJ 907(1):L1. https://doi.org/10.3847/2041-8213/abd8c6. arXiv:2101.03179 [astro-ph.GA]

Wang G, Ni WT, Han WB, Xu P, Luo Z (2021) Alternative LISA-TAIJI networks. Phys Rev D 104(2):024012. https://doi.org/10.1103/PhysRevD.104.024012. arXiv:2105.00746 [gr-qc]

Wang JS, Lai D (2020) Evolution of inspiralling neutron star binaries: effects of tidal interactions and orbital eccentricities. Phys Rev D 102:083005. https://doi.org/10.1103/PhysRevD.102.083005. arXiv:2009.08300 [astro-ph.HE]

Wang JS, Peng FK, Wu K, Dai ZG (2018) Pre-merger electromagnetic counterparts of binary compact stars. ApJ 868(1):19. https://doi.org/10.3847/1538-4357/aae531. arXiv:1810.00170 [astro-ph.HE]

Wang L, Spurzem R, Aarseth S, Nitadori K, Berczik P, Kouwenhoven MBN, Naab T (2015) NBODY6++ GPU: ready for the gravitational million-body problem. MNRAS 450(4):4070–4080. https://doi.org/10.1093/mnras/stv817. arXiv:1504.03687 [astro-ph.IM]

Wang L, Spurzem R, Aarseth S, Giersz M, Askar A, Berczik P, Naab T, Schadow R, Kouwenhoven MBN (2016) The DRAGON simulations: globular cluster evolution with a million stars. MNRAS 458(2):1450–1465. https://doi.org/10.1093/mnras/stw274. arXiv:1602.00759 [astro-ph.SR]

Wang L, Greene JE, Ju W, Rafikov RR, Ruan JJ, Schneider DP (2017) Searching for binary supermassive black holes via variable broad emission line shifts: low binary fraction. ApJ 834(2):129. https://doi.org/10.3847/1538-4357/834/2/129. arXiv:1611.00039 [astro-ph.GA]

Wang Y, Shang Y, Babak S (2012) Extreme mass ratio inspiral data analysis with a phenomenological waveform. Phys Rev D 86(10):104050. https://doi.org/10.1103/PhysRevD.86.104050. arXiv:1207.4956 [gr-qc]

Ward WR (1988) On disk-planet interactions and orbital eccentricities. Icarus 73(2):330–348. https://doi.org/10.1016/0019-1035(88)90103-0

Ward WR (1997) Protoplanet migration by nebula tides. Icarus 126(2):261–281. https://doi.org/10.1006/icar.1996.5647

Warner B (1995) The AM Canum Venaticorum stars. Ap&SS 225(2):249–270. https://doi.org/10.1007/BF00613240

Watts AL (2019) Constraining the neutron star equation of state using pulse profile modeling. In: Xiamen-CUSTIPEN workshop on the equation of state of dense neutron-rich matter in the era of gravitational wave astronomy. American Institute of Physics conference series, vol 2127, p 020008. https://doi.org/10.1063/1.5117798. arXiv:1904.07012 [astro-ph.HE]

Webb JJ, Leigh NWC, Singh A, Ford KES, McKernan B, Bellovary J (2018) The evolution of kicked stellar-mass black holes in star cluster environments. MNRAS 474(3):3835–3846. https://doi.org/10.1093/mnras/stx3024. arXiv:1711.09100 [astro-ph.GA]

Webbink RF (1979) The evolution of low-mass close binary systems. VI. Population II W Ursae Majoris systems. ApJ 227:178–184. https://doi.org/10.1086/156717

Webbink RF (1984) Double white dwarfs as progenitors of R Coronae Borealis stars and type I supernovae. ApJ 277:355–360. https://doi.org/10.1086/161701

Webbink RF (1985) Stellar evolution and binaries. In: Pringle JE, Wade RA (eds) Interacting binary stars. Cambridge University Press, Cambridge, p 39

Weinberg MD (1986) Orbital decay of satellite galaxies in spherical systems. ApJ 300:93. https://doi.org/10.1086/163785

Weinberg MD (1989) Self-gravitating response of a spherical galaxy to sinking satellites. MNRAS 239:549–569. https://doi.org/10.1093/mnras/239.2.549

Weinberger R, Springel V, Hernquist L, Pillepich A, Marinacci F, Pakmor R, Nelson D, Genel S, Vogelsberger M, Naiman J et al (2017) Simulating galaxy formation with black hole driven thermal and kinetic feedback. MNRAS 465(3):3291–3308. https://doi.org/10.1093/mnras/stw2944. arXiv:1607.03486 [astro-ph.GA]

Weisberg JM, Huang Y (2016) Relativistic measurements from timing the binary pulsar PSR B1913+16. ApJ 829(1):55. https://doi.org/10.3847/0004-637X/829/1/55. arXiv:1606.02744 [astro-ph.HE]

Weisskopf MC, Ramsey B, O'Dell S, Tennant A, Elsner R, Soffitta P, Bellazzini R, Costa E, Kolodziejczak J, Kaspi V et al (2016) The imaging X-ray polarimetry explorer (IXPE). In: den Herder JWA,

Takahashi T, Bautz M (eds) Space telescopes and instrumentation 2016: ultraviolet to gamma ray. Society of photo-optical instrumentation engineers (SPIE) conference series, vol 9905, p 990517. https://doi.org/10.1117/12.2235240

Wen L (2003) On the eccentricity distribution of coalescing black hole binaries driven by the Kozai mechanism in globular clusters. ApJ 598(1):419–430. https://doi.org/10.1086/378794. arXiv:astro-ph/0211492 [astro-ph]

Wen L, Chen Y (2010) Geometrical expression for the angular resolution of a network of gravitational-wave detectors. Phys Rev D 81(8):082001. https://doi.org/10.1103/PhysRevD.81.082001. arXiv:1003.2504 [astro-ph.CO]

Wen L, Gair JR (2005) Detecting extreme mass ratio inspirals with LISA using time frequency methods. Class Quantum Grav 22(10):S445–S451. https://doi.org/10.1088/0264-9381/22/10/041. arXiv:gr-qc/0502100 [gr-qc]

Wesson R, Jones D, García-Rojas J, Boffin HMJ, Corradi RLM (2018) Confirmation of the link between central star binarity and extreme abundance discrepancy factors in planetary nebulae. MNRAS 480 (4):4589–4613. https://doi.org/10.1093/mnras/sty1871. arXiv:1807.09272 [astro-ph.SR]

Wetzel AR, Hopkins PF, Kim Jh, Faucher-Giguère CA, Kereš D, Quataert E (2016) Reconciling dwarf galaxies with ΛCDM cosmology: simulating a realistic population of satellites around a milky way-mass galaxy. ApJ 827(2):L23. https://doi.org/10.3847/2041-8205/827/2/L23. arXiv:1602.05957 [astro-ph.GA]

Wevers T, Torres MAP, Jonker PG, Wetuski JD, Nelemans G, Steeghs D, Maccarone TJ, Heinke C, Hynes RI, Udalski A et al (2016) Discovery of a high state AM CVn binary in the Galactic Bulge Survey. MNRAS 462(1):L106–L110. https://doi.org/10.1093/mnrasl/slw141. arXiv:1607.04262 [astro-ph.HE]

Wevers T, Stone NC, van Velzen S, Jonker PG, Hung T, Auchettl K, Gezari S, Onori F, Mata Sánchez D, Kostrzewa-Rutkowska Z et al (2019) Black hole masses of tidal disruption event host galaxies II. MNRAS 487(3):4136–4152. https://doi.org/10.1093/mnras/stz1602. arXiv:1902.04077 [astro-ph.HE]

Whalen D, Abel T, Norman ML (2004) Radiation hydrodynamic evolution of primordial H II regions. ApJ 610(1):14–22. https://doi.org/10.1086/421548. arXiv:astro-ph/0310283 [astro-ph]

Wild V, Heckman T, Charlot S (2010) Timing the starburst-AGN connection. MNRAS 405(2):933–947. https://doi.org/10.1111/j.1365-2966.2010.16536.x. arXiv:1002.3156 [astro-ph.CO]

Wilhelm MJC, Korol V, Rossi EM, D'Onghia E (2021) The Milky Way's bar structural properties from gravitational waves. MNRAS 500(4):4958–4971. https://doi.org/10.1093/mnras/staa3457. arXiv:2003.11074 [astro-ph.GA]

Will (2006) The confrontation between general relativity and experiment. Living Rev Relativ 9:3. https://doi.org/10.12942/lrr-2006-3. arXiv:gr-qc/0510072 [gr-qc]

Will CM (2014) Post-Newtonian effects in N-body dynamics: conserved quantities in hierarchical triple systems. Class Quantum Grav 31(24):244001. https://doi.org/10.1088/0264-9381/31/24/244001. arXiv:1404.7724 [astro-ph.GA]

Willems B, Kalogera V, Vecchio A, Ivanova N, Rasio FA, Fregeau JM, Belczynski K (2007) Eccentric double white dwarfs as LISA sources in globular clusters. ApJ 665(1):L59–L62. https://doi.org/10.1086/521049. arXiv:0705.4287 [astro-ph]

Williams CC, Curtis-Lake E, Hainline KN, Chevallard J, Robertson BE, Charlot S, Endsley R, Stark DP, Willmer CNA, Alberts S et al (2018) The JWST extragalactic mock catalog: modeling galaxy populations from the UV through the near-IR over 13 billion years of cosmic history. ApJS 236 (2):33. https://doi.org/10.3847/1538-4365/aabcbb. arXiv:1802.05272 [astro-ph.GA]

Wise JH, Regan JA, O'Shea BW, Norman ML, Downes TP, Xu H (2019) Formation of massive black holes in rapidly growing pre-galactic gas clouds. Nature 566(7742):85–88. https://doi.org/10.1038/s41586-019-0873-4. arXiv:1901.07563 [astro-ph.GA]

Wittor D, Gaspari M (2020) Dissecting the turbulent weather driven by mechanical AGN feedback. MNRAS 498(4):4983–5002. https://doi.org/10.1093/mnras/staa2747. arXiv:2009.03344 [astro-ph.GA]

Wong KWK, Baibhav V, Berti E (2019) Binary radial velocity measurements with space-based gravitational-wave detectors. MNRAS 488(4):5665–5670. https://doi.org/10.1093/mnras/stz2077. arXiv:1902.01402 [astro-ph.HE]

Wong KWK, Berti E, Gabella WE, Holley-Bockelmann K (2019) On the possibility of detecting ultrashort period exoplanets with LISA. MNRAS 483(1):L33–L36. https://doi.org/10.1093/mnrasl/sly208. arXiv:1808.07055 [astro-ph.EP]

Wongwathanarat A, Janka HT, Müller E (2013) Three-dimensional neutrino-driven supernovae: neutron star kicks, spins, and asymmetric ejection of nucleosynthesis products. A&A 552:A126. https://doi.org/10.1051/0004-6361/201220636. arXiv:1210.8148 [astro-ph.HE]

Woods TE, Ivanova N (2011) Can we trust models for adiabatic mass loss? ApJ 739(2):L48. https://doi.org/10.1088/2041-8205/739/2/L48. arXiv:1108.2752 [astro-ph.SR]

Woods TE, Ivanova N, van der Sluys MV, Chaichenets S (2012) On the formation of double white dwarfs through stable mass transfer and a common envelope. ApJ 744(1):12. https://doi.org/10.1088/0004-637X/744/1/12. arXiv:1102.1039 [astro-ph.SR]

Woods TE, Agarwal B, Bromm V, Bunker A, Chen KJ, Chon S, Ferrara A, Glover SCO, Haemmerlé L, Haiman Z et al (2019) Titans of the early universe: the Prato statement on the origin of the first supermassive black holes. PASA 36:e027. https://doi.org/10.1017/pasa.2019.14. arXiv:1810.12310 [astro-ph.GA]

Woosley SE (1993) Gamma-ray bursts from stellar mass accretion disks around black holes. ApJ 405:273. https://doi.org/10.1086/172359

Woosley SE, Heger A (2021) The pair-instability mass gap for black holes. ApJL 912:L31. https://doi.org/10.3847/2041-8213/abf2c4. arXiv:2103.07933 [astro-ph.SR]

Woosley SE, Blinnikov S, Heger A (2007) Pulsational pair instability as an explanation for the most luminous supernovae. Nature 450(7168):390–392. https://doi.org/10.1038/nature06333. arXiv:0710.3314 [astro-ph]

Worsley MA, Fabian AC, Bauer FE, Alexand er DM, Hasinger G, Mateos S, Brunner H, Brand t WN, Schneider DP (2005) The unresolved hard X-ray background: the missing source population implied by the Chandra and XMM-Newton deep fields. MNRAS 357(4):1281–1287. https://doi.org/10.1111/j.1365-2966.2005.08731.x. arXiv:astro-ph/0412266 [astro-ph]

Wu K, Cropper M, Ramsay G, Sekiguchi K (2002) An electrically powered binary star? MNRAS 331(1):221–227. https://doi.org/10.1046/j.1365-8711.2002.05190.x. arXiv:astro-ph/0111358 [astro-ph]

Wu XB, Wang F, Fan X, Yi W, Zuo W, Bian F, Jiang L, McGreer ID, Wang R, Yang J et al (2015) An ultraluminous quasar with a twelve-billion-solar-mass black hole at redshift 6.30. Nature 518(7540):512–515. https://doi.org/10.1038/nature14241. arXiv:1502.07418 [astro-ph.GA]

Xin C, Haiman Z (2021) Ultra-short-period massive black hole binary candidates in LSST as LISA "verification binaries". MNRAS 506(2):2408–2417. https://doi.org/10.1093/mnras/stab1856. arXiv:2105.00005 [astro-ph.HE]

Xu H, Norman ML, O'Shea BW, Wise JH (2016) Late pop III star formation during the epoch of reionization: results from the renaissance simulations. ApJ 823:140. https://doi.org/10.3847/0004-637X/823/2/140. arXiv:1604.03586

Xu W, Lai D (2017) Resonant tidal excitation of oscillation modes in merging binary neutron stars: inertial-gravity modes. Phys Rev D 96(8):083005. https://doi.org/10.1103/PhysRevD.96.083005. arXiv:1708.01839 [astro-ph.HE]

Xu XJ, Li XD (2010) On the binding energy parameter λ of common envelope evolution. ApJ 716(1):114–121. https://doi.org/10.1088/0004-637X/716/1/114. arXiv:1004.4957 [astro-ph.SR]

Yagi K, Seto N (2011) Detector configuration of DECIGO/BBO and identification of cosmological neutron-star binaries. PhRvD 83(4):044011. https://doi.org/10.1103/PhysRevD.83.044011. arXiv:1101.3940 [astro-ph.CO]

Yagi M, Yoshida M, Komiyama Y, Kashikawa N, Furusawa H, Okamura S, Graham AW, Miller NA, Carter D, Mobasher B et al (2010) A dozen new galaxies caught in the act: gas stripping and extended emission line regions in the coma cluster. AJ 140(6):1814–1829. https://doi.org/10.1088/0004-6256/140/6/1814. arXiv:1005.3874 [astro-ph.CO]

Yamaguchi MS, Kawanaka N, Bulik T, Piran T (2018) Detecting black hole binaries by Gaia. ApJ 861(1):21. https://doi.org/10.3847/1538-4357/aac5ec. arXiv:1710.09839 [astro-ph.SR]

Yang J, Wang F, Fan X, Hennawi JF, Davies FB, Yue M, Banados E, Wu XB, Venemans B, Barth AJ et al (2020) Pōniuā'ena: a luminous z = 7.5 quasar hosting a 1.5 billion solar mass black hole. ApJ 897(1):L14. https://doi.org/10.3847/2041-8213/ab9c26. arXiv:2006.13452 [astro-ph.GA]

Yang Y, Bartos I, Gayathri V, Ford KES, Haiman Z, Klimenko S, Kocsis B, Márka S, Márka Z, McKernan B et al (2019) Hierarchical black hole mergers in active galactic nuclei. Phys Rev Lett 123(18):181101. https://doi.org/10.1103/PhysRevLett.123.181101. arXiv:1906.09281 [astro-ph.HE]

Yang Y, Gayathri V, Bartos I, Haiman Z, Safarzadeh M, Tagawa H (2020) Black hole formation in the lower mass gap through mergers and accretion in AGN disks. ApJ 901(2):L34. https://doi.org/10.3847/2041-8213/abb940. arXiv:2007.04781 [astro-ph.HE]

Ye BB, Zhang X, Zhou MY, Wang Y, Yuan HM, Gu D, Ding Y, Zhang J, Mei J, Luo J (2019) Optimizing orbits for TianQin. Int J Mod Phys D 28(9):1950121. https://doi.org/10.1142/S0218271819501219

Ye CS, Fong Wf, Kremer K, Rodriguez CL, Chatterjee S, Fragione G, Rasio FA (2020) On the rate of neutron star binary mergers from globular clusters. ApJ 888(1):L10. https://doi.org/10.3847/2041-8213/ab5dc5. arXiv:1910.10740 [astro-ph.HE]

Yelda S, Ghez AM, Lu JR, Do T, Meyer L, Morris MR, Matthews K (2014) Properties of the remnant clockwise disk of young stars in the galactic center. ApJ 783(2):131. https://doi.org/10.1088/0004-637X/783/2/131. arXiv:1401.7354 [astro-ph.GA]

Yi SX, Nelemans G, Brinkerink C, Kostrzewa-Rutkowska Z, Timmer ST, Stoppa F, Rossi EM, Portegies Zwart SF (2022) The gravitational wave universe toolbox: a software package to simulate observation of the Gravitational Wave Universe with different detectors. A&A 663:A155. https://doi.org/10.1051/0004-6361/202141634. arXiv:2106.13662 [astro-ph.HE]

Yoshida N, Abel T, Hernquist L, Sugiyama N (2003) Simulations of early structure formation: primordial gas clouds. ApJ 592:645–663. https://doi.org/10.1086/375810. arXiv:astro-ph/0301645

Yu H, Weinberg NN, Fuller J (2020) Non-linear dynamical tides in white dwarf binaries. MNRAS 496 (4):5482–5502. https://doi.org/10.1093/mnras/staa1858. arXiv:2005.03058 [astro-ph.SR]

Yu Q (2002) Evolution of massive binary black holes. MNRAS 331(4):935–958. https://doi.org/10.1046/j.1365-8711.2002.05242.x. arXiv:astro-ph/0109530 [astro-ph]

Yu Q, Tremaine S (2002) Observational constraints on growth of massive black holes. MNRAS 335 (4):965–976. https://doi.org/10.1046/j.1365-8711.2002.05532.x. arXiv:astro-ph/0203082 [astro-ph]

Yu Q, Tremaine S (2003) Ejection of hypervelocity stars by the (binary) black hole in the galactic center. ApJ 599(2):1129–1138. https://doi.org/10.1086/379546. arXiv:astro-ph/0309084 [astro-ph]

Yu S, Jeffery CS (2010) The gravitational wave signal from diverse populations of double white dwarf binaries in the Galaxy. A&A 521:A85. https://doi.org/10.1051/0004-6361/201014827. arXiv:1007.4267 [astro-ph.SR]

Yu S, Lu Y, Jeffery CS (2021) Orbital evolution of neutron-star-white-dwarf binaries by Roche lobe overflow and gravitational wave radiation. MNRAS 503(2):2776–2790. https://doi.org/10.1093/mnras/stab626. arXiv:2103.01884 [astro-ph.HE]

Yuan F, Narayan R (2014) Hot accretion flows around black holes. ARA&A 52:529–588. https://doi.org/10.1146/annurev-astro-082812-141003. arXiv:1401.0586 [astro-ph.HE]

Yue XJ, Han WB (2018) Gravitational waves with dark matter minispikes: the combined effect. Phys Rev D 97(6):064003. https://doi.org/10.1103/PhysRevD.97.064003. arXiv:1711.09706 [gr-qc]

Yue XJ, Han WB, Chen X (2019) Dark matter: an efficient catalyst for intermediate-mass-ratio-inspiral events. ApJ 874(1):34. https://doi.org/10.3847/1538-4357/ab06f6. arXiv:1802.03739 [gr-qc]

Yunes N, Berti E (2008) Accuracy of the post-Newtonian approximation: optimal asymptotic expansion for quasicircular, extreme-mass ratio inspirals. Phys Rev D 77(12):124006. https://doi.org/10.1103/PhysRevD.77.124006. arXiv:0803.1853 [gr-qc]

Yunes N, Kocsis B, Loeb A, Haiman Z (2011) Imprint of accretion disk-induced migration on gravitational waves from extreme mass ratio inspirals. Phys Rev Lett 107(17):171103. https://doi.org/10.1103/PhysRevLett.107.171103. arXiv:1103.4609 [astro-ph.CO]

Yunes N, Miller MC, Thornburg J (2011) Effect of massive perturbers on extreme mass-ratio inspiral waveforms. Phys Rev D 83(4):044030. https://doi.org/10.1103/PhysRevD.83.044030. arXiv:1010.1721 [astro-ph.GA]

Yungelson LR (2008) Evolution of low-mass helium stars in semidetached binaries. Astron Lett 34 (9):620–634. https://doi.org/10.1134/S1063773708090053. arXiv:0804.2780 [astro-ph]

Yungelson LR, Lasota JP, Nelemans G, Dubus G, van den Heuvel EPJ, Dewi J, Portegies Zwart S (2006) The origin and fate of short-period low-mass black-hole binaries. A&A 454(2):559–569. https://doi.org/10.1051/0004-6361:20064984. arXiv:astro-ph/0604434 [astro-ph]

Zahn JP (1966) Les marées dans une étoile double serrée. Ann Astrophys 29:313

Zahn JP (1977) Reprint of 1977A&A....57.383Z. Tidal friction in close binary stars. A&A 500:121–132

Zana T, Dotti M, Capelo PR, Bonoli S, Haardt F, Mayer L, Spinoso D (2018) External versus internal triggers of bar formation in cosmological zoom-in simulations. MNRAS 473(2):2608–2621. https://doi.org/10.1093/mnras/stx2503. arXiv:1705.02348 [astro-ph.GA]

Zana T, Dotti M, Capelo PR, Mayer L, Haardt F, Shen S, Bonoli S (2018) Bar resilience to flybys in a cosmological framework. MNRAS 479(4):5214–5219. https://doi.org/10.1093/mnras/sty1850. arXiv:1805.03658 [astro-ph.GA]

Zelenka O, Lukes-Gerakopoulos G, Witzany V, Kopáček O (2020) Growth of resonances and chaos for a spinning test particle in the Schwarzschild background. Phys Rev D 101(2):024037. https://doi.org/10.1103/PhysRevD.101.024037. arXiv:1911.00414 [gr-qc]

Zepf SE, Stern D, Maccarone TJ, Kundu A, Kamionkowski M, Rhode KL, Salzer JJ, Ciardullo R, Gronwall C (2008) Very broad [O III] $\lambda\lambda$4959, 5007 emission from the NGC 4472 globular cluster RZ 2109 and implications for the mass of its black hole X-ray source. ApJ 683(2):L139. https://doi.org/10.1086/591937. arXiv:0805.2952 [astro-ph]

Zevin M, Pankow C, Rodriguez CL, Sampson L, Chase E, Kalogera V, Rasio FA (2017) Constraining formation models of binary black holes with gravitational-wave observations. ApJ 846:82. https://doi.org/10.3847/1538-4357/aa8408. arXiv:1704.07379 [astro-ph.HE]

Zevin M, Kremer K, Siegel DM, Coughlin S, Tsang BTH, Berry CPL, Kalogera V (2019) Can neutron-star mergers explain the r-process enrichment in globular clusters? ApJ 886(1):4. https://doi.org/10.3847/1538-4357/ab498b. arXiv:1906.11299 [astro-ph.HE]

Zevin M, Samsing J, Rodriguez C, Haster CJ, Ramirez-Ruiz E (2019) Eccentric black hole mergers in dense star clusters: the role of binary-binary encounters. ApJ 871(1):91. https://doi.org/10.3847/1538-4357/aaf6ec. arXiv:1810.00901 [astro-ph.HE]

Zhang S, Santangelo A, Feroci M, Xu Y, Lu F, Chen Y, Feng H, Zhang S, Brandt S, Hernanz M et al (2019) The enhanced X-ray timing and polarimetry mission–eXTP. Sci China Phys Mech Astron 62 (2):29502. https://doi.org/10.1007/s11433-018-9309-2. arXiv:1812.04020 [astro-ph.IM]

Zhang Z, Yunes N, Berti E (2011) Accuracy of the post-Newtonian approximation. II. Optimal asymptotic expansion of the energy flux for quasicircular, extreme mass-ratio inspirals into a Kerr black hole. Phys Rev D 84(2):024029. https://doi.org/10.1103/PhysRevD.84.024029. arXiv:1103.6041 [gr-qc]

Zhao H, Silk J (2005) Dark minihalos with intermediate mass black holes. Phys Rev Lett 95(1):011301. https://doi.org/10.1103/PhysRevLett.95.011301. arXiv:astro-ph/0501625 [astro-ph]

Zhu XJ, Thrane E (2020) Toward the unambiguous identification of supermassive binary black holes through Bayesian inference. ApJ 900(2):117. https://doi.org/10.3847/1538-4357/abac5a. arXiv:2004.10944 [astro-ph.HE]

Zinn R, West MJ (1984) The globular cluster system of the Galaxy. III. Measurements of radial velocity and metallicity for 60 clusters and a compilation of metallicities for 121 clusters. ApJS 55:45–66. https://doi.org/10.1086/190947

Ziosi BM, Mapelli M, Branchesi M, Tormen G (2014) Dynamics of stellar black holes in young star clusters with different metallicities—II. Black hole-black hole binaries. MNRAS 441(4):3703–3717. https://doi.org/10.1093/mnras/stu824. arXiv:1404.7147 [astro-ph.GA]

Zorotovic M, Schreiber MR, Gänsicke BT, Nebot Gómez-Morán A (2010) Post-common-envelope binaries from SDSS. IX: constraining the common-envelope efficiency. A&A 520:A86. https://doi.org/10.1051/0004-6361/200913658. arXiv:1006.1621 [astro-ph.SR]

Zorotovic M, Schreiber MR, Gänsicke BT (2011) Post common envelope binaries from SDSS. XI. The white dwarf mass distributions of CVs and pre-CVs. A&A 536:A42. https://doi.org/10.1051/0004-6361/201116626. arXiv:1108.4600 [astro-ph.SR]

Zorotovic M, Schreiber MR, García-Berro E, Camacho J, Torres S, Rebassa-Mansergas A, Gänsicke BT (2014) Monte Carlo simulations of post-common-envelope white dwarf + main sequence binaries: the effects of including recombination energy. A&A 568:A68. https://doi.org/10.1051/0004-6361/201323039. arXiv:1407.3301 [astro-ph.SR]

Zubovas K, King AR (2012) The M-σ relation in different environments. MNRAS 426(4):2751–2757. https://doi.org/10.1111/j.1365-2966.2012.21845.x. arXiv:1208.1380 [astro-ph.GA]

Zuckerman B, Melis C, Klein B, Koester D, Jura M (2010) Ancient planetary systems are orbiting a large fraction of white dwarf stars. ApJ 722(1):725–736. https://doi.org/10.1088/0004-637X/722/1/725. arXiv:1007.2252 [astro-ph.SR]

Zurek DR, Knigge C, Maccarone TJ, Dieball A, Long KS (2009) An ultracompact X-ray binary in the globular cluster NGC 1851. ApJ 699(2):1113–1118. https://doi.org/10.1088/0004-637X/699/2/1113. arXiv:0905.0145 [astro-ph.HE]

Zurek DR, Knigge C, Maccarone TJ, Pooley D, Dieball A, Long KS, Shara M, Sarajedini A (2016) A far-ultraviolet variable with an 18-minute period in the globular cluster NGC 1851. MNRAS 460 (4):3660–3668. https://doi.org/10.1093/mnras/stw1190. arXiv:1605.04827 [astro-ph.SR]

Zwick L, Capelo PR, Bortolas E, Mayer L, Amaro-Seoane P (2020) Improved gravitational radiation time-scales: significance for LISA and LIGO-Virgo sources. MNRAS 495(2):2321–2331. https://doi.org/10.1093/mnras/staa1314. arXiv:1911.06024 [astro-ph.GA]

Zwick L, Capelo PR, Bortolas E, Vázquez-Aceves V, Mayer L, Amaro-Seoane P (2021) Improved gravitational radiation time-scales II: spin-orbit contributions and environmental perturbations. MNRAS 506(1):1007–1018. https://doi.org/10.1093/mnras/stab1818. arXiv:2102.00015 [astro-ph. GA]

Authors and Affiliations

Pau Amaro-Seoane[1,2,3,4,182] · Jeff Andrews[5,6] · Manuel Arca Sedda[7] · Abbas Askar[8] · Quentin Baghi[9] · Razvan Balasov[10,11] · Imre Bartos[12] · Simone S. Bavera[13,14] · Jillian Bellovary[15,16,17] · Christopher P. L. Berry[5,6,18] · Emanuele Berti[19] · Stefano Bianchi[20] · Laura Blecha[12] · Stéphane Blondin[21] · Tamara Bogdanović[22] · Samuel Boissier[21] · Matteo Bonetti[23] · Silvia Bonoli[24,25] · Elisa Bortolas[26,27] · Katelyn Breivik[176] · Pedro R. Capelo[28] · Laurentiu Caramete[29] · Federico Cattorini[26,27,30] · Maria Charisi[31] · Sylvain Chaty[32] · Xian Chen[33] · Martyna Chruślińska[34] · Alvin J. K. Chua[35] · Ross Church[36] · Monica Colpi[37] · Daniel D'Orazio[38] · Camilla Danielski[39] · Melvyn B. Davies[40] · Pratika Dayal[41] · Alessandra De Rosa[42] · Andrea Derdzinski[28] · Kyriakos Destounis[43] · Massimo Dotti[26,27,44] · Ioana Duțan[45] · Irina Dvorkin[46] · Gaia Fabj[47,48] · Thierry Foglizzo[49] · Saavik Ford[50,51,52,53] · Jean-Baptiste Fouvry[54] · Alessia Franchini[26,27] · Tassos Fragos[14,55] · Chris Fryer[56] · Massimo Gaspari[57,58] · Davide Gerosa[26,27,59] · Luca Graziani[60,61,62] · Paul Groot[34,63,64,65] · Melanie Habouzit[66,67] · Daryl Haggard[68] · Zoltan Haiman[69] · Wen-Biao Han[70] · Alina Istrate[34] · Peter H. Johansson[71] · Fazeel Mahmood Khan[72] · Tomas Kimpson[73] · Kostas Kokkotas[74] · Albert Kong[75] · Valeriya Korol[76,181] · Kyle Kremer[77,78] · Thomas Kupfer[79] · Astrid Lamberts[80] · Shane Larson[5,6] · Mike Lau[81,82] · Dongliang Liu[83] · Nicole Lloyd-Ronning[84] · Giuseppe Lodato[85] · Alessandro Lupi[26,27] · Chung-Pei Ma[86] · Tomas Maccarone[87] · Ilya Mandel[81,82,88] · Alberto Mangiagli[89] · Michela Mapelli[90,91,92] · Stéphane Mathis[93] · Lucio Mayer[28] · Sean McGee[94] · Berry McKernan[179] · M. Coleman Miller[95] · David F. Mota[96] · Matthew Mumpower[97] · Syeda S. Nasim[98,99] · Gijs Nelemans[34,100,101] · Scott Noble[102] · Fabio Pacucci[103,104] · Francesca Panessa[105] · Vasileios Paschalidis[106] · Hugo Pfister[107,108] · Delphine Porquet[21] · John Quenby[109] · Angelo Ricarte[178] · Friedrich K. Röpke[110,111] · John Regan[112] · Stephan Rosswog[113] · Ashley Ruiter[114] · Milton Ruiz[115] · Jessie Runnoe[116] · Raffaella Schneider[117,118,119,120] · Jeremy Schnittman[121] · Amy Secunda[122] · Alberto Sesana[26,27] · Naoki Seto[123] · Lijing Shao[124] · Stuart Shapiro[125] · Carlos Sopuerta[126,127] · Nicholas C. Stone[128] · Arthur Suvorov[43] · Nicola Tamanini[129] · Tomas Tamfal[28] · Thomas Tauris[130] · Karel Temmink[131] · John Tomsick[132] · Silvia Toonen[133] · Alejandro Torres-

Orjuela[134] · Martina Toscani[129,135] · Antonios Tsokaros[125] ·
Caner Unal[136] · Verónica Vázquez-Aceves[137] · Rosa Valiante[138] ·
Maurice van Putten[139] · Jan van Roestel[140] · Christian Vignali[141,142] ·
Marta Volonteri[143] · Kinwah Wu[144] · Ziri Younsi[145] · Shenghua Yu[83] ·
Silvia Zane[146] · Lorenz Zwick[147] · Fabio Antonini[148] · Vishal Baibhav[149] ·
Enrico Barausse[150,151,152] · Alexander Bonilla Rivera[153] · Marica Branchesi[180] ·
Graziella Branduardi-Raymont[154] · Kevin Burdge[155] · Srija Chakraborty[156] ·
Jorge Cuadra[157] · Kristen Dage[158,159] · Benjamin Davis[160] ·
Selma E. de Mink[161] · Roberto Decarli[162] · Daniela Doneva[163] ·
Stephanie Escoffier[164] · Poshak Gandhi[165] · Francesco Haardt[166] ·
Carlos O. Lousto[167] · Samaya Nissanke[177] · Jason Nordhaus[168] ·
Richard O'Shaughnessy[168] · Simon Portegies Zwart[170] · Adam Pound[169] ·
Fabian Schussler[9] · Olga Sergijenko[171,172] · Alessandro Spallicci[173] ·
Daniele Vernieri[174] · Alejandro Vigna-Gómez[175]

✉ Lucio Mayer
lmayer@physik.uzh.ch

Pau Amaro-Seoane
amaro@riseup.net

Jeff Andrews
jeffrey.andrews@northwestern.edu

Manuel Arca Sedda
m.arcasedda@gmail.com

Abbas Askar
askar@astro.lu.se

Quentin Baghi
quentin.baghi@cea.fr

Razvan Balasov
rabalasov@spacescience.ro

Imre Bartos
imrebartos@ufl.edu

Simone S. Bavera
simone.bavera@unige.ch

Jillian Bellovary
jbellovary@amnh.org

Christopher P. L. Berry
christopher.berry.2@glasgow.ac.uk

Emanuele Berti
berti@jhu.edu

Stefano Bianchi
bianchi@fis.uniroma3.it

Laura Blecha
lblecha@ufl.edu

Stéphane Blondin
stephane.blondin@lam.fr

Tamara Bogdanović
tamarab@gatech.edu

Samuel Boissier
samuel.boissier@lam.fr

Matteo Bonetti
matteo.bonetti@unimib.it

Silvia Bonoli
silvia.bonoli@dipc.org

Elisa Bortolas
elisa.bortolas@unimib.it

Pedro R. Capelo
pcapelo@physik.uzh.ch

Laurentiu Caramete
lcaramete@spacescience.ro

Federico Cattorini
fcattorini@uninsubria.it

Maria Charisi
maria.charisi@nanograv.org

Sylvain Chaty
sylvain.chaty@u-paris.fr

Xian Chen
xian.chen@pku.edu.cn

Martyna Chruślińska
mchruslinska@mpa-garching.mpg.de

Alvin J. K. Chua
achua@caltech.edu

Ross Church
ross@astro.lu.se

Monica Colpi
monica.colpi@unimib.it

Daniel D'Orazio
daniel.dorazio@nbi.ku.dk

Camilla Danielski
cdanielski@iaa.es

Melvyn B. Davies
melvyn_b.davies@math.lu.se

Pratika Dayal
p.dayal@rug.nl

Alessandra De Rosa
alessandra.derosa@inaf.it

Andrea Derdzinski
andrea@ics.uzh.ch

Kyriakos Destounis
kyriakos.destounis@uni-tuebingen.de

Massimo Dotti
massimo.dotti@unimib.it

Ioana Duţan
idutan@spacescience.ro

Irina Dvorkin
dvorkin@iap.fr

Gaia Fabj
gaia.fabj@stud.uni-heidelberg.de

Thierry Foglizzo
thierry.foglizzo@cea.fr

Saavik Ford
sford@amnh.org

Jean-Baptiste Fouvry
fouvry@iap.fr

Alessia Franchini
alessia.franchini@unimib.it

Tassos Fragos
anastasios.fragkos@unige.ch

Chris Fryer
fryer@lanl.gov

Massimo Gaspari
massimo.gaspari@inaf.it

Davide Gerosa
davide.gerosa@unimib.it

Luca Graziani
luca.graziani@uniroma1.it

Paul Groot
p.groot@astro.ru.nl

Melanie Habouzit
habouzit.astro@gmail.com

Daryl Haggard
daryl.haggard@mcgill.ca

Zoltan Haiman
zoltan@astro.columbia.edu

Wen-Biao Han
wbhan@shao.ac.cn

Alina Istrate
a.istrate@astro.ru.nl

Peter H. Johansson
Peter.Johansson@helsinki.fi

Fazeel Mahmood Khan
khanfazeel.ist@gmail.com

Tomas Kimpson
tom.kimpson.16@ucl.ac.uk

Kostas Kokkotas
kostas.kokkotas@uni-tuebingen.de

Albert Kong
akong@gapp.nthu.edu.tw

Valeriya Korol
korol@star.sr.bham.ac.uk

Kyle Kremer
kkremer@caltech.edu

Thomas Kupfer
tkupfer@ttu.edu

Astrid Lamberts
astrid.lamberts@oca.eu

Shane Larson
s.larson@northwestern.edu

Dongliang Liu
dlliu@bao.ac.cn

Nicole Lloyd-Ronning
lloyd-ronning@lanl.gov

Giuseppe Lodato
giuseppe.lodato@unimi.it

Alessandro Lupi
alessandro.lupi@unimib.it

Chung-Pei Ma
cpma@berkeley.edu

Tomas Maccarone
thomas.maccarone@ttu.edu

Ilya Mandel
ilya.mandel@monash.edu

Alberto Mangiagli
mangiagli@apc.in2p3.fr

Michela Mapelli
michela.mapelli@unipd.it

Stéphane Mathis
stephane.mathis@cea.fr

Sean McGee
smcgee@star.sr.bham.ac.uk

M. Coleman Miller
miller@astro.umd.edu

David F. Mota
d.f.mota@astro.uio.no

Matthew Mumpower
mumpower@lanl.gov

Syeda S. Nasim
ssnkct@mst.edu

Gijs Nelemans
nelemans@astro.ru.nl

Scott Noble
scott.c.noble@nasa.gov

Fabio Pacucci
fabio.pacucci@cfa.harvard.edu

Francesca Panessa
francesca.panessa@inaf.it

Vasileios Paschalidis
vpaschal@email.arizona.edu

Hugo Pfister
pfisterastro@gmail.com

Delphine Porquet
delphine.porquet@lam.fr

John Quenby
j.quenby@imperial.ac.uk

Friedrich K. Röpke
friedrich.roepke@h-its.org

John Regan
john.regan@mu.ie

Stephan Rosswog
stephan.rosswog@astro.su.se

Ashley Ruiter
ashley.ruiter@adfa.edu.au

Milton Ruiz
ruizm@illinois.edu

Jessie Runnoe
jessie.c.runnoe@vanderbilt.edu

Raffaella Schneider
raffaella.schneider@uniroma1.it

Jeremy Schnittman
jeremy.schnittman@nasa.gov

Amy Secunda
asecunda@princeton.edu

Alberto Sesana
alberto.sesana@unimib.it

Naoki Seto
seto@tap.scphys.kyoto-u.ac.jp

Lijing Shao
lshao@pku.edu.cn

Stuart Shapiro
slshapir@illinois.edu

Carlos Sopuerta
carlos.f.sopuerta@csic.es

Nicholas C. Stone
nicholas.stone@mail.huji.ac.il

Arthur Suvorov
arthur.suvorov@tat.uni-tuebingen.de

Nicola Tamanini
nicola.tamanini@l2it.in2p3.fr

Tomas Tamfal
tomas.tamfal@uzh.ch

Thomas Tauris
tauris@mp.aau.dk

Karel Temmink
Karel.Temmink@ru.nl

John Tomsick
jtomsick@berkeley.edu

Silvia Toonen
toonen@uva.nl

Alejandro Torres-Orjuela
atorreso@mail.sysu.edu.cn

Martina Toscani
martina.toscani@l2it.in2p3.fr

Antonios Tsokaros
tsokaros@illinois.edu

Caner Unal
unalx005@umn.edu

Verónica Vázquez-Aceves
veronica@nao.cas.cn

Rosa Valiante
rosa.valiante@inaf.it

Maurice van Putten
mvp@sejong.ac.kr

Jan van Roestel
jvanroes@caltech.edu

Christian Vignali
cristian.vignali@unibo.it

Marta Volonteri
martav@iap.fr

Kinwah Wu
kinwah.wu@ucl.ac.uk

Ziri Younsi
z.younsi@ucl.ac.uk

Shenghua Yu
shenghuayu@bao.ac.cn

Silvia Zane
s.zane@ucl.ac.uk

Lorenz Zwick
zwicklo@ics.uzh.ch

Fabio Antonini
antoninif@cardiff.ac.uk

Vishal Baibhav
baibhavv@gmail.com

Enrico Barausse
barausse@sissa.it

Alexander Bonilla Rivera
alex.acidjazz@gmail.com

Graziella Branduardi-Raymont
g.branduardi-raymont@ucl.ac.uk

Kevin Burdge
kburdge@caltech.edu

Srija Chakraborty
srija.chakraborty@sns.it

Jorge Cuadra
jcuadra@npf.cl

Kristen Dage
dagek@physics.mcgill.ca

Benjamin Davis
ben.davis@nyu.edu

Selma E. de Mink
sedemink@mpa-garching.mpg.de

Roberto Decarli
roberto.decarli@inaf.it

Daniela Doneva
daniela.doneva@uni-tuebingen.de

Stephanie Escoffier
escoffier@cppm.in2p3.fr

Poshak Gandhi
poshak.gandhi@soton.ac.uk

Francesco Haardt
haardt@uninsubria.it

Carlos O. Lousto
colsma@rit.edu

Jason Nordhaus
nordhaus@astro.rit.edu

Richard O'Shaughnessy
richard.oshaughnessy@ligo.org

Simon Portegies Zwart
spz@strw.leidenuniv.nl

Adam Pound
a.pound@soton.ac.uk

Fabian Schussler
fabian.schussler@cea.fr

Olga Sergijenko
olga.sergijenko.astro@gmail.com

Alessandro Spallicci
spallicci@cnrs-orleans.fr

Daniele Vernieri
daniele.vernieri@unina.it

Alejandro Vigna-Gómez
avignagomez@nbi.ku.dk

[1]   Institute of Multidisciplinary Mathematics, Universitat Politécnica de Valéncia, Valencia, Spain

[2] Lanzhou Center for Theoretical Physics, Key Laboratory of Theoretical Physics of Gansu Province, School of Physical Science and Technology, Lanzhou University, Lanzhou 730000, People's Republic of China

[3] Institute of Theoretical Physics and Research Center of Gravitation, Lanzhou University, Lanzhou 730000, People's Republic of China

[4] Kavli Institute for Astronomy and Astrophysics, Beijing, China

[5] Center for Interdisciplinary Exploration and Research in Astrophysics (CIERA), Evanston, USA

[6] Department of Physics and Astronomy, Northwestern University, 1800 Sherman Ave, Evanston, IL 60201, USA

[7] Astronomisches Rechen Institut (University of Heidelberg), Heidelberg, Germany

[8] Lund Observatory, Department of Astronomy, and Theoretical Physics, Lund University, Box 43, 221 00 Lund, Sweden

[9] IRFU, CEA, Université Paris-Saclay, 91191 Gif-sur-Yvette, France

[10] Institute of Space Science, Măgurele, Romania

[11] Faculty of Physics, University of Bucharest, Bucharest, Romania

[12] Department of Physics, University of Florida, PO Box 118440, Gainesville, FL 32611-8440, USA

[13] Geneva Observatory, University of Geneva, Chemin Pegasi 51, 1290 Versoix, Switzerland

[14] Gravitational Wave Science Center (GWSC), Université de Genève, 1211 Geneva, Switzerland

[15] CUNY - Queensborough Community College, Queens, USA

[16] American Museum of Natural History, New York, USA

[17] CUNY Graduate Center, New York, USA

[18] SUPA, School of Physics and Astronomy, University of Glasgow, Kelvin Building, University Ave, Glasgow G12 8QQ, UK

[19] Johns Hopkins University, Baltimore, USA

[20] Dipartimento di Matematica e Fisica, Università degli Studi Roma Tre, via della Vasca Navale 84, 00146 Rome, Italy

[21] Aix Marseille Univ, CNRS, CNES, LAM, Marseille, France

[22] School of Physics and Center for Relativistic Astrophysics, 837 State St NW, Georgia Institute of Technology, Atlanta, GA 30332, USA

[23] Dipartimento di Fisica "G. Occhialini", Università degli Studi di Milano-Bicocca, Piazza della Scienza 3, 20126 Milan, Italy

[24] Donostia International Physics Centre (DIPC), Paseo Manuel de Lardizabal 4, 20018 Donostia-San Sebastian, Spain

[25] IKERBASQUE, Basque Foundation for Science, 48013 Bilbao, Spain

[26] Dipartimento di Fisica "G. Occhialini", Università degli Studi di Milano-Bicocca, Piazza della Scienza 3, 20126 Milan, Italy

[27] INFN, Sezione di Milano-Bicocca, Piazza della Scienza 3, 20126 Milan, Italy

[28] Center for Theoretical Astrophysics and Cosmology, Institute for Computational Science, University of Zurich, Winterthurerstrasse 190, 8057 Zürich, Switzerland

[29] Institute of Space Science, Magurele, Romania

[30] DiSAT, Università degli studi dell'Insubria, Via Valleggio, 11, 22100 Como, Italy

31 Department of Physics and Astronomy, Vanderbilt University, 2301 Vanderbilt Place, Nashville, TN 37235, USA

32 CNRS, AstroParticule et Cosmologie, Université de Paris, 75013 Paris, France

33 Astronomy Department, School of Physics, Peking University, Beijing 100871, People's Republic of China

34 Department of Astrophysics/IMAPP, Radboud University, P.O. Box 9010, 6500 GL Nijmegen, The Netherlands

35 Theoretical Astrophysics Group, California Institute of Technology, Pasadena, CA 91125, USA

36 Lund Observatory, Lund, Sweden

37 Department of Physics, University of Milano Bicocca, Milan, Italy

38 Niels Bohr International Academy, Niels Bohr Institute, Blegdamsvej 17, 2100 Copenhagen, Denmark

39 Instituto de Astrofísica de Andalucía (IAA-CSIC), Glorieta de la Astronomía S/N, 18008 Granada, Spain

40 Centre for Mathematical Sciences, Lund University, Box 118, 221 00 Lund, Sweden

41 Kapteyn Astronomical Institute, University of Groningen, P.O. Box 800, 9700 AV Groningen, The Netherlands

42 INAF - Istituto di Astrofisica e Planetologia Spaziali, via Fosso del Cavaliere, 133 Roma, Italy

43 Theoretical Astrophysics, IAAT, University of Tübingen, 72076 Tübingen, Germany

44 INAF, Osservatorio Astronomico di Brera, Via E. Bianchi 46, 23807 Merate, Italy

45 Institute of Space Science, Atomiştilor 409, 077125 Măgurele, Romania

46 Institut d'Astrophysique de Paris, Sorbonne Université & CNRS, UMR 7095, 98 bis bd Arago, 75014 Paris, France

47 Astronomisches Rechen-Institut, Zentrum für Astronomie, Universität Heidelberg, 69120 Heidelberg, Germany

48 Department of Astrophysics, American Museum of Natural History, New York, NY 10024, USA

49 AIM, CEA, CNRS, Université Paris-Saclay, Université Paris Diderot, Sorbonne Paris Cité, 91191 Gif-sur-Yvette, France

50 Department of Astrophysics, American Museum of Natural History, New York, NY 10024, USA

51 Center for Computational Astrophysics, Flatiron Institute, New York, NY 10010, USA

52 Graduate Center, City University of New York, 365 5th Avenue, New York, NY 10016, USA

53 Department of Science, BMCC, City University of New York, New York, NY 10007, USA

54 CNRS and Sorbonne Université, UMR 7095, Institut d'Astrophysique de Paris, 98 bis Boulevard Arago, 75014 Paris, France

55 Département d'Astronomie, Université de Geneve, Chemin Pegasi 51, 1290 Versoix, Switzerland

56 Center for Theoretical Astrophysics, Los Alamos National Laboratory, Los Alamos, NM 87545, USA

57 INAF - Osservatorio di Astrofisica e Scienza dello Spazio, via P. Gobetti 93/3, 40129 Bologna, Italy

58 Department of Astrophysical Sciences, Princeton University, 4 Ivy Lane, Princeton, NJ 08544-1001, USA

59 School of Physics and Astronomy, Institute for Gravitational Wave Astronomy, University of Birmingham, Birmingham B15 2TT, UK

[60] Dipartimento di Fisica, Sapienza, Università di Roma, Piazzale Aldo Moro 5, 00185 Rome, Italy

[61] INFN, Sezione di Roma I, P.le Aldo Moro 2, 00185 Rome, Italy

[62] INAF/Osservatorio Astrofisico di Arcetri, Largo E. Femi 5, 50125 Florence, Italy

[63] Department of Astronomy, University of Cape Town, Private Bag X3, Rondebosch 7701, South Africa

[64] South African Astronomical Observatory, P.O. Box 9, Observatory 7935, South Africa

[65] The Inter-University Institute for Data Intensive Astronomy, University of Cape Town, Private Bag X3, Rondebosch 7701, South Africa

[66] Max-Planck-Institut für Astronomie, Königstuhl 17, 69117 Heidelberg, Germany

[67] Zentrum für Astronomie der Universität Heidelberg, ITA, Albert-Ueberle-Str. 2, 69120 Heidelberg, Germany

[68] McGill Space Institute and Department of Physics, McGill University, 3600 rue University, Montréal, QC H3A 2T8, Canada

[69] Columbia University, New York, USA

[70] Shanghai Astronomical Observatory, CAS, 80 Nandan Road, Shanghai 200030, China

[71] Department of Physics, University of Helsinki, Gustaf Hällströmin katu 2, 00014 Helsinki, Finland

[72] Department of Space Science, Institute of Space Technology, Islamabad 44000, Pakistan

[73] Mullard Space Science Laboratory, University College London, Holmbury St. Mary, Dorking, Surrey RH5 6NT, UK

[74] Theoretical Astrophysics, University of Tuebingen, Tübingen, Germany

[75] Institute of Astronomy, National Tsing Hua University, Hsinchu 30013, Taiwan

[76] Institute for Gravitational Wave Astronomy, School of Physics and Astronomy, University of Birmingham, Birmingham B15 2TT, UK

[77] TAPIR, California Institute of Technology, Pasadena, CA 91125, USA

[78] The Observatories of the Carnegie Institution for Science, Pasadena, CA 91101, USA

[79] Department of Physics and Astronomy, Texas Tech University, PO Box 41051, Lubbock, TX 79409, USA

[80] Observatoire de la Côte d'Azur, CNRS, Laboratoire Lagrange, Laboratoire Artémis, Université Côte d'Azur, Bd de l'Observatoire,CS 34229, 06304 Nice Cedex 4, France

[81] Monash Centre for Astrophysics, School of Physics and Astronomy, Monash University, Clayton, VIC 3800, Australia

[82] OzGrav, Australian Research Council Centre of Excellence for Gravitational Wave Discovery, Clayton, Australia

[83] National Astronomical Observatories, Chinese Academy of Sciences, Beijing, People's Republic of China

[84] Los Alamos National Lab, The University of New Mexico, Albuquerque, USA

[85] Università degli Studi di Milano, Milan, Italy

[86] Department of Astronomy and Physics, University of California at Berkeley, Berkeley, CA 94720, USA

[87] Department of Physics and Astronomy, Texas Tech University, Box 41051, Lubbock, TX 79409-1051, USA

88 Institute of Gravitational Wave Astronomy, School of Physics and Astronomy, University of Birmingham, Birmingham B15 2TT, UK

89 APC, AstroParticule et Cosmologie, Université de Paris, CNRS, 75013 Paris, France

90 Physics and Astronomy Department Galileo Galilei, University of Padova, Vicolo dell'Osservatorio 3, 35122 Padua, Italy

91 INFN–Padova, Via Marzolo 8, 35131 Padua, Italy

92 INAF–Osservatorio Astronomico di Padova, Vicolo dell'Osservatorio 5, 35122 Padua, Italy

93 Département d'Astrophysique-AIM, CEA/DRF/IRFU, CNRS/INSU, Université Paris-Saclay, Université Paris-Diderot, Université De Paris, 91191 Gif-sur-Yvette, France

94 School of Physics and Astronomy, University of Birmingham, Edgbaston, Birmingham B15 2TT, UK

95 Department of Astronomy, University of Maryland, College Park, MD 20742-2421, USA

96 Institute of Theoretical Astrophysics, University of Oslo, PO Box 1029, Blindern, Oslo 0315, Norway

97 Los Alamos National Laboratory, Los Alamos, USA

98 Missouri University of Science and Technology, Rolla, MO, USA

99 American Museum of Natural History, New York, NY, USA

100 SRON, Netherlands Institute for Space Research, Sorbonnelaan 2, 3584 CA Utrecht, The Netherlands

101 Institute of Astronomy, KU Leuven, Celestijnenlaan 200D, 3001 Leuven, Belgium

102 Gravitational Astrophysics Laboratory, NASA Goddard Space Flight Center, Greenbelt, MD 20771, USA

103 Center for Astrophysics | Harvard & Smithsonian, Cambridge, MA 02138, USA

104 Black Hole Initiative, Harvard University, Cambridge, MA 02138, USA

105 INAF - Istituto di Astrofisica e Planetologia Spaziali, via Fosso del Cavaliere 100, 00133 Rome, Italy

106 Departments of Astronomy and Physics, University of Arizona, Tucson, AZ 85719, USA

107 Department of Physics, The University of Hong Kong, Pokfulam Road, Hong Kong, China

108 DARK, Niels Bohr Institute, University of Copenhagen, Jagtvej 128, 2200 Copenhagen, Denmark

109 Imperial College, London, UK

110 Zentrum für Astronomie der Universität Heidelberg, Institut für Theoretische Astrophysik, Heidelberg, Germany

111 Heidelberg Institute for Theoretical Studies, Heidelberg, Germany

112 Department of Theoretical Physics, Maynooth University, Maynooth, Ireland

113 The Oskar Klein Centre, Department of Astronomy, Stockholm University, Stockholm, Sweden

114 University of New South Wales (Canberra), Sydney, Australia

115 Department of Physics, University of Illinois at Urbana-Champaign, Urbana, IL 61801, USA

116 Department of Physics and Astronomy, Vanderbilt University, 6301 Stevenson Center, Nashville, TN 37235, USA

117 Dipartimento di Fisica, Universita di Roma La Sapienza, Piazzale Aldo Moro 2, 00185 Rome, Italy

[118] Sapienza School for Advanced Studies, Viale Regina Elena 291, 00161 Rome, Italy

[119] Istituto Nazionale di Astrofisica/Osservatorio Astronomico di Roma, via Frascati 33, Monte Porzio Catone, 00078 Rome, Italy

[120] Istituto Nazionale di Fisica Nucleare, Sezione di Roma1, Piazzale Aldo Moro 2, 00185 Rome, Italy

[121] NASA Goddard Space Flight Center, 8800 Greenbelt Rd, Greenbelt, MD 20771, USA

[122] Department of Astrophysical Sciences, Princeton University, Peyton Hall, Princeton, NJ 08544, USA

[123] Department of Physics, Kyoto University, Kyoto 606-8502, Japan

[124] Kavli Institute for Astronomy and Astrophysics, Peking University, Beijing 100871, China

[125] University of Illinois at Urbana-Champaign, Urbana, USA

[126] Institut de Ciéncies de l'Espai (ICE, CSIC), Campus UAB, Carrer de Can Magrans s/n, 08193 Cerdanyola del Vallés, Spain

[127] Institut d'Estudis Espacials de Catalunya (IEEC), Edifici Nexus, Carrer del Gran Capitá 2-4, despatx 201, 08034 Barcelona, Spain

[128] The Hebrew University of Jerusalem, Jerusalem, Israel

[129] Laboratoire des 2 Infinis - Toulouse (L2IT-IN2P3), Université de Toulouse, CNRS, UPS, 31062 Toulouse Cedex 9, France

[130] Department of Materials and Production, Aalborg University, Aalborg, Denmark

[131] Department of Astrophysics/IMAPP, Radboud University Nijmegen, Nijmegen, The Netherlands

[132] Space Sciences Laboratory, University of California, 7 Gauss Way, Berkeley, CA 94720-7450, USA

[133] Anton Pannekoek Institute for Astronomy, University of Amsterdam, 1090 GE Amsterdam, The Netherlands

[134] MOE Key Laboratory of TianQin Mission, TianQin Research Center for Gravitational Physics & School of Physics and Astronomy, Frontiers Science Center for TianQin, CNSA Research Center for Gravitational Waves, Sun Yat-Sen University (Zhuhai Campus), Zhuhai 519082, China

[135] Dipartimento di Fisica, Università Degli Studi di Milano, Via Celoria, 16, Milan 20133, Italy

[136] CEICO, Institute of Physics of the Czech Academy of Sciences, Na Slovance 1999/2, 182 21 Praha 8, Czechia

[137] Institute of Applied Mathematics, Academy of Mathematics and Systems Science, Chinese Academy of Sciences, Beijing 100190, China

[138] INAF-Osservatorio Astronomico di Roma, via di Frascati 33, 00078 Monte Porzio Catone, Italy

[139] Physics and Astronomy, Sejong University, 209 Neungdong-ro, Gwangjin-gu, Seoul 143-747, South Korea

[140] Caltech, 1201 E. California Blvd, Pasadena, CA 91125, USA

[141] Dipartimento di Fisica e Astronomia "Augusto Righi", Università degli Studi di Bologna, Via Gobetti 93/2, 40129 Bologna, Italy

[142] INAF – Osservatorio di Astrofisica e Scienza dello Spazio di Bologna (OAS), Via Gobetti 93/3, 40129 Bologna, Italy

[143] CNRS, UMR 7095, Institut d'Astrophysique de Paris, Sorbonne Université, 98 bis bd Arago, 75014 Paris, France

[144] Mullard Space Science Laboratory, University College London, Holmbury St Mary, Surrey RH5 6NT, UK

[145] Mullard Space Science Laboratory, University College London, Holmbury St. Mary, Dorking, Surrey RH5 6NT, UK

[146] Mullard Space Science Laboratory, University College London, Holmbury St. Mary, Dorking, Surrey RH5 6NT, UK

[147] Centre for Theoretical Astrophysics and Cosmology, University of Zürich, Zürich, Switzerland

[148] Gravity Exploration Institute, School of Physics and Astronomy, Cardiff University, Cardiff CF24 3AA, UK

[149] Department of Physics and Astronomy, Johns Hopkins University, 3400 N. Charles St, Baltimore, MD 21218, USA

[150] SISSA, Via Bonomea 265, 34136 Trieste, Italy

[151] INFN Sezione di Trieste, Trieste, USA

[152] IFPU - Institute for Fundamental Physics of the Universe, Via Beirut 2, 34014 Trieste, Italy

[153] Departamento de Física, Universidade Federal de Juiz de Fora, Juiz de Fora, MG 36036-330, Brazil

[154] Mullard Space Science Laboratory, University College London, London, UK

[155] Division of Physics, Mathematics and Astronomy, California Institute of Technology, Pasadena, CA 91125, USA

[156] Scuola Normale Superiore, Pisa, Italy

[157] Departamento de Ciencias, Facultad de Artes Liberales, Universidad Adolfo Ibáñez, Padre Hurtado 750, Viña del Mar, Chile

[158] Department of Physics, McGill University, 3600 University Street, Montréal, QC H3A 2T8, Canada

[159] McGill Space Institute, McGill University, 3550 University Street, Montréal, QC H3A 2A7, Canada

[160] Center for Astro, Particle, and Planetary Physics, New York University Abu Dhabi, Abu Dhabi, United Arab Emirates

[161] Max-Planck-Institut für Astrophysik, Karl-Schwarzschild-Straße 1, 85741 Garching, Germany

[162] INAF – Osservatorio di Astrofisica e Scienza dello Spazio di Bologna, via Gobetti 93/3, 40129 Bologna, Italy

[163] University of Tübingen, Tübingen, Germany

[164] CNRS/IN2P3, CPPM, Aix Marseille Univ, Marseille, France

[165] School of Physics and Astronomy, University of Southampton, Southampton SO17 1BJ, UK

[166] Dipartimento di Scienza e Alta Tecnologia, Università degli Studi dell'Insubria, via Valleggio 11, 22100 Como, Italy

[167] CCRG, Rochester Institute of Technology, New York, USA

[168] Center for Computational Relativity and Gravitation, Rochester Institute of Technology, Rochester, NY 14623, USA

[169] School of Mathematical Sciences and STAG Research Centre, University of Southampton, Southampton SO17 1BJ, UK

[170] Leiden Observatory, Leiden, the Netherlands

[171] Astronomical Observatory of Taras Shevchenko National University of Kyiv, Observatorna str., 3, Kyiv 04053, Ukraine

[172] Main Astronomical Observatory of the National Academy of Sciences of Ukraine, Zabolotnoho str., 27, Kyiv 03680, Ukraine

[173] Université d'Orléans - Centre National de la Recherche Scientifique, Orléans, France

[174] Dipartimento di Fisica "E. Pancini", Università di Napoli "Federico II" and INFN, Sezione di Napoli, Compl. Univ. di Monte S. Angelo, Edificio G, Via Cinthia, 80126 Naples, Italy

[175] DARK, Niels Bohr Institute, University of Copenhagen, Jagtvej 128, 2200 Copenhagen, Denmark

[176] Department of Physics, Carnegie Mellon University, Wean Hall, 5000 Forbes Ave Pittsburgh, Pittsburgh, PA 15213-3890, USA

[177] University of Amsterdam, Science Park 904, Postbus, 94485, 1090 GL, Amsterdam, The Netherlands

[178] Harvard-Smithsonian Center for Astrophysics, Harvard University, 60 Garden Street, MS-51 Cambridge, MA 02138, USA

[179] Borough of Manhattan Community College, The City University of New York, 199 Chambers Street, New York, NY 10007, USA

[180] Gran Sasso Science Institute, viale Francesco Crispi, viale Francesco Crispi, 7 - 67100, L' Aquila (AQ), Italy

[181] Max Planck Institute for Astrophysics, Karl-Schwarzschild-Straße 1, 85748 Garching bei München, Germany

[182] Institute for Multidisciplinary Mathematics, Universita' Politecnica of Valencia, Camí de Vera, s/n, 46022 Valencia, Spain